A biological signature of stress resilience: Immunization with either *Mycobacterium vaccae* NCTC 11659 or *M. vaccae* ATCC 15483 prevents stress-induced changes to proteomic, metabolomic, lipidomic, and immunological profiles in adult male rodent models

By

Kelsey Marie Loupy

M.S., University of Colorado Boulder, 2018

B.S., California Polytechnic State University, 2015

A thesis submitted to the Faculty of the Graduate School
of the University of Colorado in partial fulfillment of the
requirement for the degree of Doctor of Philosophy
Department of Integrative Physiology
2021

Committee Members:
Christopher A. Lowry
Benjamin N. Greenwood
Steven F. Maier
Robert L. Spencer
Tor D. Wager

Abstract

Loupy, Kelsey Marie (Ph.D., Integrative Physiology)

A biological signature of stress resilience: Immunization with either *Mycobacterium vaccae* NCTC 11659 or *M. vaccae* ATCC 15483 prevents stress-induced changes to proteomic, metabolomic, lipidomic, and immunological profiles in adult male rodent models

IACUC Protocol #2620

Dissertation directed by Associate Professor Christopher A. Lowry.

Stress-related psychiatric disorders, including anxiety disorders, affective disorders, and trauma- and stressor-related disorders like posttraumatic stress disorder (PTSD), are characterized by chronic, low-grade inflammation and dysregulated neuroimmune signaling. In particular, increased activation of the sympathetic nervous system (SNS), decreased activation of the parasympathetic nervous system (PNS), and disrupted glucocorticoid signaling are common among persons with PTSD. In recent years, microbial-based therapeutics have gained attention for their potential to prevent and treat stress-related psychiatric disorders such as PTSD by mediating microbiome-gut-brain axis pathways. We have previously described stress-resilience and anti-inflammatory effects of a heat-killed preparation of *Mycobacterium vaccae* NCTC 11659 in rodent models. For the first time, I demonstrate that immunization with a heat-killed preparation of *M. vaccae* ATCC 15483 is as effective as *M. vaccae* NCTC 11659 at preventing anxiety-like defensive behavioral responses 24 hours after exposure to inescapable tail shock stress (IS) in adult male rats. Using proteomic, metabolomic, lipidomic, and gene expression data, I show that immunization with either *M. vaccae* strain promotes stress resilience at a physiological level as well as a behavioral level and that these two strains might generally

converge on their mechanisms of action. Together, these data suggest that immunization with either *M. vaccae* strain attenuates SNS-induced release of proinflammatory monocytes from the bone marrow and monocyte/macrophage trafficking into the brain. These effects are associated with the prevention of IS-induced endothelial dysfunction, metabolic dysregulation, and neuroinflammation by both *M. vaccae* strains. These findings describe, for the first time, biological signatures of IS associated with anxiety-like behaviors and biological signatures of stress resilience. These results contribute to our understanding of mechanisms underlying stress vulnerability versus resilience and may provide novel targets for the prevention and treatment of stress-related psychiatric disorders. Collectively, data in this dissertation indicate that microbial-based interventions like *M. vaccae* NCTC 11659 or *M. vaccae* ATCC 15483 may be promising, novel therapeutics for use in clinical studies of stress-related psychiatric disorders.

Dedicated to my family.

Acknowledgements

First, I would like to thank my mentor, Dr. Christopher Lowry. Thank you for giving me the opportunity to find myself as a scientist, providing me the space to grow independently, and for your encouragement and guidance along the way. I am grateful that we have been able to develop such a productive and positive working relationship.

Thank you to everyone in the Behavioral Neuroendocrinology Laboratory. I learned a lot from interacting with and working beside each of my colleagues. I must give a big thank you to Dr. Cristian Zambrano for getting this experiment off the ground. Likewise, thank you, Kristin Cler and Brandon Marquart, for your efforts in helping to complete the original experiment in an accelerated timeline, which included some very late-night flow cytometry.

I would like to thank all my generous collaborators, especially Dr. Matthew Frank, for his continued assistance throughout the chapters of this dissertation, and Heather D'Angelo, for her contributions in the laboratory. This project would not be possible without Dr. Thomas Lee and Dr. Christopher Ebmeier at the Central Analytical Laboratory and Mass Spectrometry Facility at the University of Colorado Boulder, nor would it be possible without Dr. Julie Haines and Francesca Cendali at the Mass Spectrometry Metabolomics Shared Resource Facility at the University of Colorado Anschutz Medical Campus.

Thank you to my dissertation committee: Dr. Steven Maier, Dr. Robert Spencer, Dr. Benjamin Greenwood, and Dr. Tor Wager. I thank you all for your interest in my work, for prompting me to examine the big picture, and for engaging me to think outside of my field.

A special thank you to Dr. Mathew Arnold for advocating for me. In times of uncertainty, you pulled back the curtain and showed me that I can do more and be more than I thought.

Finally, a great deal of love and gratitude goes out to my family and friends (near and far). Mom, Dad, Bryan, and Anne, you are the reason I am here today; you nurtured my earliest desires to pursue the sciences and inspired me to be self-motivated, determined, and confident. With your unwavering strength and support, I feel unstoppable.

TABLE OF CONTENTS

LIST OF FIGURES

LIST OF TABLES

LIST OF ABBREVIATIONS

5-HT, 5-hydroxytryptamine, serotonin

A0A0G2JTG4, Ig-like domain containing protein A0A0G2JTG4

A0A0G2K3A6, Ig-like domain containing protein A0A0G2K3A6

A0A0G2K6T8, uncharacterized protein A0A0G2K6T8

A0A0G2K975, uncharacterized protein A0A0G2K975, similar to complement factor H-related protein

A0A0G2K980, Ig-like domain containing protein A0A0G2K980

AA, arachidonic acid

Ali3, gene encoding alpha-1-inhibitor 3 (alpha 1 I3)

A1m, gene encoding alpha-1-macroglobulin (alpha-1-M)

A2m, gene encoding alpha-2-macroglobulin (alpha-2-M)

ABCB9, ATP-binding cassette sub-family B member 9

Acta1, gene encoding alpha-actin 1/2 (α-actin 1/2)

Actb, gene encoding beta-actin (β-actin)

Acyl-C2, acylcarnitine C2:0; acetylcarnitine

Acyl-C3, acylcarnitine C3:0; propionylcarnitine

Acyl-C4, butanoylcarnitine

Acyl-C4-DC, acyl-C4-dicarboxylcarnitine, also known as methylmalonylcarnitine

Acyl-C8, acylcarnitine C8:0; octanoylcarnitine

Acyl-C8:1, octenoylcarnitine

Acyl-C10:1, acylcarnitine C10:1; decenoylcarnitine

Acyl-C14, tetradecanoylcarnitine, also known as myristoyllevocarnitine

Acyl-C20:4, arachidonoylcarnitine

Adipoq, adiponectin

AGP, alpha-1-acid glycoprotein, also known as orosomucoid

Ahsg, gene encoding alpha-2-HC-glycoprotein (also known as 59 kDa bone sialic acid-containing protein; BSP)

AK1, adenylate kinase isoenzyme 1

Ak1, gene encoding adenylate kinase isoenzyme (AK1)

Alb, gene encoding albumin

Alb, gene encoding albumin

Aldh9a, gene encoding for aldehyde dehydrogenase 9 family, A1

AldoA, fructose-bisphosphate aldolase A

Aldoa, gene encoding fructose-bisphosphate aldolase A (AldoA)

AldoC, fructose-bisphosphate aldolase C

Aldoc, gene encoding fructose-bisphosphate aldolase C (AldoC)

Alpha 1 I3, alpha-1-inhibitor 3

Alpha-1-M, alpha-1-macroglobulin

Alpha-1-MAP, major acute phase protein, also known as thiostatin or T-kininogen 1

Alpha-2-M, alpha-2-macroglobulin

AMP, adenosine monophosphate

ANG-1, angiopoetin-1

ANGL-6, angiopoetin-like 6

Angpt1, gene encoding angiopoetin-1 (AG-1)

Angptl6, gene encoding angiopoietin-like protein 6 (ANGL-6)

ANS, autonomic nervous system

ApoA-I, apolipoprotein A-I

Apoa1, gene encoding apolipoprotein A-I (ApoA-I)

ApoA-II, apolipoprotein A-II

Apoa2, gene encoding apolipoprotein A-II (ApoA-II)

ApoA-IV, apolipoprotein A-IV

ApoA-V, apolipoprotein A-V

Apoa5, gene encoding apolipoprotein A-V (ApoA-V)

ApoC-I, apolipoprotein C-I

ApoC-II, apolipoprotein C-II

Apoc2, gene encoding apolipoprotein C-II (ApoC-II)

ApoE, apolipoprotein E

Apoe, gene encoding apolipoprotein E (ApoE)

ApoM, apolipoprotein M

Apom, gene encoding apolipoprotein M

ApoN, apolipoprotein N

AST, aspartate aminotransferase

ATCC, American Tissue Culture Company; *Mycobacterium vaccae* ATCC 15483

ATP, adenosine triphosphate

BBB, blood-brain barrier

BBS, borate-buffered saline

BCSFB, blood-cerebrospinal fluid barrier

BiP, endoplasmic reticulum chaperone BiP (BiP, binding immunoglobulin protein; also known as heat shock protein 70 family protein 5)

BSH, bile salt hydrolase

BSP, 59 kDa bone sialic acid-containing protein

C1r, complement C1r

C1s, complement C1s subcomponent

C1s, gene encoding complement C1s subcomponent (C1s)

C4, complement C4

C4a, complement C4a

C4a, gene encoding complement C4a (C4a)

C4b, complement C4b

C4b, gene encoding complement C4b (C4b)

C4BPa, complement component C4b-binding protein alpha chain

C4bpa, gene encoding complement C4b-binding protein alpha chain (C4Bpa)

C4BPb, complement component C4b-binding protein beta chain

C4bpb, gene encoding complement C4b-binding protein beta chain (C4BPb)

C5, complement C5

C5, gene encoding complement component C5 (C5)

C8, complement C8

C8a, complement C8 alpha chain

C9, complement C9

C9, gene encoding complement C9 (C9)

Calm1/2/3, gene encoding calmodulin matching isoforms 1, 2, and 3 (CaM)

CaM, calmodulin

CCK, cholecystokinin

CCL2, C-C motif chemokine ligand 2

Ccl2, gene encoding C-C motif chemokine ligand 2

CCR1, C-C motif chemokine receptor 1

CCR2L, C-C motif chemokine receptor 2-like

Cd, gene encoding cluster of differentiation (CD)

CD, cluster of differentiation (CD)

Cd3e, CD3, epsilon chain

CD5L, CD5 molecule like

Cd5l, gene encoding CD5 molecule like (CD5L)

CD99, CD99 molecule (Xg blood group)

CDCA, chenodeoxycholic acid

Cdh17, gene encoding cadherin-17

CDR, chronic disruption of rhythms

Ces1C, carboxylesterase 1C

Ces1c, gene encoding carboxylesterase 1C (Ces1C)

CFHL1, complement component factor h-like 1

Cfhr1, gene encoding complement component factor h-like 1 (CFHL1)

CFU, colony-forming unit

CgA, chromogranin A

CGP-39, cartilage glycoprotein 39

ChemR23, chemokine-like receptor 1 (chemerin receptor)

Chga, gene encoding chromogranin A (CgA)

Chi3l1, chitinase-3-like protein 1

Ckm, gene encoding creatine kinase M-type (M-CK)

ClAA, 2-chloroacetamide

CL-L1, collectin subfamily member 10 (also known as collectin liver protein 1; collectin-10)

CMP, cytidine monophosphate

CNS, central nervous system

CNTN2, contactin-2

Cntn2, gene encoding contactin-2 (CNTN2)

CoA, coenzyme A

Colec10, gene encoding collectin liver protein 1 (CL-L1)

Colec11, gene encoding collectin 11

Collectin-11, collectin subfamily member 11

COX, cyclooxygenase

CPE, carboxypeptidase E

CTRP3, C1q and tumor necrosis factor-related 3 protein

CRP, C-reactive protein

Crp, C-reactive protein

Cryab, alpha-crystallin B chain

Cryab, gene encoding alpha-crystallin B chain (Cryab)

CSF, cerebrospinal fluid

CSC, chronic subordinate colony housing

CXCL4, C-X-C motif chemokine ligand 4

D3ZBB2, Ig-like domain containing protein D3ZBB2

D6D, delta-6-desaturase

DAMP, damage-associated molecular pattern

DAVID, Database for Annotation, Visualization and Integrated Discovery

DC, dendritic cell

DCA, deoxycholic acid

DHA, docosahexaenoic acid

DPA, docosapentaenoic acid

DR, dorsal raphe nucleus

DSM-5, *Diagnostic and Statistical Manual of Mental Disorders*, 5th Edition

DSS, dextran sulfate sodium

DnaJC16, DnaJ homolog subfamily C member 16

EET, epoxyeicosatrienoic acid

EF-1-alpha-1, elongation factor 1-alpha 1

Efemp1, gene encoding fibulin-3 (FIBL-3)

ELISA, enzyme-linked immunosorbent assay

EPA, eicosapentaenoic acid

ETA, eicosatrienoic acid

F1LXY6, Ig-like domain containing protein F1LXY6

F1M1R0, Ig-like domain containing protein F1M1R0

F1M299, Ig-like domain containing protein F1M299

F1MAE7, Ig-like domain containing protein F1MAE7

Factor XIIIa, coagulation factor XIII A chain

Factor IX, coagulation factor IX

Factor X, coagulation factor X

Fbln1, gene encoding fibulin-1 (FIBL-1)

FDR, false discovery rate

FGA, fibrinogen alpha chain

Fga, gene encoding fibrinogen alpha chain (FGA)

FGB, fibrinogen beta chain

Fgb, gene encoding fibrinogen beta chain (FGB)

FGG, fibrinogen gamma chain

Fgg, gene encoding fibrinogen gamma chain (FGG)

FGL-1, fibrinogen-like protein 1

FIBL-1, fibulin-1

FIBL-3, fibulin-3, also known as EGF-containing fibulin-like extracellular matrix protein 1

FoxP3, forkhead box P3

FRRS1L, DOMON domain-containing protein FRRS1L

G3V9J1 (uncharacterized protein G3V9J1; annotated by the DAVID database as alpha-1-inhibitor 3)

GALT, gut-associated lymphoid tissue

Gc, gene encoding vitamin D-binding protein (VDB)

GGH, gamma-glutamyl hydrolase

GLM, generalized linear model

GLP-1, glucagon-like peptide-1

GPCR158, G-protein coupled receptor 158

Gpld1, gene encoding phosphatidylinositol-glycan-specific phospholipase D (PI-G PLD)

GPx, glutathione peroxidase

GPx1, glutathione peroxidase 1

Gpx3, gene encoding glutathione peroxidase matching isoforms 3, 5, and 6 (GPx3/5/6)

GPx3/5/6, glutathione peroxidase (matching isoforms 3, 5, and 6)

GSH, glutathione

GSSG, glutathione disulfide

HBA-1/2, hemoglobin subunit alpha 1/2

HBB-1, hemoglobin subunit beta-1

Hbb-b1, gene encoding hemoglobin subunit beta 1 (HBB-1)

HBB-2, hemoglobin subunit beta-2

Hbb-b2, gene encoding hemoglobin subunit beta 2 (HBB-2)

HBE-1, hemoglobin subunit epsilon 1

Hbe1, gene encoding hemoglobin subunit epsilon 1 (HBE-1)

HC, home cage control conditions

HDL, high-density lipoprotein

HEPE, hydroxyeicosapentaenoic acid

HETE, hydroxyeicosatetraenoic acid

Hp, gene encoding haptoglobin

HPA, hypothalamic-pituitary-adrenal

HPETE, hydroperoxyeicosatetraenoic acid

HODE, hydroxyoctadecadienoic acid

HOTrE, hydroxy-10E,12Z,15Z-octadecatrienoic acid

Hsp70-5, heat shock protein 70 family protein 5, encoded by *HspA5*

Hspa5, gene encoding heat shock protein 70 family protein 5

IBD, inflammatory bowel disease

IDO, indoleamine 2,3-dioxygenase

IFN, interferon

IFN- γ, interferon gamma

Ig, immunoglobulin

IGF-I, insulin-like growth factor I

Igf1, gene encoding insulin-like growth factor I (IGF-I)

IGFALS, insulin-like growth factor-binding protein complex acid labile subunit

Igfals, gene encoding insulin-like growth factor-binding protein complex acid labile subunit (IGFALS)

IGFBP-5, insulin-like growth factor-binding protein 5

IGFBP-6, insulin-like growth factor-binding protein 6

Igfbp6, gene encoding insulin-like growth factor-binding protein 6 (IGFBP-6)

IgG-1, Ig gamma-1 chain C region

IgG-2a, Ig-gamma-2A chain C region

Igg-2a, gene encoding Ig-gamma-2A chain C region (IgG-2a)

IgG-2c, Ig gamma-2C chain C region

IgH-1a, immunoglobulin heavy chain 1a (also mapped as Ig gamma 2b)

Igh-1a, gene encoding immunoglobulin heavy chain 1a (IgH-1a)

Ighg1, gene encoding Ig gamma-1 chain C region (IgG-1)

IGHM, immunoglobulin heavy constant mu

IgK, Ig kappa chain C region

Igkc, gene encoding Ig kappa chain C region (IgK)

IgL-2, Ig lambda-2 chain C region

IL, interleukin

IL-6, interleukin 6

Il6, gene encoding interleukin 6

IL-10, interleukin 10

IMP, inosine monophosphate

inositol 1,2,3,5,6-PP, inositol 1,2,3,5,6-pentakisphosphate

IS, inescapable tail shock stress

ITI, inter-trial interval

ITIH4, inter-alpha trypsin inhibitor heavy chain 4

Itih4, gene encoding inter-alpha trypsin inhibitor heavy chain 4 (ITIH4)

J-chain, immunoglobulin joining chain

Jchain, gene encoding immunoglobulin joining chain (J-chain)

JSE, juvenile social exploration

KAT, kynurenine aminotransferase

KEGG, Kyoto Encyclopedia of Genes and Genomes

KBP, kallikrein-binding protein

KNG1, T-kininogen 1

Kng1, alias for gene encoding T-kininogen 1 (KNG1; also mapped as *Map1* by DAVID and *Kng1* by STRING)

KNG1L1, kininogen 1-like 1, T-kininogen 2

KNG2, T-kininogen 2

Kng2, gene encoding T-kininogen 2 (KNG2; also mapped as *Kng1l1* by DAVID and *Kng2* by STRING)

KYNU, kynureninase

LBP, lipopolysaccharide binding protein

Lbp, gene encoding lipopolysaccharide binding protein (LBP)

LC-MS/MS, liquid chromatography-tandem mass spectrometry

LDLR, low-density lipoprotein receptor

LFNG, beta-1,3-N-acetylglucosaminyltransferase lunatic fringe

LIMMA, linear models for microarray analysis

LOC259246, gene encoding major urinary protein (also known as alpha-2u globulin PGCL1; MUP)

LOX, lipoxygenase

LOXL1, lysyl oxidase-like 1

Loxl1, gene encoding lysyl oxidase-like 1 (LOXL1)

LPA, lysophosphatidic acid

lp-PLA2, lipoprotein-associated phospholipase A2

LPS, lipopolysaccharide

LRR, leucine-rich repeat

Lyz2, gene encoding lysozyme M0R789, uncharacterized protein M0R789

M cell, microfold cell

M. vaccae, *Mycobacterium vaccae*

M0RA79, uncharacterized protein M0RA79

M0RE02, uncharacterized protein M0RE02

MAC, membrane attack complex

MAMP, microbe-associated molecular pattern

MASP-2, mannan-binding lectin serine protease 2

Masp2, gene encoding mannan-binding lectin serine protease 2 (MASP-2)

MBP-A, mannose-binding protein A, also known as mannose-binding lectin or mannan-binding lectin

Mbl1, gene encoding mannose-binding protein A (MBP-A)

M-CK, creatine kinase M-type

MDD, major depressive disorder

MGB, microbiome-gut-brain

MLN, mesenteric lymph nodes

MS, mass spectrometry

MTHF, methenyltetrahydrofolate

Mug1, murinoglobulin-1, also known as alpha-1 inhibitor 3 variant I

Mug1, gene encoding murinoglobulin 1 (Mug1)

MUP, major urinary protein

MYDGF, myeloid-derived growth factor

Myh1/2, gene encoding myosin heavy chain matching isoforms 1 and 2 (MyHC-1/2)

Myh4, gene encoding myosin heavy chain 4 (MyHC-4)

Myh6/7, gene encoding myosin heavy chain matching isoforms 6 and 7 (MyHC-6/7)

MyHC-1/2, myosin heavy chain matching isoform 1 and 2

MyHC-4, myosin heavy chain 4

MyHC-6/7, myosin heavy chain matching isoforms 6 and 7

Myl2/3/4, gene encoding myosin light chain matching isoforms 1, 3, and 4 (MyLC-1/3/4)

MyLC-1/3/4, myosin light chain (matching isoforms 1, 3, and 4)

MyLC-2, myosin light chain 2

Mylpf, gene encoding myosin regulatory light chain 2 (MyLC-2)

n-3, omega-3

n-6, omega-6

NAD+, nicotinamide adenine dinucleotide (oxidized)

NADH, nicotinamide adenine dinucleotide (reduced)

NCAM1, neural cell adhesion molecule 1

Ncam1, gene encoding neural cell adhesion molecule 1 (NCAM1)

NCAM2, neural cell adhesion molecule 2

Ncam2, gene encoding neural cell adhesion molecule 2 (NCAM2)

NCTC, National Collection of Type Cultures, *Mycobacterium vaccae* NCTC 11659

NDK A/B, nucleoside diphosphate kinase (matching isoforms A and B)

Nfkbia, nuclear factor κB inhibitor α

NLRP3, NOD-, LRR- and pyrin domain-containing protein 3

Nme1/2, NME/NM23 nucleoside diphosphate kinase 1 gene, encoding NDK A/B, nucleoside diphosphate kinase (matching isoforms A and B)

NOD, nucleotide oligomerization domain

NPTXR, neuronal pentraxin receptor

Nr2f2, nuclear receptor 2, factor 2

NS, neuroserpin

Ntm, neurotrimin

Ntm, gene encoding neurotrimin (Ntm)

Ogn, osteoglycin

Ogn, gene encoding osteoglycin (Ogn)

Orm1, gene encoding alpha-1-acid glycoprotein (AGP)

P450, cytochrome P450

PAF-AH, platelet-activating factor acetylhydrolase

PAMP, pathogen-associated molecular pattern

PBMC, peripheral blood mononuclear cell

PC, principal component

PCA, principal component analysis

PF-4, platelet factor 4*Pf4*, gene encoding platelet factor 4 (PF-4)

PGA1, prostaglandin A1

PGB1, prostaglandin B1

PGB2, prostaglandin B2

PGD2, prostaglandin D2

PGD3, prostaglandin D3

PGE2, prostaglandin E2

PGLYRP2, peptidoglycan recognition protein 2

Pglyrp2, gene encoding peptidoglycan recognition protein 2 (PGLYRP2)

PI3K, phosphoinositide-3-kinase

PI-G PLD, phosphatidylinositol-glycan-specific phospholipase D

PIK3IP1, phosphoinositide-3-kinase-interacting protein 1

Pik3ip1, gene encoding phosphoinositide-3-kinase-interacting protein 1 (PIK3IP1)

PKM, pyruvate kinase

PLA_2, phospholipase A2

Pla2g7, gene encoding platelet-activating factor acetylhydrolase (PAF-AH)

PLS-DA, partial least squares-discriminant analysis

PLTP, phospholipid transfer protein

Pltp, gene encoding phospholipid transfer protein (PLTP)

PNS, parasympathetic nervous system

PON 1, serum paraoxonase/arylesterase 1

Pon1, gene encoding serum paraoxonase/arylesterase (PON 1)

PPAR, peroxisome proliferator-activated receptor

PPARα, peroxisome proliferator-activated receptor α

Ppara, gene encoding peroxisome proliferator-activated receptor α

Ppard, gene encoding peroxisome proliferator-activated receptor δ

PPARγ, peroxisome proliferator-activated receptor γ

Pparg, gene encoding peroxisome proliferator-activated receptor γ

Prg4, gene encoding proteoglycan 4

pro-MCH, pro-melanin-concentrating hormone

Proz, gene encoding protein Z

Psap, gene encoding sulfated glycoprotein 1 (SGP-1)

PSMA7, proteasome subunit alpha type-7

PSMB6, proteasome subunit beta type-6

PTSD, posttraumatic stress disorder

PUFA, polyunsaturated fatty acid

Pvalb, parvalbumin alpha

Pvalb, gene encoding parvalbumin alpha (Pvalb)

PYG, glycogen phosphorylase

Pygm, gene encoding glycogen phosphorylase (PYG)

pyridoxamine 5'-P, pyridoxamine 5'-phosphate

QPRT, quinolinic acid phosphoribosyltranferase

Rarres2, gene encoding retinoic acid receptor responder 2 (also known as chemerin)

RBEC, rat brain microvascular endothelial cell

RGD1310507, gene encoding uncharacterized protein A0A0G2K896 (similar to RIKEN cDNA)

rOSOX, sulfhydryl oxidase 1

RT-qPCR, quantitative real-time polymerase chain reaction

SAA4, serum amyloid A protein

Saa4, gene encoding serum amyloid A protein (SAA4)

Sbsn, gene encoding suprabasin

s.c., subcutaneous

SCFA, short-chain fatty acid

SDS, sodium dodecyl sulfate

Serpin A3C, serine proteinase inhibitor, clade A, member 3C

Serpina3c, gene encoding serine proteinase inhibitor, clade A, member 3C (Serpin A3C)

Serpin A3K, serine protease inhibitor A3K (also known as kallikrein-binding protein, KBP)

Serpin A3L, serine protease inhibitor A3L

Serpina3l, gene encoding serine protease inhibitor A3L (Serpin A3L)

Serpin A3M, serine protease inhibitor A3M

Serpina3m, gene encoding serine protease inhibitor A3M (Serpin A3M) Serpin A3N, serine protease inhibitor A3N

Serpin A3N, serine protease inhibitor A3N

Serpina3n, gene encoding serine protease inhibitor A3N (Serpin A3N)

Serpin G1, plasma protease C1 inhibitor

SGP-1, sulfated glycoprotein 1, also known as prosaposin

SNS, sympathetic nervous system

SP3, Single Pot Solid Phase Sample Preparation

TCA, tricarboxylic acid

TCDCA, taurochenodeoxycholic acid

TCEP, tris(2-carboxyethyl)phosphine

TDCA, taurodeoxycholic acid

TDO, tryptophan 2,3 dioxygenase

TF, tissue factor, also known as F3, coagulation factor III

TfR1, transferrin receptor protein 1

TGF-β, transforming growth factor- β

TGN38, trans-Golgi network integral membrane protein TGN38

Th17, T-helper 17

TLR, toll-like receptor

TMT, Tandem Mass Tags

TNF, tumor necrosis factor

Tph2, gene encoding tryptophan hydroxylase 2 (TPH2)

Tpm1, tropomyosin alpha-1 chain

Tpm1, gene encoding tropomyosin 1

Tpm4, tropomyosin alpha-4 chain

Tpm4, gene encoding tropomyosin 4

TRAPPC4, trafficking protein particle complex subunit 4

Treg, regulatory T cell

Trfc, gene encoding transferrin receptor protein 1 (TfR1)

TRIM33, tripartite motif-containing 33

tRNA, transfer ribonucleic acid

TUDCA, tauroursodeoxycholic acid

UDCA, ursodeoxycholic acid

UDP, uridine diphosphate

UHPLC, ultra high pressure liquid chromatography

Vanin-3, vascular non-inflammatory molecule 3

Vcl, gene encoding vinculin

VDB, vitamin D-binding protein

VIP, variable importance in projection

Vnn3, gene encoding vascular non-inflammatory molecule 3 (Vanin-3)

VSTM2B, V-set and transmembrane domain containing 2B

VWF, von Willebrand factor

Vwf, gene encoding von Willebrand factor (VWF)

WRS, tryptophanyl-tRNA synthetase

YIPF3, YIP1 family member 3

YWHAE, 14-3-3 protein epsilon

Ywhae, gene encoding 14-3-3 protein epsilon (YWHAE)

YWHAG, 14-3-3 protein gamma

Ywhag, gene encoding 14-3-3 protein gamma (YWHAG)

Chapter 1. Introduction: Posttraumatic stress disorder and the gut microbiome

Citation

Loupy, K.M., Lowry, C.A. (2020). Posttraumatic stress disorder and the gut microbiome. *The Oxford Handbook of the Microbiome-Gut-Brain Axis*, Oxford University Press, available online. DOI: 10.1093/oxfordhb/9780190931544.013.1.

Authors' names

Kelsey M. Loupy[a] and Christopher A. Lowry[a,b,c,d,e,f,g]

Authors' affiliations

[a]Department of Integrative Physiology, University of Colorado Boulder, Boulder, CO 80309, USA

[b]Center for Neuroscience and Center for Microbial Exploration, University of Colorado Boulder, Boulder, CO 80309, USA

[c]Department of Physical Medicine and Rehabilitation and Center for Neuroscience, University of Colorado, Anschutz Medical Campus, Aurora, CO 80045, USA

[d]Veterans Health Administration, Rocky Mountain Mental Illness Research Education and Clinical Center, Denver, CO 80045, USA

[e]Military and Veteran Microbiome Consortium for Research and Education (MVM-CoRE), Denver, CO 80045, USA

[f]Senior Fellow, inVIVO Planetary Health, of the Worldwide Universities Network (WUN), West New York, NJ 07093, USA

1.1 Abstract

Posttraumatic stress disorder (PTSD) is a trauma- and stressor-related disorder that is often associated with the dysregulation of multiple physiological systems, including autonomic nervous system functioning, glucocorticoid signaling, and chronic low-grade inflammation. Recent evidence suggests that persons with a diagnosis of PTSD also exhibit alterations in the composition of gut microbiomes compared to people who are trauma-exposed but do not develop PTSD. The bidirectional communication between the gut microbiome, the gut, and the brain, deemed the microbiome-gut-brain (MGB) axis, is composed of neural, neuroendocrine, and immune processes that both impact and respond to the structure of the gut microbiome. This chapter aims to outline (1) the ways in which trauma and stressor exposure may impact the gut microbiome; (2) the ways in which gut microbiome composition may influence brain function, including anxiety, and fear responses; and (3) how the bidirectional MGB axis, through interactions with several physiological circuits, may determine individual variability in resilience versus vulnerability to development of PTSD after trauma exposure.

1.2 Introduction

Posttraumatic stress disorder (PTSD) is a trauma- and stressor-related disorder. Both the risk of development of PTSD and the persistence of PTSD symptoms may be influenced by the bidirectional signaling of the microbiome-gut-brain (MGB) axis. We begin by defining PTSD and its economic and social costs and then define the gut microbiome. We then describe

physiological mechanisms through which trauma and stressor exposures can impact the gut microbiome. Finally, we describe physiological mechanisms through which the gut microbiome signals to the central nervous system (CNS) to influence the risk of developing PTSD and maintenance of PTSD symptoms. We then conclude by highlighting future directions in this expanding and rapidly progressing field of research.

1.3 PTSD as a trauma- and stressor-related disorder

Posttraumatic stress disorder is a trauma- and stressor-related disorder characterized by behavioral symptoms that include re-experiencing a traumatic event, avoidance of trauma-related stimuli, negative alterations of cognitions and mood, and alterations of arousal and reactivity following the experience of a traumatic event (American Psychiatric Association, 2013). PTSD is often comorbid with other psychological and physiological disorders, such as anxiety disorders, depression, diabetes, hypertension, and substance abuse (Reisman, 2016). Taken together, the economic burden of PTSD is high. Among US veterans alone, the annual health care cost was estimated to be more than $16,000 per person (Wang, Li, Zhou, Pandya, & Baser, 2016); to put this in perspective, in 2012, PTSD was the third most prevalent disability in US veterans (Reisman, 2016). The National Center for PTSD has estimated that 50% of all people living in the United States, citizens and military persons alike, will experience a traumatic event at some point in their lives, yet only 7–8% of the population will develop PTSD (National Center for Posttraumatic Stress Disorder., 2018). Although the prevalence of PTSD is higher among those exposed to military combat—approaching 20% (Hoge et al., 2014)—individual variability exists in risk of development of PTSD following exposure to trauma. This may be due to a variety of risk factors, including genetic and environmental predispositions.

The human microbiome has recently gained attention for its potential contribution to individual variability in risk of development of PTSD following exposure to trauma, due to its many interactions with the host, including effects on neural, neuroendocrine, and immune signaling (Figure 1.1). Persons with a diagnosis of PTSD show alterations in their gut microbiota relative to trauma-exposed controls (Hemmings et al., 2017), as well as in their autonomic nervous system (ANS) (Park et al., 2017), neuroendocrine (Wichmann et al., 2017), and immune (Eswarappa et al., 2018) signaling. For the purposes of this chapter, we highlight the role of the gut microbiome and its interactions with efferent and afferent signaling mechanisms in overlapping physiological processes. It is worth noting, however, that microbiomes associated with other ecological niches of the human body (such as the skin, mouth, and respiratory tracts) may also be relevant to human health and may contribute to the risk of development of psychiatric disorders like PTSD.

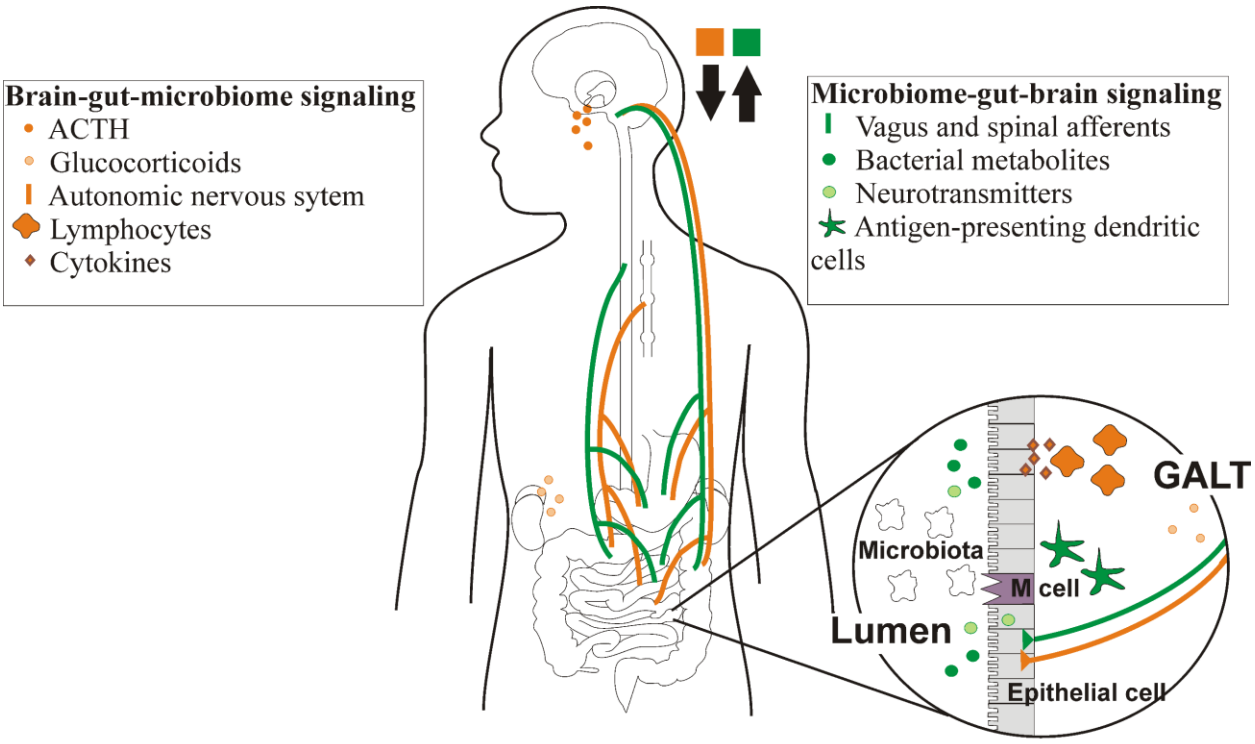

Figure 1.1 Proposed pathways for the bidirectional microbiome-gut-brain (MGB) axis. Interactions among the microbiome and autonomic, neuroendocrine, and immune systems of the host may influence stress resilience and vulnerability to the development of trauma- and stressor-related disorders such as posttraumatic stress disorder (PTSD). Abbreviations: ACTH, adrenocorticotropic hormone; GALT, gut-associated lymphoid tissue; M cell, microfold cell.

1.4 The gut microbiome

The gut microbiome consists of all microorganisms and their genes residing in the gut, whereas "gut microbiota" refers only to the living microorganisms (Turnbaugh et al., 2007). The microbiota-derived metabolome consists of all metabolite products that are synthesized by microbiota and may or may not be released extracellularly (Mashego et al., 2007; Turnbaugh et al., 2007). Commensal microbiota, one category of "Old Friends," are thought to be vital for modern human health, since long-standing evolutionary relationships have developed between commensal microorganisms and humans (Rook et al., 2013a; Rook and Lowry, 2008). The

compositions of individual microbiomes arise through a complex interplay between genetics and environment, although emerging evidence suggests that environment plays a dominating role in establishing resident and transient microbiota (Rothschild et al., 2018; Tasnim et al., 2017). Therefore, the microbiome is dynamic, with the potential to shift rapidly in accordance with the host's environment and lifestyle factors (David et al., 2014). We are now beginning to understand how differences in the number or types of microorganisms that constitute the microbiota may contribute to differences in physical health, behavior, and affect (Valles-Colomer et al., 2019). Likewise, gut dysbiosis, or an imbalance in the composition of the gut microbiota, may lead to alterations in the types and abundances of active compounds released by the microbiota into the gut, which may consequently affect gut permeability, neuronal excitability, and chemical signaling in the host (Valdes et al., 2018), discussed in more detail in the sections that follow. It is important to note that the composition of the gut microbiota includes all taxonomic domains of life: archaea, bacteria, viruses, and eukaryotes, such as fungi; however, the relative abundance of these is dominated by bacteria (Marchesi, 2010). Thus, for the purposes of this chapter, we will focus on bacterial contributions to the gut microbiome and their interactions with host physiology and behavior.

It is estimated that more than 1,000 different bacterial species colonize the human gut with at least 160 different species per individual, and, collectively, these bacteria house approximately 150 times more genetic information than the human host (Qin et al., 2010). More recently, it has been estimated that the number of bacterial cells residing in the gut equals the total number of human cells of the host (Sender et al., 2016). These bacteria exist across many phyla, the most abundant of which are Firmicutes, Bacteriodetes, Proteobacteria, and Actinobacteria (Eckburg et

al., 2005), and they produce a multitude of compounds that interact with the host physiology, including fatty acids, secondary bile acids, and neurotransmitters (Koh et al., 2016; Ramírez-Pérez et al., 2017; Strandwitz, 2018). These metabolites can interact with gut epithelial cells, stimulate afferent neural fibers traveling in sympathetic and parasympathetic nerve bundles, enter the bloodstream to travel to distant sites, and activate immune cells.

In more recent years, scientists have uncovered many mechanisms through which the CNS communicates with the gut (and vice versa) and how this bidirectional signaling both influences and is influenced by the gut microbiota. Thus, the MGB axis comprises a set of bidirectional communication pathways and employs multiple physiological systems, including neural, metabolite/endocrine/neuroendocrine, and immune systems.

1.5 PTSD and the gut microbiome

Evidence suggests that the composition of the gut microbiome is different in persons with a diagnosis of PTSD, relative to trauma-exposed controls. For example, a recent study found differences in the relative abundance of a consortium of three phyla between persons with a diagnosis of PTSD and trauma-exposed controls, although there were no significant differences in overall microbial alpha or beta diversity measures between PTSD and trauma-exposed control groups (Hemmings et al., 2017). The three phyla (Actinobacteria, Lentisphaerae, and Verrucomicrobia) were correlated with higher Clinician-Administered Posttraumatic Stress Disorder Scale (CAPS) scores, where lower abundances of these phyla correlated with higher CAPS scores, suggesting an important role of these phyla in distinguishing trauma-exposed individuals with and without a diagnosis of PTSD (Hemmings et al., 2017). The current literature

points to a diverse gut microbial community as having a fundamental association with positive health and affect (Lloyd-Price et al., 2016). Thus, interest in studying the relevance of gut microbiome dysbiosis, or imbalance, in the context of the development and persistence of PTSD symptoms is growing (Leclercq et al., 2016).

It is well understood that the CNS controls gastrointestinal function in the gut, but much less is known about how the gut environment, including the microbiota, may influence brain function, particularly in the realm of psychiatric disorders. Brain-gut-microbiome signaling pathways, including efferent neural, neuroendocrine, and immune pathways activated by the CNS, work in parallel to mediate homeostatic responses in the gut; likewise, MGB signaling pathways, including afferent neural, metabolite/endocrine, and immune pathways activated by changes in the gut environment can modify functioning of the CNS. Regarding MGB signaling, it has been shown that intestinal microbial content, as studied using germ-free and specific pathogen-free mice, can alter CNS activity and behavior, favoring a more anxiogenic or anxiolytic phenotype, depending on microbiome composition (Bercik et al., 2011a; Neufeld-Cohen et al., 2012). Changes in the function of specific brain regions due to microbiome imbalances may be important in determining behavioral outcomes. Hoban et al. (2018) found that, in mice, the gut microbiome composition alters the expression of genes relating to neuronal activity in the amygdala, a brain region frequently associated with anxiety disorders and trauma-and stressor-related disorders like PTSD (Hoban et al., 2018). Furthermore, microbiome composition effectively alters fear recall behaviors (Hoban et al., 2018) and fear extinction learning (Chu et al., 2019). Next, we outline (1) ways in which trauma or stressor exposure impacts the

microbiome throughout the lifespan; and (2) ways in which dysbiosis of the gut microbiome may occur and how it may impact CNS functioning relevant to PTSD.

1.6 Effects of early-life stressors on the gut microbiome and PTSD risk

Early-life stress is associated with increased risk for later development of PTSD (Koenen et al., 2007). For example, family stressors in childhood are associated with increased risk of development of PTSD after trauma exposure in adulthood (Koenen et al., 2007). In another study, traumatic experiences in adolescence were associated with adult dysregulation of physiological functions that are present in PTSD, including dysregulation of hypothalamic-pituitary-adrenal (HPA) axis and ANS functioning (Heim et al., 2000). Importantly, early-life stressors can also alter the gut microbiome. Maternal stress during pregnancy, as assessed by self-report and plasma cortisol concentrations, was shown to alter the infant microbiome throughout the first 110 days after birth. Microbiota dysregulation was characterized by increased relative abundances of gram-negative bacteria from the phylum Proteobacteria and lower relative abundances of lactic acid bacteria (i.e., *Lactobacillus*, *Lactococcus*, *Aerococcus*) and bifidobacteria, a pattern that was proposed to potentially reflect increased bias toward inflammation (Box 1) (Zijlmans et al., 2015). Importantly, maternal stress exposure was also linked to increases in maternally reported infant inflammatory responses (gastrointestinal and allergy symptoms), which are often exaggerated in persons with psychopathology, such as PTSD (Zijlmans et al., 2015). In a mouse model of early-life stress, maternal separation caused microbial dysbiosis, enhanced HPA axis activation, and increased anxiety-like defensive behavioral responses during adulthood (De Palma et al., 2015). Together, these studies suggest

that early-life stress may initiate long-lasting physiological alterations that increase vulnerability for the development of PTSD later in life.

Box 1. Definitions and Biomarkers of Inflammation

Inflammation	"The condition, usually involving redness, warmth, swelling, and pain, produced locally in the tissues [including blood] as a reaction to injury, infection, etc." (Brown, 1993). The physiological response to foreign antigens, especially pathogens, characterized by recruitment of immune cells and their secretion of chemokines and cytokines (Chen and Nuñez, 2010)
Sterile inflammation	Initiation of a proinflammatory response in the absence of pathogens or microorganisms (i.e., stress-induced) (Chen and Nuñez, 2010)
Common biomarkers of inflammation	C-reactive protein (CRP), interleukin (IL) 1β, IL-6, tumor necrosis factor (TNF)

1.7 Effects of trauma and stressor exposure during adulthood on the gut microbiome

Persons with stress-related psychiatric disorders including depression and anxiety exhibit altered microbiota abundance and increased gut permeability (Jiang et al., 2018; Stevens et al., 2018). In a recent study, persons with depression consistently displayed decreased abundances of *Coprococcus* and *Dialister* species from the phylum Firmicutes (Valles-Colomer et al., 2019).

Chronic stress has also been shown to be a potent indicator of irritable bowel syndrome (IBS) symptom severity in adults (E. J. Bennett, Tennant, Piesse, Badcock, & Kellow, 1998). Additionally, traumatic physical stressors are associated with major alterations to the gut flora, wherein changes take place within 72 hours of the injury (Howard et al., 2017). Together, these results provide some evidence that trauma and stressor exposure can lead to shifts in the microbiome in humans. However, studies using animal models are imperative to understanding the mechanisms by which stressor exposures may contribute to dysbiosis.

It is well-established that stress promotes gut dysbiosis, increases gut permeability, and increases circulating proinflammatory cytokine concentrations in rodents (Bharwani et al., 2017; O'Mahony et al., 2009; Reber et al., 2016b; van de Wouw et al., 2018; Zheng et al., 2017). Stress also activates the HPA axis and leads to increased secretion of glucocorticoids, which in turn can cause dysbiosis (Huang et al., 2015; Noguera et al., 2018). Chronic psychosocial stress paradigms, such as chronic social defeat or chronic subordinate colony housing, are proposed as valid models of PTSD in rodents (Reber et al., 2016a; Whitaker et al., 2014), and these stress paradigms are associated with increased gut dysbiosis coinciding with proliferation of effector T cells and proinflammatory cytokines and decreases in regulatory T cells (Treg) (Bharwani et al., 2017; Langgartner et al., 2017; Reber et al., 2016b). In one study, the microbiome of mice was shown to be dramatically altered after continuous exposure to an aggressor (Gautam et al., 2018). Following exposure to an aggressor for 10 days, these mice exhibited an increased ratio of Firmicutes/Bacteroidetes in gut microbiota compared to control animals. Exposure to stress or trauma releases a variety of host-derived endogenous molecules called damage-associated molecular patterns (DAMPs), which prepare the body for danger and activate the immune system

by synthesizing inflammasome complexes (Bortolotti et al., 2018; Fleshner et al., 2017). Interestingly, both microbe-associated molecular patterns (MAMPs) and pathogen-associated patterns (PAMPs) are increased after tail-shock stress in mice (Maslanik et al., 2012), which may be indicative of stress-induced gut dysbiosis.

1.8 PTSD, the ANS, and the gut microbiome

The ANS is a branch of the peripheral nervous system, comprised of efferent effector fibers that control involuntary homeostatic processes through two divisions: the "fight-or-flight" sympathetic nervous system (SNS) and the "rest-and-digest" parasympathetic nervous system (PNS). Imbalances in ANS functioning associated with trauma- and stressor-related disorders like PTSD are characterized by increased SNS activation and decreased PNS activation (H. Cohen et al., 2000; Dennis et al., 2016; Hopper, Spinazzola, Simpson, & van der Kolk, 2006; Park et al., 2017; Ulmer, Hall, Dennis, Beckham, & Germain, 2018). Low efferent vagal tone has been implicated in sensitivity to stress-induced psychopathology of youth (McLaughlin et al., 2015), including PTSD (Jenness et al., 2018). Increased plasma levels of catecholamines like norepinephrine are also associated with PTSD development (Pervanidou et al., 2007). In this section, we provide evidence for regulation of microbiome dynamics by the ANS.

While the vagus nerve is primarily responsible for parasympathetic innervation, the sympathetic nerve branches originate from the spinal cord to produce physiological states of arousal (McCorry, 2007). Activation of sympathetic efferent neurons innervating the gut suppresses digestion and prevents the movement of food through the digestive tract. Thus, the SNS is antagonized by the PNS and may be regulated by vagus nerve stimulation (Ylikoski et al., 2017).

Stress activates the SNS (Yaribeygi et al., 2017). In humans, the stress response is consistently associated with a decrease in PNS activity and a corresponding increase in SNS activity (H.-G. Kim et al., 2018; Lischke et al., 2018). Continuous SNS stimulation can change microbial composition in the gut and increase gut permeability (Houlden et al., 2016; Santisteban et al., 2017). One reason for this may be the increase in catecholamines released by the adrenal gland and sympathetic nerve terminals in response to SNS stimulation (McCorry, 2007). Lyte and colleagues have demonstrated that epinephrine and norepinephrine can induce proliferation of a variety of gram-negative bacteria, particularly *Escherichia coli*, in culture (Lyte & Ernst, 1992). *Escherichia coli* also proliferates after injury-induced release of norepinephrine in vivo, implicating SNS activity as a key player in intestinal colonization of gram-negative bacteria and gut dysbiosis (Lyte & Bailey, 1997).

Circulating microbial metabolites can also increase or decrease action potentials in sympathetic efferent neurons to regulate energy expenditure and energy homeostasis (Kimura et al., 2011). Emerging evidence suggests that microbiota may even influence the actions of SNS stimulants, such as angiotensin II (Karbach et al., 2016).

1.9 PTSD, neuroendocrine systems, and the gut microbiome

Persons with a diagnosis of PTSD exhibit dysregulated glucocorticoid signaling and altered sensitivity of glucocorticoid-mediated negative feedback to the HPA axis (de Kloet et al., 2007; Olff and van Zuiden, 2017; Pan et al., 2018; Wichmann et al., 2017; Yehuda et al., 1995). The HPA axis is known for its homeostatic regulation of glucocorticoids, including the stress

hormone cortisol (or corticosterone in rodents). Dysbiosis of the microbiome is tightly linked with stress responses and activation of the HPA axis, characterized by altered glucocorticoid levels and altered HPA axis sensitivity (Fukui et al., 2018; Pellissier et al., 2014; Reber et al., 2016b).

Stress-induced increases in glucocorticoid secretion and alterations in glucocorticoid receptor sensitivity may be important mediators of inflammatory dysbiosis because of the potent anti-inflammatory effects of glucocorticoids. Blunted HPA axis responses leading to lower levels of glucocorticoids or glucocorticoid resistance may potentiate dysbiosis, as is seen in inflammatory bowel disease models (Reber, 2012). Importantly, chronic stressors can decrease circulating glucocorticoid concentrations, decrease glucocorticoid sensitivity, and increase inflammation (Bunea, Szentágotai-Tătar, & Miu, 2017; S. Cohen et al., 2012; Gao et al., 2018).

1.10 PTSD, inflammation, and the gut microbiome

Stress induces inflammatory responses, which may persist in chronically stressed individuals and contribute to psychiatric disorders (Eraly et al., 2014; Pace et al., 2006). In humans, the Trier Social Stress Test (TSST) increases plasma levels of the proinflammatory cytokine interleukin 6 (IL-6), an effect that persists for hours after the stressor exposure (Böbel et al., 2018). Men with major depressive disorder and a history of early-life stress exhibit exaggerated release of IL-6 into the plasma after the TSST (Pace et al., 2006). A meta-analysis found that trauma exposure in humans is associated with chronic low-grade inflammation, as indicated by increased inflammatory biomarkers, such as C-reactive protein, interleukin 1β (IL-1β), IL-6, and tumor necrosis factor (TNF) (Tursich et al., 2014). Other studies have affirmed that people with a

diagnosis of stress-related psychiatric disorders, including PTSD, are more likely to develop inflammatory diseases (O'Donovan et al., 2015; Song et al., 2018).

Stress-induced increases in inflammatory markers are associated with changes in the microbiome and anxiety- and depressive-like behavioral responses in rodents (Wong et al., 2016). The immune system is capable of impacting the microbiome, most likely working in parallel with, rather than simply as a result of, microbial dysbiosis. For example, neutrophils are recruited to the intestinal epithelium during gastric inflammation where they are activated to release antimicrobial agents and may contribute to epithelial damage (Luissint et al., 2016; Zhou and Liu, 2017). Interestingly, a recent study has shown that mice infected with the respiratory virus influenza A have less microbial diversity in the gut, allowing pathogenic bacteria to colonize (Yildiz et al., 2018). These results suggest that there is a tight interplay between immune and microbial interactions and that both may influence each other. Interestingly, immune and microbial dysfunction are both exaggerated by trauma and psychosocial stressors (Bharwani et al., 2016; Langgartner et al., 2018; Reber et al., 2006). It is thought that the propensity for excessive inflammatory responses may increase vulnerability to development of stress-related psychiatric disorders such as PTSD (Eraly et al., 2014; Hodes et al., 2014).

Features of chronic low-grade inflammation are present in PTSD (Eswarappa et al., 2018; Gola et al., 2013; Michopoulos et al., 2017, 2015; Tursich et al., 2014). Indeed, persons with a diagnosis of PTSD reliably display increases of the proinflammatory marker, C-reactive protein, in the circulating plasma (Eraly et al., 2014; Michopoulos et al., 2015; Rosen et al., 2017). It is unclear whether this inflammation contributes to changes in the microbiome or if it is a product

of an altered microbiome, but it is likely a combination of both. PTSD is comorbid with a number of autoimmune diseases, implicating a stress-induced dysregulation of immune function (O'Donovan et al., 2015). In fact, veterans diagnosed with PTSD have higher risk of developing any autoimmune disease relative to their undiagnosed veteran counterparts, including those with other psychiatric disorders (O'Donovan et al., 2015). Compared with veterans with a diagnosis of other psychiatric disorders, veterans with PTSD had significantly increased relative risk for the development of inflammatory bowel diseases, thyroiditis, and rheumatoid arthritis, making PTSD particularly unique in its strong association with these particular types of inflammatory disorders (O'Donovan et al., 2015). Persons with PTSD also show consistently different patterns of lipopolysaccharide (LPS)-stimulated plasma cytokine production by freshly isolated peripheral blood mononuclear cells compared to healthy controls, although this has yet to be linked to the microbiome (Gola et al., 2013). One potential mechanism underlying inappropriate inflammation is a decrease in the number or function of Tregs, which release anti-inflammatory cytokines, promote immunoregulation, and suppress inappropriate inflammation. In fact, Treg cell abundances were found to be decreased in people with PTSD relative to healthy controls, suggesting that immunoregulatory circuits are disrupted (Morath et al., 2014; Sommershof et al., 2009).

1.11 Stress-induced gut dysbiosis, afferent neural signaling, and PTSD

The enteric nervous system is a division of the ANS, a network containing both SNS and PNS innervation that exists throughout the gastrointestinal tract. Recent work has revealed the critical impact of microbiota on development and maintenance of the enteric nervous system, implying that these interactions begin early and persist throughout adulthood (De Vadder et al., 2018;

Kabouridis et al., 2015). Sensory afferents traveling in sympathetic and parasympathetic nerve bundles send information about the gut to the brain for integration. Here, we describe ways in which the microbiome may regulate these interactions and may contribute to increased vulnerability to negative outcomes following exposure to traumatic stress.

The vagus nerve has been implicated as one of the predominant mediators of afferent neural signaling between the gut and brain. More than 80% of vagal nerve fibers are afferent fibers. These fibers travel from the gastrointestinal tract via the nodose and jugular ganglia to the nucleus of the solitary tract (NTS) in the brainstem, which, in turn, projects to many different brain regions involved in anxiety and stress-related circuits, such as the locus coeruleus, hypothalamus, bed nucleus of the stria terminalis, and amygdala (Berthoud and Neuhuber, 2000; Bonaz et al., 2018; Breit et al., 2018). These fibers are activated by chemoreceptors and mechanoreceptors located in the digestive tract. Probiotic treatment or modifications of the gut's microbial communities and subsequent production of various metabolic byproducts may alter the firing rate of vagal afferent nerves and signaling to the CNS (Bonaz et al., 2018; Breit et al., 2018), although results have been conflicting (Bercik et al., 2011b; Bercik et al., 2010). In one study, anxiety induced by experimental colitis was completely abolished with vagotomy (Bercik et al., 2011b). In line with this work, Bercik et al. (2011b) found that anxiolytic effects induced by *Bifidobacterium longum* NCC3001 required an intact vagus nerve. Administration of the probiotic *Lactobacillus rhamnosus* JB-1 (Table 1.1) was shown to differentially alter gamma-aminobutyric acid (GABA) expression in the brain and induce antidepressant-like behaviors, both of which were abolished with vagotomy (Bravo et al., 2011). Indeed, ex vivo intraluminal administration of *Lactobacillus rhamnosus* JB-1 increased afferent mesenteric neural activity,

which was dependent on vagus nerve integrity (Perez-Burgos et al., 2013). In vitro, the addition of human microbial communities to nodose ganglia, wherein a majority of vagal afferent cell bodies reside, increased excitability of these neurons, an effect that was blocked by protease inhibitors, establishing microbial proteases as a necessary component for vagal afferent stimulation (Pradhananga et al., 2018). On the contrary, Bercik and colleagues demonstrated that antibiotic-induced changes in microbial community structure, shifting toward higher abundance of Actinobacteria and lower abundance of Proteobacteria, increased exploratory behavior in mice (Bercik et al., 2011a). However, mice receiving vagotomy or sympathectomy prior to antibiotic treatment showed the same alterations in behavior, revealing that microbiota may affect behavior through ANS-independent mechanisms and implicating other processes as critical mediators of MGB axis signaling (Bercik et al., 2011a).

Input from vagal afferents may affect downstream parasympathetic efferent responses via a vago-vagal reflex (Ghia et al., 2006). Likewise, microbial metabolites that enter the bloodstream and cross the blood-brain barrier may contribute to changes in parasympathetic control of host metabolism, such as pancreatic insulin release (Perry et al., 2016). Long-term gut dysbiosis, as found in patients with Crohn’s disease, is associated with vagal output dysregulation (Engel et al., 2015), while dysbiosis of gut bacteria has been linked to decreased vagal efferent firing in humans (Pellissier et al., 2014). In addition, experimental colitis in rats was associated with decreased vagal output and increased sympathetic output (Ciesielczyk et al., 2017). Importantly, decreases in vagal tone are also evident in persons with PTSD and accompany increases in the SNS activity (Hopper et al., 2006; Park et al., 2017).

Spinal afferent fibers, though largely unstudied, also play a major role in MGB axis communication. Spinal afferent fibers travel in sympathetic nerve bundles and have cell bodies within dorsal root ganglia. These afferents innervate lamina I of the spinal cord, where signals are relayed to spinoparabrachial and spinothalamic pathways. Spinothalamic afferents extend to the thalamus, where input is relayed to important emotional centers such as the anterior cingulate cortex (Mayer, 2011). Experimentally induced intestinal inflammation in guinea pigs prompted a robust increase in excitability of dorsal root ganglion (sensory) neurons innervating the intestinal tract (Moore et al., 2002). Interestingly, this hypersensitivity can be transferred from humans with IBS to germ-free rats by fecal transplant, implicating direct influence of the microbiome on spinal afferents (Crouzet et al., 2013). Hypersensitivity was also linked to higher relative abundance of Enterobacteriaceae (a family within the Proteobacteria phylum) and lower *Bifidobacterium* (a genus within the Actinobacteria phylum) (Crouzet et al., 2013). Similarly, persons with IBS show signs of general afferent dysregulation, including altered gastrointestinal reflexes (Mayer, 2011). It is important to note that spinal afferent hypersensitivity is increased not only in IBS but also after antibiotic treatment (Verdú et al., 2006) or by chronic stress (Ait-Belgnaoui et al., 2018) and may be attenuated by treatment with a probiotic containing *Lactobacillus paracasei* NCC2461 or *Lactobacillus helveticus* R0052 and *Bifidobacterium longum* R0175, respectively.

1.12 Stress-induced gut dysbiosis, microbial metabolites, and PTSD

Persons with a diagnosis of PTSD exhibit altered plasma metabolite profiles, including changes in fatty acids and bile acids, which are influenced by the gut microbiota (Karabatsiakis et al., 2015). The gut microbiota are mostly commensal, in that they thrive off of the host environment

while simultaneously providing the host with enzymes and metabolites that break down indigestible foods, such as fiber and cellulose, with evolutionarily favorable energetic consequences for the host (Rowland et al., 2018; Valdes et al., 2018). They also aid in general digestion and nutrient absorption, antioxidant production, insulin sensitivity, and overall gut health (Rowland et al., 2018; Valdes et al., 2018). As such, microbiota produce a vast array of metabolites that interact with host physiological processes. These metabolites interact with epithelial cells that line the gut lumen, afferent enteric nervous system fibers that innervate the gut, mucosal immune cells, and, when taken up into the bloodstream, can affect different target tissues and cell types, as discussed later. In the following discussion, we highlight some important metabolites produced by microbiota, and we touch on their specific interactions with host physiological systems to understand how dysregulation of microbial metabolites can contribute to the risk of development of PTSD or persistence of PTSD symptoms.

Short-chain fatty acids (SCFAs) are important byproducts of carbohydrate and protein fermentation by gut microbiota across many phyla, most notably Firmicutes (Koh et al., 2016). SCFAs, including acetate, butyrate, and propionate, act as signaling molecules that can modify the homeostatic energy metabolism of the host (Hu et al., 2018; van de Wouw et al., 2018), initiate immunoregulation through the proliferation of Tregs (Smith et al., 2013), activate afferent neurons, activate the ANS (Goswami et al., 2018; Kimura et al., 2011), and influence the circadian clock of peripheral tissues (Tahara et al., 2018). In rodent and human studies, diet has been shown to alter gut microbial communities, which are associated with changes in SCFA type and abundance (Bishehsari et al., 2018; Nishitsuji et al., 2017; Russell et al., 2011). High-fat diets and obesity may contribute to changes in the microbial community structure and decrease

SCFAs (Bishehsari et al., 2018; Nishitsuji et al., 2017). Treatment with prebiotics can also alter complex carbohydrate fermentation activity in vitro and increase SCFA production (Sanchez et al., 2009). The potential for SCFAs to alter brain signaling is indicated by studies of germ-free C57BL/6J mice, which show increased blood-brain barrier permeability. Increased blood-brain barrier permeability in germ-free mice is attenuated by the colonization of the germ-free mice with bacterial strains known to produce SCFAs, *Clostridium tyrobutyricum* DSM 2637 and *Bacteriodes thetaiotaomicron*, or oral administration of SCFAs (Braniste et al., 2014). Germ-free and altered Schaedler flora (ASF) mice also exhibit malformation and dysfunction of neurons and glia; cohousing with specific pathogen-free mice and oral administration of SCFAs reverses this phenotype (Erny et al., 2015). SCFAs can stimulate sensory fibers of the vagus nerve to mediate CNS-regulated behaviors, including feeding (Goswami et al., 2018). Expression of the SCFA receptor, G protein-coupled receptor 41 (encoded by *Gpr41*/*Ffar3*) is found in nodose ganglion cells (Egerod et al., 2018), suggesting that SCFAs can act through G protein-coupled receptor signaling mechanisms to directly alter the excitability of vagal afferents. Likewise, intraperitoneal injections of SCFAs modify gastrointestinal/gastric motility, an ANS-regulated process, although results suggest both excitatory and inhibitory functions of SCFAs on gastrointestinal/gastric motility (Hurst et al., 2014). In diabetic or ketogenic states, SCFAs may even directly mediate the activity of SNS output by acting on GPR41 (Kimura et al., 2011). More studies are required to further elucidate the role of diet and microbiota on the production of SCFAs, and how different types of SCFAs may affect physiological processes involved in the etiology of PTSD.

Bile acids are produced by the host's liver, stored in the gall bladder, then released into the gastrointestinal tract and modified into secondary bile acids by gut microbiota such as *Lactobacillus, Bifidobacterium,* and *Clostridium* species (Ridlon et al., 2006). Bile acids are a critical component of the bile secreted from the gall bladder into the small intestine, allowing for the digestion of lipids. They can both affect and be affected by gut microbiota species (Buffie et al., 2015; Cheng et al., 2018; Just et al., 2018; C. Y. Li et al., 2018a; Martin et al., 2018). Fecal transplants from healthy human donors to persons infected by *Clostridioides difficile*, a bacterium that may cause colitis, improved primary and secondary bile acid balance, as well as fatty acid levels (Brown et al., 2018). Not only do gut microbiota modify existing bile acid structures (Martin et al., 2018), but they also can regulate the expression of enzymes involved in the original synthesis of bile acids in the liver, as well as regulate the expression of bile acid reabsorption transporters in the lumen (Cheng et al., 2018; C. Y. Li et al., 2018a; Sayin et al., 2013). Bile acids are potent regulators of the immune system and thus may prove to be an important link between changes in microbiota composition and inflammation (Ma et al., 2018).

Microbial metabolites may also influence the release of chemical signals produced by enteroendocrine cells that line the lumen of the gastrointestinal tract. These cells sense the gut environment and secrete gastrointestinal hormones, peptides, and neurotransmitters to elicit a physiological response (Kaelberer et al., 2018). Indeed, these cells are thought to be at the forefront of the gut-brain connection (Latorre et al., 2016). The release of regulatory molecules and digestive hormones from enteroendocrine cells includes the release of appetitive hormones that help to regulate food intake (Latorre et al., 2016). The hormone cholecystokinin (CCK) is secreted in response to the consumption of fats and proteins and stimulates the release of bile for

the digestion of these macronutrients. In combination with CCK, peptide YY (PYY) and glucagon-like peptide-1 (GLP-1) are secreted after eating to increase satiety and decrease food intake (Hornigold et al., 2018; Iwasaki et al., 2018; Reidelberger et al., 2013). CCK and GLP-1 are also important signaling molecules in the brain, and a mutation in the CCK gene promoter is associated with PTSD diagnosis (Badour et al., 2015). More recent studies suggest that CCK may play an important role in gene by environment interactions of anxiety states (Weidner et al., 2019). It is proposed that all three of these chemicals promote anorexigenic states by activating vagal afferents in the gut (Iwasaki et al., 2018; Kaelberer et al., 2018; Newman et al., 2017). SCFAs were determined to increase PYY release from human enteroendocrine cells in vitro (Larraufie et al., 2018). Another study found that diets high in fermentable carbohydrates increased the number of PYY-secreting cells in the intestine, undoubtedly through microbial-driven production of SCFAs (Brooks et al., 2017). Interestingly, enteroendocrine cells can also communicate directly with vagal nodose neurons by release of the neurotransmitter glutamate (Kaelberer et al., 2018). Microbiota may influence the amount of glutamate in the gut through glutamate dehydrogenase activity (Girinathan et al., 2016; Kolmeder et al., 2016; Tanca et al., 2017). This direct communication is rapid (within 1 second), compared to CCK-stimulation of nodose ganglia that takes several minutes, implicating enteroendocrine cells as an integral component of afferent MGB axis signaling and allowing for near-immediate CNS responses to the gut environment (Kaelberer et al., 2018).

Microbial metabolites can mediate the function of specialized neuroendocrine cells called enterochromaffin cells (Reigstad et al., 2015; Yano et al., 2015). Over 90% of the neurotransmitter serotonin (5-hydroxytryptamine; 5-HT) in the human body is synthesized in the

gut by enterochromaffin cells and enteric neurons (Banskota et al., 2018). Enterochromaffin cells release 5-HT in response to ingesting food, promoting secretion, absorption, and peristaltic reflexes during digestion (Banskota et al., 2018). Proper 5-HT signaling is critical to enteric nervous system development (De Vadder et al., 2018; Li et al., 2011; Margolis et al., 2016), and more recently implicated in gut homeostasis. 5-HT dysregulation has been associated with gut dysbiosis disorders, which are associated with altered cognitive function and behaviors (Margolis et al., 2016; Shajib et al., 2018; Xu et al., 2017). Importantly, the microbiome can regulate the production of 5-HT, implicating the microbiome in the control of host metabolic processes (De Vadder et al., 2018; Hata et al., 2017; Yano et al., 2015). The presence of gut microbiota increases the amount of 5-HT in the intestinal lumen (Hata et al., 2017). It was discovered that some SCFAs produced by the gut microbiota can stimulate the expression of tryptophan hydroxylase 1 (Tph1), an enzyme involved in the rate-limiting step of serotonin synthesis, in enterochromaffin cells, providing one possible explanation for the relationship between the gut microbiota and 5-HT signaling by enterochromaffin cells (Reigstad et al., 2015; Yano et al., 2015). The gut microbiota may also modulate glucose metabolism (Soto et al., 2018; Suez et al., 2014; Zarrinpar et al., 2018), which in turn influences the release of 5-HT from enterochromaffin cells (Zelkas et al., 2015).

Changes in microbial metabolites may influence the integrity of the epithelial barrier and induce secretion of specific cytokines from epithelial cells (Muñoz et al., 2018; Wang et al., 2018). One study supporting this idea found that stimulus-induced IL-6 cytokine production was associated with changes in several microbial metabolites involved in L-arginine depletion (Schirmer et al., 2016). The epithelial cells in the gut can respond to changes in the microbiome and communicate

with immune cells, such as T-helper 17 (Th17) cells (Atarashi et al., 2015). Thus, the secretion of cytokines from intestinal epithelial cells may contribute to an altered immune response. Increases in SCFAs are thought to have an immunoregulatory effect on epithelial cells, blunting cytokine release (Wang et al., 2018).

1.13 Stress-induced gut dysbiosis, immune signaling from the periphery to the central nervous system, and PTSD

The gut microbiome may communicate with the immune system directly by interaction with dendritic cells that contact the gut lumen, directly by contacting leukocytes after translocation across the epithelial barrier, or indirectly by interacting with intestinal epithelial cells (Chieppa et al., 2006; Coombes and Powrie, 2008; Nicoletti et al., 2009). Ongoing studies seek to understand how the microbiome might cause the development of systemic inflammatory diseases (Clemente et al., 2018). Exposure to a diverse microbial environment may be an important determinant of immune activation. One study found that people who were raised in an urban environment with less microbial diversity had a more exaggerated immune response to a psychosocial stressor than people raised in a rural environment with exposure to farm animals until the age of 15 (Böbel et al., 2018). The importance of microbiome health is evident in the gut, where dysbiosis of the gut microbiome is highly associated with inflammatory bowel disease (IBD), including Crohn's disease or ulcerative colitis (Henson and Phalak, 2017; Morgan et al., 2012; Sokol et al., 2018). A study of discordant twins has suggested that an important environmental component to the development of IBD is early gastrointestinal infection or antibiotic treatment (Halfvarson et al., 2006); moreover, fecal microbiota transplantation has been shown to be successful in the treatment of IBD (Sun et al., 2016). Gut dysbiosis is correlated with increased circulating plasma levels of proinflammatory cytokines (Knoop et al., 2016), C-reactive protein (Yamashiro et al.,

2017), and inflammatory phenotypes of IBD (Kellermayer et al., 2012; Shen et al., 2018). Interestingly, gut dysbiosis, like PTSD, is associated with several other autoimmune diseases, including multiple sclerosis and thyroiditis, implicating the microbiome in overall immune regulation (de Oliveira, Leite, Higuchi, Gonzaga, & Mariano, 2017; Haghikia et al., 2015; Hebbandi Nanjundappa et al., 2017; Li, Selmi, Tang, Gershwin, & Ma, 2018; Opazo et al., 2018; Zhao et al., 2018).

Recently, Schirmer et al. (2016) linked gut microbiome composition to variability in stimulated inflammatory responses (Schirmer et al., 2016). In this study, fecal samples from 500 people were analyzed for microbiome content, and blood samples were taken to investigate cytokine production. Blood samples were exposed to a variety of microbial stimuli ex vivo, two of which were bacterial in origin and two that were fungal. This study found significant correlations between stimulated cytokine production, stimulus type, and bacterial species abundance in the gut, as well as a species by stimulus interaction (Schirmer et al., 2016).

Hodes and colleagues found that inflammatory hypersensitivity to LPS, a component of the outer cell wall of gram-negative bacteria, was predictive of anxiety- and depression-like behaviors in mice following repeated social defeat, a psychosocial stressor; specifically, these stress-vulnerable animals produced higher circulating plasma levels of the cytokine IL-6 when challenged with a dominant aggressor than animals that were resilient to behavioral changes (Hodes et al., 2014). Irradiated mice reconstituted with bone marrow from susceptible mice also showed greater vulnerability to stress-induced anxiety- and depression-like behaviors than control chimeras (Hodes et al., 2014). These results suggest that inappropriate inflammation,

particularly inappropriate release of IL-6, may contribute to the susceptibility of stress-induced behavioral dysregulation.

In general, differences in the composition of the gut microbiome are associated with differences in plasma concentrations and stimulated release of cytokines, including IL-6 (Moya-Pérez et al., 2017; Schirmer et al., 2016). One of the ways in which dysbiosis may initiate inflammation is by increasing the permeability of the intestinal epithelium, so-called "leaky gut," allowing for the passage of bacteria and bacterial products into the body (Fukui et al., 2018; Knoop et al., 2016; Muñoz et al., 2018; Thevaranjan et al., 2017). Major stressors linked to microbial dysbiosis are also associated with increased gut permeability in rats. Gut permeability, for instance, is increased following treatment with *Escherichia coli* (Wang et al., 2018) or LPS (Nighot et al., 2017). Imbalances in microbiota composition or metabolite production, tipping toward a gram-negative bacterial environment, may promote increased permeability of tight junctions that sit between epithelial cells lining the intestinal lumen (Nighot et al., 2017; Simeonova et al., 2018). Indeed, high abundance of gram-negative bacteria and low abundance of gram-positive bacteria is associated with increased gut permeability in young adults exposed to chronic stress (Karl et al., 2017). Normally, the microbiome is physically isolated in a manner that allows communication only with specialized cells of the intestine; however, increased intestinal permeability allows for enteric microbiota to migrate to other areas of the body, including the liver, kidney, spleen, and mesenteric lymphoid complex (Berg, 1999), where immune cells may directly interact with microbial recognition patterns, MAMPs and PAMPs to initiate an immune response. MAMPs and PAMPs can stimulate the production of inflammasome complexes (Fleshner et al., 2017). Similarly, increased intestinal permeability allows microbial products to

more easily pass into the bloodstream to influence the function of leukocytes and promote proinflammatory responses (Thevaranjan et al., 2017).

Intestinal microfold (M) cells are specialized epithelial cells that transport microbial antigens from the lumen of the intestine to the gut-associated lymphoid tissue (GALT). Very little has been reported on the contribution of these cells to dysbiosis-generated inflammation, although evidence suggests that these cells proliferate during intestinal inflammation (Bennett et al., 2016; Parnell, Walch, & Lo, 2017). M cells have been shown to differentially activate and alter gene expression in the presence of specific bacteria, and further, these cells disparately transport certain species of commensal bacteria (Lapthorne et al., 2012). For instance, Lapthorne and colleagues showed that *Escherichia coli* and *Bacteriodes fragilis* could translocate across M cells more efficiently than *Lactobacillus salivarius* using an in vitro model and confirmed differential activation of M cells in vivo (Lapthorne et al., 2012). M cells can also rapidly translocate mycobacteria into the body (Fujimura, 1986; Nair et al., 2016). On the other side of the M cell-mucosal barrier are dendritic cells (DCs) residing in the GALT. DCs identify microbes via pattern recognition receptors that interact with cell wall components serving as MAMPs, and evidence suggests that specific subtypes of DCs perform different antigen-presenting duties to elicit immune responses (Hammer et al., 2016; Liang et al., 2016; Tytgat et al., 2016). One hypothesis is that gut dysbiosis creates an imbalance of microbiota and associated antigens that are disproportionately picked up and translocated across the mucosa and presented to DCs, which are then activated to initiate proinflammatory immune responses. Likewise, M cells, in concert with DCs, could be important mediators of the immunoregulatory effects of some

probiotics by translocating bacteria across the intestinal barrier to stimulate Treg differentiation (Perdigòn et al., 2000).

1.14 Microbiome impacts on stress-related behavioral responses

Traumatic stress precedes the onset of clinical PTSD (American Psychiatric Association, 2013). However, only a subset of individuals that experience trauma go on to develop PTSD, suggesting that genetic or environmental factors contribute to vulnerability or resilience to PTSD. We hypothesize that differences in physiological functioning may contribute vulnerability or resistance to the risk of developing PTSD. The gut microbiome may contribute to stress vulnerability or resistance by modifying the integrity of the gut epithelial barrier, interacting with neural afferents, influencing HPA axis and ANS responses, or inducing inflammatory or immunoregulatory responses. Likely, the gut microbiome is working with these systems in a complex and multi-factorial way. In many ways, stress modulates the gut microbiome or exacerbates dysbiosis, and it may impact individual responsivity to traumatic stressors.

Studies of germ-free mice have shown that stress behaviors are partially gut microbiota-dependent (Bercik et al., 2011a; Collins, Kassam, & Bercik, 2013; De Palma et al., 2017; Li, Guo, et al., 2018). Compared to conventionally-raised mice, germ-free mice exhibit decreased fear retention after a fear conditioning paradigm, whereas germ-free mice colonized with the microbiome of conventional mice present similar fear-retention behavior as conventional mice (Hoban et al., 2018). The gut microbiota can also modulate anxiety- and depression-like behaviors (Bravo et al., 2011; Huo et al., 2017; Moya-Pérez et al., 2017). Germ-free mice given a fecal transplant from a low-anxiety mouse strain begin to adopt anxiolytic behaviors of the

donor mice (Premysl Bercik et al., 2011). Likewise, germ-free mice given a fecal transplant from humans with IBD or humans with major depressive disorder exhibit increased anxiety-like and depressive-like behaviors (De Palma et al., 2017; Li, Guo, et al., 2018). Importantly, treatment with certain bacterial species can shift the balance of T cells towards the proliferation of Treg in both rodents and humans, promoting an immunoregulatory phenotype that corresponds with decreases in anxiety-like defensive behavioral responses and depressive-like behaviors (Bharwani et al., 2017; Konieczna et al., 2012; Luo et al., 2017; Reber et al., 2016b; Savino et al., 2018).

Interestingly, cortisol release in pregnant women following an acute psychosocial stressor was associated with the abundance of several members of the Firmicutes and Bacteroidetes phyla in the gut (Hantsoo et al., 2018). Indeed, gut microbiota have been shown to modulate HPA axis function in mice, although the mechanism is unknown (Bravo et al., 2011; Huo et al., 2017; Moya-Pérez et al., 2017). Chemically-induced gut dysbiosis potentiates stress-induced glucocorticoid release in mice (Reichmann et al., 2015). Although the HPA axis is highly connected to other physiological systems, there is evidence to suggest that the gut environment can directly influence HPA axis function by modifying gut epithelial production of corticosterone and its release into the bloodstream (Hussain, 2013).

1.15 Pathobionts as a risk factor for stress-induced gut dysbiosis, inflammation, and PTSD

Pathobionts are microorganisms that are normally harmless and commonly present in healthy individuals but may activate an inflammatory immune response given certain genetic or physiological states. Research has shown that pathobionts can induce inflammatory responses

under the right conditions. In genetically susceptible mice, the translocation of gut pathobionts such as *Enterococcus gallinarum* across the intestinal barrier to the liver triggered the onset of autoimmune diseases, showing that native bacteria can capitalize on the host's genetic predisposition to produce a proinflammatory response (Fine et al., 2018; Manfredo Vieira et al., 2018). In IL-10-deficient mice, intraperitoneal injection or oral gavage of *Helicobacter* species induces colitis, while a probiotic treatment of *Lactobacillus paracasei* 1602 and *Lactobacillus reuteri* 6798 may attenuate the *Helicobacter*-induced intestinal inflammation (Fox et al., 1999; Peña et al., 2005). Additionally, the pathobiont *Helicobacter bilis* has been shown to induce chronic inflammatory disease after pretreatment with a sub-pathological treatment of a chemical colitogen, implicating that the proinflammatory phenotype of pathobionts may be specially mediated by the environment (Gomes-Neto et al., 2017). Further, exposure to certain pathobionts may contribute to individual variability in physiology and behavior after a stressor or trauma, where pathobiont exposure confers development of colitis and anxiety-like defensive behavioral responses (Langgartner et al., 2017; Reber et al., 2016b).

Importantly, the human pathobiont *Helicobacter pylori* proliferates in the stomach of mice after exposure to chronic restraint stress (Guo et al., 2009). In this study, psychological stress exacerbated the gastric mucosal damage due to *Helicobacter pylori* and produced gastric ulcers. Treatment with a glucocorticoid receptor antagonist reduced *Helicobacter pylori* colonization and mitigated gastric damage caused by stress and *Helicobacter pylori*. These results argue that the release of glucocorticoids in response to chronic, repeated stressors may be mediating the colonization of pathobionts, possibly by interacting with immune cells in the mucosa (Guo et al., 2009).

With evidence suggesting that pathobionts contribute to variability in the development of immunodysregulation, it is possible that pathobionts represent a risk factor for the development of PTSD. One hypothesis is that the presence of pathobionts in some individuals predisposes those individuals to proinflammatory consequences after a trauma. That is to say, traumatic events may kick off physiological homeostatic dysregulation and characteristic inflammatory cascades that contribute to the development of PTSD in individuals with resident pathobionts.

Predisposition to a proinflammatory milieu may be a risk factor for development of PTSD and may contribute to the individual variability in development of PTSD following exposure to trauma (Eraly et al., 2014; Eswarappa et al., 2018; Michopoulos et al., 2015). As inflammation is tightly linked to microbiome composition, we would expect to see differences in microbial or metabolic content as a biomarker for the onset of PTSD. However, variability between individual microbiomes is very high (Schirmer et al., 2016), and evidence suggests that variability in treatment efficacy between people may be dependent on these individual microbiomes (Suwal et al., 2018). Thus, more effort should be directed towards understanding factors contributing to individual variability in the composition and diversity of the microbiome, inflammation, and response to stress. Likewise, more studies are needed to explore mechanisms of microbe-host interactions with respect to efficacy of probiotics for the prevention or treatment of trauma- and stressor-related disorders like PTSD.

1.16 Microbiome-based interventions for prevention and treatment of PTSD

Probiotics show promise in maintaining a variety of physiological functions relevant to PTSD, including ANS activity, endocrine function, and inflammation. See Table 1.1 for a list of preclinical probiotic and heat-killed bacteria studies mentioned in this chapter. More studies are needed to explore the potential benefits of probiotics used as a treatment and as a prevention strategy for the development of PTSD.

Vagus nerve stimulation, which reduces SNS hypersensitivity, has been proposed as a possible treatment for people with PTSD (McIntyre, 2018; Noble et al., 2017, 2019). Intriguingly, probiotics show promising results to influence vagus nerve activity in rodents (Bercik et al., 2011b; Bravo et al., 2011; Perez-Burgos et al., 2013; Yamano et al., 2006). Thus, modulation of the gut microbiome may be critical for the maintenance of vagus nerve signaling and potentially useful for prevention and treatment of PTSD.

Probiotics have been shown to attenuate stress-induced increases in HPA axis activity and plasma corticosterone in rodents (Ait-Belgnaoui et al., 2012, 2014, 2018; Bravo et al., 2011; Fukui et al., 2018; Moya-Pérez et al., 2017). In one study, a probiotic treatment of *Lactobacillus farciminis* mitigated stress-induced HPA axis activity, an effect that was associated with decreased proinflammatory cytokines in the hippocampus and reduced gut permeability (Ait-Belgnaoui et al., 2012). In another study, *Bifidobacterium pseudocatenulatum* CECT 7765 prevented stress-induced HPA axis sensitivity (Moya-Pérez et al., 2017). A combination probiotic of *Lactobacillus helveticus* R0052 and *Bifidobacterium longum* R0175 alleviated chronic stress-induced alterations in glucocorticoid receptors in the hypothalamus (Ait-Belgnaoui et al., 2018).

Maintaining a properly balanced microbiome is essential for supporting an immunoregulatory phenotype (Ohnmacht et al., 2015; Sefik et al., 2015). Indeed, probiotics are becoming popular therapeutic strategies for the treatment of inflammatory diseases. A number of probiotics have been shown to be effective treatments for IBD, reducing inflammation and improving symptoms (Jonkers et al., 2012; Saez-Lara et al., 2015; Wasilewski et al., 2015). Currently, probiotics are being sought out to treat autoimmune diseases (de Oliveira et al., 2017). Molecular studies are providing the backbone of support for utilizing therapeutic probiotics as treatments for inflammatory disease. Pretreatment with the probiotic *Lactobacillus plantarum* ZLP001 mitigated *Escherichia coli*-induced cytokine production in intestinal epithelial cells, possibly through the production of SCFAs (Wang et al., 2018). Indeed, as mentioned earlier, SCFAs have been shown to increase Treg (Arpaia et al., 2013; Furusawa et al., 2013; Smith et al., 2013; Zeng and Chi, 2015), but have also been shown to prevent intestinal (Singh et al., 2014), systemic (Li, van Esch, Henricks, Folkerts, & Garssen, 2018), autoimmune (Haghikia et al., 2015), and even neuroinflammatory responses (Matt et al., 2018). As mentioned earlier, plasma levels of C-reactive protein are a potential biomarker for propensity to develop PTSD (Eraly et al., 2014; Michopoulos et al., 2015; Rosen et al., 2017; Tursich et al., 2014). A multitude of studies have shown that probiotics (mostly consisting of *Lactobacillus* and *Bifidobacterium* species) decrease plasma C-reactive protein concentrations in diseased and healthy persons (Mazidi et al., 2017).

Cognitive and physiological benefits of probiotics and prebiotics are also often attributed to the immunoregulatory effects of these bacteria (Bharwani et al., 2017; Chunchai et al., 2018; Frank et al., 2019; Lowry et al., 2016; Reber et al., 2016b; Ren et al., 2018). Some bacteria in the

Actinobacteria phylum proliferate in response to galactooligosaccharide prebiotics (Davis, Martínez, Walter, Goin, & Hutkins, 2011), and their presence in the gut is often associated with positive neuroimmune function. This could be due in part to the diverse antimicrobial effects of Actinobacteria (Elbendary et al., 2018; Mohamed et al., 2017; Verma et al., 2018), which may target pathogenic species to prevent colonization and dysbiosis. As mentioned earlier, Actinobacteria diversity and abundance, particularly *Bifidobacterium* spp., is associated with reductions in stress-induced gut permeability (Karl et al., 2017). The presence of *Bifidobacterium* spp. has been implicated in phenotypes resilient to chronic stress (Yang et al., 2017), and treatment with *Bifidobacterium pseudocatenulatum* CECT 7765 mitigated anxiety-like defensive behavioral responses (Moya-Pérez et al., 2017). *Bifidobacterium* has also been shown to mitigate anxiety-like defensive behavioral responses associated with chemically-induced colitis (Bercik et al., 2011b). *Mycobacterium vaccae* NCTC 11659, when injected subcutaneously, prevents stress-induced increases in corticotropin-releasing hormone in the central nucleus of the amygdala and bed nucleus of the stria terminalis, two brain regions directly involved with the expression of anxiety- and fear-related defensive behavioral responses (Loupy et al., 2018). *Mycobacterium vaccae* also prevents stress-induced colitis and has been shown to promote an anti-inflammatory environment in both the periphery and the brain (Fonken et al., 2018; Frank et al., 2019, 2018b; Reber et al., 2016b). Both *Bifidobacterium bifidum* (Verma et al., 2018) and *Mycobacterium vaccae* (Zuany-Amorim et al., 2002) may induce the proliferation of Treg cells, which may explain their roles in attenuating stress-related inflammation.

Similarly, probiotics containing some Firmicutes have shown promise in the treatment of neuroimmune dysregulation across species. Oral treatment with *Lactobacillus rhamnosus* JB-1

prevented stress-induced alterations in behavior and immune function in mice, simultaneously promoting increases in the anti-inflammatory cytokine, interleukin 10 (IL-10), and producing Tregs (Bharwani et al., 2017). Likewise, *Lactobacillus helveticus* NS8 increased circulating levels of IL-10 in plasma and attenuated anxiety-like defensive behavioral responses after chronic stress in rats (Liang et al., 2015). *Lactobacillus plantarum* USDA-ARS protected against stress-induced gut dysbiosis and stress-response hypersensitivity in a zebrafish model (Davis et al., 2016). Some *Clostridium* species are immunoregulatory, producing SCFAs and stimulating the proliferation of Tregs (Vital et al., 2014). Indeed, the Firmicutes phylum is recognized for producing the majority of the SCFA butyrate, which is thought to be an immunoregulatory metabolite (Koh et al., 2016). Recently, a study in mice found that treatment with SCFAs alone reduced stress-induced gut permeability as well as stress responsiveness (van de Wouw et al., 2018). In humans, supplementation with *Lactobacillus plantarum* P8 for 12 weeks decreased plasma concentrations of proinflammatory cytokines and cortisol, reduced scores of self-reported stress, and enhanced memory (Lew et al., 2018). *Lactobacillus reuteri* DSM 17938 has shown promise in preventing stress-related inflammation in humans (Brenner et al., 2017).

Table 1.1. Physiological and behavioral outcomes of preclinical probiotic and heat-killed bacterium studies.[1]

Bacteria	Administration	Outcome	Model	Publication
Bifidobacterium bifidum G9-1	Oral gavage, 1.0×10^8 CFU, 16 days	Attenuated HPA axis stress response; maintained gut integrity	Rat	Fukui et al., 2018
Bifidobacterium breve	Oral gavage, 1.0×10^{10}, 10^9, 10^7, and 10^5 CFU, 43 days	Mitigated inflammatory response; promoted immunoregulation	Mouse	Ren et al., 2018

Bifidobacterium longum NCC3001	Intragastric gavage, 1.0×10^{10} CFU/mL, 14 days	Reduced colitis-induced anxiogenic behavior	Mouse	Bercik et al., 2011b
Bifidobacterium longum JDM 301	Oral gavage, 1.0×10^{9} CFU, 3 days	Mitigated inflammatory response; maintained gut integrity	Mouse	Suwal et al., 2018
Bifidobacterium pseudocatenulatum CECT 7765	Oral gavage, 1.0×10^{8} CFU, 21 days	Reduced stress-induced behaviors; mitigated inflammatory response; attenuated HPA axis stress response	Mouse	Moya-Pérez et al., 2017
Lactobacillus farciminis	Oral gavage, 1.0×10^{11} CFU, 14 days	Attenuated HPA axis stress response; maintained gut integrity	Rat	Ait-Belgnaoui et al., 2012
Lactobacillus helveticus NS8	Oral, water, 1.0×10^{9} CFU/mL, 26 days	Reduced stress-induced behaviors; attenuated HPA axis stress response; promoted immunoregulation	Rat	Liang et al., 2015
Lactobacillus johnsonii La1	Oral, water, 7.56×10^{7} CFU/mL, 14 days	Decreased ANS hyperactivity; augmented glucose tolerance	Rat	Yamano et al., 2006
Lactobacillus paracasei HII01	Oral, 1.0×10^{8} CFU, 12 weeks	Mitigated inflammatory response; treated metabolic syndrome; improved cognitive behavioral tasks	Rat	Chunchai et al., 2018
Lactobacillus paracasei NCC2461	Oral gavage, 1.0×10^{9} CFU, 10 days	Mitigated inflammatory response; decreased ANS hyperactivity	Mouse	Verdú et al., 2006
Lactobacillus plantarum	tank supplement, 1.0×10^{6} CFU/mL, 30 days	Reduced stress-induced behaviors	Zebrafish	Davis et al., 2016

Lactobacillus plantarum ZLP001	Oral, feed, 5.0 × 10^9 CFU/g, 30 days; *in vitro*, 1.0 x 10^8 CFU/mL	Mitigated inflammatory response; maintained gut integrity	Piglet	Wang et al., 2018
Lactobacillus rhamnosus JB-1	Oral gavage, 1.0 × 10^9 CFU, 28 days	Reduced stress behaviors; attenuated HPA axis stress response	Mouse	Bravo et al., 2011
Lactobacillus rhamnosus JB-1	Oral gavage, 1.67 × 10^9 CFU, 28 days	Reduced stress-induced behaviors; promoted immunoregulation	Rat	Bharwani et al., 2017
mixed, *Lactobacillus helveticus* R0052 and *Bifidobacterium longum* R0175	Oral gavage, 1.0 × 10^9 CFU, 14 days	Attenuated HPA axis stress response; decreased ANS hyperactivity; maintained gut integrity	Mouse	Ait-Belgnaoui et al., 2014, 2018
Mycobacterium vaccae NCTC 11659	Subcutaneous injection, 0.1 mg, once per week, 3 weeks	Mitigated peripheral and neural inflammatory responses; promoted immunoregulation; maintained gut integrity; decreased corticotropin-releasing hormone	Rat	Fonken et al., 2018; Fox et al., 2017; Frank et al., 2018; Loupy et al., 2018; Reber, Siebler, et al., 2016

[1]Abbreviations: ANS, autonomic nervous system; CFU, colony-forming units; HPA, hypothalamic-pituitary-adrenal.

1.17 Clinical relevance

The use of microbiome-based interventions, including prebiotics, probiotics, synbiotics, and postbiotics, has potential for development in the prevention and treatment of PTSD. Prebiotics are compounds that are carbohydrates that are nondigestible by humans but cause proliferation of certain bacteria that utilize them, while synbiotics are combinations of prebiotics and probiotics. Postbiotics are known microbial metabolites that are beneficial to host physiology (Aguilar-

Toalá et al., 2018; Wasilewski et al., 2015). Large randomized, double-blind, placebo-controlled clinical trials are still needed to understand the benefits of using probiotics and related bioactive compounds for the prevention and treatment of trauma- and stressor-related psychiatric disorders such as PTSD. Already, some clinical results are promising. Treatment with a general probiotic containing several different *Lactobacillus* and *Bifidobacterium* species was shown to shift microbial communities and improve mood and memory in healthy humans (Bagga et al., 2018); likewise, *Lactobacillus plantarum* P8 improved cognition and reduced feelings of stress and anxiety in a high-stress group (Lew et al., 2018). In a sample of people with mild to moderate depression, a probiotic of *Lactobacillus helveticus* R0052 and *Bifidobacterium longum* R0175 reduced depression scores (as measured by the Beck Depression Inventory) in addition to reducing the kynurenine/tryptophan ratio in serum, a potential indicator of gut microbial activity (Kazemi et al., 2018). Another study found that, in persons with IBS, treatment with *Bifidobacterium longum* NCC3001 reduced depression scores (using the Hospital Anxiety and Depression scale) and reduced brain activity in the amygdala, frontal cortex, and temporal cortex in response to fearful stimuli (Pinto-Sanchez et al., 2017). A clinical trial is currently underway to investigate the potential therapeutic benefit of *Lactobacillus reuteri* DSM 17938 on gut permeability, biological signatures of peripheral inflammation, and measures of stress resilience in veterans with PTSD and mild traumatic brain injury (Brenner et al., 2017).

1.18 Conclusions

Persons with a diagnosis of PTSD exhibit altered gut microbiome composition relative to trauma-exposed controls without a diagnosis of PTSD (Hemmings et al., 2017). In addition, persons with a diagnosis of PTSD exhibit dysregulated glucocorticoid signaling (Wichmann et

al., 2017), sympathetic/parasympathetic nervous system imbalances (Park et al., 2017), and chronic low-grade inflammation (Eswarappa et al., 2018). Evidence suggests that traumatic stressors can induce or enhance microbial dysbiosis, which in turn interacts with many physiological pathways in the host, contributing to the development of PTSD. It is also possible that the preexisting gut microbiome predisposes individuals to the development of PTSD after exposure to trauma. However, further studies are required to describe how the gut microbiome contributes to changes in physiological systems in the context of PTSD and to explore the possible role of the microbiome as a mediator of risk for development of PTSD and persistence of PTSD symptoms.

1.19 Future directions

First and foremost, there is a critical need to study the gut microbiome in individuals with a diagnosis of PTSD. Appropriate controls include individuals who were not exposed to trauma, as well as trauma-exposed individuals, matched according to time since trauma and potential microbiome confounders (Falony et al., 2016), such as age, diet, drug usage, comorbid diagnoses, and pharmaceutical treatments. In line with this, studies should explore the potential benefits of prebiotics, probiotics, synbiotics, and postbiotics (or combinations of these) for the prevention and treatment of PTSD. Due to the complexity and variability of individual microbiomes, power analyses are imperative to design studies that are likely to obtain valid results; thus, these studies should incorporate a statistically relevant number of samples per group.

One difficult problem to address is the relative contribution of each of the several pathways simultaneously working within the bidirectional MGB axis. These mechanisms are likely to be massively redundant, parallel, and convergent at the level of the CNS. Multiple factors influencing afferent signaling mechanisms should be studied, including bacterial metabolites, gut permeability, afferent neural activation, afferent endocrine/chemical signaling mechanisms, and immune signaling from the periphery to the CNS. Functional magnetic resonance imaging could be one way to visualize the neuronal activation in association with changes in the gut microbiome composition, or microbiome-based interventions (see, for example, Tillisch et al., 2013). Longitudinal studies of military and combat personnel, as well as other high-risk groups, may help us understand how the microbiome and its associated pathways change over time, notably before and after trauma, and may help us identity specific vulnerabilities for the development of PTSD and the persistence of PTSD symptoms. Finally, additional work is needed to understand how brain injury, such as traumatic brain injury, affects these mechanisms and outcomes.

1.20 Acknowledgements

We are grateful to Zachary D. Barger for proofreading the manuscript.

1.21 Disclosures

C.A.L. serves on the Scientific Advisory Board of Immodulon Therapeutics, Ltd.

Chapter 2. Comparing the effects of two different strains of mycobacteria, *Mycobacterium vaccae* NCTC 11659 and *M. vaccae* ATCC 15483, on stress-resilient behaviors and lipid-immune signaling in rats

Citation

Loupy, K.M., Cler, K.E., Marquart, B.M., Yifru, T.W., D'Angelo, H.M., Arnold, M.R., Elsayed, A.I., Gebert, M.J., Fierer, N., Fonken, L.K., Frank, M.G., Zambrano, C.A., Maier, S.F., Lowry, C.A. (2021). Comparing the effects of two different strains of mycobacteria, *Mycobacterium vaccae* NCTC 11659 and *M. vaccae* ATCC 15483, on stress-resilient behaviors and lipid-immune signaling in rats. *Brain, Behavior, and Immunity*, 91: 212-229.

Authors' names

Kelsey M. Loupy[a], Kristin E. Cler[a], Brandon M. Marquart[a], Tumim W. Yifru[a], Heather M. D'Angelo[b], Mathew R. Arnold[a,c], Ahmed I. Elsayed[a], Matthew J. Gebert[d,e], Noah Fierer[d,e], Laura K. Fonken[f], Matthew G. Frank[b,c], Cristian A. Zambrano[a], Steven F. Maier[b,c], Christopher A. Lowry[a,c,e,g,h,i,j,*]

Authors' affiliations

[a]Department of Integrative Physiology, University of Colorado Boulder, Boulder, CO 80309, USA

[b]Department of Psychology and Neuroscience, University of Colorado Boulder, Boulder, CO 80309, USA

[c]Center for Neuroscience, University of Colorado Boulder, Boulder, CO 80309, USA

[d]Department of Ecology and Evolutionary Biology, Cooperative Institute for Research in Environmental Sciences (CIRES), University of Colorado Boulder, Boulder, CO 80309, USA

[e]Center for Microbial Exploration, University of Colorado Boulder, Boulder, CO 80309, USA

[f]Division of Pharmacology and Toxicology, University of Texas at Austin, Austin, TX 78712, USA

[g]Department of Physical Medicine and Rehabilitation and Center for Neuroscience, University of Colorado Anschutz Medical Campus, Aurora, CO 80045, USA

[h]Veterans Health Administration, Rocky Mountain Mental Illness Research Education and Clinical Center (MIRECC), Rocky Mountain Regional Veterans Affairs Medical Center (RMRVAMC), Aurora, CO 80045, USA

[i]Military and Veteran Microbiome: Consortium for Research and Education (MVM-CoRE), Aurora, CO 80045, USA

[j]inVIVO Planetary Health, of the Worldwide Universities Network (WUN), West New York, NJ 07093, USA

2.1 Abstract

Stress-related disorders, such as posttraumatic stress disorder (PTSD), are highly prevalent and often difficult to treat. In rodents, stress-related, anxiety-like defensive behavioral responses may be characterized by social avoidance, exacerbated inflammation, and altered metabolic states. We have previously shown that, in rodents, subcutaneous injections of a heat-killed preparation

of the soil-derived bacterium *Mycobacterium vaccae* NCTC 11659 promotes stress resilience effects that are associated with immunoregulatory signaling in the periphery and the brain. In the current study, we sought to determine whether treatment with a heat-killed preparation of the closely related *M. vaccae* type strain, *M. vaccae* ATCC 15483, would also promote stress-resilience in adult male rats, likely due to biologically similar characteristics of the two strains. Here we show that immunization with either *M. vaccae* NCTC 11659 or *M. vaccae* ATCC 15483 prevents stress-induced increases in hippocampal interleukin 6 mRNA expression, consistent with previous studies showing that *M. vaccae* NCTC 11659 prevents stress-induced increases in peripheral IL-6 secretion and prevents exaggeration of anxiety-like defensive behavioral responses assessed 24 h after exposure to inescapable tail shock stress (IS) in adult male rats. Analysis of mRNA expression, protein abundance, and flow cytometry data demonstrate overlapping but also unique effects of treatment with the two *M. vaccae* strains on immunological and metabolic signaling in the host. These data support the hypothesis that treatment with different *M. vaccae* strains may immunize the host against stress-induced dysregulation of physiology and behavior.

2.2 Introduction

Stress-related psychiatric disorders, including anxiety, depression, and posttraumatic stress disorder (PTSD), contribute exceptional social and economic burdens in the U.S. and worldwide (Dieleman et al., 2016; Judd et al., 1996; Kessler, 2000; Konnopka and König, 2020; Roehrig, 2016). Stress-related psychiatric disorders are commonly associated with chronic low-grade inflammation and altered metabolic function (Gao et al., 2018; Rohleder, 2014; Schultebraucks et al., 2020; Van Der Kooij et al., 2018; Xu et al., 2020). Recently, the microbiome has gained

attention for its ability to mediate and modulate stress-related behavioral responses through the regulation of inflammatory and metabolic signaling, posing an exciting new frontier for the prevention and treatment of psychiatric and neurological disorders (for review, see Cryan et al., 2019; Lowry et al., 2016; Miller and Raison, 2016).

The "old friends" hypothesis proposes that exposure to a diverse set of microbes may help prepare the immune system for and stabilize inflammatory processes during sterile (nonpathogenic) inflammatory events, such as stress, promoting a resilient behavioral phenotype (Böbel et al., 2018; Langgartner et al., 2019; Lowry et al., 2016; Rook, 2013; Rook et al., 2014, 2013a, 2013b, 2004; Rook and Brunet, 2005; Rook and Lowry, 2008). For over a decade, our laboratory has shown that subcutaneous immunization with a heat-killed preparation of the environmental bacterium *Mycobacterium vaccae* NCTC 11659 can attenuate anxiety- and fear-related behaviors in a variety of contexts that involve stress-induced inflammation in rodents, possibly through the activation of immune-responsive mesolimbocortical brain serotonergic systems in the dorsal raphe nucleus (DR) (Amoroso et al., 2020; Fonken et al., 2018; Fox et al., 2017; Frank et al., 2018b; Hassell et al., 2019; Lowry et al., 2007; Reber et al., 2016b). Most notably, immunization with *M. vaccae* NCTC 11659 prevents stress-induced reductions in exploratory behavior in the juvenile social exploration (JSE) paradigm after exposure to inescapable tail shock (IS) (Frank et al., 2018b). In rodents, stress-induced anxiety- and depressive-like behaviors are at least partly regulated by inflammatory signaling, notably interleukin (IL)-6 signaling, in the periphery and the brain (Hodes et al., 2016, 2014). In association with stress-resilience behavior in the chronic subordinate colony (CSC) housing paradigm, immunization with *M. vaccae* NCTC 11659 prevents stress-induced colitis and stress-

induced increases in secretion of proinflammatory cytokines, IL-6 and interferon (IFN)-γ, from freshly isolated mesenteric lymph node cells stimulated with anti-CD3 antibody ex vivo (Amoroso et al., 2020; Reber et al., 2016b). Stress-resilient, anxiolytic behaviors are also observed in *M. vaccae*-treated animals after CSC exposure, as measured by the elevated plus-maze, novel object, and social preference/avoidance tests (Amoroso et al., 2020; Reber et al., 2016b). Immunization with *M. vaccae* NCTC 11659 prior to or after fear conditioning enhances fear extinction in the fear-potentiated startle paradigm (Fox et al., 2017; Hassell et al., 2019), and analysis of brain tissue collected following fear extinction suggests that *M. vaccae* NCTC 11659 may reduce corticotropin-releasing hormone (*Crh*) mRNA expression in the extended amygdala in association with decreased anxiety- and fear-related behaviors (Loupy et al., 2018).

Although the mechanisms through which immunization with *M. vacca*e NCTC 11659 promotes stress resilience are not known, evidence suggests that induction of persistent increases in immunoregulation may play an important role. In a mouse model of allergic pulmonary inflammation, treatment with *M. vaccae* NCTC 11659 increases the number of regulatory T cells (Tregs) in the spleen (Zuany-Amorim et al., 2002). Reber and colleagues have also shown that treatment with an anti-CD25 antibody could, in part, prevent the anxiolytic behaviors induced by *M. vaccae* 11659 after exposure to CSC stress, implicating $CD25^+$ Tregs as a mechanism through which *M. vaccae* NCTC 11659 promotes stress-resilience behaviors (Reber et al., 2016b). Collectively, these data suggest that *M. vaccae* may provide long-term protection as a “stress immunizing” agent with therapeutic potential for the prevention and treatment of stress-induced inflammation stress-induced increases in anxiety-like defensive behavioral responses.

Importantly, immune signaling during stress is intimately tied to metabolic function, and microbiome-host interactions can alter both immune and metabolic signaling within the host (Kishino et al., 2013; Lathrop et al., 2011). Probiotics alter peroxisome proliferator-activated receptor (PPAR) signaling to mitigate inflammation and dyslipidemia (Goto et al., 2015; Mencarelli et al., 2011; Nepelska et al., 2017; Wa et al., 2019; Y. Wang et al., 2016). Evidence suggests that alterations in PPARγ expression in adipose tissue may play a primary role in susceptibility to stress-induced behaviors (Guo et al., 2017), and activation of PPARγ by probiotics may prevent stress-induced pathology by regulating inflammatory and metabolic signaling (Hsieh et al., 2018; Ryan et al., 2012; Sun et al., 2013). A free fatty acid isolated from *M. vaccae* NCTC 11659, 10(*Z*)-hexadecenoic acid, specifically activates PPARα to block lipopolysaccharide (LPS)-stimulated secretion of IL-6 from macrophages in vitro (Smith et al., 2019). Thus, in this study, we sought to examine markers of both immune and metabolic signaling after immunization with *M. vaccae* NCTC 11659 and exposure to IS.

The ability of bacterial strains to induce mental health benefits are thought to be strain specific, and, at this time, there is no theoretical basis to predict which strains have stress resilience effects (Sarkar et al., 2016; Savignac et al., 2014). Therefore, empirical data are required to determine if different strains of bacteria, including different strains of mycobacteria, can confer stress resilience effects. Considering the genetic similarity among different *M. vaccae* strains (Gupta et al., 2018; Nouioui et al., 2018), we investigated the behavioral, immunological, and metabolic effects of *M. vaccae* NCTC 11659 and *M. vaccae* ATCC 15483 in adult male rats after exposure to IS. Here, we show that both strains increase stress-resilience in a rat model of inescapable stress. Results from this study show that both *M. vaccae* NCTC 11659 and *M. vaccae* ATCC

15483 prevent stress-induced anxiety-like defensive behavioral responses, which may be mediated by lipid and immune signaling in the periphery. This is the first study to demonstrate different mycobacterial strains may be physiologically relevant for the prevention and treatment of stress- and anxiety-related disorders.

2.3 Materials and methods

2.3.1 Animals

For an experimental timeline, please see Figure 2.1. Adult male Sprague Dawley® rats (Hsd:Sprague Dawley® SD®; Envigo, Indianapolis, IN, USA) weighing 250-265 g upon arrival were pair-housed in Allentown micro-isolator filter-topped caging [259 mm (W) × 476 mm (L) × 209 mm (H); cage model #PC10198HT, cage top #MBT1019HT; Allentown, NJ, USA] containing an approximately 2.5 cm-deep layer of bedding (cat. no. 7090; Teklad Sani-Chips; Harlan Laboratories, Indianapolis, IN, USA). This species, strain, and supplier were chosen due to previous studies evaluating stress resilience effects of *M. vaccae* NCTC 11659 that were conducted with these animals (Frank et al., 2018b). All rats were kept under standard laboratory conditions (12-h light/dark cycle, lights on at 0700 h, 22 °C) and had free access to bottled reverse-osmosis water and standard rat diet (Harlan Teklad 2918 Irradiated Rodent Chow, Envigo, Huntingdon, United Kingdom). Cages were changed once per week. The research described here was conducted in compliance with the ARRIVE Guidelines for Reporting Animal Research (Kilkenny et al., 2010), and all studies were consistent with the National Institutes of Health *Guide for the Care and Use of Laboratory Animals*, Eighth Edition (National Research Council, 2011). The Institutional Animal Care and Use Committee at the University of Colorado

Boulder approved all procedures. All efforts were made to limit the number of animals used and their suffering.

2.3.2 Reagents

This study used a whole cell heat-killed preparation of *M. vaccae* NCTC 11659 [IMM-201; alternative designations and different preparations and production processes of *M. vaccae* NCTC 11659 used in clinical trials or preclinical studies include: DAR-901 (Lahey et al., 2016), DarDar tuberculosis vaccine (Von Reyn et al., 2010), MV001 (Waddell et al., 2000), MV 007 (Vuola et al., 2003), *M. vaccae* SRL 172 (Von Reyn et al., 2010), *M. vaccae* SRP 299 (Lowry et al., 2007); V7 (Bourinbaiar et al., 2020) is a hydrolyzed version of heat-killed *M. vaccae* NCTC 11659]; 10 mg/ml solution; strain National Collection of Type Cultures (NCTC) 11659, batch C079-ENG#1, provided by BioElpida (Lyon, France), diluted to 1 mg/ml in 100 µl sterile borate-buffered saline (BBS) for injections]. This study also employed the use of a whole heat-killed preparation of *M. vaccae* ATCC 15483 suspension. *M. vaccae* ATCC 15483 was purchased from American Type Culture Collection (ATCC) (Bonicke and Juhasz (ATCC® 15483), Manassas, VA, USA). *M. vaccae* ATCC 15483 was cultured in ATCC® Medium 1395: Middlebrook 7H9 broth with ADC enrichment at 37 °C, then centrifuged at 3000 x g at 4 °C for ten minutes to pellet the cells, growth media was removed, and cells were weighed and resuspended in sterile borate-buffered saline to a concentration of 10 mg/ml. Cells were transferred to a sealed sterile glass container and autoclaved at 121 °C for 15 minutes. Heat-killed bacterial stock was stored at 4 °C. *M. vaccae* ATCC 15483 was further diluted to 1 mg/ml in 100 µl sterile BBS for injections.

2.3.3 Mycobacterium vaccae (M. vaccae) NCTC 11659, ATCC 15483, and vehicle immunization

Experimental rats received 3 subcutaneous (s.c.) immunizations of: 1) 0.1 mg of a heat-killed preparation of *M. vaccae* NCTC 11659; or 2) 0.1 mg of a heat-killed preparation of *M. vaccae* ATCC 15483; or 3) 100 µl of the vehicle, sterile BBS, using 21-gauge needles and injection sites between the scapulae, between the hours of 12 pm and 4 pm. Injections occurred on days –21, –14, and –7 prior to stress exposure, which occurred on day 0. The dose used in these experiments (0.1 mg) was 1/10 of the dose used in human studies (1 mg) (O'Brien et al., 2004) and identical to the dose used in previous studies in mice and rats (Amoroso et al., 2020; Fonken et al., 2018; Fox et al., 2017; Frank et al., 2018b; Hassell et al., 2019; Loupy et al., 2018; Lowry et al., 2007; Reber et al., 2016b; Siebler et al., 2018). Figure 2.1 provides a timeline of *M. vaccae* treatments and stress exposure in relation to behavioral testing and tissue collection.

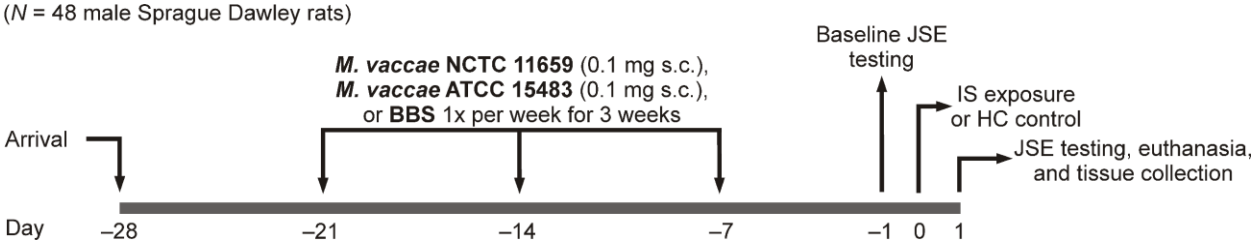

Figure 2.1 Experimental timeline.
This schematic represents the experimental timeline for *M. vaccae* NCTC 11659, *M. vaccae* ATCC 15483, or vehicle (borate-buffered saline [BBS]) treatment in relation to exposure to inescapable shock, as well as behavioral testing, (juvenile social exploration [JSE]) and euthanasia and tissue collection. *N* = 48 adult male Sprague Dawley® rats (Hsd: Sprague Dawley® SD®, Envigo, Indianapolis, IN, USA) weighing between 250-265 g, received three immunizations (s.c.) with either: 1) vehicle control (borate-buffered saline [BBS]); 2) *M. vaccae* NCTC 11659; or 3) *M. vaccae* ATCC 15483 on days –21, –14, and –7 and were subsequently exposed to IS or home cage (HC) control conditions on day 0. Abbreviations: BBS, borate-buffered saline; HC, home cage control conditions; IS, inescapable shock; JSE, juvenile social exploration.

2.3.4 Inescapable tail shock (IS)

IS was performed as previously described (Frank et al., 2018b). Briefly, rats were placed in Plexiglas® tubes (23.4 cm in length × 7 cm in diameter) and exposed to 100 1.6 mA, 5-s tail shocks with a variable inter-trial interval (ITI) ranging from 30 to 90 s (average ITI = 60 s). All inescapable shock (IS) treatments occurred between 09:00 and 11:00 h. IS animals were returned to their home cages immediately after termination of the shock. Home cage control (HC) animals remained undisturbed in their home cages.

2.3.5 Juvenile social exploration (JSE)

Inescapable tail shock (IS) exposure produces robust decreases in JSE (Christianson et al., 2008), which is a widely used and validated measure of anxiety (File and Seth, 2003) and is sensitive to the neuroinflammatory effects of stress (Goshen and Yirmiya, 2009). Here, JSE was measured 24 hours prior to IS (baseline) and 24 h after IS (test) (i.e., between 9:00 and 10:00 h). Each experimental subject was transferred to a novel cage with shaved wood bedding in a dimly lit room (40 lux). After a 15-min habituation period, a 28–32 day-old juvenile male rat was introduced to the subject's cage for 5 min. Exploratory behaviors of the adult (sniffing, pinning, licking and allo-grooming of the juvenile) were timed by an observer blind to treatment condition. After the test, the juvenile was removed and the experimental adult rat was returned to its home cage. Although juvenile stimulus rats were reused for multiple tests, the adult was never retested with the same juvenile. For each animal, JSE test data were quantified as a percent of baseline JSE. Due to technical issues, a total of four animals were removed from the JSE paradigm and subsequent behavioral analysis and our final group sample sizes prior to outlier analysis were BBS/HC, $n = 8$; BBS/IS, $n = 6$; NCTC/HC, $n = 8$; NCTC/IS, $n = 8$; ATCC/HC, $n = 8$; ATCC/IS, $n = 6$.

2.3.6 Euthanasia and tissue collection

Rats were euthanized eight days following the last injection, immediately after JSE testing (10:00-13:00 h MST), using an overdose of sodium pentobarbital (Fatal Plus®, Vortech Pharmaceuticals Ltd., Dearborn, MI, USA; 200 mg/kg, i.p.); the descending aorta was clamped and the brain was perfused with ice-cold 0.9% saline to remove peripheral leukocytes from brain vasculature. The spleen was removed and placed in ice cold phosphate-buffered saline for downstream flow cytometry analysis. The right median lobe of the liver was cut and placed on dry ice for downstream analysis. After perfusion, whole hippocampus was dissected from both left and right hemispheres, separated into dorsal and ventral regions, and immediately placed in liquid nitrogen; all tissue was stored at −80 °C until used for downstream analyses. Due to technical issues during tissue collection or downstream processing, our final sample sizes for dorsal hippocampus mRNA expression prior to outlier analysis were BBS/HC, n = 7; BBS/IS, n = 8; NCTC/HC, n = 7; NCTC/IS, n = 8; ATCC/HC, n = 8; ATCC/IS, n = 8. Our final sample sizes for ventral hippocampus mRNA expression prior to outlier analysis were BBS/HC, n = 7; BBS/IS, n = 6; NCTC/HC, n = 6; NCTC/IS, n = 7; ATCC/HC, n = 8; ATCC/IS, n = 7. Our final sample sizes for dorsal hippocampus IL-4 protein expression prior to outlier analysis were BBS/HC, n = 6; BBS/IS, n = 5; NCTC/HC, n = 7; NCTC/IS, n = 8; ATCC/HC, n = 7; ATCC/IS, n = 7.

2.3.7 Single-cell splenocyte suspension and antibody staining

Briefly, single-cell suspensions of spleen were made by mechanical disruption of the lymphatic tissue filtered through a 40 μm cell strainer (cat. no. 10199-655, VWR International, Radnor, PA,

USA). Cell suspensions were centrifuged at 300 *g* for five minutes at 4 ºC and supernatant was removed; the pellet was resuspended in 20 mL of ammonium-chloride-potassium (ACK) lysing buffer for five minutes at room temperature, and the reaction was terminated by adding 25 mL of PBS. The solution was filtered again through a fresh cell strainer, centrifuged at 300 *g* for five minutes at 4 ºC and washed with 10 ml PBS. Cells were counted using a Neubauer cell counting chamber (cat. no. 717810, BRAND GMBH + CO KG, Wertheim, Germany) and volumes were determined to aliquot $1.0 \times l0^6$ cells for each corresponding sample. LIVE/DEAD Fixable Near-IR Dead Cell Stain Kit (cat. no. L10119, ThermoFisher Scientific, Waltham, MA, USA) was used according to the manufacturer's instructions. $CD4^+$ cells were stained using a CD4 monoclonal antibody conjugated to a FITC fluorophore (OX35, cat. no. 11004082, eBioscience, Inc., San Diego, CA, USA) at the recommended concentration of 0.25 µg/100 µL of flow cytometry staining buffer consisting of 2% fetal bovine serum (FBS; Cat. No. F9423, Sigma-Aldrich, Saint Louis, MO, USA) in PBS. Cells were fixed and permeabilized overnight using the FoxP3/Transcription Factor Staining Kit (cat. no. 00552300, eBioscience, Inc.) according to the manufacturer's instructions. $FoxP3^+$ cells were stained using a monoclonal antibody conjugated to a PE fluorophore (FJK-16s, cat. no. 12577382, eBioscience, Inc.) at the recommended concentration of 1 µg/100 µL of 1X permeabilization buffer. Single-label controls were stained using UltraComp eBeads™ Compensation Beads (cat. no. 01-2222-41, Invitrogen, Carlsbad, CA, USA) for each fluorescent-labeled antibody at the same staining concentration as samples to control for fluorescence spillover. Single-label cells and fluorescence minus one (FMO)-stained cells served as controls to set thresholds for positive and negative cell gates.

2.3.8 Flow cytometry and cell gating strategies

BD Special Order FACSArray™ Bioanalyzer machine (serial no. W91100224, BD Biosciences, Franklin Lakes, NJ, USA) was used to detect fluorescence of stained markers. All downstream analysis was carried out using the FlowJo Software (version 10.1, FlowJo, LLC., Ashland, OR, USA). Compensation was set in FlowJo and was confirmed using single-label control cells by determining the median fluorescence of the negative and positive population of each fluorophore in each of the spillover channels. A general cell gate was placed around the entire population of cells to exclude debris from the analysis, followed by a singlet gate to exclude doublets or clumps of cells. Live cells were gated for negative fluorescence of the near-infrared (NIR) dye, and $CD4^+$ and $FoxP3^+$ cells were gated using FMO and single label controls for positive fluorescence. For a detailed description of the gating procedure, please see Supplementary Figure 2.1.

2.3.9 Real time RT-qPCR semi-quantitative analysis of hippocampal mRNA expression

Quantitative real time RT-qPCR was performed as described previously (Frank et al., 2007). Total RNA was isolated from the left whole hippocampus utilizing a standard method of phenol:chloroform extraction (Chomczynski and Sacchi, 1987). cDNA sequences were obtained from Genbank at the National Center for Biotechnology Information (NCBI; www.ncbi.nlm.nih.gov) (GenBank, 1982). Primer sequences were designed using the Operon Oligo Analysis Tool (http://www.operon.com/technical/toolkit.aspx) or the Integrated DNA Technologies (IDT) PrimerQuest tool (https://www.idtdna.com/pages/tools/primerquest). *Crp* primer sequences were gathered from previously published data (Terra et al., 2009). All primers were tested for sequence specificity using the Basic Local Alignment Search Tool (BLAST) at NCBI (Altschul et al., 1997). Primers were obtained from Invitrogen (*Actb, Cd200, Cd200r1*,

Cd3e, *Crp*, *Il1b*, *Il4*, *Il6*, *Cd206* (*Mrc1*), *Nfkbia*, *Nr2f2*) or IDT (*Adipoq*, *Apoa1*, *Ppara*, *Ppard*, and *Pparg*). Primer specificity was verified by melt curve analyses. All primers were designed to span exon/exon boundaries and thus exclude amplification of genomic DNA (see Supplementary Table 2.1 for primer description and sequences). PCR amplification of cDNA was performed using the QuantiTect SYBR Green PCR Kit (cat. no. 204056, Qiagen, Hilden, Germany). Formation of PCR product was monitored in real time using the MyiQ Single-Color Real-Time PCR Detection System (Bio-Rad, Hercules, CA, USA). Relative mRNA expression was determined by the $2^{-\Delta\Delta Cq}$ method, relative to β-actin, for all genes except those that were highly expressed (*Crp* and *Apoa1* in liver). For these highly expressed genes, relative gene expression was determined by taking the linear expression ratio of the gene of interest to β-actin.

2.3.10 Enzyme-linked immunosorbent assay (ELISA)

Hippocampus was sonicated in a mixture containing extraction buffer (cat. no. FNN0071, Invitrogen) and protease inhibitors (cat. no. P2714, Sigma-Aldrich, St. Louis, MO, USA). Ice-cold tissue sonicates were centrifuged at 14,000 rpm for 10 min at 4 °C. The supernatant was removed and the total protein concentration for each sample was quantified using the Bradford method. Rat IL-4 (cat. no. R4000, R & D Systems, Minneapolis, MN, USA) protein was measured using a standard colorimetric sandwich ELISA according to the manufacturer's instructions. Protein was quantified as pg/100 μg total protein.

2.3.11 Statistical analysis

Statistical analyses for JSE, hippocampal mRNA expression, hippocampal IL-4 protein, flow cytometry, and liver mRNA expression were performed using the software package IBM

Statistical Package for the Social Sciences (version 26.0, SPSS Inc., Chicago, IL, USA). Data were analyzed for extreme outliers using Grubbs' test for single outliers (Grubbs, 1969), and extreme outliers were removed from data sets prior to graphical representation of the data and statistical analysis. 2 x 3 ANOVAs were conducted first to determine effects of treatment, stress, or treatment x stress interactions on mRNA expression. If an effect of one or more factors was found, post hoc pairwise comparisons were made using Fisher's least significant difference (LSD) test. Effect sizes represented by partial eta-squared (η^2_p) for significant effects in the 2 x 3 ANOVA and Cohen's d for significant post hoc pairwise comparisons (Schäfer and Schwarz, 2019) are given in Supplementary Table 2. Paired samples *t*-tests were run to determine gene expression differences between dorsal and ventral hippocampus dissections; homogeneity of variance was analyzed by Levene's Test for Equality of Variance. If variance was unequal, the adjusted *p*-value (obtained from Welch's *t*-test) from the SPSS output was used. In all bar graphs, bars represent the mean + standard error of the mean. Analysis of correlations between dependent variables were performed using R Statistical Programming (version 3.6.1 for Windows), conducted using the Pearson correlation method and false discovery rate (FDR) adjusted *p*-values.

2.4 Results

2.4.1 Effect of M. vaccae NCTC 11659 and ATCC 15483 on stress-induced anxiety-like behavior

Previously published data have shown that *M. vaccae* NCTC 11659 prevents stress-induced exaggeration of anxiety-like defensive behavioral responses (Frank et al., 2018b; Reber et al., 2016b) including in the JSE paradigm (Frank et al., 2018b), and enhances fear extinction (Fox et al., 2017; Hassell et al., 2019; Loupy et al., 2018). Here, we sought to determine if a different

strain of *M. vaccae*, specifically the type strain *M. vaccae* ATCC 15483, also prevents stress-induced exaggeration of anxiety-like defensive behavioral responses in the IS/JSE paradigm. The 2 x 3 ANOVA revealed an effect of stress on JSE behavior ($F = 12.967$; $p < 0.001$; Figure 2.2). Post hoc analysis revealed that among BBS-treated animals, IS decreased juvenile social exploration behavior in the JSE paradigm ($p < 0.01$; Figure 2.2). Immunization with *M. vaccae* NCTC 11659 prevented a stress-induced decrease in JSE behavior, replicating results from Frank et al. (2018) (Figure 2.2). Immunization with *M. vaccae* ATCC 15483 also prevented a stress-induced decrease in JSE behavior (Figure 2.2).

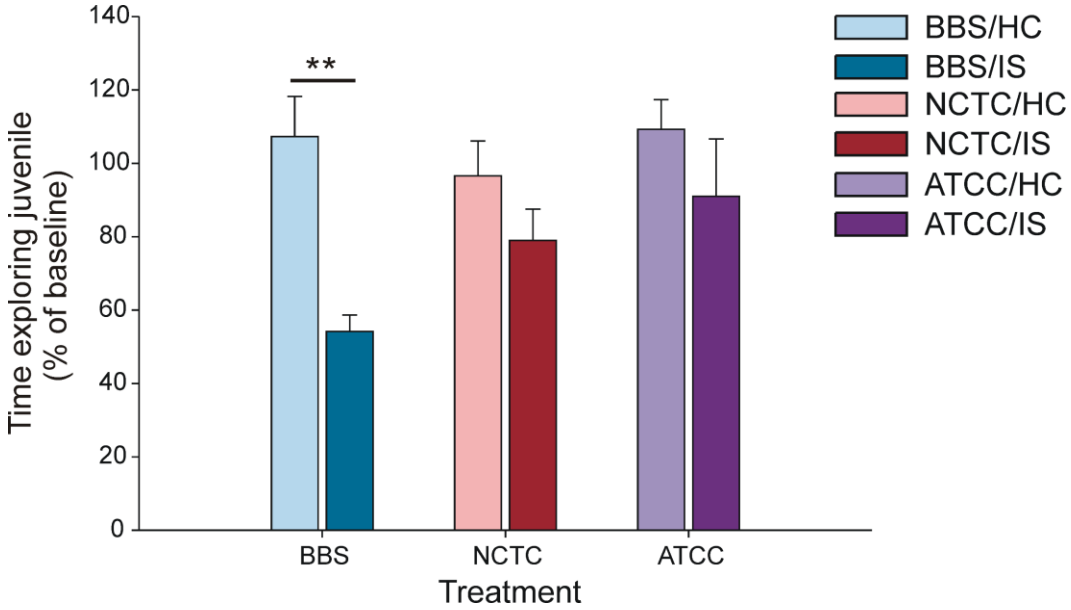

Figure 2.2 Immunization with either *M. vaccae* NCTC 11659 (NCTC) or *M. vaccae* ATCC 15483 (ATCC) prevents stress-induced exaggeration of anxiety-like defensive behavioral responses as assessed by the juvenile social exploration (JSE) paradigm 24 h after inescapable tail shock stress (IS).

Six days after rats received the third injection, i.e., on day –1, baseline JSE was measured in all rats. Twenty-four hours after baseline JSE testing, on day 0, rats were exposed to IS or home cage control conditions. Twenty-four hours after IS, on day 1, rats were tested in the JSE test again. Sample sizes: BBS/HC, $n = 8$; BBS/IS, $n = 6$; NCTC/HC, $n = 8$; NCTC/IS, $n = 8$; ATCC/HC, $n = 7$; ATCC/IS, $n = 6$. Data are presented as a percent of baseline JSE. Bars represent the mean + SEM. Post hoc testing was conducted using Fisher's least significant difference (LSD) test. $^{**}p < 0.01$. Abbreviations: ATCC, *M. vaccae* ATCC 15483; BBS, borate-

buffered saline; HC, home cage control conditions; IS, inescapable tail shock; NCTC, *M. vaccae* NCTC 11659.

2.4.2 Confirmation of dorsal hippocampus dissection

We are interested in understanding how *M. vaccae*-induced immune signaling in the periphery translates to altered immune signaling, neural activity, and behavior. We hypothesize that this may take place through structures with reduced blood-brain barrier function, including the choroid plexus (Baruch and Schwartz, 2013; Strominger et al., 2018). The dorsal hippocampus is of particular interest due to its physical proximity to the choroid plexus and abundance of parenchymal T cells, identified by the high expression, relative to the ventral hippocampus, of *Cd3e* (encoding CD3, epsilon chain) mRNA (Supplementary Figure 2.2) (Frank et al., 2018b; Lee et al., 2017). *Cd3e* mRNA may indicate migratory $CD4^+$ T cells have crossed into the parenchyma from the choroid plexus through a chemokine- and adhesion molecule-dependent process (Strominger et al., 2018). For analysis of all subsequent mRNA expression, we focused on the dorsal hippocampus, as we have shown previously that the effects of *M. vaccae* NCTC 11659 were most evident in the dorsal hippocampus, relative to the intermediate or ventral hippocampus (Frank et al., 2018).

To validate our dissections of the dorsal and ventral hippocampus, we assessed expression of two genes previously shown to be differentially expressed in these hippocampal subregions. Previous studies have shown that dorsal hippocampus is characterized by relatively high expression of *Cd3e* and low expression of *Nr2f2* (encoding nuclear factor 2, receptor 2, NR2F2) mRNA compared to the ventral hippocampus (Frank et al., 2018b; Lee et al., 2017). Paired samples *t*-tests revealed greater *Cd3e* mRNA expression in the dorsal hippocampus compared to ventral

hippocampus (t = 14.623, $p < 0.001$) and lower expression of *Nr2f2* in the dorsal hippocampus compared to ventral hippocampus (t = –16.744, $p < 0.001$); these results confirm the expected pattern of gene expression following dissection of the dorsal and ventral subdivisions of the hippocampus (Supplementary Figure 2.2).

In the dorsal hippocampus, the 2 x 3 ANOVA revealed an effect of stress on *Cd3e* mRNA expression ($F_{(1, 40)} = 4.609$, $p < 0.05$). Mean relative *Cd3e* mRNA expression in home cage control rats was 3215 ± 215, whereas mean *Cd3e* mRNA expression in IS-exposed rats was 2537 ± 233. However, post hoc pairwise comparisons did not reveal differences between any of the IS groups relative to the HC control groups (Supplementary Figure 2.2, showing the relative expression as a fraction of home-cage control gene expression in ventral hippocampus). The 2 x 3 ANOVA did not reveal an effect of treatment, stress, or a treatment x stress interaction on *Nr2f2* mRNA expression in the dorsal hippocampus, consistent with Frank et al., (2018) (Supplementary Figure 2.2).

2.4.3 Effect of M. vaccae NCTC 11659 and ATCC 15483 on expression of inflammatory signaling genes in the dorsal hippocampus

Potent stressors such as IS increase proinflammatory responses in the periphery and the brain (Johnson et al., 2002) and lead to hippocampal microglial priming (Frank et al., 2018b; Weber et al., 2015). IS increases the expression of *Il1b* and *Nfkbia* mRNA in hippocampal microglia challenged with LPS ex vivo, and this effect is attenuated by immunization with *M. vaccae* NCTC 11659 (Frank et al., 2018b). Here, we assessed the effects of *M. vaccae* NCTC 11659 and *M. vaccae* ATCC 15483 on expression of genes involved in inflammatory signaling, including *Il6, Il1b,* and *Nfkbia*, under IS and HC conditions. The 2 x 3 ANOVA revealed an effect of

treatment ($F_{(2, 40)} = 3.441$, $p < 0.05$) and an effect of stress ($F_{(1, 40)} = 7.268$, $p < 0.05$; Figure 2.3A) on *Il6* mRNA expression in the dorsal hippocampus. Post hoc analysis revealed that among home cage control animals, immunization with *M. vaccae* NCTC 11659 increased *Il6* mRNA expression in the dorsal hippocampus (Figure 2.3A). Among BBS-treated animals, IS increased *Il6* mRNA in the dorsal hippocampus (Figure 2.3A). Immunization with either *M. vaccae* NCTC 11659 or *M. vaccae* ATCC 15483 prevented the stress-induced increase in *Il6* mRNA expression (Figure 2.3A). Although JSE behavior did not correlate with *Il6* mRNA expression in the dorsal hippocampus across all groups ($r = –0.405$; $p > 0.05$; Figure 2.7), JSE behavior negatively correlated with *Il6* mRNA expression among BBS-treated animals only ($r = –0.563$; $p < 0.05$; Supplementary Figure 2.3A) and among animals immunized with *M. vaccae* ATCC 11659 only ($r = –0.564$; $p < 0.05$; Supplementary Figure 2.3C); however, JSE behavior did not correlate with *Il6* mRNA expression among animals immunized with *M. vaccae* NCTC 11659 only ($r = –0.123$; $p > 0.05$; Supplementary Figure 2.3B).

The 2 x 3 ANOVA did not reveal an effect of treatment, stress, or a treatment x stress interaction on either *Il1b* (Figure 2.3B) or *Nfkbia* (Figure 2.3C) mRNA expression in the dorsal hippocampus.

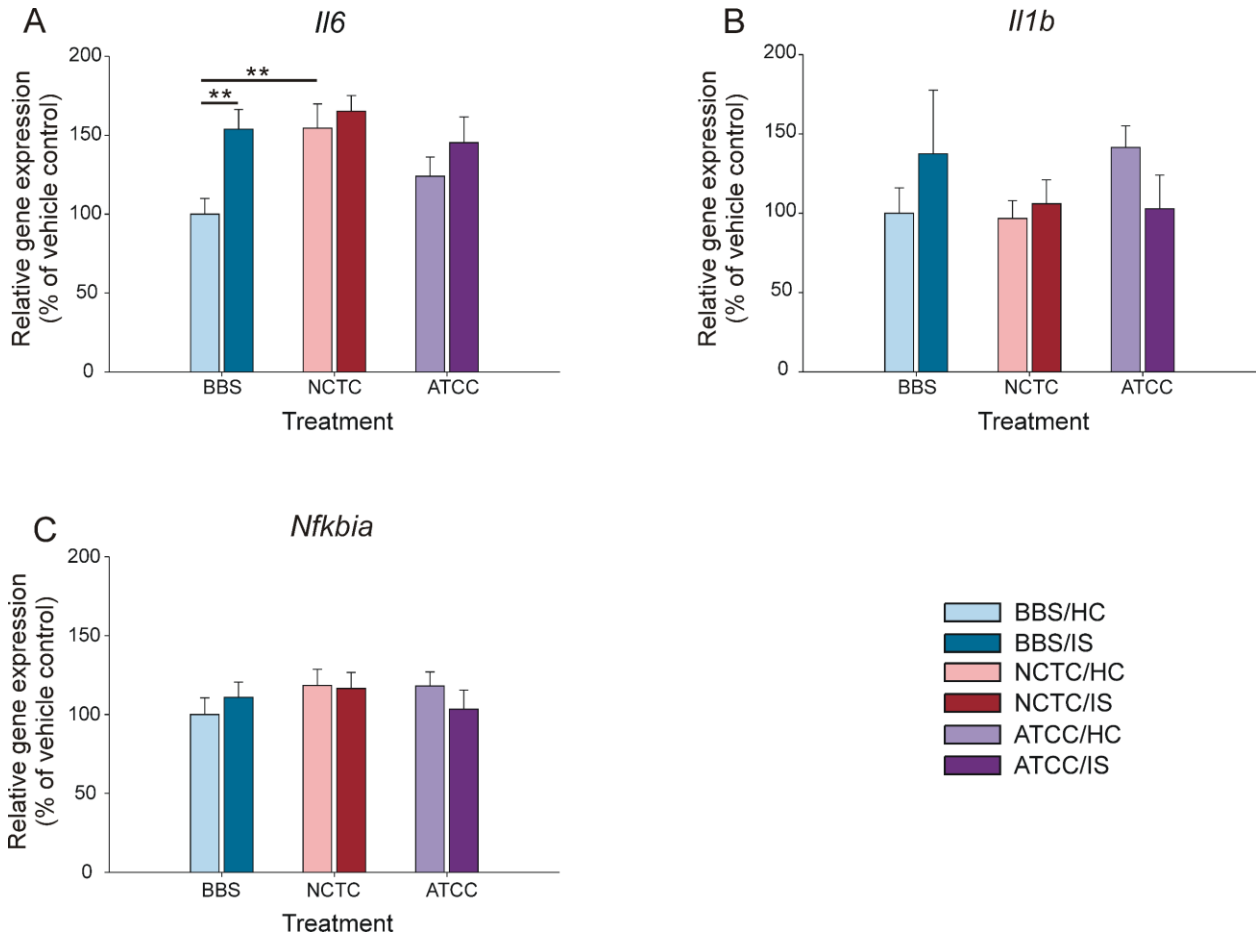

Figure 2.3 Immunization with either *M. vaccae* NCTC 11659 (NCTC) or *M. vaccae* ATCC 15483 (ATCC) prevents stress-induced increases of *Il6* mRNA expression in the dorsal hippocampus 24 h after inescapable tail shock stress (IS).

Sample sizes: *Il6* (BBS/HC, *n* = 7; BBS/IS, *n* = 8; NCTC/HC, *n* = 7; NCTC/IS, *n* = 8; ATCC/HC, *n* = 8; ATCC/IS, *n* = 8); *Il1b* (BBS/HC, *n* = 6; BBS/IS, *n* = 8; NCTC/HC, *n* = 6; NCTC/IS, *n* = 8; ATCC/HC, *n* = 7; ATCC/IS, *n* = 8); *Nfkbia (*BBS/HC, *n* = 7; BBS/IS, *n* = 8; NCTC/HC, *n* = 7; NCTC/IS, *n* = 8; ATCC/HC, *n* = 8; ATCC/IS, *n* = 8). Expression of *Il6*, *Il1b*, and *Nfkbia* mRNA was measured using quantitative real-time polymerase chain reaction (RT-qPCR), with beta-actin as a reference. Bars represent the mean + SEM. Post hoc testing was conducted using Fisher's least significant difference (LSD) test. ***p* <0.01. Abbreviations: ATCC, *M. vaccae* ATCC 15483; BBS, borate-buffered saline; HC, home cage control conditions; *Il*, interleukin; IS, inescapable tail shock; NCTC, *M. vaccae* NCTC 11659; *Nfkbia*, NF-κB inhibitor α.

2.4.4 Effect of M. vaccae NCTC 11659 and ATCC 15483 on expression of Il4 mRNA and IL-4 responsive genes in dorsal hippocampus

Previous studies have shown that in addition to dampening proinflammatory responses to stress, immunization with *M. vaccae* NCTC 11659 increases expression of genes involved in anti-inflammatory signaling in the hippocampus, including *Il4* and the IL-4-responsive genes *Cd206* (*Mrc1*, encoding mannose receptor C-type 1) and *Cd200r1*, without affecting *Cd200* expression (Frank et al., 2018). These findings prompted us to compare the effects of *M. vaccae* NCTC 11659 and *M. vaccae* ATCC 15483 on expression of *Il4*, *Cd206* (*Mrc1*), *Cd200r1*, and *Cd200* in the dorsal hippocampus under IS and control conditions.

Il4

Unexpectedly, and in contrast to previous studies (Frank et al., 2018b), the 2 x 3 ANOVA did not reveal an effect of treatment, stress, or a treatment x stress interaction on *Il4* mRNA expression in the dorsal hippocampus (Figure 2.4A).

Cd206

The 2 x 3 ANOVA revealed an effect of stress on *Cd206* mRNA expression in the dorsal hippocampus ($F_{(1, 38)} = 6.638$, $p < 0.05$; Figure 2.4B). In contrast with previous studies (Frank et al., 2018b), *M. vaccae* NCTC 11659 did not increase *Cd206* mRNA in the dorsal hippocampus. Among animals immunized with *M. vaccae* ATCC 15483, IS decreased *Cd206* mRNA expression ($p < 0.01$; Figure 2.4B).

Cd200

Previous studies have shown that *M. vaccae* NCTC 11659 has no effect on hippocampal *Cd200* mRNA expression (Frank et al., 2018b). Consistent with these previous studies, the 2 x 3

ANOVA revealed that there was no effect of treatment, stress, or a treatment x stress interaction on *Cd200* mRNA expression in the dorsal hippocampus, although a main effect of stress approached significance ($F_{(1, 39)} = 3.083$, $p = 0.087$; Figure 2.4C).

Cd200r1

Previous studies have shown that IS decreases *Cd200r1* mRNA expression in the dorsal hippocampus and in freshly isolated hippocampal microglia; conversely, immunization with *M. vaccae* increases *Cd200r1* mRNA expression in the dorsal hippocampus in home cage control animals and IS-exposed animals and, furthermore, prevents the IS-induced decreases in *Cd200r1* in freshly isolated hippocampal microglia (Frank et al., 2018b). As noted previously, CD200R1, which is expressed almost exclusively on microglia as well as other CNS macrophages (Koning et al., 2009; Wright et al., 2000), plays a prominent role in microglial immunomodulation. In the CNS microenvironment, microglia are maintained in a surveillant or quiescent state of activation through several inhibitory signaling dyads (Hoarau et al., 2011; Ransohoff and Cardona, 2010) including the CD200:CD200R1 ligand/receptor dyad. CD200R1 inhibits myeloid cell function through interaction with its ligand CD200 (Gorczynski, 2005), which is expressed on endothelial cells, oligodendrocytes, and neurons. In agreement with previous studies (Frank et al., 2018b), the 2 x 3 ANOVA revealed an effect of stress on *Cd200r1* mRNA expression in the dorsal hippocampus ($F_{(1, 39)} = 12.819$, $p < 0.01$; Figure 2.4D). Post hoc analysis revealed that among BBS-treated animals, IS decreased *Cd200r1* mRNA expression ($p < 0.01$; Figure 2.4D). In agreement with previous studies (Frank et al., 2018b), despite the lack of effect of *M. vaccae* NCTC 11659 on *Il4* mRNA expression in the dorsal hippocampus in this study, immunization with *M. vaccae* NCTC 11659 prevented IS-induced decreases in *Cd200r1* mRNA expression

(Figure 2.4D). In contrast, the *M. vaccae* ATCC 15483 type strain did not prevent the IS-induced decrease in *Cd200r1* mRNA expression in the dorsal hippocampus ($p < 0.01$; Figure 2.4D).

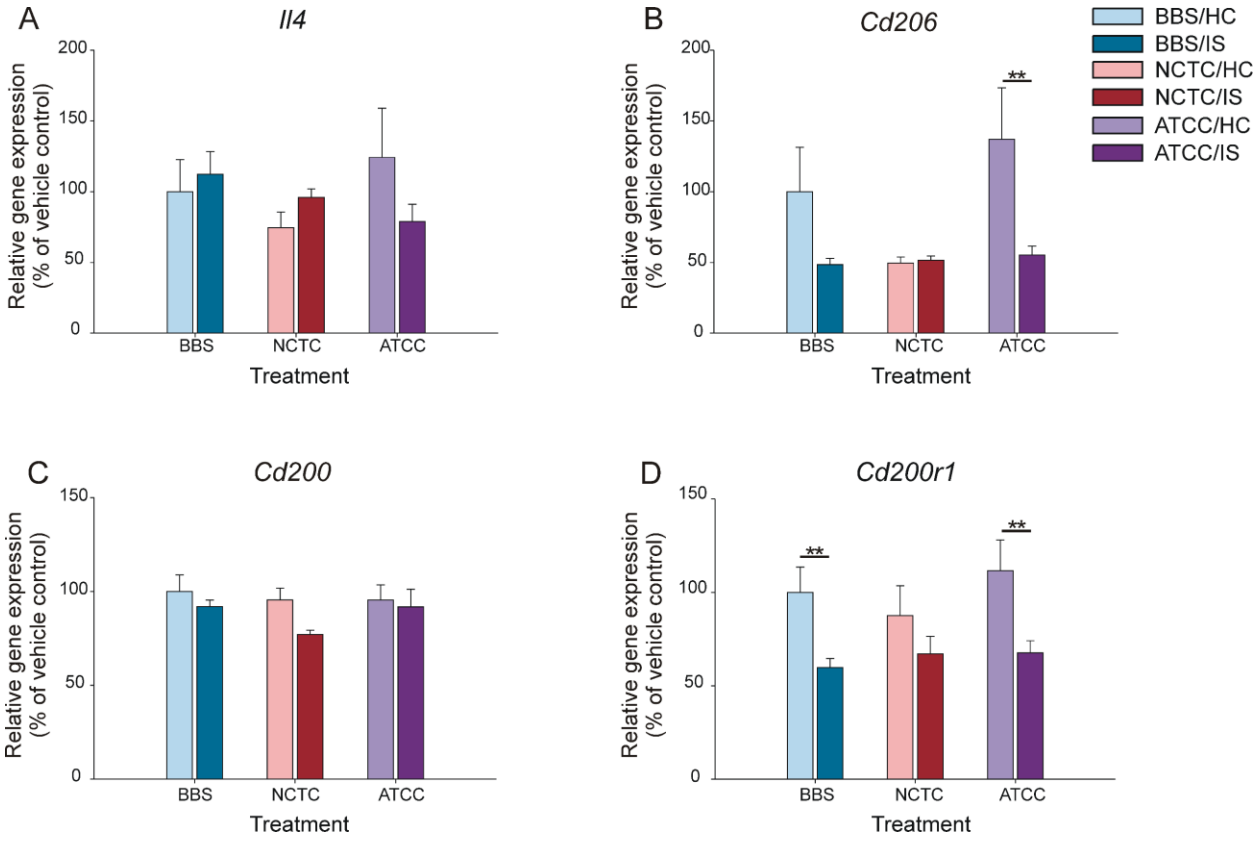

Figure 2.4 Immunization with *M. vaccae* NCTC 11659 (NCTC), but not immunization with *M. vaccae* ATCC 15483 (ATCC), prevents stress-induced decreases of *Cd200r1* mRNA expression in the dorsal hippocampus 24 h after inescapable tail shock stress (IS).

Sample sizes: *Il4* (BBS/HC, *n* = 7; BBS/IS, *n* = 8; NCTC/HC, *n* = 7; NCTC/IS, *n* = 8; ATCC/HC, *n* = 8; ATCC/IS, *n* = 8); *Cd206* (BBS/HC, *n* = 7; BBS/IS, *n* = 7; NCTC/HC, *n* = 6; NCTC/IS, *n* = 8; ATCC/HC, *n* = 8; ATCC/IS, *n* = 8); *Cd200* (BBS/HC, *n* = 7; BBS/IS, *n* = 8; NCTC/HC, *n* = 7; NCTC/IS, *n* = 7; ATCC/HC, *n* = 8; ATCC/IS, *n* = 8); *Cd200r1* (BBS/HC, *n* = 7; BBS/IS, *n* = 7; NCTC/HC, *n* = 7; NCTC/IS, *n* = 8; ATCC/HC, *n* = 8; ATCC/IS, *n* = 8). Expression of (A) *Il4*, (B) *Cd206*, (C) *Cd200*, and (D) *Cd200r1* mRNA was measured using quantitative real-time polymerase chain reaction (RT-qPCR), with beta-actin as a reference. Bars represent the mean + SEM. Post hoc testing was conducted using Fisher's least significant difference (LSD) test. $^{**}p < 0.01$. Abbreviations: ATCC, *M. vaccae* ATCC 15483; BBS, borate-buffered saline; *Cd*, cluster of differentiation; HC, home cage control conditions; *Il*, interleukin; IS, inescapable tail shock; NCTC, *M. vaccae* NCTC 11659.

2.4.5 Effect of M. vaccae on IL-4 protein in the dorsal hippocampus

Previous studies have reported that immunization with *M. vaccae* NCTC 11659 can increase hippocampal IL-4 protein expression in home cage control animals (Frank et al., 2018). In alignment with findings outlined above with *Il4* mRNA expression, but contrary to prior published findings (Frank et al., 2018), the 2 x 3 ANOVA did not reveal an effect of treatment, stress, or a treatment x stress interaction on IL-4 protein in the dorsal hippocampus (Supplementary Figure 2.4).

2.4.6 Effect of M. vaccae on regulatory T cell flow cytometry in the spleen

A study by Zuany-Amorim et al. (2002) suggests that treatment with *M. vaccae* NCTC 11659 may activate a specific population of $CD4^{+}CD45RB^{Lo}$ Tregs in mice. However, the 2 x 3 ANOVA did not reveal an effect of treatment, stress, or a treatment x stress interaction on percent $CD4^{+}$ cells, percent $CD4^{+}/FoxP3^{+}$ cells of total cells, or percent $FoxP3^{+}$ cells of $CD4^{+}$ cells in the spleen (Supplementary Figure 2.5A-C).

2.4.7 Effect of M. vaccae on expression of lipid and immune signaling genes in the liver

Liver tissue was chosen for investigation of metabolic and immune signaling effects of *M. vaccae* NCTC 11659 and *M. vaccae* ATCC 15483 treatment due to prior studies showing that a free-fatty acid isolated from *M. vaccae* NCTC 11659, 10(*Z*)-hexadecenoic acid, stimulates PPARα signaling in freshly isolated peritoneal macrophages ex vivo (Smith et al., 2019), and expression of PPARα, a regulator of immune and metabolic signaling, is highest in the liver (Abbott et al., 1987; Braissant et al., 1996). Given that *M. vaccae* NCTC 11659 and *M. vaccae* ATCC 15483 were administered subcutaneously, *M. vaccae* may drive long-lasting changes in

the liver via secretions from adipose tissue, including cytokines and free fatty acids (Coelho et al., 2013; Reilly et al., 2015).

Previous studies have identified an association between psychological distress and liver disease mortality (Russ et al., 2015). However, the effects of IS on liver function, including lipid and immune signaling, have not been studied. Here, we assessed the effects of IS on expression of genes involved in hepatic lipid (i.e., *Ppara*, *Ppard*, and *Pparg*, *Adipoq*) and immune (i.e., *Crp*, *Nfkbia*, *Il4*, *Il6*, *l1b*, and *Cd206*) signaling and the effects of immunization with *M. vaccae* NCTC 11659 or *M. vaccae* ATCC 15483 on these responses.

Ppara, Ppard, and Pparg

Ppara, Ppard, and *Pparg* encode the peroxisome proliferator-activated receptors α, δ, and γ, respectively, which are ligand-activated transcription factors that play a regulatory role in energy homeostasis and metabolic function. Previous studies have suggested that *M. vaccae* NCTC 11659 may attenuate inflammatory responses by activating the PPARα signaling pathway in freshly isolated peritoneal macrophages (Smith et al., 2019) or may alter the abundance of immune signaling and lipid metabolism proteins associated with the PPARγ pathway in the plasma and CSF of rats (Loupy et al., 2020). Here, we measured the relative abundance of *Ppara*, *Ppard*, and *Pparg* mRNA expression in the liver, a metabolic tissue that has high expression of all three genes. The 2 x 3 ANOVA did not reveal an effect of treatment, stress, or a treatment x stress interaction on *Ppara* (Figure 2.5A) or *Ppard* (Figure 2.5B) mRNA expression in the right median lobe of the liver. However, the 2 x 3 ANOVA revealed an effect of treatment ($F_{(2, 41)} = 4.913$, $p < 0.05$) and an effect of stress ($F_{(1, 41)} = 13.466$, $p < 0.01$; Figure 2.5C) on

Pparg mRNA expression in the right median lobe of the liver. Post hoc analysis revealed that, among home cage control rats, immunization with either *M. vaccae* NCTC 11659 ($p < 0.05$; Figure 2.5C) or *M. vaccae* ATCC 15483 ($p < 0.05$; Figure 2.5C) decreased *Pparg* mRNA expression compared to BBS-treated rats. Among BBS-treated rats, IS decreased *Pparg* mRNA expression ($p < 0.01$; Figure 2.5C). Similarly, among animals preimmunized with *M. vaccae* ATCC 15483, IS decreased *Pparg* mRNA expression ($p < 0.05$; Figure 2.5C). However, immunization with *M. vaccae* NCTC 11659 prevented a stress-induced decrease in *Pparg* mRNA expression.

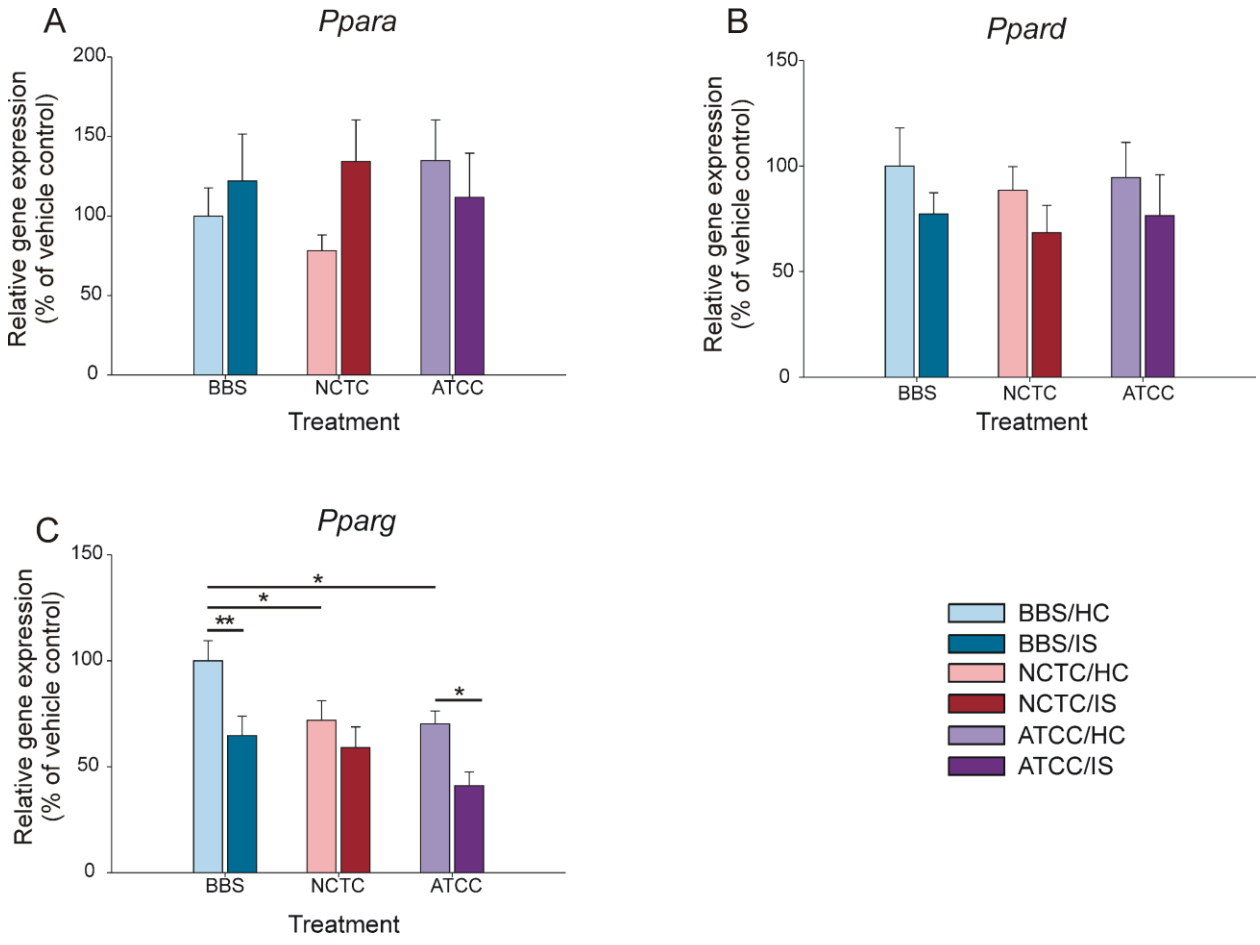

Figure 2.5 Immunization with either *M. vaccae* NCTC 11659 (NCTC) or *M. vaccae* ATCC 15483 (ATCC) decreases *Pparg* mRNA expression in the liver among home cage

control animals, but only immunization with *M. vaccae* NCTC 11659 prevents stress-induced decreases in *Pparg* mRNA expression.

Sample sizes: *Ppara* (BBS/HC, *n* = 8; BBS/IS, *n* = 7; NCTC/HC, *n* = 7; NCTC/IS, *n* = 8; ATCC/HC, *n* = 8; ATCC/IS, *n* = 8); *Ppard (*BBS/HC, *n* = 8; BBS/IS, *n* = 8; NCTC/HC, *n* = 8; NCTC/IS, *n* = 8; ATCC/HC, *n* = 8; ATCC/IS, *n* = 8); *Pparg* (BBS/HC, *n* = 8; BBS/IS, *n* = 8; NCTC/HC, *n* = 8; NCTC/IS, *n* = 8; ATCC/HC, *n* = 8; ATCC/IS, *n* = 7). Expression of *Ppara*, *Ppard*, and *Pparg* mRNA was measured using quantitative real-time polymerase chain reaction (RT-qPCR), with beta-actin as a reference. Bars represent the mean + SEM. Post hoc testing was conducted using Fisher's least significant difference (LSD) test. **p* < 0.05, ***p* <0. 01. Abbreviations: ATCC 15483, *M. vaccae* ATCC 15483; BBS, borate-buffered saline; HC, home cage control conditions; IS, inescapable tail shock; NCTC 11659, *M. vaccae* NCTC 11659; *Ppara*, peroxisome proliferator-activated receptor α; *Ppard*, peroxisome proliferator-activated receptor δ; *Pparg*, peroxisome proliferator-activated receptor γ.

PPAR signaling pathway-associated genes

Adiponectin is an anti-inflammatory hormone that activates PPARα, which in turn has anti-inflammatory effects in the liver (Masaki et al., 2004; Neumeier et al., 2006). In line with the absence of effects of IS or *M. vaccae* strains on PPARα mRNA expression, the 2 x 3 ANOVA did not reveal an effect of treatment, stress, or a treatment x stress interaction on *Adipoq* (encoding adiponectin) mRNA expression in the right median lobe of the liver (Supplementary Figure 2.6A).

Likewise, the 2 x 3 ANOVA did not reveal an effect of treatment, stress, or a treatment x stress interaction on *Apoa1* (encoding apolipoprotein A-I, a PPARα-responsive gene (Vu-Dac et al., 1998)) in the right median lobe of the liver (Supplementary Figure 2.6B).

Crp

Given the liver's prevalence of resident macrophages, called Kupffer cells, and monocyte-derived macrophages, which play important roles in inflammation related to stress and injury (Guillot and Tacke, 2019), we measured the mRNA expression of a panel of immune signaling

molecules in the liver that are associated with either *M. vaccae* NCTC 11659 immunization, stress-induced inflammation, or both: *Crp*, *Nfkbia*, *Il4*, *Il6*, *Il1b*, and *Cd206* (Fonken et al., 2018; Frank et al., 2018b; Reber et al., 2016b; Tursich et al., 2014). CRP is an acute-phase protein synthesized in the liver that increases following induction by IL-6 (Pepys and Hirschfield, 2003). CRP is strongly associated with stress-induced proinflammatory responses in the periphery, and elevated levels of CRP are thought to be a risk factor for the development of stress-related disorders (Eraly et al., 2014; Michopoulos et al., 2015). The 2 x 3 ANOVA revealed an effect of stress on *Crp* mRNA expression in the right median lobe of the liver ($F_{(1, 41)} = 9.135$, $p < 0.01$). Post hoc analysis revealed that, among rats immunized with *M. vaccae* ATCC 15483, IS increased *Crp* mRNA expression ($p < 0.01$; Figure 2.6A).

Nfkbia

The 2 x 3 ANOVA revealed an effect of stress on *Nfkbia* mRNA expression in the right median lobe of the liver ($F_{(1, 41)} = 6.154$, $p < 0.05$). A treatment x stress interaction on *Nfkbia* mRNA ($F_{(2, 41)} = 2.816$, $p = 0.071$; Figure 2.6B) approached significance. Among rats immunized with *M. vaccae* NCTC 11659, IS decreased *Nfkbia* mRNA expression ($p < 0.01$; Figure 2.6B).

Il4

The 2 x 3 ANOVA did not reveal an effect of treatment, stress, or a treatment x stress interaction on *Il4* mRNA expression in the right median lobe of the liver, although an effect of stress approached statistical significance ($F_{(1, 39)} = 3.926$, $p = 0.055$; Figure 2.6C).

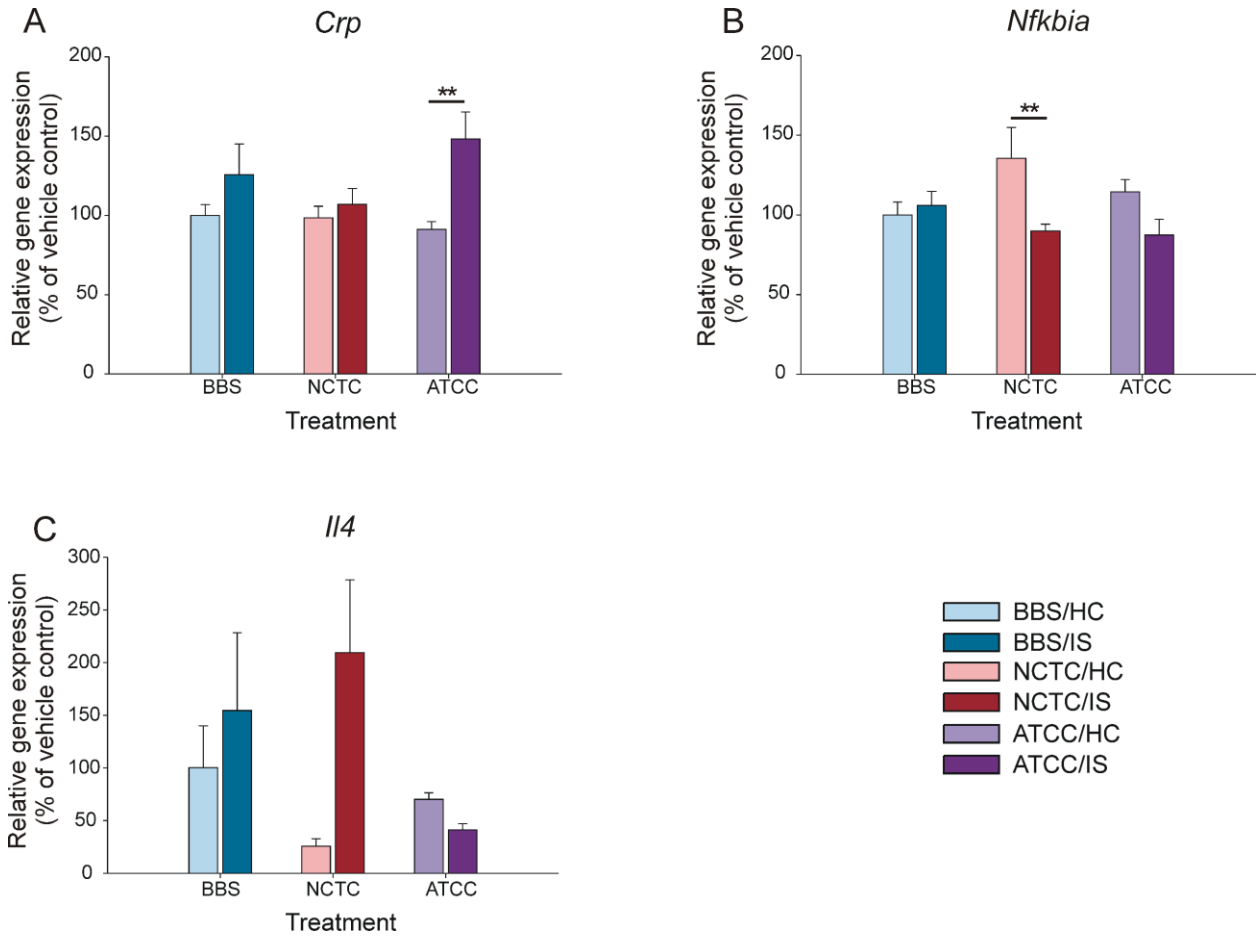

Figure 2.6 Immunization with either *M. vaccae* NCTC 11659 (NCTC) or *M. vaccae* ATCC 15483 (ATCC) and exposure to inescapable tail shock stress (IS) differentially alters immune signaling genes in the liver.

Data represent (A) *Crp*, (B) *Nfkbia*, and (C) *Il4* mRNA expression in the right median lobe of the liver. Sample sizes: *Crp* (BBS/HC, *n* = 8; BBS/IS, *n* = 8; NCTC/HC, *n* = 8; NCTC/IS, *n* = 7; ATCC/HC, *n* = 8; ATCC/IS, *n* = 8); *Nfkbia* (BBS/HC, *n* = 8; BBS/IS, *n* = 8; NCTC/HC, *n* = 8; NCTC/IS, *n* = 7; ATCC/HC, *n* = 8; ATCC/IS, *n* = 8); *Il4* (BBS/HC, *n* = 8; BBS/IS, *n* = 7; NCTC/HC, *n* = 7; NCTC/IS, *n* = 8; ATCC/HC, *n* = 7; ATCC/IS, *n* = 8). Expression of *Crp*, *Nfkbia*, and *Il4* mRNA were measured using quantitative real-time polymerase chain reaction (RT-qPCR), with beta-actin as a reference. Bars represent the mean + SEM. Post hoc testing was conducted using Fisher's least significant difference (LSD) test. **p* < 0.05, ***p* <0.01. Abbreviations: ATCC, *M. vaccae* ATCC 15483; BBS, borate-buffered saline; *Crp*, C-reactive protein; HC, home cage control conditions; *Il*, interleukin; IS, inescapable tail shock; NCTC, *M. vaccae* NCTC 11659; *Nfkbia*, NF-κB inhibitor α.

Il6, Il1b, and Cd206

The 2 x 3 ANOVA did not reveal an effect of treatment, stress, or a treatment x stress interaction on *Il16* (Supplementary Figure 2.6C) or *Il1b* (Supplementary Figure 2.6D) mRNA expression in the right median lobe of the liver.

The 2 x 3 ANOVA did not reveal an effect of treatment, stress, or treatment x stress on *Cd206* mRNA expression in the right median lobe of the liver (Supplementary Figure 2.6E).

2.4.8 Correlations among biological signatures of lipid and immune signaling

To determine possible relationships among lipid metabolism, immune signaling, and behavior, a correlation matrix containing all experimental endpoints was created. Pearson's correlation *r* and FDR-adjusted *p*-values were determined and are presented in Figure 2.7. Although *Ppara* mRNA expression in the liver was not different among groups (Figure 2.5B), *Ppara* mRNA expression in the liver positively correlated to both *Il4* mRNA expression in the liver ($r = 0.932$, $p < 0.001$; Figure 2.7; Figure 2.8A; Table 2.1) and *Il4* mRNA expression in the dorsal hippocampus ($r = 0.419$, $p < 0.05$; Figure 2.7; Figure 2.8B; Table 2.1). *Ppara* mRNA expression in the liver also positively correlated to *Apoa1* ($r = 0.612$, $p < 0.001$; Table 2.1) and *Adipoq* ($r = 0.401$, $p < 0.05$; Table 2.1) mRNA expression in the liver, two markers of lipid metabolism. Furthermore, *Apoa1* and *Adipoq* mRNA expression in the liver were positively correlated with each other ($r = 0.695$, $p < 0.001$; Figure 2.7; Table 2.1). *Apoa1* mRNA expression in the liver was correlated with *Il4* mRNA expression in the liver ($r = 0.518$, $p < 0.01$; Figure 2.7; Table 2.1), whereas *Adipoq* mRNA expression in the liver was positively correlated with *Il4* mRNA expression in the dorsal hippocampus ($r = 0.564$, $p < 0.001$; Figure 2.7; Table 2.1). Interestingly, *Ppara*, *Apoa1*, *Adipoq*, and *Il4* mRNA expression in the liver all positively correlated with *Nfkbia* mRNA expression in

the dorsal hippocampus (respectively, $r = 0.525$, $p < 0.01$; $r = 0.639$, $p < 0.001$; $r = 0.432$, $p < 0.05$; $r = 0.394$, $p < 0.05$; Figure 2.7; Table 2.1). Table 2.1 lists a subset of the aforementioned genes measured in the liver and dorsal hippocampus whose relative expressions are correlated with one another and whose correlations cluster hierarchically, regardless of significant differences in the expression of these genes between experimental groups. Since the correlations exist across the experimental groups, these genes represent possible lipid-immune signaling pathways that may be relevant to individual variability of biomarkers assessed after *M. vaccae* NCTC 11659 immunizations, *M. vaccae* ATCC 15483 immunizations, and IS.

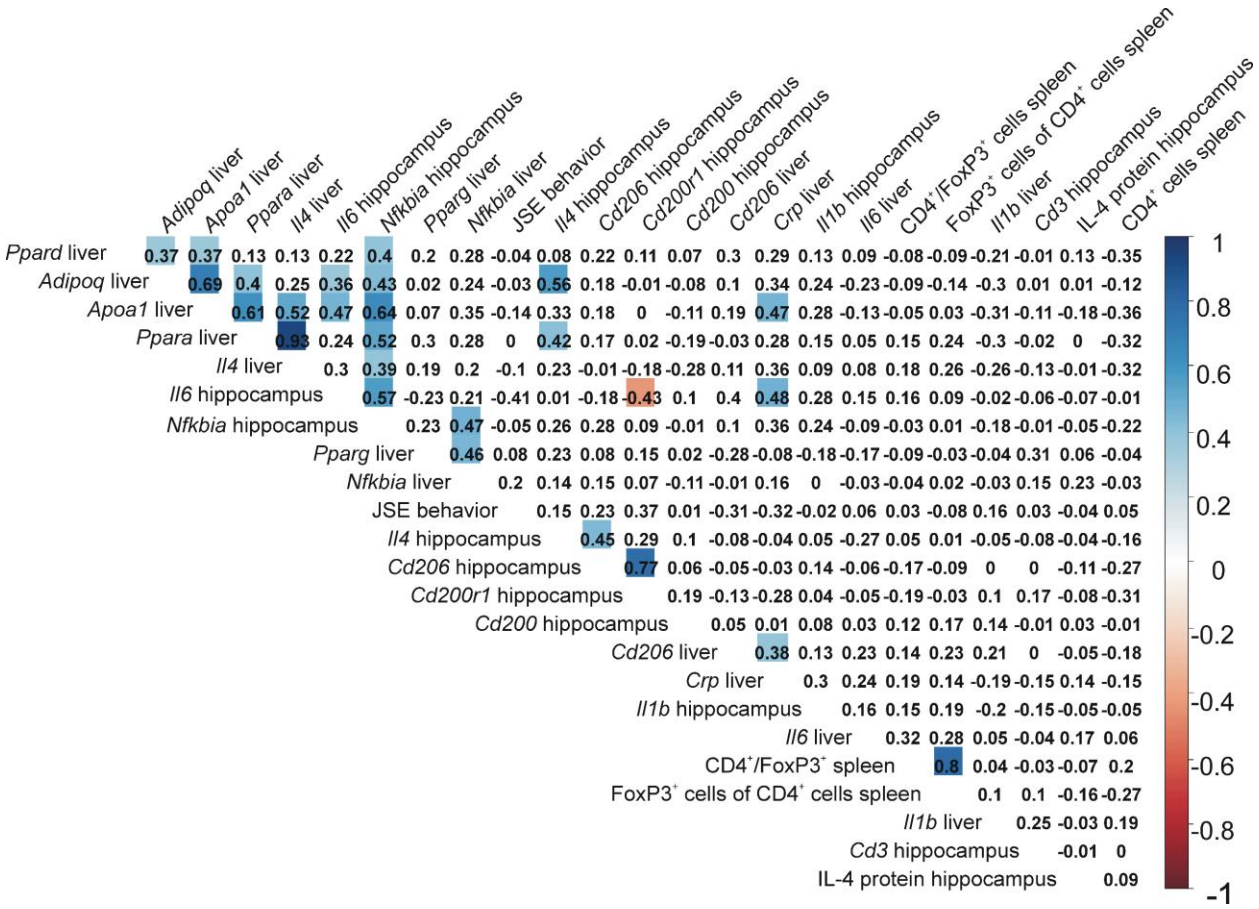

Figure 2.7 Heat map of correlations among all major endpoints, ordered by hierarchical clustering of correlations, shows clustering between lipid and immune signaling genes. Values indicate Pearson's correlation *r*.

Colored squares represent false discovery rate-adjusted *p* values < 0.05. Heat legend is provided on the right, indicating blue colors as positive correlations and red colors as negative correlations, where the darkness of color represents the strength of the correlation. Sample sizes: *Ppard* in liver, *N* = 48; *Adipoq* in liver, *N* = 46; *Apoa1* in liver, *N* = 48; *Ppara* in liver, *N* = 46; *Il4* in liver, *N* = 45; *Il6* in dorsal hippocampus, *N* = 46; *Nfkbia* in dorsal hippocampus, *N* = 46; *Pparg* in liver, *N* = 47; *Nfkbia* in liver, *N* = 47; JSE behavior, *N* = 43; *Il4* in dorsal hippocampus, *N* = 46; *Cd206* in dorsal hippocampus, *N* = 44; *Cd200r1* in dorsal hippocampus, *N* = 45; *Cd200* in dorsal hippocampus, *N* = 45; *Cd206* in liver, *N* = 48; *Crp* in liver, *N* = 47; *Il1b* in dorsal hippocampus, *N* = 43; *Il6* in liver, *N* = 45; $CD4^+/FoxP3^+$ cells as percent of total cells in spleen, *N* = 47; $FoxP3^+$ cells as percent of $CD4^+$ cells in spleen, *N* = 48; *Il1b* in liver, *N* = 47; *Cd3* in dorsal hippocampus, *N* = 46; IL-4 protein in dorsal hippocampus, *N* = 40; $CD4^+$ cells as percent of total cells in spleen, *N* = 46. Abbreviations: *Adipoq*, adiponectin; *Apoa1*, apolipoprotein A-I; *Cd*, cluster of differentiation; FoxP3, forkhead box P3; *Il*, interleukin; JSE, juvenile social exploration; *Nfkbia*, NF-κB inhibitor α; *Ppara*, peroxisome proliferator-activated receptor α; *Ppard*, peroxisome proliferator-activated receptor δ; *Pparg*, peroxisome proliferator-activated receptor γ.

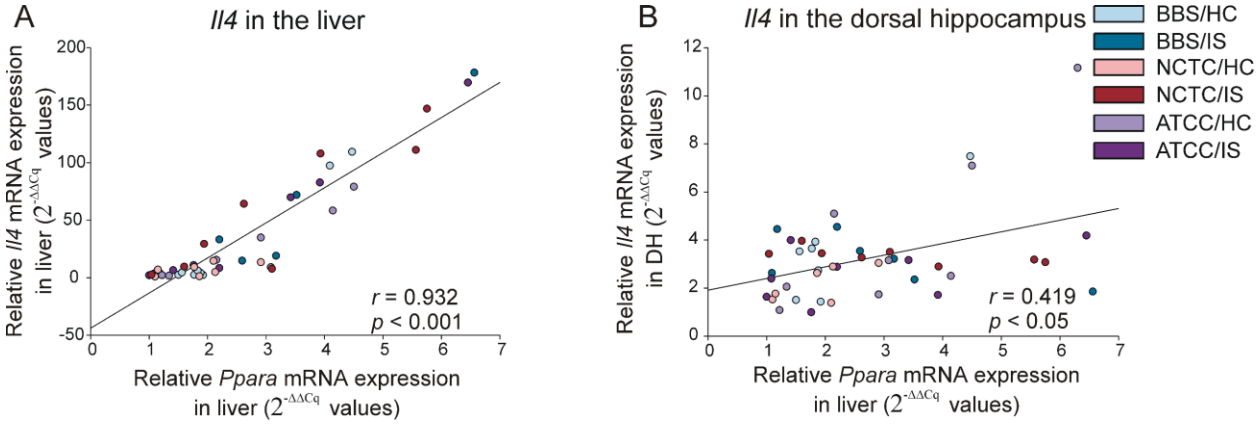

Figure 2.8 *Ppara* mRNA expression in the liver positively correlates with *Il4* mRNA expression in the liver and dorsal hippocampus.

Data represent correlations between *Ppara* mRNA expression in the right median lobe of the liver and (A) *Il4* mRNA expression in the right median lobe of the liver, and (B) *Il4* mRNA expression in the dorsal hippocampus. Sample sizes: *Ppara* mRNA expression in the liver (BBS/HC, *n* = 8; BBS/IS, *n* = 7; NCTC/HC, *n* = 7; NCTC/IS, *n* = 8; ATCC/HC, *n* = 8; ATCC/IS, *n* = 8); *Il4* mRNA expression in the liver (BBS/HC, *n* = 8; BBS/IS, *n* = 7; NCTC/HC, *n* = 7; NCTC/IS, *n* = 8; ATCC/HC, *n* = 7; ATCC/IS, *n* = 8); *Il4* mRNA expression in the dorsal hippocampus (BBS/HC, *n* = 7; BBS/IS, *n* = 8; ATCC/HC, *n* = 8; ATCC/IS, *n* = 8; NCTC/HC, *n* = 7; NCTC/IS, *n* = 8). *Ppara* and *Il4* mRNA expression in the liver and *Il4* mRNA expression in the dorsal hippocampus were measured using quantitative real-time polymerase chain reaction (RT-qPCR), with beta-actin as a reference, and data are presented as raw $2^{-\Delta\Delta Cq}$ values. Post hoc testing was conducted using Fisher's least significant difference (LSD) test. Pearson's correlation coefficient and *p*-values are given. Abbreviations: ATCC, *M. vaccae* ATCC 15483; BBS, borate-buffered saline; DH, dorsal hippocampus; HC, home cage control conditions; *Il*, interleukin; IS,

inescapable tail shock; NCTC, *M. vaccae* NCTC 11659; *Ppara*, peroxisome proliferator-activated receptor α.

Table 2.1. Correlations between lipid metabolism gene expression in the liver and immune isignaling gene expression in the liver and dorsal hippocampus.

Gene[1]	*Ppara* liver	*Apoa1* liver	*Adipoq* liver	*Il4* liver	*Il4* DH	*Nfkbia* DH
***Ppara* liver**	1	0.612***	0.401*	0.932***	0.419*	0.525**
***Apoa1* liver**	0.612***	1	0.695***	0.518**	0.328	0.639***
***Adipoq* liver**	0.401*	0.695***	1	0.247	0.564***	0.432*
***Il4* liver**	0.932***	0.518**	0.247	1	0.232	0.394*

[1]Abbreviations: *Apoa1*, apolipoprotein A-I; *Adipoq*, adiponectin; DH, dorsal hippocampus; *Il*, interleukin; *Nfkbia*, NF-κB inhibitor α; *Ppara*, peroxisome proliferator-activated receptor α.
*$p < 0.05$; **$p < 0.01$; ***$p < 0.001$; values indicate Pearson's correlation coefficient *r*.

2.5 Discussion

Immunization with either *M. vaccae* NCTC 11659 or *M. vaccae* ATCC 15483 prevented IS-induced increases in anxiety-like defensive behavioral responses as measured by the JSE paradigm, demonstrating that the stress-protective effects of heat-killed preparations of mycobacteria are not limited to a single strain. These effects were associated with altered metabolic-immune signaling that may mediate the stress-protective effects of heat-killed preparations of *M. vaccae* strains. In particular, both *M. vaccae* NCTC 11659 and *M. vaccae* ATCC 15483 prevented stress-induced biological signatures of inflammation in the dorsal hippocampus, including stress-induced increases in hippocampal *Il6* mRNA expression.

2.5.1 Both M. vaccae NCTC 11659 and M. vaccae ATCC 15483 promoted stress resilient behavior

Inescapable stress increased anxiety-like defensive behavioral responses as measured by the JSE paradigm (i.e., exposure to IS decreased juvenile social exploration assessed 24 h later). It is thought that the anxiogenic and exaggeration of fear-conditioning effects of IS are part of a larger set of behavioral effects called “learned helplessness” (Maier and Seligman, 1976), which may work through a fear-sensitizing circuit that includes serotonergic neurons within the dorsal raphe nucleus (Christianson et al., 2008; Maier and Watkins, 2005). Immunization with either *M. vaccae* NCTC 11659 or *M. vaccae* ATCC 15483 prevented stress-induced anxiety-like defensive behavioral responses as measured by the JSE paradigm. Previous work has already demonstrated the stress resilience behavioral effects of repeated immunization with *M. vaccae* NCTC 11659 in a variety of contexts (Amoroso et al., 2020; Fonken et al., 2018; Fox et al., 2017; Frank et al., 2018b; Hassell et al., 2019; Loupy et al., 2018; Reber et al., 2016b), including JSE (Frank et al., 2018b). This is the first study to show that the *M. vaccae* type strain, *M. vaccae* ATCC 15483, also confers anxiolytic, behavioral resilience effects in rats. Our molecular evidence suggests that the two strains have overlapping, but distinct, spectra of effects on markers of immune and lipid signaling in the brain and periphery.

2.5.2 Both M. vaccae NCTC 11659 and M. vaccae ATCC 15483 prevented stress-induced biological signatures of inflammation in the dorsal hippocampus

Immunization with either *M. vaccae* NCTC 11659 or *M. vaccae* ATCC 15483 prevented stress-induced increases in biological signatures of inflammation, including *Il6* mRNA expression, in the dorsal hippocampus. These findings are consistent with previous studies in mice in which immunization with *M. vaccae* NCTC 11659 prevented psychosocial stress-induced increases in IL-6 secretion from freshly isolated mesenteric lymph node cells stimulated with anti-CD3 antibody ex vivo (Reber et al., 2016b). Interestingly, in both the study by Reber and colleagues

in mice, and in our study, immunization with *M. vaccae* NCTC 11659, in the absence of stress exposure, increased IL-6 or *Il6* mRNA expression, respectively. This may reflect a general immune activation by *M. vaccae* NCTC 11659. Increased *Il6* mRNA expression could be a biological marker of immune activation characteristic of mycobacterial species. *Mycobacterium tuberculosis* and several of its isolated proteins, for example, signal through toll-like receptors (TLRs), which can stimulate the maturation of dendritic cells (DCs) and the release of IL-6 (Basu et al., 2012; Jang et al., 2004). *M. vaccae* NCTC 11659 can signal through TLR2 in DCs in vitro (Le Bert et al., 2011). Interestingly, the *M. tuberculosis*-induced TLR2-mediated release of IL-6 in DCs is mediated by NF-κB (Basu et al., 2012; Jang et al., 2004). Recent studies have shown that immunization of mice with an *M. vaccae* vaccine 3, 17, and 31 days following infection with *M. tuberculosis* H37Rv strain, results in upregulation of TLR2 signaling in peripheral blood mononuclear cells (PBMCs) in association with upregulation of genes encoding inflammatory cytokines, including IL-6, and Nfκbia, via an MyD88-dependent TLR signaling pathway, assessed eight weeks after the final immunization with *M. vaccae* (Gong et al., 2020). In our study, *Il6* mRNA expression in the dorsal hippocampus was correlated with *Nfkbia* mRNA expression, a marker of NFκ-B activity, in the dorsal hippocampus. Nevertheless, in the study by Reber and colleagues (2016) in mice, and in our study in rats, immunization with *M. vaccae* NCTC 11659 prevented stress-induced increases in IL-6 protein or *Il6* mRNA expression, respectively. *M. vaccae* ATCC 15483 also prevented stress-induced increases in *Il6* mRNA expression in the dorsal hippocampus. However, it is also possible that the prevention of stress-induced increases in *Il6* mRNA expression observed among *M. vaccae* NCTC 11659- or *M. vaccae* ATCC 15483-treated animals was the result of a ceiling effect; in other words, *M. vaccae* NCTC 11659 increased expression of *Il6* mRNA among home cage control animals to

maximal levels, preventing any further IS-induced increases in *Il6* mRNA expression. Nevertheless, these findings are consistent with previous studies of *M. vaccae* NCTC 11659 in a chronic psychosocial stress model in mice, in which *M. vaccae* NCTC 11659 increased ex vivo stimulated release of IL-6 from mesenteric lymph node cells in single housed control mice, but prevented further stress-induced increases in IL-6 secretion (Reber et al., 2016b).

IL-6 is tightly linked to stress-related psychopathologies (for review, see Michopoulos et al., 2017). Mice that are more susceptible to stress-induced anxiety-like defensive behavioral responses, such as decreased social interaction, present with higher peripheral levels of IL-6 post-stressor exposure than mice that are more resilient to behavioral changes (Hodes et al., 2014). A potential causal role of IL-6 in individual vulnerability to stress-induced anxiety is supported by findings that transplanting hematopoietic progenitor cells from stress-susceptible mice releasing high IL-6 increases stress-induced anxiety, while transplanting these cells from IL-6 knockout (IL-$6^{-/-}$) mice, or treatment with an anti-IL-6 monoclonal antibody, decreases stress-induced anxiety (Hodes et al., 2014; for review, see Ménard et al., 2017). In line with these findings, rats exposed to inescapable shock and were susceptible to escape deficits, measured three days later, show elevated plasma IL-6 concentrations relative to both control and stress resilient rats (Yang et al., 2015). Consequently, the ability of *M. vaccae* NCTC 11659 to prevent stress-induced increases in peripheral IL-6 secretion (Reber et al., 2016b) and the ability of both *M. vaccae* NCTC 11659 and *M. vaccae* ATCC 15483 to prevent stress-induced increases in hippocampal *Il6* mRNA expression may be central to the ability of these strains to prevent stress-induced increases in anxiety-like defensive behavioral responses. The dependence of the stress-resilience effects of *M. vaccae* NCTC 11659 and *M. vaccae* ATCC 15483 on suppression of

stress-induced increases in peripheral and hippocampal IL-6 protein levels should be evaluated in future studies.

In addition to preventing stress-induced increases in *Il6* mRNA expression, encoding the proinflammatory cytokine IL-6, immunization with *M. vaccae* NCTC 11659, but not immunization with *M. vaccae* ATCC 15483, prevented a stress-induced decrease in the expression of the IL-4-responsive gene, *Cd200r1*, in the dorsal hippocampus. These data are in line with Frank et al. (2018a), showing that IS reduces *Cd200r1* mRNA in the hippocampus and that immunization with *M. vaccae* NCTC 11659 prevents this reduction, functionally buffering against the stress-induced disinhibition of microglia (Frank et al., 2018a, 2018b). In the current study, stress decreased the expression of *Cd200r1* mRNA in both BBS- and *M. vaccae* ATCC 15483-treated animals, whereas *Cd200r1* mRNA expression did not change among animals immunized with *M. vaccae* NCTC 11659. In addition to *Cd200r1*, stress also reduced *Cd206* mRNA expression among animals immunized with *M. vaccae* ATCC 15483. Of note, a stress-induced decrease in *Cd206* mRNA expression among BBS-treated animals approached statistical significance ($p = 0.093$). There was no stress-induced decrease in *Cd206* mRNA expression in *M. vaccae* NCTC 11659-treated rats. Interestingly, there was a strong correlation between *Cd200r1* and *Cd206* mRNA expression in the dorsal hippocampus ($r = 0.773$, $p < 0.001$; Figure 2.7). Collectively, these data are consistent with previous studies showing that immunization with *M. vaccae* NCTC 11659 prevents stress-induced reduction in hippocampal *Cd200r1* mRNA expression in freshly isolated and LPS-stimulated hippocampal microglia (Frank et al., 2018b). The finding that *M. vaccae* ATCC 15483 did not prevent stress-induced reductions of IL-4 responsive genes supports a hypothesis that the two strains may differentially affect stress-

induced neuroimmunological responses. Indeed, various strains of the *Mycobacterium tuberculosis* complex can induce different immunological responses in the host (for review, see Tientcheu et al., 2017), while different strains of nontuberculous mycobacteria also elicit different immunologic responses in a human monocytic cell line (Yuksel et al., 2011). This may be due to a diverse range of lipids and phospholipids found on the surface of the bacterial cell wall that interact with the host, although isolation and characterization of such membrane lipids has yet to be performed for either strain of *M. vaccae* (Collins et al., 2018; for review, see Sia and Rengarajan, 2019). However, these data might also suggest that the specific neuroimmunological changes uniquely associated with *M. vaccae* NCTC 11659 in the dorsal hippocampus are not necessary to produce the behavioral effects induced by both strains of *M. vaccae*. Additional experiments are needed to examine immunoregulatory signaling in alternative brain regions that may be associated with the regulation of anxiety-related defensive behavioral responses, such as the prefrontal cortex, ventral hippocampus, amygdala, and dorsal raphe nucleus (Qi et al., 2018; Wood et al., 2015).

2.5.3 Effects of M. vaccae NCTC 11659 and M. vaccae ATCC 15483 on splenic CD4+FoxP3+ Treg following inescapable stress

Stress susceptibility is associated with reduced numbers of splenic $CD4^{+}FoxP3^{+}$ Treg in mice (Ambrée et al., 2019). In contrast to our expectations, exposure to IS had no effect on the abundance of splenic $CD4^{+}FoxP3^{+}$ Treg, and neither *M. vaccae* NCTC 11659 nor *M. vaccae* ATCC 15483 increased splenic $CD4^{+}FoxP3^{+}$ Treg abundance. There is evidence that *M. vaccae* NCTC 11659 increases Tregs characterized by $CD4^{+}CD45RB^{Lo}$ in mice (Zuany-Amorim et al., 2002), and further, depleting $CD25^{+}$ cells inhibits anxiolytic behaviors induced by *M. vaccae* NCTC 11659 (Reber et al., 2016b). However, to date there have been no studies to confirm that

M. vaccae NCTC 11659 increases traditional FoxP3$^+$ Treg in young adult rats. In fact, although *M. vaccae* NCTC 11659 increases *Foxp3* mRNA expression in hippocampus of aged rats, there is no effect of *M. vaccae* NCTC 11659 on *Foxp3* mRNA expression in adult (non-aged) rats, eight days after the last injection and after laparotomy surgery stress or sham surgery (Fonken et al., 2018). It could be that *M. vaccae* NCTC 11659 and *M. vaccae* ATCC 15483 activate alternative Tregs that do not express FoxP3. Indeed, a number of cell types with regulatory properties, besides the CD4$^+$CD25$^+$Foxp3$^+$ Treg subset, have been described (Adams et al., 2004; Chen et al., 1994; Groux et al., 1997; Huang et al., 2004; Iwasaki and Kelsall, 1999; McMenamin et al., 1991; Perdomo et al., 2016; Polanski et al., 1997; Vicente et al., 2016; Zuany-Amorim et al., 2002). Alternatively, our CD4$^+$FoxP3$^+$ markers may be too broad to capture any changes in specific subtypes of cells; for example, CD4$^+$FoxP3$^+$ cell populations may include both CD25$^+$ and CD25$^-$ cell types (Nishioka et al., 2006). Prior studies with *M. vaccae* NCTC 11659 and some probiotic strains suggest that CD25$^+$ cells are at least partially required for stress resilience (Liu et al., 2020; Reber et al., 2016b). It is also important to point out that this study only targets one time point for the Treg cell analysis and that this time point occurs eight days after the final injection and after behavioral analysis; it could be that measuring Treg abundance at earlier or later time points would reveal differences between vehicle and *M. vaccae*-treated animals. Future studies are required to determine the role of CD4$^+$CD25$^+$Foxp3$^+$ and alternative Treg cells in the stress-resilience effects of *M. vaccae* treatment.

2.5.4 M. vaccae NCTC 11659 and M. vaccae ATCC 15483 altered hepatic biological signatures of lipid-immune signaling

Here, immunization with either *M. vaccae* NCTC 11659 or *M. vaccae* ATCC 15483 reduced *Pparg* mRNA expression in the liver among home cage control animals. In line with these

findings, probiotics containing *Lactobacillus* species (H. Li et al., 2020; Zhao et al., 2019) and bifidobacteria-fermented herbs (Choi et al., 2020) decrease hepatic and adipose *Pparg* mRNA expression in mice fed high fat diets. It is important to note that protein expression may be different from mRNA expression; likewise, we should recognize that our time point of tissue collection represents a long-term effect of *M. vaccae* NCTC 11659 and *M. vaccae* ATCC 15483 on gene expression of *Pparg*.

IS strongly decreased *Pparg* mRNA expression, while *M. vaccae* NCTC 11659, but not *M. vaccae* ATCC 15483, prevented a stress-induced decrease in *Pparg* mRNA expression. Previous studies have shown that PPARγ agonists can shift production from proinflammatory mediators to anti-inflammatory mediators, including increased CD206 expression, by nonparenchymal liver cells (Morán-Salvador et al., 2013), including Kupffer cells (Linares et al., 2018). Indeed, disruption of PPARγ expression selectively in macrophages increases inflammatory damage and fibrogenesis in a chronic constriction injury model in mice. Disruption of PPARγ selectively in liver Kupffer cells exaggerates proinflammatory responses to lipopolysaccharide, including increases in IL-1β, effects that can be attenuated using PPARγ agonists (Morán-Salvador et al., 2013). IS increases circulating LPS, suggestive of "leaky gut" and increased systemic commensal bacteria or their byproducts (Maslanik et al., 2012). Thus, the IS-induced increases in LPS, in association with IS-induced decreases in *Pparg* mRNA expression in liver, would be expected to exaggerate proinflammatory responses by Kuppfer cells in the liver. It will be important to confirm that IS-induced decreases in *Pparg* mRNA expression as shown here are associated with decreases in liver PPARγ protein expression.

PPARγ may also play an important role in stress-related behavioral responses. In one study, mice that were susceptible to stress-induced anxiety-like behaviors as measured by a social interaction test (i.e., those with low social interaction scores after chronic social defeat stress) showed a reduction of *Pparg* mRNA expression in adipose tissue, whereas resilient mice (i.e., those with high social interaction scores after chronic social defeat stress) did not present with a reduction of *Pparg* in adipose tissue (Guo et al., 2017). Recently, agonists of PPARs such as PPARγ have gained attention for their potential therapeutic benefit in the treatment of psychiatric disorders including posttraumatic stress disorder (PTSD) (Bersani et al., 2020; Rolland et al., 2013). In line with our results, probiotics may prevent gut epithelial barrier disruption, subsequent hepatic inflammation, and a reduction of PPARγ protein expression in the liver in rodent models of sepsis (Ewaschuk et al., 2007; Y. Wang et al., 2016). Our data support the idea that both *M. vaccae* type strains alter PPARγ signaling in the liver, and, like IL-4-responsive genes, only *M. vaccae* NCTC 11659 buffered against stress-induced decreases in *Pparg* mRNA expression. Furthermore, these data suggest that immunization with *M. vaccae* NCTC 11659 may prevent stress-induced decreases in *Pparg* mRNA expression, thus preventing stress-induced exaggeration of proinflammatory responses by liver Kupffer cells following “leaky gut” (Ewaschuk et al., 2007; Linares et al., 2018; Maslanik et al., 2012; Morán-Salvador et al., 2013).

Unlike *Pparg*, there were no effects of treatment or IS on *Ppara* mRNA expression in the liver; however, *Ppara* expression was correlated with expression of several genes associated with lipid metabolism and immunoregulatory responses, and this correlation was particularly evident for *Il4* mRNA expression in the liver and dorsal hippocampus. PPARα is thought to play a role in host anti-mycobacterial immune defenses, simultaneously suppressing aberrant inflammation

and reducing lipid droplet formation during mycobacterial infection in macrophages derived from mice (Kim et al., 2017). In this study, *Ppara* mRNA expression correlated with *Apoa1* (encoding apolipoprotein A-I), *Adipoq* (encoding adiponectin), and *Il4* mRNA expression in the liver and *Il4* mRNA expression in the dorsal hippocampus. The strength of the correlation between *Ppara* mRNA and *Il4* mRNA in the liver implies the likely interaction of *Ppara* and *Il4* mRNA expression in our study, under the influence of factors that were not controlled for in the experimental design, and also suggests that there may be a biological reason for the variability in *Il4* mRNA expression that is not controlled for in the experimental design. Indeed, PPARα activation can promote IL-4 secretion in splenocytes, including T cells (Cunard et al., 2002; Dasgupta et al., 2007; Gocke et al., 2009; Lovett-Racke et al., 2004).

Nfkbia mRNA expression in the dorsal hippocampus was correlated with *Ppara*, *Apoa1*, *Adipoq*, and *Il4* mRNA in the liver. Analysis of these five genes using the Database for Annotation, Visualization, and Integrated Discovery (DAVID) revealed two KEGG pathways to be significantly enriched in the gene list, based on the Benjamini-adjusted *p*-value (Dennis et al., 2003); these pathways were "PPAR signaling pathway," which included *Ppara*, *Apoa1*, and *Adipoq* and "adipocytokine signaling pathway" which included *Ppara*, *Adipoq*, and *Nfkbia* (Supplementary Table 2.3). It is likely that external environmental factors that were not controlled for by our experimental design contributed to the individual variability among these genes, accounting for the correlations observed between markers of lipid and immune signaling, including between the periphery and the CNS, in the absence of any effects of treatment or IS on *Ppara* mRNA expression. Nonetheless, these data provide an interesting pattern showing a relationship between expression of lipid-immune signaling genes in the liver that should be

further explored, in particular because *M. vaccae* NCTC 11659, and presumably *M. vaccae* ATCC 15483, contains a lipid that binds host PPARα receptors (Smith et al., 2019). Tissue-specific changes of mRNA expression and protein associated with lipid-immune pathways should be investigated in future experiments.

2.5.5 Potential roles of immune stimulation in the prevention of stress-induced exaggerated inflammatory responses and stress-resilient behaviors following immunization with either M. vaccae NCTC 11659 or M. vaccae ATCC 15483

In the current study, we show that immunization with either strain of *M. vaccae* promotes behavioral and physiological stress-resilience. However, we also provide evidence that treatment with *M. vaccae* NCTC 11659 or *M. vaccae* ATCC 15483 may promote immunogenic responses among home cage control animals, either by decreasing anti-inflammatory signaling pathways (i.e, *Pparg*) in the liver, or by increasing expression of proinflammatory cytokines (i.e. *Il6* mRNA expression) in the brain. Although we primarily focus on the immunoregulatory benefits of "old friends", mycobacteria interact with dendritic cells through a T helper 1 (Th1)-mediated pathway (Covián et al., 2019; Le Bert et al., 2011; Maeda et al., 2003). For example, immunization with the anti-tuberculosis Bacille Calmette-Guérin (BCG) vaccine stimulates secretion of Th1 cytokines such as interferon γ (IFNγ) (Abebe, 2012; Freyne et al., 2020; Shibata, 2005). In contrast, BCG also stimulates immunometabolic pathways that promote glycolysis in T cells (Russell et al., 2019) and monocytes (Arts et al., 2016) and induces Treg differentiation for protection against autoimmune diseases like multiple sclerosis and type 1 diabetes (Covián et al., 2019; Ristori et al., 2018). Similarly, both live and heat-killed preparations of *M. vaccae*, although showing anti-inflammatory and immunoregulatory properties, also increase IFNγ and Th1 signaling in mice (Gong et al., 2020; Lahey et al., 2016;

Smith et al., 2019, 2020; Zhang et al., 2016). This is one of the many reasons *M. vaccae* NCTC 11659 is being developed as an anti-TB immunotherapy alongside first-line anti-TB drug therapy (Bourinbaiar et al., 2020). Interestingly, IFNγ expression is required for social behavior, which we measured here using the JSE paradigm, possibly arising from meningeal T cells and acting on both microglia and neurons in the brain (Filiano et al., 2016). Such immune "training" (Kleen et al., 2020), i.e., stimulation and subsequent immunoregulation, may be the reason why prior exposure to "old friends" is important for stabilizing the immune response to stress (Böbel et al., 2018; Rook, 2013; Rook et al., 2013a, 2013b).

2.5.6 Limitations

While assessing these results, a few limitations should be addressed. First, it is important to recognize that our molecular data were collected at a single time point, immediately after behavioral testing. This design only allowed us to examine one snapshot along the complex (and unknown) time courses for immune and metabolic signaling, and we cannot establish causal relationships between molecular data and behavior. It is also important to recognize that mRNA expression is not a perfect predictor of protein expression; thus, further research measuring protein abundance is warranted. It is also important to consider that adult male rats were used for this study and that results may likely be different in experiments conducted in female or in adolescent or aged rats.

2.5.7 Clinical implications

The findings reported here may be relevant to anxiety disorders, affective disorder, or trauma and stressor-related disorders such as PTSD. PTSD is a trauma- and stressor-related disorder

characterized by the Diagnostic and Statistical Manual of Mental Disorders, 5th edition (DSM-5) as exhibiting symptoms across four major criteria following exposure to a traumatic event: intrusions, avoidance, negative alterations in mood and cognition, and alterations in arousal or reactivity (American Psychiatric Association, 2013) (see Supplementary Table 2.4). The prevalence of PTSD, especially among war Veterans, is very high (up to 18%) (Ginzburg et al., 2010; Hoge et al., 2014; Knowles et al., 2019), and rates of PTSD co-occurring with anxiety and depressive disorders is often more common (up to 30% in Veterans) than PTSD alone (Ginzburg et al., 2010; Knowles et al., 2019). Recent evidence points toward immune and metabolic dysregulations as potential risk factors for the development of PTSD (Bersani et al., 2020; Eraly et al., 2014; Kim et al., 2020; Mellon et al., 2018; Schultebraucks et al., 2020). The use of whole cell heat-killed preparations of bacteria or probiotics to treat PTSD and comorbid disorders in Veterans is promising and in its early stages of clinical trials (Brenner et al., 2017; Hoisington et al., 2018b). Preclinical studies using subcutaneous injections of *M. vaccae* NCTC 11659 in rodent models have been shown to attenuate behaviors associated with three of the four symptomatic criteria of PTSD (avoidance, negative alterations in mood and cognition, and alterations in arousal or reactivity) as designated by the DSM-5 (Amoroso et al., 2020; Bowers et al., 2017, 2019, 2018; Fonken et al., 2018; Fox et al., 2017; Frank et al., 2018b; Hassell et al., 2019; Lambert et al., 2017; Reber et al., 2016b) (Table S4). Our present study provides evidence that the type strain, *M. vaccae* ATCC 15483, also mitigates anxiety-like defensive behavioral responses in rodents that may be relevant to anxiety disorders, affective disorder, or trauma- and stressor-related disorders such as PTSD. Further, our study reveals novel molecular effects (involving immune and metabolic signaling) of *M. vaccae* NCTC 11659 and *M. vaccae* ATCC 15483 in vivo that are associated with stress-resilience behaviors. Results from this experiment

are encouraging, as they demonstrate the promise of *M. vaccae* NCTC 11659, *M. vaccae* ATCC 15483, or related interventions for the prevention and treatment of stress-related disorders.

2.5.8 Conclusions and future directions

In this study we have confirmed that both *M. vaccae* NCTC 11659 and *M. vaccae* ATCC 15483 prevent stress-induced anxiety-like defensive behavioral responses. These behavioral effects were associated with alterations in lipid and immune signaling. Previous studies using *Lactobacillus* spp. and *Bifidobacterium* spp. have found that probiotics with "psychobiotic" properties, i.e., the ability to impact brain and behavior, and to increase stress resilience, are highly species- and strain-specific (Sarkar et al., 2016; Savignac et al., 2015, 2014; Stenman et al., 2020); thus, the finding that both *M. vaccae* NCTC 11659 and *M. vaccae* ATCC 15483 show stress resilience effects in this study should not be extrapolated to all species and strains of environmental mycobacteria, or to all physiological or behavioral outcomes relevant to stress resilience. These questions will need to be addressed empirically in future studies. Nevertheless, the ability to reproduce the behavioral outcomes of *M. vaccae* NCTC 11659 treatment using *M. vaccae* ATCC 15483 implies that stress-resilience effects of environmental mycobacteria may not be unique to one mycobacterial strain. To understand the physiological impact of immunization with *M. vaccae*, future mechanistic experiments are required. Future studies should further investigate the effects of *M. vaccae* NCTC 11659 and *M. vaccae* ATCC 15483 on proteomic and metabolomic signaling in the host in the context of stress. Studies designed to compare the behavioral and molecular effects across mycobacterial strains may be useful for development of novel approaches to the prevention and treatment of a variety of inflammatory

disorders, as well as psychiatric and neurological disorders where inflammation is a risk factor for the development of the disorder or persistence of symptoms.

2.6 Acknowledgements, author contributions, and conflicts of interest

Acknowledgements

These studies were funded by the National Institute of Mental Health (NIMH) award (R21MH116263A) to C.A.L., S.F.M., M.G.F. (PIs), and L.K.F. (Co-I), a Biological Sciences Initiative (BSI) Scholars Award at the University of Colorado Boulder to B.M.M. (2019 – 2020), and a Dell Scholarship to T.W.Y. (2019 – 2020). We gratefully acknowledge Lauren M. Oko and the Anschutz Flow Cytometry Core at the University of Colorado Anschutz Medical Campus for assistance with experimental design and analysis of flow cytometry results. We acknowledge Catherine M. Nicholls for her assistance with tissue collection, flow cytometry, and RT-qPCR.

Author contributions

Study design was conceived by K.M.L., L.K.F., M.G.F., C.A.Z., S.F.M., and C.A.L. *M. vaccae* NCTC 11659 and *M. vaccae* ATCC 15483 injections were performed by B.M.M., A.I.E., and C.A.Z. JSE and IS were performed by H.M.D. Tissue collection was conducted by K.M.L., K.E.C., B.M.M., T.W.Y., M.G.F., and C.A.Z. Flow cytometry was performed by K.M.L., K.E.C., B.M.M., T.W.Y., and C.A.Z. Real time qRT-PCR was performed by K.M.L., K.E.C., B.M.M., T.W.Y., H.M.D., M.R.A., and C.A.Z. ELISA was carried out by M.G.F. Data analysis and statistical analysis were carried out by K.M.L. Figures and figure legends were produced by K.M.L., K.E.C., B.M.M., and T.W.Y. Manuscript preparation was conducted by K.M.L., K.E.C.,

B.M.M., and T.W.Y. Editing and review was contributed by K.M.L., K.E.C., B.M.M., T.W.Y., H.M.D., M.R.A., T.W.Y., A.I.E., L.K.F., M.G.F., C.A.Z., S.F.M., and C.A.L.

Conflicts of interest

C.A.L. serves on the Scientific Advisory Board of Immodulon Therapeutics, Ltd., is Cofounder and Chief Scientific Officer of Mycobacteria Therapeutics Corporation, and serves as an unpaid scientific consultant to Aurum Switzerland A.G. and is a member of the faculty of the Integrative Psychiatry Institute, Boulder, Colorado, USA.

Chapter 3. Comparing the effects of two different strains of mycobacteria, *Mycobacterium vaccae* NCTC 11659 and *M. vaccae* ATCC 15483, on stress-induced changes in the proteome of adult male rats: I. plasma.

Citation

Loupy, K.M., Ebmeier, C.C., Lee, T., D'Angelo, H.M., Elsayed, A.I., Cler, K.E., Marquart, B.M., Fonken, L.K., Frank, M.G., Arnold, M.R., Zambrano, C.A., Maier, S.F., Lowry, C.A. Comparing the effects of two different strains of mycobacteria, *Mycobacterium vaccae* NCTC 11659 and *M. vaccae* ATCC 15483, on stress-induced changes in the proteome of adult male rats: I. plasma. Manuscript in preparation.

Authors' names

Kelsey M. Loupy[a], Christopher C. Ebmeier[b], Thomas Lee[b], Heather M. D'Angelo[c], Ahmed I. Elsayed[a], Kristin E. Cler[a], Brandon M. Marquart[a], Laura K. Fonken[d], Matthew G. Frank[c,e], Mathew R. Arnold[a,e], Cristian A. Zambrano[a], Steven F. Maier[c,e], Christopher A. Lowry[a,e,f,g,h,i,j]∗

Authors' affiliations

[a]Department of Integrative Physiology, University of Colorado Boulder, Boulder, CO 80309, USA

[b]Center for Neuroscience and Center for Microbial Exploration, University of Colorado Boulder, Boulder, CO 80309, USA

[c]Department of Physical Medicine and Rehabilitation and Center for Neuroscience, University of Colorado, Anschutz Medical Campus, Aurora, CO 80045, USA

[d]Veterans Health Administration, Rocky Mountain Mental Illness Research Education and Clinical Center, Denver, CO 80045, USA

[e]Military and Veteran Microbiome Consortium for Research and Education (MVM-CoRE), Denver, CO 80045, USA

[f]Senior Fellow, inVIVO Planetary Health, of the Worldwide Universities Network (WUN), West New York, NJ 07093, USA

3.1 Abstract

Anxiety disorders, affective disorders, and trauma- and stressor-related disorders such as posttraumatic stress disorder (PTSD) are common across the worldwide population and are especially prevalent among war Veterans. Currently, there are few effective treatments for PTSD. Microbial-based treatments targeting the microbiome-gut-brain axis have gained attention in recent years for their potential modulation of physiology and behavior, including their potential for modulation of stress resilience versus vulnerability. We have previously demonstrated the stress resilient physiological and behavioral effects of immunization with the soil-derived bacterium, *Mycobacterium vaccae* NCTC 11659, and the related strain, *M. vaccae* ATCC 15483 in adult male rats exposed to inescapable tail shock stress (IS). Immunization with either *M. vaccae* strain prevent IS-induced increases in neuroinflammation and anxiety-like defensive behavioral responses in the juvenile social exploration paradigm. Here, we use an

untargeted proteomics approach to characterize the plasma proteome of the rats used in the original study [Loupy et al., 2021, *Brain, Behavior, and Immunity*, 91: 212–229], assessed 24 hours after IS. We describe changes to the relative abundances of 57 circulating proteins after IS, including those associated with cardiovascular function, immune signaling (including the "complement and coagulation cascades" pathway, and a biological signature of inflammatory monocytes), phospholipid metabolism, and energetic homeostasis. We show that immunization with either *M. vaccae* strain modulates the effect of IS on the plasma proteome. Specifically, data show that immunization with *M. vaccae* strains attenuates IS-induced activation of complement and coagulation cascades (possibly by preventing IS-induced changes in intestinal epithelial barriers and gut-vascular barriers), attenuation of IS-induced increases in acute-phase response proteins, and IS-induced increases in a biological signature of inflammatory monocytes. Using functional enrichment analyses, we outline physiological processes that are associated with the vulnerability or resilience to developing stress-induced exaggeration of anxiety-like behavior. This study reveals complex biological signatures of trauma and stress vulnerability versus resilience, and results from this study may aid researchers in the development of novel targets for the prevention and treatment of stress-related disorders including PTSD.

3.2 Introduction

Stress-related psychiatric disorders, including anxiety disorders, affective disorders, and trauma- and stressor-related disorders are highly prevalent. For example, the weighted prevalence of developing PTSD after exposure to a trauma is 4% worldwide, although risk for developing PTSD is dependent on trauma type (Kessler et al., 2017; Liu et al., 2017). It is estimated that

20% of war Veterans are diagnosed with PTSD, often comorbid with other mood and anxiety disorders (Hoge et al., 2014).

Trauma is associated in a transdiagnostic manner with chronic increases in inflammation (Tursich et al., 2014). For example, PTSD diagnosis is associated with increased inflammatory signaling and the development of concurrent inflammatory disorders like autoimmune disorders (O'Donovan et al., 2015), cardiovascular disease (O'Donovan et al., 2012), and metabolic syndromes (Heppner et al., 2009). Higher plasma levels of C-reactive protein (CRP) in soldiers prior to deployment are associated with increased risk of developing PTSD after combat exposure (Eraly et al., 2014). In addition to CRP, metabolites like citrate, glutamine, and eicosanoids (e.g., prostaglandins and leukotrienes) are biomarkers that may be predictive of PTSD in combat soldiers prior to deployment (Schultebraucks et al., 2020); other biomarkers that are associated with PTSD diagnosis in war Veterans include heart rate, albumin, insulin, low-density lipoprotein, lactate/citrate ratio, and global arginine bioavailability ratio (defined as arginine/[ornithine + citrulline]) (Dean et al., 2020; Schultebraucks et al., 2020). Many of the circulating metabolites might be attributed, in part, to circulating blood monocytes, which are a predictive marker of PTSD development (Schultebraucks et al., 2020). Increases in numbers of circulating monocytes are thought to reflect chronic inflammation, and have been identified, among the white blood cell subtype counts, to be an independent predictor of cardiovascular disease risk (Kim et al., 2019). Meanwhile, monocyte:lymphocyte ratios have also been shown to be predictive of a chronic inflammatory state (Cherfane et al., 2015), and the inflammatory state of monocytes has been linked to depression severity, childhood adversity, suicide risk, and PTSD

(Keaton et al., 2019; Kuan et al., 2019; Lynall et al., 2020; Miller and Raison, 2016; Neylan et al., 2011; Nowak et al., 2019; Schiweck et al., 2020; Serafini et al., 2020).

Dysregulated neuroimmune signaling is commonly observed in individuals with PTSD, including increased sympathetic nervous system (SNS) activation (Cohen et al., 2000; Dennis et al., 2016; Park et al., 2017), decreased parasympathetic nervous system (PNS) activation (Hopper et al., 2006; Jenness et al., 2018; Ulmer et al., 2018), and altered glucocorticoid secretion or receptor sensitivity (Pan et al., 2018; Yehuda et al., 2014). Altered glucocorticoid sensitivity (Breen et al., 2019; de Kloet et al., 2007; van Zuiden et al., 2012; Yehuda et al., 1995) and enhanced proinflammatory phenotypes (Gola et al., 2013; Kuan et al., 2019; Neylan et al., 2011) of peripheral blood mononuclear cells (PBMCs) are associated with a diagnosis of PTSD. Increased SNS activity, decreased PNS activity, decreased cortisol secretion, and increased sensitivity of glucocorticoids in peripheral immune cells may be important features of, or risk factors for, inflammation associated with PTSD (Brudey et al., 2015; Michopoulos et al., 2017; Olff and van Zuiden, 2017); stress-induced hyperactivation of neuroimmune pathways stimulates the release and trafficking of proinflammatory bone marrow-derived monocytes from the periphery to the central nervous system via the blood circulation (Niraula et al., 2018; Wohleb et al., 2014, 2013, 2011).

Individual differences in stress-related inflammatory responses associated with PTSD might be influenced by microbial exposures and microbiome composition, acting through the microbiome-gut-brain axis (for review, see Cryan et al., 2020; Leclercq et al., 2016; Long-Smith et al., 2020; Loupy and Lowry, 2020; Lowry et al., 2016; Malan-Muller et al., 2018). The “old friends”

hypothesis suggests that microbial interactions with the immune system (for example, in the gut) help stabilize the immune system's reaction to aversive proinflammatory events, such as trauma (for review, see Langgartner et al., 2019; Lowry et al., 2016; Rook, 2013; Rook et al., 2014, 2013a, 2013b, 2004; Rook and Brunet, 2005; Rook and Lowry, 2008). Currently, microbial-based therapeutics (i.e., prebiotics, probiotics, parabiotics, postbiotics) are being researched and developed for possible treatment of stress-related psychiatric disorders (Brenner et al., 2020, 2017; Hoisington et al., 2018b; Long-Smith et al., 2020; Lowry et al., 2016).

For the last fifteen years, immunization with a heat-killed preparation of the soil-derived bacterium *Mycobacterium vaccae* NCTC 11659 has been studied in rodent models as a microbe-based approach to enhance stress resilience. Adult male rats preimmunized with *M. vaccae* NCTC 11659 are more resilient to developing anxiety-like defensive behaviors after exposure to inescapable tail shock stress (IS) (Frank et al., 2018b; Loupy et al., 2021), a model of traumatic stress and "learned helplessness" (Maier and Seligman, 1976; Seligman and Maier, 1967; van der Kolk et al., 1985). Immunization with *M. vaccae* NCTC 11659, either before or after fear conditioning, promotes fear extinction in the fear-potentiated startle (FPS) paradigm among adult male rats (Fox et al., 2017; Hassell et al., 2019). Among aged rats, immunization with *M. vaccae* NCTC 11659 attenuates neuroinflammation and prevents cognitive impairment in a model of post-operative cognitive dysfunction (Fonken et al., 2018). Immunization with *M. vaccae* NCTC 11659 also promotes proactive coping behaviors in the chronic subordinate colony (CSC) housing paradigm (Amoroso et al., 2020; Reber et al., 2016b) and an acute social defeat paradigm paired with sleep disruption stress (Bowers et al., 2020; Foxx et al., 2021) in mice. The effects of *M. vaccae* NCTC 11659 are associated with anti-inflammatory and immunoregulatory

effects in the periphery and in the brain (Bowers et al., 2020; Fonken et al., 2018; Frank et al., 2018b; Loupy et al., 2021; Reber et al., 2016b; Smith et al., 2020) and may prevent dysregulation of immune and endocrine signaling associated with stress vulnerability (for review, see Olff and van Zuiden, 2017). For example, immunization with *M. vaccae* NCTC 11659 prior to stress exposure reduces *Crh* (encoding corticotropin-releasing hormone) mRNA expression in the extended amygdala following fear extinction in the FPS paradigm, which aligns with increased fear extinction behavior (Loupy et al., 2018). It is also possible that immunization with *M. vaccae* NCTC 11659 alters the composition of the gut microbiome (Foxx et al., 2021) or strengthens the integrity of the gut endothelial or epithelial barriers (Amoroso et al., 2019; Reber et al., 2016b) as mechanisms that contribute to stress resilience. *M. vaccae* NCTC 11659 immunizations may not only exert prophylactic stress-resilience effects; treatment with *M. vaccae* NCTC 11659 during CSC (Amoroso et al., 2020) or after FPS conditioning (Hassell et al., 2019) also supports stress resilient behaviors. Studies using probiotics that contain *Lactobacillus* spp. and *Bifidobacterium* spp. have reported that behavioral and physiological effects of these bacteria are strain-specific (Sarkar et al., 2016; Savignac et al., 2015, 2014; Stenman et al., 2020). It is currently unknown how many mycobacterial species possess "psychobiotic" properties that replicate those of *M. vaccae* NCTC 11659.

We recently demonstrated that immunization with a different mycobacterial strain, *M. vaccae* ATCC 15483, decreases anxiety-like defensive behavioral responses in the juvenile social exploration (JSE) paradigm 24 hours after exposure to IS (Loupy et al., 2021). Comparing the two *M. vaccae* strains, we found that immunization with either *M. vaccae* NCTC 11659 or *M. vaccae* ATCC 15483 prevents IS-induced increases of *Il6* (encoding the proinflammatory

cytokine interleukin [IL]-6) mRNA expression in the dorsal hippocampus; however, the two strains differed in their effects on IS-stimulated gene expression of other immune signaling markers in the hippocampus (*Cd206*) and liver (*Pparg, Crp, Nfkbia*), suggesting that behavioral resilience to stress may be more profoundly associated with the prevention of proinflammatory IL-6 signaling in the brain (Loupy et al., 2021). This finding is corroborated by previous reports that suggest that increased IL-6 secretion from blood leukocytes might indicate greater vulnerability to developing stress-related behaviors (Hodes et al., 2014; Niraula et al., 2019), and that increased cerebrospinal fluid levels of IL-6 correspond to PTSD symptom severity (Kim et al., 2020); collectively, these data support the hypothesis that stress-induced exaggeration of anxiety-like behaviors are mediated by induction of release of monocytes from bone marrow into the general circulation that then traffic to the brain (Niraula et al., 2019, 2018; Reader et al., 2015; Weber et al., 2017; Wohleb et al., 2015, 2014, 2013, 2011). It is possible that *M. vaccae* strains work in similar and overlapping ways to stimulate anti-inflammatory signaling and prevent the release or trafficking of proinflammatory monocytes (Loupy et al., 2021). In order to further investigate mechanisms through which *M. vaccae* strains promote stress resilience, we employed the use of untargeted proteomics followed by pathway enrichment and protein interaction analyses to integrate the complex physiological effects of immunization with either *M. vaccae* NCTC 11659, *M. vaccae* ATCC 15483, and IS in vivo.

In the current study, we analyzed the plasma proteome of the same rats from Loupy et al. (2021). The aim of our experiment was to: 1) identify plasma proteins that are altered by IS and thus may inform mechanisms underlying stress-induced anxiety-like behavioral responses; and 2) associate plasma proteins to the stress resilient behavioral and immunological effects of *M.*

vaccae strains. To the best of our knowledge, this is the first study to quantify the plasma proteome of IS-exposed animals relative to control animals; this study is also the first to quantify relative abundances of plasma proteins using mass spectrometry proteomics after a three-week protocol of *M. vaccae* NCTC 115649 or *M. vaccae* ATCC 15483 immunizations followed by IS or home cage control conditions (HC). By using an untargeted approach, our findings may help uncover novel biomarkers of traumatic stress that may contribute to stress-related behaviors; considering that the periphery and brain communicate via the transport of cells and molecules through blood circulation, our results might provide insight into the complex physiological changes to peripheral-brain axes, such as the microbiome-gut-brain axis (Cryan et al., 2020; Long-Smith et al., 2020; Loupy and Lowry, 2020; Lowry et al., 2016) or immune-brain axis (Wohleb et al., 2015), after IS. Likewise, by comparing the effects of the two *M. vaccae* strains on the plasma proteome after IS, our results may shed light on novel biological markers or physiological processes that may be targeted in future experiments to enhance stress resilience.

3.3 Materials and methods

3.3.1 Animals

For an experimental timeline, please see Figure 3.1 (adapted from Loupy et al. [2021]). The data reported in this study are derived from the same rats used in a previous report, which investigated the effects of immunization with *Mycobacterium vaccae* strains and stress exposure on behavioral outcomes and molecular signaling in the liver, spleen, and hippocampus (Loupy et al., 2021). In the current study, proteomic profiles in plasma of these rats are reported. Adult male Sprague Dawley® rats (Hsd:Sprague Dawley® SD®; Envigo, Indianapolis, IN, USA) weighing 250-265 g upon arrival were pair-housed in Allentown micro-isolator filter-topped

caging [259 mm (W) × 476 mm (L) × 209 mm (H); cage model #PC10198HT, cage top #MBT1019HT; Allentown, NJ, USA] containing an approximately 2.5 cm-deep layer of bedding (Cat. No. 7090; Teklad Sani-Chips; Harlan Laboratories, Indianapolis, IN, USA). This species, strain, and supplier were chosen due to previous studies evaluating stress resilience effects of *M. vaccae* NCTC 11659 that were conducted with these animals (Frank et al., 2018b). All rats were kept under standard laboratory conditions (12-h light/dark cycle, lights on at 0700 h, 22 °C) and had free access to bottled reverse-osmosis water and standard rat diet (Harlan Teklad 2918 Irradiated Rodent Chow, Envigo, Huntingdon, United Kingdom). Cages were changed once per week. The research described here was conducted in compliance with the ARRIVE 2.0 Guidelines for Reporting Animal Research (Kilkenny et al., 2010; Percie du Sert et al., 2020), and all studies were consistent with the National Institutes of Health *Guide for the Care and Use of Laboratory Animals*, Eighth Edition (National Research Council, 2011). The Institutional Animal Care and Use Committee at the University of Colorado Boulder approved all procedures. All efforts were made to limit the number of animals used and their suffering.

3.3.2 Reagents

This study used a whole cell heat-killed preparation of *M. vaccae* NCTC 11659 [IMM-201; alternative designations and different preparations and production processes of *M. vaccae* NCTC 11659 used in clinical trials or preclinical studies include: DAR-901 (Lahey et al., 2016), DarDar tuberculosis vaccine (Von Reyn et al., 2010), MV001 (Waddell et al., 2000), MV 007 (Vuola et al., 2003), *M. vaccae* SRL 172 (Von Reyn et al., 2010), and *M. vaccae* SRP 299 (Lowry et al., 2007); V7 (Bourinbaiar et al., 2020) is a hydrolyzed version of heat-killed *M. vaccae* NCTC 11659; *M. vaccae* NCTC 11659 has recently been classified as *M. kyogaense* sp. nov. (NCTC

11659; CECT 9646; DSM 107316) (Nouioui et al., 2018) (but see also Gupta et al., 2018); 10 mg/ml solution; strain National Collection of Type Cultures (NCTC) 11659, batch C079-ENG#1, provided by BioElpida (Lyon, France), diluted to 1 mg/ml in 100 µl sterile borate-buffered saline (BBS) for injections]. This study also employed the use of a whole heat-killed preparation of *M. vaccae* American Type Culture Collection (ATCC) 15483 suspension. *M. vaccae* ATCC 15483 was purchased from ATCC (Bonicke and Juhasz (ATCC® 15483, Manassas, VA, USA). *M. vaccae* ATCC 15483 was cultured in ATCC® Medium 1395: Middlebrook 7H9 broth (Cat. No. M0178-500G; Sigma-Aldrich; St. Louis, MO, USA) with ADC enrichment at 37 °C, then centrifuged at 3000 x g at 4 °C for ten minutes to pellet the cells, growth media was removed, and cells were weighed and resuspended in sterile BBS to a concentration of 10 mg/ml. Cells were transferred to a sealed sterile glass container and autoclaved at 121 °C for 15 minutes. Heat-killed bacterial stock was stored at 4 °C. *M. vaccae* ATCC 15483 was further diluted to 1 mg/ml in 100 µl sterile BBS for injections.

3.3.3 Mycobacterium vaccae (M. vaccae) NCTC 11659, M. vaccae ATCC 15483, and vehicle immunization

Experimental rats received 3 subcutaneous (s.c.) immunizations of: 1) 0.1 mg of a heat-killed preparation of *M. vaccae* NCTC 11659 (estimated to be 1 x 10^8 cells); 2) 0.1 mg of a heat-killed preparation of *M. vaccae* ATCC 15483 (estimated to be 1 x 10^8 cells); or 3) 100 µl of the vehicle, sterile BBS, using 21-gauge needles and injection sites between the scapulae, between the hours of 12 pm and 4 pm. Injections occurred on days –21, –14, and –7 prior to stress exposure, which occurred on day 0. The dose used in these experiments (0.1 mg) was 1/10 of the dose used in human studies (1 mg) (O'Brien et al., 2004) and identical to the dose used in previous studies in mice and rats (Amoroso et al., 2020; Fonken et al., 2018; Fox et al., 2017; Frank et al., 2018b;

Hassell et al., 2019; Loupy et al., 2018; Lowry et al., 2007; Reber et al., 2016b; Siebler et al., 2018). Figure 3.1 provides a timeline of *M. vaccae* treatments and stress exposure in relation to tissue collection.

Figure 3.1 Experimental timeline.
This schematic represents the experimental timeline for immunization with *M. vaccae* NCTC 11659, *M. vaccae* ATCC 15483, or vehicle (borate-buffered saline [BBS]), exposure to inescapable tail shock stress (IS), behavioral testing (juvenile social exploration [JSE]), and euthanasia. Behavioral results have been published separately in Loupy et al. (2021). Abbreviations: BBS, borate-buffered saline; HC, home cage control conditions; IS, inescapable tail shock stress; JSE, juvenile social exploration. Adapted, with permission, from Loupy et al. (2021).

3.3.4 Inescapable tail shock stress (IS)

IS was performed as previously described (Frank et al., 2018b). Briefly, rats were placed in Plexiglas® tubes (23.4 cm in length × 7 cm in diameter) and exposed to 100 1.6 mA, 5-s tail shocks with a variable inter-trial interval (ITI) ranging from 30 to 90 s (average ITI = 60 s). All IS treatments occurred between 09:00 and 11:00 h. IS animals were returned to their home cages immediately after termination of the shock. Home cage control (HC) animals remained undisturbed in their home cages.

3.3.5 Juvenile social exploration (JSE)

IS exposure produces robust decreases in JSE (Christianson et al., 2008), which is a widely used and validated measure of anxiety (File and Seth, 2003) and is sensitive to the neuroinflammatory effects of stress (Goshen and Yirmiya, 2009). Here, JSE was measured 24 h prior to IS (baseline) and 24 h after IS (test) (i.e., between 9:00 and 10:00 h). Each experimental subject was transferred to a novel cage with shaved wood bedding in a dimly lit room (40 lx). After a 15-min habituation period, a 28–32 day-old juvenile male rat was introduced to the subject's cage for 5 min. Exploratory behaviors of the adult (sniffing, pinning, licking and allo-grooming of the juvenile) were timed by an observer blind to treatment condition. After the test, the juvenile was removed and the experimental adult rat was returned to its home cage. Although juvenile stimulus rats were reused for multiple tests, the adult was never retested with the same juvenile. For each animal, JSE test data were quantified as a percent of baseline JSE. Due to technical issues, a total of four animals were removed from the JSE paradigm and subsequent behavioral analysis and our final group sample sizes prior to outlier analysis were BBS/HC, n = 8; BBS/IS, n = 6; NCTC/HC, n = 8; NCTC/IS, n = 8; ATCC/HC, n = 8; ATCC/IS, n = 6. Behavioral results have been published separately in Loupy et al. (2021).

3.3.6 Euthanasia and tissue and plasma collection

Rats were euthanized eight days following the last injection using an overdose of sodium pentobarbital (Fatal Plus®, Vortech Pharmaceuticals Ltd., Dearborn, MI, USA; 200 mg/kg, i.p.). After euthanasia, blood was collected by opening the thoracic cavity and inserting a 21-gauge needle into the right atrium of the heart and slowly drawing up 1 mL of blood. Blood was gently released into a BD Vacutainer® blood collection tube containing EDTA (Cat. No. 367835; Becton, Dickinson, and Company; Franklin Lakes, NJ, USA) and spun down at 1500 × g for 10

min; the plasma supernatant was collected and stored at −80 °C. Due to loss of samples during plasma collection, final sample sizes for plasma analysis were BBS/HC, *n* = 8; BBS/IS, *n* = 6; NCTC/HC, *n* = 8; NCTC/IS, *n* = 8; ATCC/HC, *n* = 7; ATCC/IS, *n* = 8.

3.3.7 Protein enrichment of plasma

Protein enrichment allows for greater resolution of low abundance proteins in downstream analyses of plasma samples. Samples were thawed on ice and 200 µL was taken for enrichment of low-abundance proteins using ProteoMiner™ Small Capacity Kit (Cat. No 163-3006, Bio-Rad Laboratories, Inc., Hercules, CA, USA). Samples were immediately processed for liquid chromatography-tandem mass spectrometry (LC-MS/MS) at the Central Analytical Mass Spectrometry Facility, University of Colorado Boulder.

3.3.8 Plasma sample preparation for quantitative mass spectrometry proteomics

Rat enriched plasma in 8 M urea was diluted 25-fold with 4% (w/v) SDS, 10mM TCEP, 40 mM 2-chloroacetamide (ClAA), and incubated at ambient temperature for an excess of 60 minutes to reduce and alkylate all plasma proteins. Sample preparation for mass spectrometry analyses was performed using the Single Pot Solid Phase Sample Preparation (SP3) method (Hughes et al., 2014). Briefly, 4-12 µg protein in 100 µL plasma was added to 100 µg Sera-Mag SpeedBeads Carboxylate Magnetic Beads (Cytiva, Marlborough, MA, USA) and mixed thoroughly. Acetonitrile was added to 80% (v/v) and mixed for an excess of 10 minutes to precipitate protein with the beads. Tubes were placed on a magnet and the supernatant was removed. Beads were then washed two times with 80% (v/v) ethanol in water and two times with 100% acetonitrile, sonicating 2 minutes with each wash. Protease digestion was performed with 0.5 µg of a

LycC/Trypsin mix (Promega, Madison, WI, USA) in 25 µL 50mM HEPES pH 8.0 mixing overnight at 37 °C. Tryptic digest supernatants were removed using a magnet and peptide concentrations were determined by tryptophan fluorescence (Wiśniewski and Gaugaz, 2015). Each of eight rat cohorts was multiplexed using 6-plex Tandem Mass Tags (6-plex TMT) (Thermo Scientific, Waltham, MA, USA), each including a control and two treatments for two different conditions (i.e., one sample from each of six experimental groups). Out of eight rat cohorts for each treatment group, two samples were missing for plasma, the BBS/IS cohort #2 and ATCC/HC cohort #4. These samples were replaced by mixing equal amounts of the same samples from the remaining six cohorts, for complete TMT 6-plexes for each cohort. TMT reagent was dissolved in anhydrous acetonitrile and added to tryptic peptides in 50 mM HEPES pH 8.0 and vortexed, then incubated at ambient temperature for 1 hour. Labeling reactions were quenched with the addition of hydroxylamine, vortexed, and incubated at ambient temperature for 15 minutes. Each sample in each cohort was labeled separately with one of the six TMT reagents in each 6-plex, and these multiplexed samples were desalted using an Oasis HLB 1 cc (10 mg) extraction cartridge (Waters, Milford, MA, USA) according to the manufacturer's instructions. Desalted multiplexed samples were dried completely using a speedvac vacuum concentrator.

3.3.9 Liquid chromatography/mass spectrometry analyses of 6-plex TMT-labeled rat plasma samples

Multiplexed samples were suspended in 3% (v/v) acetonitrile, 0.1% (v/v) trifluoracetic acid and 1 µg was loaded directly onto an ACQUITY UPLC M-class Peptide CSH reversed-phase C18, 130Å, 1.7µm, 75 µm X 250 mm column (cat. no. 186007478; Waters) using an Ultimate 3000 RSLCnano UPLC (Thermo Scientific). Peptides were eluted into a Q-Exactive HF-X Hybrid

Orbitrap mass spectrometer (Thermo Scientific) at 300 nL/minute with a gradient from 5% to 20% (v/v) acetonitrile in water over 115 minutes. Precursor mass spectra (MS1) were acquired at a resolution of 60,000 from 380 to 1580 m/z with an AGC target of 3E6 ions and a maximum injection time of 45 milliseconds. Dynamic exclusion was set for 25 seconds with a mass tolerance of +/– 10 ppm. Precursor peptide ion isolation window width for MS2 scans was 0.7 m/z with a +0.2 m/z offset. The top 12 most intense ions were selected for MS2 sequencing using higher-energy collisional dissociation (HCD) at 30% normalized collision energy. An AGC target of 1E5 ions and 100 milliseconds maximum injection time was used for all MS2 scans. Orbitrap MS data were searched against the Uniprot *Rattus norvegicus* database, downloaded 01/22/2019, using Maxquant version 1.6.3.4 for reporter ion MS2 quantification of 6-plex TMT with isotopic purity corrections from the product data sheet. Protease digestion was Trypsin/P with a maximum of two missed cleavages and a minimum peptide length of 7 amino acids. Cysteine carbamidomethylation was a fixed modification, while methionine oxidation and protein N-terminal acetylation were variable modifications. First search mass tolerance was 20 ppm and the main search tolerance was 4.5 ppm with a 20 ppm MS/MS mass tolerance. False discovery rates (FDR) for peptide and protein identifications were 1%.

3.3.10 Statistical Analysis

Proteomics analyses were performed for plasma using R Statistical Programming (version 3.5.3 for Windows). Abundance of each protein was measured by reporter ion-corrected values. To correct for potential noise in the MS/MS detection, reporter ion-corrected values were removed for any proteins that had a reporter intensity count less than two. Contaminants were also removed from the dataset. Peak intensities were log2-transformed and normalized across the

dataset using the normalizeBetweenArrays function and the cyclic loess method within the linear models for microarray analysis (LIMMA) package. Two analyses were run on the data: 1) generalized linear model (GLM) was performed to understand the general effects of treatment and stress on proteomic profiles in the plasma, and 2) LIMMA analysis using the empirical Bayes method was performed to directly compare treatment groups of interest. GLM analysis was performed on log2-transformed normalized peak intensity for each protein, with treatment, stress, and treatment x stress as factors. Cohort (i.e., TMT batch) was also included as a factor in the GLM analysis to better control for any batch effects of the 6-plex TMT. Fold change values and pairwise comparison *p*-values were analyzed from the LIMMA output. For both GLM and LIMMA analyses, two-tailed significance was set at $\alpha = 0.1$ and an adjusted *p*-value was not calculated due to low power (Pascovici et al., 2016). Statistical analysis was only performed on proteins wherein each treatment group sample size was greater than or equal to $n = 3$. Proteins that were found to be significantly different between treatment and control as well as proteins with a fold-change (up or downregulated) greater than two were used in downstream pathway analysis via the Database for Annotation, Visualization and Integrated Discovery (DAVID, version 6.8) (Huang et al., 2009a, 2009b) using UniProt accession IDs (The UniProt Consortium, 2019) for gene labeling and *Rattus norvegicus* as species. Analyses of correlations between dependent variables were performed using R Statistical Programming (version 3.6.1 for Windows), conducted using the Pearson correlation method and FDR adjusted *p*-values. For protein interaction analysis, STRING database (version 11) was used (Szklarczyk et al., 2019). The Kyoto encyclopedia of genes and genomes (KEGG) (Kanehisa and Goto, 2000), Harmonizome (Rouillard et al., 2016), and UniProt (The UniProt Consortium, 2019) databases were used for additional pathway analysis and gene ontology.

3.4 Results

3.4.1 General effects of M. vaccae strain, IS, and interactions of M. vaccae strain x IS on protein relative abundances in the plasma

To understand the overall effect of IS and either *M. vaccae* NCTC 11659 or *M. vaccae* ATTC 15483 treatment on protein abundance in the plasma, we ran GLMs with *M. vaccae* strain and IS as factors and *M. vaccae* strain x IS as an interaction factor. Effects of *M. vaccae* NCTC 11659 or *M. vaccae* ATTC 15483, and their interactions with IS, were analyzed separately. To control for batch effect of the 6-plex TMT, batch was included as an additional factor in the GLM.

Effects of M. vaccae NCTC 11659 and IS on protein relative abundances in the plasma

We investigated the effects of immunization with *M. vaccae* NCTC 11659 and IS on relative protein abundances in the plasma. The GLM revealed an interaction effect of *M. vaccae* NCTC 11659 x IS on sixteen of 230 proteins: angiopoetin-1 (ANG-1), angiopoietin-like 6 (ANGL-6), apolipoprotein A-V (ApoA-V), β-actin, complement C4 (C4), complement C4a (C4a), complement C4b (C4b), endoplasmic reticulum chaperone BiP (also known as heat shock protein 70 family protein 5; binding immunoglobulin protein BiP; Hsp70-5, encoded by *Hspa5*), coagulation factor XIII A chain (factor XIIIa), immunoglobulin heavy chain 1a (also mapped as Ig gamma 2b; IgH-1a), an Ig-like domain containing protein (Ig-like, UniProt ID F1M1R0), insulin-like growth factor-binding protein 6 (IGFBP-6), proteasome subunit beta type-6 (PSMB6), serine protease inhibitor A3K (also known as kallikrein-binding protein; Serpin A3K; KBP), and tropomyosin alpha-1 chain (Tpm1). In addition, there were main effects of *M. vaccae* NCTC 11659 on twelve proteins: ANG-1, ANGL-6, ApoA-V, factor XIIIa, C4, C4b, IgH-1a, Ig-like protein F1M1R0, Tpm1, and uncharacterized protein with UniProt ID A0A0G2K6T8. The

GLM revealed an effect of IS on 57 proteins: albumin, alpha-1-inhibitor 3 (alpha 1 I3), ANGL-6, apolipoprotein A-I (ApoA-I), apolipoprotein A-II, apolipoprotein A-IV (ApoA-IV), apolipoprotein A-V (ApoA-V), apolipoprotein C-II (ApoC-II), apolipoprotein E (ApoE), apolipoprotein N (ApoN), ATP-binding cassette sub-family B member 9 (ABCB9), α-actin-1/2, β-actin, coagulation factor X (factor X), complement component factor h-like 1 (CFHL1; also known as complement factor H-related protein 1), complement C1r (C1r), complement C1s subcomponent (C1s), C4a, C4b, complement component C4b-binding protein alpha chain (C4BPa), complement C8 alpha chain (C8a), complement component C9 (C9), factor XIIIa, fibrinogen beta chain (FGB), fibrinogen gamma chain (FGG), fibrinogen-like protein 1 (FGL-1), fibulin-3 (also known as EGF-containing fibulin-like extracellular matrix protein 1; FIBL-3), glutathione peroxidase (matching isoforms 3, 5, and 6; GPx3/5/6), hemoglobin subunit alpha 1/2 (HBA-1/2), IgH-1a, insulin-like growth factor-binding protein complex acid labile subunit (IGFALS), IGFBP-6, Ig kappa chain C region (IgK), Ig-like domain-containing protein (Ig-like, UniProt ID A0AG2K3A6), inter-alpha trypsin inhibitor heavy chain 4 (ITIH4), kallikrein, T-kininogen 1 (also known as major acute phase protein or thiostatin; KNG1; alpha-1-MAP; also mapped as *Map1* by DAVID and *Kng1* by STRING), T-kininogen 2 (also mapped as kininogen 1-like 1 or kininogen 1; KNG2; KNG1L1; also mapped as *Kng1l1* by DAVID and *Kng2* by STRING), lipase, lipopolysaccharide (LPS) binding protein (LBP), lysyl oxidase-like 1 (LOXL1), mannose-binding protein A (MBP-A; also known as mannose-binding lectin, or MBL), myosin heavy chain matching isoforms 6 and 7 (MyHC-6/7), myosin light chain (matching isoforms 1, 3, and 4; MyLC-1/3/4), platelet factor 4 (PF-4; also known as C-X-C motif chemokine ligand 4, or CXCL4), peptidoglycan recognition protein 2 (PGLYRP2), phosphatidylinositol-glycan-specific phospholipase D (PI-G PLD), serum

paraoxonase/arylesterase 1 (PON 1), proteoglycan 4, PSMB6, prosaposin (also known as sulfated glycoprotein 1; SGP-1), serum amyloid A protein (SAA4), Serpin A3K, serine protease inhibitor A3N (Serpin A3N), von Willebrand factor (VWF), and 14-3-3 protein gamma (YWHAG).

Effects of M. vaccae ATCC 15483 and IS on protein relative abundances in the plasma

We investigated the effects of immunization with *M. vaccae* ATCC 15483 and IS on relative protein abundance in the plasma. The GLM revealed an interaction effect of *M. vaccae* ATCC 15483 x IS on 22 of 230 proteins: BiP, CD5 molecule like (CD5L), C1q and tumor necrosis factor-related 3 protein (CTRP3), C4b, complement component C4b-binding protein beta chain (C4BPb), creatine kinase M-type (M-CK), DnaJ homolog subfamily C member 16 (DnaJC16), IgH-1a, three Ig-like domain containing proteins (Ig-like, UniProt IDs D3ZBB2, F1M229, and F1LXY6), IGFBP-6, LBP, PON 1, protein Z, proteasome subunit alpha type-7 (PSMA7), PSMB6, SAA4, suprabasin, Tpm1, 14-3-3 protein epsilon (YWHAE), and YWHAG. There was an effect of *M. vaccae ATCC 15483* on 23 proteins: BiP, calmodulin (matching isoforms 1, 2, and 3; CaM), CD5L, CL-L1, CTRP3, C4BPb, C8a, IgH-1a, Ig-like D3ZBB2, Ig-like F1M229, Ig-like F1LXY6, IGFBP-6, KNG1, KNG2, LBP, PON 1, PSMA7, PSMB6, SAA4, serine protease inhibitor A3L (Serpin A3L), plasma protease C1 inhibitor (Serpin G1), Tpm1, YWHAE, and YWHAG. There was an effect of IS on 34 proteins: ABCB9, ApoA-I, apolipoprotein A-II (ApoA-II), ApoN, CFHL1, C1s, C4BPb, complement C5 (C5), complement C8 (C8), C9, FIBL-3, FGB, FGG, FGL-1, IgH-1a, Ig-like F1LXY6, IGFBP-6, ITIH4, KNG1, KNG2, lipase, MBP-A, MyLC-1/3/4, PF-4, PGLYRP2, PI-G PLD, pyruvate kinase (PKM), PON 1, PSMB6, Serpin A3K, Serpin A3N, Serpin G1, SGP-1.

3.4.2 Individual pairwise comparisons of protein abundances in the plasma

To directly compare protein abundances between each experimental group, we first analyzed our data using an average fold change analysis, indicating which proteins had a fold change (upregulated or downregulated) equal to or greater than two. We then ran a separate linear model analysis, investigating pairwise comparisons for each protein using the linear models for microarray data (limma) package in R. We first report the effects of *M. vaccae* NCTC 11659 on protein relative abundances in the plasma of home cage control animals; we then report effects of IS on protein relative abundances in the plasma of vehicle-treated animals; we then report effects of immunization with *M. vaccae* NCTC 11659 on protein relative abundances in the plasma of IS-exposed animals; and finally, we report the effects of stress on protein relative abundances in the plasma of animals immunized with *M. vaccae* NCTC 11659. Data are then reported in a similar manner for *M. vaccae* ATCC 15483.

3.4.3 Pairwise comparisons with M. vaccae NCTC 11659

Effects of immunization with M. vaccae NCTC 11659 on protein relative abundances in the plasma of home cage control animals

Fold change analysis revealed that, among home cage control animals, immunization with *M. vaccae* NCTC 11659 did not increase or decrease the abundance of any protein in the plasma by two-fold (Figure 3.2A).

The pairwise comparison analysis found a significant difference in abundance of three proteins in the plasma between *M. vaccae* NCTC 11659-treated and BBS-treated home cage animals. Among home cage animals, immunization with *M. vaccae* NCTC 11659 increased the

abundances of ANGL-6, β-actin, and an uncharacterized protein with UniProt ID A0A0G2K6T8 (Figure 3.2A). There were no proteins significantly downregulated in the plasma after immunization with *M. vaccae* NCTC 11659 among home cage animals (Figure 3.2A).

Effects of stress on protein relative abundances in the plasma of vehicle-treated animals

Fold change analysis revealed that, among BBS-treated animals, IS increased the abundance of twelve proteins in the plasma by two-fold: ABCB9, FGL-1, KNG2, LBP, myosin heavy chain matching isoforms 1 and 2 (MyHC-1/2), myosin heavy chain 4 (MyHC-4), MyHC-6/7, MyLC-1/3/4, glycogen phosphorylase (matching isoforms M and B; PYG), Tpm1, trafficking protein particle complex subunit 4 (TRAPPC4), and YWHAG (Figure 3.2B; Figure 3.3B). Among BBS-treated animals, IS decreased the abundance of one protein by two-fold: PF-4 (Figure 3.2B; Figure 3.3B).

The pairwise comparison analysis found a significant difference in abundance of 64 proteins in the plasma between IS-exposed and home cage animals treated with BBS. Among BBS-treated animals, IS increased the abundance of ABCB9, alpha-1-acid glycoprotein (also known as orosomucoid; AGP), fructose-bisphosphate aldolase A (AldoA), ANGL-6, α-actin-1/2, β-actin, CFHL1, C1s, C4BPa, C4BPb, C5, C9, FGB, FGG, FGL-1, IGFBP-6, IgH-1a, ITIH4, KNG1 , KNG2, LBP, lipase, MyHC-1/2, MyHC-6/7, MyLC-1/3/4, PKM, proteoglycan 4, PYG, SAA4, Serpin A3N, Tpm1, and VWF (Figure 3.2B; Figure 3.3B). Among BBS-treated animals, IS significantly decreased the abundance of albumin, alpha 1 I3, ApoA-I, ApoA-II, ApoA-IV, ApoC-II, ApoE, ApoN, C4a, C4b, C8a, cadherin-17, chemerin, CL-L1, FIBL-3, GPx3/5/6, HBA-1/2, IGFALS, Ig gamma-2A chain C region (IgG-2a), IgK, two Ig-like domain-containing

proteins (Ig-like, UniProt IDs A0AG2K3A6 and A0A0G2K980), LOXL1, MBP-A, murinoglobulin-1 (also known as alpha-1 inhibitor 3 variant I; Mug1), PF-4, PGLYRP2, PI-G PLD, phospholipid transfer protein (PLTP), PON 1, Serpin A3K, SGP-1, and tropomyosin alpha-4 chain (Tpm4) (Figure 3.2B; Figure 3.3B).

Effects of immunization with M. vaccae NCTC 11659 on protein relative abundances in the plasma of IS-exposed animals

Fold change analysis revealed that, among IS-exposed animals, immunization with *M. vaccae* NCTC 11659 increased the abundance of two proteins in the plasma by two-fold: Ig-like protein F1M1R0 and PF-4 (Figure 3.2C). Among IS-exposed animals, immunization with *M. vaccae* NCTC 11659 did not decrease the abundance of any proteins by two-fold (Figure 3.2C).

The pairwise comparison analysis found a significant difference in abundance of eight proteins in the plasma between *M. vaccae* NCTC 11659-treated and BBS-treated animals exposed to IS. Among IS-exposed animals, immunization with *M. vaccae* NCTC 11659 increased the abundance of C4a, Ig-like protein F1M1R0, lysozyme, Serpin A3K, and an uncharacterized protein similar to complement factor H-related protein (UniProt ID A0A0G2K975) (Figure 3.2C). Among IS-exposed animals, immunization with *M. vaccae* NCTC 11659 decreased the abundances of ANGL-6, IGFBP-6, and IgH-1a compared to BBS-treated animals (Figure 3.2C).

Effects of stress on protein relative abundances in the plasma of animals immunized with M. vaccae NCTC 11659

Fold change analysis revealed that, among animals immunized with *M. vaccae* NCTC 11659, IS increased the abundance of eight proteins in the plasma by two-fold: AldoA, FGL-1, Ig-like

protein F1M1R0, PYG, LBP, MyHC-1/2, MyHC-4, and Tpm1 (Figure 3.2D). Among animals immunized with *M. vaccae* NCTC 11659, IS did not decrease the abundance of any proteins by two-fold (Figure 3.2D).

The pairwise comparison analysis found a significant difference in abundance of 58 proteins in the plasma between IS-exposed and home cage animals immunized with *M. vaccae* NCTC 11659. Among animals immunized with *M. vaccae* NCTC 11659, IS increased the abundance of AGP, AldoA, ANG-1, α-actin-1/2, CFHL1, C1s, C4, C4BPa, C4BPb, fibrinogen alpha chain (FGA), FGB, FGG, FGL-1, haptoglobin (also known as liver regeneration-related protein), Ig-like protein F1M1R0, ITIH4, LBP, lipase, lysozyme, KNG1, M-CK, MyHC-1/2, MyHC-6/7, MyLC-1/3/4, myosin regulatory light chain 2 (MyLC-2), PKM, PYG, SAA4, Serpin A3N, Tpm1, tripartite motif-containing 33 (TRIM33), vitamin D-binding protein (VDB), YWHAG, and an uncharacterized protein similar to complement factor H-related protein (UniProt ID A0A0G2K975) (Figure 3.2D). Immunization with *M. vaccae* NCTC 11659 prevented a stress-induced increase of ABCB9, ANGL-6, β-actin, C5, C9, IGFBP-6, IgH-1a, KNG2, proteoglycan 4, TRAPPC4, and VWF; however, immunization with *M. vaccae* NCTC 11659 may have promoted a stress-induced increase of several additional proteins, including ANG-1, C4, FGA, haptoglobin, Ig-like protein F1M1R0, lysozyme, M-CK, MyLC-2, TRIM33, VDB, and an uncharacterized protein with UniProt ID A0A0G2K975 (i.e., compare Figure 3.2B and Figure 3.2D). Among animals immunized with *M. vaccae* NCTC 11659, IS decreased the abundance of ANGL-6, ApoA-I, ApoA-II, ApoA-IV, ApoC-II, ApoE, apolipoprotein M (ApoM), ApoN, C8a, chromogranin-A (CgA), CL-L1, C8a, GPx3/5/6, IgG-2a, immunoglobulin heavy constant mu (IGHM), IgK, Ig lambda-2 chain C region (IgL-2), immunoglobulin joining chain (J-chain),

LOXL1, PGLYRP2, PI-G PLD, PLTP, PON 1, Serpin A3K, transferrin receptor protein 1 (TfR1), and an uncharacterized protein with UniProt ID G3V9J1 (annotated by the DAVID database as alpha-1-inhibitor 3) (Figure 3.2D). Immunization with *M. vaccae* NCTC 11659 prevented a stress-induced decrease of albumin, alpha 1 I3, cadherin-17, chemerin, C4a, C4b, FIBL-3, HBA-1/2, IGFALS, Ig-like proteins A0AG2K3A6 and A0A0G2K980, MBP-A, Mug1, PF-4, SGP-1, and Tpm4; however, immunization with *M. vaccae* NCTC 11659 may have promoted a stress-induced decrease of ANGL-6, ApoM, CgA, IGHM, IgL-2, J-chain, TfR1, and an uncharacterized protein with UniProt ID G3V9J1.

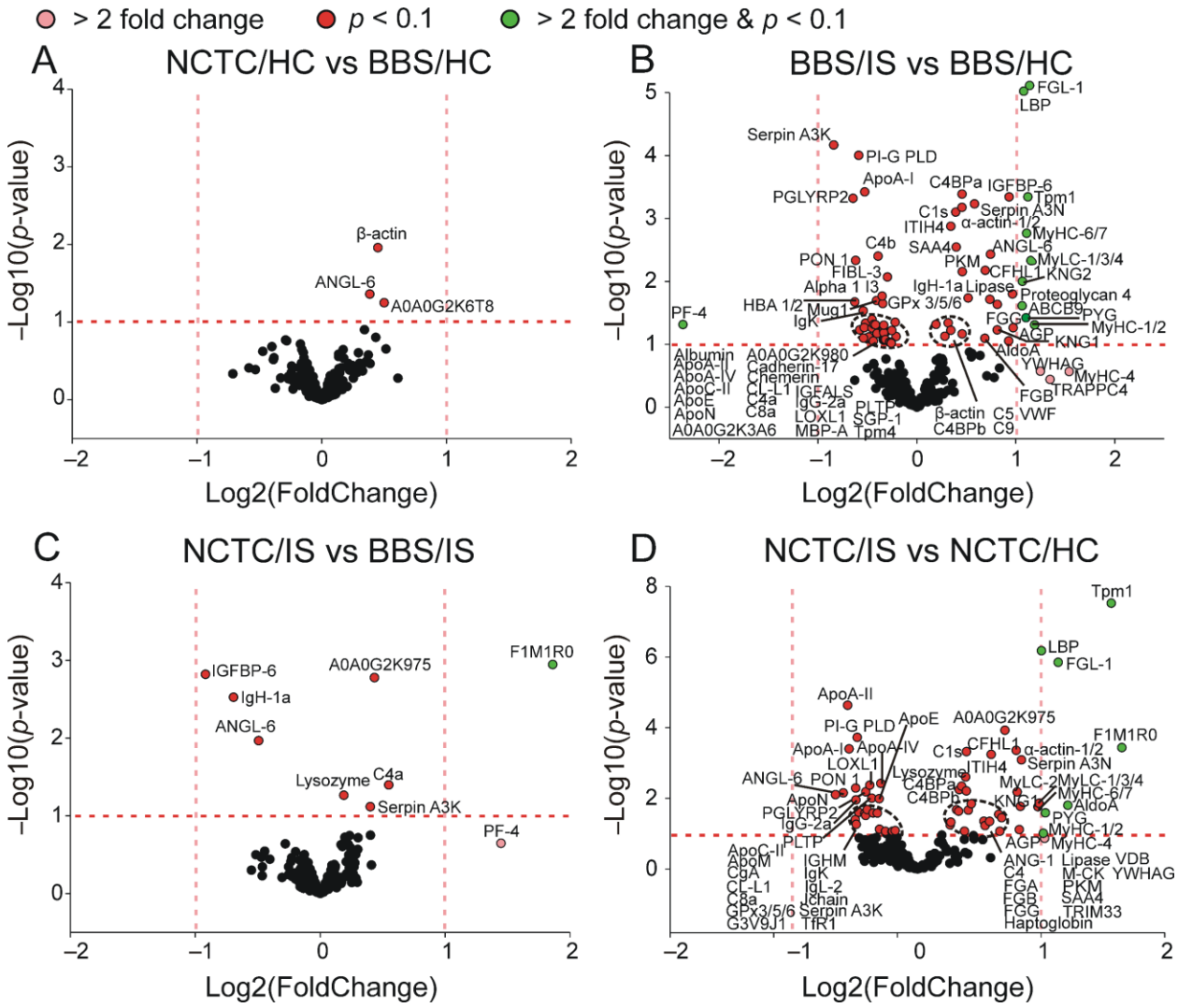

Figure 3.2 Volcano plot showing effects of immunization with *Mycobacterium vaccae* NCTC 11659 and inescapable tail shock stress (IS) on plasma proteomics as measured by liquid chromatography-tandem mass spectrometry (LC-MS/MS).

The pink vertical dashed lines represent the thresholds for greater than two-fold change in average corrected peak intensity, corresponding to proteins labeled pink, and the red horizontal dashed line represents the threshold for significance at a *p*-value less than 0.1, corresponding to proteins labeled red. Proteins labeled green had both a two-fold difference in abundance and a *p*-value less than 0.1. Panel B from Figures 2 and 3 are the same, duplicated for reference. Final sample sizes for plasma analysis: BBS/HC, *n* = 8; BBS/IS, *n* = 6; NCTC/HC, *n* = 8; NCTC/IS, *n* = 8. Abbreviations: A0A0G2K3A6, Ig-like domain containing protein; A0A0G2K6T8, uncharacterized protein; A0A0G2K975, uncharacterized protein similar to complement factor H-related protein; A0A0G2K980, Ig-like domain containing protein; ABCB9, ATP-binding cassette sub-family B member 9; AGP, alpha-1-acid glycoprotein; AldoA, fructose-bisphosphate aldolase A; alpha 1 I3, alpha-1-inhibitor 3; ANG-1, angiopoietin-1, ANGL-6, angiopoietin-like 6; ApoA-I, apolipoprotein A-I; ApoA-II, apolipoprotein A-II; ApoA-IV, apolipoprotein A-IV; ApoA-V, apolipoprotein A-V; ApoC-II, apolipoprotein C-II; ApoE, apolipoprotein E; ApoM, apolipoprotein M; ApoN, apolipoprotein N; ATCC, *M. vaccae* ATCC 15483; BBS, borate-buffered saline; C1s, complement C1s subcomponent; C4a, complement C4a; C4b, complement C4b; C4BPa, complement C4b-binding protein alpha chain; C5, complement C5; C8a, complement C8 alpha chain; C9, complement C9; CFHL1, complement component factor h-like 1; CgA, chromogranin-A; CL-L1, collectin liver protein 1 (collectin-10); F1M1R0, Ig-like domain containing protein; FGA, fibrinogen alpha chain; FGB, fibrinogen beta chain; FGG, fibrinogen gamma chain; FGL-1, fibrinogen-like protein 1; FIBL-3, fibulin-3; GPx3/5/6, glutathione peroxidase matching isoforms 3, 5, and 6; HBA 1/2, hemoglobin subunit alpha 1/2; HC, home cage control; IGFALS, insulin-like growth factor-binding protein complex acid labile subunit; IGFBP-6, insulin-like growth factor-binding protein 6; IgG-2a, Ig-gamma-2A chain C region; IgH-1a, immunoglobulin heavy chain 1a; IGHM, immunoglobulin heavy constant mu; IgK, Ig kappa chain C region; IgL-2, Ig lambda-2 chain C region; IS, inescapable tail shock; ITIH4, inter-alpha trypsin inhibitor heavy chain 4; J-chain, immunoglobulin joining chain; KNG1, T-kininogen 1; KNG2, T-kininogen 2; LBP, lipopolysaccharide binding protein; LOXL1, lysyl oxidase-like 1; MBP-A, mannose-binding protein A; M-CK, creatine kinase M-type; Mug1, murinoglobulin-1; MyHC-1/2, myosin heavy chain matching isoforms 1 and 2; MyHC-4, myosin heavy chain 4; MyHC-6/7, myosin heavy chain matching isoforms 6 and 7; MyLC-1/3/4, myosin light chain matching isoforms 1, 3, and 4; MyLC-2, myosin regulatory light chain 2; NCTC, *M. vaccae* NCTC 11659; PF-4, platelet factor 4; PGLYRP2, peptidoglycan recognition protein 2; PI-G PLD, phosphatidylinositol-glycan-specific phospholipase D; PKM, pyruvate kinase; PLTP, phospholipid transfer protein; PON 1, paraoxonase/arylesterase 1; PYG, glycogen phosphorylase; SAA4, serum amyloid A protein; Serpin A3K, serine protease inhibitor A3K; Serpin A3N, serine protease inhibitor A3N; SGP-1, sulfated glycoprotein 1; TfR1, transferrin receptor protein 1; Tpm1, tropomyosin alpha-1 chain; Tpm4, tropomyosin alpha-4 chain; TRAPPC4, trafficking protein particle complex subunit 4; TRIM33, tripartite motif-containing 33; VDB, vitamin-D binding protein; VWF, von Willebrand factor; YWHAG, 14-3-3 protein gamma.

3.4.4 Pairwise comparisons with M. vaccae ATCC 15483

Effects of immunization with M. vaccae ATCC 15483 on protein abundances in the plasma of home cage control animals

Fold change analysis revealed that, among home cage animals, immunization with *M. vaccae* ATCC 15483 did not increase the abundance of any proteins in the plasma by two-fold (Figure 3.3A). Among home cage animals, immunization with *M. vaccae* ATCC 15483 decreased the abundance of two proteins in the plasma by two-fold: PF-4 and YWHAG (Figure 3.3A).

The pairwise comparison analysis found a significant difference in abundance of twelve proteins in the plasma between *M. vaccae* ATCC 15483-treated and BBS-treated home cage animals. Among home cage animals, immunization with *M. vaccae* ATCC 15483 increased the abundance of IGFBP-6, Ig-like proteins F1M229 and F1LXY6, KNG1, and KNG2 compared to BBS-treated animals (Figure 3.3A). Among home cage animals, immunization with *M. vaccae* ATCC 15483 decreased the abundances of ApoN, C4BPb, FIBL-3, PF-4, Serpin A3L, Tpm1, and YWHAG (Figure 3.3A).

Effects of immunization with M. vaccae ATCC 15483 on protein relative abundances in the plasma of IS-exposed animals

Fold change analysis revealed that, among IS-exposed animals, immunization with *M. vaccae* ATCC 15483 increased the abundance of PF-4 in the plasma by two-fold. Among IS-exposed animals, immunization with *M. vaccae* ATCC 15483 decreased the abundance of IGFBP-6 in the plasma by two-fold (Figure 3.3C).

The pairwise comparison analysis found a significant difference in abundance of four proteins in the plasma between *M. vaccae* ATCC 15483-treated and BBS-treated animals exposed to IS.

Among IS-exposed animals, immunization with *M. vaccae* ATCC 15483 increased the abundances of M-CK and suprabasin compared to BBS-treated animals (Figure 3.3C). Among IS-exposed animals, immunization with *M. vaccae* ATCC 15483 decreased the abundances of IGFBP-6 and IgH-1a (Figure 3.3C).

Effects of stress on protein relative abundances in the plasma of animals immunized with M. vaccae ATCC 15483

Fold change analysis revealed that, among animals immunized with *M. vaccae* ATCC 15483, IS increased the abundance of thirteen proteins in the plasma by two-fold: AGP, AldoA, FGL-1, LBP, M-CK, MyHC-1/2, MyHC-4, MyHC-6/7, proteoglycan 4, PYG, Tpm1, TRAPPC4, and YWHAG (Figure 3.3D). Among animals immunized with *M. vaccae* ATCC 15483, IS decreased the abundance of one protein by two fold: an uncharacterized protein with UniProt ID M0R789 (Figure 3.3D).

The pairwise comparison analysis found a significant difference in abundance of 72 proteins in the plasma between IS-exposed and home cage animals immunized with *M. vaccae* ATCC 15483. Among animals immunized with *M. vaccae* ATCC 15483, IS increased the abundance of ABCB9, AGP, AldoA, ANGL-6, ApoA-V, α-actin-1/2, CaM, CFHL1, collectin subfamily member 11 (collectin-11), C1s, C4BPa, C4BPb, DnaJC16, FGB, FGG, FGL-1, ITIH4, LBP, KNG1, mannan-binding lectin serine protease 2 (MASP-2), M-CK, MyHC-6/7, MyLC-1/3/4, MyLC-2, protein Z (a vitamin K-dependent plasma glycoprotein), proteoglycan 4, PYG, SAA4, Serpin A3N, suprabasin, Tpm1, TRIM33, YWHAE, YWHAG, and uncharacterized protein with UniProt ID A0A0G2K975 (Figure 3.3D). Immunization with *M. vaccae* ATCC 15483, like immunization with *M. vaccae* NCTC 11659, prevented the stress-induced increase of β-actin,

C5, C9, IGFBP-6, IgH-1a, KNG2, and VWF; additionally, *M. vaccae* ATCC 15483 prevented the stress-induced increase of lipase and PKM. Immunization with *M. vaccae* ATCC 15483, like immunization with *M. vaccae* NCTC 11659, may have promoted a stress-induced increase of M-CK, MyLC-2, TRIM33, and an uncharacterized protein with UniProt ID A0A0G2K975; additionally, *M. vaccae* ATCC 15483 may have promoted the stress-induced increase of ApoA-V, CaM, collectin-11, DnaJC16, MASP-2, protein Z, suprabasin, and YWHAE. Among animals immunized with *M. vaccae* ATCC 15483, IS decreased the abundance of albumin, alpha 1 I3, ApoA-I, ApoA-II, apolipoprotein C-I (ApoC-I), ApoC-II, ApoE, ApoM, ApoN, CD5L, carboxylesterase 1C (Ces1C), GPx3/5/6, IGFALS, IGFBP-6, IGHM, Ig gamma-1 chain C region (IgG-1), IgG-2a, IgH-1a, IgL-2, IgK, Ig-like domain containing proteins (Ig-like, UniProt IDs A0A0G2JTG4, A0AG2K3A6, D3ZBB2, F1LXY6, F1MAE7, F1M229), LOXL1, Mug1, PGLYRP2, PI-G PLD, Serpin A3K, serine protease inhibitor A3M (Serpin A3M), SGP-1, and uncharacterized proteins with UniProt IDs G3V9J1 (annotated by the DAVID database as alpha-1-inhibitor 3), M0R789, M0RA79, M0RE02, and (Figure 3.3D). Immunization with *M. vaccae* ATCC 15483, like immunization with *M. vaccae* NCTC 11659, prevented the stress-induced decrease of cadherin-17, chemerin, C4a, C4b, FIBL-3, HBA-1/2, MBP-A, PF-4, and Tpm4; additionally, *M. vaccae* ATCC 15483 prevented the stress-induced decrease of ApoA-IV, CL-L1, C8a, PLTP, and PON 1. Immunization with *M. vaccae* ATCC 15483, like immunization with *M. vaccae* NCTC 11659, may have promoted a stress-induced decrease of ApoM, IGHM, Ig-L2, and an uncharacterized protein with UniProt ID G3V9J1; additionally, *M. vaccae* ATCC 15483 may have promoted the stress-induced decrease of ApoC-I, CD5L, Ces1C, IGFBP-6, IgG-1, IgH-1a, Ig-like proteins A0A0G2JTG4, D3ZBB2, F1LXY6, F1MAE7, F1M229, Serpin A3M, and uncharacterized proteins M0RA79, M0RE02, and M0R789.

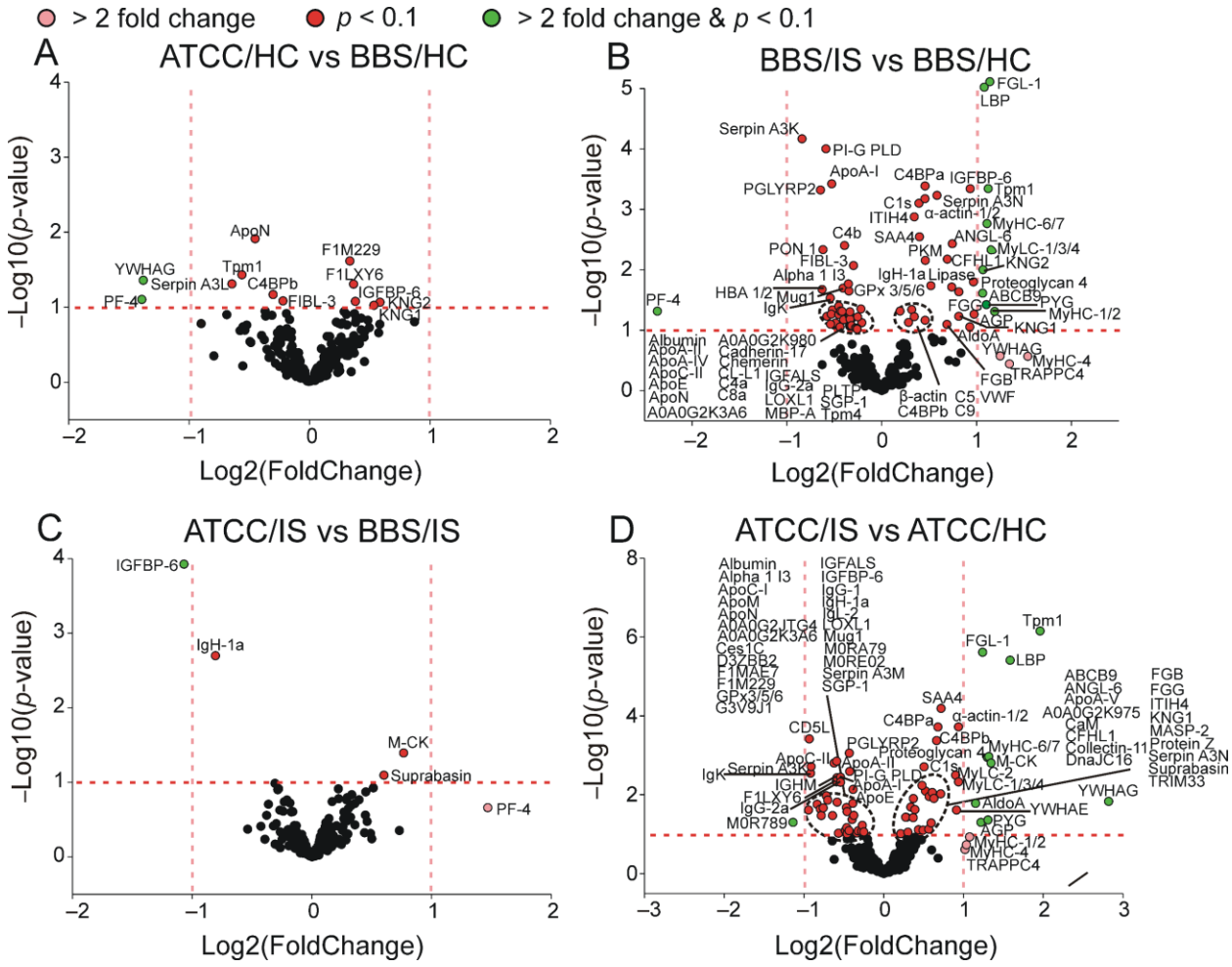

Figure 3.3 Volcano plot showing effects of immunization with *Mycobacterium vaccae* ATCC 15483 and inescapable tail shock stress (IS) on plasma proteomics as measured by liquid chromatography-tandem mass spectrometry (LC-MS/MS).

The pink vertical dashed lines represent the thresholds for greater than two-fold change in average corrected peak intensity, corresponding to proteins labeled pink, and the red horizontal dashed line represents the threshold for significance at a *p*-value less than 0.1, corresponding to proteins labeled red. Proteins labeled green had both a two-fold difference in abundance and a *p*-value less than 0.1. Panel B from Figures 2 and 3 are the same, duplicated for reference. Final sample sizes for plasma analysis: BBS/HC, *n* = 8; BBS/IS, *n* = 6; ATCC/HC, *n* = 7; ATCC/IS, *n*= 8. Abbreviations: A0A0G2JTG4, Ig-like domain containing protein; A0A0G2K3A6, Ig-like domain containing protein; A0A0G2K6T8, uncharacterized protein; A0A0G2K975, uncharacterized protein similar to complement factor H-related protein; ABCB9, ATP-binding cassette sub-family B member 9; AGP, alpha-1-acid glycoprotein; AldoA, fructose-bisphosphate aldolase A; alpha 1 I3, alpha-1-inhibitor 3; ANG-1, angiopoietin-1, ANGL-6, angiopoietin-like 6; ApoA-I, apolipoprotein A-I; ApoA-II, apolipoprotein A-II; ApoA-IV, apolipoprotein A-IV; ApoA-V, apolipoprotein A-V; ApoC-I, apolipoprotein C-I; ApoC-II, apolipoprotein C-II; ApoE, apolipoprotein E; ApoM, apolipoprotein M; ApoN, apolipoprotein N; ATCC, *M. vaccae* ATCC 15483; BBS, borate-buffered saline; CaM , calmodulin; CD5L, CD5 molecule like; Ces1C,

carboxylesterase 1C; CFHL1, complement component factor h-like 1; CL-L1, collectin liver protein 1 (collectin-10); C1s, complement C1s subcomponent; C4b, complement C4b; C4BPa, complement component C4b-binding protein alpha chain; C8a, complement C8 alpha chain; C9, complement C9; DnaJC16, DnaJ homolog subfamily C member 16; F1LXY6, Ig-like domain containing protein; F1M229, Ig-like domain containing protein; F1MAE7, Ig-like domain containing protein; FGB, fibrinogen beta chain; FGG, fibrinogen gamma chain; FGL-1, fibrinogen-like protein 1; FIBL-3, fibulin-3; GPx3/5/6, glutathione peroxidase matching isoforms 3, 5, and 6; HBA 1/2, hemoglobin subunit alpha 1/2; HC, home cage control; IGFALS, insulin-like growth factor-binding protein complex acid labile subunit; IGFBP-6, insulin-like growth factor-binding protein 6; IgG-1, Ig gamma-1 chain C region; IgG-2a, Ig-gamma-2A chain C region; IgH-1a, immunoglobulin heavy chain 1a; IGHM, immunoglobulin heavy constant mu; IgK, Ig kappa chain C region; IgL-2, Ig lambda-2 chain C region; IS, inescapable tail shock; ITIH4, inter-alpha trypsin inhibitor heavy chain 4; KNG1, T-kininogen 1; KNG2, T-kininogen 2; LBP, lipopolysaccharide binding protein; LOXL1, lysyl oxidase-like 1; M0R789, uncharacterized protein M0R789; M0RA79, uncharacterized protein; M0RE02, uncharacterized protein; MASP-2, mannan-binding lectin serine protease 2; MBP-A, mannose-binding protein A; M-CK, creatine kinase M-type; Mug1, murinoglobulin-1; MyHC-1/2, myosin heavy chain matching isoforms 1 and 2; MyHC-4, myosin heavy chain 4; MyHC-6/7, myosin heavy chain matching isoforms 6 and 7; MyLC-1/3/4, myosin light chain matching isoforms 1, 3, and 4; ; NCTC, *M. vaccae* NCTC 11659; Ogn, osteoglycin; PF-4, platelet factor 4; PGLYRP2, peptidoglycan recognition protein 2; PI-G PLD, phosphatidylinositol-glycan-specific phospholipase D; PKM, pyruvate kinase; PLTP, phospholipid transfer protein; PON 1, paraoxonase/arylesterase 1; PYG, glycogen phosphorylase; SAA4, serum amyloid A protein; Serpin A3K, serine protease inhibitor A3K; Serpin A3M, serine protease inhibitor A3M; Serpin A3N, serine protease inhibitor A3N; SGP-1, sulfated glycoprotein 1; Tpm1, tropomyosin alpha-1 chain; TRAPPC4, trafficking protein particle complex subunit 4; TRIM33, tripartite motif-containing 33; VWF, von Willebrand factor; YWHAG, 14-3-3 protein gamma.

3.4.5 Functional enrichment analysis of plasma proteomics

To better understand how *M. vaccae* strains might be altering different biological functions in plasma to promote stress-resilience behavior, functional enrichment gene analyses, including pathway analysis and gene ontology (GO) analyses, were performed separately on subsets of proteins that were upregulated or downregulated (as measured by two-fold change and *p*-value) by immunization with *M. vaccae* NCTC 11659 or *M. vaccae* ATCC 15483 in home cage control rats (Supplementary Table 3.1), IS exposure in BBS-treated rats (Supplementary Table 3.2), proteins that were prevented from increasing or decreasing after IS in rats immunized with *M. vaccae* NCTC 11659 (Supplementary Table 3.3), proteins that increased or decreased after IS

only in rats immunized with *M. vaccae* NCTC 11659 (Supplementary Table 3.3), proteins that were prevented from increasing or decreasing after IS in rats immunized with *M. vaccae* ATCC 15483 (Supplementary Table 3.4), and proteins that increased or decreased after IS only in rats immunized with *M. vaccae* ATCC 15483 (Supplementary Table 3.4). All functional enrichment results for plasma, including pathway analysis and gene ontology annotations, can be found in Supplementary Tables 3.1–3.4.

There were no pathways enriched nor gene ontology annotations for the two proteins altered in the plasma eight days after the final immunization with *M. vaccae* NCTC 11659; although there were no pathways enriched for the subset of proteins altered in the plasma eight days after the final immunization with *M. vaccae* ATCC 15483, all gene ontology annotations can be found in Supplementary Table 3.1. Among BBS-treated rats, the subset of proteins increased after IS was enriched for ten pathways. The top five pathways were "complement and coagulation cascades," "pertussis," "platelet activation," "*Staphylococcus aureus* infection," "cardiac muscle contraction," and "hypertrophic cardiomyopathy" (Supplementary Table 3.2). The subset of proteins decreased after IS was enriched for six pathways: "complement and coagulation cascades," "peroxisome proliferator-activated receptor (PPAR) signaling pathway," "vitamin digestion and absorption," "African trypanosomiasis," "fat digestion and absorption," and "*Staphylococcus aureus* infection" (Supplementary Table 3.2). Immunization with *M. vaccae* NCTC 11659 prevented stress-induced increases in proteins enriched for the pathway "complement and coagulation cascades," "prion diseases," "systemic lupus erythematosus," and "platelet activation," (Supplementary Table 3.3). Additionally, immunization with *M. vaccae* NCTC 11659 promoted the stress-induced increase of proteins enriched for the pathway

"complement and coagulation cascades" (Supplementary Table 3.3). Immunization with *M. vaccae* NCTC 11659 prevented the stress-induced decrease in proteins enriched for the pathways "complement and coagulation cascades" and "*Staphylococcus aureus* infection" (Supplementary Table 3.3). However, there were no pathways enriched by those proteins whose stress-induced decrease was promoted by immunization with *M. vaccae* NCTC 11659 (Supplementary Table 3.3). Immunization with *M. vaccae* ATCC 15483, like immunization with *M. vaccae* NCTC 11659, prevented the stress-induced increases in proteins enriched for the pathway "complement and coagulation cascades," "prion diseases," "systemic lupus erythematosus," and "platelet activation," implicating that preimmunization with either *M. vaccae* strain prevented stress-induced inflammatory pathways in the plasma (Supplementary Table 3.4). Immunization with *M. vaccae* ATCC 15483 promoted the stress-induced increases in proteins enriched for the pathway "oocyte meiosis" and "neurotrophin signaling pathway" (Supplementary Table 3.4). Immunization with *M. vaccae* ATCC 15483, like immunization with *M. vaccae* NCTC 111659, also prevented the stress-induced decreases of proteins enriched for the pathways "complement and coagulation cascades" and "*Staphylococcus aureus* infection," further suggesting that both *M. vaccae* strains altered the stress-induced immune response in the plasma. There were no pathways enriched by those proteins whose stress-induced decrease was promoted by immunization with *M. vaccae* ATCC 15483 (Supplementary Table 3.4).

3.4.6 Protein-protein interaction (PPI) network analysis of plasma proteomics

To better visualize the effects of IS on the plasma proteome, including how IS may affect proteins enriched for pathway and GO annotations, protein-protein network analysis using STRING (v. 11) was performed individually on the subset of proteins increased or the subset of

proteins decreased after IS among BBS-treated rats, and the networks were mapped using k-means clustering within four or five clusters, respectively.

Within the subset of proteins increased after IS, STRING revealed a significant number of protein interactions, with 31 nodes and 50 association edges (PPI enrichment *p*-value < 1.0E-16) (Figure 3.4A). Immunization with either *M. vaccae* NCTC 11659 or *M. vaccae* ATCC 15483 prevented the stress-induced increase in proteins involved in all five network clusters, which are associated with several enriched KEGG pathways: complement and coagulation cascades, platelet activation, cardiac muscle contraction, and adrenergic signaling in cardiomyocytes (Figure 3.4A; Figure 3.5A; Supplementary Tables 3.2–3.4). Within the subset of proteins decreased after IS, STRING revealed a significant number of protein interactions, with 32 nodes and 72 association edges (PPI enrichment *p*-value < 1.0E-16) (Figure 3.4B). Immunization with either *M. vaccae* NCTC 11659 or *M. vaccae* ATCC 15483 prevented the stress-induced decrease in proteins involved in all five network clusters, which are associated with several enriched KEGG pathways and GO annotations: complement and coagulation cascades, fat digestion and absorption, and PPAR signaling pathway (Figure 3.4B; Figure 3.5B; Supplementary Tables 3.2–3.4). In addition, the STRING database associated the subset of proteins downregulated by IS with a curated pathway from Reactome that was not annotated by DAVID: regulation of IGF by IGFBP, which includes ApoA-I, ApoA-II, ApoE, C4a, C4b, and IGFALS proteins; notably, immunization with either *M. vaccae* NCTC 11659 or *M. vaccae* ATCC 15483 prevented the stress-induced decrease in C4a, C4b, and/or IGFALS (Figure 3.4B; Supplementary Tables 3.3–3.4).

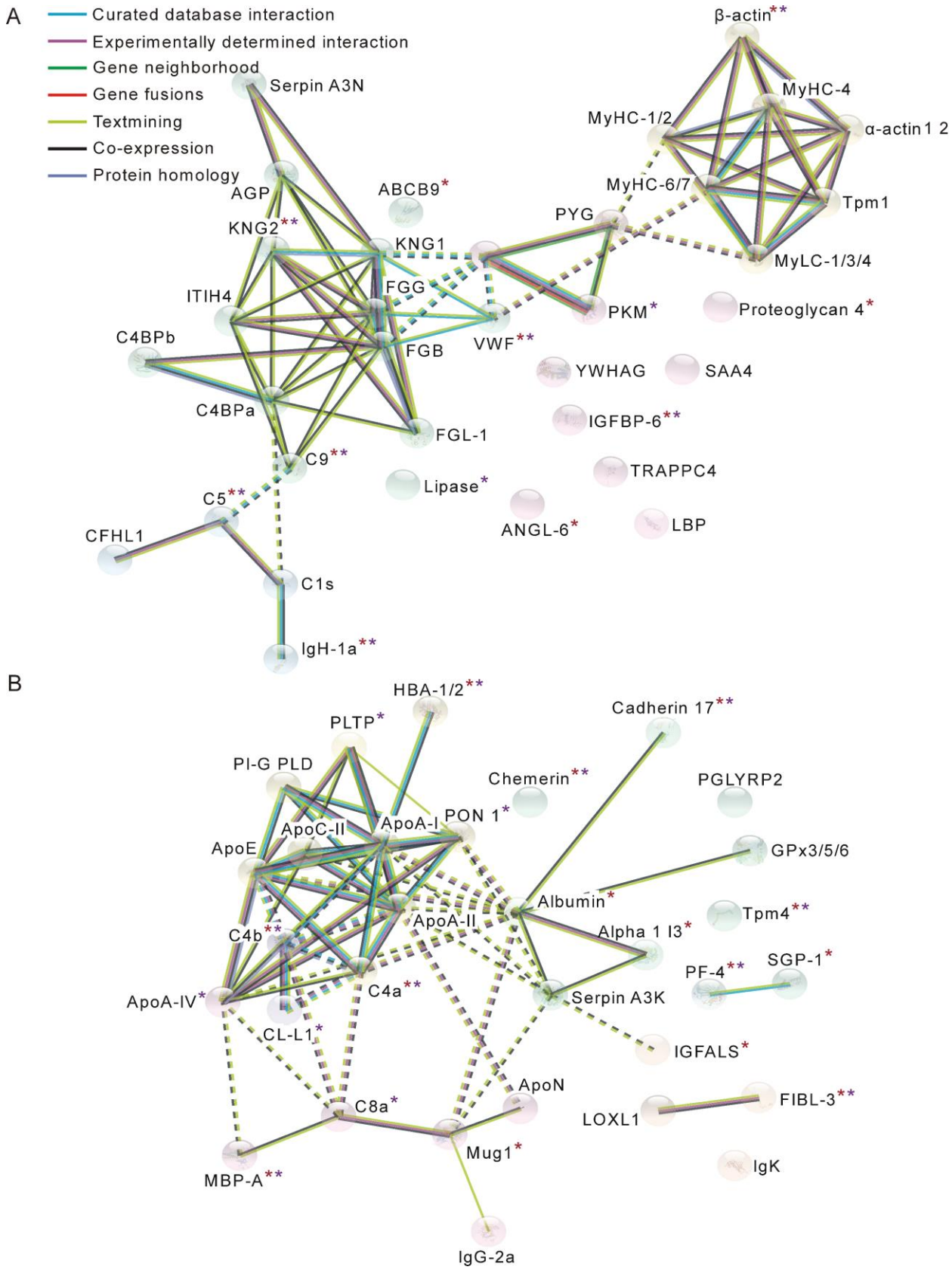
A
Curated database interaction
Experimentally determined interaction
Gene neighborhood
Gene fusions
Textmining
Co-expression
Protein homology
Serpin A3N
AGP
ABCB9*
KNG2**
KNG1
ITIH4
FGG
FGB
C4BPb
C4BPa
C9**
C5**
CFHL1
C1s
IgH-1a**
β-actin**
MyHC-4
MyHC-1/2
α-actin1 2
MyHC-6/7
Tpm1
PYG
MyLC-1/3/4
PKM*
Proteoglycan 4*
VWF**
YWHAG
SAA4
IGFBP-6**
FGL-1
TRAPPC4
Lipase*
ANGL-6*
LBP
B
HBA-1/2**
PLTP*
Cadherin 17**
PI-G PLD
Chemerin**
PGLYRP2
PON 1*
ApoA-I
ApoC-II
ApoE
GPx3/5/6
Albumin*
Tpm4**
ApoA-II
C4b**
Alpha 1 I3*
PF-4**
SGP-1*
C4a**
ApoA-IV*
Serpin A3K
CL-L1*
IGFALS*
ApoN
C8a*
LOXL1
FIBL-3**
Mug1*
IgK
MBP-A**
IgG-2a

Figure 3.4 Protein-protein interaction networks for proteins whose relative abundances (A) increased or (B) decreased in the plasma after inescapable tail shock stress (IS) among BBS-treated control animals, clustered by a k-means algorithm within five clusters.

Asterisks in dark red indicate proteins whose stress-induced increase or decrease was prevented by immunization with *M. vaccae* NCTC 11659 and asterisks in purple indicate proteins whose stress-induced increase or decrease was prevented by immunization with *M. vaccae* ATCC 15483. Associations were computed by STRING database (v.11). Solid lines represent associations within clusters and dashed lines represent associations between clusters. Final sample sizes for plasma analysis were BBS/HC, $n = 8$, BBS/IS, $n = 6$; NCTC/HC, $n = 8$; NCTC/IS, $n = 8$; ATCC/HC, $n = 7$; ATCC/IS, $n = 8$. Abbreviations: ABCB9, ATP-binding cassette sub-family B member 9; AGP, alpha-1-acid glycoprotein; AldoA, fructose-bisphosphate aldolase A; alpha 1 I3, alpha-1-inhibitor 3; ANG-1, angiopoietin-1, ANGL-6, angiopoietin-like 6; ApoA-I, apolipoprotein A-I; ApoA-II, apolipoprotein A-II; ApoA-IV, apolipoprotein A-IV; ApoC-II, apolipoprotein C-II; ApoE, apolipoprotein E; ApoN, apolipoprotein N; C1s, complement C1s subcomponent; C4b, complement C4b; C4BPa, complement C4b-binding protein alpha chain; C8a, complement C8 alpha chain; C9, complement C9; CFHL1, complement component factor h-like 1; CL-L1, collectin liver protein 1 (collectin-10); FGB, fibrinogen beta chain; FGG, fibrinogen gamma chain; FGL-1, fibrinogen-like protein 1; FIBL-3, fibulin-3; GPx3/5/6, glutathione peroxidase matching isoforms 3, 5, and 6; IGFALS, insulin-like growth factor-binding protein complex acid labile subunit; IGFBP-6, insulin-like growth factor-binding protein 6; IgG-2a, Ig-gamma-2A chain C region; IgH-1a, immunoglobulin heavy chain 1a; IgK, Ig kappa chain C region; ITIH4, inter-alpha trypsin inhibitor heavy chain 4; KNG1, T-kininogen 1; KNG2, T-kininogen 2; LBP, lipopolysaccharide binding protein; LOXL1, lysyl oxidase-like 1; MBP-A, mannose-binding protein A; Mug1, murinoglobulin-1; MyHC-1/2, myosin heavy chain matching isoforms 1 and 2; MY-HC-4, myosin heavy chain 4; MyHC-6/7, myosin heavy chain matching isoforms 6 and 7; MyLC-1/3/4, myosin light chain matching isoforms 1, 3, and 4; PF-4, platelet factor 4; PGLYRP2, peptidoglycan recognition protein 2; PI-G PLD, phosphatidylinositol-glycan-specific phospholipase D; PKM, pyruvate kinase; PLTP, phospholipid transfer protein; PON 1, paraoxonase/arylesterase 1; PYG, glycogen phosphorylase; SAA4, serum amyloid A protein; Serpin A3K, serine protease inhibitor A3K; Serpin A3N, serine protease inhibitor A3N; SGP-1, sulfated glycoprotein 1; Tpm1, tropomyosin alpha-1 chain; TRAPPC4, trafficking protein particle complex subunit 4; VWF, von Willebrand factor; YWHAG, 14-3-3 protein gamma.

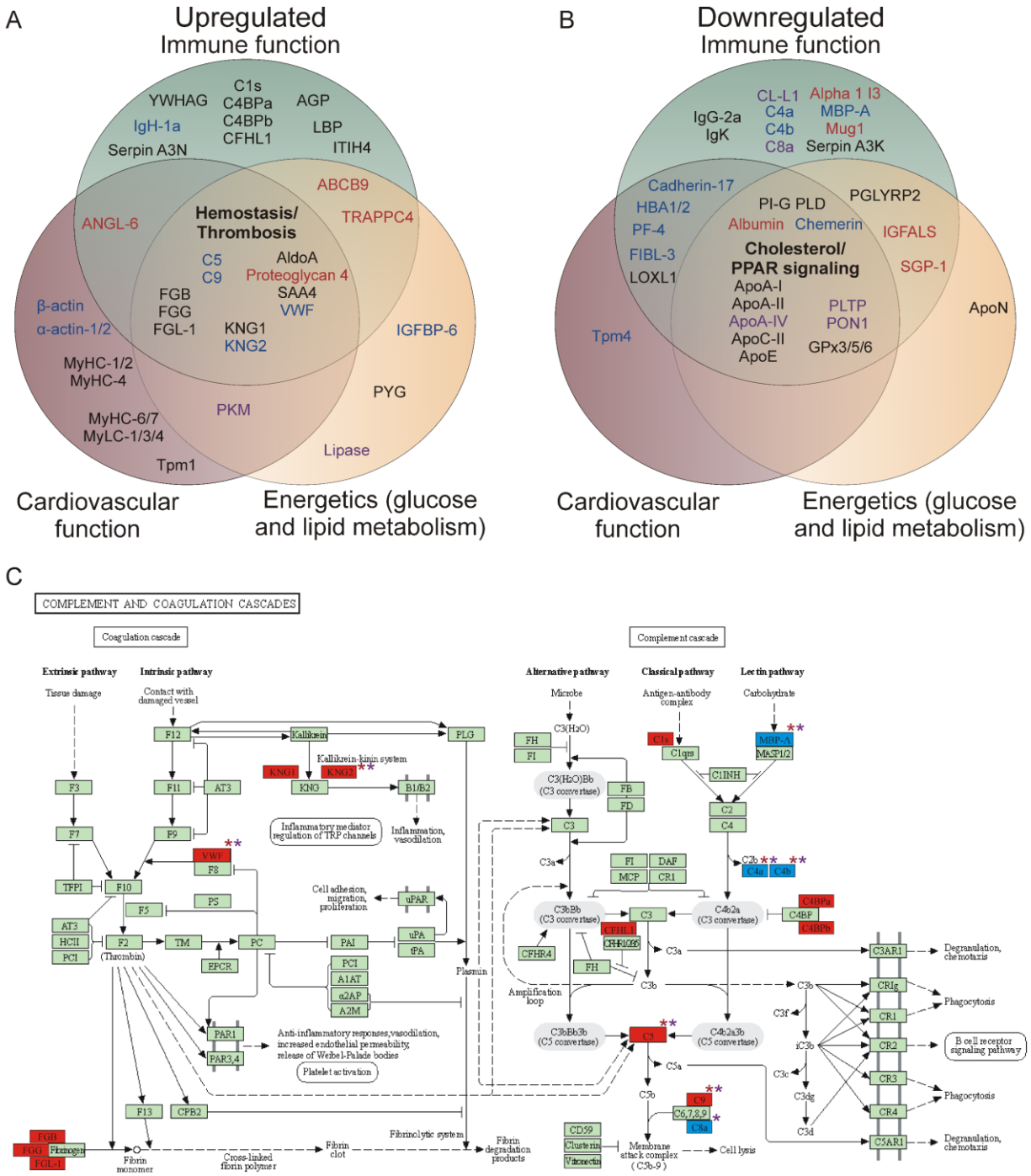

Figure 3.5 Functional categorization of proteins whose relative abundances (A) increased or (B) decreased after inescapable tail shock stress (IS) among BBS-treated control animals, and (C) a diagram showing proteome enrichment of the Kyoto encyclopedia of genes and genomes (KEGG) pathway, "complement and coagulation cascades" (KEGG rno04610).

In (A) and (B), proteins are organized by function into three general categories (indicated by green, immune function; crimson, cardiovascular function; and yellow, energetics (glucose and lipid metabolism) circles) based on gene ontology analyses from UniProt and the Harmonizome databases; overlapping protein functions are indicated in the diagram using bold letters. Protein names in dark red indicate proteins whose stress-induced increase or decrease was prevented by immunization with *M. vaccae* NCTC 11659, protein names in purple indicate proteins whose stress-induced increase or decrease was prevented by immunization with *M. vaccae* ATCC 15483, and protein names in dark blue indicate proteins whose stress-induced increase or decrease was prevented by immunization with both *M. vaccae* strains. In (C), the pathway was adapted, with permission, from the KEGG database (Kanehisa and Goto, 2000). Red boxes indicate proteins whose abundances were increased by IS among BBS-treated animals, and blue boxes indicate proteins whose abundances were decreased by IS among BBS-treated animals. Asterisks in dark red indicate proteins whose stress-induced increase or decrease was prevented by immunization with *M. vaccae* NCTC 11659 and asterisks in purple indicate proteins whose stress-induced increase or decrease was prevented by immunization with *M. vaccae* ATCC 11659. Abbreviations: Abbreviations: ABCB9, ATP-binding cassette sub-family B member 9; AGP, alpha-1-acid glycoprotein; AldoA, fructose-bisphosphate aldolase A; alpha 1 I3, alpha-1-inhibitor 3; ANG-1, angiopoietin-1, ANGL-6, angiopoietin-like 6; ApoA-I, apolipoprotein A-I; ApoA-II, apolipoprotein A-II; ApoA-IV, apolipoprotein A-IV; ApoC-II, apolipoprotein C-II; ApoE, apolipoprotein E; ApoM, apolipoprotein M; ApoN, apolipoprotein N; C1s, complement C1s subcomponent; C4b, complement C4b; C4BPa, complement C4b-binding protein alpha chain; C4BPb, complement C4b-binding protein beta chain; C8a, complement C8 alpha chain; C9, complement C9; CFHL1, complement component factor h-like 1; CL-L1, collectin liver protein 1 (collectin-10); FGB, fibrinogen beta chain; FGG, fibrinogen gamma chain; FGL-1, fibrinogen-like protein 1; FIBL-3, fibulin-3; F13, coagulation factor XIIIa; GPx3/5/6, glutathione peroxidase matching isoforms 3, 5, and 6; IGFALS, insulin-like growth factor-binding protein complex acid labile subunit; IGFBP-6, insulin-like growth factor-binding protein 6; IgG-2a, Ig-gamma-2A chain C region; IgH-1a, immunoglobulin heavy chain 1a; IgK, Ig kappa chain C region; ITIH4, inter-alpha trypsin inhibitor heavy chain 4; KNG1, T-kininogen 1; KNG2, T-kininogen 2; LBP, lipopolysaccharide binding protein; LOXL1, lysyl oxidase-like 1; MBP-A, mannose-binding protein A; Mug1, murinoglobulin-1; MyHC-1/2, myosin heavy chain matching isoforms 1 and 2; MyHC-6/7, myosin heavy chain matching isoforms 6 and 7; MyLC-1/3/4, myosin light chain matching isoforms 1, 3, and 4; PF-4, platelet factor 4; PGLYRP2, peptidoglycan recognition protein 2; PI-G PLD, phosphatidylinositol-glycan-specific phospholipase D; PKM, pyruvate kinase; PLTP, phospholipid transfer protein; PON 1, paraoxonase/arylesterase 1; SAA4, serum amyloid A protein; Serpin A3K, serine protease inhibitor A3K; Serpin A3N, serine protease inhibitor A3N; SGP-1, sulfated glycoprotein 1; Tpm1, tropomyosin alpha-1 chain; TRAPPC4, trafficking protein particle complex subunit 4; VWF, von Willebrand factor.

3.5 Discussion

IS altered the abundance of proteins associated with immune response, cardiovascular function, and metabolic function, including those related to the “complement and coagulation cascades”

pathway, when assessed 24 h following the stressor. Interestingly, prior immunization with either *M. vaccae* NCTC 11659 or *M. vaccae* ATCC 15483 largely prevented stress-induced alterations in the complement cascade, consistent with the anti-inflammatory and immunoregulatory effects of the two mycobacterial strains. Our data may also suggest a role for *M. vaccae* strains in the protection of intestinal epithelial and vascular endothelial barriers such as at the gut-vascular barrier. Alternatively—or in parallel—*M. vaccae* strains may confer protection against the activation, migration, or differentiation of proinflammatory bone marrow-derived monocytes, which traffic from the bone marrow into the vasculature after stress, driving arterial cholesterol metabolism and promoting atherosclerosis. Immunization with *M. vaccae* strains might help to regulate the metabolic processes in the plasma that are disrupted after exposure to IS, although the mechanisms by which *M. vaccae* NCTC 11659 and *M. vaccae* ATCC 15483 influence metabolic homeostasis may differ. Collectively, our study provides evidence that immunization with either *M. vaccae* NCTC 11659 or *M. vaccae* ATCC 15483 promotes resilience to IS-induced changes in the plasma proteome that are associated with the enhancement of anxiety-like defensive behavioral responses.

3.5.1 Evidence that IS altered the abundance of proteins associated with immune response (including those related to the "complement and coagulation cascades" pathway and a biological signature of inflammatory monocytes), cardiovascular function, and metabolic function in plasma, when assessed 24 h following the stressor

IS altered the abundance of proteins associated with cardiovascular function, immune signaling (especially proteins related to the "complement and coagulation cascades" pathway and a biological signature of inflammatory monocytes), and energetic homeostasis in plasma, when

assessed 24 h after stressor exposure (Figure 5; Supplementary Table 2; KEGG pathway rno04610).

Coagulation cascades are activated by two pathways: the tissue factor (TF, also known as F3, coagulation factor III, or extrinsic) pathway, which can be activated by inflammatory monocytes during times of hypoxia, tissue damage, endotoxemia, or sepsis (for review, see Pawlinski and Mackman, 2010; Smith et al., 2015), and the contact (intrinsic) pathway, which is activated by the kininogen-kallikrein pathway during times of cellular apoptosis and pathogen infection, including sepsis (Smith et al., 2015). Increased cardiovascular output, hyperventilation, and vascular endothelial or myocardial injury can contribute to activation of coagulation pathways, such as during physical or emotional trauma (Gao et al., 2020; Satyam et al., 2019; Turdi et al., 2012; Von Känel et al., 2006). Among the pathways that were enriched in our protein set altered by IS were “cardiac muscle contraction,” “hypertrophic cardiomyopathy,” “dilated cardiomyopathy,” and “adrenergic signaling in cardiomyocytes” which might suggest increased sympathetic nervous system activity, increased muscle contraction, cardiomyocyte contractile dysfunction, or myocardial injury/autophagy due to stress (Chiong et al., 2011; Gao et al., 2020; Turdi et al., 2012). The proteins involved in these pathways, namely actin, myosin, and tropomyosin proteins, were increased after IS regardless of pretreatment, implicating a general physiological trauma response to the IS paradigm (Verbitsky et al., 2020). Likewise, the coagulation-promoting fibrinogen subunits involved in both TF and contact pathways, FGB, FGG, FGL-1, were increased after IS regardless of pretreatment.

Of the proteins altered in our dataset, at least 36 proteins are found in the secretome of human inflammatory bone marrow-derived monocytes or monocyte-derived cells, consistent with the hypothesis that stressor or trauma exposure activates the SNS and induces release of inflammatory monocytes from the bone marrow that subsequently traffic to different organ systems, including the central nervous system (Ciborowski et al., 2007; Garcia-Sabaté et al., 2020; Lubbers et al., 2017; Oh et al., 2016; Sintiprungrat et al., 2010). Hypertension is associated with the trafficking of monocytes to the brain, inducing peripheral and neural inflammatory events (Santisteban et al., 2017). As mentioned above, increases in numbers of circulating monocytes are thought to reflect chronic inflammation, and have been identified, among the white blood cell subtype counts, to be an independent predictor of cardiovascular disease risk (Kim et al., 2019). Meanwhile, monocyte:lymphocyte ratios have also been shown to be predictive of a chronic inflammatory state (Cherfane et al., 2015), and the inflammatory state of monocytes has been linked to depression severity, childhood adversity, suicide risk, and PTSD (Keaton et al., 2019; Kuan et al., 2019; Miller and Raison, 2016; Neylan et al., 2011; Nowak et al., 2019; Schiweck et al., 2020; Serafini et al., 2020). It has been previously demonstrated that peripheral monocyte abundance is a biomarker of PTSD risk (Schultebraucks et al., 2020), while increased SNS activation may be responsible for the development of hypertension and cardiovascular disease in persons with PTSD (Brudey et al., 2015; Park et al., 2017).

Finally, IS exposure in BBS-treated control animals altered phospholipid metabolism and other metabolic homeostatic processes. Prominent in these effects, based on gene ontology, biological process analysis, were effects on “phospholipid efflux,” “cholesterol efflux,” “phosphatidylcholine metabolic process,” “cholesterol metabolic process,” “triglyceride

homeostasis," and "lipoprotein metabolic process." Together, these findings are consistent with activation of phospholipid and lipid metabolism, important for energetic homeostasis following stress exposure, and activation of the arachidonic acid cascade, which has been implicated in stress-induced inflammation and inflammatory depression (Suneson et al., 2021).

These effects of IS on cardiovascular function, immune signaling (including the "complement and coagulation cascades" pathway, and a biological signature of inflammatory monocytes), phospholipid metabolism, and energy homeostasis, will be discussed in detail below, in the context of the potential for *M. vaccae* NCTC 11659 or *M. vaccae* ATCC 15483 to attenuate the effects of IS and promote stress resilience.

3.5.2 Evidence that immunization with M. vaccae strains prevent IS-induced changes in complement and coagulation cascades

As mentioned above, immunization with *M. vaccae* strains prevented IS-induced changes in complement and coagulation cascades. Specifically, immunization with either *M. vaccae* strain prevented the IS-induced increases of KNG2 (also mapped as kininogen-like 1 (KNG1L1) or kininogen 1) and VWF, two major players in the contact pathway of the coagulation cascade (Figure 3.5C). These findings might suggest that, although *M. vaccae* strains did not necessarily prevent increases of the TF pathway (i.e., extrinsic pathway), prior immunization with *M. vaccae* strains prevented stress-induced increases of the contact pathway (i.e., intrinsic pathway). Interestingly, it is the contact pathway, rather than the TF pathway, that tends to positively correlate with symptoms of posttraumatic stress disorder (PTSD) (Ho et al., 2016), and increases of VWF are most commonly associated with PTSD (Robicsek et al., 2011; Von Känel et al., 2006). This is particularly interesting in the context that immunization with *M. vaccae* NCTC

11659 has been shown to prevent development of a PTSD-like syndrome in a mouse model of PTSD, the chronic subordinate colony housing model (Langgartner et al., 2019; Reber et al., 2016b, 2016a).

There was also a significant interaction effect of *M. vaccae* NCTC 11659 x IS on the abundance of factor XIIIa (F13 in Figure 3.5C), a protein critical to the formation of fibrin clots (Figure 3.5C) and directly activated by thrombin, based on our GLM. Upon closer inspection of pairwise comparisons, we found that IS tended to increase the abundance of factor XIIIa ($\log_2$[fold change] = 0.50); however, among animals immunized with either *M. vacccae* NCTC 11659 or *M. vaccae* ATCC 15483, IS tended to decrease the abundance of factor XIIIa ($\log_2$[fold change] = –0.40 and $\log_2$[fold change] = –0.27, respectively).

These results might suggest that immunization with *M. vaccae* strains generally decreased the overall severity of the coagulation cascades induced by IS, possibly by mitigating coagulation initiated by the contact pathway. This might suggest that *M. vaccae* strains attenuate IS-induced damage to blood vessels, bacterial leakage into the blood (i.e., from the gut), or both. Considering that immunization with *M. vaccae* NCTC 11659 protects rodents from stress-induced inflammation (Amoroso et al., 2019; Fonken et al., 2018; Frank et al., 2018b; Loupy et al., 2021; Reber et al., 2016b; Smith et al., 2020), it could be that *M. vaccae* strains specifically attenuate the proinflammatory mediators that contribute to aberrant signaling of the contact pathway by protecting blood vessel endothelium from injury.

Interestingly, prior immunization with either *M. vaccae* NCTC 11659 or *M. vaccae* ATCC 15483 largely prevented stress-induced alterations in the complement cascade, consistent with the anti-inflammatory effects of the two mycobacterial strains (Loupy et al., 2021). The complement cascade is an innate immune response to pathogens and is activated upon recognition of pathogenic moieties or tissue damage (for review, see Dunkelberger and Song, 2010). Three pathways have been described: classical, lectin, and alternative pathways (Figure 3.5C). However, all pathways lead to, among other things, the creation of the membrane attack complex (MAC) for the destruction of pathogens via the "terminal pathway" (i.e. from the formation of C5 convertase, encompassing the sequence of interactions between components C5b, C6, C7, C8 and C9, leading to the production of a MAC that has the ability to disrupt cell membranes) (Dunkelberger and Song, 2010). Dysregulation of complement cascades (i.e., altered abundance or function of complement proteins) has been linked to trauma- and stress-related psychiatric disorders, including PTSD (Hovhannisyan et al., 2010; Oganesyan et al., 2009) and depression (Crider et al., 2018). Studies have suggested that persons with PTSD exhibit a shift in baseline plasma hemolytic activity featuring hyperactivity of the classical complement pathway, hypoactivity of the alternative complement pathway, and hyperactivity of the terminal pathway (Hovhannisyan et al., 2010; Oganesyan et al., 2009). In our study, IS decreased C4a, C4b, C8a, and MBP-A, consistent with altered classical and lectin pathways, but IS increased C1s, C4Bpa, C4BPb, C5, C9, and CFHL1, suggesting that stress promoted a physiological shift toward increased activation of the terminal pathways (Figure 3.5C). In all, prior immunization with *M. vaccae* strains prevented the stress-induced alteration of five out of the ten (50%) complement proteins.

Prior immunization with either *M. vaccae* NCTC 11659 or *M. vaccae* ATCC 15483 prevented the IS-induced decrease of C4a, C4b, MBP-A and the IS-induced increase of C5 and C9. However, immunization with either *M. vaccae* strain did not prevent the stress-induced increase of C4BPa and C4BPb, which inhibit activation of the C3 convertase within classical and lectin pathways, nor CFHL1, which inhibits activation of C5 convertase within the alternative pathway (Heinen et al., 2009) (Figure 3.5C). However, among rats immunized with *M. vaccae* NCTC 11659 or *M. vaccae* ATCC 15483, IS increased the abundance of an uncharacterized protein with UniProt ID A0A0G2K975, similar to complement factor H (CFH)-related protein. Although its function is unknown, the additional CFH family member is predicted by the Reactome Pathway (version 75) to play a role in regulating the complement cascade (Fabregat et al., 2018). Our data that IS induces complement and coagulation cascade signaling, perhaps in response to translocation of bacteria from the gut lumen into the circulation, consistent with the increases in circulating LPS 24 h after IS (Maslanik et al., 2012), and our own finding of increased plasma LBP concentrations 24 after IS. Furthermore, our data suggest that immunization with *M. vaccae* strains attenuates IS-induced complement and coagulation signaling. However, one hypothesis is that immunization with *M. vaccae* strains prevents IS-induced changes in intestinal epithelial and gut-vascular barriers (see below). It remains to be determined how immunization with *M. vaccae* strains attenuates IS-induced complement and coagulation signaling, as well as how immunization with *M. vaccae* strains might mitigate IS-induced damage to blood vessel endothelium, effectively preventing activation of the contact pathway.

3.5.3 Evidence that immunization with M. vaccae strains prevents IS-induced changes in intestinal epithelial and gut-vascular barriers

Our data may also suggest a role for *M. vaccae* strains in the protection of intestinal epithelial and vascular endothelial barriers such as at the gut-vascular endothelial barrier. Acute psychological stress and injury-induced disturbance of gut permeability are well described in the literature, often corresponding to proinflammatory signaling in the vasculature (Ait-Belgnaoui et al., 2012, 2005; Alsaigh, 2015). Consistent with the hypothesis that IS induces a "leaky gut", previous studies have shown increased plasma LPS concentrations 24 h following exposure of rats to IS (Maslanik et al., 2012). Upon release of glucocorticoids like corticosterone, intestinal permeability is increased by glucocorticoid actions at cell-cell junctions (Meddings and Swain, 2000; Zheng et al., 2017). Previous studies show that preimmunization with *M. vaccae* NCTC 11659 prevents stress-induced colitis in mice in the chronic subordinate colony housing (CSC) paradigm (Amoroso et al., 2019; Reber et al., 2016b). In the current study, we observed that IS decreased the abundance of plasma cadherin-17 and that immunization with *M. vaccae* strains prevented this effect. Cadherin-17 is a specialized adhesive protein for intestinal epithelium, and knockout of cadherin-17 causes increased susceptibility to dextran sulfate sodium (DSS)-induced colitis in mice (Chang et al., 2018). Immunization with *M. vaccae* strains also prevented the stress-induced alteration of plasma proteins that affect the function and integrity of the vascular endothelium. Gut permeability is, in part, dependent upon the gut-vascular barrier, which has emerged as a secondary filtration system to the epithelial barrier that regulates the translocation of bacteria or corresponding antigens into the bloodstream (Spadoni et al., 2015). Immunization with *M. vaccae* NCTC 11659 promoted a stress-induced increase of proteins associated with the GO biological process annotation "negative regulation of endothelial cell apoptotic process", which included the proteins ANG-1 and FGA (Supplementary Table 3.3). ANG-1, increased after IS only among rats immunized with *M. vaccae* NCTC 11659, enhances endothelial barrier

function by stabilizing cell-cell junctions (Gaonac'h-Lovejoy et al., 2020; Pizurki et al., 2003). Many proinflammatory proteins involved in coagulation cascades, promoted by IS but prevented by *M. vaccae* immunizations, such as kininogen-1, platelet-activating factor, or thrombin, increase permeability of the vascular endothelium (for review, see Wettschureck et al., 2019), as do increases in VWF (Kawecki et al., 2017). Likewise, immunization with *M. vaccae* strains prevented the IS-induced decrease of a number of proteins that may be important for function, growth, and integrity of the vasculature, like chemerin (Zhao and Wang, 2011), HBA-1/2 (Straub et al., 2012), FIBL-3 (Lin et al., 2016), and Tpm4 (Jeong et al., 2017; Ziegler et al., 2012).

By buffering against the disruption of epithelial and vascular barriers after IS, immunization with *M. vaccae* NCTC 11659 and *M. vaccae* ATCC 15483 might help mitigate stress-induced translocation of gut microbes, including gram-negative, LPS-carrying bacteria, into gut mucosal tissues, or into systemic circulation. These effects of *M. vaccae* are likely mediated through the attenuation of stress-induced inflammatory responses that would lead to increased intestinal permeability or "leaky gut" (Amoroso et al., 2019; Reber et al., 2016b), and thus we would expect *M. vaccae* strains to also mitigate downstream immune activation caused by microbial translocation into mucous tissues and into the blood. This hypothesis is supported by the finding that immunization with *M. vaccae* NCTC 11659 prior to CSC stress and administration of DSS in a murine model of inflammatory bowel disease decreases the number of viable mesenteric lymph node cells and prevents stress-induced increases in anti-CD3 stimulated release of interferon gamma and interleukin 6 from freshly isolated mesenteric lymph node cells (Reber et al.,2016). Furthermore, through similar mechanisms, immunization with *M. vaccae* strains may attenuate IS-induced secretion of acute phase response proteins from the liver, and attenuate

proinflammatory activation of circulating bone marrow-derived monocytes (Miller and Raison, 2016), which are thought to traffic to the central nervous system and drive neuroinflammation (discussed further below).

3.5.4 Evidence that immunization with M. vaccae strains attenuates IS-induced secretion of acute-phase response proteins

Of the proteins altered by IS, AGP (also known as orosomucoid), AldoA, chemerin, C4BPa, FGG, HBA1/2, IgG-2a, IgH-1a, IgK, LBP, LOXL1, MBP-A, PGLYRP2, Serpin A3N, and VWF are annotated by either UniProt or the Harmonizome databases as acute-phase response proteins that are increased following exposure to bacteria or LPS. Positive acute-phase proteins serve as part of the innate immune system response to microbes or microbe-associated molecular patterns (MAMPs).

Evidence of IS-induced increases in MAMPs include increases in LBP, which is increased after IS regardless of immunization with *M. vaccae* strains. Plasma LBP negatively correlated with juvenile social exploration (JSE) behavior, wherein increased abundances of LBP in the plasma corresponded to decreased social interaction after IS (Supplementary Table 3.5), and we recently reported that prior immunization with either *M. vaccae* strain prevents IS-induced reductions of JSE behavior (Loupy et al., 2021). Abundances of KNG1 and KNG2, which increased in plasma after IS, also negatively correlated with JSE behavior (Supplementary Table 3.5). It is also thought that KNG1 and KNG2, by acting in the kallikrein-kinin pathway, may be produced in response to microbes, as an anti-bacterial and anti-fungal proteins (Cagliani et al., 2013; Ding et al., 2018; Köhler et al., 2020; Nordahl et al., 2005), although the extent to which KNG1 and KNG2 prevent or promote inflammation in this context is debated (Ding et al., 2018; Köhler et

al., 2020). In line with these findings, although not significant in our pairwise comparison testing, there was a significant effect of IS on kallikrein protein abundance based on our GLM. The stress-induced increase of KNG2 was completely prevented by immunization with either *M. vaccae* type strain, while the stress-induced increase of KNG1, although not prevented by prior immunization with either of the *M. vaccae* strains, was much smaller among animals immunized with *M. vaccae* strains (i.e., not a two-fold change greater) compared to BBS-treated animals. PF-4 is an anti-microbial peptide most commonly secreted by platelets that helps to opsonize gram-positive and gram-negative bacteria for destruction by host immune cells (Palankar et al., 2018). Of particular significance are the complement proteins C5 and C9, which are critical players in the formation of the MAC (Dunkelberger and Song, 2010); prior immunization with either *M. vaccae* NCTC 11659 or *M. vaccae* ATCC 15483 prevented the IS-induced increases in C5 and C9. In all, immunization with *M. vaccae* NCTC 11659, immunization with *M. vaccae* ATCC 15483, or immunization with both *M. vaccae* strains, prevents the stress-induced alteration of nine out of a total of 20 (45%) of these microbe-responsive proteins. GO and pathway analyses of proteins altered after IS also suggested enrichment for processes involved in pathogenic infection, including pathways such as “African Trypanosomiasis,” “*Staphylococcus aureus* infection,” and “pertussis” and biological processes including several responses to complement cascades as well as “response to lipopolysaccharide” (Supplementary Table 3.2); immunization with *M. vaccae* strains largely prevented IS-induced changes to the abundance of proteins involved in host antimicrobial response.

3.5.5 Evidence that immunization with M. vaccae strains prevents release or migration of inflammatory monocytes from bone marrow into systemic circulation

M. vaccae strains may confer protection against the release, differentiation, or migration of proinflammatory bone marrow-derived monocytes, which, following stimulation by the sympathetic nervous system, traffic from the bone marrow into the vasculature after stress, driving arterial cholesterol metabolism and promoting atherosclerosis (for review, see Miller and Raison, 2016; Pennings et al., 2006; Shashkin et al., 2005). For example, IS-induced changes in abundances of both C5 and MBP-A are prevented by prior immunization with either strain of *M. vaccae*. C5 and MBP-A, described above as players in the complement cascade, are independently critical for the migration of hematopoietic stem/progenitor cells (including monocytes) from the bone marrow into the vasculature (Adamiak et al., 2017; Lee et al., 2009; Ratajczak et al., 2018). Complement cascade pathways and monocyte infiltration are highly integrated pathways that are initiated by the innate immune system. Complement proteins can be further secreted by monocytes or monocyte-derived macrophages that are activated by damage-associated molecular patterns (DAMPs) from injured tissue or by pathogen-associated molecular patterns (PAMPs) from "leaky gut" (Lubbers et al., 2017; Weber et al., 2017; Wohleb et al., 2015). ATP, which is released during stress (for review, see Fleshner et al., 2017), including LPS-induced inflammatory stress (Cauwels et al., 2014), is an important DAMP that can activate the NOD-, LRR- and pyrin domain-containing protein 3 (NLRP3) inflammasome-producing interleukin (IL)-1β pathway; it can also bind to MBP-A to promote monocyte transendothelial migration from the bone marrow into the systemic circulation (Ratajczak et al., 2018). Likewise, LPS itself is a well-described PAMP that promotes monocyte release into the systemic circulation (Fleshner et al., 2017). Once activated by DAMPs or PAMPs and translocated from bone marrow into the blood, inflammatory bone-marrow derived monocytes can differentiate into macrophages, phagocytosing cholesterol in the blood and promoting atherosclerosis

(Maguire et al., 2019). Additionally, inflammatory monocytes might migrate into the brain to perpetuate anxiety- and depressive-like behavior in rodents (Miller and Raison, 2016; Reader et al., 2015; Weber et al., 2017; Wohleb et al., 2013).

It could be that IS activated bone marrow-derived monocytes and induced monocyte infiltration into the systemic circulation and differentiation to macrophages regardless of pretreatment, but that prior immunization with either *M. vaccae* NCTC 11659 or *M. vaccae* ATCC 15483 primed monocytic cells toward an alternative or immunoregulatory phenotype. Monocytes stimulated with different immune adjuvants will produce and secrete unique proteomes containing varying abundances of proteins that are classically associated with inflammatory monocytes and those that are not (Oh et al., 2016); likewise, monocytes can be classically or alternatively activated to differentiate into a variety of macrophage phenotypes commonly classified as M1 (classic) or M2 (alternative) (Orecchioni et al., 2019). Indeed, prior administration of *M. vaccae* NCTC 11659 prevents the stress-induced exaggeration of secretion of IL-6 and IFN-γ from mesenteric lymph node cells isolated from CSC-exposed mice and treated with an anti-CD3 antibody (Reber et al., 2016b). In addition, a free fatty acid isolated from *M. vaccae* NCTC 11695, 10(*Z*)-hexadecenoic acid, shifts murine peritoneal macrophages toward an anti-inflammatory phenotype via PPARα activation; pretreatment with 10(*Z*)-hexadecenoic acid one hour prior to LPS treatment decreases LPS-induced secretion of IL-6 and stimulates differential expression of 203 genes, primarily associated with immune and metabolic functions, compared to untreated macrophages stimulated with LPS (Smith et al., 2019).

Supporting the idea that IS generally promoted monocyte infiltration and differentiation, we found that 24 hours after IS, among BBS-treated rats, *M. vaccae* NCTC 11659-treated rats, or *M. vaccae* ATCC 15483-treated rats, abundances of several apolipoproteins (i.e., ApoA-I, ApoA-II, ApoA-IV, ApoC-I, ApoC-II, ApoE, ApoM, and ApoN) were dramatically decreased in plasma, consistent with enhanced macrophage lipid and cholesterol metabolism (Remmerie and Scott, 2018; Shashkin et al., 2005). Furthermore, ABCB9, which was increased in plasma after IS among BBS and *M. vaccae* ATCC 15483-treated animals but not among *M. vaccae* NCTC 11659-treated animals (log2[fold change] = 0.45, $p = 0.11$), is highly increased among monocyte-derived macrophages and dendritic cells compared to undifferentiated monocytes (Demirel et al., 2007). YWHAG, which, in our study, was also increased in plasma 24 hours after IS regardless of pretreatment, is secreted from HIV-1-infected monocyte-derived macrophages (Ciborowski et al., 2007). Of the proteins altered in our dataset, at least 36 proteins including albumin, AldoA, AGP, ApoA-I, ApoA-II, ApoA-IV, ApoC-II, ApoE, β-actin, BiP, C1s, C4, C4a, C5, C8, C9, factor XIIIa, FGA, FGB, FIBL, haptoglobin, IgG, IgK, LOXL1, kallikrein, PKM, PSMA7, PF-4, PYG, serine proteinase inhibitors, TfR1, Tpm4, YWHAE, YWHAG, VDB, VWF are found in the secretome of human monocytes, monocyte-derived dendritic cells, or monocyte-derived macrophages, and thus their secreted abundance may be altered depending on the specific mechanism of monocyte activation and differentiation into dendritic cells and macrophages (Ciborowski et al., 2007; Garcia-Sabaté et al., 2020; Lubbers et al., 2017; Oh et al., 2016; Sintiprungrat et al., 2010). Two subsets of circulating monocytes are observed in humans and rodents (Gordon and Taylor, 2005) (characterized by differential CD14 and CD16 expression in humans (Passlick et al., 1989), CCR2, CX3CR1 and Ly6C in mice (Serbina and Pamer, 2006; Tsou et al., 2007), and CD43 expression in rats (Ahuja et al., 1995;

Barnett-Vanes et al., 2016)). In rats, CD43 Hi and Lo monocytes are thought to be analogous to the Ly6C Lo (non-classical) and Hi (classical; i.e. inflammatory) murine monocytes, respectively (Strauss-Ayali et al., 2007; Sunderkötter et al., 2004). It is likely that immunization with *M. vaccae* strains and subsequent exposure to IS differentially influenced monocyte-derived macrophage protein expression and secretomes in vivo (Reber et al., 2016b; Smith et al., 2019). For example, expression of *Apoc2* (encoding ApoC-II), *Hp* (encoding haptoglobin), *Orm1* (encoding AGP), and *Saa3* (encoding a serum amyloid A protein) were increased in LPS-stimulated peritoneal macrophages pretreated with the anti-inflammatory, *M. vaccae* NCTC 11659-derived lipid, 10(*Z*)-hexadecenoic acid, compared to LPS-stimulated macrophages that were previously untreated (Smith et al., 2019). Given our experimental design, it will be difficult to discern exactly which proteins are attributable to inflammatory or alternatively activated monocytes and how exactly monocytes might be alternatively activated by *M. vaccae* strains and stress in vivo.

Nevertheless, it is telling that, compared to BBS-treated animals, rats immunized with either *M. vaccae* NCTC 11659 or *M. vaccae* ATCC 15483 exhibited differential plasma proteomes associated with monocyte-derived macrophages, most notably 24 hours after IS. For instance, the IS-induced increase of the proinflammatory mediators C5, C9, KNG2, and VWF, associated with the secretomes of monocytes, monocyte-derived dendritic cells, or monocyte-derived macrophages, were prevented by immunization with *M. vaccae* strains. Of the proteins upregulated by IS and secreted by monocytes, PKM, SAA4, Serpin A3N, and Tpm1 were negatively correlated with JSE behavior (Supplementary Table 3.5), and among the proteins downregulated by IS, LOXL1 was positively correlated with JSE behavior (Supplementary Table

3.5). Although immunization with *M. vaccae* strains did not prevent stress-induced changes in the abundance of many of these proteins, correlations between these proteins and JSE behavior would suggest, based on the finding that *M. vaccae* immunizations prevented stress-induced reductions in exploratory behavior, that *M. vaccae* strains may have exerted some stress-buffering effects on the abundance of monocyte-secreted proteins (Supplementary Table 3.5). Among the proteins decreased by IS, we found that prior immunization with *M. vaccae* strains prevented stress-induced decreases of PF-4 and the adipokine chemerin, which both play a role in monocyte signaling, including migration and adhesion, via C-C motif chemokine receptor 1 (CCR1) and chemokine-like receptor 1 (ChemR23; chemerin receptor), respectively (Dimitriadis et al., 2018; Fox et al., 2018). PF-4 is one of few growth factors that can induce the differentiation of monocytes into macrophages that are thought to play a role in atherosclerosis, and PF-4 stimulation in monocytes promotes the differentiation of macrophages with unique phenotypes consisting of both M1 and M2 characteristics (Gleissner et al., 2010). Interestingly, gene expression profiling of monocytes among males with PTSD show reduced expression of both the *PF4* and *PSAP* genes, but a decrease of *PF4* was reported in two separate studies (Kuan et al., 2019; Neylan et al., 2011). Chemerin binds to C-C motif chemokine receptor 2-like (CCRL2) located on monocyte cells, but does not promote signaling cascades, thereby preventing excessive inflammatory signaling in monocytes (Regan-Komito et al., 2017). Additionally, TRIM33, which is increased after IS among rats immunized with *M. vaccae* strains, is a regulator of transforming growth factor-β (TGF-β) signaling that is expressed in blood monocytes; it is thought that monocytic expression of TRIM33 is imperative for protection against colitis (Petit et al., 2019).

3.5.6 Evidence that differential effects of M. vaccae strains on lipid homeostasis may be due to unique interactions with the host

In addition to regulating inflammatory processes, monocytes and macrophages are major contributors to lipid metabolism and cholesterol homeostasis (Fernandez-Ruiz et al., 2016; Remmerie and Scott, 2018). Monocytes and macrophages participate in "lipid loading" of cholesterol, cholesteryl esters, and lysophosphatidylcholine to produce foam cells, which produce atherosclerotic lesions (Pennings et al., 2006; Shashkin et al., 2005). Cholesterol is taken up through low-density lipoprotein receptors (LDLRs), LDL receptor-related protein (LRP), or very-low-density lipoprotein receptor (VLDLR) (Pennings et al., 2006). Depending on how they are activated (i.e., classically or alternatively), monocytes and macrophages can differentially express metabolic processing proteins, receptors, and enzymes (Batista-Gonzalez et al., 2020; Fernandez-Ruiz et al., 2016; Viola et al., 2019); simultaneously, the cholesterol products taken up, combined with environmental signaling input, can modify foam cell formation (Shashkin et al., 2005).

Evidence suggests that IS alters phospholipid metabolism. Biological processes downregulated by IS in BBS-treated animals included "phospholipid efflux", "phosphatidylcholine metabolic process", "phosphatidylcholine-sterol O-acyltransferase activator activity", and "phosphatidylcholine binding." One hypothesis is that IS induces activation of the arachidonic acid cascade, leading to synthesis of inflammatory lipids, including eicosanoids, a process that has been suggested to contribute to inflammatory depression (Suneson et al., 2021). IS-induced decreases in "phosphatidylcholine metabolic process" were prevented by immunization with *M. vaccae* ATCC 15483. Meanwhile, a previous study in mice found that immunization with *M. vaccae* NCTC 11659 increases a family of lysophospholipids, including lysophosphocholine

(22:6) (Foxx et al., 2021). Thus, *M. vaccae* strains may alter the phospholipid metabolism, including the balance of inflammatory and anti-inflammatory lipid signaling molecules that are derived from phospholipids (Suneson et al., 2021).

PPAR signaling, especially PPARγ, play a prominent role in determining the outcome of macrophage metabolism (Batista-Gonzalez et al., 2020; Chinetti et al., 2001; Shashkin et al., 2005; Viola et al., 2019). Polarized macrophage phenotypes will also exhibit differential rates of glycolysis, fatty acid oxidation, eicosanoid production, and tryptophan metabolism, contributing to organismal energetics (Batista-Gonzalez et al., 2020; Shashkin et al., 2005; Viola et al., 2019). Our data suggest that *M. vaccae* strains may help to regulate the metabolic processes in the plasma that are disrupted after exposure to IS, although the mechanisms by which *M. vaccae* NCTC 11659 and *M. vaccae* ATCC 15483 influence metabolic homeostasis may differ. Prior proteomic analyses have shown that one week following immunization with *M. vaccae* NCTC 11659, rats exhibit evidence of altered lipid metabolism in plasma and CSF among home cage control animals (Loupy et al., 2020). It is also known that 10(*Z*)-hexadecenoic acid isolated from *M. vaccae* NCTC 11659 activates PPARα signaling in peritoneal macrophages (Smith et al., 2019). We recently reported that, among home cage control animals, immunization with either *M. vaccae* strain decreased *Pparg* (encoding PPARγ) mRNA expression in the liver, but only *M. vaccae* NCTC 11659 prevented a further stress-induced decrease of *Pparg* mRNA expression (Loupy et al., 2021). Here, in the plasma proteome, we found that IS decreased the abundance of proteins associated with PPAR signaling; however, our data suggest that only *M. vaccae* ATCC 15483 partially prevents stress-induced reductions of these proteins in plasma, namely ApoA-IV, PLTP, and PON 1. One hypothesis is that lipids located on the mycobacterial cell wall can

contribute to the alternative activation or reprogramming of monocytes or monocyte-derived macrophages to alter plasma metabolism, possibly through PPAR signaling. Further experiments should explore the plasma metabolomes and lipidomes of animals immunized with *M. vaccae* type strains and exposed to IS.

3.5.7 Limitations

Although our study is the first to demonstrate effects of IS and *M. vaccae* strains on the plasma proteome, there are a number of limitations of the study that should be considered. It is important to point out that any functional associations of proteins are speculative in nature because we did not measure the activity of enzymes in specific pathways. Likewise, although associations can be made between our independent variables and protein abundance in plasma, our data do not establish direct causal relationships. Proteins detected by mass spectrometry were those whose abundance was above the detection limit, and thus not all proteins in plasma were captured; it will be important for future studies to target specific proteins of interest based on the exploratory proteomics results. This is especially important for the plasma proteome, in which several physiological systems (i.e., immune, endocrine, neural, etc) may influence the abundance and function of plasma proteins; many proteins have multiple functions, and thus their altered abundance may be context specific. Future experiments should investigate ex vivo and in vitro models to study individual organs and cell types that may contribute to the effects described in this paper. In addition, in our study the effects of immunization with *M. vaccae* and IS are restricted to a single time point of tissue collection, eight days following immunization with *M. vaccae* and 24 hours after stress; considering that our results may have been influenced by immune activation and resolution of inflammation (not measured here), future experiments

should explore time-dependent changes on the plasma proteome following final immunizations of *M. vaccae* strains and following IS. Another limitation of our study is that nutrition intake and physical activity were not monitored after exposure to IS and may have been additional variables that contributed to an altered plasma proteome. Also, our experiment was conducted only in adult male rats, and future studies should include female rats to determine if *M. vaccae* administration and/or IS may produce differential effects on the plasma proteome dependent on sex (Koeken et al., 2020). Similarly, immune response to IS and *M. vaccae* strains may be altered in juvenile or aged rats, and future experiments should investigate these differences.

3.5.8 Conclusions

Collectively, our study provides evidence that immunization with either *M. vaccae* NCTC 11659 or *M. vaccae* ATCC 15483 promotes resilience to IS-induced changes in the plasma proteome that are associated with the IS-induced enhancement of anxiety-like defensive behavioral responses. The data presented here argue that immunization with *M. vaccae* strains can shift the immunological milieu to attenuate IS-induced disruption of the gut barrier, activation of coagulation and complement cascades, increases in acute-phase response proteins, and/or stimulation of bone marrow-derived monocytes and circulating macrophages toward a proinflammatory phenotype that induces trafficking to the central nervous system. To further investigate these possible mechanisms of *M. vaccae* strains, and to see if *M. vaccae* strains can mitigate IS-induced increases of biological signatures of inflammation in the brain, we next evaluated the CSF proteome of the same rats in this study (see part II of this article).

3.6 Acknowledgements, author contributions, and conflicts of interest

Acknowledgements

These studies were funded by the National Institute of Mental Health (NIMH) R21 grant (R21MH116263) awarded to C.A.L., S.F.M., M.G.F. (PIs), and L.K.F. (Co-I). We gratefully acknowledge the Central Analytical Laboratory and Mass Spectrometry Facility at the University of Colorado Boulder for their services. Purchase of a Thermo Q-Exactive HF-X mass spectrometer was made possible with a grant from the National Institute of Health (S10-OD025267).

Author contributions

Study design was conceived by K.M.L., C.A.Z., and C.A.L. Preparation of heat-killed *M. vaccae* ATCC 15483 was conducted by C.A.Z. *M. vaccae* injections were performed by A.I.E, B.M.M., and C.A.Z. Inescapable tail shock was conducted by H.M.D. Tissue collection for plasma was conducted by K.M.L, K.E.C., B.M.M., M.G.F., and C.A.Z. Proteomics sample preparation was performed by K.M.L., C.C.E., T.L., and A.I.E. LC/MS-MS was performed by C.C.E. and T.L. Data analysis and statistical analysis was carried out by K.M.L. and C.C.E. Figures and figure legends were produced by K.M.L. and K.E.C. Manuscript preparation was conducted by K.M.L. Editing and review was contributed by K.M.L, C.C.E., T.L., A.I.E., K.E.C., B.M.M., L.K.F., M.G.F., C.A.Z., S.F.M., and C.A.L

Conflicts of interest

CAL serves on the Scientific Advisory Board of Immodulon Therapeutics, Ltd, is Cofounder and Chief Scientific Officer of Mycobacterium Therapeutics Corporation, and serves as an unpaid

scientific consultant to Aurum Switzerland A.G., and is member of the faculty of the Integrative Psychiatry Institute, Boulder, CO, USA

Chapter 4. Comparing the effects of two different strains of mycobacteria, *Mycobacterium vaccae* NCTC 11659 and *M. vaccae* ATCC 15483, on stress-induced changes in the proteome of adult male rats: II. cerebrospinal fluid.

Citation

Loupy, K.M., Ebmeier, C.C., Lee, T., D'Angelo, H.M., Elsayed, A.I., Cler, K.E., Marquart, B.M., Fonken, L.K., Frank, M.G., Arnold, M.R., Zambrano, C.A., Maier, S.F., Lowry, C.A. Comparing the effects of two different strains of mycobacteria, *Mycobacterium vaccae* NCTC 11659 and *M. vaccae* ATCC 15483, on stress-induced changes in the proteome of adult male rats: II. cerebrospinal fluid. Manuscript in preparation.

Authors' names

Kelsey M. Loupy[a], Christopher C. Ebmeier[b], Thomas Lee[b], Heather M. D'Angelo[c], Ahmed I. Elsayed[a], Kristin E. Cler[a], Brandon M. Marquart[a], Laura K. Fonken[d], Matthew G. Frank[c,e], Mathew R. Arnold[a,e], Cristian A. Zambrano[a], Steven F. Maier [c,e], Christopher A. Lowry[a,e,f,g,h,i,j]*

Authors' affiliations

[a]Department of Integrative Physiology, University of Colorado Boulder, Boulder, CO 80309, USA

[b]Center for Neuroscience and Center for Microbial Exploration, University of Colorado Boulder, Boulder, CO 80309, USA

[c]Department of Physical Medicine and Rehabilitation and Center for Neuroscience, University of Colorado, Anschutz Medical Campus, Aurora, CO 80045, USA

[d]Veterans Health Administration, Rocky Mountain Mental Illness Research Education and Clinical Center, Denver, CO 80045, USA

[e]Military and Veteran Microbiome Consortium for Research and Education (MVM-CoRE), Denver, CO 80045, USA

[f]Senior Fellow, inVIVO Planetary Health, of the Worldwide Universities Network (WUN), West New York, NJ 07093, USA

4.1 Abstract

Individuals with anxiety disorders, affective disorders, and trauma- and stressor-related disorders such as posttraumatic stress disorder (PTSD) exhibit dysregulated neuroimmune functions, including aggravated sympathetic nervous system activation and exaggerated proinflammatory signaling. There is increasing interest in using microbial-based therapeutics to help prevent or treat neuroimmune dysfunctions associated with stress-related disorders. We recently reported that immunization with either of two heat-killed preparations of mycobacteria, either *Mycobacterium vaccae* NCTC 11659 or *M. vaccae* ATCC 15483, prevents the stress-induced increases of interleukin 6 mRNA expression in the dorsal hippocampus and stress-induced exaggeration of anxiety-like defensive behavioral responses, assessed 24 h after inescapable tail shock stress (IS). In part I of this article, we used an untargeted proteomics approach to characterize the plasma proteome of the rats used in the original study [Loupy et al., 2021, *Brain,*

Behavior, and Immunity, 91: 212–229]. Here, we describe effects of IS on the cerebrospinal fluid (CSF) proteome, and we demonstrate that immunization with either *M. vaccae* strain protects against IS-induced alterations to the CSF proteome. Specifically, immunization with either *M. vaccae* strain prevents development of a biological signature of inflammatory monocytes in the CSF, possibly by preventing vascular endothelial injury and/or monocyte trafficking. This study builds upon part I of this article to reveal biological signatures of trauma and stress vulnerability versus resilience in the central nervous system (CNS). Results from this study may aid researchers in the development of novel targets for the prevention and treatment of anxiety disorders, affective disorders, and trauma and stressor-related disorders like PTSD.

4.2 Introduction

Stress-related psychiatric disorders include anxiety disorders, affective disorders, and trauma- and stressor-related disorders. Posttraumatic stress disorder (PTSD) is a trauma- and stressor-related disorder that is diagnosed according to the *Diagnostic and Statistical Manual of Mental Disorders*, 5th Edition (DSM-5) using four major symptom criteria: 1) intrusions, or re-experiencing a traumatic event, 2) avoidance of trauma-related stimuli, 3) negative alterations of cognitions and mood, and 4) alterations of arousal and reactivity following the experience of a traumatic event (American Psychiatric Association, 2013). Physiologically, trauma and stressor-related psychiatric disorders like PTSD are characterized in part by hyperactivity of the sympathetic nervous system (SNS) and chronic low-grade inflammation (for review, see Michopoulos et al., 2017). It is thought that increased activation of the SNS initiates proinflammatory signaling, while insufficient glucocorticoid secretion, as observed among persons with PTSD, is unable to mitigate these processes (Michopoulos et al., 2017). However, it

is also thought that inflammation prior to trauma exposure might be a risk factor for the development of PTSD; higher concentrations of plasma C-reactive protein (CRP) in soldiers prior to deployment may be a reliable biomarker of increased risk to develop PTSD post-deployment (Eraly et al., 2014). Supporting this claim, based on machine learning approaches to study active-duty military personnel, biological signatures of inflammation, including elevated levels of plasma CRP, eicosanoids, and absolute numbers of circulating monocytes assessed prior to deployment rank among the highest features that predict provisional PTSD diagnosis 90-180 days after deployment (Schultebraucks et al., 2020). Proinflammatory signaling is also described in the central nervous system (CNS) of individuals with PTSD, wherein PTSD symptom severity is positively correlated with increased abundance of interleukin (IL)-6 in cerebrospinal fluid (CSF) (Kim et al., 2020).

Stress-induced activation of the SNS causes proinflammatory phenotypes associated with the onset of complement and coagulation pathways by the innate immune system (for review, see Von Känel, 2015) (see also part I of this article). Individuals with PTSD exhibit increased circulating markers of coagulation, including fibrinogen (Eswarappa et al., 2018; Von Känel et al., 2006), which may be predicted by measures of hyperarousal (Von Känel et al., 2006). Consequently, persons with PTSD are at a higher risk of developing cardiovascular disease (Brudey et al., 2015) or ischemic stroke (Rosman et al., 2019). Rodent models have shown that chronic social defeat stress (CSD) alters gene expression of cerebrovascular endothelial cells consistent with hypertension, neuroinflammation, and disruption of the blood-brain barrier (BBB) (Lehmann et al., 2020; Menard et al., 2017a). Furthermore, CSD induces cerebrovascular microbleeds and increases fibrinogen deposition in the brain (Lehmann et al., 2020). It was

suggested that endothelial dysfunction in the CSD model is driven by SNS and glucocorticoid release (Lehmann et al., 2020).

SNS activity also initiates the transmigration of monocytes from the bone marrow to the circulation (Wohleb et al., 2015). Monocytes that are activated by damage-associated molecular patterns (DAMPs), pathogen-associated molecular patterns (PAMPs), or microbe-associated molecular patterns (MAMPs) subsequent to cellular injury, leaky gut, or release of metabolic products will then traffic to the brain and contribute to the development of anxiety-like behaviors by promoting neuroinflammatory processes (Wohleb et al., 2015, 2014, 2013, 2011). Peripheral blood mononuclear cells (PBMCs) taken from individuals with PTSD spontaneously secrete more IL-6 ex vivo than PBMCs from healthy controls (Gola et al., 2013); other studies have shown that investigating four different immune cell types ($CD4^+$ T cells, $CD8^+$ T cells, B cells, and monocytes) from individuals with PTSD compared to trauma-exposed controls, differential gene expression was most pronounced in monocytes (Kuan et al., 2019; Neylan et al., 2011). These experiments indicate that monocytes are involved in the long-term inflammatory changes associated with PTSD (Kuan et al., 2019; Neylan et al., 2011). Similar arguments have been made for other stress-related psychiatric disorders, including affective disorders (Grosse et al., 2015; Lynall et al., 2020; Miller and Raison, 2016).

The “old friends” hypothesis proposes that, from an evolutionary perspective, greater exposure to diverse microbial environments, particularly at a young age, might suppress aberrant inflammatory responses (for review, see Langgartner et al., 2019; Lowry et al., 2016; Rook, 2013; Rook et al., 2014, 2013b, 2013a, 2004; Rook and Brunet, 2005; Rook and Lowry, 2008).

Exposure to a diverse microbial environment is thought to benefit the immune system by "training" it to respond to stimuli with a healthy balance of inflammatory and anti-inflammatory processes, including a balanced expression of effector and regulatory T cells, also called immunoregulation. In fact, gut microbiome-based therapeutics (i.e., prebiotics, probiotics, parabiotics, and postbiotics) are gaining attention for their potential to prevent and treat stress-related psychiatric disorders (Brenner et al., 2017; for review, see Loupy and Lowry, 2020). Although the "old friends" hypothesis has, in the past, largely focused on the ability of microbes to interact with the immune system (Rook et al., 2013a), it is likely that these microbes also influence autonomic nervous system signaling (Bermúdez-Humarán et al., 2019; Bravo et al., 2011; Brenner et al., 2020; Loupy and Lowry, 2020). We have previously described in detail the promising therapeutic effects of immunization with a heat-killed preparation of *Mycobacterium vaccae* NCTC 11659, an environmental saprophyte with anti-inflammatory and immunoregulatory properties, for stress-related psychiatric disorders (Amoroso et al., 2020; Bowers et al., 2020; Fonken et al., 2018; Fox et al., 2017; Foxx et al., 2021; Frank et al., 2018b; Hassell et al., 2019; Loupy et al., 2021, 2018; Reber et al., 2016b), including therapeutic effects across three of the four major diagnostic criteria for PTSD (see Supplementary Table 4 in Loupy et al., 2021). More recently, we have reported similar effects using *M. vaccae* ATCC 15483 (Loupy et al., 2021) (see also part I of this article).

In part I of this article, we observed that IS evokes a proteomic signature of thrombosis, but that prior immunization with *M. vaccae* strains attenuates these effects; we also suggested that immunization with *M. vaccae* strains promote gut endothelial or epithelial barrier integrity (see part I of this article). Finally, we hypothesized that immunization with *M. vaccae* strains prevents

monocyte/macrophage trafficking or may shift activation from a proinflammatory (M1) phenotype toward an anti-inflammatory (M2) phenotype (see part I of this article). Both blood filtrates and immune cells, including monocytes, can traffic to the CSF through the choroid plexus, a highly vascularized structure that is responsible for the formation of CSF (Ge et al., 2017; Herz et al., 2017; Kierdorf et al., 2019; Mottahedin et al., 2019; Nishihara et al., 2020; Steinmann et al., 2013; Strominger et al., 2018). Here, we describe the effects of IS on the CSF proteome, and we evaluate the therapeutic effects of prior immunization with *M. vaccae* strains. Our results validate our findings from part I of this article and provide further evidence that *M. vaccae* strains promote stress-resilience by preserving the integrity of endothelial barriers at the blood-brain barrier and protecting the brain from an influx of proinflammatory monocytes, possibly by preventing their release or migration, or by promoting a phenotypic shift toward M2 macrophages.

4.3 Materials and methods

4.3.1 Animals

For an experimental timeline, please see Figure 4.1 (adapted from Loupy et al. [2021]). The data reported in this study are derived from the same rats used in a previous report, which investigated the effects of immunization with *Mycobacterium vaccae* strains and stress exposure on behavioral outcomes and molecular signaling in the liver, spleen, and hippocampus (Loupy et al., 2021). In the current study, proteomic profiles in plasma of these rats are reported. Adult male Sprague Dawley® rats (Hsd:Sprague Dawley® SD®; Envigo, Indianapolis, IN, USA) weighing 250-265 g upon arrival were pair-housed in Allentown micro-isolator filter-topped caging [259 mm (W) × 476 mm (L) × 209 mm (H); cage model #PC10198HT, cage top

#MBT1019HT; Allentown, NJ, USA] containing an approximately 2.5 cm-deep layer of bedding (Cat. No. 7090; Teklad Sani-Chips; Harlan Laboratories, Indianapolis, IN, USA). This species, strain, and supplier were chosen due to previous studies evaluating stress resilience effects of *M. vaccae* NCTC 11659 that were conducted with these animals (Frank et al., 2018b). All rats were kept under standard laboratory conditions (12-h light/dark cycle, lights on at 0700 h, 22 °C) and had free access to bottled reverse-osmosis water and standard rat diet (Harlan Teklad 2918 Irradiated Rodent Chow, Envigo, Huntingdon, United Kingdom). Cages were changed once per week. The research described here was conducted in compliance with the ARRIVE 2.0 Guidelines for Reporting Animal Research (Kilkenny et al., 2010; Percie du Sert et al., 2020), and all studies were consistent with the National Institutes of Health *Guide for the Care and Use of Laboratory Animals*, Eighth Edition (National Research Council, 2011). The Institutional Animal Care and Use Committee at the University of Colorado Boulder approved all procedures. All efforts were made to limit the number of animals used and their suffering.

4.3.2 Reagents

This study used a whole cell heat-killed preparation of *M. vaccae* NCTC 11659 [IMM-201; alternative designations and different preparations and production processes of *M. vaccae* NCTC 11659 used in clinical trials or preclinical studies include: DAR-901 (Lahey et al., 2016), DarDar tuberculosis vaccine (Von Reyn et al., 2010), MV001 (Waddell et al., 2000), MV 007 (Vuola et al., 2003), *M. vaccae* SRL 172 (Von Reyn et al., 2010), and *M. vaccae* SRP 299 (Lowry et al., 2007); V7 (Bourinbaiar et al., 2020) is a hydrolyzed version of heat-killed *M. vaccae* NCTC 11659*; M. vaccae* NCTC 11659 has recently been classified as *M. kyogaense* sp. nov. (NCTC 11659; CECT 9646; DSM 107316) (Nouioui et al., 2018) (but see also Gupta et al., 2018);

10 mg/ml solution; strain National Collection of Type Cultures (NCTC) 11659, batch C079-ENG#1, provided by BioElpida (Lyon, France), diluted to 1 mg/ml in 100 µl sterile borate-buffered saline (BBS) for injections]. This study also employed the use of a whole heat-killed preparation of *M. vaccae* American Type Culture Collection (ATCC) 15483 suspension. *M. vaccae* ATCC 15483 was purchased from ATCC (Bonicke and Juhasz (ATCC® 15483, Manassas, VA, USA). *M. vaccae* ATCC 15483 was cultured in ATCC® Medium 1395: Middlebrook 7H9 broth (Cat. No. M0178-500G; Sigma-Aldrich; St. Louis, MO, USA) with ADC enrichment at 37 °C, then centrifuged at 3000 x g at 4 °C for ten minutes to pellet the cells, growth media was removed, and cells were weighed and resuspended in sterile BBS to a concentration of 10 mg/ml. Cells were transferred to a sealed sterile glass container and autoclaved at 121 °C for 15 minutes. Heat-killed bacterial stock was stored at 4 °C. *M. vaccae* ATCC 15483 was further diluted to 1 mg/ml in 100 µl sterile BBS for injections.

4.3.3 Mycobacterium vaccae (M. vaccae) NCTC 11659, M. vaccae ATCC 15483, and vehicle immunization

Experimental rats received 3 subcutaneous (s.c.) immunizations of: 1) 0.1 mg of a heat-killed preparation of *M. vaccae* NCTC 11659 (estimated to be 1 x 10^8 cells); 2) 0.1 mg of a heat-killed preparation of *M. vaccae* ATCC 15483 (estimated to be 1 x 10^8 cells); or 3) 100 µl of the vehicle, sterile BBS, using 21-gauge needles and injection sites between the scapulae, between the hours of 12 pm and 4 pm. Injections occurred on days –21, –14, and –7 prior to stress exposure, which occurred on day 0. The dose used in these experiments (0.1 mg) was 1/10 of the dose used in human studies (1 mg) (O'Brien et al., 2004) and identical to the dose used in previous studies in mice and rats (Amoroso et al., 2020; Fonken et al., 2018; Fox et al., 2017; Frank et al., 2018b; Hassell et al., 2019; Loupy et al., 2018; Lowry et al., 2007; Reber et al., 2016b; Siebler et al.,

2018). Figure 4.1 provides a timeline of *M. vaccae* treatments and stress exposure in relation to tissue collection.

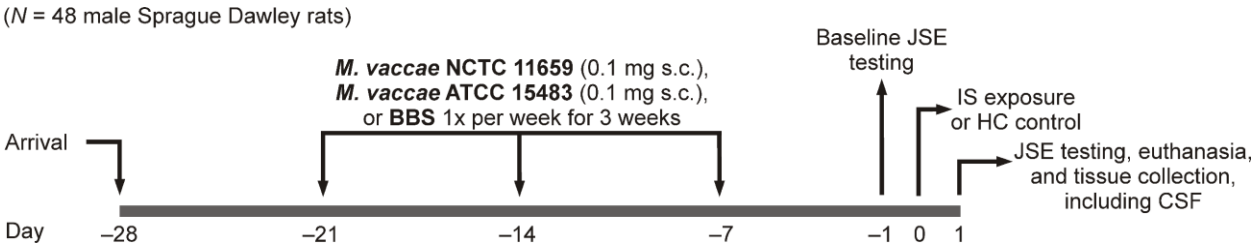

Figure 4.1 Experimental timeline.
This schematic represents the experimental timeline for immunization with *M. vaccae* NCTC 11659, *M. vaccae* ATCC 15483, or vehicle (borate-buffered saline [BBS]), exposure to inescapable tail shock stress (IS), behavioral testing (juvenile social exploration [JSE]), and euthanasia. Behavioral results have been published separately in Loupy et al. (2021). Abbreviations: BBS, borate-buffered saline; CSF, cerebrospinal fluid; HC, home cage control conditions; IS, inescapable tail shock stress; JSE, juvenile social exploration. Adapted, with permission, from Loupy et al. (2021).

4.3.4 Inescapable tail shock stress (IS)

IS was performed as previously described (Frank et al., 2018b). Briefly, rats were placed in Plexiglas® tubes (23.4 cm in length × 7 cm in diameter) and exposed to 100 1.6 mA, 5-s tail shocks with a variable inter-trial interval (ITI) ranging from 30 to 90 s (average ITI = 60 s). All IS treatments occurred between 09:00 and 11:00 h. IS animals were returned to their home cages immediately after termination of the shock. Home cage control (HC) animals remained undisturbed in their home cages.

4.3.5 Juvenile social exploration (JSE)

IS exposure produces robust decreases in JSE (Christianson et al., 2008), which is a widely used and validated measure of anxiety (File and Seth, 2003) and is sensitive to the neuroinflammatory effects of stress (Goshen and Yirmiya, 2009). Here, JSE was measured 24 h prior to IS (baseline)

and 24 h after IS (test) (i.e., between 9:00 and 10:00 h). Each experimental subject was transferred to a novel cage with shaved wood bedding in a dimly lit room (40 lx). After a 15-min habituation period, a 28–32 day-old juvenile male rat was introduced to the subject's cage for 5 min. Exploratory behaviors of the adult (sniffing, pinning, licking and allo-grooming of the juvenile) were timed by an observer blind to treatment condition. After the test, the juvenile was removed and the experimental adult rat was returned to its home cage. Although juvenile stimulus rats were reused for multiple tests, the adult was never retested with the same juvenile. For each animal, JSE test data were quantified as a percent of baseline JSE. Due to technical issues, a total of four animals were removed from the JSE paradigm and subsequent behavioral analysis and our final group sample sizes prior to outlier analysis were BBS/HC, $n = 8$; BBS/IS, $n = 6$; NCTC/HC, $n = 8$; NCTC/IS, $n = 8$; ATCC/HC, $n = 8$; ATCC/IS, $n = 6$. Behavioral results have been published separately in Loupy et al. (2021).

4.3.6 Euthanasia and tissue and plasma collection

Rats were euthanized eight days following the last injection using an overdose of sodium pentobarbital (Fatal Plus®, Vortech Pharmaceuticals Ltd., Dearborn, MI, USA; 200 mg/kg, i.p.). Immediately after euthanasia, CSF was collected, as described previously (Fonken et al., 2016). Briefly, the dorsal aspect of the skull was shaved and swabbed with 70% ethanol. A sterile 26-gauge needle attached via PE50 tubing to a sterile 1 mL syringe was inserted into the cisterna magna, and 0.2 mL of clear CSF was drawn into the syringe. CSF was then spun down at 1000 × g for 10 min, and the supernatant was collected and stored at –80 °C. Due to loss of samples

during CSF collection, final sample sizes for CSF analysis were BBS/HC, *n* = 7; NCTC/HC, *n* = 8; ATCC/HC, *n* = 8; BBS/IS, *n* = 7; NCTC/IS, *n* = 7; ATCC/IS, *n* = 8.

4.3.7 CSF sample preparation for quantitative mass spectrometry proteomics

A stock solution of freshly prepared sodium dodecyl sulfate (SDS), tris(2 carboxyethyl)phosphine (TCEP) and 2-chloroacetamide (ClAA) was added to rat CSF for a final concentration of 2% (w/v) SDS, 10 mM TCEP and 40 mM ClAA, then boiled at 95 °C for 10 minutes to reduce and alkylate all CSF proteins. Sample preparation for mass spectrometry analyses was performed using the Single Pot Solid Phase Sample Preparation (SP3) method (Hughes et al., 2014). Briefly, 4-33 µg protein in 110 µL CSF was added to 100 µg Sera-Mag SpeedBeads Carboxylate Magnetic Beads (Cytiva, Marlborough, MA, USA) and mixed thoroughly. Acetonitrile was added to 80% (v/v) and mixed for an excess of 10 minutes to precipitate protein with the beads. Tubes were placed on a magnet and the supernatant was removed. Beads were then washed two times with 80% (v/v) ethanol in water and two times with 100% acetonitrile, sonicating 2 minutes with each wash. Protease digestion was performed with 0.5 µg of a LycC/Trypsin mix (Promega, Madison, WI, USA) in 25 µL 50 mM HEPES pH 8.0 mixing overnight at 37 °C. Tryptic digest supernatants were removed using a magnet and peptide concentrations were determined by tryptophan fluorescence (Wiśniewski and Gaugaz, 2015). Each of eight rat cohorts was multiplexed using 6-plex Tandem Mass Tags (6-plex TMT) (Thermo Scientific, Waltham, MA, USA), each including a control and two treatments for two different conditions (i.e., one sample from each of six experimental groups). Out of eight rat cohorts for each treatment group, two samples were missing for CSF, the BBS/HC cohort #1 and NCTC/IS cohort #2. These samples were replaced by mixing equal amounts of the same samples

from the remaining six cohorts, for complete TMT 6-plexes for each cohort. TMT reagent was dissolved in anhydrous acetonitrile and added to tryptic peptides in 50 mM HEPES pH 8.0 and vortexed, then incubated at ambient temperature for 1 hour. Labeling reactions were quenched with the addition of hydroxylamine, vortexed, and incubated at ambient temperature for 15 minutes. Each sample in each cohort was labeled separately with one of the six TMT reagents in each 6-plex, and these multiplexed samples were desalted using an Oasis HLB 1 cc (10 mg) extraction cartridge (Waters, Milford, MA, USA) according to the manufacturer's instructions. Desalted multiplexed samples were dried completely using a speedvac vacuum concentrator.

4.3.8 Liquid chromatography/mass spectrometry analyses of 6-plex TMT-labeled rat CSF samples

Multiplexed samples were suspended in 3% (v/v) acetonitrile, 0.1% (v/v) trifluoracetic acid and 1 µg was loaded directly onto an ACQUITY UPLC M-class Peptide CSH reversed-phase C18, 130Å, 1.7 µm, 75 µm X 250 mm column (cat. no. 186007478; Waters) using an Ultimate 3000 RSLCnano UPLC (Thermo Scientific). Peptides were eluted into a Q-Exactive HF-X Hybrid Orbitrap mass spectrometer (Thermo Scientific) at 300 nL/minute with a gradient from 5% to 20% (v/v) acetonitrile in water over 115 minutes. Precursor mass spectra (MS1) were acquired at a resolution of 60,000 from 380 to 1580 m/z with an AGC target of 3E6 ions and a maximum injection time of 45 milliseconds. Dynamic exclusion was set for 25 seconds with a mass tolerance of +/– 10 ppm. Precursor peptide ion isolation window width for MS2 scans was 0.7 m/z with a +0.2 m/z offset. The top 12 most intense ions were selected for MS2 sequencing using higher-energy collisional dissociation (HCD) at 30% normalized collision energy. An AGC target of 1E5 ions and 100 milliseconds maximum injection time was used for all MS2 scans. Orbitrap MS data were searched against the Uniprot *Rattus norvegicus* database,

downloaded 01/22/2019, using Maxquant version 1.6.3.4 for reporter ion MS2 quantification of 6-plex TMT with isotopic purity corrections from the product data sheet. Protease digestion was Trypsin/P with a maximum of two missed cleavages and a minimum peptide length of 7 amino acids. Cysteine carbamidomethylation was a fixed modification, while methionine oxidation and protein N-terminal acetylation were variable modifications. First search mass tolerance was 20 ppm and the main search tolerance was 4.5 ppm with a 20 ppm MS/MS mass tolerance. False discovery rates (FDR) for peptide and protein identifications were 1%.

4.3.9 Statistical analysis

Proteomics analyses were performed for CSF using R Statistical Programming (version 3.5.3 for Windows). Abundance of each protein was measured by reporter ion-corrected values. To correct for potential noise in the MS/MS detection, reporter ion-corrected values were removed for any proteins that had a reporter intensity count less than two. Contaminants were also removed from the dataset. Peak intensities were log2-transformed and normalized across the dataset using the normalizeBetweenArrays function and the cyclic loess method within the linear models for microarray analysis (LIMMA) package. Two analyses were run on the data: 1) generalized linear model (GLM) was performed to understand the general effects of treatment and stress on proteomic profiles in the CSF, and 2) LIMMA analysis using the empirical Bayes method was performed to directly compare treatment groups of interest. GLM analysis was performed on log2-transformed normalized peak intensity for each protein, with treatment, stress, and treatment x stress as factors. Cohort (i.e., TMT batch) was also included as a factor in the GLM analysis to better control for any batch effects of the 6-plex TMT. Fold change values and pairwise comparison *p*-values were analyzed from the LIMMA output. For both GLM and

LIMMA analyses, two-tailed significance was set at $\alpha = 0.1$ and an adjusted *p*-value was not calculated due to low power (Pascovici et al., 2016). Statistical analysis was only performed on proteins wherein each treatment group sample size was greater than or equal to $n = 3$. Proteins that were found to be significantly different between treatment and control as well as proteins with a fold-change (up or downregulated) greater than two were used in downstream pathway analysis via the Database for Annotation, Visualization and Integrated Discovery (DAVID, version 6.8) using UniProt accession IDs (The UniProt Consortium, 2019) for gene labeling and *Rattus norvegicus* as species. Analyses of correlations between dependent variables were performed using R Statistical Programming (version 3.6.1 for Windows), conducted using the Pearson correlation method and FDR adjusted *p*-values. For protein interaction analysis, STRING database (version 11) was used (Szklarczyk et al., 2019). The Kyoto encyclopedia of genes and genomes (KEGG) (Kanehisa and Goto, 2000) and the Gene Ontology and GO Annotations (QuickGO) (Huntley et al., 2015) databases were used for additional pathway analysis and gene ontology.

4.4 Results

4.4.1 General effects of M. vaccae strain, IS, and interactions of M. vaccae strain x IS on protein relative abundances in the CSF

To understand the overall effect of IS and either *M. vaccae* NCTC 11659 or *M. vaccae* ATTC 15483 treatment on protein abundances in the CSF, we ran GLMs with *M. vaccae* strain and IS as factors and *M. vaccae* strain x IS as an interaction factor. Effects of *M. vaccae* NCTC 11659 or *M. vaccae* ATTC 15483, and their interactions with IS, were analyzed separately. To control for batch effect of the 6-plex TMT, batch was included as an additional factor in the GLM.

Effects of M. vaccae NCTC 11659 and IS on protein relative abundances in the CSF

We investigated the effects of immunization with *M. vaccae* NCTC 11659 and IS on relative protein abundance in the CSF. The GLM revealed an interaction effect of *M. vaccae* NCTC 11659 x IS on six of 257 proteins: apolipoprotein M (ApoM), complement 9 (C9), neural cell adhesion molecule 1 (NCAM1), serum amyloid A protein (SAA4), V-set and transmembrane domain containing 2B (VSTM2B), and 14-3-3 protein gamma (YWHAG). In addition, there were main effects of *M. vaccae* NCTC 11659 on three proteins: apolipoprotein A-I (ApoA-I), ApoM, and SAA4. The GLM revealed a main effect of IS on seventeen proteins. These were: albumin, alpha-1-acid glycoprotein (AGP), ApoM, chromogranin A (CgA), carboxypeptidase E (CPE), C9, DOMON domain-containing protein FRRS1L (FRRS1L), T-kininogen 1 (also known as major acute phase protein or thiostatin; KNG1; alpha-1-MAP; mapped as *Map1* by DAVID and *Kng1* by STRING), T-kininogen 2 (also mapped as kininogen 1-like 1 or kininogen 1 by UniProt; KNG2; KNG1L1; also mapped as *Kng1l1* by DAVID and *Kng2* by STRING), neuroserpin (NS), neurotrimin (Ntm), platelet-activating factor acetylhydrolase (PAF-AH; also known as lipoprotein-associated phospholipase A2; lp-PLA2), SAA4, serine protease inhibitor A3N (Serpin A3N), tropomyosin alpha-1 chain (Tpm1), VSTM2B, and YWHAG.

Effects of M. vaccae ATCC 15483 and IS on protein relative abundances in the CSF

We investigated the effects of immunization with *M. vaccae* ATCC 15483 and IS on relative protein abundance in the CSF. The GLM revealed an interaction effect of *M. vaccae* ATCC 15483 x IS on seven of 257 proteins: apolipoprotein C2 (ApoC-II), CD99 molecule (Xg blood group) (CD99), chitinase-3-like protein 1 (Chi3l1; also known as cartilage glycoprotein 39; CGP-39), FRRS1L, gamma-glutamyl hydrolase (GGH), insulin-like growth factor I (IGF-I), and

YWHAG. There was a main effect of *M. vaccae* ATCC 15483 on four proteins: CD99, FRRS1L, GGH, and IGF-I. There was a main effect of IS on eleven proteins: albumin, ApoC-II, CD99, CGP-39, FRRS1L, GGH, hemoglobin subunit beta-1 (HBB-1), hemoglobin subunit beta-2 (HBB-2), an Ig-like domain containing protein (UniProt ID F1LTY5), T-kininogen 2, and YWHAG.

4.4.2 Individual pairwise comparisons of protein abundances in the CSF

To directly compare protein abundances between each experimental group, we first analyzed our data using an average fold change analysis, indicating which proteins had a fold change (upregulated or downregulated) equal to or greater than two. We then ran a separate linear model analysis, investigating pairwise comparisons for each protein using the linear models for microarray data (LIMMA) package in R. We first report the effects of *M. vaccae* NCTC 11659 on protein relative abundances in the CSF of home cage control animals; we then report effects of IS on protein relative abundances in the CSF of vehicle-treated animals; we then report effects of immunization with *M. vaccae* NCTC 11659 on protein relative abundances in the CSF of IS-exposed animals; and finally, we report the effects of stress on protein relative abundances in the CSF of animals immunized with *M. vaccae* NCTC 11659. Data are then reported in a similar manner for *M. vaccae* ATCC 15483.

4.4.3 Pairwise comparisons with M. vaccae NCTC 11659

Effects of immunization with M. vaccae NCTC 11659 on protein relative abundances in the CSF of home cage control animals

Fold change analysis revealed that, among home cage control rats, immunization with *M. vaccae* NCTC 11659 increased the relative abundances of three proteins in the CSF by two-fold: alpha-

1-macroglobulin (Alpha-1-M), ApoC-II, and vinculin (Figure 4.2A). Among home cage control animals, immunization with *M. vaccae* NCTC 11659 decreased the abundance of two proteins by two-fold: serine proteinase inhibitor, clade A, member 3C (Serpin A3C) and vascular non-inflammatory molecule 3 (vanin-3) (Figure 4.2A).

The pairwise comparison analysis found a significant difference in abundance of three proteins in the CSF between *M. vaccae* NCTC 11659-treated and BBS-treated home cage control rats. Among home cage animals, immunization with *M. vaccae* NCTC 11659 increased the abundances of Alpha-1-M, ApoA-I, and complement C4a (C4a) compared to BBS-treated rats (Figure 4.2A). There were no proteins significantly downregulated in the CSF after immunization with *M. vaccae* NCTC 11659 among home cage control rats (Figure 4.2A).

Effects of stress on protein relative abundances in the CSF of vehicle-treated animals

Fold change analysis revealed that, among BBS-treated rats, IS increased the abundance of ten proteins in the CSF by two-fold: ATP-binding cassette sub-family B member 9 (ABCB9), adenylate kinase isoenzyme 1 (AK1), ApoC-II, HBB-1, HBB-2, hemoglobin subunit epsilon 1 (HBE-1), T-kininogen 2, Tpm1, VSTM2B, and YWHAG (Figure 4.2B; Figure 4.3B). Among BBS-treated animals, IS decreased the abundance of one protein by two-fold: NCAM1 (Figure 4.2B; Figure 4.3B).

The pairwise comparison analysis found a significant difference in abundance of twenty proteins in the CSF between IS-exposed and home cage control rats treated with BBS. Among BBS-treated animals, IS increased the abundance of AGP, ApoC-II, HBB-1, HBB-2, HBE-1, T-

kininogen 1 (KNG1), T-kininogen 2 (KNG2), nucleoside diphosphate kinase (matching isoforms A and B); NDK A/B), SAA4, Serpin A3N, Tpm1, VSTM2B, and YWHAG (Figure 4.2B). Among BBS-treated animals, IS significantly decreased the abundance of eight proteins, including albumin, CgA, FRRS1L, NCAM1, Ntm, osteoglycin (Ogn), PAF-AH (lp-PLA2), and phosphoinositide-3-kinase-interacting protein 1 (PIK3IP1) (Figure 4.2B). Of note, ABCB9, AGP, T-kininogen 1, T-kininogen 2, SAA4, Serpin A3N, Tpm1, and YWHAG were also upregulated, and albumin was also downregulated, in the plasma of BBS-treated rats after exposure to IS (see part I of this article).

Effects of immunization with M. vaccae NCTC 11659 on protein relative abundances in the CSF of IS-exposed animals

Fold change analysis revealed that, among IS-exposed rats, immunization with *M. vaccae* NCTC 11659 increased the abundance of one protein in the CSF by two-fold: trans-Golgi network integral membrane protein TGN38 (TGN38) (Figure 4.2C). Among IS-exposed animals, immunization with *M. vaccae* NCTC 11659 decreased the abundance of four proteins by two-fold: HBE-1, vinculin, VSTM2B, and YWHAG (Figure 4.2C).

The pairwise comparison analysis found a significant difference in abundance of five proteins in the CSF between *M. vaccae* NCTC 11659-treated and BBS-treated rats exposed to IS. Immunization with *M. vaccae* NCTC 11659 did not increase the abundance of any proteins among IS-exposed animals (Figure 4.2C). Among IS-exposed animals, immunization with *M. vaccae* NCTC 11659 decreased the abundance of five proteins, including contactin-2 (CNTN2), T-kininogen 2, NCAM1, VSTM2B, and YWHAG compared to BBS-treated rats (Figure 4.2C).

Effects of stress on protein relative abundances in the CSF of animals immunized with M. vaccae NCTC 11659

Fold change analysis revealed that, among rats immunized with *M. vaccae* NCTC 11659, IS increased the abundance of four proteins in the CSF by two-fold: alpha-crystallin B chain (Cryab), TGN38, Tpm1, and Serpin A3C (Figure 4.2D). Among animals immunized with *M. vaccae* NCTC 11659, IS decreased the abundance of two proteins by two-fold: NCAM1 and vinculin (Figure 4.2D).

The pairwise comparison analysis found a significant difference in abundance of eleven proteins in the CSF between IS-exposed and home cage control rats immunized with *M. vaccae* NCTC 11659. Among animals immunized with *M. vaccae* NCTC 11659, IS increased the abundance of six proteins including AGP, alpha-2-macroglobulin (Alpha-2-M), an Ig-like domain containing protein (UniProt ID A0A0G2JTG4), T-kininogen 2, Serpin A3N, and Tpm1 in the CSF (Figure 4.2D). Of note, immunization with *M. vaccae* NCTC 11659 prevented a stress-induced increase of ABCB9, AK1, ApoC-II, HBB-1, HBB-2, HBE-1, T-kininogen 1, NDK A/B, SAA4, VSTM2B, and YWHAG; however, *M. vaccae* NCTC 11659 may have promoted a stress-induced increase of alpha-2-M, Cryab, Ig-like protein A0A0G2JTG4, Serpin A3C, and TGN38. Among animals immunized with *M. vaccae* NCTC 11659, IS decreased the abundance of alpha-2-HC-glycoprotein (also known as 59 kDa bone sialic acid-containing protein; BSP), major urinary protein (MUP; also known as alpha-2u globulin PGCL1), NCAM1, and uncharacterized proteins with UniProt IDs A0A0G2K896 (similar to RIKEN cDNA) and F1M2W3 (Figure 4.2D). Immunization with *M. vaccae* NCTC 11659 prevented a stress-induced decrease of albumin, CgA, FRRS1L, Ntm, Ogn, PAF-AH, and PIK3IP1; however, *M. vaccae* NCTC 11659

may have promoted a stress-induced decrease of BSP, MUP, vinculin, and uncharacterized proteins with UniProt IDs A0A0G2K896 and F1M2W3.

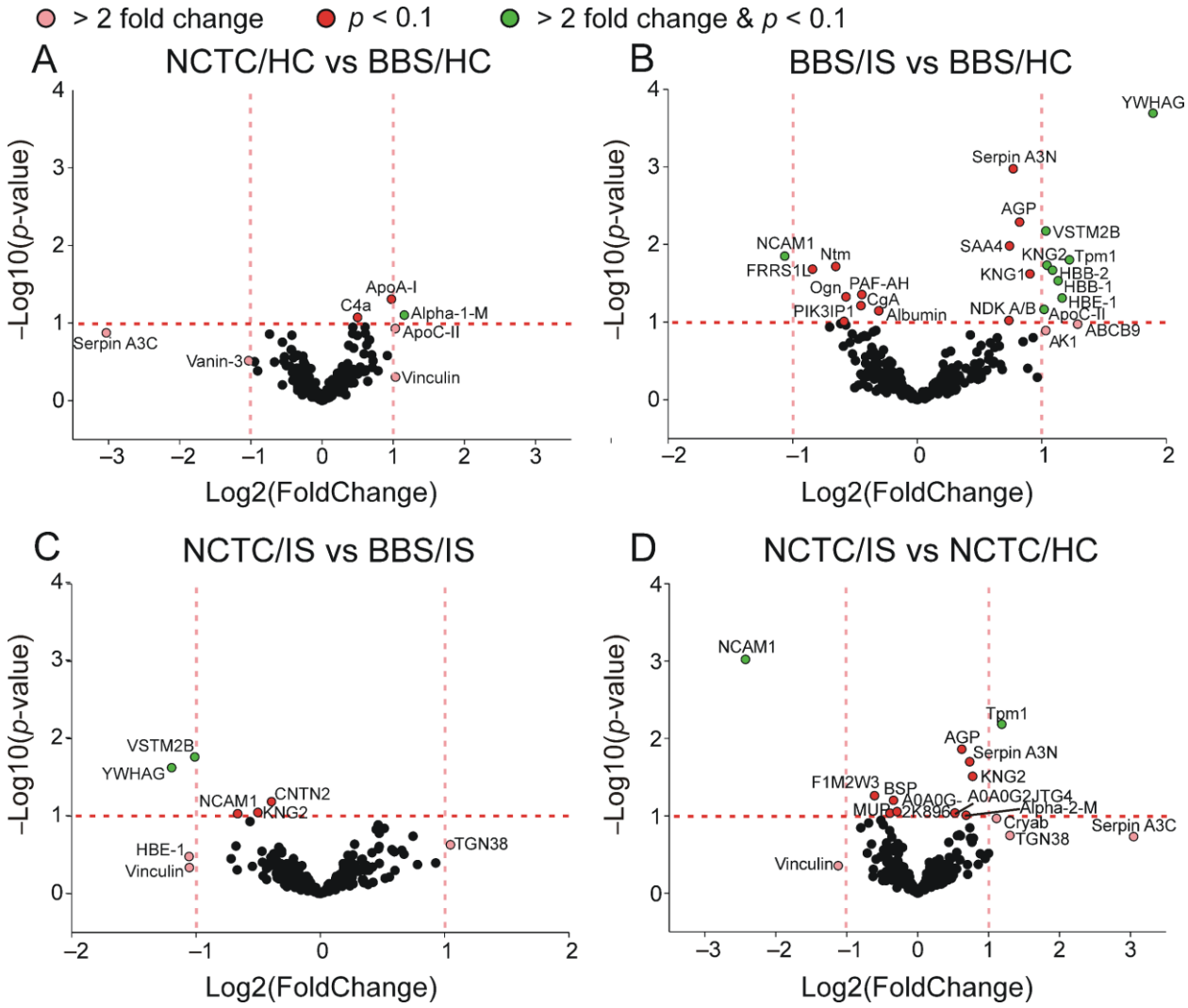

Figure 4.2 Volcano plot showing effects of immunization with *Mycobacterium vaccae* NCTC 11659 and inescapable tail shock stress (IS) on the cerebrospinal fluid (CSF) proteome of adult male rats, as measured by liquid chromatography-tandem mass spectrometry (LC-MS/MS).

The pink vertical dashed lines represent the thresholds for greater than two-fold change in average corrected peak intensity, corresponding to proteins labeled pink, and the red horizontal dashed line represents the threshold for significance at a *p*-value less than 0.1, corresponding to proteins labeled red. Proteins labeled green had both a two-fold difference in abundance and a *p*-value less than 0.1. Panel B from Figures 2 and 3 are the same, duplicated for reference. Final sample sizes for CSF analysis: BBS/HC, *n* = 7; NCTC/HC, *n* = 8; BBS/IS, *n* = 7; NCTC/IS, *n* = 7. Abbreviations: ABCB9, ATP-binding cassette sub-family B member 9; AGP, alpha-1-acid

glycoprotein; AK1, adenylate kinase isoenzyme 1; alpha-1-M, alpha-1-macroglobulin; alpha-2-M, alpha-2-macroglobulin; ApoA-I, apolipoprotein A-I; ApoC-II, apolipoprotein C-II; ATCC, *M. vaccae* ATCC 15483; BBS, borate-buffered saline; BSP, alpha-2-HC-glycoprotein (also known as 59 kDa bone sialic acid-containing protein); CgA, chromogranin-A; Cryab, alpha-crystallin B chain; C4a, complement C4a; FRRS1L, DOMON domain-containing protein FRRS1L; HBB-1, hemoglobin subunit beta 1; HBB-2, hemoglobin subunit beta 2; HBE-1, hemoglobin subunit epsilon 1; HC, home cage control; IS, inescapable tail shock; MUP, major urinary protein; NCAM1, neural cell adhesion molecule 1; NCTC, *M. vaccae* NCTC 11659; NDK A/B, nucleoside diphosphate kinase A/B; Ntm, neurotrimin; Ogn, osteoglycin; PAF-AH, platelet-activating factor acetylhydrolase; PIK3IP1, phosphoinositide-3-kinase-interacting protein 1; SAA4, serum amyloid A protein; Serpin A3C, serine proteinase inhibitor, clade A, member 3C; TGN38, trans-Golgi network integral membrane protein TGN38; Tpm1, tropomyosin alpha-1 chain; Vanin-3, vascular non-inflammatory molecule 3; VSTM2B, V-set and transmembrane domain containing 2B; YWHAG, 14-3-3 protein gamma.

4.4.4 Pairwise comparisons with M. vaccae ATCC 15483

Effects of immunization with M. vaccae ATCC 15483 on protein abundances in the CSF of home cage control animals

Fold change analysis revealed that, among home cage control rats, immunization with *M. vaccae* ATCC 15483 did not increase nor decrease the abundance of any proteins in the CSF by two-fold (Figure 4.3A).

Likewise, the pairwise comparison analysis did not find a significant difference in the abundance of any proteins in the CSF between *M. vaccae* ATCC 15483-treated and BBS-treated home cage animals (Figure 4.3A).

For effects of stress on protein relative abundances in the CSF of vehicle-treated animals, see previous section entitled, “Effects of stress on protein relative abundances in the CSF of vehicle-treated animals” (Figure 4.2B; Figure 4.3B).

Effects of immunization with M. vaccae ATCC 15483 on protein relative abundances in the CSF of IS-exposed animals

Fold change analysis revealed that, among IS-exposed rats, immunization with *M. vaccae* ATCC 15483 did not increase the abundance of any proteins in the CSF by two-fold (Figure 4.3C). Among IS-exposed animals, immunization with *M. vaccae* ATCC 15483 decreased the abundance of six proteins by two-fold: fructose-bisphosphate aldolase C (AldoC), ApoC-II, fibulin-1 (FIBL-1), YWHAG, an uncharacterized protein with UniProt ID A0A0G2JX36, and an uncharacterized protein with UniProt ID A0A0G2JY98 (Figure 4.3C).

The pairwise comparison analysis found a significant difference in abundance of five proteins in the CSF between *M. vaccae* ATCC 15483-treated and BBS-treated rats exposed to IS. Among IS-exposed animals, immunization with *M. vaccae* ATCC 15483 increased the abundance of CD99 and FRRS1L compared to BBS-treated animals (Figure 4.3C). Among IS-exposed animals, immunization with *M. vaccae* ATCC 15483, like immunization with *M. vaccae* NCTC 11659, decreased the abundance of YWHAG (Figure 4.3C). Additionally, immunization with *M. vaccae* ATCC 15483 decreased the abundance of ApoC-II and an uncharacterized protein with UniProt ID A0A0G2JY98 among IS-exposed rats (Figure 4.3C).

Effects of stress on protein relative abundances in the CSF of animals immunized with M. vaccae ATCC 15483

Fold change analysis revealed that, among rats immunized with *M. vaccae* ATCC 15483, IS increased the abundance of four proteins in the CSF by two-fold: AGP, HBE-1, Tpm1, and VSTM2B (Figure 4.3D). Among animals immunized with *M. vaccae* ATCC 15483, IS decreased

the abundance of four proteins by two-fold: AldoC, FIBL-1, NCAM1, and parvalbumin alpha (Pvalb) (Figure 4.3D).

The pairwise comparison analysis found a significant difference in abundance of ten proteins in the CSF between IS-exposed and home cage control rats immunized with *M. vaccae* ATCC 15483. Among animals immunized with *M. vaccae* ATCC 15483, IS increased the abundance of seven proteins: AGP, CD99, CNTN2, HBE-1, Serpin A3N, Tpm1, and VSTM2B (Figure 4.3D). Immunization with *M. vaccae* ATCC 15483, like immunization with *M. vaccae* NCTC 11659, prevented the stress-induced increase of ABCB9, AK1, ApoC-II, HBB-1, HBB-2, T-kininogen 1, NDK A/B, SAA4, and YWHAG; additionally, *M. vaccae* ATCC 15483 prevented the stress-induced increase of T-kininogen 2. Immunization with *M. vaccae* ATCC 15483 may have promoted a stress-induced increase of CD99 and CNTN2. Among animals immunized with *M. vaccae* ATCC 15483, IS decreased the abundance of three proteins: carboxylesterase 1C (Ces1C), IGF-I, and NCAM1 (Figure 4.3D). Immunization with *M. vaccae* ATCC 15483, like immunization with *M. vaccae* NCTC 11659, prevented the stress-induced decrease of albumin, CgA, FRRS1L, Ntm, Ogn, PAF-AH, and PIK3IP1. Immunization with *M. vaccae* ATCC 15483 may have promoted a stress-induced decrease of AldoC, Ces1C, FIBL-1, IGF-I, and Pvalb.

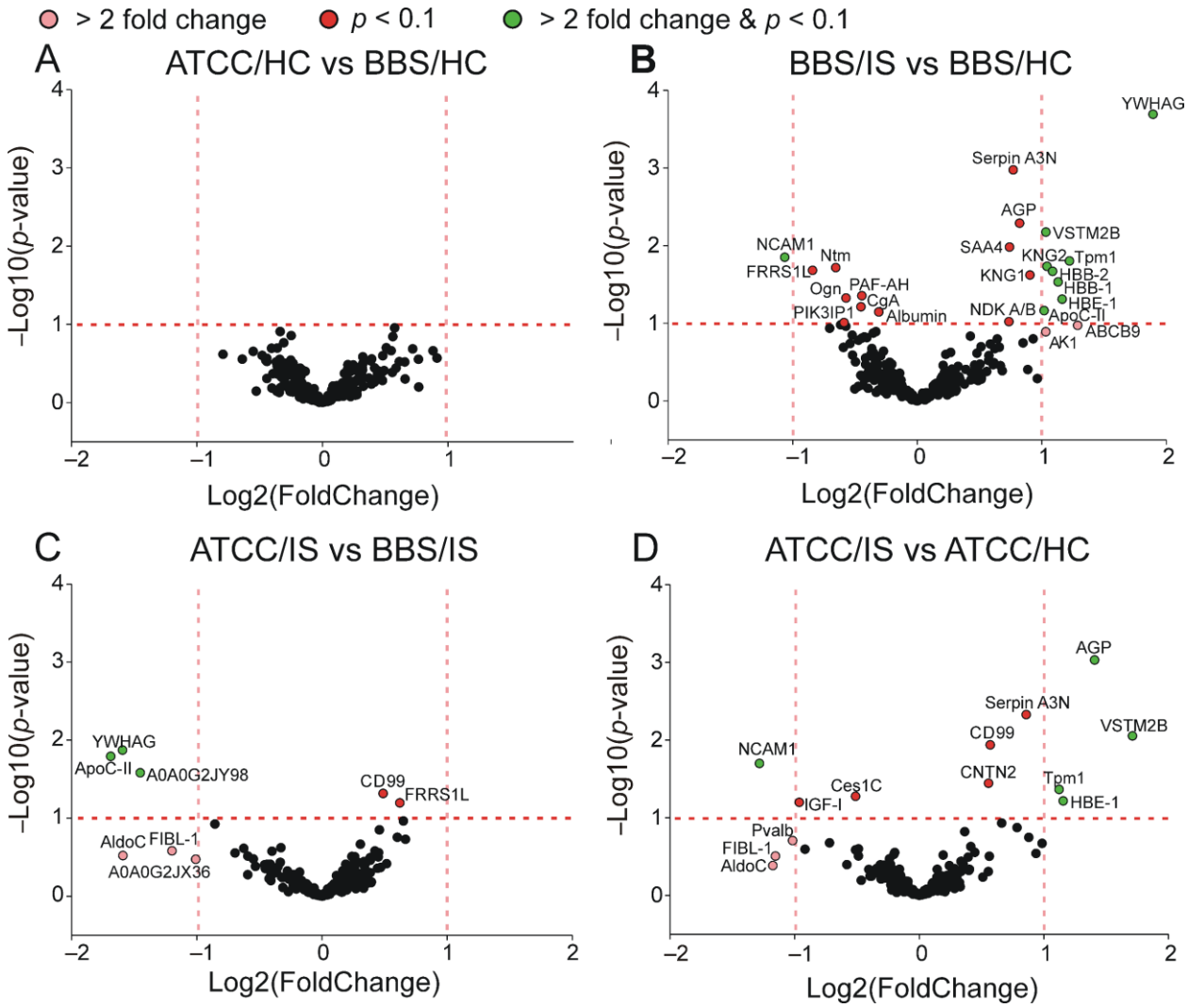

Figure 4.3 Volcano plot showing effects of immunization with *Mycobacterium vaccae* ATCC 15483 and inescapable tail shock stress (IS) on cerebrospinal fluid (CSF) proteome of adult male rats, as measured by liquid chromatography-tandem mass spectrometry (LC-MS/MS).

The pink vertical dashed lines represent the thresholds for greater than two-fold change in average corrected peak intensity, corresponding to proteins labeled pink, and the red horizontal dashed line represents the threshold for significance at a *p*-value less than 0.1, corresponding to proteins labeled red. Proteins labeled green had both a two-fold difference in abundance and a *p*-value less than 0.1. Panel B from Figures 2 and 3 are the same, duplicated for reference. Final sample sizes for CSF analysis: BBS/HC, *n* = 7; ATCC/HC, *n* = 8; BBS/IS, *n* = 7; ATCC/IS, *n* = 8. Abbreviations: ABCB9, ATP-binding cassette sub-family B member 9; AGP, alpha-1-acid glycoprotein; AK1, adenylate kinase isoenzyme 1; AldoC, fructose-bisphosphate aldolase C; ApoC-II, apolipoprotein C-II; ATCC, *M. vaccae* ATCC 15483; BBS, borate-buffered saline; BSP, alpha-2-HC-glycoprotein (also known as 59 kDa bone sialic acid-containing protein); CD, cluster of differentiation; CgA, chromogranin-A; FIBL-1, fibulin 1; FRRS1L, DOMON domain-containing protein FRRS1L; HBB-1, hemoglobin subunit beta 1; HBB-2, hemoglobin subunit beta 2; HBE-1, hemoglobin subunit epsilon 1; HC, home cage control; IS, inescapable tail shock; NCAM1, neural cell adhesion molecule 1; NCTC, *M. vaccae* NCTC 11659; NDK A/B, nucleoside diphosphate kinase A/B; Ntm, neurotrimin; Ogn, osteoglycin; PAF-AH, platelet-activating factor acetylhydrolase; PIK3IP1, phosphoinositide-3-kinase-interacting protein 1; Pvalb, parvalbumin alpha;

SAA4, serum amyloid A protein; Serpin A3N, serine protease inhibitor A3N; TGN38, trans-Golgi network integral membrane protein TGN38; Tpm1, tropomyosin alpha-1 chain; VSTM2B, V-set and transmembrane domain containing 2B; YWHAG, 14-3-3 protein gamma.

4.4.5 Functional enrichment analysis of CSF proteomics

To better understand how *M. vaccae* strains might be altering different biological functions in CSF to prevent stress-induced increases in hippocampal *Il6* mRNA expression and promote stress-resilience behavior, functional enrichment gene analyses, including pathway analysis and gene ontology (GO) analyses, were performed separately on: 1) subsets of proteins that were upregulated or downregulated (as measured by two-fold change and *p*-value) by immunization with *M. vaccae* NCTC 11659 or *M. vaccae* ATCC 15483 in home cage control rats (Supplementary Table 4.1); 2) subsets of proteins that were upregulated or downregulated (as measured by two-fold change and *p*-value) by IS exposure in BBS-treated rats (Supplementary Table 4.2); 3) proteins that were prevented from increasing or decreasing after IS in rats immunized with *M. vaccae* NCTC 11659 (Supplementary Table 4.3); 4) proteins that increased or decreased after IS only in rats immunized with *M. vaccae* NCTC 11659 (Supplementary Table 4.3); 5) proteins that were prevented from increasing or decreasing after IS in rats immunized with *M. vaccae* ATCC 15483 (Supplementary Table 4.4); and 6) proteins that increased or decreased after IS only in rats immunized with *M. vaccae* ATCC 15483 (Supplementary Table 4.4). Interestingly, among BBS-treated rats, IS increased proteins involved in "acute-phase response" (*Kng1*, *Kng2*, *Orm1*, *Saa4*), "nucleoside triphosphate biosynthetic process" (*Ak1*, *Ndk1/2*) "cellular response to glucocorticoid stimulus" (*Orm1*, *Serpina3n*), and "negative regulation of cell adhesion" (*Kng1*, *Kng2*), as annotated by the GO analysis for biological processes; likewise, IS decreased proteins involved in "cell adhesion" (*Ncam1, Ntm*) (Supplementary Table 4.2). Additionally, IS increased proteins associated with "blood

microparticle" (*Hbb-b2, Hbe1, Kng1, Kng2, Orm1*) and increased and decreased proteins associated with "extracellular exosome" (increased: *Ak1, Apoc2, Kng1, Kng2, Nme1/2, Orm1, Ywhag*; decreased: *Alb, Ncam1, Ogn, Pik3ip1*), as annotated by the GO analysis for cellular component. All functional enrichment results for CSF can be found in Supplementary Tables 4.1–4.4.

Although there were no pathways enriched for the subset of proteins altered in the CSF eight days after the final immunization with *M. vaccae* NCTC 11659, all gene ontology annotations can be found in Supplementary Table 4.1; there were no proteins altered in the CSF eight days after the final immunization with *M. vaccae* ATCC 15483. The subset of proteins increased among BBS-treated rats 24 hours after IS was enriched for two pathways: "African trypanosomiasis" and "malaria" (Supplementary Table 4.2). There were no pathways enriched by the subset of proteins decreased after IS (Supplementary Table 4.2). Immunization with *M. vaccae* NCTC 11659 prevented the stress-induced increase of proteins enriched for the pathways "African trypanosomiasis" and "malaria" (Supplementary Table 4.3). There were no pathways enriched by those proteins whose stress-induced increase was promoted by immunization with *M. vaccae* NCTC 11695, and there were no pathways enriched by those proteins whose stress-induced decrease was promoted by immunization with *M. vaccae* NCTC 11659 (Supplementary Table 4.3). Immunization with *M. vaccae* ATCC 15483, like immunization with *M. vaccae* NCTC 11659, prevented the stress-induced increase of proteins enriched for the pathways "African trypanosomiasis" and "malaria" (Supplementary Table 4.4). There were no pathways enriched by those proteins whose stress-induced increase was promoted by immunization with *M. vaccae* ATCC 15483, and there were no pathways enriched by those proteins whose stress-

induced decrease was promoted by immunization with *M. vaccae* ATCC 15483 (Supplementary Table 4.4).

4.4.6 Protein-protein interaction (PPI) network analysis of CSF proteomics

To better visualize the effects of IS on the plasma proteome, including how IS may affect proteins enriched for pathway and GO annotations, protein-protein network analysis using STRING (v. 11) was performed individually on the subset of proteins increased or the subset of proteins decreased after IS among BBS-treated animals, and the networks were created using k-means clustering within two clusters.

Within the subset of proteins increased after IS, STRING revealed a significant number of protein-protein interactions, with fifteen nodes and six association edges (PPI enrichment *p*-value = 9.5E-05) (Figure 4.4A). Immunization with either *M. vaccae* NCTC 11659 or *M. vaccae* ATCC 15483 prevented the stress-induced increase in proteins involved in all four network clusters including the primary cluster containing AGP, T-kininogen 1, T-kininogen 2, and Serpin A3N.

Within the subset of proteins decreased after IS, STRING did not reveal a significant number of protein-protein interactions (PPI enrichment *p*-value = 0.11). The PPI network analysis established only eight nodes and two association edges between the eight proteins (Figure 4.4B).

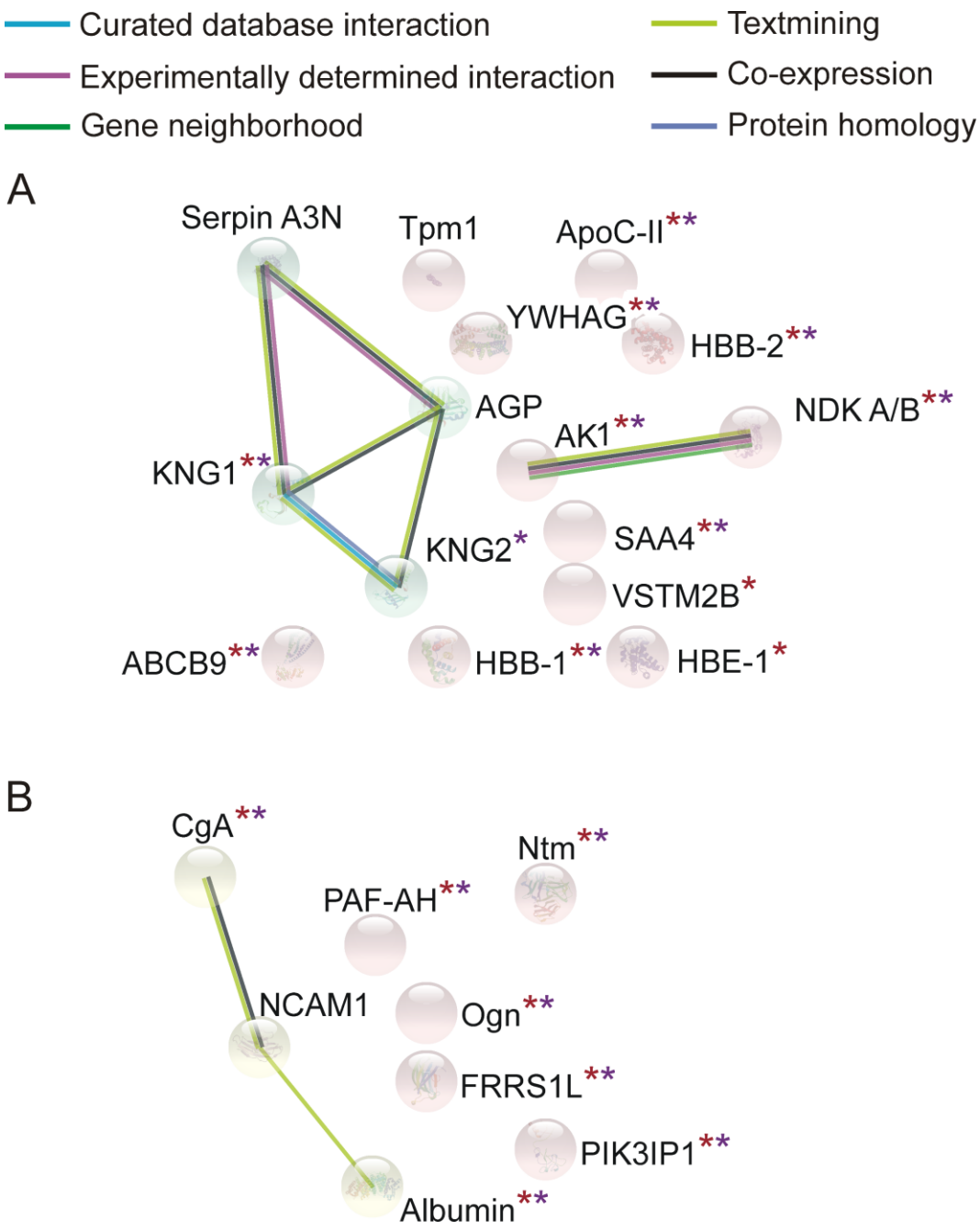

Figure 4.4 Protein-protein interaction networks for proteins (A) increased and (B) decreased in the CSF after IS among BBS-treated rats, clustered by a k-means algorithm within five clusters.

Asterisks in red indicate proteins whose stress-induced increase or decrease was prevented by immunization with *M. vaccae* NCTC 11659 and asterisks in purple indicate proteins whose stress-induced increase or decrease was prevented by immunization with *M. vaccae* ATCC 15483. Associations were computed by STRING database (v.11). Solid lines represent associations within clusters. Final sample sizes for plasma analysis were BBS/HC, $n = 7$, BBS/IS, $n = 7$. Abbreviations: ABCB9, ATP-binding cassette sub-family B member 9; AGP, alpha-1-acid glycoprotein; AK1, adenylate kinase isoenzyme 1; ApoC-II, apolipoprotein C-II;

CgA, chromogranin A; FRRS1L, DOMON domain-containing protein FRRS1L; HBB-1, hemoglobin subunit beta 1; HBB-2, hemoglobin subunit beta 2; HBE-1, hemoglobin subunit epsilon 1; NCAM1, neural cell adhesion molecule 1; NDK A/B, nucleoside diphosphate kinase A/B; Ntm, neurotrimin; Ogn, osteoglycin; PAF-AH, platelet-activating factor acetylhydrolase; PIK3IP1, platelet-activating factor acetylhydrolase; SAA4, serum amyloid A protein; Serpin A3N, serine protease inhibitor A3N; Tpm1, tropomyosin alpha-1 chain; VSTM2B, V-set and transmembrane domain containing 2B; YWHAG, 14-3-3 protein gamma.

4.4.7 Correlations between the CSF proteome and Il6 mRNA expression in the dorsal hippocampus

We previously showed that immunization with either *M. vaccae* NCTC 11659 or *M. vaccae* ATCC 15483 can prevent stress-induced anxiety-like defensive behavioral responses as measured by the juvenile social exploration (JSE) paradigm one day following inescapable tail shock (Loupy et al., 2021). These behavioral effects coincided with the expression of *Il6* mRNA in the dorsal hippocampus, and immunization with either strain of *M. vaccae* prevented stress-induced increases in *Il6* mRNA (Loupy et al., 2021). Considering that the CSF collected in this study was taken from the same rats, we wanted to investigate whether changes in the CSF proteome correlated with either behavior or *Il6* mRNA expression. There were no proteins whose abundance correlated with JSE behavior. However, out of 262 proteins, there were 20 proteins whose relative abundance correlated with the relative expression of *Il6* mRNA in the dorsal hippocampus (FDR-adjusted $p < 0.1$). The relative abundance of the following 15 proteins positively correlated with *Il6* mRNA expression in the dorsal hippocampus: ABCB9, augurin, aspartate aminotransferase (AST), CPE, fibulin-5, G-protein coupled receptor 158 (GPCR158), insulin-like growth factor-binding protein 5 (IGFBP-5), beta-1,3-N-acetylglucosaminyltransferase lunatic fringe (LFNG), neural cell adhesion molecule 2 (NCAM2), neuronal pentraxin receptor (NPTXR), Ntm, pro-melanin-concentrating hormone (pro-MCH), sulfhydryl oxidase 1 (rQSOX), VSTM2B, and YIP1 family member 3 (YIPF3)

(Supplementary Table 4.5). In contrast, the relative abundance of the following five proteins negatively correlated with *Il6* mRNA expression in the dorsal hippocampus: elongation factor 1-alpha 1 (EF-1-alpha-1), glutathione peroxidase 1 (GPx1), Ig gamma-2C chain C region (IgG-2c), myeloid-derived growth factor (MYDGF), and an uncharacterized protein with UniProt ID A0A0G2JXF0 (Supplementary Table 4.5). Interestingly, of the proteins that correlated with *Il6* mRNA expression, four of them were found to be significantly altered by treatment, stress, or treatment x stress in our current study: ABCB9, CPE, Ntm, and VSTM2B (Supplementary Table 4.5). Correlations between each of these four proteins and *Il6* mRNA in the dorsal hippocampus can be found in Supplementary Figure 4.1. Considering that YWHAG is associated with inflammatory monocyte-derived macrophages, we were surprised to find that YWHAG did not correlate with *Il6* mRNA expression in the dorsal hippocampus among all groups. This led us to investigate correlations between YWHAG and *Il6* mRNA expression separated by treatment (i.e. BBS, *M. vaccae* NCTC 11659, and *M. vaccae* ATCC 15483) as done previously (Loupy et al., 2021). Indeed, CSF YWHAG strongly positively correlated with *Il6* mRNA in the dorsal hippocampus among BBS-treated animals ($r = 0.708$; $p < 0.01$) but not among animals previously immunized with either strain of *M. vaccae* ($p > 0.05$; Supplementary Figure 4.2).

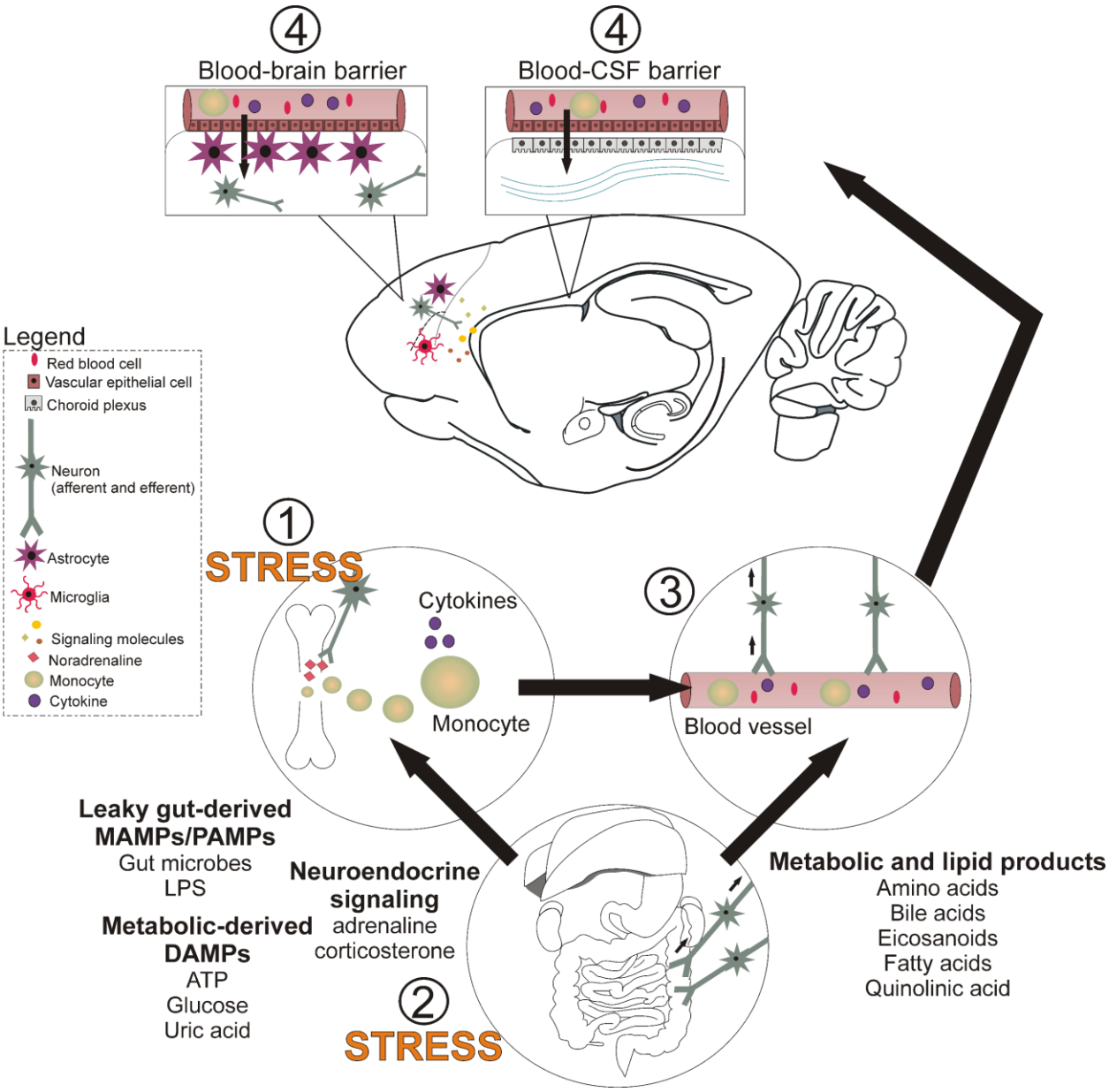

Figure 4.5 General overview of stress signaling and monocyte trafficking from the periphery to the brain, including: 1) release of monocytes from the bone marrow stimulated by sympathetic nervous system (SNS) release of noradrenaline; 2) induction of a proinflammatory monocyte phenotype by effects of danger-associated molecular patterns (DAMPs), microbe-associated molecular patterns (MAMPs), and pathogen-associated molecular patterns (PAMPs), and neuroendocrine signaling molecules on circulating monocytes; 3) vascular-mediated trafficking of monocytes to the brain; and 4) transmigration of monocytes across the blood-brain barrier (BBB) and blood-cerebrospinal fluid barrier (BCSFB).

Stress-induced alterations to immune, metabolic, enteric nervous system, or vascular signaling may induce monocytes toward a proinflammatory state or compromise the endothelial integrity at the BBB and BCSFB. In our study, we found that prior immunization with *M. vaccae* NCTC

11659 or *M. vaccae* ATCC 15483 largely attenuates inescapable tail shock (IS)-induced physiological responses as measured in the plasma and CSF proteome, which are associated with prevention of IS-induced hippocampal *Il6* mRNA expression and promotion of stress-resilient behaviors. Abbreviations: ATP, adenosine triphosphate; CSF, cerebrospinal fluid; DAMPs, danger-associated molecular patterns, LPS, lipopolysaccharide; MAMPs, microbe-associated molecular patterns; PAMPs, pathogen-associated molecular patterns.

4.5 Discussion

IS altered the CSF proteome measured 24 hours after stress exposure, but prior immunization with *M. vaccae* NCTC 11659 or *M. vaccae* ATCC 15483 prevented the IS-induced increases and decreases of a large subset of CSF proteins. Functional enrichment analysis revealed that IS increased proteins in CSF associated with the acute phase response and blood microparticles. Immunization with either *M. vaccae* NCTC 11659 or *M. vaccae* ATCC 15483 attenuated the IS-induced alteration of nine proteins involved in vascular endothelial function: CgA, HBB-1, HBB-2, HBE-1, KNG1, KNG2, Ntm, Ogn, SAA4; these results might suggest that *M. vaccae* strains mitigate stress-induced impairments in the BBB or blood-CSF barrier (BCSFB). Another set of proteins (ABCB9, AK1, ApoC-II, NDK A/B, SAA4, YWHAG) whose stress-induced increase was prevented with prior immunization with *M. vaccae* strains are associated with inflammatory monocyte-derived macrophages, which traffic from the bone marrow to the central nervous system (CNS) following stress and drive central neuroinflammatory responses. In contrast, two proteins (PAF-AH, PIK3IP1) whose stress-induced decrease was prevented with prior immunization of *M. vaccae* strains are negative immune regulators associated with inflammation-resolving macrophages. Together, these data align with the hypothesis that stress-induced increases in anxiety-like defensive behavioral responses are driven by translocation of interleukin (IL)-6-secreting inflammatory monocytes that, following stress-induced activation of the sympathetic nervous system, traffic from the bone marrow to the CNS, which may be aided

by stress-induced disruption of the BBB or BCSFB. Our data would also support the hypothesis that immunization with *M. vaccae* strains interferes with the infiltration or differentiation of inflammatory monocyte-derived macrophages in the CNS, consistent with the stress-resilient behavioral effects of *M. vaccae* strains.

4.5.1 Evidence that M. vaccae strains induce persistent changes in the CSF proteome in the absence of stress exposure

There was little evidence that *M. vaccae* strains induced persistent changes in the CSF proteome in the absence of stress exposure. Indeed, *M. vaccae* ATCC 15483 had no significant effect on any CSF protein assessed eight days following the final immunization. This suggests that *M. vaccae* strains do not have major persistent effects on baseline functioning within the CSF compartment, but instead, perhaps through persistent anti-inflammatory and immunoregulatory effects, alter the acute physiological and behavioral response to trauma or stressor exposures.

4.5.2 Evidence that IS alters the CSF proteome

Data reported here provide evidence that IS exposure altered the CSF proteome assessed 24 h after IS. Briefly, evidence suggests that IS: 1) disrupted the BBB or BCSFB functioning; 2) induced cerebral microvascular endothelial injury or remodeling; 3) induced a biological signature of complement and coagulation cascades; 4) induced trafficking of inflammatory bone marrow-derived monocytes to the CNS, followed by differentiation of inflammatory, M1-type, monocyte-derived macrophages; and 5) altered lipid-immune signaling in the CNS. Each of these effects of IS will be discussed in detail below in the context of the degree to which prior immunization with *M. vaccae* NCTC 11659 and *M. vaccae* ATCC 15483 prevented these effects.

4.5.3 Evidence that immunization with M. vaccae strains prevent IS-induced disruption of the BBB or BCSFB

As mentioned above, IS altered the CSF proteome measured 24 h after stress exposure, but prior immunization with *M. vaccae* NCTC 11659 or *M. vaccae* ATCC 15483 prevented the IS-induced increases and decreases of a large subset of CSF proteins. Furthermore, immunization with either *M. vaccae* NCTC 11659 or *M. vaccae* ATCC 15483 attenuated the IS-induced alteration of nine proteins involved in vascular endothelial function: CgA, HBB-1, HBB-2, HBE-1, KNG1, KNG2, Ntm, Ogn, SAA4; these results might suggest that *M. vaccae* strains mitigate stress-induced impairments in the BBB or BCSFB. Stress-induced damage to the BBB and BCSFB are well described in the literature (Dudek et al., 2020; Lehmann et al., 2020; Welcome and Mastorakis, 2020; Xu et al., 2019), and disruption at the vascular endothelial junction of the BBB or BCSFB after IS might explain the increased filtration or secretion of plasma proteins from blood to the CSF (Lehmann et al., 2020). Indeed, recent studies have demonstrated that social stress in mice disrupts the integrity of the BBB through loss of tight junction protein claudin-5 (Cldn5), promoting translocation of peripheral IL-6 across the BBB, resulting in a depressive-like phenotype (Menard et al., 2017a). Furthermore, Cldn5 downregulation was sufficient to induce depression-like behavioral responses following subthreshold social stress while chronic antidepressant treatment rescued Cldn5 loss and promoted stress resilience (Menard et al., 2017a). CLDN5 expression was also decreased in the brains of depressed patients (Menard et al., 2017a). Interestingly, data from the plasma proteome of these same rats also demonstrated changes to the abundance of proteins involved in maintaining the function and integrity of the vascular endothelium 24 hours after IS; these effects were largely attenuated in rats immunized with *M. vaccae* strains (see part I of this article). In the current study, among BBS-treated rats, IS increased the abundances of KNG1 and KNG2, which are involved in

"negative cell adhesion," and decreased the abundances of NCAM1 and Ntm, which are associated with "cell adhesion," as annotated by GO analysis of biological processes. Immunization with *M. vaccae* strains attenuated the IS-induced alteration of three (KNG1, KNG2, Ntm) of these four proteins. Simultaneously, among rats immunized with *M. vaccae* ATCC 15483, IS increased the abundance of CD99 and CNTN2, proteins important for the maintenance of endothelial cell tight junctions and neuronal cell adhesion, respectively (KEGG rno04514). NCAM1, which is expressed in neurons and plays an important role in synaptogenesis (Sytnyk et al., 2017), learning and memory (Lüthi et al., 1994; Vukojevic et al., 2020), and dopamine signaling (Xiao et al., 2009), was decreased after IS regardless of treatment, suggesting a general effect of IS on neuronal structure or function that may warrant further investigation.

Nonetheless, data reported here suggest that immunization with *M. vaccae* type strains appears to specifically buffer against IS-induced changes in the abundance of vascular endothelial proteins in the CSF, which may be required for the previously reported stress-resilient behavioral effects of *M. vaccae* treatment (Loupy et al., 2021). Prior studies demonstrate that social defeat stress causes cerebrovascular dysfunction (Lehmann et al., 2020; Menard et al., 2017a) and alters the expression of vascular endothelial proteins to promote monocyte trafficking into the CNS (Menard et al., 2017b; Sawicki et al., 2015). Social stress (Stankiewicz et al., 2014) and chronic unpredictable mild stress (Ma et al., 2016) increase *Hba-a1*, *Hba-a2*, *Hbb-b1* and *Hbb-b2* mRNA expression in prefrontal cortex of mice, although the reason for this is still unclear. Interestingly, hemoglobin is implicated in matrix metalloproteinase 9 activation and subsequent BBB and BCSFB dysfunction following vascular injury and erythrocyte lysis in the brain (Gram

et al., 2014; Katsu et al., 2010). Similarly, SAA4, which is released after stress-induced sympathetic nervous system activation (Konstandi et al., 2019), can impair the BBB by reducing tight junctions of microvascular endothelial cells (Matsumoto et al., 2020); of particular interest, SAA4 decreases the expression of claudin-5 in rat brain microvascular endothelial cells (RBECs). SAA4 was also increased in the plasma proteome following IS, but its stress-induced increase was only prevented by *M. vaccae* strains in the CSF proteome. Ogn is an important component of the endothelial glycocalyx, which is disrupted during inflammatory events (Kolářová et al., 2014), and CgA can protect the endothelium against vascular leakage due to inflammation (Ferrero et al., 2002); immunization with *M. vaccae* strains prevented the IS-induced decrease of both of these proteins. Likewise, the pathway "African trypanosomiasis" was enriched in our dataset of proteins increased after IS, including HBB-1, HBB-2, and HBE-1, which were annotated by DAVID, but also complement component C9 and kininogen-1 (KEGG rno05143). Among these proteins, immunization with *M. vaccae* prevented IS-induced increases of HBB-1, HBB-2, HBE-1, and KNG1; immunization with *M. vaccae* ATCC 15483 prevented IS-induced increases of KNG2, and among rats exposed to IS, the abundance of KNG2 was decreased in the CSF of animals previously immunized with *M. vaccae* NCTC 11659 compared to vehicle-treated animals. Although not significant in our pairwise comparison testing, there was a significant interaction effect of *M. vaccae* NCTC 11659 x IS on C9, where IS tended to increase the abundance of factor C9 ($\log_2$[fold change] = 0.43, $p = 0.13$), but prior immunization with either *M. vaccae* NCTC 11659 or *M. vaccae* ATCC 15483 prevented this effect of IS ($\log_2$[fold change] = –0.052 and $p = 0.88$; $\log_2$[fold change] = 0.16 and $p = 0.71$, respectively). Interestingly, African trypanosomiasis pathology is associated with endothelial dysfunction at the BBB or BCSFB (Grab and Kennedy, 2008; Lonsdale-Eccles and Grab, 2002), and evidence

suggests that parasitic trypanosomes might cross directly into the CSF via the BCSFB (Mogk et al., 2014).

To further investigate the possibility of increased BCSFB permeability, we analyzed the albumin CSF/plasma ratio of BBS-treated rats exposed to IS versus home cage control animals (Musaeus et al., 2020). An independent samples *t*-test revealed that the relative abundance of albumin CSF/plasma ratio was not significantly different between BBS/IS and BBS/HC groups (t = 0.417; p = 0.685). This is likely because albumin levels decreased in both plasma and CSF, and thus is not a stable marker to determine leakiness of the BCSFB barrier. Although, in plasma, the abundance of albumin decreased 24 hours after IS among both BBS- and *M. vaccae* ATCC 15483-treated rats, in CSF, the abundance of albumin was only decreased after IS among vehicle-treated rats. Considering that albumin is decreased in response to inflammation (Ambrus and Westling, 2019; Hübner et al., 2016; Kaysen et al., 2004) and is filtered into the CSF from the blood (Musaeus et al., 2020; Pisani et al., 2012), this finding is consistent with the hypothesis that immunization with *M. vaccae* strains protects the CNS from inflammatory responses after stress, possibly by promoting BBB or BCSFB integrity.

4.5.4 Evidence that immunization with M. vaccae strains prevent IS-induced cerebrovascular injury

One possibility is that stress promoted microvascular endothelial injury (Menard et al., 2017b, 2017a) or remodeling (Lehmann et al., 2020; Pearson-Leary et al., 2017; Sawicki et al., 2015) associated with bacterial translocation from the gut to the brain (Al-Obaidi and Desa, 2018; Banks et al., 2015). In line with this idea, AST, which positively correlated with *Il6* mRNA expression in the dorsal hippocampus, is associated with brain ischemia and BBB disruption

(Kelbich et al., 2020). We also found increased abundances of C9, KNG1, and KNG2 in the CSF proteome of BBS-treated rats 24 hours after IS, replicating our results in the plasma proteome (see part I of this article); these proteins are involved in complement and coagulation cascades (KEGG rno04610) as a defense response to pathogens and/or endothelial damage (Cagliani et al., 2013; Ding et al., 2018; Dunkelberger and Song, 2010; Köhler et al., 2020; Nordahl et al., 2005). In the CSF, prior immunization with either *M. vaccae* NCTC 11659 or *M. vaccae* ATCC 15483 attenuated the stress-induced increase of these proteins. NDK A/B and AK1, which also increased after IS among BBS-treated rats but not animals previously immunized with *M. vaccae* strains, are important kinases for the biosynthesis of adenosine triphosphate (ATP) (GO:0009142) and may act as intracellular sensors for energy homeostasis of cells (Dzeja and Terzic, 2009; Lacombe et al., 2018). The release of ATP and associated purinergic enzymes might be a sign of microvasculature cell lysis (Allard et al., 2005; Büttner et al., 1986; Gross et al., 2017). Likewise, extracellular purinergic signaling might be indicative of anti-microbial activity in the CNS (Alves et al., 2020; Z. Zhang et al., 2019). For example, NDK A secretion from the choroid plexus is increased after a treatment with the endotoxin component of lipopolysaccharide (LPS), lipid A (Takano et al., 2014); furthermore, NDK isoforms are secreted from pathogenic bacteria, including *Mycobacterium* species (Chopra et al., 2003; H. Yu et al., 2017), and host-targeted lysis of pathogenic mycobacterial cells promotes release of AK1 from host cells (Forbes et al., 2015). Notably, ATP acts as a damage-activated molecular pattern (DAMP) that promotes monocyte migration from the bone marrow into the peripheral circulation (for review, see Fleshner et al., 2017) and activates proinflammatory signaling cascades toward a T helper 17 cell (Th17)-inducing pathway (Lee et al., 2018; Paustian et al., 2013). The hallmark features of African trypanosomiasis infection, a pathway enriched in our dataset among BBS-

treated animals 24 hours after IS, are both impaired BBB function and increase of macrophage transmigration into the CNS (KEGG rno rno05143) (Lonsdale-Eccles and Grab, 2002; Mogk et al., 2014). Macrophages can reside in the perivascular spaces of the brain, the choroid plexus, or transmigrate into the CSF (for review, see Herz et al., 2017; Kierdorf et al., 2019). Previous work describes monocyte-derived macrophages that traffic to the brain can lead to disruption of BCSFB vasculature in a mouse model of cerebral ischemia (Ge et al., 2017). Thus, our dataset might reflect increased monocyte-derived macrophage transmigration to the CNS, altering the secretion of endothelial cells, neural resident cells, and macrophages themselves, in parallel with, or due to, disruption of the BBB or BCSFB.

4.5.5 Evidence that immunization with M. vaccae strains prevent trafficking of inflammatory monocytes to the CNS

A striking finding is that another set of proteins whose stress-induced increase was prevented by prior immunization of mice with *M. vaccae* strains are associated with inflammatory monocyte-derived macrophages, which traffic from the bone marrow to the CNS following stress and drive central neuroinflammatory responses (Menard et al., 2017b; Niraula et al., 2019, 2018; Reader et al., 2015; Weber et al., 2017; Wohleb et al., 2013, 2011). These include ABCB9 (Demirel et al., 2007), AK1 (Kuehnel et al., 2009), ApoC-II (Wallner et al., 2014; Wolska et al., 2017), NDK A (Farkas et al., 2019), SAA4 (Jumeau et al., 2019; Song et al., 2009), and YWHAG (Ciborowski et al., 2007). Expression of ABCB9 (Demirel et al., 2007) and ApoC-II (Wallner et al., 2014) are increased upon monocyte differentiation to macrophages, while YWHAG is specifically expressed in inflammatory HIV-1 infected monocyte-derived macrophages, relative to uninfected controls (Ciborowski et al., 2007). AK1 (Kuehnel et al., 2009) and NDK A (Farkas et al., 2019) are important for macrophage phagocytotic processes, and during these events AK1 is

secreted from the macrophage (Kuehnel et al., 2009). In addition, macrophages can release ATP, synthesized by AK1 and NDK A, to promote the assembly of the NOD-, LRR- and pyrin domain-containing protein 3 (NLRP3) inflammasome and subsequent release of IL-1β from macrophages (Lee et al., 2018; Piccini et al., 2008). One study found that serum amyloid A proteins can perpetuate cytokine release from monocyte-derived macrophages through the PI3K pathway (Song et al., 2009), which aligns with the observation that PI3KIP1, a protein involved in PI3K pathway inhibition (GO, biological process; GO:0043553), is decreased in CSF after IS. The finding that immunization with either *M. vaccae* NCTC 11659 or *M. vaccae* ATCC 15483 prevented IS-induced alteration of these proteins in the CSF, which was not observed in the plasma proteome of the same animals, might suggest that *M. vaccae* may be working at the BBB or BCSFB to prevent inflammatory monocyte-derived macrophage infiltration or differentiation in the brain. As increases in release of IL-6 from monocyte-derived macrophages trafficking to the CNS have been proposed to mediate stress-induced increases in anxiety (Menard et al., 2017b, 2017a; Niraula et al., 2019; Wohleb et al., 2014), this effect may contribute to the exaggerated anxiety-like defensive behavioral responses in these animals (Loupy et al., 2021). These results provide evidence that prior immunization with either *M. vaccae* NCTC 11659 or *M. vaccae* ATCC 15483 prevented proinflammatory pathways related to monocyte-derived macrophage trafficking to the CNS, associated with the stress resilience properties of these mycobacteria (Loupy et al., 2021).

Monocytes are released from the bone marrow upon stress-induced activation of the sympathetic nervous system and release of noradrenaline at nerve terminals (Wohleb et al., 2011) as well as glucocorticoid secretion stimulated by the hypothalamic-pituitary-adrenal (HPA) axis (Niraula et

al., 2018). Monocytes and circulating macrophages are further induced toward a proinflammatory and migratory state by 1) neuroimmune signals such as adrenaline or glucocorticoids; 2) proinflammatory signaling, including cytokines and chemokines 3) cell injury, releasing DAMPs; and 4) increased intestinal permeability, leaking microbial contents such as PAMPs into the vasculature from the gut (Fleshner et al., 2017; Frank et al., 2015; Reader et al., 2015; van de Wouw et al., 2019; Weber et al., 2017; Wohleb et al., 2015) (Figure 4.5). Once monocyte-derived macrophages have trafficked into the brain, macrophages release a number of proinflammatory cytokines, enhancing microglial responses and influencing anxiety-like behavior (Menard et al., 2017b, 2017a; Reader et al., 2015; Wohleb et al., 2014). For example, stress-induced increases in anxiety-like defensive behavioral responses in rodents are associated with IL-6-primed monocyte trafficking to the brain, presenting with increased expression of mRNA encoding IL-1β, tumor necrosis factor (TNF), and IL-6 in $CD11b^{+}$ cells isolated from the brain. (Menard et al., 2017b, 2017a; Niraula et al., 2019, 2018). We have previously shown that prior immunization with *M. vaccae* NCTC 11659 prevents NLRP3-related microglial priming and associated reductions in juvenile social exploration 24 hours after IS (Frank et al., 2018b). More recently, we reported that immunization with either *M. vaccae* NCTC 11659 or *M. vaccae* ATCC 15483 prevents IS-induced increases of *Il6* mRNA expression in the dorsal hippocampus, and that *Il6* expression correlates with anxiety-like defensive behavioral responses 24 hours after IS (Loupy et al., 2021). Here, we show that the hippocampal *Il6* mRNA expression positively correlated with the monocyte-derived macrophage-associated proteins ABCB9 and YWHAG. Of note, YWHAG abundance in the CSF strongly (r = 0.71) correlated with hippocampal *Il6* mRNA expression only among BBS-treated rats, but not among animals immunized with *M. vaccae* strains, suggesting that immunization with *M. vaccae* interrupted a

stress-related relationship between YWHAG and *Il6*, which may be facilitated by monocyte-derived macrophages. IL-6, derived, in part, from inflammatory monocytes that traffic to the brain, is thought to drive anxiety-like defensive behavioral responses in rodents (Hodes et al., 2016; Menard et al., 2017b, 2017a; Niraula et al., 2019). One study demonstrated that prenatal stress in mice causes microbiome-dependent activation and transmigration of monocytes to the intrauterine environment, promoting IL-6-mediated neuroinflammation and altered serotonin synthesis in the fetal brain (Chen et al., 2020). Interestingly, YWHAG binds with and activates phosphorylated tryptophan hydroxylase, and may play a role in stress-induced, monocyte-mediated, activation of tryptophan hydroxylase activity following IS (Ichimura et al., 1995).

4.5.6 Evidence that immunization with M. vaccae strains stabilize lipid-immune signaling in the CNS

In contrast, a few proteins whose stress-induced decrease was prevented with prior immunization of mice with *M. vaccae* strains are negative immune regulators associated with inflammation-resolving, M2-type, macrophages. The secretion and/or expression of PAF-AH (Stafforini et al., 1990; Van Ginderachter et al., 2006; Yagnik, 2014) from polarized macrophages, and PIK3IP1 from T cells and macrophages (Chen et al., 2019; Defrances et al., 2012; Kang et al., 2017; Uche et al., 2018) are important for immune suppression and resolution, and their reduced abundance in the CSF after IS exposure may indicate diminished immunoregulatory signaling in the CNS. Expression of *Pla2g7*, the gene encoding PAF-AH (Van Ginderachter et al., 2006) and *Pik3ip1* (Kang et al., 2017) has been associated with alternatively activated (M2) macrophages, and inflammatory cytokines decrease macrophage expression of PAF-AH (Cao et al., 1998) and PIK3IP1 (Kang et al., 2017). We have previously shown that *M. vaccae* NCTC 11659 may increase the relative abundance of PAF-AH in CSF among home cage animals, one week

following the last immunization (Loupy et al., 2020). Likewise, we have shown that a free fatty acid isolated from *M. vaccae* NCTC 11659, 10(*Z*)-hexadecenoic acid, increases expression of *Pla2g7*, the gene encoding PAF-AH, among isolated peritoneal macrophages stimulated with LPS, presumably through peroxisome proliferator-activated receptor alpha (PPARα) activation (Smith et al., 2019). In the plasma proteome, our pathway analysis revealed "PPAR signaling pathway" to be downregulated after IS among BBS-treated animals. The ability of *M. vaccae* strains to prevent stress-induced reductions in PAF-AH, and PIK3IP1 may, in part, be due to *M. vaccae*'s ability to prime monocytes toward an anti-inflammatory phenotype via the activation of PPARs (Bouhlel et al., 2007; Smith et al., 2019). PAF-AH, also known as phospholipase A2 group VII, in turn, may be responsible for cleavage of free fatty acids from phospholipids, generating lysophospholipids and anti-inflammatory lipids that resolve inflammation (Suneson et al., 2021); such a mechanism may account for previous observations that both *M. vaccae* NCTC 11659 (Foxx et al., 2021) and *M. tuberculosis* (Collins et al., 2018) infection increase lysophospholipid metabolites in plasma. This is not unlike other species of mycobacteria that have been shown to recruit immunoregulatory monocytes to the CNS, mitigating inflammation in neurological disorders (Zuo et al., 2017). The apparent ability of *M. vaccae* strains to maintain the integrity of the blood-brain barrier (BBB) during stress in our current study—possibly through activation of PPARs—might additionally help to mitigate the translocation of inflammatory monocytes into the brain (Huang et al., 2008; Ramirez et al., 2008).

Macrophages are, in fact, major contributors to an organism's lipid and cholesterol metabolism, and they are highly responsive to PPAR agonists. The translocation of monocyte-derived macrophages to the choroid plexus after IS may explain the alteration of several lipid metabolism

proteins in CSF, which is prevented by prior immunization with *M. vaccae* strains (ApoC-II, PAF-AH, PIK3IP1, SAA4). During stress, lipids are mobilized for energy utilization, and proatherosclerotic macrophages, activated in response to cardiovascular distress, phagocytose cholesterol products in a process called “lipid loading” (Pennings et al., 2006; Remmerie and Scott, 2018; Shashkin et al., 2005). SAA4, for example, is synthesized in macrophages and prevents the efflux of high-density lipoprotein (HDL) cholesterol (Getz and Reardon, 2019). The plasma proteome of BBS-treated rats 24 hours after IS exhibited increased abundance of proteins associated with complement and coagulation cascades and decreased abundance of apolipoproteins, consistent with the functional activities contributed by macrophage differentiation due to myocardial injury, leading to atherosclerosis (see part I of this article). In the current study, we observed IS-induced changes in abundances of lipid metabolism-related proteins that were not altered in the plasma, namely, PAF-AH and PIK3IP1; PAF-AH and PIK3IP1 were not altered in the plasma but were decreased in CSF following IS exposure. Interestingly, ApoC-II was decreased in plasma 24 hours after IS across all treatment groups, but it was increased in CSF only among BBS-treated rats and not animals previously immunized with *M. vaccae* strains. This finding may implicate a role for increased transport of lipoproteins via the low-density lipoprotein receptor (LDLR), as is used, for example, by LPS endotoxin to enter the brain (Vargas-Caraveo et al., 2017); likewise, this finding may reflect increased macrophage metabolism in the CNS (Wolska et al., 2017).

4.5.7 Evidence that immunization with M. vaccae strains promotes the trafficking of alternatively activated monocytes to the CNS after stress

Interestingly, in the plasma, ABCB9, KNG1, SAA4, and YWHAG were increased 24 hours after IS regardless of vehicle or *M. vaccae* treatment (see part I of this article); however, in the CSF,

these proteins were only altered after IS among BBS-treated animals and not *M. vaccae*-treated animals. Similarly, albumin, CgA, and ApoC-II were decreased in plasma 24 hours after IS regardless of treatment (see part I of this article); however, these proteins were only altered in CSF among BBS-treated animals exposed to IS and not *M. vaccae*-treated animals exposed to IS. These results suggest that, in the periphery, IS exerted generalizable effects (i.e., unaffected by *M. vaccae* treatment) on inflammatory pathways, including hemostasis and monocyte mobilization (see part I of this article). However, preimmunization with either *M. vaccae* NCTC 11659 or *M. vaccae* ATCC 15483 prevented the transfer of these changes into the CSF proteome, which may reflect a reduction of monocyte trafficking across the BBB or BCSFB. It could also be that *M. vaccae* strains, like other mycobacteria, recruit alternatively activated (anti-inflammatory) monocytes to the CNS, mitigating inflammation due to stress (Zuo et al., 2017); thus, differences in the abundance of inflammatory markers may be reflective of the polarization of different macrophage phenotypes in the CNS. For example, in the cardiac infarction model of vascular injury, MYDGF (also known as C19orf10) is secreted by macrophages to promote tissue healing and resolve inflammation through a phosphatidylinositol 3-kinase (PI3K)-Akt pathway (Korf-Klingebiel et al., 2015); in our study, we found that MYDGF negatively correlated with *Il6* mRNA in the dorsal hippocampus. Furthermore, previous studies using *M. vaccae* NCTC 11659 or its derivative, 10(*Z*)-hexadecenoic acid, provide evidence that treatment with *M. vaccae* NCTC 11659 primes immune cells, including macrophages, toward an anti-inflammatory phenotype; immunization with *M. vaccae* in mice suppresses the stress-induced exaggeration of ex vivo anti-CD3 antibody-stimulated secretion of IL-6 and interferon (IFN)-γ from freshly isolated mesenteric lymph node cells (Reber et al., 2016b), and in vitro incubation of freshly-isolated peritoneal macrophages with 10(*Z*)-hexadecenoic acid attenuates LPS-induced

expression of *Il6* and *Ccl2* (encoding C-C motif chemokine ligand 2, or CCL2) (Smith et al., 2019). These are significant findings because CCL2 expression is considered a primary marker of proinflammatory, or M1, macrophages that travel to the brain and mediate anxiety-like behavior by secreting IL-6 (Niraula et al., 2019; Wohleb et al., 2014, 2013). In vivo, prior immunization with *M. vaccae* NCTC 11659 prevents an IS-induced increase of the alarmin high mobility group box 1 (HMGB1) in the hippocampus, which may be mediated by IL-4 secreting cell types that are activated by *M. vaccae* in home cage control conditions (Frank et al., 2018b).

4.5.8 Limitations

Although our study is the first to demonstrate the effects of IS and *M. vaccae* strains on the CSF proteome, as well as associations between the stress-resilient behavioral effects of *M. vaccae* strains with physiological effects on the CSF proteome, there are limitations to our experimental design that should be considered for future experiments. It is important to point out that any functional associations of proteins are speculative in nature because we did not measure the activity of enzymes or other proteins in specific pathways. Likewise, although associations can be made between our independent variables and protein abundance in plasma, our data do not establish direct causal relationships. Proteins detected by mass spectrometry were those whose abundance was above the detection limit, and thus not all proteins in CSF were captured; it will be important for future studies to target specific proteins of interest based on the exploratory proteomics results. Many proteins have multiple functions, and thus their altered abundance may be context specific. Future experiments should investigate ex vivo and in vitro models to study individual organs and cell types that may contribute to the effects described in this paper. In addition, in our study the effects of immunization with *M. vaccae* and IS are restricted to a single

time point of tissue collection, eight days following immunization with *M. vaccae* and 24 hours after stress; considering that our results may have been influenced by immune activation and resolution of inflammation (not measured here), future experiments should explore time-dependent changes on the CSF proteome following final immunizations of *M. vaccae* strains and following IS. Another limitation of our study is that nutrition intake and physical activity were not monitored after exposure to IS and may have been additional variables that contributed to an altered CSF proteome. Also, our experiment was conducted only in adult male rats, and future studies should include female rats to determine if *M. vaccae* administration and/or IS may produce differential effects on the CSF proteome dependent on sex (Koeken et al., 2020). Similarly, immune response to *M. vaccae* strains may be altered in juvenile or aged rats, and future experiments should investigate these differences.

4.5.9 Conclusions

Together, these data align with the hypothesis that stress-induced increases in anxiety-like defensive behavioral responses are driven by translocation of IL-6-secreting inflammatory monocytes that traffic from the bone marrow to the CNS, which may be aided by disruption of the BBB or BCSFB (an overview of these pathways is displayed in Figure 4.5). Our data would also support the hypothesis that immunization with *M. vaccae* strains interferes with the infiltration or differentiation of inflammatory monocyte-derived macrophages in the CNS, consistent with the stress-resilient behavioral effects of *M. vaccae* strains. These results will be important for understanding the biological mechanisms of trauma- and stressor-related behaviors in preclinical models. Our study also provides a hypothetical framework for understanding how *M. vaccae* strains prevent IS-induced anxiety-like defensive behavioral responses in rodents and

may provide a novel therapeutic direction for the prevention or treatment of anxiety disorders, affective disorders, and trauma- and stressor-related disorders, such as PTSD. In line with the 2013 review entitled, “Harnessing monocyte-derived macrophages to control central nervous system pathologies: no longer ‘if’ but ‘how’” by Shechter and Schwartz, we provide evidence that microbial-derived interventions might prove to be a promising approach to mediate macrophage signaling to the CNS for the therapeutic treatment of neuroinflammatory conditions, including psychiatric disorders (Shechter and Schwartz, 2013).

4.6 Acknowledgements, author contributions, and conflicts of interest

Acknowledgements

These studies were funded by the National Institute of Mental Health (NIMH) R21 grant (R21MH116263) awarded to C.A.L., S.F.M., M.G.F. (PIs), and L.K.F. (Co-I). We gratefully acknowledge the Central Analytical Laboratory and Mass Spectrometry Facility at the University of Colorado Boulder for their services. Purchase of a Thermo Q-Exactive HF-X mass spectrometer was made possible with a grant from the National Institute of Health (S10-OD025267).

Author contributions

Study design was conceived by K.M.L., C.A.Z., and C.A.L. Culture of *M. vaccae* ATCC 15483 was performed by M.J.G. and N.F. Preparation of heat-killed *M. vaccae* ATCC 15483 was conducted by C.A.Z. *M. vaccae* injections were performed by A.I.E, B.M.M., and C.A.Z. Inescapable tail shock was conducted by H.M.D. Tissue collection for CSF was conducted by K.M.L, K.E.C., B.M.M., M.G.F., and C.A.Z. Proteomics sample preparation was performed by

K.M.L., C.C.E., T.L., and A.I.E. LC/MS-MS was performed by C.C.E. and T.L. Data analysis and statistical analysis were carried out by K.M.L. and C.C.E. Figures and figure legends were produced by K.M.L. and K.E.C. Manuscript preparation was conducted by K.M.L. Editing and review was contributed by K.M.L, C.C.E., T.L., A.I.E., K.E.C., B.M.M., L.K.F., M.G.F., C.A.Z., S.F.M., and C.A.L.

Conflicts of interest

CAL serves on the Scientific Advisory Board of Immodulon Therapeutics, Ltd, is Cofounder and Chief Scientific Officer of Mycobacterium Therapeutics Corporation, serves as an unpaid scientific consultant to Aurum Switzerland A.G., and is member of the faculty of the Integrative Psychiatry Institute, Boulder, CO, USA.

Chapter 5. Immunization with either *Mycobacterium vaccae* NCTC 11659 or *M. vaccae* ATCC 15483 prevents stress-induced changes to neuroactive metabolites in the plasma of adult male rats: I. targeted metabolomics.

Citation

Loupy, K.M., Cendali, F., Reisz, J.A., D'Angelo, H.M., Arnold, M.R., Elsayed, A.I., Marquart, B.M., Cler, K.E., Fonken, L.K., Frank, M.G., Zambrano, C.A., Maier, S.F., Lowry, C.A. Immunization with either *Mycobacterium vaccae* NCTC 11659 or *M. vaccae* ATCC 15483 prevents stress-induced changes to neuroactive metabolites in the plasma of adult male rats: I. targeted metabolomics. Manuscript in preparation.

Authors' names

Kelsey M. Loupy[a], Francesca Cendali[b], Julie A. Reisz[b], Heather M. D'Angelo[c], Mathew R. Arnold[a,d], Ahmed I. Elsayed[a], Brandon M. Marquart[a], Kristin E. Cler[a], Laura K. Fonken[e], Matthew G. Frank[c,d], Cristian A. Zambrano[a], Steven F. Maier [c,d], Christopher A. Lowry[a,d,f,g,h,i,j]*

Authors' affiliations

[a]Department of Integrative Physiology, University of Colorado Boulder, Boulder, CO 80309, USA

[b]Department of Biochemistry and Molecular Genetics, University of Colorado Anschutz Medical Campus, Aurora, CO 80045, USA

[c]Department of Psychology and Neuroscience, University of Colorado Boulder, Boulder, CO 80309, USA

[d]Center for Neuroscience, University of Colorado Boulder, Boulder, CO 80309, USA

[e]Division of Pharmacology and Toxicology, University of Texas at Austin, Austin, TX 78712, USA.

[f]Center for Microbial Exploration, University of Colorado Boulder, Boulder, CO 80309, USA

[g]Department of Physical Medicine and Rehabilitation and Center for Neuroscience, University of Colorado Anschutz Medical Campus, Aurora, CO 80045, USA

[h]Veterans Health Administration, Rocky Mountain Mental Illness Research Education and Clinical Center (MIRECC), Rocky Mountain Regional Veterans Affairs Medical Center (RMRVAMC), Aurora, CO 80045, USA

[i]Military and Veteran Microbiome: Consortium for Research and Education (MVM-CoRE), Aurora, CO 80045, USA

[j]Senior Fellow, inVIVO Planetary Health, of the Worldwide Universities Network (WUN), West New York, NJ 07093, USA

5.1 Abstract

Stress-related psychiatric disorders, including anxiety disorders, affective disorders, and trauma and stressor-related disorders, such as posttraumatic stress disorder (PTSD), are prevalent and result in significant socioeconomic burden. Although the mechanisms underlying the etiology and pathophysiology of these disorders are not fully understood, recent studies suggest that

biological signatures of peripheral inflammation are among the best predictors of PTSD. Consequently, microbiome-based interventions that increase anti-inflammatory and immunoregulatory signaling might help to prevent or treat behavioral and physiological symptoms associated with PTSD. Using a rat model of inescapable stress, we previously demonstrated that immunization with heat-killed preparations of either *Mycobacterium vaccae* NCTC 11659 or *M. vaccae* ATCC 15483 prevents stress-induced neuroinflammation and anxiety-like defensive behavioral responses 24 hours after inescapable tail shock stress (IS) [Loupy et al., 2021, Brain, Behavior, and Immunity, 91: 212–229]. Here, we investigated the effects of immunization with *M. vaccae* strains and IS on the rat plasma metabolome, performing a targeted analysis of 152 metabolites, associated with stress vulnerability versus resilience. Exposure to IS induced biomarkers of sympathetic nervous system activation and altered tryptophan metabolism and immunometabolic pathways consistent with a biological signature of inflammatory, interleukin 6-secreting, bone marrow-derived monocytes that have previously been demonstrated to traffic to the central nervous system and increase anxiety-like defensive behavioral responses. Prior immunization with either *M. vaccae* NCTC 11659 or *M. vaccae* ATCC 15483 prevented IS-induced induction of biomarkers of sympathetic nervous system activation and the biological signature of inflammatory bone marrow-derived monocytes. These data support the hypothesis that heat-killed preparations of *M. vaccae* NCTC 11659 and *M. vaccae* ATCC 15483, bacterial strains with anti-inflammatory and immunoregulatory properties, have promise as novel, multitargeted therapeutic strategies for the prevention and treatment of stress-related psychiatric disorders, including PTSD.

5.2 Introduction

Stress-related psychiatric disorders include anxiety disorders, affective disorders, and trauma and stressor-related disorders, including posttraumatic stress disorder (PTSD). Stress-related disorders are prevalent and account for significant socioeconomic costs (Kessler, 2000; Kessler et al., 2017; Koenen et al., 2017; Roehrig, 2016; L. Wang et al., 2016). For example, the lifetime prevalence of PTSD is estimated at about 4% worldwide (Kessler et al., 2017; Liu et al., 2017) and around 7% in the United States (Goldstein et al., 2016; Kessler et al., 2005, 1995). However, there is individual variability in responses to trauma, with only a subset of individuals responding with subsequent development of PTSD. Although the lifetime prevalence of trauma exposure is about 70% (Kessler et al., 2017), on average less than 10% of exposed persons go on to develop PTSD, with the likelihood of an eventual PTSD diagnosis dependent upon trauma type (Kessler et al., 2017, 1995; Liu et al., 2017). Among individuals exposed to war, including Veterans and war civilians, the risk of developing PTSD is much higher than average, closer to 20-25% (Hoge et al., 2014; Hoppen and Morina, 2019). Worldwide, this equates to hundreds of millions of persons presently living with PTSD, often comorbid with other psychiatric disorders, including major depressive disorder (MDD) (Hoppen and Morina, 2019). Factors that determine an individual's vulnerability or resilience to developing trauma- and stressor-related disorders like PTSD are currently unknown; studying biological signatures that are associated with stress-related disorders will be valuable for enhancing preventative and personalized medicine.

Increased activity of the sympathetic nervous system (SNS) activity, corresponding to decreased activity of the parasympathetic nervous system (PNS), is one physiological symptom of PTSD (for review, see Fonkoue et al., 2020; Michopoulos et al., 2017). In contrast, decreased glucocorticoid release and increased glucocorticoid resistance have also been implicated in the

etiology of PTSD symptoms (Breen et al., 2019; de Kloet et al., 2007; Olff and van Zuiden, 2017; van Zuiden et al., 2012; Yehuda et al., 1995). Hyperactivity of the SNS increases proinflammatory signaling, while a reduced biological response to glucocorticoids prevents homeostatic attenuation of inflammation. Together, these phenomena result in a persistent state of low-grade inflammation. This may explain why individuals with PTSD are also at higher risk of developing cardiovascular disease (for review, see Brudey et al., 2015) or metabolic syndromes (for review, see Michopoulos et al., 2016) that are associated with aberrant inflammation. It has been suggested that proinflammatory markers such as C-reactive protein (Eraly et al., 2014; Michopoulos et al., 2015; Rosen et al., 2017; Schultebraucks et al., 2020), interleukin (IL)-6 (Gill et al., 2008; Kim et al., 2020), and monocyte abundance or activity (Kuan et al., 2019; Neylan et al., 2011; Schultebraucks et al., 2020) might be biomarkers that indicate greater risk for developing PTSD after exposure to a trauma. It could be that SNS activation and subsequent inflammation polarize bone-marrow derived monocytes toward an immunophenotype typical of proinflammatory monocytes/macrophages, and that infiltration of monocytes into the central nervous system (CNS) contribute to the manifestation of PTSD (for review, see Hodes et al., 2016; Menard et al., 2017b, 2017a; Reader et al., 2015; Weber et al., 2017; Wohleb et al., 2015).

Monocytes/macrophages are largely responsible for both innate immune signaling and energy homeostasis (for review, see Remmerie and Scott, 2018; Shashkin et al., 2005); therefore trauma-induced dysregulation of the activation, metabolism, and function of monocytes/macrophages would be consistent with the pathophysiology of PTSD in rodent models (Niraula et al., 2019; Wohleb et al., 2014, 2013, 2011) and human studies (Gola et al.,

2013; Kuan et al., 2019; Neylan et al., 2011; Schiweck et al., 2020; Schultebraucks et al., 2020). Changes to monocyte/macrophage metabolism might indicate shifts toward proinflammatory signaling, monocyte/macrophage trafficking to the brain, and risk for stress-related psychiatric disorders. For example, proinflammatory cytokines like interferon gamma (IFNγ) increase tryptophan metabolism in monocytes, monocyte-derived macrophages, and macrophages toward the production of neurotoxic quinolinic acid via the kynurenine pathway (Guillemin et al., 2003; Jones et al., 2015), although this effect is commonly cited in studies of MDD (for review, see Ruddick et al., 2006; Savitz, 2017; Won and Kim, 2016), whereas few studies have examined tryptophan metabolism in PTSD (for review, see Kim and Jeon, 2018; O'Farrell and Harkin, 2017). Production of quinolinic acid is driven by bone-marrow derived monocytes/macrophages more than any other immune cell type (Guillemin et al., 2003; Jones et al., 2015). Other metabolic pathways driven by monocytes/macrophages, such as arachidonic acid metabolism, terminate in proinflammatory eicosanoids as well as free radicals and oxidative stress (Das, 2018; Martinez et al., 2006; Shashkin et al., 2005), which are also associated with anxiety and depressive disorders (Lehmann et al., 2019; for review, see Suneson et al., 2021). A potential role for inflammatory monocyte-derived macrophages in determining risk of development of PTSD is indicated by the recent finding that pre-deployment absolute monocyte numbers and plasma eicosanoid concentrations are among the highest ranking features, based on machine learning approaches, predicting provisional PTSD diagnosis 90-180 days following deployment (Schultebraucks et al., 2020). Immunometabolism profiling might help indicate stress-vulnerable and stress-resilient populations by describing monocyte/macrophage polarization towards inflammatory (M1) or immunoregulatory (M2) functions (Abuawad et al., 2020; Batista-Gonzalez et al., 2020; Martinez et al., 2006; Suneson et al., 2021; Viola et al., 2019).

New therapies for PTSD, including peroxisome proliferator-activated receptor (PPAR) agonists, might target macrophages and lymphocytes to either inhibit inflammation or shift their actions toward inflammation resolution and tissue repair (Penas et al., 2015). Recent research also suggests that anti-inflammatory vagal nerve stimulation may be a promising therapy for the treatment of PTSD (Noble et al., 2019, 2017; Souza et al., 2020, 2019; Wittbrodt et al., 2020). Considering that PTSD is comorbid with MDD 25-50% of the time (Armenta et al., 2019; Flory and Yehuda, 2015; Hoppen and Morina, 2019; Knowles et al., 2019), and that vagal nerve stimulation is already approved for persons with treatment-resistant depression (Dell'Osso et al., 2018) or as an adjunctive therapy for persons with MDD (Aaronson et al., 2017), vagal nerve stimulation may also prove to be an effective treatment for individuals with PTSD or PTSD comorbid with MDD. Vagal nerve stimulation may benefit persons with aberrant sympathetic nervous system signaling by decreasing SNS activity and might help to regulate downstream autonomic nervous system responses that are disrupted in PTSD (Cacioppo et al., 1995; Won and Kim, 2016). Indeed, vagal nerve stimulation suppresses M1 macrophages and may even polarize macrophages toward an M2-like phenotype (for review, see Kalkman and Feuerbach, 2016).

It is thought that the intestinal microbes and their metabolites might also play a role in altering immune activation and metabolic states, either by direct contact with immune cells or by stimulating afferent branches of the vagus nerve (for review, see Loupy and Lowry, 2020). A variety of microbial-based therapeutics, including "psychobiotics," are an intriguing new branch of research for the prevention and treatment of stress-related disorders like PTSD (Bermúdez-Humarán et al., 2019; Brenner et al., 2020, 2017; Hoisington et al., 2018b, 2018a; Long-Smith et

al., 2020; Loupy and Lowry, 2020). Microbial-based interventions have been shown to attenuate inflammation, maintain energy homeostasis, and enhance endothelial barrier function at both the gut-vascular barrier and blood-CNS barriers (for review, see Bermúdez-Humarán et al., 2019; Long-Smith et al., 2020; Loupy and Lowry, 2020). We recently demonstrated the stress-resilience effects of heat-killed preparations of two different strains of mycobacteria, *Mycobacterium vaccae* NCTC 11659 and *M. vaccae* ATCC 15483, in adult male rats (Loupy et al., 2021). Immunizations with either *M. vaccae* strain prevented IS-induced increases of *Il6* mRNA in the dorsal hippocampus (Loupy et al., 2021) and prevented stress-induced anxiety-like defensive behavioral responses 24 hours after inescapable tail shock (IS) (Loupy et al., 2021).

In the current study, we sought to determine the effects of *M. vaccae* strains and IS on the plasma metabolome, associating neuroactive metabolites with stress-related behaviors (behavioral results published separately in Loupy et al., 2021). We utilized a targeted approach for the analysis of 152 metabolites and incorporated pathway analyses to understand functional changes in the plasma, 8 days following the final immunization with *M. vaccae* strains and/or 24 hours after IS. Results from this study support the hypotheses that: 1) IS induces activation of the sympathetic nervous system induces mobilization of inflammatory bone marrow-derived macrophages into systemic circulation; and 2) immunization with *M. vaccae* strains effectively prevent the adverse physiological changes associated with stress-related behavior 24 hours after IS. Specifically, our data provide evidence that immunization with *M. vaccae* attenuates the IS-induced SNS response and promotes inflammation resolution metabolic phenotypes.

5.3 Materials and methods

5.3.1 Animals

For an experimental timeline, please see Figure 5.1. The data reported in this study are derived from the same rats used in a previous report, which investigated the effects of immunization with *M. vaccae* NCTC 11659 and *M. vaccae* ATCC 15483 strains and exposure to IS on behavioral outcomes and molecular signaling in the liver, spleen, and hippocampus (Loupy et al., 2021). In the current study, metabolomic profiles in plasma of these rats are reported. Adult male Sprague Dawley® rats (Hsd:Sprague Dawley® SD®; Envigo, Indianapolis, IN, USA) weighing 250-265 g upon arrival were pair-housed in Allentown micro-isolator filter-topped caging [259 mm (W) × 476 mm (L) × 209 mm (H); cage model #PC10198HT, cage top #MBT1019HT; Allentown, NJ, USA] containing an approximately 2.5 cm-deep layer of bedding (Cat. No. 7090; Teklad Sani-Chips; Harlan Laboratories, Indianapolis, IN, USA). This species, strain, and supplier were chosen due to previous studies evaluating stress resilience effects of *M. vaccae* NCTC 11659 that were conducted with these animals (Frank et al., 2018b). All rats were kept under standard laboratory conditions (12-h light/dark cycle, lights on at 0700 h, 22 °C) and had free access to bottled reverse-osmosis water and standard rat diet (Harlan Teklad 2918 Irradiated Rodent Chow, Envigo, Huntingdon, United Kingdom). Cages were changed once per week. The research described here was conducted in compliance with the ARRIVE 2.0 Guidelines for Reporting Animal Research (Percie du Sert et al., 2020), and all studies were consistent with the National Institutes of Health *Guide for the Care and Use of Laboratory Animals*, Eighth Edition (National Research Council, 2011). The Institutional Animal Care and Use Committee at the University of Colorado Boulder approved all procedures. All efforts were made to limit the number of animals used and their suffering.

5.3.2 Reagents

This study used a whole cell heat-killed preparation of *M. vaccae* NCTC 11659 [IMM-201; alternative designations and different preparations and production processes of *M. vaccae* NCTC 11659 used in clinical trials or preclinical studies include: DAR-901 (Lahey et al., 2016), DarDar tuberculosis vaccine (Von Reyn et al., 2010), MV001 (Waddell et al., 2000), MV 007 (Vuola et al., 2003), *M. vaccae* SRL 172 (O'Brien et al., 2004; Von Reyn et al., 2010), and *M. vaccae* SRP 299 (Lowry et al., 2007); V7 (Bourinbaiar et al., 2020) is a hydrolyzed version of heat-killed *M. vaccae* NCTC 11659*; M. vaccae* NCTC 11659 has recently been classified as *M. kyogaense* sp. nov. (NCTC 11659; CECT 9646; DSM 107316) (Nouioui et al., 2018) (but see also Gupta et al., 2018)]; 10 mg/ml solution; strain National Collection of Type Cultures (NCTC) 11659, batch C079-ENG#1, provided by BioElpida (Lyon, France), diluted to 1 mg/ml in 100 µl sterile borate-buffered saline (BBS) for injections]. This study also employed the use of a whole cell heat-killed preparation of *M. vaccae* American Type Culture Collection (ATCC) 15483 suspension. *M. vaccae* ATCC 15483 was purchased from ATCC (Bonicke and Juhasz (ATCC® 15483), Manassas, VA, USA). *M. vaccae* ATCC 15483 was cultured in ATCC® Medium 1395: Middlebrook 7H9 broth with ADC enrichment at 37 °C, then centrifuged at 3000 x g at 4 °C for ten minutes to pellet the cells, growth media was removed, and cells were weighed and resuspended in sterile BBS to a concentration of 10 mg/ml. Cells were transferred to a sealed sterile glass container and autoclaved at 121 °C for 15 minutes. Heat-killed bacterial stock was stored at 4 °C. *M. vaccae* ATCC 15483 was further diluted to 1 mg/ml in 100 µl sterile BBS for injections.

5.3.3 Mycobacterium vaccae (M. vaccae) NCTC 11659, M. vaccae ATCC 15483, and vehicle immunization

Experimental rats received 3 subcutaneous (s.c.) immunizations of: 1) 0.1 mg of a heat-killed preparation of *M. vaccae* NCTC 11659 (estimated to be 1 x 10^8 cells); 2) 0.1 mg of a heat-killed preparation of *M. vaccae* ATCC 15483 (estimated to be 1 x 10^8 cells); or 3) 100 µl of the vehicle, sterile BBS, using 21-gauge needles and injection sites between the scapulae, between the hours of 12 pm and 4 pm. Injections occurred on days –21, –14, and –7 prior to stress exposure, which occurred on day 0. The dose used in these experiments (0.1 mg) was 1/10 of the dose used in human studies (1 mg) (O'Brien et al., 2004) and identical to the dose used in previous studies in mice and rats (Amoroso et al., 2020; Bowers et al., 2020; Fonken et al., 2018; Fox et al., 2017; Foxx et al., 2021; Frank et al., 2018b; Hassell et al., 2019; Loupy et al., 2021, 2020, 2018; Lowry et al., 2007; Reber et al., 2016b; Siebler et al., 2018; Smith et al., 2020). Figure 5.1 provides a timeline of *M. vaccae* treatments and stress exposure in relation to tissue collection.

Figure 5.1 Experimental timeline.
This schematic represents the experimental timeline for immunization with *Mycobacterium vaccae* NCTC 11659, *M. vaccae* ATCC 15483, or vehicle (borate-buffered saline [BBS]), exposure to inescapable tail shock stress (IS), behavioral testing (juvenile social exploration [JSE], and euthanasia. Behavioral results have been published separately in Loupy et al. [2021]). Abbreviations: BBS, borate-buffered saline; HC, home cage control conditions; IS, inescapable tail shock stress; JSE, juvenile social exploration. Adapted from Loupy et al. (2021).

5.3.4 Inescapable tail shock stress (IS)

IS was performed as previously described (Frank et al., 2018b; Loupy et al., 2021). Briefly, rats were placed in Plexiglas® tubes (23.4 cm in length × 7 cm in diameter) and exposed to 100 1.6

mA, 5-s tail shocks with a variable inter-trial interval (ITI) ranging from 30 to 90 s (average ITI = 60 s). All IS treatments occurred between 09:00 and 11:00 h. IS animals were returned to their home cages immediately after termination of the shock. Home cage control (HC) animals remained undisturbed in their home cages.

5.3.5 Juvenile social exploration (JSE)

IS exposure produces robust decreases in JSE (Christianson et al., 2008), which is a widely used and validated measure of anxiety (File and Seth, 2003) and is sensitive to the neuroinflammatory effects of stress (Goshen and Yirmiya, 2009). Here, JSE was measured 24 h prior to IS (baseline) and 24 h after IS (test) (i.e., between 9:00 and 10:00 h). Each experimental subject was transferred to a novel cage with shaved wood bedding in a dimly lit room (40 lx). After a 15-min habituation period, a 28–32 day-old juvenile male rat was introduced to the subject's cage for 5 min. Exploratory behaviors of the adult (sniffing, pinning, licking and allo-grooming of the juvenile) were timed by an observer blind to treatment condition. After the test, the juvenile was removed and the experimental adult rat was returned to its home cage. Although juvenile stimulus rats were reused for multiple tests, the adult was never retested with the same juvenile. For each animal, JSE test data were quantified as a percent of baseline JSE. Due to technical issues, a total of four animals were removed from the JSE paradigm and subsequent behavioral analysis and our final group sample sizes prior to outlier analysis were BBS/HC, n = 8; BBS/IS, n = 6; NCTC/HC, n = 8; NCTC/IS, n = 8; ATCC/HC, n = 8; ATCC/IS, n = 6. Behavioral results have been published separately in Loupy et al. (2021).

5.3.6 Euthanasia and plasma collection

Rats were euthanized eight days following the last injection using an overdose of sodium pentobarbital (Fatal Plus®, Vortech Pharmaceuticals Ltd., Dearborn, MI, USA; 200 mg/kg, i.p.). After euthanasia, blood was collected by opening the thoracic cavity and inserting a 21-gauge needle into the right atrium of the heart and slowly drawing up 1 mL of blood. Blood was gently released into a BD Vacutainer® blood collection tube containing EDTA (Cat. No. 367835; Becton, Dickinson, and Company; Franklin Lakes, NJ, USA) and spun down at 1500 × g for 10 min; the plasma supernatant was collected and stored at −80 °C. Due to loss of samples during plasma collection, final sample sizes for plasma analysis were BBS/HC, n = 8; BBS/IS, n = 6; NCTC/HC, n = 8; NCTC/IS, n = 8; ATCC/HC, n = 7; ATCC/IS, n = 8.

5.3.7 Plasma metabolite extraction, mass spectrometry (MS), and targeted analysis

Plasma samples were thawed on ice. Metabolites from plasma (20 uL) were extracted at 4 °C in the presence of 5:3:2 MeOH:MeCN:water (v/v/v, 480 μL), and the resulting supernatant was analyzed on a Thermo Vanquish ultra high pressure liquid chromatography (UHPLC) coupled to a Thermo Q Exactive MS as previously described in detail (Nemkov et al., 2019). For targeted analyses, .raw files were converted to .mzXML using RawConverter 1.1.0.21. Metabolites were assigned and peaks were integrated using Maven (Princeton University) (Clasquin et al., 2012; Melamud et al., 2010) in conjunction with the Kyoto Encyclopedia of Genes and Genomes (KEGG) database (Kanehisa and Goto, 2000) and an in-house standard library. Quality control was assessed using technical replicates run at the beginning, end, and middle of each sequence as previously described (Nemkov et al., 2017). In all, 152 metabolites were assigned in this study.

5.3.8 Statistical analysis

Metabolomics analyses were performed using R Statistical Programming (version 3.5.3 for Windows) and MetaboAnalyst 4.0 (https://www.metaboanalyst.ca/home.xhtml) (Chong et al., 2019, 2018). Zero values were imputed with one fifth of the lowest value detected for that metabolite. Data were normalized using log transformation and two analyses were run on the data: 1) generalized linear model (GLM) was performed in R in order to explore the general effects of treatment, stress, and their interaction on the plasma metabolome, and 2) pairwise comparison analyses were performed in MetaboAnalyst to directly compare treatment groups of interest. Specifically, GLM analysis was performed on log-transformed peak intensities for each metabolite with treatment, stress, and treatment x stress as factors. Fold change values and pairwise comparison *p*-values were analyzed in MetaboAnalyst. For both GLM and pairwise analyses, two-tailed significance was set at $\alpha = 0.1$. Pairwise analyses utilized false discovery rate (FDR)-adjusted *p*-values. Metabolites that were found to be significantly different between groups as well as metabolites with a fold change (up or downregulated) greater than two were used in downstream pathway analysis, utilizing the MetaboAnalyst Pathway Analysis with KEGG IDs for metabolite labeling and *Rattus norvegicus* as species, hypergeometric testing for overrepresentation analysis, and relative-betweenness centrality for pathway topology analysis. Kynurenine/tryptophan ratios were analyzed using the software package IBM Statistical Package for the Social Sciences (version 26.0, SPSS Inc., Chicago, IL, USA) using a two-tailed significance set at $\alpha = 0.05$. Correlations among all groups were performed in R, using the Pearson method and FDR-adjusted p-value < 0.05; correlations within treatment groups were performed in SPSS, using the Pearson method and two-tailed p-value < 0.05.

5.4 Results

5.4.1 Analysis of effects of M. vaccae strains and IS on the plasma metabolome using GLM analysis

To understand the overall effect of immunization with *M. vaccae* NCTC 11659 or *M. vaccae* ATCC 15483 treatment and IS on the plasma metabolome, we ran a generalized linear model (GLM) using treatment (*M. vaccae* NCTC 11659, *M. vaccae* ATCC 15483, or BBS), stress (IS or HC), and treatment x stress as factors in our model, using two-tailed $p < 0.1$ as performed previously (Loupy et al., 2021). Analysis at the GLM level revealed altered metabolic signatures of altered tryptophan, glucose, and fatty acid immunometabolism implicated in polarization of proinflammatory (M1) and anti-inflammatory/pro-resolving (M2) macrophages (Rattigan et al., 2018; Viola et al., 2019). Specifically, analysis using GLM identified main effects of treatment for nine metabolites, main effects of stress for 33 metabolites, and treatment x stress interactions for six metabolites (Supplementary Figure 5.1; Supplementary Table 5.1). These results warranted further analysis using pairwise comparisons. To directly compare abundances between experimental groups, we first utilized an average fold change analysis for metabolites with a fold change of magnitude greater than or equal to two. We also ran independent samples *t*-tests, using FDR-adjusted $p < 0.1$. Below we report the results for the effects of treatment with either *M. vaccae* NCTC 11659 or *M. vaccae* ATCC 15483 among home cage control animals. Then, we report the results for the effects of stress without and with immunization with either *M. vaccae* NCTC 11659 or *M. vaccae* ATCC 15483. Finally, we report the results for the effects of treatment with either *M. vaccae* NCTC 11659 or *M. vaccae* ATCC 15483 among IS-exposed rats.

5.4.2 Effects of immunization with M. vaccae NCTC 11659 or M. vaccae ATCC 15483 on the plasma metabolome of home cage control rats

Among home cage control rats, immunization with either *M. vaccae* NCTC 11659 or *M. vaccae* ATCC 15483 altered many of the same metabolites in plasma, twelve of which were increased by both strains and two of which were decreased by both strains (Supplementary Figure 5.2).

M. vaccae NCTC 11659

Fold change analysis revealed that, among home cage control rats, immunization with *M. vaccae* NCTC 11659 increased the abundance of 2',3'-cyclic cytidine monophosphate (CMP), 2-aminomuconate, 3-sulfocatechol, 4-phosphopantothenate, 5-hydroxykynurenamine, decenoylcarnitine (acyl-C10:1), dopamine, γ-glutamyl-γ-aminobutyrate, glycolate, inositol 1,2,3,5,6-pentakisphosphate, mercaptopyruvate, *N*-acetylcitrulline, nicotinate ribonucleotide, pyridoxamine 5'-phosphate, and spermine by two fold (see Figure 5.2A for a heat map of the top 50 most differentially abundant metabolites based on partial least squares-discriminant analysis [PLS-DA] variable importance in projection [VIP] analysis; Supplementary Figure 5.2; Supplementary Table 5.2). Immunization with *M. vaccae* NCTC 11659 decreased the abundance of 5-hydroxyindoleacetate and indole-3-acetaldehyde by two-fold (Figure 5.2A; Supplementary Figure 5.2; Supplementary Table 5.2). It should be noted that the peak intensity values for pyridoxamine 5'-phosphate and 5-hydroxyindoleacetate were below the detectable threshold for the majority of samples, and although the presence or absence (above the detectable limit) of these metabolites might be biologically relevant, these findings should be scrutinized with caution. Independent samples *t*-tests found that there were no metabolites whose abundance in plasma was significantly altered by *M. vaccae* NCTC 11659. The only KEGG database pathway that was significantly enriched in the plasma in response to *M. vaccae* NCTC 11659 was tryptophan metabolism (FDR-adjusted $p < 0.1$), based on four metabolites that were altered: 2-

aminomuconate, 5-hydroxyindoleacetate, 5-hydroxykynurenamine, and indole-3-acetaldehyde, (Figure 5.2B). Anthranilate, a metabolite in the kynurenine pathway of tryptophan metabolism (Ruddick et al., 2006), was increased by immunization with *M. vaccae* strains, based on main effects of treatment in the GLM ($p < 0.1$; Supplementary Figure 5.1; Supplementary Table 5.1). Generally, tryptophan metabolites involved in the kynurenine pathway of tryptophan metabolism (including 2-aminomuconate [Supplementary Figure 5.2; Supplementary Table 5.2] and anthranilate [Supplementary Figure 5.1; Supplementary Table 5.1]) were increased in *M. vaccae* NCTC 11659-immunized rats under home cage control conditions. In contrast, tryptophan metabolites associated with other pathways of tryptophan metabolism (e.g. 5-hydroxyindoleacetate, indole-3-acetaldehyde) tended to be decreased in *M. vaccae* NCTC 11659-immunized rats under home cage control conditions, suggesting a shift toward the kynurenine pathway of tryptophan metabolism in *M. vaccae* NCTC 11659-immunized rats under home cage control conditions.

M. vaccae ATCC 15483

Fold change analysis revealed that, among home cage control rats, immunization with *M. vaccae* ATCC 15483, like immunization with *M. vaccae* NCTC 11659, increased the abundance of 2',3'-cyclic CMP, 2-aminomuconate, 3-sulfocatechol, 5-hydroxykynurenamine, dopamine, γ-glutamyl-γ-aminobutyrate, glycolate, inositol 1,2,3,5,6-pentakisphosphate, mercaptopyruvate, *N*-acetylcitrulline, nicotinate ribonucleotide, pyridoxamine 5'-phosphate, and spermine by two-fold (see Figure 5.2C for a heat map of the top 50 most differentially abundant metabolites based on PLS-DA VIP analysis; Supplementary Figure 5.2; Supplementary Table 5.2). Additionally, immunization with *M. vaccae* ATCC 15483 increased the abundance of 2-

hydroxyglutarate/citramalate, 2-oxoglutaramate, 4-acetamidobutanoate, 4-pyridoxate, propionylcarnitine (acyl-C3), acyl-C4-dicarboxylcarnitine (DC), and itaconate by two-fold (Figure 5.2C; Supplementary Figure 5.2; Supplementary Table 5.2). Immunization with *M. vaccae* ATCC 15483, like immunization with *M. vaccae* NCTC 11659, decreased the abundance of 5-hydroxyindoleacetate and indole-3-acetaldehyde by two-fold (Figure 5.2C; Supplementary Figure 5.2; Supplementary Table 5.2). Additionally, *M. vaccae* ATCC 15483 decreased the abundance of adenosine monophosphate (AMP) and kynurenine by two-fold (Figure 5.2C; Supplementary Figure 5.2; Supplementary Table 5.2). However, independent samples *t*-tests found that there were no metabolites whose abundance in plasma was significantly altered by *M. vaccae* ATCC 15483. Similar to the results discovered with *M. vaccae* NCTC 11659 immunization, the most enriched pathway covered in this analysis was "tryptophan metabolism" (FDR-adjusted $p < 0.05$) based on five metabolites that were altered: 2-aminomuconate, 5-hydroxyindoleacetate, 5-hydroxykynurenamine, indole-3-acetaldehyde, and kynurenine (Figure 5.2D). As with *M. vaccae* NCTC 11659, note that anthranilate, a metabolite in the kynurenine pathway of tryptophan metabolism, was increased by immunization with *M. vaccae* strains, based on main effects of treatment in the GLM (Supplementary Figure 5.1; Supplementary Table 5.1). Generally, tryptophan metabolites involved in the kynurenine pathway of tryptophan metabolism (including 2-aminomuconate [Supplementary Figure 5.2; Supplementary Table 5.2] and anthranilate [Supplementary Figure 5.1; Supplementary Table 5.1]) tended to be increased in *M. vaccae* ATCC 15483-immunized rats under home cage control conditions. In contrast, tryptophan metabolites associated with other pathways of tryptophan metabolism (e.g. 5-hydroxyindoleacetate, indole-3-acetaldehyde) tended to be decreased in *M. vaccae* ATCC 15483-immunized rats under home cage control conditions, suggesting a shift toward the

kynurenine pathway of tryptophan metabolism in *M. vaccae* ATCC 15483-immunized rats under home cage control conditions.

Vitamin B6 metabolism (vitamin B6; pyridoxine, 4,5-bis(hydroxymethyl)-2-methylpyridin-3-ol) also emerged as a potential hub of metabolic changes (raw $p < 0.01$; FDR-adjusted $p > 0.1$; Supplementary Table 5.4) based on two metabolites that were altered: 4-pyridoxate and pyridoxamine 5'-phosphate (Figure 5.2D). Vitamin B6 and its derivative pyridoxal 5'-phosphate (PLP), the bioactive form of vitamin B6, are essential for many enzymatic reactions; of note, PLP is required for the activity of key enzymes in the kynurenine pathway of tryptophan metabolism, including kynurenine aminotransferase (KAT) and kynureninase (KYNU) (the latter responsible for the conversion of kynurenine to anthranilate). Increased activity through PLP could account for both the decrease in kynurenine (Figure 5.2C; Supplementary Figure 5.2; Supplementary Table 5.2) and increase in anthranilate and 2-aminomuconate, thought to maintain adequate NAD^+ formation from tryptophan (KEGG R01937, R01938, R03889), in response to *M. vaccae* strains in home cage control rats. Indeed, vitamin B6 inadequacy is thought to contribute to immune activation and inflammation (for review, see Lotto et al., 2011). *M. tuberculosis* synthesizes PLP, which is thought to be essential for survival of *M. tuberculosis* in vivo (Dick et al., 2010). Thus, the effects of *M. vaccae* strains on tryptophan metabolism and vitamin B6 metabolism appear to be linked.

The possibility that *M. vaccae* strains may affect functionally related pathways under home cage control conditions is further supported by identification of "nicotinate and nicotinamide metabolism" as a pathway potentially affected by both *M. vaccae* NCTC 11659 and *M. vaccae*

ATCC 15483 based on the increase in nicotinate ribonucleotide (Figure 5.2B, 5.2D; raw $p < 0.1$; FDR-adjusted $p > 0.1$). NAD^+ is considered the final metabolic product of the kynurenine pathway of tryptophan metabolism involving conversion of quinolinic acid to NAD^+ by quinolinic acid phosphoribosyltranferase (QPRT) (Ruddick et al., 2006), which converts quinolinic acid to nicotinate ribonucleotide (increased following administration of *M. vaccae* NCTC 11659 or *M. vaccae* ATCC 15483 (Figures 5.2A, 5.2C; Supplementary Figure 5.2; Supplementary Table 5.2; *M. vaccae* NCTC 11659, 48.8 fold change; 5.61 Log2[fold change]; *M. vaccae* ATCC 15483, 53.3 fold change; 5.74 Log2[fold change]), which in turn is converted to deamino-NAD^+ and ultimately to NAD^+ via NAD^+ synthase (KEGG rno00380). Indeed, nicotinate ribonucleotide was the highest ranked feature based on fold change and Log2(fold change) for both *M. vaccae* NCTC 11659 and *M. vaccae* ATCC 15483 under home cage control conditions (Supplementary Figure 5.2; Supplementary Table 5.2), effects that may be related to the persistent increase in IFNγ induced by *M. vaccae* strains (see Discussion) (Grant, 2018; Moon and Minhas, 2018).

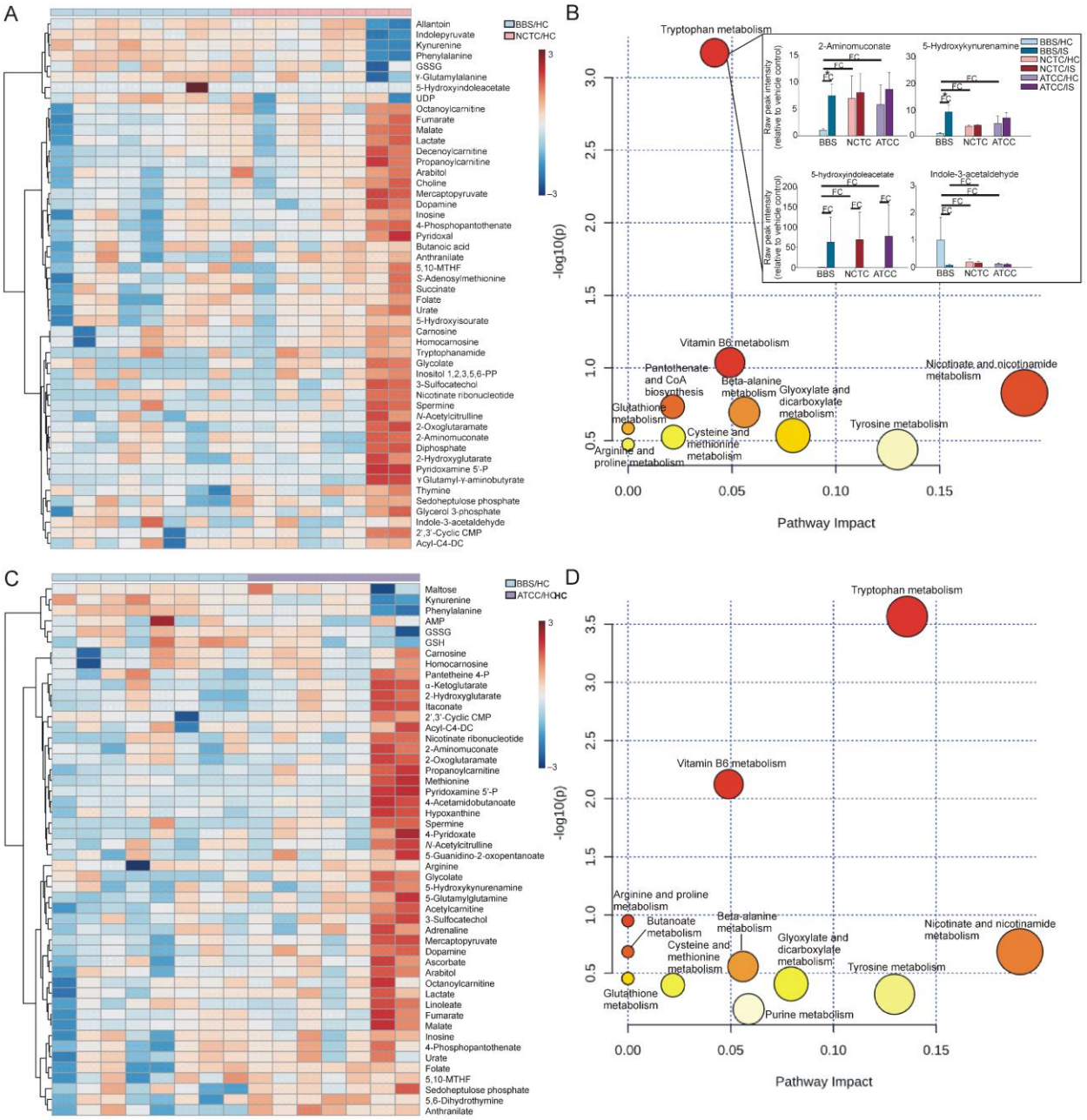

Figure 5.2 Effects of immunization with either (A, B) *M. vaccae* NCTC 11659 or (C, D) *M. vaccae* ATCC 15483 on the plasma metabolome among home cage control adult male rats. Panels A and C depict clustered heat maps of the top 50 most differentially abundant metabolites across each sample in *M. vaccae*- and BBS-treated animals ranked by the partial least squares discriminant analysis (PLS-DA) variable importance in projection (VIP), the range of color depicting a scale relative to the normalized abundance of metabolites.

Heat maps were clustered hierarchically using Ward's method with Euclidian distances (dendrogram trees shown to the left of each heat map). Panels B and D depict pathway analyses from MetaboAnalyst, showing raw *p*-values and impact values for each pathway; darker red circles indicate a smaller *p*-value, larger circles indicate a greater impact. Abbreviations: acyl-

C4-DC, acyl-C4-dicarboxylcarnitine; AMP, adenosine monophosphate; ATCC, *M. vaccae* ATCC 15483; BBS, borate-buffered saline; CMP, cytidine monophosphate; GSH, glutathione; GSSG, glutathione disulfide; HC, home cage control; inositol 1,2,3,5,6-PP, inositol 1,2,3,5,6-pentakisphosphate; MTHF, methenyltetrahydrofolate; NCTC, *M. vaccae* NCTC 11659; pyridoxamine 5'-P, pyridoxamine 5'-phosphate; UDP, uridine diphosphate.

5.4.3 Effects of stress on the plasma metabolome of vehicle-treated rats

Among BBS-treated rats, IS increased the abundance of 32 metabolites and decreased the abundance of eleven metabolites in plasma based on fold change analysis (Figure 5.3; Supplementary Figure 5.3; Supplementary Table 5.3). Independent samples *t*-tests determined that IS increased the abundance of 20 metabolites and decreased the abundance of fifteen metabolites in plasma with statistical significance (Figure 5.3; Supplementary Figure 5.3; Supplementary Table 5.3). IS-induced changes to the plasma metabolome among vehicle-treated rats are associated with the development of anxiety-like behaviors 24 hours after IS exposure in these same rats (see Loupy et al., 2021 for behavioral assessment).

Fold change analysis revealed that, among BBS-treated rats, IS increased the abundance of 2',3'-cyclic CMP, 2-aminomuconate, 2-oxoglutaramate, 3-sulfocatechol, 4-phosphopantothenate, 5-hydroxyindoleacetate, 5-hydroxykynurenamine, 6-phosphogluconate, acyl-C3, acyl-C4-DC, octanoylcarnitine (acyl-C8), acyl-C10:1, adrenaline, creatine, diphosphate, dopamine, folate, γ-glutamyl-γ-aminobutyrate, glycolate, hexadecenoic acid, inosine, inositol 1,2,3,5,6-pentakisphosphate, leucine and isoleucine (co-eluting isomers), linoleate, mercaptopyruvate, methionine, *N*-acetylcitrulline, nicotinate ribonucleotide, phosphoserine, pyridoxamine 5'-phosphate, spermine, and tetradecenoic acid (see Figure 5.3A for a principal component analysis plot and Figure 5.3B for a heat map of the top 50 most differentially abundant metabolites based on PLS-DA VIP analysis; Supplementary Figure 5.3; Supplementary Table 5.3). IS decreased

the abundance of allantoin, AMP, citrate, citrulline, glutamate, glutathione disulfide (GSSG), indolepyruvate, indole-3-acetaldehyde, kynurenine, phenylalanine, and putrescine by two-fold (Figure 5.3A-B; Supplementary Figure5. 3; Supplementary Table 5.3).

Independent samples *t*-tests found that IS increased the abundance of select amino acids (histidine, leucine and isoleucine [co-eluting isomers], and methionine); acylcarnitines (acetylcarnitine and propionylcarnitine); nucleotides (2',3'-cyclic CMP, 3',5'-cyclic inosine monophosphate [IMP], cytosine, pyridoxal, and pyridoxamine 5'-phosphate); neurotransmitters, including catecholamines (acetylcholine, adrenaline, and dopamine); tryptophan metabolites (2-aminomuconate and 5-hydroxykynurenamine); and other metabolites that might be associated with increased energy expenditure (choline, creatine, creatinine, phosphoserine, and spermine). (Figure 5.3A-B; Supplementary Figure 5.3; Supplementary Table 5.3). IS decreased the abundance of a subset of amino acids (asparagine, aspartate, citrulline, glutamate, glutamine, phenylalanine, serine, and threonine) and tryptophan metabolites (indolepyruvate and kynurenine) (Figure 5.3A-B; Supplementary Figure 5.3; Supplementary Table 5.3); other metabolites that were decreased by IS include 5-oxoproline, citrate, γ-glutamyl-alanine, guanidinoacetate, and allantoin (Figure 5.3A-B; Supplementary Figure 5.3; Supplementary Table 5.3).

Pathway analysis determined that the most critical metabolic changes due to IS (FDR-adjusted $p < 0.1$) occurred at the level of free amino acids and tryptophan metabolism (Figure 5.3C-D; Supplementary Table 5.4). All pathways associated with metabolites altered by IS are listed in Supplementary Table 5.4.

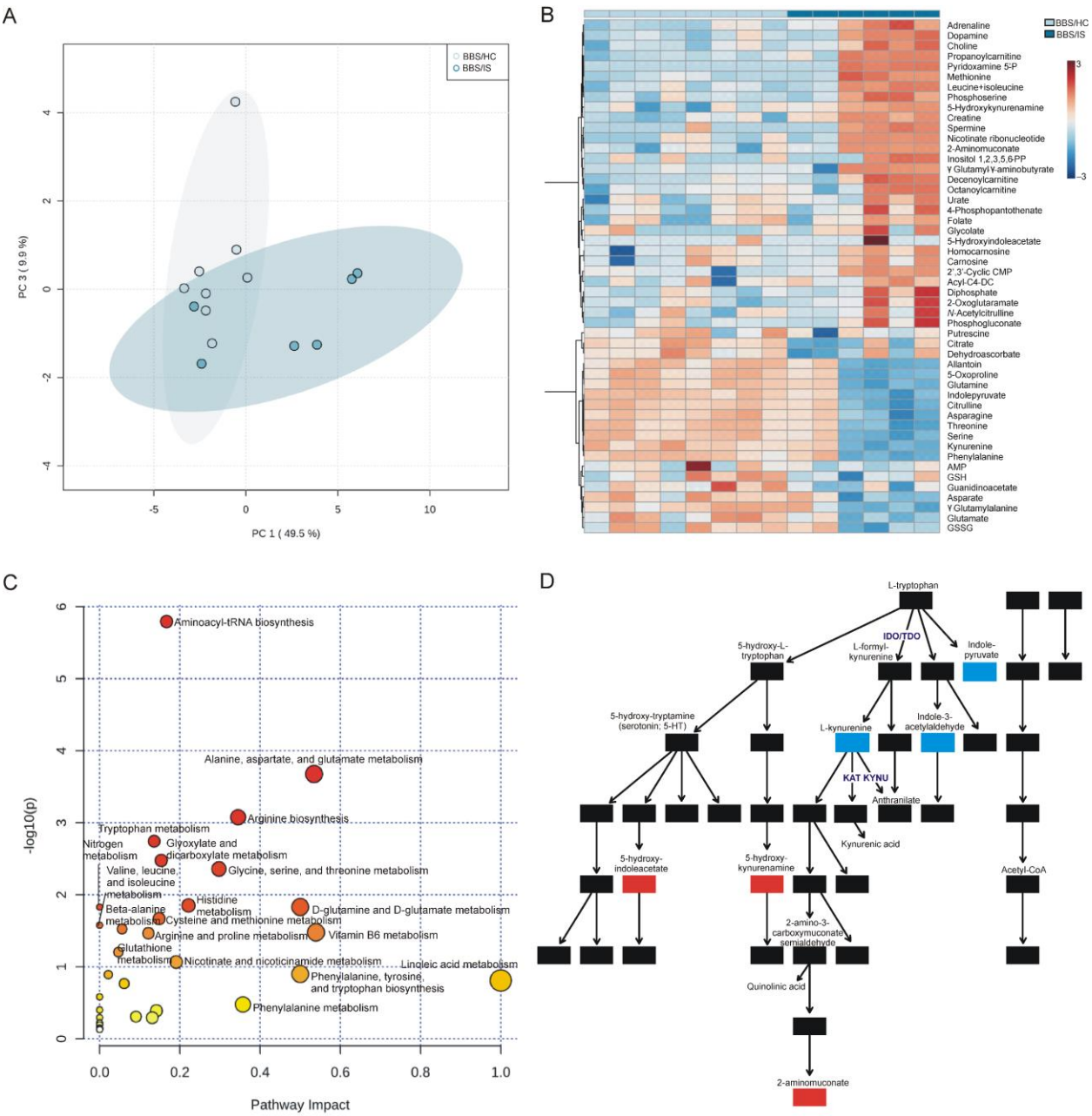

Figure 5.3 Effects of inescapable tail shock (IS), relative to home cage control conditions, on the plasma metabolome of adult male rats treated with borate-buffered saline (BBS; vehicle control).

Panel A depicts a principal component analysis (PCA) plot of IS- and home cage (HC)-exposed animals, showing PC 3 versus PC 1. Panel B depicts a clustered heat map of the top 50 most differentially abundant metabolites across each sample in IS- and HC-exposed animals ranked by the partial least squares discriminant analysis (PLS-DA) variable importance in projection (VIP) and clustered hierarchically using Ward's method with Euclidian distances (dendrogram trees

shown to the left of each heat map), the range of color depicting a scale relative to the normalized abundance of metabolites. Panel C depicts pathway analysis from MetaboAnalyst, showing raw *p*-values and impact values for each pathway; darker red circles indicate a smaller *p*-value, larger circles indicate a greater impact, and pathways with raw *p*-value < 0.1 or impact > 0.2 are labeled. Panel D depicts the "tryptophan metabolism" pathway, with each significant metabolite colored (red, increased; blue, decreased) and only relevant metabolites labeled; enzymes highlighted in this paper are in purple. Abbreviations: AMP, adenosine monophosphate; BBS, borate-buffered saline; GSH, glutathione; GSSG, glutathione disulfide; HC, home cage control; IDO, indoleamine 2,3-dioxygenase; inositol 1,2,3,5,6-PP, inositol 1,2,3,5,6-pentakisphosphate; IS, inescapable tail shock; KAT, kynurenine aminotransferase; KYNU, kynureninase; pyridoxamine 5'-P, pyridoxamine 5'-phosphate; PC, principal component; TDO, tryptophan 2,3 dioxygenase.

5.4.4 Effects of stress, relative to home cage control conditions, on the plasma metabolome of rats immunized with M. vaccae NCTC 11659 or M. vaccae ATCC 15483

Considering the stress-resilience behavioral effects of both *M. vaccae* strains (Loupy et al., 2021), we next sought to determine metabolites and pathways altered by IS among rats immunized by *M. vaccae* NCTC 11659 or *M. vaccae* ATCC 15483.

Effects of stress, relative to home cage control conditions, on the plasma metabolome of rats immunized with M. vaccae NCTC 11659

Fold change analysis revealed that among rats immunized with *M. vaccae* NCTC 11659, IS increased the abundance of hexadecenoic acid and 5-hydroxyindoleacetate (see Figure 5.4A for a heat map of the top 50 most differentially abundant metabolites based on PLS-DA VIP analysis; Supplementary Figure 5.3; Supplementary Table 5.5). IS decreased the abundance of AMP, citrate, glutathione (GSH), guanidinoacetate, and succinate (Supplementary Figure 5.3; Supplementary Table 5.5), and independent samples *t*-tests found only guanidinoacetate to be significantly decreased by IS ($t = 4.54$; FDR-adjusted $p < 0.1$) (Figure 5.4A; Supplementary Figure 5.3). There were no pathways that were significantly enriched in the plasma (FDR-adjusted $p > 0.1$) based on the metabolites altered by IS, among animals immunized with *M.*

vaccae NCTC 11659, although TCA cycle (raw $p < 0.01$; FDR-adjusted $p > 0.1$) and alanine, aspartate and glutamate metabolism (raw $p < 0.01$; FDR-adjusted $p > 0.1$) emerged as potential pathways based on altered levels of citrate and succinate (Figure 5.4B).

Effects of stress, relative to home cage control conditions, on the plasma metabolome of rats immunized with M. vaccae ATCC 15483

Fold change analysis revealed that, among rats immunized with *M. vaccae* ATCC 15483, IS increased the abundance of diphosphate, 4-phosphopantothenate, homocarnosine, maltose, glycero-3-phosphoethanolamine, and 6-phosphogluconate (see Figure 5.4C for a heat map of the top 50 most differentially abundant metabolites based on PLS-DA VIP analysis; Supplementary Figure 5.3; Supplementary Table 5.5). Among rats immunized with *M. vaccae* ATCC 15483, like rats immunized with *M. vaccae* NCTC 11659, IS decreased the abundance of citrate and guanidinoacetate; additionally, IS decreased the abundance of dehydroascorbate among animals immunized with *M. vaccae* ATCC 15483 (Supplementary Figure 5.3; Supplementary Table 5.5), and independent samples *t*-tests found only guanidinoacetate to be significantly decreased by IS ($t = 5.48$; FDR-adjusted $p < 0.05$), replicating the effects of IS among animals immunized with *M. vaccae* NCTC 11659 (Figure 5.4C; Supplementary Figure 5.3). There were no pathways that were significantly enriched in the plasma (FDR-adjusted $p > 0.1$) based on the metabolites altered by IS, among animals immunized with *M. vaccae* ATCC 15483, although "arginine and proline metabolism" (raw $p < 0.05$; FDR-adjusted $p > 0.1$) emerged as a potential pathway based on altered levels of homocarnosine and guanidinoacetate (Figure 5.4D). Importantly, among animals that were previously immunized with either *M. vaccae* NCTC 11659 or *M. vaccae* ATCC 15483, IS did not alter metabolites involved in the tryptophan metabolism pathway (Figure 5.4B, 5.4D; Supplementary Figure 5.3). Additionally, among animals immunized with

either *M. vaccae* strain, IS did not increase the catecholamines adrenaline or dopamine, nor did it increase acetylcholine (Figure 5.5).

5.4.5 Effects of immunization with M. vaccae NCTC 11659 or M. vaccae ATCC 15483, relative to BBS-treated animals, on the plasma metabolome of rats exposed to IS

Considering the stress-resilience behavioral effects of both *M. vaccae* strains (Loupy et al., 2021), we determined plasma metabolic alterations induced by *M. vaccae* NCTC 11659 or *M. vaccae* ATCC 15483 among rats exposed to IS.

Effects of immunization with M. vaccae NCTC 11659, relative to BBS-treated animals, on the plasma metabolome of rats exposed to IS

Fold change analysis revealed that among rats exposed to IS, prior immunization with *M. vaccae* NCTC 11659 increased the abundance of allantoin, indole-3-acetylaldehyde, and mercaptopyruvate, compared to BBS-treated animals (Supplementary Table 5.6). Among rats exposed to IS, prior immunization with *M. vaccae* NCTC 11659 decreased the abundance of inositol 1-2-3-5-6-pentakisphosphate, pyridoxamine 5'-phosphate, and tetradecenoic acid by two-fold (Supplementary Table 5.6). Independent samples *t*-tests using FDR-adjusted $p < 0.1$ found that there were no metabolites whose abundance in plasma was significantly altered by prior immunization with *M. vaccae* NCTC 11659, compared to BBS-treated animals, among rats exposed to IS. Pathway analysis found that there were no major alterations to metabolic pathways in plasma (FDR-adjusted $p > 0.1$).

Effects of immunization with M. vaccae ATCC 15483, relative to BBS-treated animals, on the plasma metabolome of rats exposed to IS

Fold change analysis revealed that among rats exposed to IS, prior immunization with *M. vaccae* ATCC 15483, like immunization with *M. vaccae* NCTC 11659, increased the abundance of mercaptopyruvate; additionally, among rats exposed to IS, prior immunization with *M. vaccae* ATCC 15483 increased the abundance of 4-pyridoxate, GSSG, maltose, and tryptophanamide compared to BBS-treated animals (Supplementary Table 5.6). There were no metabolites whose abundance in plasma was decreased two-fold. Independent samples *t*-tests using FDR-adjusted $p < 0.1$ found that there were no metabolites whose abundance in plasma was significantly altered by prior immunization with *M. vaccae* ATCC 15483, compared to BBS-treated animals, among rats exposed to IS. Pathway analysis found that there were no major alterations to metabolic pathways in the plasma (FDR-adjusted $p > 0.1$).

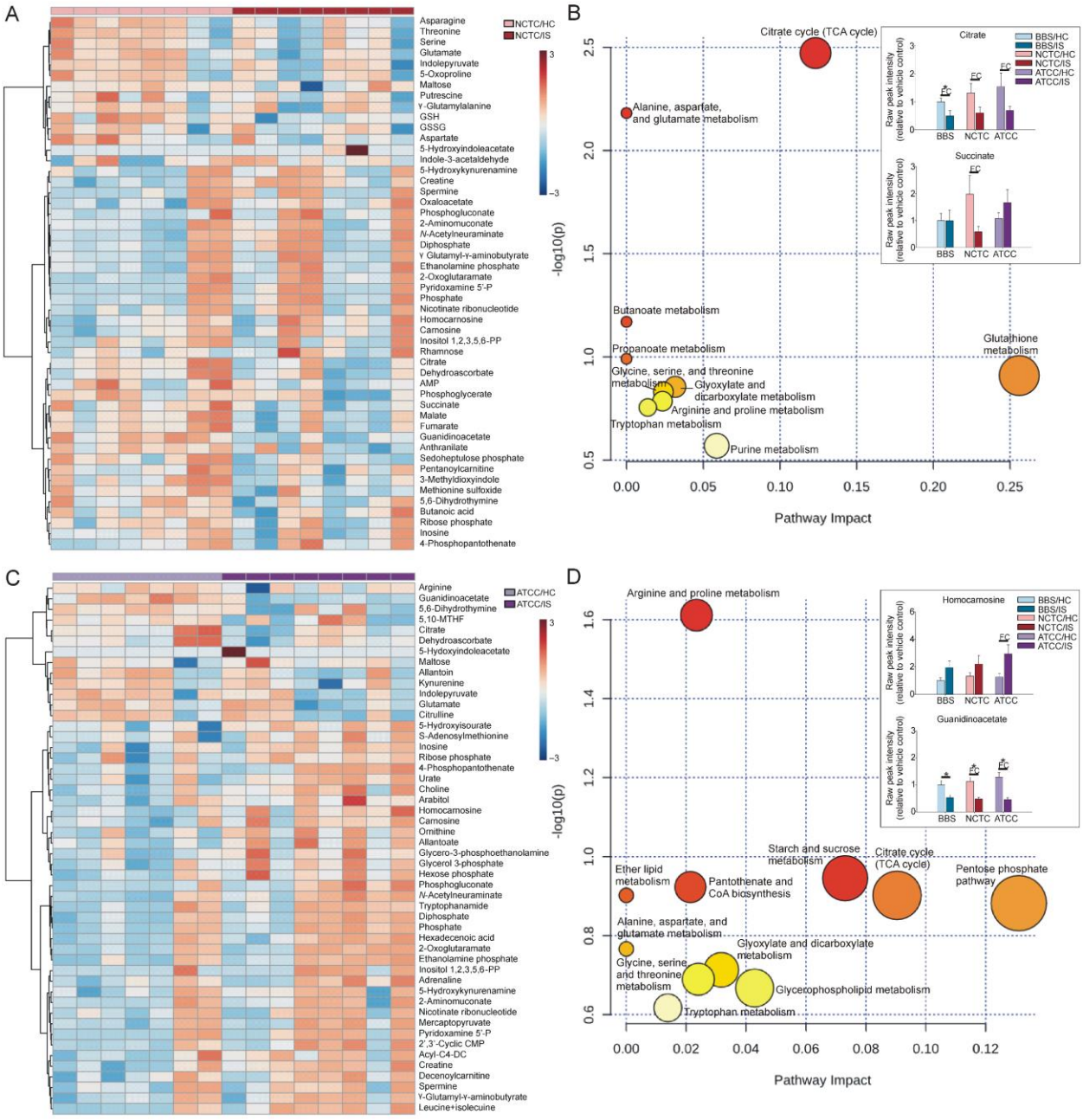

Figure 5.4 Effects of inescapable tail shock (IS) on the plasma metabolome of adult male rats immunized with either (A, B) *M. vaccae* NCTC 11659 or (C, D) *M. vaccae* ATCC 15483 on the plasma metabolome among home cage control animals.

Panels A and C depict clustered heat maps of the top 50 most differentially abundant metabolites across each sample in IS- and home cage (HC)-exposed animals ranked by the partial least squares discriminant analysis (PLS-DA) variable importance in projection (VIP), the range of color depicting a scale relative to the normalized abundance of metabolites. Heat maps were clustered hierarchically using Ward's method with Euclidian distances (dendrogram trees shown to the left of each heat map). Panels B and D depict pathway analyses from MetaboAnalyst, showing raw *p*-values and impact values for each pathway; darker red circles indicate a smaller

p-value, larger circles indicate a greater impact. Abbreviations: acyl-C4-DC, acyl-C4-dicarboxylcarnitine; AMP, adenosine monophosphate; ATCC, *M. vaccae* ATCC 15483; BBS, borate-buffered saline; CMP, cytidine monophosphate; GSH, glutathione; GSSG, glutathione disulfide; HC, home cage control; inositol 1,2,3,5,6-PP, inositol 1,2,3,5,6-pentakisphosphate; IS, inescapable tail shock; MTHF, methenyltetrahydrofolate; NCTC, *M. vaccae* NCTC 11659; pyridoxamine 5'-P, pyridoxamine 5'-phosphate.

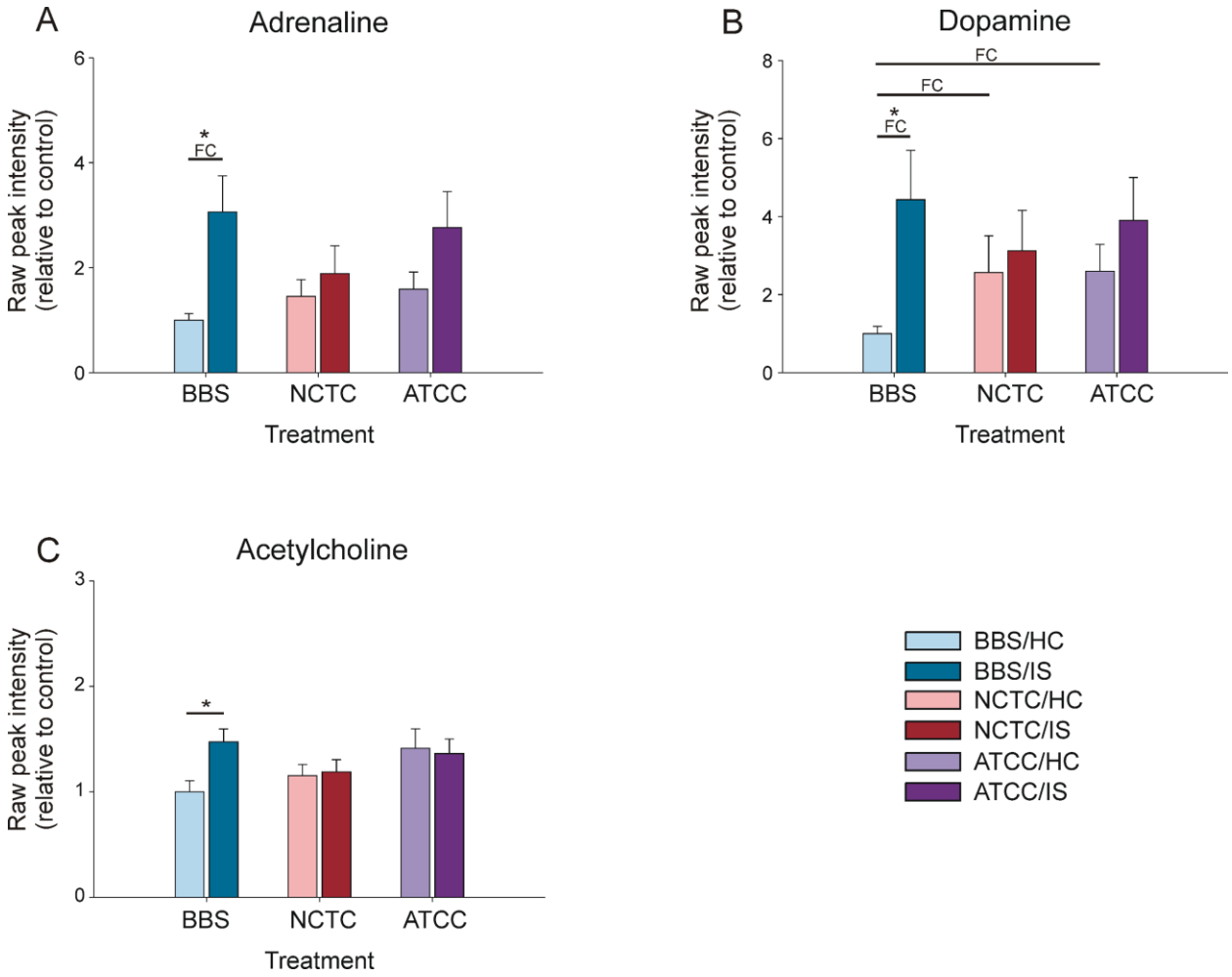

Figure 5.5 Effects of immunization with either *M. vaccae* NCTC 11659 (NCTC) or *M. vaccae* ATCC 15483 (ATCC) and inescapable tail shock (IS) on abundances of (A) adrenaline, (B) dopamine, and (C) acetylcholine in the plasma.

Bars represent the mean + standard error of the mean (SEM) of raw peak intensities of metabolites relative to vehicle control (BBS/HC). Sample sizes: BBS/HC, $n = 8$; BBS/IS, $n = 6$; NCTC/HC, $n = 8$; NCTC/IS, $n = 8$; ATCC/HC, $n = 7$; ATCC/IS, $n = 8$. FC, fold change difference. *FDR-adjusted $p < 0.1$. Abbreviations: ATCC, *M. vaccae* ATCC 15483; BBS, borate-buffered saline; HC, home cage control conditions; IS, inescapable tail shock; NCTC, *M. vaccae* NCTC 11659.

5.4.6 Effects of immunization with either M. vaccae NCTC 11659 or M. vaccae ATCC 15483 and IS exposure on tryptophan metabolism

Our results have revealed that among home cage animals, immunization with either *M. vaccae* NCTC 11659 or *M. vaccae* ATCC 11659 altered tryptophan metabolism in the plasma of home cage control rats (Supplementary Table 5.2; Figure 5.2B-C). Among BBS-treated animals, IS altered tryptophan metabolism toward decreased kynurenine concentrations (Supplementary Tables 5.3 and 5.4; Figure 5.3C-D). Interestingly, increased plasma kynurenine levels correlate with inflammation and are suggestive of impaired immunoregulation (Lin et al., 2010; Zuo et al., 2016). We did not see any alteration in tryptophan metabolism after exposure to IS among animals immunized with *M. vaccae* NCTC 11659 or *M. vaccae* ATCC 15483 (Figure 5.4B, 5.4D). These findings led us to analyze the ratio of kynurenine/tryptophan, a well-documented measure of indoleamine 2,3-dioxygenase (IDO) activity, the rate-limiting enzyme in tryptophan metabolism that oxidized tryptophan to yield formylkynurenine, promoting catabolism toward kynurenine, and a measure commonly associated with stress-related disorders such as depression (Badawy and Guillemin, 2019). The activity of IDO and its analog tryptophan 2,3-dioxygenase (TDO) have been implicated in numerous inflammatory conditions including breast cancer (D'Amato et al., 2015; Greene et al., 2019; Rogers et al., 2019), non-small cell lung cancer (Kocher et al., 2021), sepsis (Suchard and Savulescu, 2021), Down syndrome/trisomy 21 (Powers et al., 2019), and COVID-19 (Thomas et al., 2020). Independent samples *t*-tests found that, among home cage control animals, immunization with *M. vaccae* ATCC 15483 decreased the plasma kynurenine/tryptophan ratio compared to BBS-treated animals ($t = –3.73$; $p < 0.01$; Figure 5.6), consistent with previous studies showing that immunization with *M. vaccae* NCTC 11659 decreases plasma kynurenine concentrations in mice (Reber et al., 2016b). Elevated plasma concentrations of kynurenine are considered a biomarker of inflammation (Zuo et al.,

2016), and part of a biological signature of impaired immunoregulation (Lin et al., 2010). Immunization with *M. vaccae* NCTC did not alter the kynurenine/tryptophan ratio, although this result approached statistical significance ($t = –2.08$; $p = 0.057$; Figure 5.6). Among BBS-treated animals, IS decreased the plasma kynurenine/tryptophan ratio ($t = –3.00$; $p < 0.05$; Figure 5.6); however, preimmunization with either *M. vaccae* NCTC 11659 or *M. vaccae* ATCC 15483 prevented the stress-induced decrease of the plasma kynurenine/tryptophan ratio, perhaps because *M. vaccae* NCTC 11659 and *M. vaccae* ATCC 15483, by themselves, tended to decrease the kynurenine/tryptophan ratio, in line with the stress resilience behavioral effects of these mycobacteria ($p > 0.05$; Figure 5.6).

5.4.7 Tryptophan metabolism and IS-induced monocyte-derived macrophage trafficking to the brain

Considering the relevance of the kynurenine/tryptophan ratio in stress-induced behavior, and the idea that stress-induced inflammation drives tryptophan metabolism and monocyte trafficking to the brain, we correlated raw kynurenine/tryptophan ratios with anxiety-like defensive behavioral responses as measured by the juvenile social exploration (JSE) paradigm (Loupy et al., 2021), interleukin 6 (*Il6*) mRNA expression in the dorsal hippocampus, which was associated with JSE behavior (Loupy et al., 2021), and abundance of ATP-binding cassette sub-family B member 9 (ABCB9) and 14-3-3 protein gamma (YWHAG) in the cerebrospinal fluid (CSF), two markers of monocyte-derived macrophages upregulated after IS (Loupy, unpublished data). Correlations between dependent variables were separated based on treatment (i.e., BBS, *M. vaccae* NCTC 11659, and *M. vaccae* ATCC 15483) in order to control for stress-resilience effects of *M. vaccae* that may skew correlations (Loupy et al., 2021).

Among BBS-treated animals, abundance of YWHAG in the CSF ($r = –0.596$; $p < 0.05$; Supplementary Figure 5.4) and *Il6* mRNA in the dorsal hippocampus ($r = –0.627$; $p < 0.05$; Supplementary Figure 5.4) negatively correlated with plasma kynurenine/tryptophan ratios. However, among animals immunized with either *M. vaccae* NCTC 11659 or *M. vaccae* ATCC 15483, there were no correlations between CNS markers of inflammation and plasma kynurenine/tryptophan ratios, further supporting a hypothesis that *M. vaccae* treatment disrupts stress-induced inflammation regulating tryptophan metabolism and monocyte trafficking to the brain (Supplementary Figure 5.4) (Loupy, unpublished data). Neither JSE behavior nor CSF ABCB9 correlated with raw kynurenine/tryptophan ratios in the plasma among any treatment group ($p > 0.05$).

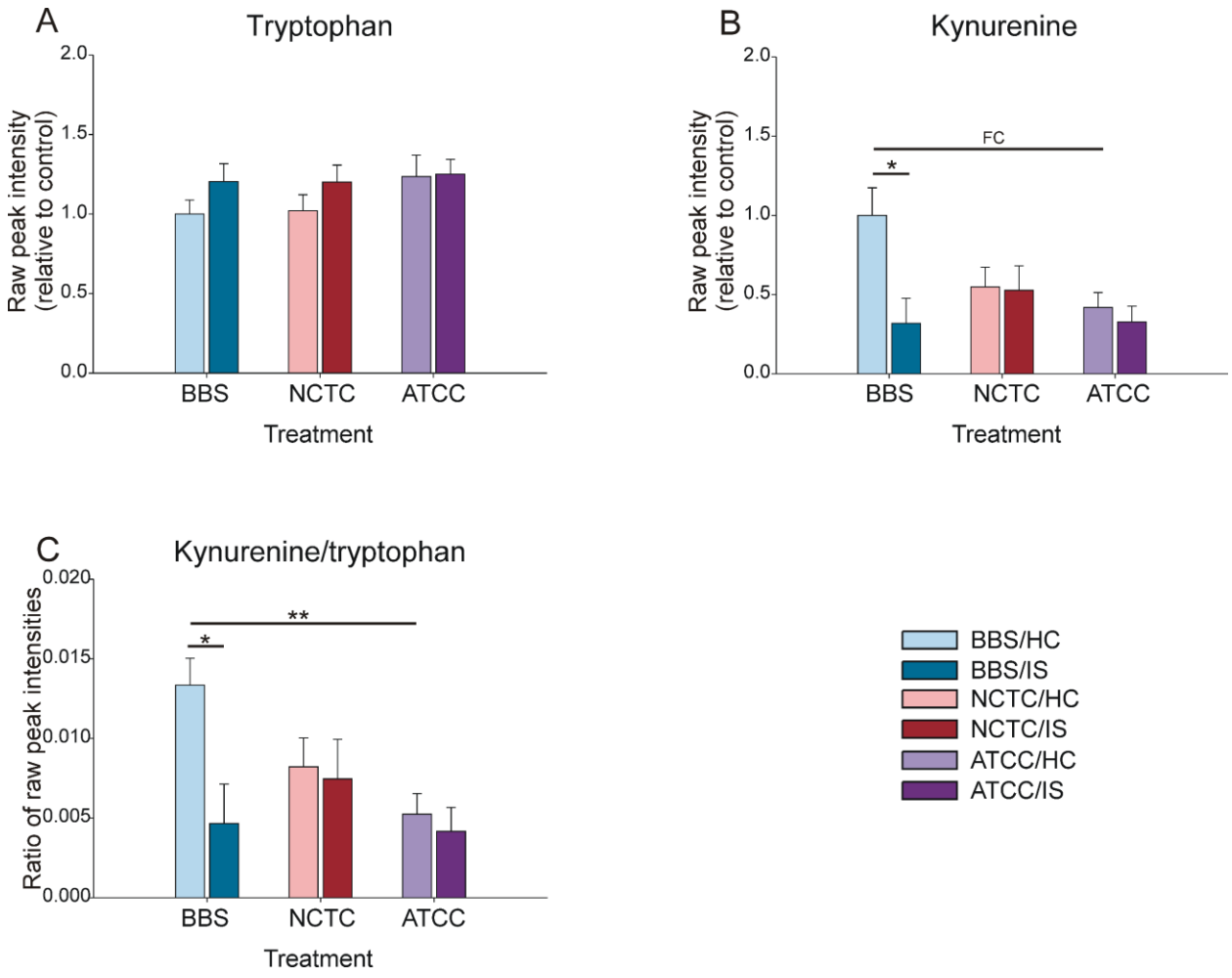

Figure 5.6 Effects of immunization with either *M. vaccae* NCTC 11659 (NCTC) or *M. vaccae* ATCC 15483 (ATCC) and inescapable tail shock (IS) on markers of tryptophan metabolism in the plasma.

Bars represent the mean + SEM of (A) raw peak intensities of tryptophan relative to vehicle control (BBS/HC), (B) raw peak intensities of kynurenine relative to vehicle control (BBS/HC), and (C) ratios of the raw peak intensities of kynurenine/tryptophan. Sample sizes: BBS/HC, n = 8; BBS/IS, n = 6; NCTC/HC, n = 8; NCTC/IS, n = 8; ATCC/HC, n = 7; ATCC/IS, n = 8. Independent samples t-tests were run on each of the metabolites targeted in the plasma. FC, fold change difference. *$p < 0.05$, **$p < 0.01$; p-value is FDR-adjusted for panels A and B, but not for panel C. Abbreviations: ATCC, *M. vaccae* ATCC 15483; BBS, borate-buffered saline; HC, home cage control conditions; IS, inescapable tail shock; NCTC, *M. vaccae* NCTC 11659.

5.5 Discussion

Among home cage control rats, immunization with either *M. vaccae* NCTC 11659 or *M. vaccae* ATCC 15483, compared to BBS-treated rats, altered in a similar fashion the abundance of

fourteen metabolites in plasma, although immunization with the two mycobacterial strains diverged with the alteration of the abundance of ten plasma metabolites. IS dramatically modified the plasma metabolome, dysregulating the abundance of metabolites involved in the stress response, including energy utilization, amino acid metabolism, antioxidant pathways, and of particular significance, tryptophan metabolism; however, IS-induced changes in tryptophan metabolism did not occur among rats immunized with *M. vaccae* NCTC 11659 or *M. vaccae* ATCC 15483. Our data might also suggest that immunization with either *M. vaccae* strain prevented metabolic consequences of IS-induced SNS activation assessed 24 hours after IS. IS-induced changes to the plasma metabolome correlated with inflammatory biomarkers in the cerebrospinal fluid and anxiety-like defensive behaviors, but these relationships were interrupted in rats immunized with either *M. vaccae* strain, consistent with an immunoregulatory phenotype in these animals. Collectively, this study demonstrates that prior immunization with *M. vaccae* strains attenuate stress-related proinflammatory processes that cause widespread changes to bidirectional physiological processes between the CNS and periphery.

5.5.1 Effects of M. vaccae strains on the plasma metabolome in rats under home cage control conditions

Below we describe the effects of immunization with either *M. vaccae* NCTC 11659 or *M. vaccae* ATCC 15483 on the plasma metabolome of home cage control rats. Immunization with either *M. vaccae* strain altered the plasma metabolome to reflect changes in tryptophan metabolism, immunometabolism, gut microbe-derived metabolites, and parasympathetic (vagal) nerve stimulation. The changes invoked among home cage control animals immunized with *M. vaccae* strains may provide some insight into the protective mechanisms of *M. vaccae* immunizations prior to stress exposure.

5.5.2 Immunization with M. vaccae strains alters tryptophan metabolism in rats under home cage control conditions

Among home cage control rats, immunization with either *M. vaccae* NCTC 11659 or *M. vaccae* ATCC 15483, compared to BBS-treated rats, altered in a similar fashion the abundance of fourteen metabolites in plasma, although immunization with the two mycobacterial strains diverged with the alteration of the abundance of ten plasma metabolites. Among home cage control rats, immunization with *M. vaccae* strains altered tryptophan metabolism by increasing abundances of plasma 2-aminomuconate and 5-hydroxykynurenamine and decreasing indole-3-acetaldehyde and 5-hydroxyindoleacetate. Immunization with *M. vaccae* ATCC 15483 also decreased the abundance of kynurenine, while immunization with *M. vaccae* NCTC 11659 tended to decrease kynurenine, although these results were not significant based on fold change or independent samples *t*-tests (Figure 6B and 6C). These results are consistent with the findings from Reber and colleagues (2016), who also showed that immunization with *M. vaccae* NCTC 11659 induces a long-term decrease of plasma kynurenine, but not tryptophan, among home cage control animals (Reber et al., 2016b). The rate-limiting enzyme for the production of kynurenine is tryptophan 2,3 dioxygenase (TDO) in the liver or IDO extrahepatically, enzymes that catalyze the conversion of tryptophan to formylkynurenine, the direct precursor of kynurenine (for review, see Murakami and Saito, 2013; Ruddick et al., 2006); TDO expression is increased by stimulation with glucocorticoids such as corticosterone, while IDO is activated by proinflammatory cytokines such as IFNγ (Murakami and Saito, 2013; Ruddick et al., 2006). Innate immune cells like macrophages highly express kynurenine metabolism enzymes, including IDO, kyunreninase, and kynurenine 3-hydroxylase (Guillemin et al., 2003); the expression and activity of these enzymes are influenced by the binding of pro- and anti-

inflammatory molecules (Regan et al., 2018). It might be that, under home cage conditions, immunization with *M. vaccae* strains inhibit IDO activity by acting on circulating immune cells to promote immunoregulatory signaling (Regan et al., 2018). Previous ex vivo studies of dendritic cells show increased IDO1 gene expression 24 hours after a single *M. vaccae* NCTC 11659 injection, modeling an immune adjuvant (Le Bert et al., 2011); our current in vivo study may reflect a complex interaction of *M. vaccae* and IDO activity that is dependent on experimental model, treatment concentration, number of treatments, and length of time until endpoint measurement. Indeed, Zhang and colleagues (2016) have shown that infection with *M. vaccae* increases both tissue $CD3^{+}CD4^{+}IFN\gamma^{+}$ cells and $CD4^{+}CD25^{+}Foxp3^{+}$ Treg cells, with maximal increases three to four weeks following infection (Zhang et al., 2016).

Interestingly, 5-hydroxyindoleacetate, the primary metabolite of serotonin, was also decreased in plasma of home cage control rats immunized with either *M. vaccae* strain, which could suggest decreased peripheral catabolism of serotonin, and may indicate either decreased or increased abundance of circulating serotonin at our time point of measurement (not measured in this study). Prior studies indicate that immunization with *M. vaccae* NCTC 11659 alters serotonergic neuron activation in the dorsal raphe nucleus of the rodent brainstem 24 hours (Lowry et al., 2007) and one week or more after a final immunization (Fox et al., 2017; Foxx et al., 2021; Reber et al., 2016b); it may not be surprising that *M. vaccae* alters serotonergic metabolism in the periphery, and further studies should investigate mechanisms involved. Dendritic cells, monocyte-derived macrophages, and T-cells take up free serotonin via the serotonin transporter and initiate its catabolism to 5-hydroxindoleacetate (for review, see Herr et al., 2017). By stimulating immune cell types, treatment with *M. vaccae* strains may shift serotonergic

metabolism. In addition, serotonin, released by platelets or enterochromaffin cells of the gut, could possible mediate the release of cytokines from monocytes (Herr et al., 2017) and regulate macrophage polarization to M2 phenotype (de las Casas-Engel et al., 2013). Further research should investigate which cell types respond to treatment with *M. vaccae* strains and might contribute to the alterations in plasma tryptophan metabolism as described here.

Altered abundances of tryptophan metabolites may indicate *M. vaccae*-induced changes in cellular homeostatic and energetic pathways among home cage control animals. For example, although quinolinic acid was not present in our dataset, the increase in abundance of nicotinate ribonucleotide, a metabolite of quinolinic acid, might suggest that immunization with *M. vaccae* strains increased kynurenine catabolism toward quinolinic acid production and the nicotinate (vitamin B3), nicotinamide, and nicotinamide adenine dinucleotide (NAD+) metabolism pathways among home cage control animals (Ruddick et al., 2006). The nicotinate and nicotinamide metabolism pathway is important for energy homeostasis because it ends in the production of NAD+, which is utilized throughout the TCA cycle and reduced to NADH for subsequent use during oxidative phosphorylation and production of cellular energy (for review, see Fernie et al., 2004). The kynurenine metabolite 2-aminomuconate, which was also increased upon immunization with *M. vaccae* strains, can be further metabolized to acetyl-CoA (for review, see Badawy, 2017) for entrance into the TCA cycle (Fernie et al., 2004).

5.5.3 M. vaccae strains alter plasma metabolites associated with the metabolic phenotype of alternatively activated (M2) macrophages in rats under home cage control conditions

Studies that have characterized the metabolic phenotype of M2 (alternatively activated) macrophages describe increased kynurenine metabolism and a shift toward predominant utilization of the TCA cycle, oxidative phosphorylation, and fatty acid oxidation, compared to M1 (classically activated) macrophages (for review, see Batista-Gonzalez et al., 2020; Viola et al., 2019). Our results provide some evidence that *M. vaccae* strains increase metabolites associated with multiple points along the TCA cycle, including itaconate, 2-hydroxyglutarate/citramalate, and 2-oxoglutaramate, as well as 4-pantothenate and spermine, which are involved in the synthesis of coenzyme A; however, treatment with each of the *M. vaccae* strains differentially increased these metabolites among home cage control animals. Immunization with *M. vaccae* strains produces differential abundances of acylcarnitine derivates among home cage control animals eight days following the final injection, which may reflect differences in the lipid composition of the mycobacterial cell walls of the two strains, contributing to differences in lipid metabolism; immunization with *M. vaccae* NCTC 11659 shifts the plasma metabolome toward an increase in medium-chain acylcarnitines (acyl-C10:1; acylcarnitine C10:1; decenoylcarnitine), while *M. vaccae* ATCC 15483 shifted the plasma metabolome toward an increase in short-chain acylcarnitines (acyl-C3; acylcarnitine C3:0; propionylcarnitine and acyl-C4-DC; acylcarnitine C4-DC; methylmalonylcarnitine). Acylcarnitines are involved in fatty-acid oxidation toward the production of acetyl-CoA, upstream of the TCA cycle (Förster and Staib, 1992). Collectively, increases of TCA cycle metabolites and β-oxidation intermediates might highlight metabolic changes that are characteristic of M2 macrophages. We previously hypothesized that immunization with *M. vaccae* strains can alternatively activate monocytes/macrophages toward an anti-inflammatory or inflammation-resolving (M2) phenotype, buffering against stress or lipopolysaccharide (LPS)-

induced inflammation (Loupy, unpublished data) (Fonken et al., 2018; Frank et al., 2018b; Reber et al., 2016b; Smith et al., 2019). Our current findings might support this hypothesis considering that *M. vaccae*-induced changes in plasma included altered (possibly increased) kynurenine metabolism, increased TCA cycle, and increased fatty acid oxidation, hallmarks of M2 macrophage metabolism.

It could be that immunization with *M. vaccae* strains alternatively activate circulating monocytes/macrophages, or possibly other tissue-resident macrophages, to promote anti-inflammatory signaling pathways that influence the metabolomic environment of plasma (Regan et al., 2018; Viola et al., 2019). We have previously shown that prior immunization with *M. vaccae* NCTC 11659 prevents stress-induced exaggeration of IFNγ and interleukin 6 (IL-6) secretion from anti-CD3-stimulated murine mesenteric lymph node cells ex vivo, which may be indicative of anti-inflammatory priming of macrophages (Reber et al., 2016b). Similarly, we have also shown that treatment with 10(*Z*)-hexadecenoic acid, a free-fatty acid derivative of *M. vaccae* NCTC 11659, prevents subsequent LPS-induced expression of proinflammatory mediators in murine peritoneal macrophages (Smith et al., 2019); furthermore, pretreatment with 10(*Z*)-hexadecenoic acid increases LPS-induced expression of *Aldh9a*, encoding for aldehyde dehydrogenase 9 family, A1, which catabolizes 5-hydroxyindoleacetylaldehyde to 5-hydroxyindoleacetate (KEGG rno00380) (Smith et al., 2019). The effects of 10(*Z*)-hexadecenoic acid on macrophages are mediated by activation of the peroxisome proliferator-activated receptor α (PPARα) (Smith et al., 2019). We recently showed that immunization with either *M. vaccae* strain decreases *Pparg* (encoding PPARγ) mRNA expression in the liver among home cage control animals (Loupy et al., 2021), immunization with *M. vaccae* NCTC 11659 prevents

IS-induced reductions in *Pparg* mRNA expression in liver (Loupy et al., 2021), and immunization with *M. vaccae* ATCC 15483 partially prevents the IS-induced decrease of plasma proteins associated with the PPAR signaling pathway (Loupy, unpublished data). These findings suggest that, in vivo, *M. vaccae* strains may be inducing alternatively activated macrophages, reflecting the changes seen in tryptophan metabolites.

5.5.4 Evidence that immunization with M. vaccae strains alters the gut microbiome in rats under home cage control conditions

Another interesting finding is that metabolites altered among home cage control rats immunized with either *M. vaccae* NCTC 11659 or *M. vaccae* ATCC15483 might be associated with "microbial metabolism in diverse environments" pathway (KEGG map01120), although this was not mapped by the pathway analysis feature of MetaboAnalyst. Glycolate and 3-sulfocatechol were specifically annotated by the KEGG database as being associated with "microbial metabolism in diverse environments," but other metabolites may also fall into this category simply for being part of generalized metabolic pathways. For instance, it is not surprising that microbial metabolism includes energetic pathways such as "Vitamin B6 metabolism," "nicotinate and nicotinamide metabolism," "glyoxylate and dicarboxylate metabolism," and "TCA cycle" (KEGG map01120). In fact, the gut microbiome plays a major role in the creation of the plasma metabolome, and the gut microbiome may be responsible for altering a large portion of circulating amino acids, tryptophan metabolites, short-chain fatty acids, and influencing bile acid homeostasis (Tang et al., 2019; Wikoff et al., 2009; Wilmanski et al., 2019). We also found increased abundances of dopamine and spermine eight days following the final injection of *M. vaccae* strains, which, among other things, are involved in the "bile secretion" pathway (KEGG rno04976). Bile acid synthesis (C. Y. Li et al., 2018b), secretion (Cheng et al.,

2018), and metabolism (Brown et al., 2018; Ma et al., 2018) pathways are regulated by the gut microbiome. Further, immunization with *M. vaccae* NCTC 11659 may have increased butanoic acid (also known as butyrate), among home cage control rats as indicated by the heat map of the top 50 most differentially abundant metabolites, although this result was not significant (Supplementary Figure 5.5). Upon further inspection, we found that butyrate tended to increase among home cage control rats immunized with either *M. vaccae* NCTC 11659 and *M. vaccae* ATCC 15483 (Supplementary Figure 5.5). Butyrate is a short-chain fatty acid (SCFA) produced exclusively by gut microbes, and therefore is a reliable marker of microbiome structure or function (Bishehsari et al., 2018); likewise, butyrate catabolism is thought to coincide with gut epithelial cell energetics (Donohoe et al., 2011). Immunization with *M. vaccae* ATCC 15483 increased the abundance of 4-acetamidobutanoate, a precursor of microbial butyrate synthesis associated with *Lactobacillus* spp. probiotic administration, among home cage control rats; in fact, immunization with *M. vaccae* strains either increased several butyrate and propionate metabolites among home cage control animals or prevented IS-induced decreases of these metabolites, including synthesis (4-acetamidobutanoate, glutamate) or β-oxidation (propionylcarnitine, methylmalonylcarnitine) pathways via bacterial or epithelial cells, respectively (for review, see Belizário et al., 2018; Esquivel-Elizondo et al., 2017; Flint et al., 2014; Selkrig et al., 2014; Trefely et al., 2020).

By influencing the host's physiology, including the plasma metabolome, the gut microbiome may contribute to the development of stress-related behaviors or stress-induced psychiatric disorders (Bassett et al., 2019; Foxx et al., 2021; K. Zhang et al., 2019). We recently reported a main effect of immunization with *M. vaccae* NCTC 11659 on gut microbial diversity measures,

and we described that prior immunization with *M. vaccae* NCTC 11659 prevented reductions in alpha diversity caused by chronic psychosocial stress (Reber et al., 2016b), and prevented reductions in alpha diversity caused by chronic disruption of rhythms (CDR) or a "double hit" model of stress combining CDR and social defeat stressors (Foxx et al., 2021). It may be that immunization with *M. vaccae* strains influences the structure of the host's gut microbiome, which may be associated with plasma metabolome changes and stress-resilient behaviors (Loupy et al., 2021).

5.5.5 Evidence that immunization with M. vaccae strains increase parasympathetic tone in rats under home cage control conditions

Results from the GLM also provide evidence that there was a main effect of treatment on anthranilate (Supplementary Figure 5.1; Supplementary Table 5.1), wherein under home cage control conditions, animals immunized with *M. vaccae* strains may have increased anthranilate. Anthranilate is a derivative of kynurenine that is increased in plasma upon vagal nerve stimulation in children with intractable epilepsy (Klinkenberg et al., 2014, 2012). It may be that, through interactions with neuroendocrine, gut barrier, immune, or vagal pathways, immunization with *M. vaccae* strains produces an increased parasympathetic tone among home cage control conditions. It is possible that increasing parasympathetic tone is a function of the inflammatory reflex, induced by alternative activation of circulating monocyte/macrophages (Pavlov and Tracey, 2012). Increased vagal output would also align with altered tryptophan metabolism (Bellono et al., 2017; Klinkenberg et al., 2014), changes to the gut microbiome (for review, see Bonaz et al., 2018; Breit et al., 2018), and modified bile secretion (for review, see Mizuno and Ueno, 2017).

5.5.6 IS alters the plasma metabolome in rats

Previous studies using models of inescapable tail shock have described proinflammatory effects of IS, including 1) increased expression of the tryptophan hydroxylase 2 (*Tph2*) enzyme (Donner et al., 2012) and activation of serotonin neurons (Benjamin N Greenwood et al., 2003) in the dorsal raphe nucleus, 2) evidence for monocyte trafficking and proinflammatory signaling in the brain (Frank et al., 2018b, 2007; Maslanik et al., 2013; Wohleb et al., 2015), 3) increased circulation of damage-associated molecular patterns (DAMPs) and pathogen-associated molecular patterns (PAMPs), such as LPS leakage from the gut (Beninson et al., 2014; Maslanik et al., 2013, 2012; Speaker et al., 2014; Weber et al., 2015), and 4) increased SNS activity (Greenwood et al., 2003b; Weiss and Simson, 1986). Here, we describe the functional implications of IS effects on the plasma metabolome in the context of the previously established effects of IS outlined above. IS-induced changes to the plasma metabolome among vehicle-treated rats are associated with the development of anxiety-like behaviors 24 hours after IS exposure in these same rats (see Loupy et al., 2021).

5.5.7 IS alters tryptophan metabolism among vehicle-treated rats

Alteration of tryptophan metabolism is highly associated with major depressive disorder (Clark et al., 2016; Colle et al., 2020; Kazemi et al., 2018; Messaoud et al., 2019; Savitz, 2017) and anxiety disorders (Kim and Jeon, 2018). In our study, we found that IS increased the abundance of 2-aminomuconate, 5-hydroxyindoleacetate, and 5-hydroxykynurenamine, but IS decreased abundance of kynurenine, indole-3-acetylaldehyde, and indolepyruvate. Of special interest is the metabolite 5-hyroxyindoleacetate, which is produced directly by catabolism of serotonin (not measured in this study). Increased abundance of the 5-hydroxyindoleacetate might therefore

indicate increased abundances of serotonin or increased enzymatic activity promoting increased catabolism. Serotonin is largely produced by enterochromaffin cells in the gut, which synthesize more than 90% of the body's serotonin (Bellono et al., 2017). Enterochromaffin cells act as an energetic sensor, releasing serotonin upon stimulation with adrenaline (Bellono et al., 2017) or mechanical disruption, such as that which occurs during dysregulation of gut epithelial or vascular endothelial permeability (Alcaino et al., 2018; Linan-Rico et al., 2016). Circulating platelets acquire serotonin from the gut and release serotonin upon vascular tissue injury (for review, see Watts et al., 2012), influencing blood pressure and heart rate (Pérgola and Alper, 1992; Saxena and Villalón, 1991; Watts et al., 2012) primarily by activating sympathetic nerves of blood vessels, causing vasoconstriction (Fujii et al., 2012; Watts et al., 2012). Simultaneously, phagocytic cells of the immune system, including monocytes, take up free circulating serotonin and break it down to 5-hydroxyindoleacetate (for review, see Herr et al., 2017); in times of stress, monocytes trafficking to the brain may transport serotonin or its metabolites to the vascular-CNS barriers, including the blood-brain barrier (BBB) or blood-CSF barrier (BCSFB) at the choroid plexus (Afergan et al., 2008; Ge et al., 2017).

Interestingly, kynurenine was reduced in plasma of BBS-treated rats exposed to IS. Proinflammatory signaling is thought to be a key driver of IDO activity and kynurenine production (Murakami and Saito, 2013; Ruddick et al., 2006), and thus increased kynurenine is often associated with MDD (Ruddick et al., 2006). However, some studies have reported decreased kynurenine in plasma of persons with MDD (Colle et al., 2020; Pu et al., 2020). It is possible that anti-inflammatory actions of glucocorticoids, such as corticosterone, might suppress proinflammatory mechanisms and reduce kynurenine production in circulating immune cells like

macrophages (Lim et al., 2007; Regan et al., 2018). It could also be, given increased abundance of the kynurenine metabolite 2-aminomuconate, that kynurenine metabolism has increased. Kynurenine metabolism results in the production of quinolinic acid, a neurotoxic molecule that is thought to be a critical mediator of depression (Savitz, 2017). Increased abundance of plasma nicotinate ribonucleotide would also support increased kynurenine metabolism toward production of quinolinic acid (Ruddick et al., 2006).

An unexpected finding was that among BBS-treated rats, IS altered metabolites that were highly enriched for the pathway "aminoacyl tRNA biosynthesis," which is also enriched in the blood metabolome of persons with MDD (Pu et al., 2020). Changes to this pathway implicate altered activity of aminoacyl tRNA synthetases. Aminoacyl tRNA synthetases are enzymes that bind amino acids to their respective tRNA, supporting protein synthesis (for review, see Nie et al., 2019). Interestingly, aminoacyl tRNA synthetases play a major role in the regulation of the immune response by mediating the phenotype and metabolism of immune cells like T cells and macrophages (Nie et al., 2019). For example, in response to proinflammatory signaling by IFNγ, macrophages, endothelial cells, and fibroblasts secrete the tryptophanyl-tRNA synthetase (WRS), which binds tryptophan to its tRNA; WRS can then bind toll-like receptor (TLR) 2 or 4 on circulating macrophages, promoting inflammatory polarization (Nie et al., 2019). WRS is increased in T cells during inflammatory events, mediating tryptophan metabolism alongside IDO activity and influencing T cell proliferation (for review, see Jin, 2019). Aminoacyl tRNA synthetases such as WRS have a variety of functions; indeed, WRS may also influence GSH metabolism via a glutathione *S*-transferase-like domain (Jin, 2019), can interact with the

vascular-endothelial cadherin, and might even be secreted as part of an antimicrobial mechanism in the host.

5.5.8 IS stimulates monocyte trafficking and proinflammatory signaling from the periphery to brain

Inflammatory monocytes are activated by stress-induced DAMPs released by tissue damage and PAMPs released by the gut (associated with increased intestinal permeability), following transmigration from the bone marrow upon direct stimulation by the SNS (for review, see Fleshner et al., 2017). IS-induced alteration of plasma tryptophan metabolites might be due to gut microbiome dysbiosis (Wikoff et al., 2009) or signaling cascades induced in enterochromaffin cells, either by adrenaline binding (Bellono et al., 2017) or mechanical disruption of these cells (Alcaino et al., 2018; Linan-Rico et al., 2016); intestinal barrier disruption is inflammatory, leading to the secretion of PAMPs into the circulation and the subsequent stimulation of monocytes toward a proinflammatory state (Fleshner et al., 2017). Likewise, tryptophan metabolism toward the kynurenine pathway may be performed directly by monocytes that have transmigrated into the vasculature (Viola et al., 2019); although serotonin is not produced in monocytes, it can be taken up and metabolized (Herr et al., 2017). From an immunometabolism perspective, BBS-treated rats exposed to IS exhibited plasma metabolic phenotypes that more closely resemble M1 macrophages compared to *M. vaccae*-immunized rats exposed to IS (for review, see O'Neill et al., 2016; Viola et al., 2019). M1 macrophages exhibit two major breakpoints in their TCA cycle; overall, M1 macrophages display a shift of metabolism toward glycolysis and fatty acid synthesis, coinciding with reduced TCA cycle activity (O'Neill et al., 2016; Viola et al., 2019). M1 macrophages also increase expression of COX-2 and promote synthesis of prostaglandin E2 (O'Neill et al., 2016; Viola et al., 2019).

However, among BBS-treated animals, IS may have induced a mixture of M1 and M2 macrophages based on the presence of both metabolic phenotypes in plasma, including acyl-carnitines associated with fatty acid oxidation. Considering that plasma was taken 24 hours after IS, it is likely that some monocytes were polarized toward M2 macrophages, or M1 macrophages were suppressed, after corticosterone secretion from the adrenal glands promoted deactivation of inflammatory processes and tissue remodeling (Martinez and Gordon, 2014); corticosterone levels were not examined in the current study, but prior studies report increased plasma corticosterone 24 hours after IS (Frank et al., 2018b).

In the current study, we also observed correlations between adrenaline and tryptophan metabolites across all experimental groups (Supplementary Table 5.7), which might point to an important relationship between SNS activity and tryptophan metabolism, possibly through enteric nervous system activation or stimulation of bone marrow-derived monocytes. We also discovered a negative correlation between kynurenine/tryptophan ratios and the abundance of YWHAG protein in the CSF among BBS-treated animals. Furthermore, we discovered a negative correlation between kynurenine/tryptophan ratios and *Il6* mRNA expression in the dorsal hippocampus, which was associated with the stress-induced exaggeration of anxiety-like defensive behaviors. Collectively, our results imply that SNS activation, tryptophan metabolism, and inflammatory CNS markers are interrelated. These data, combined with our findings that IS induced a shift toward an M1 macrophage-like metabolic phenotype, would support the hypothesis that monocyte/macrophage trafficking from the periphery to the brain connects SNS activation, tryptophan metabolism, and proinflammatory signaling in the brain. Our current study suggests that increased plasma adrenaline, decreased plasma kynurenine/tryptophan ratios,

monocyte trafficking to the brain, and increased expression of proinflammatory cytokines in the CNS are all part of the stress response to IS, leading to stress-induced exaggeration of anxiety-like defensive behavioral responses. This study complements previous studies by Wood and colleagues (2015) showing that inflammatory mediators in the dorsal raphe nucleus are associated with active and passive coping strategies in response to social stress (Wood et al., 2015), and our data provide insight into the peripheral signaling mechanisms by which psychological stressors might alter the environment of the central nervous system to control behavior.

5.5.9 Evidence that the effects of IS on the plasma metabolome are mediated in part by the gut microbiome

Our data provide support for the hypothesis that the alteration in the plasma metabolome after IS is due in part to the gut microbiome. The gut microbiome is a major source of metabolites that are secreted into the circulation, and these may be altered after stress-induced dysregulation of microbial abundance or diversity (Tang et al., 2019; Wikoff et al., 2009; Wilmanski et al., 2019). Furthermore, stress can increase the permeability of the gut barrier and promote microbial leakage into the circulation (Ait-Belgnaoui et al., 2012, 2005; Reber et al., 2016b; Stevens et al., 2018; van de Wouw et al., 2018; Zheng et al., 2017). We previously hypothesized, based on the plasma proteome of the same animals in the current study, that IS caused damage to the vascular barriers associated with the gut and the CNS, including the brain-cerebrospinal fluid barrier (BCSFB); prior immunization with either *M. vaccae* strain seemed to have attenuated gut and brain “leakiness” (Loupy, unpublished data). In the current study, among vehicle-treated rats, IS altered the abundance of a number of metabolites associated with the “microbial metabolism in diverse environments” pathway (KEGG map01120) or “bile secretion” pathway (KEGG

rno04976), although these were not mapped by the pathway analysis feature of MetaboAnalyst. Citrate, glycolate, phosphoserine, pyridoxal, allantoin, 2-oxoglutaramate, 3-sulfocatechol, and 6-phospho-gluconate are associated with the "microbial metabolism in diverse environments" pathway (KEGG map01120), whereas acetylcholine, choline, dopamine, folate, spermine, and 2-oxoglutaramate are associated with the "bile secretion" pathway (KEGG rno04976). Amino acids and nucleotides are also associated with the "biosynthesis of secondary metabolites" pathway (KEGG map01110), a pathway that maps metabolites produced by microbes, such as bacteria, in the gut.

5.5.10 IS produces prolonged activation of the sympathetic nervous system

IS increased the abundance of the catecholamines adrenaline and dopamine, which may be associated with increased SNS activity (Figure 5.5) (for review, see Gordan et al., 2015). Catecholamines and glucocorticoids (such as corticosterone) that are secreted during stress promote, among other things, the release of stored glucose and fatty acids for energy utilization (for review, see Jones et al., 2012; Macfarlane et al., 2008). Adrenaline and dopamine are released as part of the SNS "fight or flight" response to stress, and at higher concentrations, both metabolites can contribute to increased heart rate and vasoconstriction (for review, see Gordan et al., 2015). Although noradrenaline was not targeted in our current metabolomics dataset, it is likely that the abundance of noradrenaline was also increased after IS based on the increase of its precursor, dopamine, and its metabolite, adrenaline (Gordan et al., 2015; Wong, 2006). Acetylcholine is also released during sympathetic activation and was increased after IS among BBS-treated animals. Acetylcholine released by sympathetic preganglionic neurons stimulate postganglionic secretion of adrenaline and noradrenaline onto target tissues (for review, see

McCorry, 2007). Additionally, acetylcholine is released at the neuromuscular junction of skeletal muscles during contraction and might indicate increased muscle tone associated with freezing behaviors, reflecting the stress-induced increase of anxiety-like defensive behavioral responses (i.e., decreased social exploration) among vehicle-treated rats. This hypothesis also aligns with our finding that IS increases creatine and creatinine only among home cage control animals. However, acetylcholine can also act as an anti-inflammatory brain-immune mediator when it is released by the vagus nerve of the PNS during the inflammatory reflex: inflammatory mediators in the periphery, including LPS, activate the afferent branch of the vagus nerve, in turn triggering efferent activation in a negative feedback to suppress inflammation and inhibit cytokine release by proinflammatory macrophages (Pavlov and Tracey, 2012). In cardiac tissue, the vagus nerve releases acetylcholine to slow the heart rate (H. G. Kim et al., 2018), and as a consequence, acetylcholine can induce arrythmia (Bayer et al., 2019; Godoy et al., 1999; Sharifov et al., 2004); such dysregulation between PNS and SNS activation during stress can disrupt heart rate variability (H. G. Kim et al., 2018). Decreased heart rate variability is attributed to a shift toward greater SNS activity and is common among persons with PTSD (Cohen et al., 2000; Jenness et al., 2018; McLaughlin et al., 2015; Ulmer et al., 2018). IS also decreased the abundance of plasma glutamate, consistent with findings that both corticotropin-releasing hormone and adrenaline can reduce peripheral glutamate (Zlotnik et al., 2010) and providing further evidence that IS promoted a “fight or flight” response in rats. These results are consistent with previous studies showing that IS promotes the activation of classic autonomic and neuroendocrine stress pathways (Beninson et al., 2014; Deak et al., 1997; Frank et al., 2018b; Greenwood et al., 2003b; Maier et al., 1986; Maier and Watkins, 2005).

5.5.11 Immunization with M. vaccae strains prevents IS-induced changes in the plasma metabolome

The stress-resilient physiological effects of *M. vaccae* strains are extensive, and they coincide with previous reports of stress resilient phenotypes. For instance, we previously showed that immunization with *M. vaccae* NCTC 11659 reduces corticotropin-releasing hormone in the extended amygdala, consistent with a phenotype of stress resilience modeled by stressor controllability (Maier and Watkins, 2005); further, immunization with *M. vaccae* NCTC 11659 prevents IS-induced increases of hippocampal HMGB1 protein, while immunization with either strain of *M. vaccae* prevents IS-induced increases of hippocampal *Il6* mRNA (Loupy et al., 2021), suggesting that mediation of proinflammatory monocyte/macrophage trafficking by *M. vaccae* immunization promotes resilience to IS-induced behaviors (Frank et al., 2018b; Yang et al., 2015). Now, we demonstrate that *M. vaccae* strains might promote activation of injury-repairing macrophages, mediate microbial-derived metabolites, or attenuate SNS activity, consistent with stress-resilient mechanisms reported previously in IS models (Frank et al., 2018b; Greenwood et al., 2003b; Speaker et al., 2014; Thompson et al., 2020; Weiss and Simson, 1986).

5.5.12 Immunization with M. vaccae strains prevents IS-induced changes in tryptophan metabolism

As described above IS dramatically modified the plasma metabolome, dysregulating the abundance of metabolites involved in the stress response, including energy utilization, amino acid metabolism, antioxidant pathways, and of particular significance, tryptophan metabolism; however, IS-induced changes in tryptophan metabolism did not occur among rats immunized with *M. vaccae* NCTC 11659 or *M. vaccae* ATCC 15483. In fact, among animals exposed to IS, animals immunized with *M. vaccae* strains exhibited increases of indole-3-acetylaldehyde and

tryptophanamide; stabilized abundances of these metabolites among rats immunized with *M. vaccae* provide further evidence that *M. vaccae* strains protect against IS-induced changes to serotonin or kynurenine metabolism. The observation that prior immunization with *M. vaccae* strains largely prevented IS-induced changes in tryptophan metabolism supports previous studies that show stress-resilient behavioral effects of *M. vaccae* strains in rodents (Amoroso et al., 2020; Bowers et al., 2020; Fonken et al., 2018; Fox et al., 2017; Frank et al., 2018b; Hassell et al., 2019; Loupy et al., 2021, 2018; Lowry et al., 2007; Reber et al., 2016b; Siebler et al., 2018). It is currently unknown how *M. vaccae* strains might buffer against stress-induced changes to tryptophan metabolism, although one hypothesis might be that *M. vaccae* strains activate immune cells (i.e., monocytes/macrophages) to alter their metabolic phenotype (i.e, M2) at baseline, providing resilience to a shift in immunometabolism that is associated with proinflammatory monocytes/macrophages (i.e, M1) and is observed among BBS-treated animals after IS. It is also possible that tryptophan metabolites such as serotonin were derived from enterochromaffin cells in response to autonomic nervous system output from the PNS (i.e., due to immunization with *M. vaccae* strains) or from the SNS (i.e., due to IS) (for review, see Bellono et al., 2017), or from alterations to the gut microbiome (Reigstad et al., 2015).

Our data suggest that immunization with either *M. vaccae* NCTC 11659 or *M. vaccae* ATCC 15483 may have buffered against stress-induced increases of serotonin production, secretion, or metabolism. For example, immunization with *M. vaccae* strains decreased 5-hydroxyindoleacetate, a primary serotonin metabolite, among home cage control animals, although IS increased this metabolite regardless of pretreatment. Serotonin was not measured in this study, and we cannot determine exactly if and how serotonin was altered in plasma.

However, our data indicate that future studies should measure effects of *M. vaccae* immunizations and stress on the abundance of this important signaling molecule in the periphery.

5.5.13 Immunization with M. vaccae strains might invoke antioxidant pathways that attenuate oxidative stress induced by IS

Immunization with *M. vaccae* strains prevented IS-induced decreases of GSSG, putrescine, and 5-oxoproline, which are involved in the "glutathione metabolism" pathway (KEGG rno00480). GSH is an antioxidant molecule derived from glutamate, cysteine, and glycine that scavenges cellular free radicals (for review, see Wu et al., 2004) produced during psychological stress (Lehmann et al., 2019) or endotoxemia (Bhattacharyya et al., 2005); in this process, GSH is oxidized to form GSSG (Wu et al., 2004). We recently showed that IS decreased the relative abundance of glutathione peroxidase (GPx, matching isoforms 3, 5, and 6; GPx3/5/6) in plasma of the same rats (Loupy, unpublished data); collectively, GPx and GSH remove peroxides such as hydrogen peroxide (Wu et al., 2004). Although the relative abundance of GPx3/5/6 was decreased after IS regardless of pretreatment, our metabolomics data might suggest that stress-induced decrease of glutathione metabolism or activity is buffered among animals preimmunized with *M. vaccae* strains. For example, immunization with either strain of *M. vaccae* prevented IS-induced decreases in glutathione metabolism. Under home cage control conditions, immunization with either *M. vaccae* NCTC 11659 or *M. vaccae* ATCC 15483 increased GSSG, and among rats exposed to IS, immunization with *M. vaccae* ATCC 15483 increased the abundance of GSSG, suggesting a protective effect of *M. vaccae* on antioxidant function. Furthermore, among animals immunized with *M. vaccae* NCTC 11659, GSH decreased, possibly indicating increased antioxidant activity, since GSSG (not decreased after IS among animals immunized with *M. vaccae*) is produced via the oxidation of GSH (Wu et al., 2004). Increasing

antioxidant activity may be one way that *M. vaccae* strains protect against vascular endothelial damage and subsequent inflammatory signaling to the CNS after IS (Loupy, unpublished data) (Lehmann et al., 2019).

5.5.14 Evidence that immunization with M. vaccae strains disrupts IS-induced monocyte/macrophage trafficking to the brain

IS-induced changes to the plasma metabolome correlated with inflammatory biomarkers in the cerebrospinal fluid and anxiety-like defensive behaviors, but these relationships were interrupted in rats immunized with either *M. vaccae* strain, consistent with an immunoregulatory phenotype in these animals. Immunization with *M. vaccae* strains disrupted the negative correlation between kynurenine/tryptophan ratios and the abundance of YWHAG in the CSF as well as the negative correlation between kynurenine/tryptophan ratios and hippocampal *Il6* mRNA expression, as these relationships only existed among BBS-treated animals. Although the precise mechanisms by which *M. vaccae* strains mediate physiological stress responses are unknown, we previously hypothesized that *M. vaccae* strains attenuate the proinflammatory signaling induced by monocyte-derived macrophages trafficking to the brain (Loupy, unpublished data). It might be that, by interrupting these relationships, either by acting on circulating monocytes/macrophages or attenuating prolonged SNS activation, immunization with *M. vaccae* NCTC 11659 or *M. vaccae* ATCC 15483 prevents stress-induced behaviors. The current study, along with prior studies (Loupy, unpublished data) (Reber et al., 2016b; Smith et al., 2019), provide evidence that macrophages are alternatively activated by *M. vaccae* immunizations under home cage control conditions, suppressing successive proinflammatory responses that are initiated by IS and buffering against IS-induced monocyte migration into the brain. Further research should be conducted to investigate the origin of activated macrophages (i.e., monocyte-

derived, circulating, tissue-resident) and if other immune cell types are also being alternatively activated by subcutaneous injection with *M. vaccae* strains.

Overall, our data might imply that the metabolic phenotype of monocytes/macrophages in rats immunized with *M. vaccae* strains and exposed to IS are closer to the M2 phenotype compared to BBS-treated rats exposed to IS (Viola et al., 2019). For example, glutamine metabolism is involved in the differentiation of macrophages toward the M2 phenotype, and M2 cells induce the synthesis of glutamine (Viola et al., 2019); in our study, IS decreased plasma glutamine, but this effect was prevented by immunization with either *M. vaccae* strain (Supplementary Figure 5.3). Additionally, M2 macrophages display an intact TCA cycle and tend to shift their cellular metabolism toward fatty acid oxidation, oxidative phosphorylation, and kynurenine metabolism (Viola et al., 2019). Among rats immunized with *M. vaccae* strains, IS altered plasma metabolites enriched for "TCA cycle" (Figure 5.4B), "alanine, aspartate, and glutamate metabolism" (Figure 5.4B), "arginine and proline metabolism" (Figure 5.4D), and possibly "glycerophospholipid metabolism" (Figure 5.4D), all of which are enriched for in M2 polarized macrophages compared to unpolarized (M0) macrophages (Abuawad et al., 2020).

5.5.15 Evidence that immunization with M. vaccae strains protects against the stress-induced increase of gut barrier permeability

We recently reported that, in mice, immunization with *M. vaccae* NCTC 11659 stabilizes the composition of the gut microbiome and prevents aberrant disruptions in the microbial profile of the gut after CDR and chronic social defeat stressors (Foxx et al., 2021). We have also demonstrated that immunization with *M. vaccae* NCTC 11659. prior to chronic subordinate colony housing and dextran sulfate sodium (DSS) administration, prevents stress-induced colitis

in mice (Amoroso et al., 2020; Reber et al., 2016b). The abundance of plasma metabolites is strongly associated with the composition and function of the gut microbiome, and in our study, we found that the vast majority of metabolites, including amino acids, that were altered by IS among vehicle-treated rats were not altered by IS among animals immunized with *M. vaccae* strains. For example, "leaky gut" might be identified by the abundance of citrulline in the plasma metabolome; citrulline is a non-protein amino acid largely produced by enterocytes, the cells that line the intestinal epithelium, and decreased abundance of plasma citrulline is a biomarker of intestinal disease, enterocyte dysfunction, and decreased enterocyte mass (Crenn et al., 2003; Derikx et al., 2009; Fragkos and Forbes, 2018). Indeed, we found that, among BBS-treated rats, IS decreased plasma citrulline; however, prior immunization with *M. vaccae* strains prevented IS-induced decreases of plasma citrulline. Short chain fatty acids (SCFAs) such as butyrate enhance intestinal epithelial integrity (M. Li et al., 2018d; Miller et al., 2005; Peng et al., 2009; Wang et al., 2020) and mediate stress responses and reduce stress-related behaviors (Dalile et al., 2020; Loupy and Lowry, 2020; van de Wouw et al., 2018; J. Zhang et al., 2019); overall reductions of SCFAs are linked to increased inflammation associated with depression (Huang et al., 2018; van de Wouw et al., 2018). Butyrate (butanoic acid) was in the top 50 metabolites increased by *M. vaccae* NCTC 11659 among home cage control animals (using PLS-DA VIP analysis in the clustered heat map; see Figure 5.2A), and immunization with *M. vaccae* strains may have buffered against IS-induced increases of butyrate (Supplementary Figure 5.5), although these results were not significant. Our data support the idea that immunization with either *M. vaccae* NCTC 11659 or *M. vaccae* ATCC 15483 may protect the gut epithelium from IS-induced disruption. It will be important for future research to elucidate how exactly immunization with *M. vaccae* strains might contribute to enhanced barrier function during stress,

and further research should be done to investigate the specific involvement of gut microbiome-derived metabolites like SCFAs in the protective effects of *M. vaccae* strains. One novel hypothesis could be that microbially-derived indole/tryptophan metabolites act on the aryl hydrocarbon receptors in the gut lining to alter intestinal permeability (Hubbard et al., 2015; Lanis et al., 2017).

5.5.16 Immunization with M. vaccae strains attenuate activation of the sympathetic nervous system

Our data also suggest that immunization with either *M. vaccae* strain prevented increases in SNS activation 24 hours after IS. For instance, plasma adrenaline, dopamine, and acetylcholine were increased after IS among BBS-treated rats, but not among animals immunized with *M. vaccae* NCTC 11659 or *M. vaccae* ATCC 15483 (Figure 5.5). Interestingly, IS increased contractile fibers in the plasma proteome regardless of prior treatment, likely reflecting increased skeletal or cardiac contractions during IS (Loupy, unpublished data); however, our current metabolomics data imply that only vehicle-treated animals display sustained increases of important vasoactive neurotransmitters and hormones 24 hours after IS compared to their home cage counterparts. These data are in line with previous studies showing that the vagus nerve is required for some probiotics to produce stress resilience effects (Bravo et al., 2011).

Immunization with *M. vaccae* strains might counteract the effects of IS on SNS activation by increasing parasympathetic tone via the vagus nerve, as described among home cage control animals. Previous work shows that vagal nerve stimulation during exposure to the conditioned fear paradigm can enhance fear extinction, and vagal nerve stimulation reduces anxiety among unconditioned rats (Noble et al., 2019, 2017; Souza et al., 2020, 2019). The effects of *M. vaccae*

on the PNS and SNS under home cage control conditions may attenuate IS-induced aberrant cardiac contractile signaling and SNS-induced monocyte activation or release from bone marrow, ultimately preventing the development of IS-induced anxiety-like defensive behavioral responses. Considering that SNS activation is responsible for the release of inflammatory monocytes into the circulation (for review, see Weber et al., 2017; Wohleb et al., 2015), it could be that the stress-resilient effects of *M. vaccae* treatment on inflammatory macrophage metabolism arises, in part, from increased PNS/decreased SNS signaling in the periphery. Our findings offer one potential mechanism by which immunization with *M. vaccae* strains prevents adverse stress-induced physiological and behavioral outcomes (Loupy et al., 2021).

5.5.17 Limitations

Our study is the first to demonstrate associations between the stress-resilient behavioral effects of *M. vaccae* strains with physiological effects on the plasma metabolome, and there are limitations to our experimental design which should be considered for future experiments. It is important to point out that any functional associations of metabolites are speculative in nature because we did not measure the activity of enzymes in specific pathways. Likewise, although associations can be made between our plasma metabolites and stress behaviors, our data do not establish direct causal relationships. Considering that our metabolomics analysis was targeted, we were unable to measure the abundance of all plasma metabolites; it will be important for future studies to follow up with an untargeted metabolomics approach in order to create more complete and accurate functional networks. This is especially important for the plasma metabolome, in which several physiological systems (i.e., immune, endocrine, neural, etc) may influence the abundance and function of plasma metabolites. Future experiments should

investigate ex vivo and in vitro models to study individual organs and cell types that may contribute to the effects described in this paper. In addition, in our study the effects of immunization with *M. vaccae* and IS are restricted to a single time point of tissue collection, eight days following immunization with *M. vaccae* and 24 hours after stress; considering that our results may have been influenced by immune activation and resolution of inflammation (not measured here), future experiments should explore time-dependent changes on the plasma metabolome following final immunizations of *M. vaccae* strains and following IS. Another limitation of our study is that nutrition intake and physical activity were not monitored after *M. vaccae* immunizations or exposure to IS and may have been additional variables that contributed to an altered plasma metabolome. Also, our experiment was conducted only in adult male rats, and future studies should include female rats to determine if *M. vaccae* administration and/or IS may produce differential effects on the plasma metabolome dependent on sex. Similarly, immune response to *M. vaccae* strains may be altered in juvenile or aged rats, and future experiments should investigate these differences.

5.5.18 Conclusions

Collectively, this study demonstrates that prior immunization with *M. vaccae* strains attenuate stress-related proinflammatory processes that cause widespread changes to bidirectional physiological processes between the CNS and periphery. Immunization with either *M. vaccae* NCTC 11659 or *M. vaccae* ATCC 15483 attenuated the IS-induced increase of SNS-associated catecholamines. Immunization with *M. vaccae* strains also prevented IS-induced changes to the abundance of tryptophan metabolites; this may be associated with the mechanism by which *M. vaccae* alternatively activates the immune system at baseline, considering that *M. vaccae* strains

altered tryptophan metabolism under home cage control conditions, consistent with the well-established role of *M. vaccae* NCTC 11659 in increasing IFNγ. The kynurenine/tryptophan ratio, a readout for IDO activity, negatively correlated with adrenaline and inflammatory biomarkers in the CNS, suggesting a relationship among SNS activity, tryptophan metabolism, and neuroinflammatory signaling related to anxiety-like defensive behavioral responses; however, this relationship was only evident among vehicle-treated rats and not among animals immunized with *M. vaccae*. Such relationships may be mediated by SNS activation, leading to release of monocytes from the bone marrow, induction of M1-like monocytes/macrophages by MAMPs, PAMPs, and DAMPs, and trafficking of monocyte-derived macrophages trafficking to the brain, processes that are disrupted in rats previously immunized with *M. vaccae* strains. It could be that *M. vaccae* treatment alternatively activates patrolling monocytes/macrophages toward an M2 phenotype prior to IS stimulus, prevents the release of MAMPs, PAMPs, or DAMPs, due to increased gut permeability or damaged tissue, or promotes PNS activation via the vagus nerve to attenuate monocyte proliferation, transmigration, or polarization of monocytes/macrophages to an inflammatory M1-like phenotype.

5.6 Acknowledgements, author contributions, and conflicts of interest

Acknowledgements

These studies were funded by the National Institute of Mental Health (NIMH) R21 grant (R21MH116263) awarded to C.A.L., S.F.M., M.G.F. (PIs), and L.K.F. (Co-I). J.A.R. and F.C., on behalf of the University of Colorado School of Medicine Metabolomics Core, a shared resource of the University of Colorado Cancer Center, acknowledge partial support from a National Institute of Health P30 Cancer Center Support Grant (P30CA046934).

Author Contributions

Study design was conceived by K.M.L., C.A.Z., and C.A.L. *M. vaccae* injections were performed by A.I.E., B.M.M., and C.A.Z. Inescapable tail shock and behavioral testing were conducted by H.M.D. Tissue collection for plasma was conducted by K.M.L, B.M.M., K.E.C., M.G.F., and C.A.Z. Metabolomics sample preparation was performed by K.M.L., F.C., J.A.R., and A.I.E. Mass spectrometry data acquisition and analysis were performed by C.F. and J.A.R. Data analysis and statistical analysis were carried out by K.M.L. and M.R.A. Figures and figure legends were produced by K.M.L. Manuscript preparation was conducted by K.M.L. Editing and review was contributed by K.M.L, C.F., J.A.R., A.I.E., B.M.M., L.K.F., M.G.F., C.A.Z., S.F.M., and C.A.L.

Conflicts of interest

CAL serves on the Scientific Advisory Board of Immodulon Therapeutics, Ltd, is Cofounder and Chief Scientific Officer of Mycobacterium Therapeutics Corporation, serves as an unpaid scientific consultant to Aurum Switzerland A.G., and is a member of the faculty of the Integrative Psychiatry Institute, Boulder, CO, USA.

Chapter 6. Immunization with either *Mycobacterium vaccae* NCTC 11659 or *M. vaccae* ATCC 15483 prevents stress-induced changes to neuroactive metabolites in the plasma of adult male rats: II. targeted lipidomics.

Citation

Loupy, K.M., Cendali, F., Reisz, J.A., D'Angelo, H.M., Arnold, M.R., Elsayed, A.I., Marquart, B.M., Cler, K.E., Fonken, L.K., Frank, M.G., Zambrano, C.A., Maier, S.F., Lowry, C.A. Immunization with either *Mycobacterium vaccae* NCTC 11659 or *M. vaccae* ATCC 15483 prevents stress-induced changes to neuroactive metabolites in the plasma of adult male rats: II. targeted lipidomics. Manuscript in preparation.

Authors' names

Kelsey M. Loupy[a], Francesca Cendali[b], Julie A. Reisz[b], Heather M. D'Angelo[c], Mathew R. Arnold[a,d], Ahmed I. Elsayed[a], Brandon M. Marquart[a], Kristin E. Cler[a], Laura K. Fonken[e], Matthew G. Frank[c,d], Cristian A. Zambrano[a], Steven F. Maier [c,d], Christopher A. Lowry[a,d,f,g,h,i,j]*

Authors' affiliations

[a]Department of Integrative Physiology, University of Colorado Boulder, Boulder, CO 80309, USA

[b]Department of Biochemistry and Molecular Genetics, University of Colorado Anschutz Medical Campus, Aurora, CO 80045, USA

[c]Department of Psychology and Neuroscience, University of Colorado Boulder, Boulder, CO 80309, USA

[d]Center for Neuroscience, University of Colorado Boulder, Boulder, CO 80309, USA

[e]Division of Pharmacology and Toxicology, University of Texas at Austin, Austin, TX 78712, USA

[f]Center for Microbial Exploration, University of Colorado Boulder, Boulder, CO 80309, USA

[g]Department of Physical Medicine and Rehabilitation and Center for Neuroscience, University of Colorado Anschutz Medical Campus, Aurora, CO 80045, USA

[h]Veterans Health Administration, Rocky Mountain Mental Illness Research Education and Clinical Center (MIRECC), Rocky Mountain Regional Veterans Affairs Medical Center (RMRVAMC), Aurora, CO 80045, USA

[i]Military and Veteran Microbiome: Consortium for Research and Education (MVM-CoRE), Aurora, CO 80045, USA

[j]Senior Fellow, inVIVO Planetary Health, of the Worldwide Universities Network (WUN), West New York, NJ 07093, USA

6.1 Abstract

Stress-related psychiatric disorders, including anxiety disorders, affective disorders, and trauma and stressor-related disorders, such as posttraumatic stress disorder (PTSD), are prevalent and are a major source of socioeconomic and individual burden. Although the mechanisms underlying the etiology and pathophysiology of these disorders, including PTSD, are not known, they are often associated with dysregulated immune and metabolic signaling. Novel PTSD treatments, including microbial-based therapeutics, target pathways involved in immunometabolism. We recently demonstrated that immunization with a heat-killed preparation of either *Mycobacterium vaccae* NCTC 11659 or *M. vaccae* ATCC 15483 prevents anxiety-like defensive behavioral responses in adult male rats 24 hours following inescapable tail shock stress (IS), as measured by the juvenile social exploration paradigm [Loupy et al., 2021, Brain, Behavior, and Immunity, 91: 212–229]. In subsequent publications we showed that immunization with either *M. vaccae* strain attenuates IS-induced changes to the plasma and cerebrospinal fluid (CSF) proteomes (Loupy, unpublished data) and plasma metabolome, preventing unique biological signatures of stress associated with anxiety-like behavior (see part I of this article). Collectively, our data suggest that immunization with *M. vaccae* strains prevent prolonged activation of SNS activity after stress, consequently protecting against endothelial dysfunction, proinflammatory signaling, monocyte/macrophage trafficking to the brain, and general disruptions to immunometabolism. In the current study, we examine the effects of immunization with *M. vaccae* strains and IS exposure on the plasma lipidome of the same rats used in the aforementioned studies, employing a targeted approach. We describe differential effects of *M. vaccae* strains on the plasma lipidome and provide evidence that immunization with *M. vaccae* strains promote an anti-inflammatory plasma lipid profile, preventing IS-induced

increases in proinflammatory omega-6 fatty acid metabolism. Together, our studies reveal a comprehensive physiological signature of stress-resilience among animals immunized with either *M. vaccae* strain.

6.2 Introduction

Stress-related psychiatric disorders, including anxiety disorders, affective disorders, and trauma and stressor-related disorders, such as posttraumatic stress disorder (PTSD), are prevalent and are a major source of socioeconomic and individual burden (Kessler, 2000; Kessler et al., 2017; Koenen et al., 2017; Roehrig, 2016; L. Wang et al., 2016). Stress exposure is a risk factor for each of these disorders (Bandoli et al., 2017; McLaughlin et al., 2010), and part of the diagnostic criteria for PTSD (American Psychiatric Association, 2013). According to the *Diagnostic and Statistical Manual of Mental Disorders*, 5th Edition (DSM-5), PTSD is defined, in part, by alterations of arousal and reactivity following a trauma (American Psychiatric Association, 2013). Hyperarousal in individuals with PTSD is thought to be due to dysregulated autonomic nervous system activity following trauma; increased sympathetic nervous system (SNS) activity and decreased parasympathetic nervous system (PNS) activity are primary features of PTSD pathophysiology (Cohen et al., 2000; Dennis et al., 2016; Hopper et al., 2006; Jenness et al., 2018; Park et al., 2017; Ulmer et al., 2018). Likewise, inflammation, exacerbated by the disruption of neuroimmune signaling, is associated with the risk for developing and severity of PTSD symptoms (for review, see Loupy and Lowry, 2020; Michopoulos et al., 2017).

It has been suggested that monocytes, released from the bone-marrow upon SNS activation, traffic to the brain and contribute to stress-induced exaggeration of anxiety-like defensive

behavioral responses (Wohleb et al., 2014, 2013, 2011). Although this hypothesis has not been thoroughly explored in persons with PTSD, current data suggests that increased plasma monocytes are a risk factor for the development of PTSD (Schultebraucks et al., 2020) and that altered monocyte phenotypes and functions are associated with a diagnosis of PTSD (Gola et al., 2013; Kuan et al., 2019; Neylan et al., 2011; Schiweck et al., 2020). Monocytes and macrophages are phagocytic cells that are called upon as general "first responders" during inflammatory injury, but these cells also play important roles in lipid metabolism, including fatty acid metabolism. Monocytes/macrophages incorporate large amounts of polyunsaturated fatty acids (PUFAs) in their cellular membranes; these cells readily metabolize omega-6 (n-6) fatty acids like arachidonic acid and the omega-3 (n-3) fatty acids eicosapentaenoic acid (EPA), docosapentaenoic acid (DPA), and docosahexaenoic acid (DHA) (for review, see Ménégaut et al., 2019). Metabolism of arachidonic acid leads to the production of proinflammatory prostanoids (i.e., thromboxanes and prostaglandins) and leukotrienes via the action of cyclooxygenase (COX) and lipoxygenase (LOX) enzymes, respectively, in what has been called the arachidonic acid cascade (Suneson et al., 2021). Metabolism of n-3 PUFAs by COX and LOX enzymes primarily produces anti-inflammatory mediators like resolvins (Suneson et al., 2021). Interestingly, cyclooxygenase 2 (COX-2) inhibitors have been proposed as a possible new treatment for PTSD (for review, see Bersani et al., 2020); the effectiveness of these drugs might be derived from shifting PUFA metabolism away from n-6 and toward n-3metabolism. In one study, eicosanoids (which includes prostaglandins, leukotrienes and nonclassic eicosanoids (Needleman et al., 1986)), along with absolute numbers of monocytes, were found to be among the top fifteen biomarkers predictive of PTSD development among combat Veterans (Schultebraucks et al., 2020); similarly, combat Veterans with PTSD exhibit decreased plasma

DHA abundance compared to combat Veterans without PTSD (de Vries et al., 2016; Mellon et al., 2019). In a randomized, double-blind, placebo-controlled trial with traumatic accident survivors, treatment with n-3 fatty acids decreased heart rate after 12 weeks, suggesting an inhibitory effect on SNS activity, although the n-3 treatments did not reduce the risk for developing PTSD (Matsumura et al., 2017). However, a secondary analysis of another trial using omega-3 supplements revealed that, among those receiving n-3 supplements, changes in EPA+DHA, and EPA, as well as the EPA:arachidonic acid ratio and EPA: DHA ratio were inversely correlated with PTSD severity, whereas changes in arachidonic acid were positively correlated with PTSD severity (Matsuoka et al., 2016). It could be that tilting the balance of PUFA metabolism one way or the other, possibly by monocyte/macrophage stimulation, helps confer vulnerability to or protection against PTSD symptoms, as proposed previously for major depressive disorder (Suneson et al., 2021).

Considering the extensive overlap between immune and metabolic processes, novel therapeutics for PTSD might target pathways involved in immunometabolism. Although immunometabolism has not yet been studied in detail among individuals with PTSD, general immune dysregulation and mitochondrial or metabolic dysfunction has already been established in PTSD (Bersani et al., 2020). Interestingly, alteration of the gut microbiome has been suggested as a possible new method for regulating host immunometabolism (Bersani et al., 2020). Gut microbiota influence mood and cognition via the microbiome gut-brain axis, and the composition of the gut microbiome affects both immune function and production of neuroactive metabolites (for review, see Bermúdez-Humarán et al., 2019; Brenner et al., 2017; Cryan et al., 2020; Long-Smith et al., 2020; Loupy and Lowry, 2020; Malan-Muller et al., 2018). In addition, certain bacterial species

stimulate vagal nerve afferents as way of communication with the brain (Bermúdez-Humarán et al., 2019; Bravo et al., 2011; Brenner et al., 2020). Thus, microbial-based therapeutics like probiotics or “psychobiotics” might be effective for the prevention and treatment of trauma- and stress-related pathophysiology.

We recently reported that immunization with a whole cell heat-killed preparation of either *Mycobacterium vaccae* NCTC 11659 or *M. vaccae* ATCC 15483 prevents stress-induced neuroinflammation and stress-induced exaggeration of anxiety-like defensive behavioral responses as measured by the juvenile social exploration (JSE) paradigm 24 hours after inescapable tail shock stress (IS) (Loupy et al., 2021). In subsequent publications, we demonstrated that immunization with either *M. vaccae* strain attenuates IS-induced changes to the plasma and cerebrospinal fluid (CSF) proteomes (Loupy, unpublished data) and plasma metabolome (see part I of this article) preventing unique biological signatures of stress associated with stress vulnerability. Our results indicated that immunization with *M. vaccae* strains protects IS-exposed rats from aberrant signaling of complement and coagulation cascades and disrupted vascular endothelia, including at the blood-CSF barrier. We also hypothesized that *M. vaccae* strains prevented proinflammatory monocyte trafficking into the CNS, which was corroborated in part I of this article. Part I of this article also revealed that immunization with *M. vaccae* strains prevented the stress-induced increases of SNS activation that were observed among vehicle-treated animals 24 hours after IS, and we provided some evidence that immunization with *M. vaccae* strains may have increased vagal activity.

In the current study, we analyzed the effects of *M. vaccae* strains and IS exposure on the plasma lipidome, associated with behaviors indicative of stress vulnerability versus resilience (behavioral results from these rats are published separately in Loupy et al., 2021). We used a targeted approach and identified 47 lipids in the plasma. Interestingly, immunization with either strain of *M. vaccae* differentially affected the plasma lipidome, although both strains altered polyunsaturated fatty acid metabolism in a convergent manner. Immunization with *M. vaccae* strains increased n-3 polyunsaturated fatty acid metabolism, prevented IS-induced alterations of arachidonic acid metabolism, and did not prevent, but rather, may have promoted IS-induced increases in fatty acid β-oxidation. Further research is needed to investigate specific mechanisms through which *M. vaccae* strains increase stress resilience; however, our collective data provides a comprehensive physiological signature of stress-resilience among animals immunized with either *M. vaccae* strain.

6.3 Materials and methods

6.3.1 Animals

For an experimental timeline, please see Figure 6.1. The data reported in this study are derived from the same rats used in a previous report, which investigated the effects of immunization with *Mycobacterium vaccae* NCTC 11659 and *M. vaccae* ATCC 15483 strains and exposure to IS on behavioral outcomes and molecular signaling in the liver, spleen, and hippocampus (Loupy et al., 2021). In the current study, targeted lipidomic profiles in plasma of these rats are reported. Adult male Sprague Dawley® rats (Hsd:Sprague Dawley® SD®; Envigo, Indianapolis, IN, USA) weighing 250-265 g upon arrival were pair-housed in Allentown micro-isolator filter-topped caging [259 mm (W) × 476 mm (L) × 209 mm (H); cage model #PC10198HT, cage top

#MBT1019HT; Allentown, NJ, USA] containing an approximately 2.5 cm-deep layer of bedding (cat. no. 7090; Teklad Sani-Chips; Harlan Laboratories, Indianapolis, IN, USA). This species, strain, and supplier were chosen due to previous studies evaluating stress resilience effects of *M. vaccae* NCTC 11659 that were conducted with these animals (Frank et al., 2018b). All rats were kept under standard laboratory conditions (12-h light/dark cycle, lights on at 0700 h, 22 °C) and had free access to bottled reverse-osmosis water and standard rat diet (Harlan Teklad 2918 Irradiated Rodent Chow, Envigo, Huntingdon, United Kingdom). Cages were changed once per week. The research described here was conducted in compliance with the ARRIVE 2.0 Guidelines for Reporting Animal Research (Percie du Sert et al., 2020), and all studies were consistent with the National Institutes of Health *Guide for the Care and Use of Laboratory Animals*, Eighth Edition (National Research Council, 2011). The Institutional Animal Care and Use Committee at the University of Colorado Boulder approved all procedures. All efforts were made to limit the number of animals used and their suffering.

6.3.2 Reagents

This study used a whole cell heat-killed preparation of *M. vaccae* NCTC 11659 [IMM-201; alternative designations and different preparations and production processes of *M. vaccae* NCTC 11659 used in clinical trials or preclinical studies include: DAR-901 (Lahey et al., 2016), DarDar tuberculosis vaccine (Von Reyn et al., 2010), MV001 (Waddell et al., 2000), MV 007 (Vuola et al., 2003), *M. vaccae* SRL 172 (O'Brien et al., 2004; Von Reyn et al., 2010), and *M. vaccae* SRP 299 (Lowry et al., 2007); V7 (Bourinbaiar et al., 2020) is a hydrolyzed version of heat-killed *M. vaccae* NCTC 11659; *M. vaccae* NCTC 11659 has recently been classified as *M. kyogaense* sp. nov. (NCTC 11659; CECT 9646; DSM 107316) (Nouioui et al., 2018) (but see also Gupta et al.,

2018)]; 10 mg/ml solution; strain National Collection of Type Cultures (NCTC) 11659, batch C079-ENG#1, provided by BioElpida (Lyon, France), diluted to 1 mg/ml in 100 µl sterile borate-buffered saline (BBS) for injections]. This study also employed the use of a whole cell heat-killed preparation of *M. vaccae* strain American Type Culture Collection (ATCC) 15483 suspension. *M. vaccae* ATCC 15483 was purchased from ATCC (Bonicke and Juhasz (ATCC® 15483), Manassas, VA, USA). *M. vaccae* ATCC 15483 was cultured in ATCC® Medium 1395: Middlebrook 7H9 broth with ADC enrichment at 37 °C, then centrifuged at 3000 x g at 4 °C for ten minutes to pellet the cells, growth media was removed, and cells were weighed and resuspended in sterile BBS to a concentration of 10 mg/ml. Cells were transferred to a sealed sterile glass container and autoclaved at 121 °C for 15 minutes. Heat-killed bacterial stock was stored at 4 °C. *M. vaccae* ATCC 15483 was further diluted to 1 mg/ml in 100 µl sterile BBS for injections.

6.3.3 Mycobacterium vaccae (M. vaccae) NCTC 11659, M. vaccae ATCC 15483, and vehicle immunization

Experimental rats received 3 subcutaneous (s.c.) immunizations of: 1) 0.1 mg of a heat-killed preparation of *M. vaccae* NCTC 11659 (estimated to be 1 x 10^8 cells); 2) 0.1 mg of a heat-killed preparation of *M. vaccae* ATCC 15483 (estimated to be 1 x 10^8 cells); or 3) 100 µl of the vehicle, sterile BBS, using 21-gauge needles and injection sites between the scapulae, between the hours of 12 pm and 4 pm. Injections occurred on days –21, –14, and –7 prior to stress exposure, which occurred on day 0. The dose used in these experiments (0.1 mg) was 1/10 of the dose used in human studies (1 mg) (O'Brien et al., 2004) and identical to the dose used in previous studies in mice and rats (Amoroso et al., 2020; Bowers et al., 2020; Fonken et al., 2018; Fox et al., 2017; Foxx et al., 2021; Frank et al., 2018b; Hassell et al., 2019; Loupy et al., 2021, 2020, 2018; Lowry

et al., 2007; Reber et al., 2016b; Siebler et al., 2018; Smith et al., 2020). Figure 6.1 provides a timeline of *M. vaccae* treatments and stress exposure in relation to tissue collection.

Figure 6.1 Experimental timeline.
This schematic represents the experimental timeline for immunization with *M. vaccae* NCTC 11659, *M. vaccae* ATCC 15483, or vehicle (borate-buffered saline [BBS]), exposure to inescapable tail shock (IS), behavioral testing (juvenile social exploration [JSE], and euthanasia. Behavioral results have been published separately in Loupy et al. [2021]). Abbreviations: BBS, borate-buffered saline; HC, home cage control conditions; IS, inescapable tail shock stress; JSE, juvenile social exploration. Adapted from Loupy et al. (2021).

6.3.4 Inescapable tail shock stress (IS)

IS was performed as previously described (Frank et al., 2018b; Loupy et al., 2021). Briefly, rats were placed in Plexiglas® tubes (23.4 cm in length × 7 cm in diameter) and exposed to 100 1.6 mA, 5-s tail shocks with a variable inter-trial interval (ITI) ranging from 30 to 90 s (average ITI = 60 s). All IS treatments occurred between 09:00 and 11:00 h. IS animals were returned to their home cages immediately after termination of the shock. Home cage control (HC) animals remained undisturbed in their home cages.

6.3.5 Juvenile social exploration (JSE)

IS exposure produces robust decreases in JSE (Christianson et al., 2008), which is a widely used and validated measure of anxiety (File and Seth, 2003) and is sensitive to the neuroinflammatory effects of stress (Goshen and Yirmiya, 2009). Here, JSE was measured 24 h prior to IS (baseline)

and 24 h after IS (test) (i.e., between 9:00 and 10:00 h). Each experimental subject was transferred to a novel cage with shaved wood bedding in a dimly lit room (40 lx). After a 15-min habituation period, a 28–32 day-old juvenile male rat was introduced to the subject's cage for 5 min. Exploratory behaviors of the adult (sniffing, pinning, licking and allo-grooming of the juvenile) were timed by an observer blind to treatment condition. After the test, the juvenile was removed and the experimental adult rat was returned to its home cage. Although juvenile stimulus rats were reused for multiple tests, the adult was never retested with the same juvenile. For each animal, JSE test data were quantified as a percent of baseline JSE. Due to technical issues, a total of four animals were removed from the JSE paradigm and subsequent behavioral analysis and our final group sample sizes prior to outlier analysis were BBS/HC, n = 8; BBS/IS, n = 6; NCTC/HC, n = 8; NCTC/IS, n = 8; ATCC/HC, n = 8; ATCC/IS, n = 6. Behavioral results have been published separately in Loupy et al. (2021).

6.3.6 Euthanasia and tissue and plasma collection

Rats were euthanized eight days following the last injection using an overdose of sodium pentobarbital (Fatal Plus®, Vortech Pharmaceuticals Ltd., Dearborn, MI, USA; 200 mg/kg, i.p.). After euthanasia, blood was collected by opening the thoracic cavity and inserting a 21-gauge needle into the right atrium of the heart and slowly drawing up 1 mL of blood. Blood was gently released into a BD Vacutainer® blood collection tube containing EDTA (Cat. No. 367835; Becton, Dickinson, and Company; Franklin Lakes, NJ, USA) and spun down at 1500 × g for 10 min; the plasma supernatant was collected and stored at −80 °C. Due to loss of samples during plasma collection, final sample sizes for plasma analysis were BBS/HC, n = 8; BBS/IS, n = 6; NCTC/HC, n = 8; NCTC/IS, n = 8; ATCC/HC, n = 7; ATCC/IS, n = 8.

6.3.7 Plasma lipid extraction, mass spectrometry (MS), and targeted analysis

Plasma samples were thawed on ice. Lipids from plasma (10 μL) were extracted at 4 °C in the presence of methanol (90 μL), and the resulting supernatant was analyzed on a Thermo Vanquish ultra high pressure liquid chromatography (UHPLC) coupled to a Thermo Q Exactive MS as previously described in detail (Reisz et al., 2019). For targeted analyses, .raw files were converted to .mzXML using RawConverter 1.1.0.21. Lipids were assigned and peaks were integrated using Maven (Princeton University) (Clasquin et al., 2012; Melamud et al., 2010) in conjunction with the Kyoto Encyclopedia of Genes and Genomes (KEGG) database (Kanehisa and Goto, 2000) and an in-house standard library. Quality control was assessed using technical replicates run at beginning, end, and middle of each sequence as previously described (Nemkov et al., 2017). In all, 47 lipids were assigned in this study.

6.3.8 Statistical analysis

Lipidomics analyses were performed using R Statistical Programming (version 3.5.3 for Windows) and MetaboAnalyst 4.0 (https://www.metaboanalyst.ca/home.xhtml) (Chong et al., 2019, 2018). One sample from BBS/HC group was identified as an extreme outlier with low lipid detection and was removed from the analysis. Data were normalized using log transformation. Zero values were imputed with one fifth of the lowest value detected for that metabolite. Two separate analyses were run on the data: 1) generalized linear model (GLM) was performed in R in order to explore the general effects of treatment, stress, and their interaction on the plasma lipidome, and 2) pairwise comparison analyses were performed in MetaboAnalyst to directly compare treatment groups of interest. Specifically, GLM analysis was performed on

normalized peak intensities for each metabolite with treatment, stress, and treatment x stress as factors. Fold change values and pairwise comparison *p*-values were analyzed in MetaboAnalyst. For both GLM and pairwise analyses, two-tailed significance was set at $\alpha = 0.1$. Pairwise analyses utilized false discovery rate (FDR)-adjusted *p*-values. Lipids that were found to be significantly different between groups as well as lipids with a fold-change (up or downregulated) greater than two were used in downstream pathway analysis, utilizing the MetaboAnalyst Pathway Analysis with Human Metabolome Database (HMDB) IDs for metabolite labeling and *Rattus norvegicus* as species, hypergeometric testing for overrepresentation analysis, and relative-betweenness centrality for pathway topology analysis.

6.4 Results

6.4.1 Analysis of effects of M. vaccae strains and IS on the plasma lipidome using GLM analysis

To understand the overall effect of immunization with *M. vaccae* NCTC 11659 or *M. vaccae* ATCC 15483 treatment and IS on the plasma lipidome, we ran a generalized linear model (GLM) using treatment (*M. vaccae* NCTC 11659, *M. vaccae* ATCC 15483, or BBS), stress (IS or HC), and treatment x stress as factors in our model, using two-tailed $p < 0.1$ as performed previously (Loupy et al., 2021). Analysis at the GLM level revealed altered metabolic signatures of altered lipid metabolism. Specifically, analysis using GLM identified main effects of treatment for six metabolites, main effects of stress for four metabolites, and treatment x stress interactions for five metabolites (Supplementary Figure 6.1; Supplementary Table 6.1). These results warranted further analysis using pairwise comparisons. To directly compare abundances between experimental groups, we first utilized an average fold change analysis for lipids with a fold change of magnitude greater than or equal to two. We also ran independent samples *t*-tests,

using FDR-adjusted $p < 0.1$. Below we report the results for the effects of treatment with either *M. vaccae* NCTC 11659 or *M. vaccae* ATCC 15483 among home cage control rats. Then, we report the results for the effects of stress without and with immunization with either *M. vaccae* NCTC 11659 or *M. vaccae* ATCC 15483. Finally, we report the results for the effects of treatment with either *M. vaccae* NCTC 11659 or *M. vaccae* ATCC 15483 among IS-exposed rats.

6.4.2 Effects of immunization with M. vaccae NCTC 11659 or M. vaccae ATCC 15483 on the plasma lipidome of home cage control rats

Among home cage control rats, immunization with either *M. vaccae* NCTC 11659 or *M. vaccae* ATCC 15483 differentially altered the plasma lipidome. Among home cage control rats, two lipid metabolites were decreased by both strains: the secondary bile acid ursodeoxycholic acid (Figure 6.3) and the arachidonic acid derived eicosanoid, (±)11-hydroxyeicosatetraenoic acid (HETE) (Figure 6.4). Effects among home cage control rats on lipid metabolism that were specific to *M. vaccae* NCTC 11659 or *M. vaccae* ATCC 15483 are described separately below.

M. vaccae NCTC 11659

Fold change analysis revealed that, among home cage control rats, immunization with *M. vaccae* NCTC 11659 increased the abundance of the primary bile acid taurocholic acid (TCA) and the secondary bile acid taurodeoxycholic acid (TDCA) by two-fold (see Figure 6.2A for a heat map of the top 15 most differentially abundant lipids, ranked by *p*-values derived from independent samples *t*-tests; Figure 6.3). Among home cage control rats, immunization with *M. vaccae* NCTC 11659 decreased the abundance of a number of primary and secondary bile acids, including the primary bile acid chenodeoxycholic acid (CDCA), and the secondary bile acids

deoxycholic acid (DCA) and ursodeoxycholic acid (UDCA) (Figure 6.3). Among home cage control rats, immunization with *M. vaccae* NCTC 11659 decreased the abundance of several eicosanoids, including prostaglandin B1 (PGB1), prostaglandin B2 (PGB2), and 11-hydroxyeicosatetraenoic acid (HETE) by two-fold (Figure 6.2A; Figure 6.3; Figure 6.4). Finally, among home cage control rats, immunization with *M. vaccae* NCTC 11659 decreased the abundance of the n-3 fatty acid-derived specialized proresolving lipid mediator (±)18-hydroxyeicosapentaenoic acid (HEPE) (Figure 6.4).

Independent samples *t*-tests using FDR-adjusted $p < 0.1$ found that there were no lipids whose abundance in plasma was significantly altered by *M. vaccae* NCTC 11659. Overall, data suggest that bile acid metabolism, including primary and secondary bile acid biosynthesis, and fatty acid metabolism pathways may have been altered by immunization with *M. vaccae* NCTC 11659 (Supplementary Table 6.2). Lipids altered by *M. vaccae* NCTC 11659 are highlighted in bile acid and fatty acid metabolism pathways depicted in Figure 6.5A.

M. vaccae ATCC 15483

Fold change analysis revealed that, among home cage control rats, immunization with *M. vaccae* ATCC 15483 increased the abundance of eicosatetraenoic acid (5Z,8Z,11Z,14Z-eicosatetraenoic acid; also known as arachidonic acid), as well as the n-3 fatty acids, eicosapentaenoic acid (EPA), and (7Z,10Z,13Z,16Z,19Z)-docosa-7,10,13,16,19-pentaenoic acid (also known as n-3 DPA) by two fold (see Figure 6.2B for a heat map of the top 15 most differentially abundant lipids; Figure 6.4). Among home cage control rats, immunization with *M. vaccae* ATCC 15483, like immunization with *M. vaccae* NCTC 11659, decreased the abundance of the secondary bile

acid UDCA (Figure 6.2B; Figure 6.3). Finally, among home cage control rats, immunization with *M. vaccae* 15483 decreased the abundance of the arachidonic acid-derived eicosanoid 11-HETE by two-fold (Figure 6.2B; Figure 6.4). Independent samples *t*-tests using FDR-adjusted $p < 0.1$ found that there were no lipids whose abundance in plasma was significantly altered by *M. vaccae* ATCC 15483. Lipids altered by *M. vaccae* ATCC 15483 are highlighted in fatty acid metabolism pathways depicted in Figure 6.5A (see also Supplementary Table 6.2).

6.4.3 Effects of stress on the plasma lipidome of vehicle-treated rats

Fold change analysis revealed that, among BBS-treated rats, IS increased the abundance of arachidonic acid by two-fold (see Figure 6.2C for a heat map of the top 15 lipids; Figure 6.4). IS decreased the abundance of tetradecanoylcarnitine (acyl-C14) and the arachidonic acid-derived eicosanoid 11-HETE by two-fold (Figure 6.2C; Figure 6.4). However, independent samples *t*-tests using FDR-adjusted $p < 0.1$ found that there were no lipids whose abundances in plasma were significantly altered by IS. Lipids altered by IS are highlighted in the arachidonic acid metabolism pathway depicted in Figure 6.5B (see also Supplementary Table 6.2). IS-induced changes to arachidonic acid metabolism among vehicle-treated rats may be associated with the development of anxiety-like behaviors 24 hours after IS exposure in these same rats (see Loupy et al., 2021 for behavioral assessment).

6.4.4 Effects of stress, relative to home cage control conditions, on the plasma lipidome of rats preimmunized with M. vaccae NCTC 11659 or M. vaccae ATCC 15483

Considering the stress-resilience behavioral effects of both *M. vaccae* strains (Loupy et al., 2021), we next sought to determine metabolites and pathways altered by IS among rats immunized by *M. vaccae* NCTC 11659 or *M. vaccae* ATCC 15483.

Effects of stress, relative to home case control conditions, on the plasma metabolome of rats immunized with M. vaccae NCTC 11659

Among rats immunized with *M. vaccae* NCTC 11659, IS increased the abundance of the primary bile acids CDCA and DCA, and the secondary bile acid UDCA by two-fold (see Figure 6.2D for a heat map of the top 15 most differentially abundant lipids; Figure 6.3; Figure 6.5C). Among rats immunized with *M. vaccae* NCTC 11659, IS increased the abundance of the eicosanoid PGB1 (Figure 6.2D; Figure 6.4; Figure 6.5C). Among rats immunized with *M. vaccae* NCTC 11659, IS decreased the abundance of the acylcarnitine acyl-C14by two-fold (Figure 6.2D; Figure 6.4; Figure 6.5C).

Independent samples *t*-tests found that, among rats immunized with *M. vaccae* NCTC 11659, IS decreased the abundance of acyl-C14 ($t = 4.18$; FDR-adjusted $p < 0.05$) (Figure 6.2D; Figure 6.4; Figure 6.5C). Prior immunization with *M. vaccae* NCTC 11659 prevented the stress-induced increase of arachidonic acid and the stress-induced decrease of the arachidonic acid-derived eicosanoid 11-HETE (Figure 6.4; Figure 6.5B). Overall, data suggest that primary and secondary bile acid biosynthesis pathways may have been altered by IS among rats immunized with *M. vaccae* NCTC 11659, as depicted in Figure 6.5C (see also Supplementary Table 6.2).

Effects of stress, relative to home case control conditions, on the plasma metabolome of rats immunized with M. vaccae ATCC 15483

Among rats immunized with *M. vaccae* ATCC 15483, IS did not increase the abundance of any lipids in the plasma by two-fold, but IS decreased the abundance of the acylcarnitine acyl-C14 by two-fold (see Figure 6.2E for a heat map of the top 15 most differentially abundant lipids; Figure 6.4; Figure 6.5C).

Independent samples *t*-tests using FDR-adjusted $p < 0.1$ found that, among rats immunized with *M. vaccae* ATCC 15483, there were no lipids whose abundance in plasma was significantly altered by IS. Prior immunization with *M. vaccae* ATCC 15483, like immunization with *M. vaccae* NCTC 11659, prevented the stress-induced increase of arachidonic acid and the stress-induced decrease of the arachidonic acid-derived eicosanoid 11-HETE (Figure 6.4; Figure 6.5B).

6.4.5 Effects of immunization with M. vaccae NCTC 11659 or M. vaccae ATCC 15483, relative to BBS-treated animals, on the plasma lipidome of rats exposed to IS

Considering the stress-resilience behavioral effects of both *M. vaccae* strains (Loupy et al., 2021), we next sought to determine metabolites and pathways altered by *M. vaccae* NCTC 11659 or *M. vaccae* ATCC 15483 among rats exposed to IS.

Effects of immunization with M. vaccae NCTC 11659, relative to BBS-treated animals, on the plasma lipidome of rats exposed to IS

Fold change analysis revealed that, among rats exposed to IS, prior immunization with *M. vaccae* NCTC 11659 increased the abundance of the primary bile acids DCA and TCDCA acid by two-fold (Figure 6.3; Supplementary Table 6.3). There were no lipids whose abundance was decreased by two-fold among IS-exposed animals preimmunized with *M. vaccae* NCTC 11659. Additionally, independent samples *t*-tests using FDR-adjusted $p < 0.1$ found that there were no

lipids whose abundances in plasma were significantly altered by previous immunization with *M. vaccae* NCTC 11659 24 hours after IS.

Effects of immunization with M. vaccae ATCC 15483, relative to BBS-treated animals, on the plasma lipidome of rats exposed to IS

Fold change analysis revealed that, among rats exposed to IS, prior immunization with *M. vaccae* ATCC 15483 increased the abundance of the eicosanoids, prostaglandin E2 (PGE2), 13,14-dihydro-15-keto Prostaglandin D2 (PGD2), 13,14-dihydro-15-keto PGE2, and the n-3 polyunsaturated fatty acid derivative 18-HEPE by two-fold (Figure 6.4; Supplementary Figure 6.1; Supplementary Table 6.3). There were no lipids whose abundance was decreased by two-fold among IS-exposed animals immunized with *M. vaccae* ATCC 15483. Additionally, independent samples *t*-tests using FDR-adjusted $p < 0.1$ found that there were no lipids whose abundances in plasma were significantly altered by previous immunization with *M. vaccae* ATCC 15483 24 hours after IS.

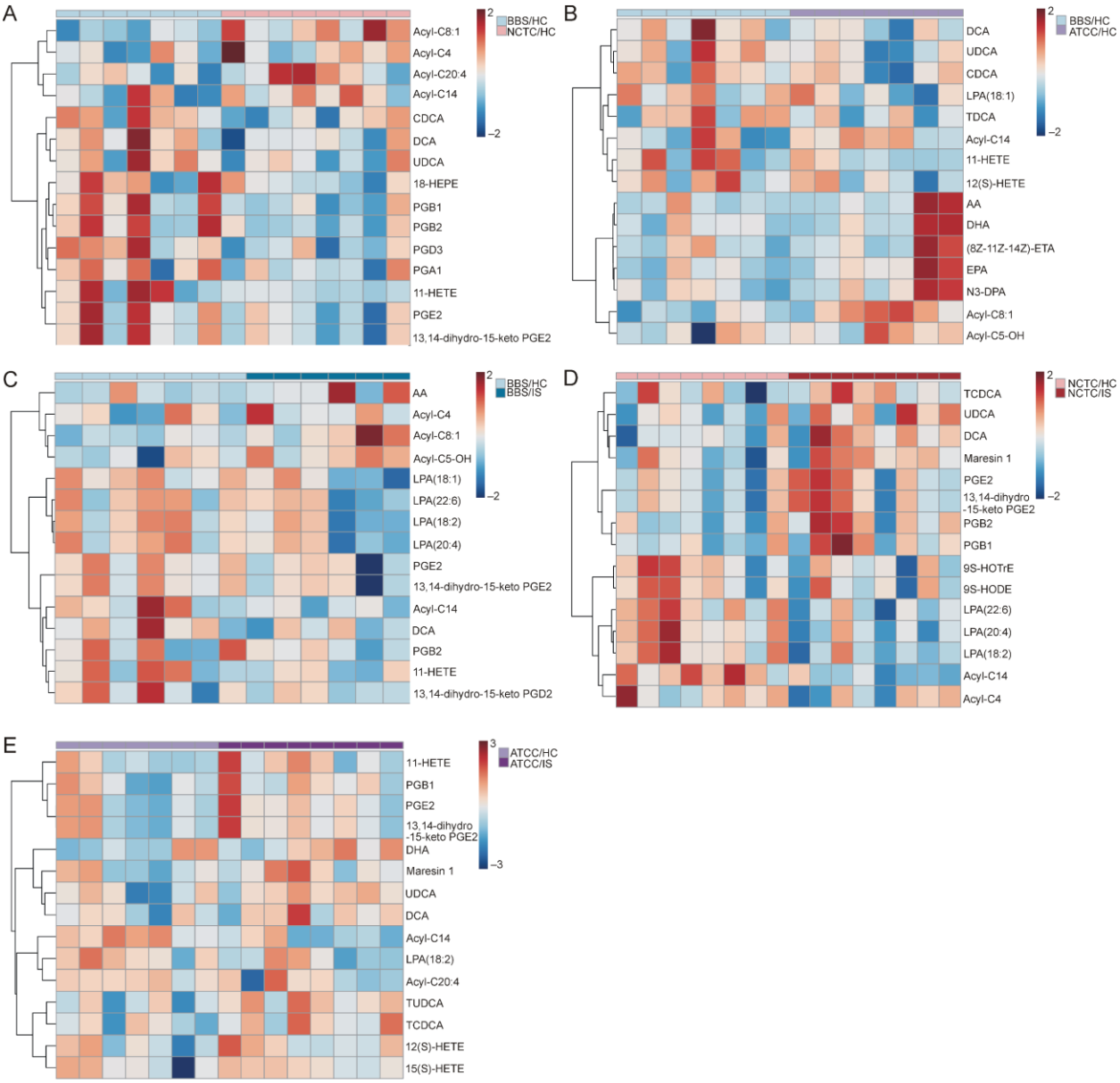

Figure 6.2 Effects of immunization with either *M. vaccae* NCTC 11659 or *M. vaccae* ATCC 15483 and inescapable tail shock stress (IS) on the plasma lipidome of adult male rats.

Each panel depicts a clustered heat map between individual pairwise comparisons, the range of color depicting a scale relative to the normalized abundance of lipids: (A) immunization with *M. vaccae* NCTC 11659 versus BBS among home cage control (HC) rats; (B) immunization with *M. vaccae* ATCC 15483 versus BBS among HC rats; (C) IS versus HC among BBS-treated rats; (D) IS versus HC among rats immunized with *M. vaccae* NCTC 11659; (E) IS versus HC among rats immunized with *M. vaccae* ATCC 15483. Heat maps show the top 15 most differentially abundant metabolites across each sample, ranked by independent samples *t*-tests, clustered hierarchically using Ward's method with Euclidian distances (dendrogram trees shown to the left of each heat map). Abbreviations: AA, arachidonic acid; Acyl-C4, butanoylcarnitine; Acyl C8:1,

octenoylcarnitine; Acyl-C14, tetradecanoylcarnitine; Acyl-C20:4, arachidonoylcarnitine; ATCC, *M. vaccae* ATCC 15483; arachidonic, arachidonic acid; BBS, borate-buffered saline; CDCA, chenodeoxycholic acid; DCA, deoxycholic acid; DHA, docosahexaenoic acid; DPA, docosapentaenoic acid; EPA, eicosapentaenoic acid; ETA, eicosatrienoic acid; HC, home cage control; HEPE, hydroxyeicosapentaenoic acid; HETE, hydroxyeicosatetraenoic acid; HODE, hydroxyoctadecadienoic acid; HOTrE, hydroxy-10E,12Z,15Z-octadecatrienoic acid; IS, inescapable tail shock stress; LPA, lysophosphatidic acid; n-3, omega-3; NCTC, *M. vaccae* NCTC 11659; PGA1, prostaglandin A1; PGB1, prostaglandin B1; PGB2, prostaglandin B2; PGD3, prostaglandin D3; PGE2, prostaglandin E2; TCDCA, taurochenodeoxycholic acid; TDCA, taurodeoxycholic acid; TUDCA, tauroursodeoxycholic acid; UDCA, ursodeoxycholic acid.

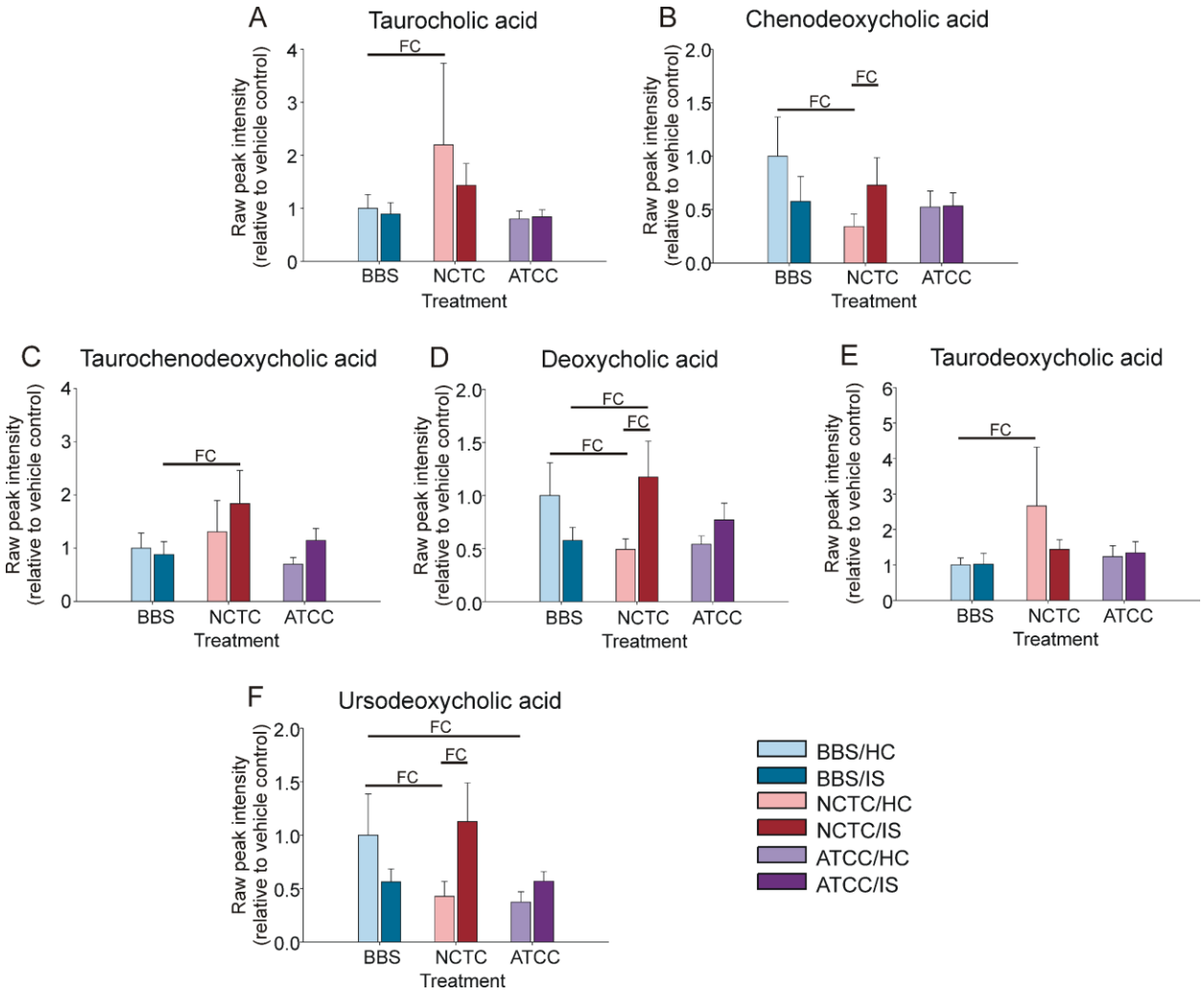

Figure 6.3 Effects of immunization with either *M. vaccae* NCTC 11659 (NCTC) or *M. vaccae* ATCC 15483 (ATCC) and inescapable tail shock stress (IS) on unconjugated primary bile acids (i.e., chenodeoxycholic acid), conjugated primary bile acids (taurocholic acid, taurochenodeoxycholic acid), unconjugated secondary bile acids

(deoxycholic acid, ursodeoxycholic acid), and conjugated secondary bile acids (taurodeoxycholic acid) in the plasma.

Data represent the mean + standard error of the mean (SEM) of raw peak intensities, relative to the vehicle control group (BBS/HC), of primary bile acids (A) taurocholic acid, (B) chenodeoxycholic acid, and (C) taurochenodeoxycholic acid and secondary bile acids (D) deoxycholic acid, (E) taurodeoxycholic acid, and (F) ursodeoxycholic acid. Sample sizes: BBS/HC, $n = 7$; BBS/IS, $n = 6$; NCTC/HC, $n = 8$; NCTC/IS, $n = 8$; ATCC/HC, $n = 7$; ATCC/IS, $n = 8$. Fold change analysis and independent samples *t*-tests were run on each of the lipids targeted in the plasma. FC, fold change difference. Abbreviations: ATCC, *M. vaccae* ATCC 15483; BBS, borate-buffered saline; HC, home cage control conditions; IS, inescapable tail shock stress; NCTC, *M. vaccae* NCTC 11659.

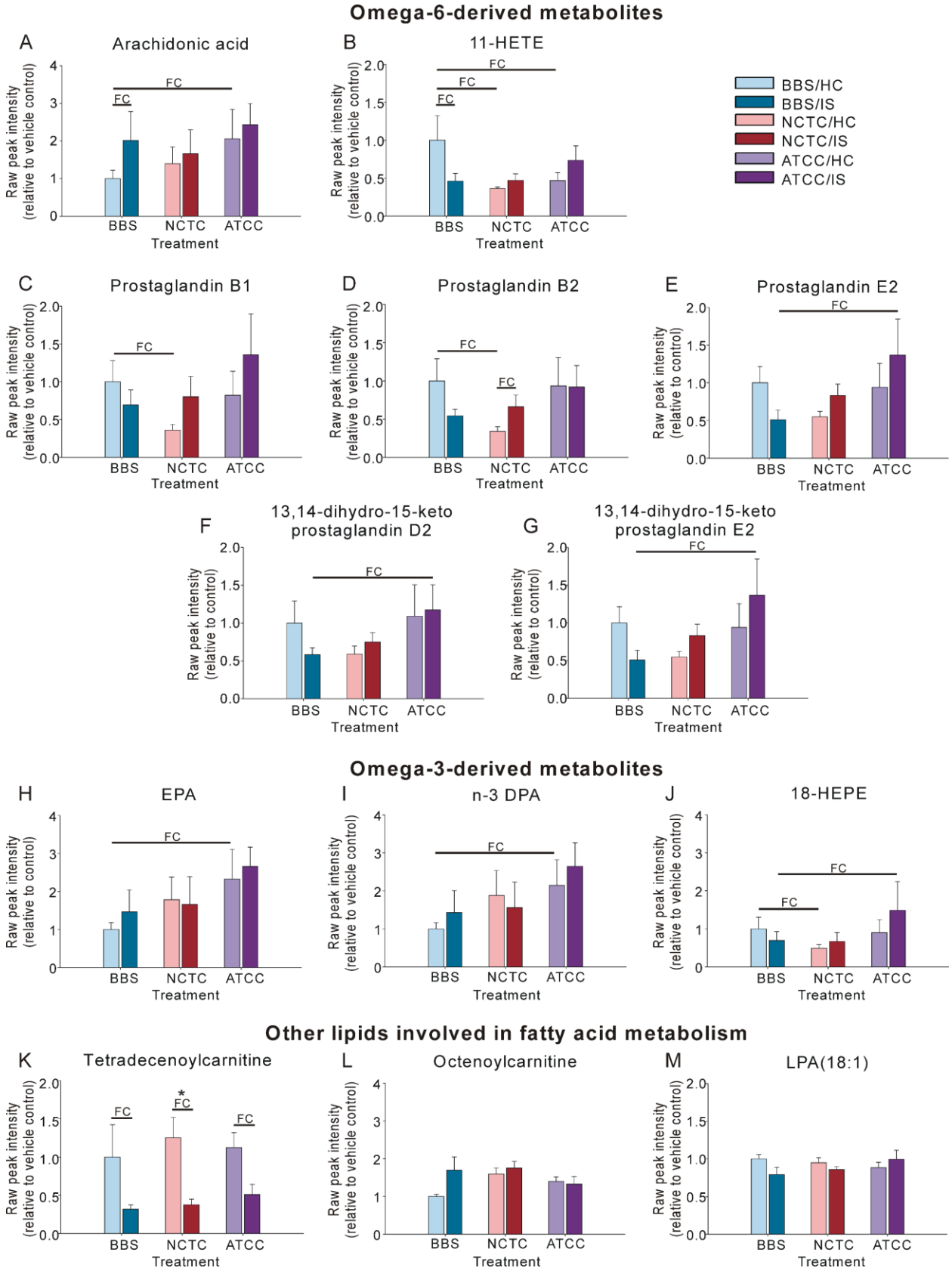
Omega-6-derived metabolites
A
Arachidonic acid
B
11-HETE
BBS/HC
BBS/IS
NCTC/HC
NCTC/IS
ATCC/HC
ATCC/IS
C
Prostaglandin B1
D
Prostaglandin B2
E
Prostaglandin E2
F
13,14-dihydro-15-keto prostaglandin D2
G
13,14-dihydro-15-keto prostaglandin E2
Omega-3-derived metabolites
H
EPA
I
n-3 DPA
J
18-HEPE
Other lipids involved in fatty acid metabolism
K
Tetradecenoylcarnitine
L
Octenoylcarnitine
M
LPA(18:1)
Raw peak intensity (relative to vehicle control)
Raw peak intensity (relative to control)
FC
*
BBS
NCTC
ATCC
Treatment

Figure 6.4 Effects of immunization with either *M. vaccae* NCTC 11659 (NCTC) or *M. vaccae* ATCC 15483 (ATCC) and inescapable tail shock stress (IS) on lipids associated with fatty acid metabolism in the plasma.

Data represent the mean + standard error of the mean (SEM) of raw peak intensities, relative to the vehicle control group (BBS/HC), of omega-6 fatty acid-derived (A) arachidonic acid, (B) 11-HETE, (C) prostaglandin B1, (D) prostaglandin B2, (E) prostaglandin E2, (F) 13,14-dihydro-15-keto prostaglandin D2, and (G) 13,14-dihydro-15-keto prostaglandin D2; omega-3 fatty acid-derived (H) EPA, (I) n-3 DPA, and (J) 18-HEPE; and other lipids involved in fatty acid metabolism, including (K) tetradecanoylcarnitine (acyl-C14), (L) octenoylcarnitine (acyl-C8:1), and (M) lysophosphatidic acid (LPA)(18:1). Sample sizes: BBS/HC, $n = 7$; BBS/IS, $n = 6$; NCTC/HC, $n = 8$; NCTC/IS, $n = 8$; ATCC/HC, $n = 7$; ATCC/IS, $n = 8$. Fold change analysis and independent samples *t*-tests were run on each of the lipids targeted in the plasma. FC, fold change difference. $*p < 0.05$; FDR-adjusted *p*-value. Abbreviations: ATCC, *M. vaccae* ATCC 15483; BBS, borate-buffered saline; DPA, docosapentaenoic acid; EPA, eicosapentaenoic acid; HC, home cage control conditions; HEPE, hydroxyeicosapentaenoic acid; HETE, hydroxyeicosatetraenoic acid; IS, inescapable tail shock stress; LPA, lysophosphatidic acid; n-3, omega-3; NCTC, *M. vaccae* NCTC 11659.

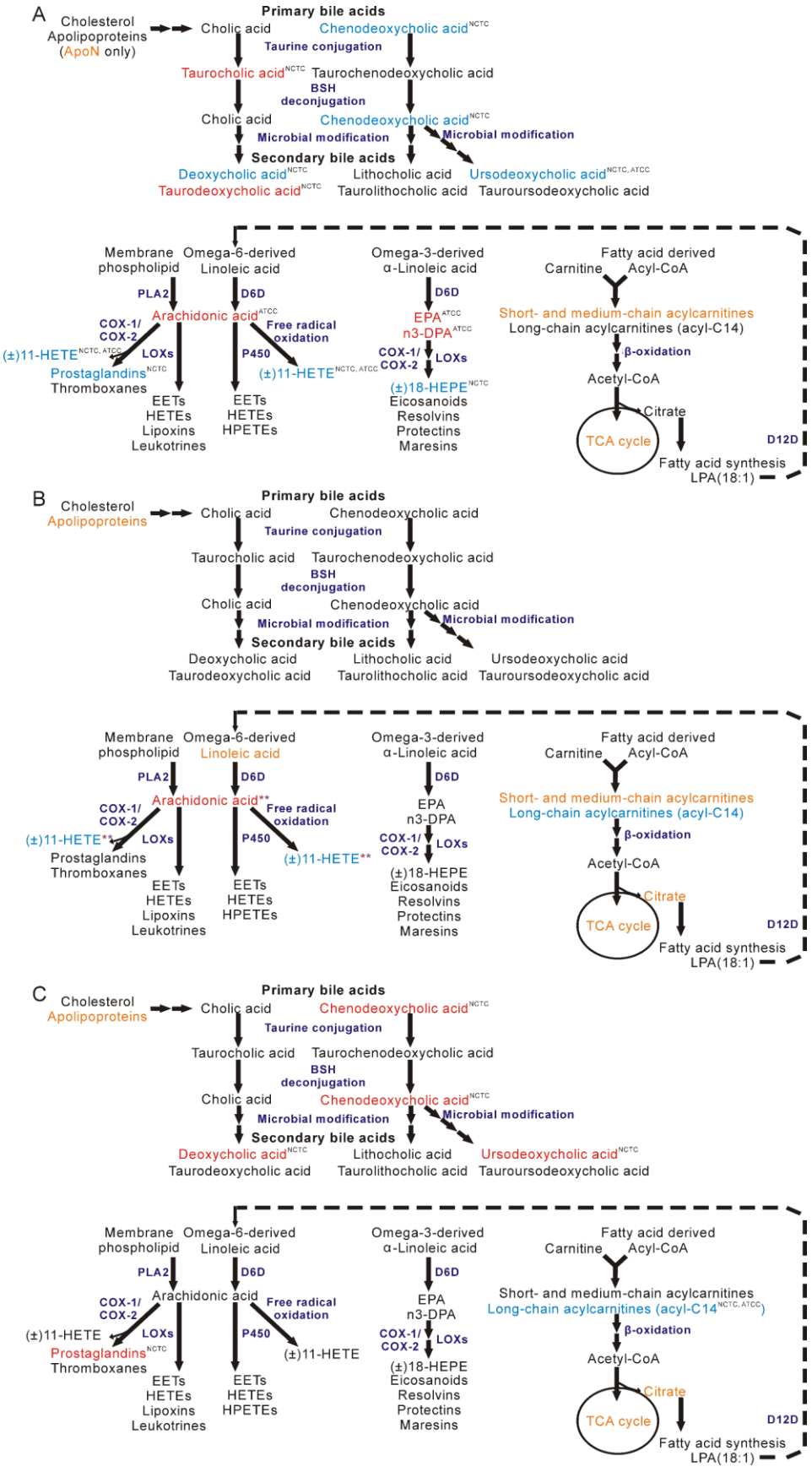
A
Cholesterol
Apolipoproteins
(ApoN only)
Primary bile acids
Cholic acid
Chenodeoxycholic acid NCTC
Taurine conjugation
Taurocholic acid NCTC
Taurochenodeoxycholic acid
BSH
deconjugation
Cholic acid
Chenodeoxycholic acid NCTC
Microbial modification
Microbial modification
Secondary bile acids
Deoxycholic acid NCTC
Taurodeoxycholic acid NCTC
Lithocholic acid
Taurolithocholic acid
Ursodeoxycholic acid NCTC, ATCC
Tauroursodeoxycholic acid
Membrane phospholipid
Omega-6-derived
Linoleic acid
PLA2
D6D
Arachidonic acid ATCC
COX-1/
COX-2
Free radical
oxidation
(±)11-HETE NCTC, ATCC
LOXs
P450
Prostaglandins NCTC
Thromboxanes
(±)11-HETE NCTC, ATCC
EETs
HETEs
Lipoxins
Leukotrines
EETs
HETEs
HPETEs
Omega-3-derived
α-Linoleic acid
D6D
EPA ATCC
n3-DPA ATCC
COX-1/
COX-2
LOXs
(±)18-HEPE NCTC
Eicosanoids
Resolvins
Protectins
Maresins
Fatty acid derived
Carnitine
Acyl-CoA
Short- and medium-chain acylcarnitines
Long-chain acylcarnitines (acyl-C14)
β-oxidation
Acetyl-CoA
Citrate
TCA cycle
D12D
Fatty acid synthesis
LPA(18:1)
B
Cholesterol
Apolipoproteins
Primary bile acids
Cholic acid
Chenodeoxycholic acid
Taurine conjugation
Taurocholic acid
Taurochenodeoxycholic acid
BSH
deconjugation
Cholic acid
Chenodeoxycholic acid
Microbial modification
Microbial modification
Secondary bile acids
Deoxycholic acid
Taurodeoxycholic acid
Lithocholic acid
Taurolithocholic acid
Ursodeoxycholic acid
Tauroursodeoxycholic acid
Membrane phospholipid
Omega-6-derived
Linoleic acid
PLA2
D6D
Arachidonic acid**
COX-1/
COX-2
Free radical
oxidation
(±)11-HETE**
LOXs
P450
Prostaglandins
Thromboxanes
(±)11-HETE**
EETs
HETEs
Lipoxins
Leukotrines
EETs
HETEs
HPETEs
Omega-3-derived
α-Linoleic acid
D6D
EPA
n3-DPA
COX-1/
COX-2
LOXs
(±)18-HEPE
Eicosanoids
Resolvins
Protectins
Maresins
Fatty acid derived
Carnitine
Acyl-CoA
Short- and medium-chain acylcarnitines
Long-chain acylcarnitines (acyl-C14)
β-oxidation
Acetyl-CoA
Citrate
TCA cycle
D12D
Fatty acid synthesis
LPA(18:1)
C
Cholesterol
Apolipoproteins
Primary bile acids
Cholic acid
Chenodeoxycholic acid NCTC
Taurine conjugation
Taurocholic acid
Taurochenodeoxycholic acid
BSH
deconjugation
Cholic acid
Chenodeoxycholic acid NCTC
Microbial modification
Microbial modification
Secondary bile acids
Deoxycholic acid NCTC
Taurodeoxycholic acid
Lithocholic acid
Taurolithocholic acid
Ursodeoxycholic acid NCTC
Tauroursodeoxycholic acid
Membrane phospholipid
Omega-6-derived
Linoleic acid
PLA2
D6D
Arachidonic acid
COX-1/
COX-2
Free radical
oxidation
(±)11-HETE
LOXs
P450
Prostaglandins NCTC
Thromboxanes
(±)11-HETE
EETs
HETEs
Lipoxins
Leukotrines
EETs
HETEs
HPETEs
Omega-3-derived
α-Linoleic acid
D6D
EPA
n3-DPA
COX-1/
COX-2
LOXs
(±)18-HEPE
Eicosanoids
Resolvins
Protectins
Maresins
Fatty acid derived
Carnitine
Acyl-CoA
Short- and medium-chain acylcarnitines
Long-chain acylcarnitines (acyl-C14 NCTC, ATCC)
β-oxidation
Acetyl-CoA
Citrate
TCA cycle
D12D
Fatty acid synthesis
LPA(18:1)

Figure 6.5 Diagram showing effects of A) immunization with either *M. vaccae* NCTC 11659 or *M. vaccae* ATCC 15483 among home cage control rats, B) inescapable tail shock stress (IS) among BBS-treated rats, or C) IS among rats immunized with either *M. vaccae* strain on bile acid metabolism (upper pathway of each panel) and fatty acid metabolism (lower pathway of each panel).

Enzymatic processes and enzymes are labeled purple. Red colored lipids are upregulated, while blue colored lipids are downregulated. In panel A and C, superscripts on either red or blue colored lipids indicate whether the effect followed immunization with *M. vaccae* NCTC 11659 (NCTC), *M. vaccae* ATCC 15483 (ATCC), or both (NCTC, ATCC). Orange colored metabolites are those that were altered in previous studies by *M. vaccae* strains, IS, or both. Abbreviations: ATCC, *M. vaccae* ATCC 15483; BSH, bile salt hydrolase; CoA, coenzyme A; COX-1, cyclooxygenase 1; COX-2, cyclooxygenase 2; DPA, docosapentaenoic acid; D6D, delta-6-desaturase; EET, epoxyeicosatrienoic acid; EPA, eicosapentaenoic acid; HEPE, hydroxyeicosapentaenoic acid; HETE, hydroxyeicosatetraenoic acid; HPETE, hydroperoxyeicosatetraenoic acid; IS, inescapable tail shock stress; LOXs, lipoxygenases (primary LOXs of interest include 5-LOX, 12-LOX, and 15-LOX); LPA, lysophosphatidic acid; NCTC, *M. vaccae* NCTC 11659; PLA2, phospholipase A2; P450, cytochrome P450; TCA, tricarboxylic acid.

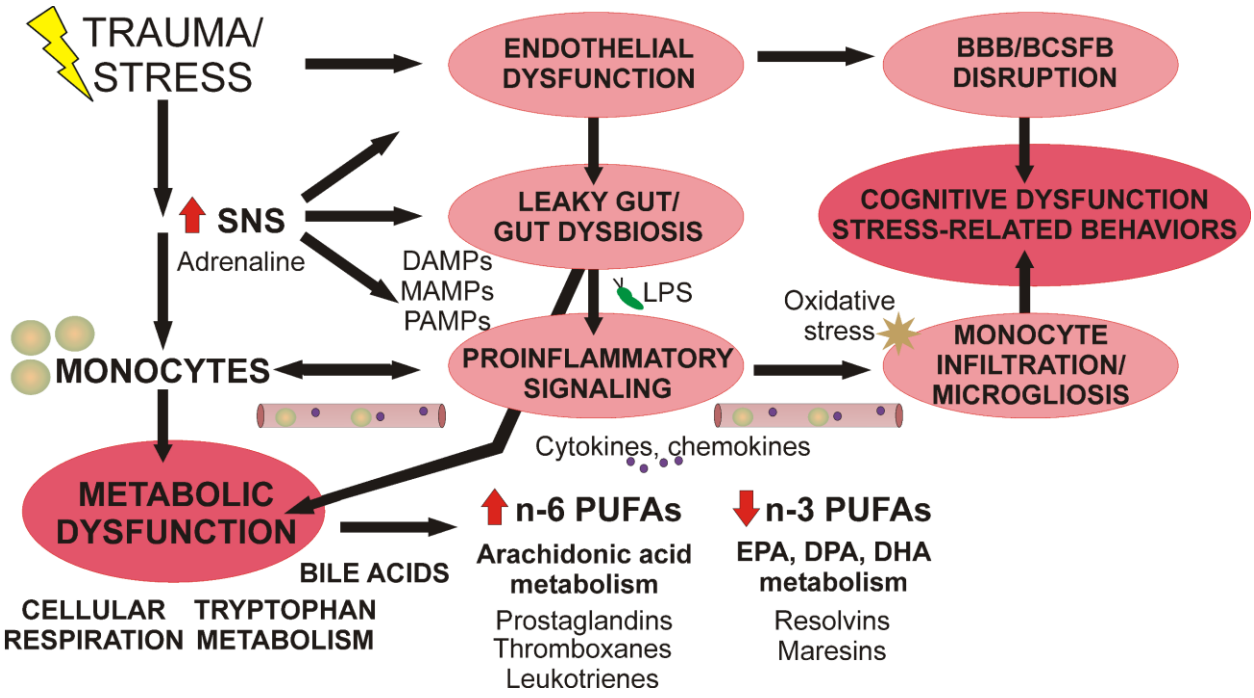

Figure 6.6 Summary figure of trauma- and stress-related pathophysiology.

Trauma leads to microbiome dysbiosis and sympathetic nervous system (SNS)-induced mobilization of monocytes from the bone marrow, leading to proinflammatory signaling that is associated with vascular endothelial dysfunction, disruption of gut and blood-central nervous system barriers, and metabolic dysfunction. Our data suggest that immunization with *M. vaccae* strains prevents prolonged activation of SNS 24 hours after inescapable tail shock stress (IS) and attenuates stress-related biological signatures of stress described here, including the arachidonic

cascade associated with synthesis of proinflammatory lipids. Abbreviations: BBB, blood-brain barrier; BCSFB, blood-cerebrospinal fluid barrier; DAMPs, damage-associated molecular patterns; LPS, lipopolysaccharide; MAMPs, microbe-associated molecular patterns; n-3, omega-3; n-6, omega-6; PAMPs, pathogen-associated molecular patterns; PUFAs, polyunsaturated fatty acids; SNS, sympathetic nervous system.

6.5 Discussion

Exposure to IS increased plasma concentrations of the omega-6 free fatty acid, arachidonic acid, the precursor of proinflammatory eicosanoid lipid signaling molecules, and decreased the pro-resolving and anti-inflammatory lipid mediator, 11-HETE assessed 24 h after IS exposure; in both cases, these IS-induced effects were prevented by immunization with *M. vaccae* NCTC 11659 or *M. vaccae* ATCC 15483. Immunization with *M. vaccae* NCTC 11659 decreased a number of proinflammatory eicosanoids, including PGB1, PGB2, and 18-HEPE in home cage control animals. In addition, *M. vaccae* ATCC 15483, and to a lesser extent *M. vaccae* NCTC 11659, increased anti-inflammatory n-3 fatty acids among home cage control animals, indicating a shift away from n-6 or toward n-3 fatty acid metabolism among rats immunized with *M. vaccae* strains. Although immunization with either *M. vaccae* NCTC 11659 or *M. vaccae* ATCC 15483 prevented IS-induced changes to arachidonic acid metabolism, immunization with either *M. vaccae* strain did not prevent the stress-induced decrease of acyl-C14, a biomarker of fatty acid oxidation. Collectively, these data suggest that immunization with individual *M. vaccae* strains may uniquely influence the plasma lipidome, but that the effects of both strains may converge on specific lipid metabolism pathways associated with stress resilience.

6.5.1 Effects of M. vaccae NCTC 11659 or M. vaccae ATCC 15483 on the plasma lipidome of home cage control rats: focus on bile acid, omega-3 fatty acid, arachidonic acid, and eicosanoid metabolism

Overall, *M. vaccae* NCTC 11659 and *M. vaccae* ATCC 15483 altered bile acid, n-3 free fatty acid, arachidonic acid, and prostaglandin metabolism in a manner consistent with a pro-resolving or anti-inflammatory immunophenotype.

6.5.2 Effects of M. vaccae NCTC 11659 or M. vaccae ATCC 15483 on bile acid metabolism

Among home cage control animals, the plasma lipidome of animals immunized with *M. vaccae* NCTC 11659 exhibited altered abundances of plasma bile acids. In particular, the plasma abundances of the bile acids TCA and TDCA were prominently and distinguishably increased only among home cage control animals immunized with *M. vaccae* NCTC 11659, as assessed eight days following the final immunization. In contrast, among home cage control animals, immunization with *M. vaccae* NCTC 11659 decreased CDCA, DCA, and UDCA. TCA is a primary bile acid—cholic acid conjugated with taurine—and called a bile salt, produced in the liver. Bile salts are released into the small intestine to enhance lipid solubility, digestion, and absorption, and are actively reabsorbed from the small intestine into the blood (for review, see Ridlon et al., 2006). Bacteria of the gut can then deconjugate and dehydroxylate primary bile salts to secondary bile acids. TDCA is a taurine-conjugated secondary bile acid, synthesized from its precursor, cholic acid. In humans, Firmicutes are well-described producers of DCA in the gut (for review, see Ridlon et al., 2014, 2006). In our study, DCA was decreased in plasma while TDCA was increased eight days following the final immunization with *M. vaccae* NCTC 11659. This might be because conjugated bile acids such as TDCA are more efficiently transported across the ileum into the blood, contributing a greater amount to the recycled bile acid pool (for review, see Dawson and Karpen, 2015; Ramírez-Pérez et al., 2017; Ridlon et al., 2006). Alternatively, unconjugated bile acids may be absorbed and re-conjugated during

transport back to the liver (for review, see Hofmann, 1999). Conjugated bile acids are more soluble at acidic pH levels (Hofmann, 1999), they are less hydrophobic and thereby less toxic to gut microbiota (Hofmann, 1999; Ridlon et al., 2006) and they are taken back up into the liver more effectively than unconjugated bile acids (Suga et al., 2017). Conjugated bile acids may also be less inflammatory due to their decreased cytotoxicity (Li et al., 2017). For example, taurocholic acid has anti-inflammatory and immunoregulatory effects on leukocytes (Talebian et al., 2020; Wang et al., 2013). While immunization with *M. vaccae* NCTC 11659 increased TDCA among home cage control rats, immunization with *M. vaccae* NCTC 11659 decreased DCA, a proinflammatory bile acid that, upon accumulation, can contribute to gut dysbiosis (Xu et al., 2021).

Bacteria associated with the *Clostridium* cluster XIVa, including bacteria from the class Clostridia and genera *Clostridium*, *Eubacterium*, *Ruminococcus*, *Coprococcus*, *Lachnospira*, *Butyrivibrio*, *Anaerostipes*, and *Roseburia* (Lopetuso et al., 2013; Van Den Abbeele et al., 2013) dehydroxylate cholic acid to produce deoxycholic acid in the gut, which can then be conjugated to produce TDCA (Ridlon et al., 2014). Bacteria of the *Clostridium* cluster XIVa readily colonize the mucin layer of the intestinal environment and are known to produce the beneficial short-chain fatty acid butyrate, as observed in an in vitro model called the mucosal-simulator of human intestinal microbial ecosystem (M-SHIME), which stimulates microbiota samples with bile salt-containing pancreatic juice (Van Den Abbeele et al., 2013). Recently, using a targeted metabolomics approach, we found that the abundance of butyrate in plasma tended to increase among home cage control rats immunized with *M. vaccae* NCTC 11659 (see part I of this article). We also recently showed that immunization with *M. vaccae* NCTC 11659 alters the

composition of the gut microbiome and stabilizes the microbial profile in both a model of chronic psychosocial stress (Reber et al., 2016b) and a “two hit” stressor model of chronic disruption of sleep rhythms (CDR) and chronic social defeat (Foxx et al., 2021). It could be that immunization with *M. vaccae* NCTC 11659 alters the gut microbial composition, contributing to increases of plasma butyrate and the secondary bile acid, TDCA.

How exactly treatment with *M. vaccae* NCTC 11659 might alter the gut microbiome is unknown, but it might be through activation of the immune system (Fonken et al., 2018; Frank et al., 2018; Loupy et al., 2021; Reber et al., 2016; Smith et al., 2019; Smith et al., 2020), chemical or neural communication with the gut barrier (Loupy, unpublished data) (see also part I of this article), or possibly bile acid production. Indeed, the upregulation of cholic acid metabolites and the downregulation of CDCA metabolites might reflect microbial-driven or host feedback regulation of bile acid synthesis and cholesterol metabolism; different bile acids and their conjugations will differentially influence the binding and activation of the farnesoid X receptor (FXR) and liver X receptor (LXR) (for review, see Chiang, 2002; Ridlon et al., 2006). Bile acids also act as signaling molecules that modulate metabolic signaling pathways, energy homeostasis, and hormone synthesis and release from a variety of tissues by binding to G protein-coupled bile acid receptor-1 (GPBAR-1, also called TGR5) in a variety of tissues and cell types, including macrophages (for review, see Di Ciaula et al., 2017).

6.5.3 Effects of M. vaccae NCTC 11659 or M. vaccae ATCC 15483 on anti-inflammatory omega-3 fatty acid metabolism

Immunization with *M. vaccae* ATCC 15483 increased the anti-inflammatory n-3 fatty acids EPA and DPA. Immunization with *M. vaccae* NCTC 11659 also tended to increase EPA (*M. vaccae*

NCTC 11659/BBS fold change fold change = 1.78) and n-3 DPA (*M. vaccae* NCTC 11659/BBS fold change fold change = 1.89), although these results were not significant based on fold change or independent *t*-test analyses. Immunization with *M. vaccae* ATCC 15483 tended to increase docosahexaenoic acid (DHA) among home cage control rats, based on the top 15 most differentially abundant lipids; upon further analysis, DHA tended to increase in plasma of rats immunized with *M. vaccae* NCTC 11659 (*M. vaccae* NCTC 11659/BBS fold change fold change = 1.80) or *M. vaccae* ATCC 15483 (*M. vaccae* ATCC 15483/BBS fold change fold change = 1.83), although these results were not significant based on fold change or independent *t*-test analyses. Diets rich in EPA have been shown to prevent stress-induced anxiety-like (Oshima et al., 2018) and depressive-like (Peng et al., 2020) behaviors in rats. These effects may be mediated by immunoregulatory effects that are stimulated by EPA. For example, diets high in EPA induce the activation of regulatory T cells (Treg) in epididymal adipose tissue of mice, mediated via adipose tissue-resident macrophages (Onodera et al., 2017). We have previously shown that preimmunization with a free-fatty acid isolated from *M. vaccae* NCTC 11659 activates the PPARα signaling pathway in isolated peritoneal murine macrophages, shifting the macrophages toward an anti-inflammatory phenotype with reduced secretion of IL-6 following LPS administration. EPA activates both PPARα (for review, see Grygiel-Górniak, 2014; Zúñiga et al., 2011) and PPARγ (Magee et al., 2012; Song et al., 2017; Sumiyoshi et al., 2015) pathways, and high dose EPA treatment reduces LPS-induced secretion of IL-6 from cultured RAW 264.7 macrophages (Honda et al., 2015). Our current data might support the idea that *M. vaccae* strains alternatively activate monocytic cells among home cage control rats, which help to reduce proinflammatory responses upon exposure to IS (Loupy, unpublished data) (see also part I of this article). These data are consistent with the hypothesis that *M. vaccae* NCTC 11569

and *M. vaccae* ATCC 15483 increase anti-inflammatory n-3 fatty acids, promoting anti-inflammatory resolvin and protectin signaling (Suneson et al., 2021).

6.5.4 Effects of M. vaccae NCTC 11659 or M. vaccae ATCC 15483 on inflammatory mediators associated with arachidonic acid and eicosanoid metabolism

As mentioned above, using a machine learning approach, eicosanoids were among the highest ranked features, when assessed pre-deployment, at predicting provisional diagnosis of PTSD 90-180 days following deployment among active military personnel (Schultebraucks et al., 2020). Eicosanoids are signaling molecules made by the enzymatic or non-enzymatic oxidation of arachidonic acid or other polyunsaturated fatty acids (PUFAs) that are, like arachidonic acid, 20 carbons in length. Eicosanoids include prostanoids, cyclopentenone prostaglandins, HETEs and oxo-ETEs, leukotrienes, lipoxins and epi-lipoxins, eoxins, and epoxyeicosanoids. In the current study, exposure to vehicle-treated rats responded to IS with increases in arachidonic acid. In contrast, rats previously immunized with *M. vaccae* NCTC 11659 or *M. vaccae* ATCC 15483 failed to respond to IS with increased arachidonic acid. Thus, *M. vaccae* strains may have buffered against the IS-induced increases in arachidonic acid metabolism observed among vehicle-treated animals. These convergent effects of *M. vaccae* strains might be indicative of alternative activation of immune cell types, such as monocyte-derived macrophages, in the blood.

Among home cage control rats, immunization with *M. vaccae* NCTC 11659 decreased abundance of specific eisocanoids, including plasma PGB1 and PGB2 (a metabolite of PGE2) by two-fold and tended to decrease PGE2 (*M. vaccae* NCTC 11659/BBS fold change = 0.55),

although this effect was not significant based on fold change or independent samples *t*-test analyses. Also among home cage control rats, although immunization with *M. vaccae* ATCC 15483 increased arachidonic acid, immunization with either *M. vaccae* NCTC 11659 or *M. vaccae* ATCC 15483 decreased the abundance of 11-HETE. Prostaglandins and 11-HETE are both produced from arachidonic acid via COX-1 and COX-2 pathways (Bailey et al., 1983; Tejera et al., 2012; Xiao et al., 1997), while 11-HETE can also be produced by free radical oxidation of arachidonic acid (Guido et al., 1993; Pickens et al., 2019; Shishehbor et al., 2006). In other words, 11-HETE is a non-enzymatically arachidonic acid-derived proinflammatory oxylipid that is a marker of lipid peroxidation (Guido et al., 1993; Pickens et al., 2017). However, recent findings also suggest that immunization with either *M. vaccae* strain increases plasma markers of antioxidant activity among home cage control rats, and these antioxidant effects might contribute to reduced 11-HETE production (see part I of this article).

Changes to the abundances of arachidonic acid metabolites in plasma may reflect an important modification in specific cell types that occurs among home cage control animals immunized with *M. vaccae* strains. Patrolling macrophages in the blood may be a major source of n-6 and n-3 fatty acid synthesis and oxidation (for review, see Batista-Gonzalez et al., 2020; Funk, 2001; Ménégaut et al., 2019; Montenegro-Burke et al., 2016; Norris and Dennis, 2014), and their metabolism of fatty acids increase upon differentiation from monocytes (Wallner et al., 2014); decreases of n-6 fatty acid metabolites (exhibited among animals immunized with *M. vaccae* NCTC 11659) or increases of n-3 metabolites (exhibited among animals immunized with *M. vaccae* ATCC 15483) might indicate a shift toward M2-like macrophages (Batista-Gonzalez et al., 2020; Funk, 2001; Ménégaut et al., 2019; Montenegro-Burke et al., 2016).

We observed that, among home cage control rats, *M. vaccae* ATCC 15483 increased arachidonic acid, and *M. vaccae* NCTC 11659 tended to do the same. Although both *M. vaccae* NCTC 11659 and *M. vaccae* ATCC 15483, under baseline, non-stressed conditions, generally appear to have anti-inflammatory and immunoregulatory properties, one exception is that, particularly well documented in the case of *M. vaccae* NCTC 11569, exposure to mycobacteria induces the canonical Th1 cytokine, IFNγ. For example, studies in humans have shown that a single intradermal injection of *M. vaccae* NCTC 11659 increases serum IFNγ one month after injection (Dlugovitzky et al., 1999), as well as antigen-stimulated IFNγ secretion from freshly isolated peripheral blood mononuclear cells one month, but not three months, following injection (Hadley et al., 2005). Consistent with these findings, in persons with moderate to advanced tuberculosis, oral administration of *M. vaccae* NCTC given on day 1, then on days 7, 14, 21, 28, 42, 56, 84, 112, and 140 increases IFNγ secretion from freshly isolated and cultured blood polymorphonuclear and mononuclear cells when tested at 2 months and 4 months (Dlugovitzky et al., 2010). This increase in IFNγ in response to *M. vaccae* NCTC 11659 and, potentially, other mycobacteria (Zhang et al., 2016), may explain some of the effects, among home cage control rats, of *M. vaccae* NCTC 11659 and *M. vaccae* ATCC 15483 on arachidonic acid. Indeed, IFNγ has been shown to induce the synthesis and prolonged activation of cytosolic phospholipase A_2 (PLA_2) (Hamilton et al., 1985; Višnjić et al., 1997; Wu et al., 1994). Despite the fact that *M. vaccae* NCTC 11659 induces a chronic increase in IFNγ under home cage control conditions, it prevents stress-induced increases in IFNγ, which coincides with the findings reported here that both *M. vaccae* NCTC 11659 and *M. vaccae* ATCC 15483 prevented stress-induced increases in arachidonic acid.

Arachidonic acid may be produced by linoleic acid metabolism, or it may be formed by the action of PLA_2 on phospholipids, cleaving phospholipids into 1) arachidonic acid (free fatty acid) and 2) lysophospholipid (the remaining component). We previously mentioned that increases of arachidonic acid among home cage control rats immunized with *M. vaccae* ATCC 15483 might be due to the action of PLA_2. Although this is the first study to demonstrate an effect of *M. vaccae* ATCC 15483 on arachidonic acid abundance in plasma, we recently demonstrated that immunization with *M. vaccae* NCTC 11659 increases plasma lysophospholipids (Foxx et al., 2021). Of interest, *M. vaccae* NCTC 11659 tended to increase lysophosphocholine (22:6) (Foxx et al., 2021). Together, our data argue that PLA_2 activity is increased with treatment of a heat-killed mycobacterial preparation. PLA_2 activity and arachidonic acid secretion is also increased in macrophages infected with *M. tuberculosis* (Duan et al., 2001; Vandal et al., 2006), and in one study investigating humans infected with *M. tuberculosis*, lysophospholipids were more abundant in plasma of persons who were infected with *M. tuberculosis* than those who were not (Collins et al., 2018). It may very well be that the effects of *M. vaccae* strains on monocyte/macrophage metabolism are generalizable to many different species of mycobacteria, and this hypothesis should be investigated in detail in future experiments.

One important finding is that *M. vaccae* ATCC 15483, and to a lesser extent *M. vaccae* NCTC 11659, increased anti-inflammatory n-3 fatty acids, also produced by PLA_2 activity (Chang et al., 2009), among home cage control animals. In the current study, altered plasma n-3 fatty acid metabolism among *M. vaccae*-treated animals might be an indication that metabolically activated

macrophages are secreting anti-inflammatory lipids into the circulation (Batista-Gonzalez et al., 2020; Ménégaut et al., 2019). Although macrophages are prolific synthesizers of n-3 fatty acids and their metabolites (Ménégaut et al., 2019; Wallner et al., 2014), it is also the case that these fatty acid metabolites can act on macrophages to shift their activity toward an M2 phenotype (Onodera et al., 2017). Alternatively activated macrophages may play a major role buffering against proinflammatory signaling during stress (Furuyashiki et al., 2019; C. Li et al., 2020; Mosser et al., 2020). In comparison to the plasma lipidome of BBS-treated rats, the plasma lipidome of rats immunized with either *M. vaccae* strain (given decreased prostaglandins and increased n-3 fatty acids) reflects enhanced anti-inflammatory signaling, tissue repair, and pro-resolving immune cell types, including M2 macrophages. It will be important for future studies to elucidate inflammation resolution time scales for immunizations with *M. vaccae* strains over the course of three weeks as well as inflammation resolution time scales for IS.

Immunization with *M. vaccae* NCTC 11659 or *M. vaccae* ATCC 15483 differentially altered the plasma lipidome of home cage control rats eight days following the final injection, where immunization with *M. vaccae* NCTC 11659 more often altered the abundance of bile acids and prostaglandins while immunization with *M. vacace* ATCC 15483 more often altered the abundance of polyunsaturated fatty acids. In plasma of home cage control animals immunized with *M. vaccae* NCTC 11659, the abundance of PGB1 and PGB2 were decreased by two-fold, while PGE2 tended to decrease in the plasma. Prostaglandins are well-studied markers of inflammation, particularly PGE2 (for review, see Ricciotti and Fitzgerald, 2011); prostaglandins are synthesized from arachidonic acid by cyclooxygenase isoenzymes 1 and 2 (COX-1 and COX-2, respectively), and increased production of PGE2 is commonly associated with

proinflammatory signaling described in stress-related psychiatric disorders and neurodegenerative diseases (Ricciotti and Fitzgerald, 2011). PGB1 and PGB2 are catabolic products of PGE1 and PGE2, respectively (for review, see Holdcroft, 1975). Non-steroidal anti-inflammatory drugs (NSAIDs) work by inhibiting COX-1 and COX-2, thereby inhibiting the production of prostaglandins among other eicosanoids, reducing neuroinflammation, and concomitantly reducing the risk of developing anxiety and depression (Hu et al., 2020; Müller, 2019) as well as dementias like Alzheimer's disease (Zhang et al., 2018); however, it should be noted that different NSAIDs work better in some contexts rather than others for reasons not yet known (Hu et al., 2020; Zhang et al., 2018). Considering that immunization with *M. vaccae* NCTC 11659: 1) promotes stress-resilient behaviors (Amoroso et al., 2020; Bowers et al., 2020; Fonken et al., 2018; Fox et al., 2017; Foxx et al., 2021; Frank et al., 2018b; Hassell et al., 2019; Loupy et al., 2021, 2020, 2018; Lowry et al., 2007; Reber et al., 2016b; Siebler et al., 2018; Smith et al., 2020); 2) decreases stress-related inflammatory processes in both the periphery and the brain (Fonken et al., 2018; Frank et al., 2018b; Loupy et al., 2021; Reber et al., 2016b); 3) prevents inflammation-related cognitive dysfunction in male rodents (Fonken et al., 2018; Foxx et al., 2021); and 4) may promote a physiological phenotype that is more resilient to the development of Alzheimer's disease (Loupy et al., 2020), our current data, showing that *M. vaccae* NCTC 11659 tended to decrease the plasma abundance of a number of COX-1 and COX-2 metabolites among home cage control rats, would support the hypothesis that immunization with *M. vaccae* NCTC 11659 induces an anti-inflammatory signature in part by inhibiting the expression or activity of COX-1 and COX-2.

It should be noted that immunization with *M. vaccae* NCTC 11659 also decreased the abundance of 18-HEPE by two-fold. 18-HEPE is produced by the action of 5-lipoxygenase (5-LOX) on the n-3 fatty acid EPA and is associated with inflammation resolution mechanisms of anti-inflammatory, alternatively-activated (M2) macrophages (for review, see Serhan and Levy, 2018). However, the enzyme 5-LOX is also responsible for metabolizing arachidonic acid to leukotrienes, which were not measured in this study. It is possible that immunization with *M. vaccae* NCTC 11659 inhibited the expression or activity of both COX-1/COX-2 and 5-LOX. Dual inhibitors of COX-2 and 5-LOX are thought to be safer and more effective than conventional COX-2 inhibitors by preventing vascular permeability and gastrointestinal damage during inflammation (Jacob et al., 2018; Martel-Pelletier et al., 2003).

6.5.5 Strain-specific effects of M. vaccae NCTC 11659 and M. vaccae ATCC 15483 on the plasma lipidome of home cage control rats

Together, our findings suggest that the two individual *M. vaccae* strains might differ in their biological effects on the host plasma lipidome; interestingly, differential effects of the two strains appear to be most notable in the current plasma lipidome dataset, rather than plasma proteome (Loupy, unpublished data) or plasma metabolome datasets (see part I of this article).

Different mycobacterial strains produce differential immunological (for review, see Tientcheu et al., 2017; Yuksel et al., 2011) and metabolic (Collins et al., 2018; for review, see Gago et al., 2018; Howard and Khader, 2020; Koo et al., 2012; Vrieling et al., 2020) responses in the host, including differential immunological and metabolic effects within monocytic cells (Gago et al., 2018; Koo et al., 2012; Vrieling et al., 2020; Yuksel et al., 2011). It is thought that mycobacterial strains may produce their differential effects via the unique composition of lipids and

phospholipids located on their bacterial cell walls (Collins et al., 2018; Gago et al., 2018; Koo et al., 2012). In our current study, both mycobacterial strains were heat-inactivated and thus were not viable to participate in metabolic processes. Their biological effects are likely mediated by a complex interaction of metabolites (including lipids) that are located on the outer cell envelope that participate in binding to immune cell receptors; it is also possible that bioactive metabolites that are located within the cytoplasmic space of these cells are released upon immune cell-mediated phagocytosis and engage in host immunometabolism. Future experiments should compare the metabolomic and lipidomic profiles of whole, heat-inactivated *M. vaccae* NCTC 11659 to those of whole, heat-inactivated *M. vaccae* ATCC 15483 to identify distinct bioactive molecules that might contribute to divergent effects of these mycobacterial strains on the plasma lipidome.

6.5.6 Effects of IS on lipid metabolism

Notably, our data suggest that there may have been a reduction of plasma bile acids among vehicle-treated rats 24 hours after IS (for an overview of stress-related pathophysiology, see Figure 6.6). Among BBS-treated rats, IS tended to decrease the primary bile acid CDCA (IS/HC fold change = 0.58), and IS tended to decrease the secondary bile acids DCA (IS/HC fold change = 0.58) and UDCA (IS/HC fold change = 0.56), although these results were not significant based on fold change analysis or independent samples *t*-tests. These effects paralleled the effects of immunization with *M. vaccae* NCTC 11659 among home cage control animals; however, one striking difference is that IS did not increase the abundance of any conjugated bile acids like immunization with *M. vaccae* NCTC 11659 did. Rather than a shift in bile acid conjugation, IS may have induced a general decrease in bile acid production, secretion, or reabsorption among

BBS-treated animals. Increased SNS activity, as exhibited in BBS-treated rats 24 hours following IS (see part I of this article), can decrease bile acid secretion (Beckh and Arnold, 1991). Bile acid metabolism may also be influenced by the composition of gut microbiota and may be altered by microbial dysbiosis (M. Yu et al., 2017). In a study using the chronic intermittent restraint stress paradigm, it was found that stress simultaneously increases bile acid excretion in feces and disrupts intestinal reabsorption of bile acids (Silvennoinen et al., 2015). An important consideration is that food consumption was not measured following exposure to IS, and long-term fasting (72 hours) has been shown to reduce bile salt synthesis and secretion in rats (Dumaswala et al., 1994).

Exposure to IS altered fatty acid metabolism assessed 24 hours later; these stress-induced changes to the plasma lipidome among vehicle-treated rats are associated with the development of anxiety-like behaviors in these same rats (see Loupy et al., 2021).. We found that, among BBS-treated rats, IS increased plasma arachidonic acid. Bone-marrow derived monocytes/macrophages and tissue-resident macrophages contain large amounts of arachidonic acid in their cellular membranes (Gil-de-Gómez et al., 2020; Sorgi et al., 2017). It could be the case that phospholipid remodeling or arachidonic acid metabolism may be altered in phagocytic cells like monocytes/macrophages (Gil-de-Gómez et al., 2020); in activated macrophages, altered arachidonic acid metabolism might be caused by changes to the availability of its precursor metabolite, linoleic acid, or changes to the expression or activity of enzymes involved in the synthesis or metabolism of arachidonic acid. For example, stress has been shown to alter the abundance of both linoleic acid and arachidonic acid in peripheral tissues (Mills et al., 1994; Williams et al., 1992). We previously showed that linoleic acid is increased in plasma 24 hours

after IS only among BBS-treated animals but not among animals previously immunized with *M. vaccae* strains (see part I of this article). These findings might suggest that increases in the abundance of arachidonic acid among vehicle-treated rats 24 hours after IS are partially due to increases of linoleic acid. However, among BBS-treated rats, IS decreased the abundance of the arachidonic acid-derived metabolite 11-HETE, and furthermore, IS tended to decrease PGB2 (IS/HC fold change = 0.54) and PGE2 (IS/HC fold change = 0.51), although these results were not significant based on fold change or independent *t*-test analyses. The finding that PGE tended to decrease 24 hours after IS was surprising considering both psychological stress and proinflammatory mediators can increase activity of COX-2, production of prostaglandins, and secretion of PGE2 from macrophages (Furuyashiki and Narumiya, 2011; Umamaheswaran et al., 2018); however, as a negative feedback mechanism, PGE2 can reduce COX-2 expression in macrophages (Tang et al., 2017). It may be the case that, 24 hours after IS, some inflammation-resolving mechanisms are taking shape to reduce the secretion of prostaglandins in the plasma.

It is important to point out that arachidonic acid metabolism also readily occurs in endothelial cells, which may be injured after IS. PLA_2 activity is increased in and arachidonic acid is secreted from vascular endothelial cells following stimulation with noradrenaline (Labelle and Polyak, 1998). In part I of this article, we found that adrenaline was increased 24 hours after IS in BBS-treated animals only, and we hypothesized that noradrenaline (not measured in the study) might also be increased. We also recently reported that IS induced proteomic markers of vascular endothelial dysfunction in plasma and CSF of the same BBS-treated rats used in the current study (Loupy, unpublished data). It is possible that, in our study, the abundance of arachidonic acid may be altered by a variety of different cell types; future studies should investigate which

cell types are responsible for changes to plasma metabolites and lipids, and accordingly, which cell types may be protected by immunization with *M. vaccae* strains.

Interestingly, IS decreased plasma acyl-C14 regardless of pretreatment. Acyl-C14 is a long-chain acylcarnitine involved in the first step of fatty acid β-oxidation (for review, see Jones and Bennett, 2017). Among BBS-treated animals, our results would suggest that decreased plasma acyl-C14 is due to increased β-oxidation, considering that short-chain and medium-chain acyl-carnitines, including the β-oxidation intermediary octanoylcarnitine (acyl-C8:1), were increased in plasma of BBS-treated rats 24 hours after IS (see part I of this article). Adrenaline and glucocorticoids released during the stress response promote the release of fatty acids for β-oxidation and cellular energy production (for review, see D'Attilio et al., 2018; Macfarlane et al., 2008). Very long-chain acyl-CoA dehydrogenase (VLCAD) is the enzyme responsible for catabolizing long-chain fatty acids containing 14-20 carbons in the first step of fatty acid oxidation, and thus acyl-C14 is increased in persons with VLCAD deficiency (Jones and Bennett, 2017; Li et al., 2015). VLCAD activity is altered in immune cells during inflammatory states, and its expression is increased in macrophages upon differentiation from monocytes (Wallner et al., 2014). It is thought that increases of arachidonic acid in monocyte-derived macrophages result from increased fatty acid oxidation and acyltransferase activity (Knottnerus et al., 2020; Kroner et al., 1981), which might also explain IS-induced increases of arachidonic acid among BBS-treated animals.

6.5.7 Effects of immunization with M. vaccae NCTC 11659 or M. vaccae ATCC 15483 on lipid metabolism among IS-exposed rats

Prior immunization with *M. vaccae* NCTC 11659 or *M. vaccae* ATCC 15483 prevented the IS-induced increase of arachidonic acid and IS-induced decrease of the arachidonic acid metabolite, 11-HETE. Immunization with *M. vaccae* ATCC 15843 increased plasma arachidonic acid among home cage control rats but immunization with either strain of *M. vaccae* prevented the IS-induced increase of arachidonic acid that was observed among vehicle-treated animals. Immunization with either *M. vaccae* NCTC 11659 or *M. vaccae* ATCC 15483 decreased plasma 11-HETE among home cage control rats but prevented the IS-induced decrease of 11-HETE that was observed among vehicle-treated animals. Furthermore, immunization with *M. vaccae* NCTC 11659 prevented IS-induced decreases of PGB2 and PGE2 that tended to occur among vehicle-treated animals. PGE2 and prostaglandin metabolites, 13,14-dihydro-15-keto PGD2 and 13,14-dihydro-15-keto PGE2, were increased only among rats previously immunized with *M. vaccae* ATCC 15483 compared to BBS-treated animals 24 hours after IS; this difference can be attributed to the IS-induced decreases of prostaglandins among BBS-treated rats, while prostaglandin abundance remained relatively stable among home cage control and IS-exposed rats immunized with *M. vaccae* ATCC 15483.

In addition, twenty-four hours after IS, EPA and n-3 DPA tended to be higher among rats previously immunized with *M. vaccae* ATCC 15483 but not those immunized with *M. vaccae* NCTC 11659, compared to BBS-treated animals. Similarly, 18-HEPE, an n-3 fatty acid metabolite released by macrophages (Endo et al., 2014), was increased in plasma of animals immunized with *M. vaccae* ATCC 15483 compared to BBS-treated animals 24 hours after IS. 18-HEPE is further metabolized to resolvin E1 and resolvin E2, two critical anti-inflammatory molecules involved in the inflammation resolution phase and tissue repair (Schwab et al., 2007;

Serhan and Levy, 2018). 18-HEPE-derived E-series resolvins can stimulate neutrophil phagocytosis (El Kebira et al., 2012; Herrera et al., 2015; Schwab et al., 2007) and inhibit polymorphonuclear leukocyte transendothelial migration into tissue (Arita et al., 2007; Serhan and Levy, 2018). In general, resolvins promote morphological shifts of macrophages toward M2 macrophage types (Kang and Lee, 2016; Schmid et al., 2016; Serhan and Levy, 2018). For example, 18-HEPE is secreted by bone marrow-derived macrophages to reduce inflammation after cardiac pressure overload in an in vivo transgenic model of n-3 fatty acid enrichment (Endo et al., 2014). In the current discussion, we hypothesize that changes to plasma n-3 and n-6 fatty acid metabolism among home cage control rats immunized with either strain of *M. vaccae* is largely a result of monocytic cell metabolism; collectively, our data might suggest that *M. vaccae* strains alternatively activate peripheral monocytes/macrophages under home cage control conditions, and that these effects help buffer against IS-induced changes to macrophage phenotypes and functions, including arachidonic acid metabolism.

Direct evidence for macrophage involvement comes from the observation that immunization with *M. vaccae* strains may have promoted an IS-induced increase of maresin 1 that was not observed among vehicle-treated animals (see Figure 6.2 for a heat map of the top 15 most differentially abundant lipids by pairwise comparison). Maresin 1 is an effective pro-resolving lipid that can induce macrophage conversion from M1 to M2 phenotype (Dalli et al., 2013; Marcon et al., 2013). Maresin 1 is also synthesized and released from *E.coli*-stimulated M2 macrophages (Werz et al., 2018) and can act as an anti-bacterial agent (C. W. Wang et al., 2016; Werz et al., 2018), including against *Mycobacterium tuberculosis* (Ruiz et al., 2019). Our data suggest that maresin 1 tended to increase after IS among animals immunized with either *M.*

vaccae NCTC 11659 (Figure 6.2D) or *M. vaccae* ATCC 15483 (Figure 6.2E) but not among animals treated with BBS (Figure 6.2B; Supplementary Figure 6.2), although these results were not significant based on fold change or independent *t*-test analyses. These findings might suggest that IS induced proinflammatory lipid signaling in plasma of BBS-treated rats and that immunization with either *M. vaccae* strain promoted an anti-inflammatory lipid profile that might be associated with an inflammation-resolving phenotype after IS. These results align with those of Wood and colleagues (2015), who showed that neuroinflammatory mediators are associated with active and passive coping strategies in response to social stress (Wood et al., 2015), and implicate peripheral mechanisms through which psychological stressors can signal to the central nervous system to control behavior. Immunization with *M. vaccae* strains may disrupt these peripheral mechanisms by promoting an anti-inflammatory peripheral immunophenotype after IS.

Although immunization with either *M. vaccae* NCTC 11659 or *M. vaccae* ATCC 15483 prevented IS-induced changes to metabolites involved in arachidonic acid metabolism, immunization with either *M. vaccae* strain did not prevent the stress-induced decrease of acyl-C14. VLCAD expression and activity is increased by PPARα agonists, a treatment commonly used for persons with VLCAD deficiency (Djouadi et al., 2005; Yang et al., 2016), and PPAR agonists may increase gene expression of the VLCAD enzyme in alternatively activated macrophages (Dai et al., 2017). Our data show that acyl-C14 was decreased after IS regardless of treatment, but that this decrease was most apparent and only statistically significant based on independent samples *t*-tests in rats previously immunized with *M. vaccae* NCTC 11659. Previous studies suggest that *M. vaccae* NCTC 11659 may activate macrophages through a PPARα

signaling pathway (Smith et al., 2019); it could be that PPAR signaling contributed to the increased fatty acid oxidation in plasma of rats immunized with *M. vaccae* NCTC 11659 and exposed to IS. In addition, increased plasma abundance of possible fatty acid oxidation substrates, namely n-6 and n-3 fatty acids, may be fueling the β-oxidation process among *M. vaccae*-treated animals. Fatty acid oxidation is also associated with increased oxidative stress; we recently found that IS decreased the relative abundance of glutathione peroxidase (GPx, matching isoforms 3, 5, and 6; GPx3/5/6), an antioxidant protein, in plasma regardless of pretreatment (Loupy, unpublished data). However, we reported that rats immunized with either *M. vaccae* strain may have had some antioxidant protection based on increased abundance of glutathione disulfide in the plasma, which may be mediated by PPAR signaling (for review, see Korbecki et al., 2019; Uppalapati et al., 2014).

IS only altered the abundance of prostaglandins and bile acids in plasma of animals immunized with *M. vaccae* NCTC 11659 but not *M. vaccae* ATCC 15483, further implicating strain-specific interactions with host physiology. All prostaglandins that decreased or tended to decrease among home cage control rats immunized with *M. vaccae* NCTC 11659 (i.e., PGB1, PGB2, and PGE2) tended to increase after IS among these animals, whereas, among BBS-treated rats, IS tended to decrease these prostaglandins. Similarly, all bile acids that were decreased by two-fold among home cage control rats immunized with *M. vaccae* NCTC 11659 (i.e., CDCA, DCA, and UDCA) were increased by two-fold after IS among these animals, whereas, among BBS-treated rats, IS tended to decrease these bile acids (CDCA [IS/HC fold change = 0.58]; DCA [IS/HC fold change = 0.58]; UDCA [IS/HC fold change = 0.56]). Additionally, TCDCA, a taurine-conjugated primary bile acid with anti-inflammatory properties (L. Li et al., 2018c), was

increased among rats immunized with *M. vaccae* NCTC 11659, relative to vehicle-treated rats, after exposure to IS. For the most part, prostaglandins and bile acids were unchanged after IS among animals immunized with *M. vaccae* ATCC 15483. The reason for these differences between *M. vaccae* strains is unknown, although it is possible that metabolites specific to *M. vaccae* NCTC 11659 can bind and activate bile-acid regulating receptors like FXR (Zhang et al., 2015). The LXR and retinoid-X-receptor (RXR) work in conjunction with FXR to mediate lipid metabolism, maintaining cholesterol and glucose homeostasis (for review, see Di Ciaula et al., 2017; Fiorucci et al., 2018; Han, 2018). Activated PPARs can form heterodimers with LXR and RXR to alter lipid metabolism and modulate bile acid synthesis (for review, see Chiang and Li, 2009; Kidani and Bensinger, 2012). We previously observed effects of *M. vaccae* strains on lipid-immune signaling in rats, but whether or not these effects are regulated by PPAR signaling is yet to be determined (Loupy et al., 2021, 2020). Bile acids can also activate additional nutrient-sensing receptors such as GPBAR-1 and vitamin D receptors (Di Ciaula et al., 2017; Duboc et al., 2014; Fiorucci et al., 2018). We recently reported that vitamin D binding protein was increased by IS only among rats immunized with *M. vaccae* NCTC 11659 (Loupy, unpublished data), and thus activation of vitamin D, possibly through alteration of bile acid secretion, might occur uniquely in animals immunized with the *M. vaccae* NCTC 11659 strain. Bile acids influence other aspects of the immune system, and they can act directly on macrophages via GPBAR-1 (Di Ciaula et al., 2017). GPBAR-1 is a dynamic receptor that initiates a variety of signaling cascades depending on the cell type that is expressing it; however, upon activation in macrophages, GPBAR-1 can reduce the LPS-induced expression of proinflammatory cytokines (Wammers et al., 2018). In fact, activation of GPBAR-1 appears to shift macrophage phenotypes from M1 to M2 (Biagioli et al., 2017; Wammers et al., 2018). The

apparent coordinated relationship between the altered abundance of bile acid metabolites and the altered abundance of macrophage-derived prostaglandins might suggest that macrophages are being activated by a specialized receptor linking lipid homeostasis with immune signaling, such as PPAR or possibly GPBAR-1, to shift their metabolic and immune phenotype. Although these types of receptors may be activated by either *M. vaccae* strain, our results reveal that bile acid and prostaglandin synthesis might be important metabolic-immune signaling biomarkers specific to *M. vaccae* NCTC 11659 immunizations.

6.5.8 Limitations

Our study is the first to demonstrate effects of IS on the plasma lipidome, and to demonstrate associations between the stress-resilient behavioral effects of *M. vaccae* strains with physiological effects on the plasma lipidome; however, there are limitations to our experimental design which should be considered for future experiments. It is important to point out that any functional associations of lipids are speculative in nature because we did not measure the activity of enzymes in specific pathways or conduct pulse-chase experiments to examine cellular processes over time. Likewise, although associations can be made between our plasma lipids and stress behaviors, our data do not establish direct causal relationships. Considering that our lipidomics analysis was targeted (limited to 47 lipids), we were unable to measure the abundance of all possible plasma lipids, and of particular interest, phosphatidylcholines; it will be important for future studies to follow up with an untargeted lipidomics approach in order to create more complete functional networks. This is especially important for the plasma lipidome, in which several physiological systems (i.e., immune, endocrine, neural, etc) may influence the abundance and function of plasma lipids. Future experiments should investigate ex vivo and in vitro models

to study individual organs and cell types that may contribute to the effects described in this paper. In addition, in our study the effects of immunization with *M. vaccae* NCTC 11569, *M. vaccae* ATCC 15483, and IS are restricted to a single time point of tissue collection, eight days following immunization with *M. vaccae* and 24 hours after stress; considering that our results may have been influenced by immune activation and resolution of inflammation (not measured here), future experiments should explore time-dependent changes on the plasma lipidome following final immunizations of *M. vaccae* strains and following IS. Another limitation of our study is that nutrition intake and physical activity were not monitored after *M. vaccae* immunizations or exposure to IS and may have been additional variables that contributed to an altered plasma lipidome. Also, our experiment was conducted only in adult male rats, and future studies should include female rats to determine if *M. vaccae* administration and/or IS may produce differential effects on the plasma lipidome dependent on sex. Similarly, immune response to *M. vaccae* strains may be altered in juvenile or aged rats, and future experiments should investigate these differences.

6.5.9 Conclusions

Collectively, these data suggest that immunization with individual *M. vaccae* strains may uniquely influence the plasma lipidome, but that the effects of both strains may converge on specific lipid metabolism pathways associated with stress resilience. However, our study revealed that rats immunized with either *M. vaccae* strain generally exhibited a plasma lipid profile akin to the inflammation-resolving metabolism of M2 macrophages by inhibiting COX-2 catabolism of arachidonic acid and increasing n-3 fatty acid metabolism toward the production of resolvins. Additional research is required to determine how each *M. vaccae* strain might induce

alternatively activated monocyte-derived macrophages, and if these macrophages are required to prevent stress-induced inflammation and anxiety-like behaviors. It will also be important to elucidate the role of bile acids and a possible role of the gut microbiome in the stress-resilience effects of *M. vaccae* strains, in particular *M. vaccae* NCTC 11659.

6.6 Acknowledgements, author contributions, and conflicts of interest

Acknowledgements

These studies were funded by the National Institute of Mental Health (NIMH) R21 grant (R21MH116263) awarded to C.A.L., S.F.M., M.G.F. (PIs), and L.K.F. (Co-I). J.A.R. and F.C., on behalf of the University of Colorado School of Medicine Metabolomics Core, a shared resource of the University of Colorado Cancer Center, acknowledge partial support from a National Institute of Health P30 Cancer Center Support Grant (P30CA046934).

Author Contributions

Study design was conceived by K.M.L., C.A.Z., and C.A.L. *M. vaccae* injections were performed by A.I.E., B.M.M., and C.A.Z. Inescapable tail shock and behavioral testing were conducted by H.M.D. Tissue collection for plasma was conducted by K.M.L, B.M.M., K.E.C., M.G.F., and C.A.Z. Metabolomics sample preparation was performed by K.M.L., F.C., J.A.R., and A.I.E. Mass spectrometry data acquisition and analysis were performed by C.F. and J.A.R. Data analysis and statistical analysis were carried out by K.M.L. and M.R.A. Figures and figure legends were produced by K.M.L. Manuscript preparation was conducted by K.M.L. Editing and review was contributed by K.M.L, C.F., J.A.R., A.I.E., B.M.M., L.K.F., M.G.F., C.A.Z., S.F.M., and C.A.L.

Conflicts of interest

CAL serves on the Scientific Advisory Board of Immodulon Therapeutics, Ltd, is Cofounder and Chief Scientific Officer of Mycobacterium Therapeutics Corporation, serves as an unpaid scientific consultant to Aurum Switzerland A.G., and is a member of the faculty of the Integrative Psychiatry Institute, Boulder, CO, USA.

Chapter 7. General discussion

7.1 Overview

Using behavioral, gene expression, and hypothesis-generating "omics" data, I have described the stress-resilience effects of immunization with a heat-killed preparation of either *Mycobacterium vaccae* NCTC 11659 or *Mycobacterium vaccae* ATCC 15483. First, I found that immunization with *M. vaccae* NCTC 11659 or *M. vaccae* ATCC 15483 prevents the stress-induced exaggeration of anxiety-like defensive behavioral responses in adult male rats 24 hours after inescapable tail shock stress (IS) using the juvenile social exploration (JSE) paradigm. Behavioral resilience was associated with the prevention of IS-induced increases of *Il6* mRNA expression in the dorsal hippocampus. In addition, I demonstrated that immunization with *M. vaccae* strains attenuated biological signatures of stress across the proteome, metabolome, and lipidome of these same rats. In the plasma proteome, immunization with *M. vaccae* strains protected rats from IS-induced increases of complement and coagulation signaling cascades, endothelial dysfunction, and monocyte/macrophage activation. In the CSF proteome, immunization with *M. vaccae* strains prevented IS-induced increases of proteins associated with proinflammatory responses in the CSF, likely by maintaining the vascular-CSF barriers and preventing the translocation of proinflammatory monocytes into the brain. In the plasma metabolome and lipidome, I found further evidence that immunization with *M. vaccae* strains prevents IS-induced alteration of monocyte/macrophage immunometabolism, most notably tryptophan metabolism and phospholipid metabolism (including omega-6) metabolism. Importantly, immunization with either strain of *M. vaccae* prevented IS-induced increases in biological markers of SNS activation and metabolites associated with energy expenditure. *M. vaccae* strains induced an anti-inflammatory immunophenotype in plasma, increasing omega-3

fatty acids and derivatives, while *M. vaccae* NCTC 11659 may have altered the gut microflora community structure or function as evidenced by changes to the plasma secondary bile acid pool. Collectively, my data demonstrate that the stress-resilience mechanisms of *M. vaccae* incorporate a multi-system framework that corroborates previously established hypotheses of anxiety disorders, affective disorders, and trauma and stressor-related disorders, such as PTSD. My studies reveal that stress-resilience may be associated with the ability to prevent proinflammatory bone marrow-derived monocyte/macrophage trafficking to the brain, either by preventing stress-induced release of monocytes or reprogramming monocytes/macrophages toward an anti-inflammatory, inflammation resolution phenotype.

7.2 Future directions

This dissertation provides evidence of specific pathways that contribute to stress-resilient behaviors; however, these data are observational in nature, and mechanistic studies are warranted. An initial experiment should examine the abundance of monocytes in blood 24 hours after IS in vehicle-treated rats and rats immunized with *M. vaccae* strains to reveal whether *M. vaccae* strains prevent IS-induced secretion of bone marrow-derived monocytes into the blood. It might also be interesting to utilize monocyte-specific knockout rodent models like CCR2-deficient mice, which show deficiencies in monocyte/macrophage trafficking (Kurihara et al., 1997; Tsou et al., 2007; Wohleb et al., 2013), to determine if monocytes are necessary to produce stress-related behaviors and pathophysiology after IS. To test if *M. vaccae* strains reduce SNS activity during or immediately following IS, direct measurements of sympathetic nerve activity and/or analyses of heart rate might be utilized (Stocker and Muntzel, 2013). To test if *M. vaccae* strains act via stimulation of the vagus nerve, studies should investigate the stress-resilience effects of *M. vaccae* strains with and without vagotomy. To test if immunization with

M. vaccae strains promotes stress resilience through the alternative activation or reprogramming of macrophages toward an inflammation resolution phenotype, it would be possible to utilize CD206-diptheria toxin receptor transgenic mice to deplete $CD206^+$ M2 macrophages prior to or immediately following immunization with *M. vaccae* strains (Kambara et al., 2015). Additional in vitro and ex vivo studies of monocyte-derived and resident macrophage cell types could help highlight the specific phenotypes (measuring gene expression, proteome, or metabolome) of cell types that confer anti-inflammatory effects and may be responsible for the large-scale "omics" changes as described in vivo in this dissertation. Furthermore, resident macrophages isolated from liver and adipose tissue should be analyzed to determine if there are widespread effects on immunometabolism and if resident macrophages from these tissue types also contribute to the effects observed in our current studies.

7.3 Conclusions

Research presented in this dissertation suggests that immunization with *M. vaccae* strains attenuates biological signatures of stress-induced proinflammatory bone marrow-derived monocytes trafficking from the periphery to the brain. Stress resilience may be achieved by preventing stress-induced proinflammatory signaling across a multi-system framework that includes monocyte trafficking, endothelial dysfunction, dysbiosis of the gut microbiome, and metabolic dysregulation.

References

Aaronson, S.T., Sears, P., Ruvuna, F., Bunker, M., Conway, C.R., Dougherty, D.D., Reimherr, F.W., Schwartz, T.L., Zajecka, J.M., 2017. A 5-year observational study of patients with treatment-resistant depression treated with vagus nerve stimulation or treatment as usual: Comparison of response, remission, and suicidality. Am. J. Psychiatry 174, 640–648. https://doi.org/10.1176/appi.ajp.2017.16010034

Abebe, F., 2012. Is interferon-gamma the right marker for bacille Calmette-Guérin-induced immune protection? The missing link in our understanding of tuberculosis immunology. Clin. Exp. Immunol. 169, 213–219. https://doi.org/10.1111/j.1365-2249.2012.04614.x

Abuawad, A., Mbadugha, C., Ghaemmaghami, A.M., Kim, D.H., 2020. Metabolic characterisation of THP-1 macrophage polarisation using LC–MS-based metabolite profiling. Metabolomics 16, 33. https://doi.org/10.1007/s11306-020-01656-4

Adamiak, M., Abdelbaset-Ismail, A., Suszynska, M., Abdel-Latif, A., Ratajczak, J., Ratajczak, M.Z., 2017. Novel evidence that the mannan-binding lectin pathway of complement activation plays a pivotal role in triggering mobilization of hematopoietic stem/progenitor cells by activation of both the complement and coagulation cascades. Leukemia 31, 262–265. https://doi.org/10.1038/leu.2016.278

Adams, V.C., Hunt, J.R.F., Martinelli, R., Palmer, R., Rook, G.A.W., Brunet, L.R., 2004. *Mycobacterium vaccae* induces a population of pulmonary CD11c $^{+}$ cells with regulatory potential in allergic mice. Eur. J. Immunol. 34, 631–638. https://doi.org/10.1002/eji.200324659

Afergan, E., Epstein, H., Dahan, R., Koroukhov, N., Rohekar, K., Danenberg, H.D., Golomb, G., 2008. Delivery of serotonin to the brain by monocytes following phagocytosis of liposomes. J. Control. Release 132, 84–90. https://doi.org/10.1016/j.jconrel.2008.08.017

Aguilar-Toalá, J.E., Garcia-Varela, R., Garcia, H.S., Mata-Haro, V., González-Córdova, A.F., Vallejo-Cordoba, B., Hernández-Mendoza, A., 2018. Postbiotics: an evolving term within the functional foods field. Trends Food Sci. Technol. 75, 105–114. https://doi.org/10.1016/J.TIFS.2018.03.009

Ahuja, V., Miller, S.E., Howell, D.N., 1995. Identification of two subpopulations of rat monocytes expressing disparate molecular forms and quantities of CD43. Cell. Immunol.

163, 59–69. https://doi.org/10.1006/cimm.1995.1099

Ait-Belgnaoui, A., Bradesi, S., Fioramonti, J., Theodorou, V., Bueno, L., 2005. Acute stress-induced hypersensitivity to colonic distension depends upon increase in paracellular permeability: Role of myosin light chain kinase. Pain 113, 141–147. https://doi.org/10.1016/j.pain.2004.10.002

Ait-Belgnaoui, A., Colom, A., Braniste, V., Ramalho, L., Marrot, A., Cartier, C., Houdeau, E., Theodorou, V., Tompkins, T., 2014. Probiotic gut effect prevents the chronic psychological stress-induced brain activity abnormality in mice. Neurogastroenterol. Motil. 26, 510–520. https://doi.org/10.1111/nmo.12295

Ait-Belgnaoui, A., Durand, H., Cartier, C., Chaumaz, G., Eutamene, H., Ferrier, L., Houdeau, E., Fioramonti, J., Bueno, L., Theodorou, V., 2012. Prevention of gut leakiness by a probiotic treatment leads to attenuated HPA response to an acute psychological stress in rats. Psychoneuroendocrinology 37, 1885–1895. https://doi.org/10.1016/J.PSYNEUEN.2012.03.024

Ait-Belgnaoui, A., Payard, I., Rolland, C., Harkat, C., Braniste, V., Théodorou, V., Tompkins, T.A., 2018. *Bifidobacterium longum* and *Lactobacillus helveticus* synergistically suppress stress-related visceral hypersensitivity through hypothalamic-pituitary-adrenal axis modulation. J. Neurogastroenterol. Motil. 24, 138–146. https://doi.org/10.5056/jnm16167

Al-Obaidi, M.M.J., Desa, M.N.M., 2018. Mechanisms of blood brain barrier disruption by different types of bacteria, and bacterial–host interactions facilitate the bacterial pathogen invading the brain. Cell. Mol. Neurobiol. 38, 1349–1368. https://doi.org/10.1007/s10571-018-0609-2

Alcaino, C., Knutson, K.R., Treichel, A.J., Yildiz, G., Strege, P.R., Linden, D.R., Li, J.H., Leiter, A.B., Szurszewski, J.H., Farrugia, G., Beyder, A., 2018. A population of gut epithelial enterochromaffin cells is mechanosensitive and requires Piezo2 to convert force into serotonin release. Proc. Natl. Acad. Sci. U. S. A. 115, E7632–E7641. https://doi.org/10.1073/pnas.1804938115

Allard, L., Burkhard, P.R., Lescuyer, P., Burgess, J.A., Walter, N., Hocnstrasser, D.F., Sanchez, J.C., 2005. PARK7 and nucleoside diphosphate kinase A as plasma markers for the early diagnosis of stroke. Clin. Chem. 51, 2043–2051. https://doi.org/10.1373/clinchem.2005.053942

Alsaigh, T., 2015. In vivo analysis of intestinal permeability following hemorrhagic shock . World J. Crit. Care Med. 4, 287. https://doi.org/10.5492/wjccm.v4.i4.287

Altschul, S.F., Madden, T.L., Schäffer, A.A., Zhang, J., Zhang, Z., Miller, W., Lipman, D.J., 1997. Gapped BLAST and PSI-BLAST: A new generation of protein database search programs. Nucleic Acids Res. 25, 3389–3402. https://doi.org/10.1093/nar/25.17.3389

Alves, V.S., Leite-Aguiar, R., Silva, J.P. da, Coutinho-Silva, R., Savio, L.E.B., 2020. Purinergic signaling in infectious diseases of the central nervous system. Brain. Behav. Immun. 89, 480–490. https://doi.org/10.1016/j.bbi.2020.07.026

Ambrée, O., Ruland, C., Zwanzger, P., Klotz, L., Baune, B.T., Arolt, V., Scheu, S., Alferink, J., 2019. Social defeat modulates T helper cell percentages in stress susceptible and resilient mice. Int. J. Mol. Sci. 20, 3512. https://doi.org/10.3390/ijms20143512

Ambrus, L., Westling, S., 2019. Inverse association between serum albumin and depressive symptoms among drug-free individuals with a recent suicide attempt. Nord. J. Psychiatry 73, 229–232. https://doi.org/10.1080/08039488.2019.1610056

American Psychiatric Association, 2013. Diagnostic and statistical manual of mental disorders (5th ed.). Arlington, VA: Author.

Amoroso, M., Böttcher, A., Lowry, C.A., Langgartner, D., Reber, S.O., 2020. Subcutaneous *Mycobacterium vaccae* promotes resilience in a mouse model of chronic psychosocial stress when administered prior to or during psychosocial stress. Brain. Behav. Immun. 87, 303–319. https://doi.org/10.1016/j.bbi.2019.12.018

Amoroso, M., Kempter, E., Eleslambouly, T., Lowry, C.A., Langgartner, D., Reber, S.O., 2019. Intranasal *Mycobacterium vaccae* administration prevents stress-induced aggravation of dextran sulfate sodium (DSS) colitis. Brain. Behav. Immun. 80, 595–604. https://doi.org/10.1016/j.bbi.2019.05.005

Arita, M., Ohira, T., Sun, Y.-P., Elangovan, S., Chiang, N., Serhan, C.N., 2007. Resolvin E1 selectively interacts with leukotriene B 4 receptor BLT1 and ChemR23 to regulate inflammation . J. Immunol. 178, 3912–3917. https://doi.org/10.4049/jimmunol.178.6.3912

Armenta, R.F., Walter, K.H., Geronimo-Hara, T.R., Porter, B., Stander, V.A., Leardmann, C.A., 2019. Longitudinal trajectories of comorbid PTSD and depression symptoms among U.S. service members and veterans. BMC Psychiatry 19, 396. https://doi.org/10.1186/s12888-019-2375-1

Arpaia, N., Campbell, C., Fan, X., Dikiy, S., van der Veeken, J., deRoos, P., Liu, H., Cross, J.R., Pfeffer, K., Coffer, P.J., Rudensky, A.Y., 2013. Metabolites produced by commensal bacteria promote peripheral regulatory T-cell generation. Nature 504, 451–455. https://doi.org/10.1038/nature12726

Arts, R.J.W., Carvalho, A., La Rocca, C., Palma, C., Rodrigues, F., Silvestre, R., Kleinnijenhuis, J., Lachmandas, E., Gonçalves, L.G., Belinha, A., Cunha, C., Oosting, M., Joosten, L.A.B., Matarese, G., van Crevel, R., Netea, M.G., 2016. Immunometabolic pathways in BCG-induced trained immunity. Cell Rep. 17, 2562–2571. https://doi.org/10.1016/j.celrep.2016.11.011

Atarashi, K., Tanoue, T., Ando, M., Kamada, N., Nagano, Y., Narushima, S., Suda, W., Imaoka, A., Setoyama, H., Nagamori, T., Ishikawa, E., Shima, T., Hara, T., Kado, S., Jinnohara, T., Ohno, H., Kondo, T., Toyooka, K., Watanabe, E., Yokoyama, S., Tokoro, S., Mori, H., Noguchi, Y., Morita, H., Ivanov, I.I., Sugiyama, T., Nuñez, G., Camp, J.G., Hattori, M., Umesaki, Y., Honda, K., 2015. Th17 cell induction by adhesion of microbes to intestinal epithelial cells. Cell 163, 367–380. https://doi.org/10.1016/j.cell.2015.08.058

Badawy, A.A.B., 2017. Kynurenine pathway of tryptophan metabolism: Regulatory and functional aspects. Int. J. Tryptophan Res. 10. https://doi.org/10.1177/1178646917691938

Badawy, A.A.B., Guillemin, G., 2019. The plasma [kynurenine]/[tryptophan] ratio and indoleamine 2,3-dioxygenase: Time for appraisal. Int. J. Tryptophan Res. 12. https://doi.org/10.1177/1178646919868978

Badour, C.L., Hirsch, R.L., Zhang, J., Mandel, H., Hamner, M., Wang, Z., 2015. Exploring the association between a cholecystokinin promoter polymorphism (rs1799923) and posttraumatic stress disorder in combat veterans. J. Anxiety Disord. 36, 78–83. https://doi.org/10.1016/J.JANXDIS.2015.09.009

Bagga, D., Reichert, J.L., Koschutnig, K., Aigner, C.S., Holzer, P., Koskinen, K., Moissl-Eichinger, C., Schöpf, V., 2018. Probiotics drive gut microbiome triggering emotional brain signatures. Gut Microbes 9, 486–496. https://doi.org/10.1080/19490976.2018.1460015

Bailey, J.M., Bryant, R.W., Whiting, J., Salata, K., 1983. Characterization of 11-HETE and 15-HETE, together with prostacyclin, as major products of the cyclooxygenase pathway in cultured rat aorta smooth muscle cells - PubMed. J. Lipid Res. 24, 1419–1428.

Bandoli, G., Campbell-Sills, L., Kessler, R.C., Heeringa, S.G., Nock, M.K., Rosellini, A.J.,

Sampson, N.A., Schoenbaum, M., Ursano, R.J., Stein, M.B., 2017. Childhood adversity, adult stress, and the risk of major depression or generalized anxiety disorder in US soldiers: A test of the stress sensitization hypothesis. Psychol. Med. 47, 2379–2392. https://doi.org/10.1017/S0033291717001064

Banks, W.A., Gray, A.M., Erickson, M.A., Salameh, T.S., Damodarasamy, M., Sheibani, N., Meabon, J.S., Wing, E.E., Morofuji, Y., Cook, D.G., Reed, M.J., 2015. Lipopolysaccharide-induced blood-brain barrier disruption: Roles of cyclooxygenase, oxidative stress, neuroinflammation, and elements of the neurovascular unit. J. Neuroinflammation 12, 223. https://doi.org/10.1186/s12974-015-0434-1

Banskota, S., Ghia, J.-E., Khan, W.I., 2018. Serotonin in the gut: Blessing or a curse. Biochimie 161, 56–64. https://doi.org/10.1016/J.BIOCHI.2018.06.008

Barbara D. Abbott, Carmen R. Wood, Andrew M. Watkins, Kaberi P. Das, Christopher S. Lau, 1987. Peroxisome proliferator-activated receptors alpha, beta, and gamma mRNA and protein expression in human fetal tisssues. PPAR Res. 2010, 2–4. https://doi.org/10.1155/2010

Barnett-Vanes, A., Sharrock, A., Birrell, M.A., Rankin, S., 2016. A single 9-colour flow cytometric method to characterise major leukocyte populations in the rat: Validation in a model of LPS-induced pulmonary inflammation. PLoS One 11, e0142520. https://doi.org/10.1371/journal.pone.0142520

Baruch, K., Schwartz, M., 2013. CNS-specific T cells shape brain function via the choroid plexus. Brain. Behav. Immun. 34, 11–16. https://doi.org/10.1016/j.bbi.2013.04.002

Bassett, S.A., Young, W., Fraser, K., Dalziel, J.E., Webster, J., Ryan, L., Fitzgerald, P., Stanton, C., Dinan, T.G., Cryan, J.F., Clarke, G., Hyland, N., Roy, N.C., 2019. Metabolome and microbiome profiling of a stress-sensitive rat model of gut-brain axis dysfunction. Sci. Rep. 9, 14026. https://doi.org/10.1038/s41598-019-50593-3

Basu, J., Shin, D.-M., Jo, E.-K., 2012. Mycobacterial signaling through toll-like receptors. Front. Cell. Infect. Microbiol. 2, 145. https://doi.org/10.3389/fcimb.2012.00145

Batista-Gonzalez, A., Vidal, R., Criollo, A., Carreño, L.J., 2020. New insights on the role of lipid metabolism in the metabolic reprogramming of macrophages. Front. Immunol. 10, 2993. https://doi.org/10.3389/fimmu.2019.02993

Bayer, J.D., Boukens, B.J., Krul, S.P.J., Roney, C.H., Driessen, A.H.G., Berger, W.R., van den

Berg, N.W.E., Verkerk, A.O., Vigmond, E.J., Coronel, R., de Groot, J.R., 2019. Acetylcholine delays atrial activation to facilitate atrial fibrillation. Front. Physiol. 10, 1105. https://doi.org/10.3389/fphys.2019.01105

Beckh, K., Arnold, R., 1991. Regulation of bile secretion by sympathetic nerves in perfused rat liver. Am. J. Physiol. - Gastrointest. Liver Physiol. 261, G775–G780. https://doi.org/10.1152/ajpgi.1991.261.5.g775

Belizário, J.E., Faintuch, J., Garay-Malpartida, M., 2018. New frontiers for treatment of metabolic diseases. Mediators Inflamm. https://doi.org/10.1155/2018/2037838

Bellono, N.W., Bayrer, J.R., Leitch, D.B., Castro, J., Zhang, C., O'Donnell, T.A., Brierley, S.M., Ingraham, H.A., Julius, D., 2017. Enterochromaffin cells are gut chemosensors that couple to sensory neural pathways. Cell 170, 185-198.e16. https://doi.org/10.1016/j.cell.2017.05.034

Beninson, L.A., Brown, P.N., Loughridge, A.B., Saludes, J.P., Maslanik, T., Hills, A.K., Woodworth, T., Craig, W., Yin, H., Fleshner, M., 2014. Acute stressor exposure modifies plasma exosome-associated heat shock protein 72 (Hsp72) and microRNA (miR-142-5p and miR-203). PLoS One 9, e108748. https://doi.org/10.1371/journal.pone.0108748

Bennett, E.J., Tennant, C.C., Piesse, C., Badcock, C.A., Kellow, J.E., 1998. Level of chronic life stress predicts clinical outcome in irritable bowel syndrome. Gut 43, 256–61. https://doi.org/10.1136/GUT.43.2.256

Bennett, K.M., Parnell, E.A., Sanscartier, C., Parks, S., Chen, G., Nair, M.G., Lo, D.D., 2016. Induction of colonic M cells during intestinal inflammation. Am. J. Pathol. 186, 1166–79. https://doi.org/10.1016/j.ajpath.2015.12.015

Bercik, Premysl, Denou, E., Collins, J., Jackson, W., Lu, J., Jury, J., Deng, Y., Blennerhassett, P., Macri, J., McCoy, K.D., Verdu, E.F., Collins, S.M., 2011. The intestinal microbiota affect central levels of brain-derived neurotropic factor and behavior in mice. Gastroenterology 141, 599-609.e3. https://doi.org/10.1053/j.gastro.2011.04.052

Bercik, P., Park, A.J., Sinclair, D., Khoshdel, A., Lu, J., Huang, X., Deng, Y., Blennerhassett, P.A., Fahnestock, M., Moine, D., Berger, B., Huizinga, J.D., Kunze, W., McLean, P.G., Bergonzelli, G.E., Collins, S.M., Verdu, E.F., 2011. The anxiolytic effect of *Bifidobacterium longum* NCC3001 involves vagal pathways for gut-brain communication. Neurogastroenterol. Motil. 23, 1132–1139. https://doi.org/10.1111/j.1365-

2982.2011.01796.x

Bercik, P., Verdú, E.F., Foster, J.A., Macri, J., Potter, M., Huang, X., Malinowski, P., Jackson, W., Blennerhassett, P., Neufeld, K.A., Lu, J., Khan, W.I., Corthesy–Theulaz, I., Cherbut, C., Bergonzelli, G.E., Collins, S.M., 2010. Chronic gastrointestinal inflammation induces anxiety-like behavior and alters central nervous system biochemistry in mice. Gastroenterology 139, 2102-2112.e1. https://doi.org/10.1053/j.gastro.2010.06.063

Berg, R.D., 1999. Bacterial translocation from the gastrointestinal tract. Adv. Exp. Med. Biol. 473, 11–30.

Bermúdez-Humarán, L.G., Salinas, E., Ortiz, G.G., Ramirez-Jirano, L.J., Morales, J.A., Bitzer-Quintero, O.K., 2019. From probiotics to psychobiotics: Live beneficial bacteria which act on the brain-gut axis. Nutrients 11, 890. https://doi.org/10.3390/nu11040890

Bersani, F.S., Mellon, S.H., Lindqvist, D., Kang, J.I., Rampersaud, R., Somvanshi, P.R., Doyle, F.J., Hammamieh, R., Jett, M., Yehuda, R., Marmar, C.R., Wolkowitz, O.M., 2020. Novel pharmacological targets for combat PTSD-metabolism, inflammation, the gut microbiome, and mitochondrial dysfunction. Mil. Med. 185, 311–318. https://doi.org/10.1093/milmed/usz260

Berthoud, H.-R., Neuhuber, W.L., 2000. Functional and chemical anatomy of the afferent vagal system. Auton. Neurosci. 85, 1–17. https://doi.org/10.1016/S1566-0702(00)00215-0

Bharwani, A., Mian, M.F., Foster, J.A., Surette, M.G., Bienenstock, J., Forsythe, P., 2016. Structural and functional consequences of chronic psychosocial stress on the microbiome and host. Psychoneuroendocrinology 63, 217–227. https://doi.org/10.1016/J.PSYNEUEN.2015.10.001

Bharwani, A., Mian, M.F., Surette, M.G., Bienenstock, J., Forsythe, P., 2017. Oral treatment with *Lactobacillus rhamnosus* attenuates behavioural deficits and immune changes in chronic social stress. BMC Med. 15, 7. https://doi.org/10.1186/s12916-016-0771-7

Bhattacharyya, J., Biswas, S., Datta, A., 2005. Mode of action of endotoxin: Role of free radicals and antioxidants. Curr. Med. Chem. 11, 359–368. https://doi.org/10.2174/0929867043456098

Biagioli, M., Carino, A., Cipriani, S., Francisci, D., Marchianò, S., Scarpelli, P., Sorcini, D., Zampella, A., Fiorucci, S., 2017. The bile acid receptor GPBAR1 regulates the M1/M2 phenotype of intestinal macrophages and activation of GPBAR1 rescues mice from murine

colitis. J. Immunol. 199, 718–733. https://doi.org/10.4049/jimmunol.1700183

Bishehsari, F., Engen, P., Preite, N., Tuncil, Y., Naqib, A., Shaikh, M., Rossi, M., Wilber, S., Green, S., Hamaker, B., Khazaie, K., Voigt, R., Forsyth, C., Keshavarzian, A., 2018. Dietary fiber treatment corrects the composition of gut microbiota, promotes SCFA production, and suppresses colon carcinogenesis. Genes (Basel). 9, 102. https://doi.org/10.3390/genes9020102

Böbel, T.S., Hackl, S.B., Langgartner, D., Jarczok, M.N., Rohleder, N., Rook, G.A.W., Lowry, C.A., Gündel, H., Waller, C., Reber, S.O., 2018. Less immune activation following social stress in rural vs. urban participants raised with regular or no animal contact, respectively. Proc. Natl. Acad. Sci. U. S. A. 115, 5259–5264. https://doi.org/10.1073/pnas.1719866115

Bonaz, B., Bazin, T., Pellissier, S., 2018. The vagus nerve at the interface of the microbiota-gut-brain axis. Front. Neurosci. 12, 49. https://doi.org/10.3389/fnins.2018.00049

Bortolotti, P., Faure, E., Kipnis, E., 2018. Inflammasomes in tissue damages and immune disorders after trauma. Front. Immunol. 9, 1900. https://doi.org/10.3389/fimmu.2018.01900

Bouhlel, M.A., Derudas, B., Rigamonti, E., Dièvart, R., Brozek, J., Haulon, S., Zawadzki, C., Jude, B., Torpier, G., Marx, N., Staels, B., Chinetti-Gbaguidi, G., 2007. PPARγ activation primes human monocytes into alternative M2 macrophages with anti-inflammatory properties. Cell Metab. 6, 137–143. https://doi.org/10.1016/j.cmet.2007.06.010

Bourinbaiar, A.S., Batbold, U., Efremenko, Y., Sanjagdorj, M., Butov, D., Damdinpurev, N., Grinishina, E., Mijiddorj, O., Kovolev, M., Baasanjav, K., Butova, T., Prihoda, N., Batbold, O., Yurchenko, L., Tseveendorj, A., Arzhanova, O., Chunt, E., Stepanenko, H., Sokolenko, N., Makeeva, N., Tarakanovskaya, M., Borisova, V., Reid, A., Kalashnikov, V., Nyasulu, P., Prabowo, S.A., Jirathitikal, V., Bain, A.I., Stanford, C., Stanford, J., 2020. Phase III, placebo-controlled, randomized, double-blind trial of tableted, therapeutic TB vaccine (V7) containing heat-killed M. vaccae administered daily for one month. J. Clin. Tuberc. Other Mycobact. Dis. 18, 100141. https://doi.org/10.1016/j.jctube.2019.100141

Bowers, S., Olker, C., Song, E., Wright, K., Fleshner, M., Lowry, C., Vitaterna, M., Turek, F., 2017. Immunization with heat-killed *Mycobacterium vaccae* increases total sleep and REM sleep, and changes NREM architecture in mice. Sleep 40, A55. https://doi.org/10.1093/sleepj/zsx050.145

Bowers, S.J., Lambert, S., He, S., Lowry, C.A., Fleshner, M., Wright Jr, K.P., Turek, F.W.,

Vitaterna, M.H., 2020. Immunization with a heat-killed bacterium, *Mycobacterium vaccae* NCTC 11659, prevents the development of cortical hyperarousal and a PTSD-like sleep phenotype after sleep disruption and acute stress in mice. Sleep. https://doi.org/10.1093/sleep/zsaa271

Bowers, S.J., Lambert, S., He, S., Olker, C.J., Song, E.J., Wright, K.P., Fleshner, M., Lowry, C.A., Turek, F.W., Vitaterna, M.H., 2019. Preimmunization with a non-pathogenic bacterium *Mycobacterium vaccae* NCTC11659 prevents the development of cortical hyperarousal and a PTSD-like sleep phenotype following sleep disruption plus acute stress in mice. Sleep 42, A94–A95. https://doi.org/10.1093/sleep/zsz067.229

Bowers, S.J., Lambert, S., Olker, C.J., Song, E.J., Wright, K.P., Fleshner, M., Lowry, C.A., Vitaterna, M.H., Turek, F.W., 2018. Effects of chronic sleep restriction on stress-induced alterations in sleep are mitigated by preimmunization with *Mycobacterium vaccae* NCTC 11659, in: Society for Research on Biological Rhythms (SRBR) M117.

Braissant, O., Foufelle, F., Scotto, C., Dauça, M., Wahli, W., 1996. Differential expression of peroxisome proliferator-activated receptors (PPARs): Tissue distribution of PPAR-α, -β, and -γ in the adult rat. Endocrinology 137, 354–366. https://doi.org/10.1210/endo.137.1.8536636

Braniste, V., Al-Asmakh, M., Kowal, C., Anuar, F., Abbaspour, A., Toth, M., Korecka, A., Bakocevic, N., Ng, L.G., Kundu, P., Gulyas, B., Halldin, C., Hultenby, K., Nilsson, H., Hebert, H., Volpe, B.T., Diamond, B., Pettersson, S., Pettersson, Sven, 2014. The gut microbiota influences blood-brain barrier permeability in mice. Sci. Transl. Med. 6, 263ra158. https://doi.org/10.1126/scitranslmed.3009759

Bravo, J.A., Forsythe, P., Chew, M. V., Escaravage, E., Savignac, H.M., Dinan, T.G., Bienenstock, J., Cryan, J.F., 2011. Ingestion of *Lactobacillus* strain regulates emotional behavior and central GABA receptor expression in a mouse via the vagus nerve. Proc. Natl. Acad. Sci. 108, 16050–16055. https://doi.org/10.1073/pnas.1102999108

Breen, M.S., Bierer, L.M., Daskalakis, N.P., Bader, H.N., Makotkine, I., Chattopadhyay, M., Xu, C., Buxbaum Grice, A., Tocheva, A.S., Flory, J.D., Buxbaum, J.D., Meaney, M.J., Brennand, K., Yehuda, R., 2019. Differential transcriptional response following glucocorticoid activation in cultured blood immune cells: a novel approach to PTSD biomarker development. Transl. Psychiatry 9, 1–13. https://doi.org/10.1038/s41398-019-

0539-x

Breit, S., Kupferberg, A., Rogler, G., Hasler, G., 2018. Vagus nerve as modulator of the brain-gut axis in psychiatric and inflammatory disorders. Front. psychiatry 9, 44. https://doi.org/10.3389/fpsyt.2018.00044

Brenner, L.A., Forster, J.E., Stearns-Yoder, K.A., Stamper, C.E., Hoisington, A.J., Brostow, D.P., Mealer, M., Wortzel, H.S., Postolache, T.T., Lowry, C.A., 2020. Evaluation of an immunomodulatory probiotic intervention for Veterans with co-occurring mild traumatic brain injury and posttraumatic stress disorder: A pilot study. Front. Neurol. 11, 1015. https://doi.org/10.3389/fneur.2020.01015

Brenner, L.A., Stearns-Yoder, K.A., Hoffberg, A.S., Penzenik, M.E., Starosta, A.J., Hernández, T.D., Hadidi, D.A., Lowry, C.A., 2017. Growing literature but limited evidence: a systematic review regarding prebiotic and probiotic interventions for those with traumatic brain injury and/or posttraumatic stress disorder. Brain. Behav. Immun. 65, 57–67. https://doi.org/10.1016/j.bbi.2017.06.003

Brooks, L., Viardot, A., Tsakmaki, A., Stolarczyk, E., Howard, J.K., Cani, P.D., Everard, A., Sleeth, M.L., Psichas, A., Anastasovskaj, J., Bell, J.D., Bell-Anderson, K., Mackay, C.R., Ghatei, M.A., Bloom, S.R., Frost, G., Bewick, G.A., 2017. Fermentable carbohydrate stimulates FFAR2-dependent colonic PYY cell expansion to increase satiety. Mol. Metab. 6, 48–60. https://doi.org/10.1016/j.molmet.2016.10.011

Brown, J.R.-M., Flemer, B., Joyce, S.A., Zulquernain, A., Sheehan, D., Shanahan, F., O'Toole, P.W., 2018. Changes in microbiota composition, bile and fatty acid metabolism, in successful faecal microbiota transplantation for Clostridioides difficile infection. BMC Gastroenterol. 18, 131. https://doi.org/10.1186/s12876-018-0860-5

Brudey, C., Park, J., Wiaderkiewicz, J., Kobayashi, I., Mellman, T., Marvar, P.J., 2015. Autonomic and inflammatory consequences of posttraumatic stress disorder and the link to cardiovascular disease. Am. J. Physiol. - Regul. Integr. Comp. Physiol. 309, R315–R321. https://doi.org/10.1152/ajpregu.00343.2014

Buffie, C.G., Bucci, V., Stein, R.R., McKenney, P.T., Ling, L., Gobourne, A., No, D., Liu, H., Kinnebrew, M., Viale, A., Littmann, E., van den Brink, M.R.M., Jenq, R.R., Taur, Y., Sander, C., Cross, J.R., Toussaint, N.C., Xavier, J.B., Pamer, E.G., 2015. Precision microbiome reconstitution restores bile acid mediated resistance to Clostridium difficile.

Nature 517, 205–208. https://doi.org/10.1038/nature13828

Bunea, I.M., Szentágotai-Tătar, A., Miu, A.C., 2017. Early-life adversity and cortisol response to social stress: a meta-analysis. Transl. Psychiatry 7, 1274. https://doi.org/10.1038/s41398-017-0032-3

Büttner, T., Hornig, C.R., Busse, O., Dorndorf, W., 1986. CSF cyclic AMP and CSF adenylate kinase in cerebral ischaemic infarction. J. Neurol. 233, 297–303. https://doi.org/10.1007/BF00314162

Cacioppo, J.T., Malarkey, W.B., Kiecolt-Glaser, J.K., Uchino, B.N., Sgoutas-Emch, S.A., Sheridan, J.F., Berntson, G.G., Glaser, R., 1995. Heterogeneity in neuroendocrine and immune responses to brief psychological stressors as a function of autonomic cardiac activation. Psychosom. Med. 57, 154–164. https://doi.org/10.1097/00006842-199503000-00008

Cagliani, R., Forni, D., Riva, S., Pozzoli, U., Colleoni, M., Bresolin, N., Clerici, M., Sironi, M., 2013. Evolutionary analysis of the contact system indicates that kininogen evolved adaptively in mammals and in human populations. Mol. Biol. Evol. 30, 1397–1408. https://doi.org/10.1093/molbev/mst054

Cao, Y., Stafforini, D.M., Zimmerman, G.A., McIntyre, T.M., Prescott, S.M., 1998. Expression of plasma platelet-activating factor acetylhydrolase is transcriptionally regulated by mediators of inflammation. J. Biol. Chem. 273, 4012–4020. https://doi.org/10.1074/jbc.273.7.4012

Cauwels, A., Rogge, E., Vandendriessche, B., Shiva, S., Brouckaert, P., 2014. Extracellular ATP drives systemic inflammation, tissue damage and mortality. Cell Death Dis. 5. https://doi.org/10.1038/cddis.2014.70

Chang, J.P.C., Chen, Y.T., Su, K.P., 2009. Omega-3 polyunsaturated fatty acids (n-3 PUFAs) in cardiovascular diseases (CVDs) and depression: The missing link? Cardiovasc. Psychiatry Neurol. 2009, 1–6. https://doi.org/10.1155/2009/725310

Chang, Y.Y., Yu, L.C.H., Yu, I.S., Jhuang, Y.L., Huang, W.J., Yang, C.Y., Jeng, Y.M., 2018. Deletion of cadherin-17 enhances intestinal permeability and susceptibility to intestinal tumour formation. J. Pathol. 246, 289–299. https://doi.org/10.1002/path.5138

Chen, G.Y., Nuñez, G., 2010. Sterile inflammation: sensing and reacting to damage. Nat. Rev. Immunol. 10, 826–837. https://doi.org/10.1038/nri2873

Chen, H.J., Antonson, A.M., Rajasekera, T.A., Patterson, J.M., Bailey, M.T., Gur, T.L., 2020. Prenatal stress causes intrauterine inflammation and serotonergic dysfunction, and long-term behavioral deficits through microbe- and CCL2-dependent mechanisms. Transl. Psychiatry 10, 191. https://doi.org/10.1038/s41398-020-00876-5

Chen, Y., Kuchroo, V.K., Inobe, J.I., Hafler, D.A., Weiner, H.L., 1994. Regulatory T cell clones induced by oral tolerance: Suppression of autoimmune encephalomyelitis. Science. 265, 1237–1240. https://doi.org/10.1126/science.7520605

Chen, Y., Wang, J., Wang, X., Li, X., Song, J., Fang, J., Liu, X., Liu, T., Wang, D., Li, Q., Wen, S., Ma, D., Xia, J., Luo, L., Zheng, S.G., Cui, J., Zeng, G., Chen, L., Cheng, B., Wang, Z., 2019. PIK3IP1 is a negative immune regulator that inhibits antitumor T-cell immunity. Clin. Cancer Res. 25, 6180–6194. https://doi.org/10.1158/1078-0432.CCR-18-4134

Cheng, S.L., Li, X., Lehmler, H.-J., Phillips, B., Shen, D., Cui, J.Y., 2018. Gut microbiota modulates interactions between polychlorinated biphenyls and bile acid homeostasis. Toxicol. Sci. 166, 269–287. https://doi.org/10.1093/toxsci/kfy208

Cherfane, C.E., Gessel, L., Cirillo, D., Zimmerman, M.B., Polyak, S., 2015. Monocytosis and a low lymphocyte to monocyte ratio are effective biomarkers of ulcerative colitis disease activity. Inflamm. Bowel Dis. 21, 1769–1775. https://doi.org/10.1097/MIB.0000000000000427

Chiang, J.Y.L., 2002. Bile acid regulation of gene expression: Roles of nuclear hormone receptors. Endocr. Rev. 23, 443–463. https://doi.org/10.1210/er.2000-0035

Chieppa, M., Rescigno, M., Huang, A.Y.C., Germain, R.N., 2006. Dynamic imaging of dendritic cell extension into the small bowel lumen in response to epithelial cell TLR engagement. J. Exp. Med. 203, 2841–2852. https://doi.org/10.1084/jem.20061884

Chinetti, G., Lestavel, S., Bocher, V., Remaley, A.T., Neve, B., Torra, I.P., Teissier, E., Minnich, A., Jaye, M., Duverger, N., Brewer, H.B., Fruchart, J.C., Clavey, V., Staels, B., 2001. PPAR-α and PPAR-γ activators induce cholesterol removal from human macrophage foam cells through stimulation of the ABCA1 pathway. Nat. Med. 7, 53–58. https://doi.org/10.1038/83348

Chiong, M., Wang, Z. V., Pedrozo, Z., Cao, D.J., Troncoso, R., Ibacache, M., Criollo, A., Nemchenko, A., Hill, J.A., Lavandero, S., 2011. Cardiomyocyte death: Mechanisms and translational implications. Cell Death Dis. https://doi.org/10.1038/cddis.2011.130

Choi, Y., Bose, S., Shin, N.R., Song, E.J., Nam, Y. Do, Kim, H., 2020. Lactate-fortified puerariae radix fermented by *Bifidobacterium breve* improved diet-induced metabolic dysregulation via alteration of gut microbial communities. Nutrients 12, 276. https://doi.org/10.3390/nu12020276

Chomczynski, P., Sacchi, N., 1987. Single-step method of RNA isolation by acid guanidinium thiocyanate-phenol-chloroform extraction. Anal. Biochem. 162, 156–159. https://doi.org/10.1006/abio.1987.9999

Chong, J., Soufan, O., Li, C., Caraus, I., Li, S., Bourque, G., Wishart, D.S., Xia, J., 2018. MetaboAnalyst 4.0: Towards more transparent and integrative metabolomics analysis. Nucleic Acids Res. 46, W486–W494. https://doi.org/10.1093/nar/gky310

Chong, J., Wishart, D.S., Xia, J., 2019. Using MetaboAnalyst 4.0 for comprehensive and integrative metabolomics data analysis. Curr. Protoc. Bioinforma. 68, e68. https://doi.org/10.1002/cpbi.86

Chopra, P., Singh, A., Koul, A., Ramachandran, S., Drlica, K., Tyagi, A.K., Singh, Y., 2003. Cytotoxic activity of nucleoside diphosphate kinase secreted from *Mycobacterium tuberculosis*. Eur. J. Biochem. 270, 625–634. https://doi.org/10.1046/j.1432-1033.2003.03402.x

Christianson, J.P., Paul, E.D., Irani, M., Thompson, B.M., Kubala, K.H., Yirmiya, R., Watkins, L.R., Maier, S.F., 2008. The role of prior stressor controllability and the dorsal raphé nucleus in sucrose preference and social exploration. Behav. Brain Res. 193, 87–93. https://doi.org/10.1016/j.bbr.2008.04.024

Chu, C., Murdock, M.H., Jing, D., Won, T.H., Chung, H., Kressel, A.M., Tsaava, T., Addorisio, M.E., Putzel, G.G., Zhou, L., Bessman, N.J., Yang, R., Moriyama, S., Parkhurst, C.N., Li, A., Meyer, H.C., Teng, F., Chavan, S.S., Tracey, K.J., Regev, A., Schroeder, F.C., Lee, F.S., Liston, C., Artis, D., 2019. The microbiota regulate neuronal function and fear extinction learning. Nature 574, 543–548. https://doi.org/10.1038/s41586-019-1644-y

Chunchai, T., Thunapong, W., Yasom, S., Wanchai, K., Eaimworawuthikul, S., Metzler, G., Lungkaphin, A., Pongchaidecha, A., Sirilun, S., Chaiyasut, C., Pratchayasakul, W., Thiennimitr, P., Chattipakorn, N., Chattipakorn, S.C., 2018. Decreased microglial activation through gut-brain axis by prebiotics, probiotics, or synbiotics effectively restored cognitive function in obese-insulin resistant rats. J. Neuroinflammation 15, 11.

https://doi.org/10.1186/s12974-018-1055-2

Ciborowski, P., Kadiu, I., Rozek, W., Smith, L., Bernhardt, K., Fladseth, M., Ricardo-Dukelow, M., Gendelman, H.E., 2007. Investigating the human immunodeficiency virus type 1-infected monocyte-derived macrophage secretome. Virology 363, 198–209. https://doi.org/10.1016/j.virol.2007.01.013

Ciesielczyk, K., Furgała, A., Dobrek, Ł., Juszczak, K., Thor, P., 2017. Altered sympathovagal balance and pain hypersensitivity in TNBS-induced colitis. Arch. Med. Sci. 13, 246–255. https://doi.org/10.5114/aoms.2015.55147

Clarendon Press, 1993. The new shorter Oxford English Dictionary on historic principles. L. Brown (Ed). Oxford: Clarendon Press.

Clark, S.M., Pocivavsek, A., Nicholson, J.D., Notarangelo, F.M., Langenberg, P., McMahon, R.P., Kleinman, J.E., Hyde, T.M., Stiller, J., Postolache, T.T., Schwarcz, R., Tonelli, L.H., 2016. Reduced kynurenine pathway metabolism and cytokine expression in the prefrontal cortex of depressed individuals. J. Psychiatry Neurosci. 41, 386–394. https://doi.org/10.1503/jpn.150226

Clasquin, M.F., Melamud, E., Rabinowitz, J.D., 2012. LC-MS data processing with MAVEN: A metabolomic analysis and visualization engine. Curr. Protoc. Bioinforma. 37, 14.11.1-14.11.23. https://doi.org/10.1002/0471250953.bi1411s37

Clemente, J.C., Manasson, J., Scher, J.U., 2018. The role of the gut microbiome in systemic inflammatory disease. BMJ 360, j5145. https://doi.org/10.1136/bmj.j5145

Coelho, M., Oliveira, T., Fernandes, R., 2013. Biochemistry of adipose tissue: An endocrine organ. Arch. Med. Sci. 9, 191–200. https://doi.org/10.5114/aoms.2013.33181

Cohen, H., Benjamin, J., Geva, A.B., Matar, M.A., Kaplan, Z., Kotler, M., 2000. Autonomic dysregulation in panic disorder and in post-traumatic stress disorder: application of power spectrum analysis of heart rate variability at rest and in response to recollection of trauma or panic attacks. Psychiatry Res. 96, 1–13. https://doi.org/10.1016/S0165-1781(00)00195-5

Cohen, S., Janicki-Deverts, D., Doyle, W.J., Miller, G.E., Frank, E., Rabin, B.S., Turner, R.B., 2012. Chronic stress, glucocorticoid receptor resistance, inflammation, and disease risk. Proc. Natl. Acad. Sci. U. S. A. 109, 5995–5999. https://doi.org/10.1073/pnas.1118355109

Colle, R., Masson, P., Verstuyft, C., Fève, B., Werner, E., Boursier-Neyret, C., Walther, B., David, D.J., Boniface, B., Falissard, B., Chanson, P., Corruble, E., Becquemont, L., 2020.

Peripheral tryptophan, serotonin, kynurenine, and their metabolites in major depression: A case–control study. Psychiatry Clin. Neurosci. 74, 112–117. https://doi.org/10.1111/pcn.12944

Collins, J.M., Walker, D.I., Jones, D.P., Tukvadze, N., Liu, K.H., Tran, V.T., Uppal, K., Frediani, J.K., Easley, K.A., Shenvi, N., Khadka, M., Ortlund, E.A., Kempker, R.R., Blumberg, H.M., Ziegler, T.R., 2018. High-resolution plasma metabolomics analysis to detect *Mycobacterium tuberculosis* associated metabolites that distinguish active pulmonary tuberculosis in humans. PLoS One 13, e0205398. https://doi.org/10.1371/journal.pone.0205398

Collins, S.M., Kassam, Z., Bercik, P., 2013. The adoptive transfer of behavioral phenotype via the intestinal microbiota: experimental evidence and clinical implications. Curr. Opin. Microbiol. 16, 240–245. https://doi.org/10.1016/J.MIB.2013.06.004

Coombes, J.L., Powrie, F., 2008. Dendritic cells in intestinal immune regulation. Nat. Rev. Immunol. 8, 435–446. https://doi.org/10.1038/nri2335

Covián, C., Fernández-Fierro, A., Retamal-Díaz, A., Díaz, F.E., Vasquez, A.E., Lay, M.K., Riedel, C.A., González, P.A., Bueno, S.M., Kalergis, A.M., 2019. BCG-induced cross-protection and development of trained immunity: Implication for vaccine design. Front. Immunol. 10, 2806. https://doi.org/10.3389/fimmu.2019.02806

Crenn, P., Vahedi, K., Lavergne-Slove, A., Cynober, L., Matuchansky, C., Messing, B., 2003. Plasma citrulline: A marker of enterocyte mass in villous atrophy-associated small bowel disease. Gastroenterology 124, 1210–1219. https://doi.org/10.1016/S0016-5085(03)00170-7

Crider, A., Feng, T., Pandya, C.D., Davis, T., Nair, A., Ahmed, A.O., Baban, B., Turecki, G., Pillai, A., 2018. Complement component 3a receptor deficiency attenuates chronic stress-induced monocyte infiltration and depressive-like behavior. Brain. Behav. Immun. 70, 246–256. https://doi.org/10.1016/j.bbi.2018.03.004

Crouzet, L., Gaultier, E., Del'Homme, C., Cartier, C., Delmas, E., Dapoigny, M., Fioramonti, J., Bernalier-Donadille, A., 2013. The hypersensitivity to colonic distension of IBS patients can be transferred to rats through their fecal microbiota. Neurogastroenterol. Motil. 25, e272–e282. https://doi.org/10.1111/nmo.12103

Cryan, J.F., O'Riordan, K.J., Sandhu, K., Peterson, V., Dinan, T.G., 2020. The gut microbiome in neurological disorders. Lancet Neurol. 19, 179–194. https://doi.org/10.1016/S1474-

4422(19)30356-4

Cunard, R., DiCampli, D., Archer, D.C., Stevenson, J.L., Ricote, M., Glass, C.K., Kelly, C.J., 2002. WY14,643, a PPARα ligand, has profound effects on immune responses in vivo. J. Immunol. 169, 6806–6812. https://doi.org/10.4049/jimmunol.169.12.6806

D'Amato, N.C., Rogers, T.J., Gordon, M.A., Greene, L.I., Cochrane, D.R., Spoelstra, N.S., Nemkov, T.G., D'alessandro, A., Hansen, K.C., Richer, J.K., 2015. A TDO2-AhR signaling axis facilitates anoikis resistance and metastasis in triple-negative breast cancer. Cancer Res. 75, 4651–4664. https://doi.org/10.1158/0008-5472.CAN-15-2011

D'Attilio, L., Santucci, N., Bongiovanni, B., Bay, M.L., Bottasso, O., 2018. Tuberculosis, the disrupted immune-endocrine response and the potential thymic repercussion as a contributing factor to disease physiopathology. Front. Endocrinol. (Lausanne). 9, 1. https://doi.org/10.3389/fendo.2018.00214

Dai, L., Bhargava, P., Stanya, K.J., Alexander, R.K., Liou, Y.H., Jacobi, D., Knudsen, N.H., Hyde, A., Gangl, M.R., Liu, S., Lee, C.H., 2017. Macrophage alternative activation confers protection against lipotoxicity-induced cell death. Mol. Metab. 6, 1186–1197. https://doi.org/10.1016/j.molmet.2017.08.001

Dalile, B., Vervliet, B., Bergonzelli, G., Verbeke, K., Van Oudenhove, L., 2020. Colon-delivered short-chain fatty acids attenuate the cortisol response to psychosocial stress in healthy men: a randomized, placebo-controlled trial. Neuropsychopharmacology 45, 2257–2266. https://doi.org/10.1038/s41386-020-0732-x

Dalli, J., Zhu, M., Vlasenko, N.A., Deng, B., Haeggström, J.Z., Petasis, N.A., Serhan, C.N., 2013. The novel 13S,14S-epoxy-maresinis converted by human macrophages to maresin 1 (MaR1), inhibits leukotriene A4 hydrolase (LTA4H), and shifts macrophage phenotype. FASEB J. 27, 2573–2583. https://doi.org/10.1096/fj.13-227728

Das, U.N., 2018. Arachidonic acid and other unsaturated fatty acids and some of their metabolites function as endogenous antimicrobial molecules: A review. J. Adv. Res. 11, 57–66. https://doi.org/10.1016/j.jare.2018.01.001

Dasgupta, S., Roy, A., Jana, M., Hartley, D.M., Pahan, K., 2007. Gemfibrozil ameliorates relapsing-remitting experimental autoimmune encephalomyelitis independent of peroxisome proliferator-activated receptor-α. Mol. Pharmacol. 72, 934–946. https://doi.org/10.1124/mol.106.033787

David, L.A., Maurice, C.F., Carmody, R.N., Gootenberg, D.B., Button, J.E., Wolfe, B.E., Ling, A. V., Devlin, A.S., Varma, Y., Fischbach, M.A., Biddinger, S.B., Dutton, R.J., Turnbaugh, P.J., 2014. Diet rapidly and reproducibly alters the human gut microbiome. Nature 505, 559–563. https://doi.org/10.1038/nature12820

Davis, D.J., Doerr, H.M., Grzelak, A.K., Busi, S.B., Jasarevic, E., Ericsson, A.C., Bryda, E.C., 2016. *Lactobacillus plantarum* attenuates anxiety-related behavior and protects against stress-induced dysbiosis in adult zebrafish. Sci. Rep. 6, 33726. https://doi.org/10.1038/srep33726

Davis, L.M.G., Martínez, I., Walter, J., Goin, C., Hutkins, R.W., 2011. Barcoded pyrosequencing reveals that consumption of galactooligosaccharides results in a highly specific bifidogenic response in humans. PLoS One 6, e25200. https://doi.org/10.1371/journal.pone.0025200

Dawson, P.A., Karpen, S.J., 2015. Intestinal transport and metabolism of bile acids. J. Lipid Res. 56, 1085–1099. https://doi.org/10.1194/jlr.R054114

de Kloet, C.S., Vermetten, E., Heijnen, C.J., Geuze, E., Lentjes, E.G.W.M., Westenberg, H.G.M., 2007. Enhanced cortisol suppression in response to dexamethasone administration in traumatized veterans with and without posttraumatic stress disorder. Psychoneuroendocrinology 32, 215–226. https://doi.org/10.1016/j.psyneuen.2006.12.009

de las Casas-Engel, M., Domínguez-Soto, A., Sierra-Filardi, E., Bragado, R., Nieto, C., Puig-Kroger, A., Samaniego, R., Loza, M., Corcuera, M.T., Gómez-Aguado, F., Bustos, M., Sánchez-Mateos, P., Corbí, A.L., 2013. Serotonin skews human macrophage polarization through HTR 2B and HTR 7 . J. Immunol. 190, 2301–2310. https://doi.org/10.4049/jimmunol.1201133

de Oliveira, G.L.V., Leite, A.Z., Higuchi, B.S., Gonzaga, M.I., Mariano, V.S., 2017. Intestinal dysbiosis and probiotic applications in autoimmune diseases. Immunology 152, 1–12. https://doi.org/10.1111/imm.12765

De Palma, G., Blennerhassett, P., Lu, J., Deng, Y., Park, A.J., Green, W., Denou, E., Silva, M.A., Santacruz, A., Sanz, Y., Surette, M.G., Verdu, E.F., Collins, S.M., Bercik, P., 2015. Microbiota and host determinants of behavioural phenotype in maternally separated mice. Nat. Commun. 6, 7735. https://doi.org/10.1038/ncomms8735

De Palma, G., Lynch, M.D.J., Lu, J., Dang, V.T., Deng, Y., Jury, J., Umeh, G., Miranda, P.M., Pigrau Pastor, M., Sidani, S., Pinto-Sanchez, M.I., Philip, V., McLean, P.G., Hagelsieb, M.-

G., Surette, M.G., Bergonzelli, G.E., Verdu, E.F., Britz-McKibbin, P., Neufeld, J.D., Collins, S.M., Bercik, P., 2017. Transplantation of fecal microbiota from patients with irritable bowel syndrome alters gut function and behavior in recipient mice. Sci. Transl. Med. 9, eaaf6397. https://doi.org/10.1126/scitranslmed.aaf6397

De Vadder, F., Grasset, E., Mannerås Holm, L., Karsenty, G., Macpherson, A.J., Olofsson, L.E., Bäckhed, F., 2018. Gut microbiota regulates maturation of the adult enteric nervous system via enteric serotonin networks. Proc. Natl. Acad. Sci. U. S. A. 115, 6458–6463. https://doi.org/10.1073/pnas.1720017115

de Vries, G.J., Mocking, R., Lok, A., Assies, J., Schene, A., Olff, M., 2016. Fatty acid concentrations in patients with posttraumatic stress disorder compared to healthy controls. J. Affect. Disord. 205, 351–359. https://doi.org/10.1016/j.jad.2016.08.021

Deak, T., Meriwether, J.L., Fleshner, M., Spencer, R.L., Abouhamze, A., Moldawer, L.L., Grahn, R.E., Watkins, L.R., Maier, S.F., 1997. Evidence that brief stress may induce the acute phase response in rats. Am. J. Physiol. Integr. Comp. Physiol. 273, R1998–R2004. https://doi.org/10.1152/ajpregu.1997.273.6.R1998

Dean, K.R., Hammamieh, R., Mellon, S.H., Abu-Amara, D., Flory, J.D., Guffanti, G., Wang, K., Daigle, B.J., Gautam, A., Lee, I., Yang, R., Almli, L.M., Bersani, F.S., Chakraborty, N., Donohue, D., Kerley, K., Kim, T.K., Laska, E., Young Lee, M., Lindqvist, D., Lori, A., Lu, L., Misganaw, B., Muhie, S., Newman, J., Price, N.D., Qin, S., Reus, V.I., Siegel, C., Somvanshi, P.R., Thakur, G.S., Zhou, Y., Baxter, D., Bierer, L., Blessing, E., Cho, J.H., Coy, M., Desarnaud, F., Fossati, S., Hoke, A., Kumar, R., Li, M., Makotkine, I., Miller, S.A., Petzold, L., Price, L., Qian, M., Scherler, K., Srinivasan, S., Suessbrick, A., Tang, L., Wu, X., Wu, G., Wu, C., Hood, L., Ressler, K.J., Wolkowitz, O.M., Yehuda, R., Jett, M., Doyle, F.J., Marmar, C., 2020. Multi-omic biomarker identification and validation for diagnosing warzone-related post-traumatic stress disorder. Mol. Psychiatry 25, 3337–3349. https://doi.org/10.1038/s41380-019-0496-z

Defrances, M.C., Debelius, D.R., Cheng, J., Kane, L.P., 2012. Inhibition of T-cell activation by PIK3IP1. Eur. J. Immunol. 42, 2754–2759. https://doi.org/10.1002/eji.201141653

Dell'Osso, B., Oldani, L., Grancini, B., Dario, A., Altamura, A.C., 2018. Ten-year outcome of vagus nerve stimulation-implanted patients with treatment-resistant depression: Two italian cases. Neuropsychiatr. Dis. Treat. 14, 915–918. https://doi.org/10.2147/NDT.S161062

Demirel, Ö., Waibler, Z., Kalinke, U., Grünebach, F., Appel, S., Brossart, P., Hasilik, A., Tampé, R., Abele, R., 2007. Identification of a lysosomal peptide transport system induced during dendritic cell development. J. Biol. Chem. 282, 37836–37843. https://doi.org/10.1074/jbc.M708139200

Dennis, G., Sherman, B.T., Hosack, D.A., Yang, J., Gao, W., Lane, H.C., Lempicki, R.A., 2003. DAVID: Database for annotation, visualization, and integrated discovery. Genome Biol. 4, R60. https://doi.org/10.1186/gb-2003-4-9-r60

Dennis, P.A., Dedert, E.A., Van Voorhees, E.E., Watkins, L.L., Hayano, J., Calhoun, P.S., Sherwood, A., Dennis, M.F., Beckham, J.C., 2016. Examining the crux of autonomic dysfunction in posttraumatic stress disorder: whether chronic or situational distress underlies elevated heart rate and attenuated heart rate variability. Psychosom. Med. 78, 805–809. https://doi.org/10.1097/PSY.0000000000000326

Derikx, J.P.M., Blijlevens, N.M.A., Donnelly, J.P., Fujii, H., Kanda, T., van Bijnen, A.A., Heineman, E., Buurman, W.A., 2009. Loss of enterocyte mass is accompanied by diminished turnover of enterocytes after myeloablative therapy in haematopoietic stem-cell transplant recipients. Ann. Oncol. 20, 337–342. https://doi.org/10.1093/annonc/mdn579

Di Ciaula, A., Garruti, G., Baccetto, R.L., Molina-Molina, E., Bonfrate, L., Wang, D.Q.H., Portincasa, P., 2017. Bile acid physiology. Ann. Hepatol. 16, s4–s14. https://doi.org/10.5604/01.3001.0010.5493

Dick, T., Manjunatha, U., Kappes, B., Gengenbacher, M., 2010. Vitamin B6 biosynthesis is essential for survival and virulence of *Mycobacterium tuberculosis*. Mol. Microbiol. 78, 980–988. https://doi.org/10.1111/j.1365-2958.2010.07381.x

Dieleman, J.L., Baral, R., Birger, M., Bui, A.L., Bulchis, A., Chapin, A., Hamavid, H., Horst, C., Johnson, E.K., Joseph, J., Lavado, R., Lomsadze, L., Reynolds, A., Squires, E., Campbell, M., DeCenso, B., Dicker, D., Flaxman, A.D., Gabert, R., Highfill, T., Naghavi, M., Nightingale, N., Templin, T., Tobias, M.I., Vos, T., Murray, C.J.L., 2016. US spending on personal health care and public health, 1996-2013. JAMA - J. Am. Med. Assoc. 316, 2627–2646. https://doi.org/10.1001/jama.2016.16885

Dimitriadis, G.K., Kaur, J., Adya, R., Miras, A.D., Mattu, H.S., Hattersley, J.G., Kaltsas, G., Tan, B.K., Randeva, H.S., 2018. Chemerin induces endothelial cell inflammation: Activation of nuclear factor-kappa beta and monocyte-endothelial adhesion. Oncotarget 9,

16678–16690. https://doi.org/10.18632/oncotarget.24659

Ding, C., van 't Veer, C., Roelofs, J.J.T.H., Shukla, M., McCrae, K.R., Revenko, A.S., Crosby, J., van der Poll, T., 2018. Limited role of kininogen in the host response during gram-negative pneumonia-derived sepsis. Am. J. Physiol. - Lung Cell. Mol. Physiol. 314, L397–L405. https://doi.org/10.1152/ajplung.00288.2017

Djouadi, F., Aubey, F., Schlemmer, D., Ruiter, J.P.N., Wanders, R.J.A., Strauss, A.W., Bastin, J., 2005. Bezafibrate increases very-long-chain acyl-CoA dehydrogenase protein and mRNA expression in deficient fibroblasts and is a potential therapy for fatty acid oxidation disorders. Hum. Mol. Genet. 14, 2695–2703. https://doi.org/10.1093/hmg/ddi303

Dlugovitzky, D., Bay, M.L., Rateni, L., Urízar, L., Rondelli, C.F.M., Largacha, C., Farroni, M.A., Molteni, O., Bottasso, O.A., 1999. In vitro synthesis of interferon-γ, interleukin-4, transforming growth factor-β and interleukin-1β by peripheral blood mononuclear cells from tuberculosis patients: Relationship with the severity of pulmonary involvement. Scand. J. Immunol. 49, 210–217. https://doi.org/10.1046/j.1365-3083.1999.00492.x

Dlugovitzky, D., Notario, R., Martinel-Lamas, D., Fiorenza, G., Farroni, M., Bogue, C., Stanford, C., Stanford, J., 2010. Immunotherapy with oral, heat-killed, *Mycobacterium vaccae* in patients with moderate to advanced pulmonary tuberculosis. Immunotherapy 2, 159–169. https://doi.org/10.2217/imt.09.90

Donner, N.C., Johnson, P.L., Fitz, S.D., Kellen, K.E., Shekhar, A., Lowry, C.A., 2012. Elevated tph2 mRNA expression in a rat model of chronic anxiety. Depress. Anxiety 29, 307–319. https://doi.org/10.1002/da.21925

Donohoe, D.R., Garge, N., Zhang, X., Sun, W., O'Connell, T.M., Bunger, M.K., Bultman, S.J., 2011. The microbiome and butyrate regulate energy metabolism and autophagy in the mammalian colon. Cell Metab. 13, 517–526. https://doi.org/10.1016/j.cmet.2011.02.018

Duan, L., Gan, H., Arm, J., Remold, H.G., 2001. Cytosolic phospholipase A 2 participates with TNF-α in the induction of apoptosis of human macrophages infected with *Mycobacterium tuberculosis* H37Ra. J. Immunol. 166, 7469–7476. https://doi.org/10.4049/jimmunol.166.12.7469

Duboc, H., Taché, Y., Hofmann, A.F., 2014. The bile acid TGR5 membrane receptor: From basic research to clinical application. Dig. Liver Dis. 46, 302–312. https://doi.org/10.1016/j.dld.2013.10.021

Dudek, K.A., Dion-Albert, L., Lebel, M., LeClair, K., Labrecque, S., Tuck, E., Perez, C.F., Golden, S.A., Tamminga, C., Turecki, G., Mechawar, N., Russo, S.J., Menard, C., 2020. Molecular adaptations of the blood–brain barrier promote stress resilience vs. depression. Proc. Natl. Acad. Sci. U. S. A. 117, 3326–3336. https://doi.org/10.1073/pnas.1914655117

Dumaswala, R., Berkowitz, D., Setchell, K.D.R., Heubi, J.E., 1994. Effect of fasting on the enterohepatic circulation of bile acids in rats. Am. J. Physiol. - Gastrointest. Liver Physiol. 267, G836–G842. https://doi.org/10.1152/ajpgi.1994.267.5.g836

Dunkelberger, J.R., Song, W.-C., 2010. Complement and its role in innate and adaptive immune responses. Cell Res. 20, 34–50. https://doi.org/10.1038/cr.2009.139

Dzeja, P., Terzic, A., 2009. Adenylate kinase and AMP signaling networks: metabolic monitoring, signal communication and body energy sensing. Int. J. Mol. Sci. 10, 1729–1772. https://doi.org/10.3390/ijms10041729

Eckburg, P.B., Bik, E.M., Bernstein, C.N., Purdom, E., Dethlefsen, L., Sargent, M., Gill, S.R., Nelson, K.E., Relman, D.A., 2005. Diversity of the human intestinal microbial flora. Science (80-.). 308, 1635–1638. https://doi.org/10.1126/science.1110591

Egerod, K.L., Petersen, N., Timshel, P.N., Rekling, J.C., Wang, Y., Liu, Q., Schwartz, T.W., Gautron, L., 2018. Profiling of G protein-coupled receptors in vagal afferents reveals novel gut-to-brain sensing mechanisms. Mol. Metab. 12, 62–75. https://doi.org/10.1016/J.MOLMET.2018.03.016

El Kebira, D., Gjorstrup, P., Filepa, J.G., 2012. Resolvin E1 promotes phagocytosis-induced neutrophil apoptosis and accelerates resolution of pulmonary inflammation. Proc. Natl. Acad. Sci. U. S. A. 109, 14983–14988. https://doi.org/10.1073/pnas.1206641109

Elbendary, A.A., Hessain, A.M., El-Hariri, M.D., Seida, A.A., Moussa, I.M., Mubarak, A.S., Kabli, S.A., Hemeg, H.A., El Jakee, J.K., 2018. Isolation of antimicrobial producing Actinobacteria from soil samples. Saudi J. Biol. Sci. 25, 44–46. https://doi.org/10.1016/J.SJBS.2017.05.003

Endo, J., Sano, M., Isobe, Y., Fukuda, K., Kang, J.X., Arai, H., Arita, M., 2014. 18-HEPE, an n-3 fatty acid metabolite released by macrophages, prevents pressure overload-induced maladaptive cardiac remodeling. J. Exp. Med. 211, 1673–1687. https://doi.org/10.1084/jem.20132011

Engel, T., Ben-Horin, S., Beer-Gabel, M., 2015. Autonomic dysfunction correlates with clinical

and inflammatory activity in patients with Crohn's disease. Inflamm. Bowel Dis. 21, 2320–2326. https://doi.org/10.1097/MIB.0000000000000508

Eraly, S.A., Nievergelt, C.M., Maihofer, A.X., Barkauskas, D.A., Biswas, N., Agorastos, A., O'Connor, D.T., Baker, D.G., Marine Resiliency Study Team, M., 2014. Assessment of plasma C-reactive protein as a biomarker of posttraumatic stress disorder risk. JAMA psychiatry 71, 423–31. https://doi.org/10.1001/jamapsychiatry.2013.4374

Erny, D., Hrabě de Angelis, A.L., Jaitin, D., Wieghofer, P., Staszewski, O., David, E., Keren-Shaul, H., Mahlakoiv, T., Jakobshagen, K., Buch, T., Schwierzeck, V., Utermöhlen, O., Chun, E., Garrett, W.S., McCoy, K.D., Diefenbach, A., Staeheli, P., Stecher, B., Amit, I., Prinz, M., 2015. Host microbiota constantly control maturation and function of microglia in the CNS. Nat. Neurosci. 18, 965–977. https://doi.org/10.1038/nn.4030

Esquivel-Elizondo, S., Ilhan, Z.E., Garcia-Peña, E.I., Krajmalnik-Brown, R., 2017. Insights into butyrate production in a controlled fermentation system via gene predictions. mSystems 2, e00051-17. https://doi.org/10.1128/msystems.00051-17

Eswarappa, M., Neylan, T.C., Whooley, M.A., Metzler, T.J., Cohen, B.E., 2018. Inflammation as a predictor of disease course in posttraumatic stress disorder and depression: a prospective analysis from the Mind Your Heart Study. Brain. Behav. Immun. 75, 220–227. https://doi.org/10.1016/J.BBI.2018.10.012

Ewaschuk, J., Endersby, R., Thiel, D., Diaz, H., Backer, J., Ma, M., Churchill, T., Madsen, K., 2007. Probiotic bacteria prevent hepatic damage and maintain colonic barrier function in a mouse model of sepsis. Hepatology 46, 841–850. https://doi.org/10.1002/hep.21750

Fabregat, A., Sidiropoulos, K., Viteri, G., Marin-Garcia, P., Ping, P., Stein, L., D'Eustachio, P., Hermjakob, H., 2018. Reactome diagram viewer: data structures and strategies to boost performance. Bioinformatics 34, 1028–1214.

Falony, G., Joossens, M., Vieira-Silva, S., Wang, J., Darzi, Y., Faust, K., Kurilshikov, A., Bonder, M.J., Valles-Colomer, M., Vandeputte, D., Tito, R.Y., Chaffron, S., Rymenans, L., Verspecht, C., De Sutter, L., Lima-Mendez, G., D'hoe, K., Jonckheere, K., Homola, D., Garcia, R., Tigchelaar, E.F., Eeckhaudt, L., Fu, J., Henckaerts, L., Zhernakova, A., Wijmenga, C., Raes, J., 2016. Population-level analysis of gut microbiome variation. Science (80-.). 352, 560–564. https://doi.org/10.1126/science.aad3503

Farkas, Z., Petric, M., Liu, X., Herit, F., Rajnavölgyi, É., Szondy, Z., Budai, Z., Orbán, T.I.,

Sándor, S., Mehta, A., Bajtay, Z., Kovács, T., Jung, S.Y., Shakir, M.A., Qin, J., Zhou, Z., Niedergang, F., Boissan, M., Takács-Vellai, K., 2019. The nucleoside diphosphate kinase NDK-1/NME1 promotes phagocytosis in concert with DYN-1/Dynamin. FASEB J. 33, 11606–11614. https://doi.org/10.1096/fj.201900220R

Fernandez-Ruiz, I., Puchalska, P., Narasimhulu, C.A., Sengupta, B., Parthasarathy, S., 2016. Differential lipid metabolism in monocytes and macrophages: Influence of cholesterol loading. J. Lipid Res. 57, 574–586. https://doi.org/10.1194/jlr.M062752

Fernie, A.R., Carrari, F., Sweetlove, L.J., 2004. Respiratory metabolism: Glycolysis, the TCA cycle and mitochondrial electron transport. Curr. Opin. Plant Biol. 7, 254–261. https://doi.org/10.1016/j.pbi.2004.03.007

Ferrero, E., Magni, E., Curnis, F., Villa, A., Ferrero, M.E., Corti, A., 2002. Regulation of endothelial cell shape and barrier function by chromogranin A, in: Annals of the New York Academy of Sciences. New York Academy of Sciences, pp. 355–358. https://doi.org/10.1111/j.1749-6632.2002.tb04495.x

File, S.E., Seth, P., 2003. A review of 25 years of the social interaction test. Eur. J. Pharmacol. 463, 35–53. https://doi.org/10.1016/S0014-2999(03)01273-1

Filiano, A.J., Xu, Y., Tustison, N.J., Marsh, R.L., Baker, W., Smirnov, I., Overall, C.C., Gadani, S.P., Turner, S.D., Weng, Z., Peerzade, S.N., Chen, H., Lee, K.S., Scott, M.M., Beenhakker, M.P., Litvak, V., Kipnis, J., 2016. Unexpected role of interferon-γ 3 in regulating neuronal connectivity and social behaviour. Nature 535, 425–429. https://doi.org/10.1038/nature18626

Fine, R., Vieira, S.M., Ruiz, D.F.Z., Kriegel, M.A., 2018. Gut pathobiont translocation induces lymphocyte migration to internal organs in autoimmunity. J. Immunol. 200, 102.16.

Fiorucci, S., Biagioli, M., Zampella, A., Distrutti, E., 2018. Bile acids activated receptors regulate innate immunity. Front. Immunol. https://doi.org/10.3389/fimmu.2018.01853

Fleshner, M., Frank, M., Maier, S.F., 2017. Danger signals and inflammasomes: stress-evoked sterile inflammation in mood disorders. Neuropsychopharmacology 42, 36–45. https://doi.org/10.1038/npp.2016.125

Flint, H.J., Duncan, S.H., Scott, K.P., Louis, P., 2014. Links between diet, gut microbiota composition and gut metabolism, in: Proceedings of the Nutrition Society. Cambridge University Press, pp. 13–22. https://doi.org/10.1017/S0029665114001463

Flory, J.D., Yehuda, R., 2015. Comorbidity between post-traumatic stress disorder and major depressive disorder: Alternative explanations and treatment considerations. Dialogues Clin. Neurosci. 17, 141–150. https://doi.org/10.31887/dcns.2015.17.2/jflory

Fonken, L.K., Frank, M.G., D'Angelo, H.M., Heinze, J.D., Watkins, L.R., Lowry, C.A., Maier, S.F., 2018. *Mycobacterium vaccae* immunization protects aged rats from surgery-elicited neuroinflammation and cognitive dysfunction. Neurobiol. Aging 71, 105–114. https://doi.org/10.1016/j.neurobiolaging.2018.07.012

Fonken, L.K., Frank, M.G., Kitt, M.M., D'Angelo, H.M., Norden, D.M., Weber, M.D., Barrientos, R.M., Godbout, J.P., Watkins, L.R., Maier, S.F., 2016. The alarmin HMGB1 mediates age-induced neuroinflammatory priming. J. Neurosci. 36, 7946–7956. https://doi.org/10.1523/JNEUROSCI.1161-16.2016

Fonkoue, I.T., Michopoulos, V., Park, J., 2020. Sex differences in post-traumatic stress disorder risk: autonomic control and inflammation. Clin. Auton. Res. 30, 409–421. https://doi.org/10.1007/s10286-020-00729-7

Forbes, L., Ebsworth-Mojica, K., DiDone, L., Li, S.-G., Freundlich, J.S., Connell, N., Dunman, P.M., Krysan, D.J., 2015. A high throughput screening assay for anti-mycobacterial small molecules based on adenylate kinase release as a reporter of cell lysis. PLoS One 10, e0129234. https://doi.org/10.1371/journal.pone.0129234

Förster, M.E.C., Staib, W., 1992. β-Oxidation as channeled reaction linked to citric acid cycle: Evidence from measurements of mitochondrial pyruvate oxidation during fatty acid degradation. Int. J. Biochem. 24, 1111–1116. https://doi.org/10.1016/0020-711X(92)90381-A

Fox, J.G., Gorelick, P.L., Kullberg, M.C., Ge, Z., Dewhirst, F.E., Ward, J.M., 1999. A novel urease-negative *Helicobacter* species associated with colitis and typhlitis in IL-10-deficient mice. Infect. Immun. 67, 1757–62.

Fox, J.H., Hassell, J.E., Siebler, P.H., Arnold, M.R., Lamb, A.K., Smith, D.G., Day, H.E.W., Smith, T.M., Simmerman, E.M., Outzen, A.A., Holmes, K.S., Brazell, C.J., Lowry, C.A., 2017. Preimmunization with a heat-killed preparation of *Mycobacterium vaccae* enhances fear extinction in the fear-potentiated startle paradigm. Brain. Behav. Immun. 66, 70–84. https://doi.org/10.1016/j.bbi.2017.08.014

Fox, J.M., Kausar, F., Day, A., Osborne, M., Hussain, K., Mueller, A., Lin, J., Tsuchiya, T.,

Kanegasaki, S., Pease, J.E., 2018. CXCL4/platelet factor 4 is an agonist of CCR1 and drives human monocyte migration. Sci. Rep. 8, 9466. https://doi.org/10.1038/s41598-018-27710-9

Foxx, C.L., Heinze, J.D., González, A., Vargas, F., Baratta, M. V., Elsayed, A.I., Stewart, J.R., Loupy, K.M., Arnold, M.R., Flux, M.C., Sago, S.A., Siebler, P.H., Milton, L.N., Lieb, M.W., Hassell, J.E., Smith, D.G., Lee, K.A.K., Appiah, S.A., Schaefer, E.J., Panitchpakdi, M., Sikora, N.C., Weldon, K.C., Stamper, C.E., Schmidt, D., Duggan, D.A., Mengesha, Y.M., Ogbaselassie, M., Nguyen, K.T., Gates, C.A., Schnabel, K., Tran, L., Jones, J.D., Vitaterna, M.H., Turek, F.W., Fleshner, M., Dorrestein, P.C., Knight, R., Wright, K.P., Lowry, C.A., 2021. Effects of immunization with the soil-derived bacterium *Mycobacterium vaccae* on stress coping behaviors and cognitive performance in a "two hit" stressor model. Front. Physiol. 11, 524833. https://doi.org/10.3389/fphys.2020.524833

Fragkos, K.C., Forbes, A., 2018. Citrulline as a marker of intestinal function and absorption in clinical settings: A systematic review and meta-analysis. United Eur. Gastroenterol. J. 6, 181–191. https://doi.org/10.1177/2050640617737632

Frank, M.G., Baratta, M. V., Sprunger, D.B., Watkins, L.R., Maier, S.F., 2007. Microglia serve as a neuroimmune substrate for stress-induced potentiation of CNS pro-inflammatory cytokine responses. Brain. Behav. Immun. 21, 47–59. https://doi.org/10.1016/J.BBI.2006.03.005

Frank, M.G., Fonken, L.K., Annis, J.L., Watkins, L.R., Maier, S.F., 2018a. Stress disinhibits microglia via down-regulation of CD200R: A mechanism of neuroinflammatory priming. Brain. Behav. Immun. 69, 62–73. https://doi.org/10.1016/j.bbi.2017.11.001

Frank, M.G., Fonken, L.K., Dolzani, S.D., Annis, J.L., Siebler, P.H., Schmidt, D., Watkins, L.R., Maier, S.F., Lowry, C.A., 2018b. Immunization with *Mycobacterium vaccae* induces an anti-inflammatory milieu in the CNS: Attenuation of stress-induced microglial priming, alarmins and anxiety-like behavior. Brain. Behav. Immun. 73, 352–363. https://doi.org/10.1016/j.bbi.2018.05.020

Frank, M.G., Fonken, L.K., Watkins, L.R., Maier, S.F., Lowry, C.A., 2019. Could probiotics be used to mitigate neuroinflammation? ACS Chem. Neurosci. 10, 13–15. https://doi.org/10.1021/acschemneuro.8b00386

Frank, M.G., Weber, M.D., Watkins, L.R., Maier, S.F., 2015. Stress sounds the alarmin: The role of the danger-associated molecular pattern HMGB1 in stress-induced neuroinflammatory

priming. Brain. Behav. Immun. 48, 1–7. https://doi.org/10.1016/j.bbi.2015.03.010

Freyne, B., Messina, N.L., Donath, S., Germano, S., Bonnici, R., Gardiner, K., Casalaz, D., Robins-Browne, R.M., Netea, M.G., Flanagan, K.L., Kollman, T., Curtis, N., 2020. Neonatal BCG vaccination reduces interferon-γ responsiveness to heterologous pathogens in infants from a randomized controlled trial - PubMed. J. Infect. Dis. 221, 1999–2009.

Fujii, H., Takatori, S., Zamami, Y., Hashikawa-Hobara, N., Miyake, N., Tangsucharit, P., Mio, M., Kawasaki, H., 2012. Adrenergic stimulation-released 5-HT stored in adrenergic nerves inhibits CGRPergic nerve-mediated vasodilatation in rat mesenteric resistance arteries. Br. J. Pharmacol. 166, 2084–2094. https://doi.org/10.1111/j.1476-5381.2012.01935.x

Fujimura, Y., 1986. Functional morphology of microfold cells (M cells) in Peyer's patches--phagocytosis and transport of BCG by M cells into rabbit Peyer's patches. Gastroenterol. Jpn. 21, 325–35.

Fukui, H., Oshima, T., Tanaka, Y., Oikawa, Y., Makizaki, Y., Ohno, H., Tomita, T., Watari, J., Miwa, H., 2018. Effect of probiotic *Bifidobacterium bifidum* G9-1 on the relationship between gut microbiota profile and stress sensitivity in maternally separated rats. Sci. Rep. 8, 12384. https://doi.org/10.1038/s41598-018-30943-3

Funk, C.D., 2001. Prostaglandins and leukotrienes: Advances in eicosanoid biology. Science (80-.). 294, 1871–1875. https://doi.org/10.1126/science.294.5548.1871

Furusawa, Y., Obata, Y., Fukuda, S., Endo, T.A., Nakato, G., Takahashi, D., Nakanishi, Y., Uetake, C., Kato, K., Kato, T., Takahashi, M., Fukuda, N.N., Murakami, S., Miyauchi, E., Hino, S., Atarashi, K., Onawa, S., Fujimura, Y., Lockett, T., Clarke, J.M., Topping, D.L., Tomita, M., Hori, S., Ohara, O., Morita, T., Koseki, H., Kikuchi, J., Honda, K., Hase, K., Ohno, H., 2013. Commensal microbe-derived butyrate induces the differentiation of colonic regulatory T cells. Nature 504, 446–450. https://doi.org/10.1038/nature12721

Furuyashiki, T., Akiyama, S., Kitaoka, S., 2019. Roles of multiple lipid mediators in stress and depression. Int. Immunol. 31, 579–587. https://doi.org/10.1093/intimm/dxz023

Furuyashiki, T., Narumiya, S., 2011. Stress responses: The contribution of prostaglandin E2 and its receptors. Nat. Rev. Endocrinol. 7, 163–175. https://doi.org/10.1038/nrendo.2010.194

Gago, G., Diacovich, L., Gramajo, H., 2018. Lipid metabolism and its implication in mycobacteria–host interaction. Curr. Opin. Microbiol. 41, 36–42. https://doi.org/10.1016/j.mib.2017.11.020

Gao, X., Cao, Q., Cheng, Y., Zhao, D., Wang, Z., Yang, H., Wu, Q., You, L., Wang, Yue, Lin, Y., Li, X., Wang, Yun, Bian, J.-S., Sun, D., Kong, L., Birnbaumer, L., Yang, Y., 2018. Chronic stress promotes colitis by disturbing the gut microbiota and triggering immune system response. Proc. Natl. Acad. Sci. U. S. A. 115, E2960–E2969. https://doi.org/10.1073/pnas.1720696115

Gao, X.L., Kim, S.J., Zhao, T., Ren, M.F., Chae, J.K., 2020. Social defeat stress induces myocardial injury by modulating inflammatory factors. J. Int. Med. Res. 48, 1–14. https://doi.org/10.1177/0300060520936903

Gaonac'h-Lovejoy, V., Boscher, C., Delisle, C., Gratton, J.-P., 2020. Rap1 is involved in angiopoietin-1-induced cell-cell junction stabilization and endothelial cell sprouting. Cells 9, 155. https://doi.org/10.3390/cells9010155

Garcia-Sabaté, A., Mohamed, W.K.E., Sapudom, J., Alatoom, A., Al Safadi, L., Teo, J.C.M., 2020. Biomimetic 3D models for investigating the role of monocytes and macrophages in atherosclerosis. Bioengineering 7, 1–20. https://doi.org/10.3390/bioengineering7030113

Gautam, A., Kumar, R., Chakraborty, N., Muhie, S., Hoke, A., Hammamieh, R., Jett, M., 2018. Altered fecal microbiota composition in all male aggressor-exposed rodent model simulating features of post-traumatic stress disorder. J. Neurosci. Res. 96, 1311–1323. https://doi.org/10.1002/jnr.24229

Ge, R., Tornero, D., Hirota, M., Monni, E., Laterza, C., Lindvall, O., Kokaia, Z., 2017. Choroid plexus-cerebrospinal fluid route for monocyte-derived macrophages after stroke. J. Neuroinflammation 14, 153. https://doi.org/10.1186/s12974-017-0909-3

GenBank [Internet], 1982. . Bethesda Natl. Libr. Med. (US), Natl. Cent. Biotechnol. Inf.

Getz, G.S., Reardon, C.A., 2019. Apoproteins E, A-I, and SAA in macrophage pathobiology related to atherogenesis. Front. Pharmacol. 10, 536. https://doi.org/10.3389/fphar.2019.00536

Ghia, J.E., Blennerhassett, P., Kumar-Ondiveeran, H., Verdu, E.F., Collins, S.M., 2006. The vagus nerve: a tonic inhibitory influence associated with inflammatory bowel disease in a murine model. Gastroenterology 131, 1122–30. https://doi.org/10.1053/j.gastro.2006.08.016

Gil-de-Gómez, L., Monge, P., Rodríguez, J.P., Astudillo, A.M., Balboa, M.A., Balsinde, J., 2020. Phospholipid arachidonic acid remodeling during phagocytosis in mouse peritoneal macrophages. Biomedicines 8, 274. https://doi.org/10.3390/BIOMEDICINES8080274

Gill, J., Vythilingam, M., Page, G.G., 2008. Low cortisol, high DHEA, and high levels of stimulated TNF-α, and IL-6 in women with PTSD. J. Trauma. Stress 21, 530–539. https://doi.org/10.1002/jts.20372

Ginzburg, K., Ein-Dor, T., Solomon, Z., 2010. Comorbidity of posttraumatic stress disorder, anxiety and depression: A 20-year longitudinal study of war veterans. J. Affect. Disord. 123, 249–257. https://doi.org/10.1016/j.jad.2009.08.006

Girinathan, B.P., Braun, S., Sirigireddy, A.R., Lopez, J.E., Govind, R., 2016. Importance of glutamate dehydrogenase (GDH) in Clostridium difficile colonization in vivo. PLoS One 11, e0160107. https://doi.org/10.1371/journal.pone.0160107

Gleissner, C.A., Shaked, I., Little, K.M., Ley, K., 2010. CXC chemokine ligand 4 induces a unique transcriptome in monocyte-derived macrophages. J. Immunol. 184, 4810–4818. https://doi.org/10.4049/jimmunol.0901368

Gocke, A.R., Hussain, R.Z., Yang, Y., Peng, H., Weiner, J., Ben, L.-H., Drew, P.D., Stuve, O., Lovett-Racke, A.E., Racke, M.K., 2009. Transcriptional modulation of the immune response by peroxisome proliferator-activated receptor-α agonists in autoimmune disease. J. Immunol. 182, 4479–4487. https://doi.org/10.4049/jimmunol.0713927

Godoy, C.M.G., Bassani, R.A., Bassani, J.W.M., 1999. Role of acetylcholine in electrical stimulation-induced arrhythmia in rat isolated atria. J. Cardiovasc. Pharmacol. 34, 475–479. https://doi.org/10.1097/00005344-199910000-00001

Gola, H., Engler, H., Sommershof, A., Adenauer, H., Kolassa, S., Schedlowski, M., Groettrup, M., Elbert, T., Kolassa, I.-T., 2013. Posttraumatic stress disorder is associated with an enhanced spontaneous production of pro-inflammatory cytokines by peripheral blood mononuclear cells. BMC Psychiatry 13, 40. https://doi.org/10.1186/1471-244X-13-40

Goldstein, R.B., Smith, S.M., Chou, S.P., Saha, T.D., Jung, J., Zhang, H., Pickering, R.P., Ruan, W.J., Huang, B., Grant, B.F., 2016. The epidemiology of DSM-5 posttraumatic stress disorder in the United States: results from the National Epidemiologic Survey on Alcohol and Related Conditions-III. Soc. Psychiatry Psychiatr. Epidemiol. 51, 1137–1148. https://doi.org/10.1007/s00127-016-1208-5

Gomes-Neto, J.C., Kittana, H., Mantz, S., Segura Munoz, R.R., Schmaltz, R.J., Bindels, L.B., Clarke, J., Hostetter, J.M., Benson, A.K., Walter, J., Ramer-Tait, A.E., 2017. A gut pathobiont synergizes with the microbiota to instigate inflammatory disease marked by

immunoreactivity against other symbionts but not itself. Sci. Rep. 7, 17707. https://doi.org/10.1038/s41598-017-18014-5

Gong, W.P., Liang, Y., Ling, Y.B., Zhang, J.X., Yang, Y.R., Wang, L., Wang, J., Shi, Y.C., Wu, X.Q., 2020. Effects of *Mycobacterium vaccae* vaccine in a mouse model of tuberculosis: Protective action and differentially expressed genes. Mil. Med. Res. 7, 25. https://doi.org/10.1186/s40779-020-00258-4

Gorczynski, R.M., 2005. CD200 and its receptors as targets for immunoregulation. Curr. Opin. Investig. Drugs 6, 483–488.

Gordan, R., Gwathmey, J.K., Xie, L.-H., 2015. Autonomic and endocrine control of cardiovascular function. World J. Cardiol. 7, 204. https://doi.org/10.4330/wjc.v7.i4.204

Gordon, S., Taylor, P.R., 2005. Monocyte and macrophage heterogeneity. Nat. Rev. Immunol. https://doi.org/10.1038/nri1733

Goshen, I., Yirmiya, R., 2009. Interleukin-1 (IL-1): A central regulator of stress responses. Front. Neuroendocrinol. 30, 30–45. https://doi.org/10.1016/j.yfrne.2008.10.001

Goswami, C., Iwasaki, Y., Yada, T., 2018. Short-chain fatty acids suppress food intake by activating vagal afferent neurons. J. Nutr. Biochem. 57, 130–135. https://doi.org/10.1016/j.jnutbio.2018.03.009

Goto, T., Kim, Y. Il, Furuzono, T., Takahashi, N., Yamakuni, K., Yang, H.E., Li, Y., Ohue, R., Nomura, W., Sugawara, T., Yu, R., Kitamura, N., Park, S.B., Kishino, S., Ogawa, J., Kawada, T., 2015. 10-oxo-12(Z)-octadecenoic acid, a linoleic acid metabolite produced by gut lactic acid bacteria, potently activates PPARγ and stimulates adipogenesis. Biochem. Biophys. Res. Commun. 459, 597–603. https://doi.org/10.1016/j.bbrc.2015.02.154

Grab, D.J., Kennedy, P.G.E., 2008. Traversal of human and animal trypanosomes across the blood-brain barrier. J. Neurovirol. 14, 344–351. https://doi.org/10.1080/13550280802282934

Gram, M., Sveinsdottir, S., Cinthio, M., Sveinsdottir, K., Hansson, S.R., Mörgelin, M., Åkerström, B., Ley, D., 2014. Extracellular hemoglobin - mediator of inflammation and cell death in the choroid plexus following preterm intraventricular hemorrhage. J. Neuroinflammation 11, 200. https://doi.org/10.1186/s12974-014-0200-9

Grant, R.S., 2018. Indoleamine 2,3-dioxygenase activity increases NAD+ production in IFN-γ-stimulated human primary mononuclear cells. Int. J. Tryptophan Res. 11, 1–8.

https://doi.org/10.1177/1178646917751636

Greene, L.I., Bruno, T.C., Christenson, J.L., D'Alessandro, A., Culp-Hill, R., Torkko, K., Borges, V.F., Slansky, J.E., Richer, J.K., 2019. A role for tryptophan-2,3-dioxygenase in CD8 T-cell suppression and evidence of tryptophan catabolism in breast cancer patient plasma. Mol. Cancer Res. 17, 131–139. https://doi.org/10.1158/1541-7786.MCR-18-0362

Greenwood, B.N., Foley, T.E., Day, H.E.W., Campisi, J., Hammack, S.H., Campeau, S., Maier, S.F., Fleshner, M., 2003a. Freewheel running prevents learned helplessness/behavioral depression: role of dorsal raphe serotonergic neurons. J. Neurosci. 23, 2889–2898.

Greenwood, B.N., Kennedy, S., Smith, T.P., Campeau, S., Day, H.E.W., Fleshner, M., 2003b. Voluntary freewheel running selectively modulates catecholamine content in peripheral tissue and c-Fos expression in the central sympathetic circuit following exposure to uncontrollable stress in rats. Neuroscience 120, 269–281. https://doi.org/10.1016/S0306-4522(03)00047-2

Gross, S., Devraj, K., Feng, Y., Macas, J., Liebner, S., Wieland, T., 2017. Nucleoside diphosphate kinase B regulates angiogenic responses in the endothelium via caveolae formation and c-Src-mediated caveolin-1 phosphorylation. J. Cereb. Blood Flow Metab. 37, 2471–2484. https://doi.org/10.1177/0271678X16669365

Grosse, L., Carvalho, L.A., Wijkhuijs, A.J.M., Bellingrath, S., Ruland, T., Ambrée, O., Alferink, J., Ehring, T., Drexhage, H.A., Arolt, V., 2015. Clinical characteristics of inflammation-associated depression: Monocyte gene expression is age-related in major depressive disorder. Brain. Behav. Immun. 44, 48–56. https://doi.org/10.1016/j.bbi.2014.08.004

Groux, H., O'Garra, A., Bigler, M., Rouleau, M., Antonenko, S., De Vries, J.E., Roncarolo, M.G., 1997. A CD4+ T-cell subset inhibits antigen-specific T-cell responses and prevents colitis. Nature 389, 737–742. https://doi.org/10.1038/39614

Grubbs, F.E., 1969. Procedures for detecting outlying observations in samples. Technometrics 11, 1–21. https://doi.org/10.1080/00401706.1969.10490657

Grygiel-Górniak, B., 2014. Peroxisome proliferator-activated receptors and their ligands: Nutritional and clinical implications - A review. Nutr. J. 13, 1–10. https://doi.org/10.1186/1475-2891-13-17

Guido, D.M., Mckenna, R., Mathews, W.R., 1993. Quantitation of hydroperoxy-eicosatetraenoic acids and hydroxy-eicosatetraenoic acids as indicators of lipid peroxidation using gas

chromatography-mass spectrometry. Anal. Biochem. 209, 123–129. https://doi.org/10.1006/abio.1993.1091

Guillemin, G.J., Smith, D.G., Smythe, G.A., Armati, P.J., Brew, B.J., 2003. Expression of the kynurenine pathway enzymes in human microglia and macrophages, in: Advances in Experimental Medicine and Biology. Kluwer Academic/Plenum Publishers, pp. 105–112. https://doi.org/10.1007/978-1-4615-0135-0_12

Guillot, A., Tacke, F., 2019. Liver macrophages: Old dogmas and new insights. Hepatol. Commun. 3, 730–743. https://doi.org/10.1002/hep4.1356

Guo, G., Jia, K.-R., Shi, Y., Liu, X.-F., Liu, K.-Y., Qi, W., Guo, Y., Zhang, W.-J., Wang, T., Xiao, B., Zou, Q.-M., 2009. Psychological stress enhances the colonization of the stomach by *Helicobacter pylori* in the BALB/c mouse. Stress 12, 478–485. https://doi.org/10.3109/10253890802642188

Guo, M., Li, C., Lei, Y., Xu, S., Zhao, D., Lu, X.Y., 2017. Role of the adipose PPAR-γ adiponectin axis in susceptibility to stress and depression/anxiety-related behaviors. Mol. Psychiatry 22, 1056–1068. https://doi.org/10.1038/mp.2016.225

Gupta, R.S., Lo, B., Son, J., 2018. Phylogenomics and comparative genomic studies robustly support division of the genus *Mycobacterium* into an emended genus *Mycobacterium* and four novel genera. Front. Microbiol. 9, 67. https://doi.org/10.3389/fmicb.2018.00067

Haghikia, A., Jörg, S., Duscha, A., Berg, J., Manzel, A., Waschbisch, A., Hammer, A., Lee, D.-H., May, C., Wilck, N., Balogh, A., Ostermann, A.I., Schebb, N.H., Akkad, D.A., Grohme, D.A., Kleinewietfeld, M., Kempa, S., Thöne, J., Demir, S., Müller, D.N., Gold, R., Linker, R.A., 2015. Dietary fatty acids directly impact central nervous system autoimmunity via the small intestine. Immunity 43, 817–829. https://doi.org/10.1016/J.IMMUNI.2015.09.007

Halfvarson, J., Jess, T., Magnuson, A., Montgomery, S.M., Orholm, M., Tysk, C., Binder, V., Järnerot, G., 2006. Environmental factors in inflammatory bowel disease: A co-twin control study of a Swedish-Danish twin population. Inflamm. Bowel Dis. 12, 925–933. https://doi.org/10.1097/01.mib.0000228998.29466.ac

Hamilton, T.A., Rigsbee, J.E., Scott, W.A., Adams, D.O., 1985. gamma-Interferon enhances the secretion of arachidonic acid metabolites from murine peritoneal macrophages stimulated with phorbol diesters. J. Immunol. 134, 2631–2636.

Hammer, G., Liang, J., Huang, H.-I., Benzatti, F., Karlsson, A., Hale, L.P., 2016. Microbiota

upregulate distinct APC functions in each intestinal dendritic cell subset, in a Myd88-independent fashion. J. Immunol. 196, 126.

Han, C.Y., 2018. Update on FXR biology: Promising therapeutic target? Int. J. Mol. Sci. 19, 2069. https://doi.org/10.3390/ijms19072069

Hantsoo, L., Criniti, S., McGeehan, B., Tanes, C., Elovitz, M., Compher, C., Wu, G., Epperson, C.N., 2018. Cortisol response to acute stress is associated with differential abundance of taxa in human gut microbiome. Biol. Psychiatry 83, S300–S301. https://doi.org/10.1016/J.BIOPSYCH.2018.02.774

Hassell, J.E., Fox, J.H., Arnold, M.R., Siebler, P.H., Lieb, M.W., Schmidt, D., Spratt, E.J., Smith, T.M., Nguyen, K.T., Gates, C.A., Holmes, K.S., Schnabel, K.S., Loupy, K.M., Erber, M., Lowry, C.A., 2019. Treatment with a heat-killed preparation of *Mycobacterium vaccae* after fear conditioning enhances fear extinction in the fear-potentiated startle paradigm. Brain. Behav. Immun. 81, 151–160. https://doi.org/10.1016/j.bbi.2019.06.008

Hata, T., Asano, Y., Yoshihara, K., Kimura-Todani, T., Miyata, N., Zhang, X.-T., Takakura, S., Aiba, Y., Koga, Y., Sudo, N., 2017. Regulation of gut luminal serotonin by commensal microbiota in mice. PLoS One 12, e0180745. https://doi.org/10.1371/journal.pone.0180745

Hebbandi Nanjundappa, R., Ronchi, F., Wang, J., Clemente-Casares, X., Yamanouchi, J., Sokke Umeshappa, C., Yang, Y., Blanco, J., Bassolas-Molina, H., Salas, A., Khan, H., Slattery, R.M., Wyss, M., Mooser, C., Macpherson, A.J., Sycuro, L.K., Serra, P., McKay, D.M., McCoy, K.D., Santamaria, P., 2017. A gut microbial mimic that hijacks diabetogenic autoreactivity to suppress colitis. Cell 171, 655-667.e17. https://doi.org/10.1016/j.cell.2017.09.022

Heim, C., Newport, D.J., Heit, S., Graham, Y.P., Wilcox, M., Bonsall, R., Miller, A.H., Nemeroff, C.B., 2000. Pituitary-adrenal and autonomic responses to stress in women after sexual and physical abuse in childhood. JAMA 284, 592–597.

Heinen, S., Hartmann, A., Lauer, N., Wiehl, U., Dahse, H.M., Schirmer, S., Gropp, K., Enghardt, T., Wallich, R., Hälbich, S., Mihlan, M., Schlötzer-Schrehardt, U., Zipfel, P.F., Skerka, C., 2009. Factor H-related protein 1 (CFHR-1) inhibits complement C5 convertase activity and terminal complex formation. Blood 114, 2439–2447. https://doi.org/10.1182/blood-2009-02-205641

Hemmings, S.M.J., Malan-Müller, S., van den Heuvel, L.L., Demmitt, B.A., Stanislawski, M.A.,

Smith, D.G., Bohr, A.D., Stamper, C.E., Hyde, E.R., Morton, J.T., Marotz, C.A., Siebler, P.H., Braspenning, M., Van Criekinge, W., Hoisington, A.J., Brenner, L.A., Postolache, T.T., McQueen, M.B., Krauter, K.S., Knight, R., Seedat, S., Lowry, C.A., 2017. The microbiome in posttraumatic stress disorder and trauma-exposed controls. Psychosom. Med. 79, 936–946. https://doi.org/10.1097/PSY.0000000000000512

Henson, M.A., Phalak, P., 2017. Microbiota dysbiosis in inflammatory bowel diseases: in silico investigation of the oxygen hypothesis. BMC Syst. Biol. 11, 145. https://doi.org/10.1186/s12918-017-0522-1

Heppner, P.S., Crawford, E.F., Haji, U.A., Afari, N., Hauger, R.L., Dashevsky, B.A., Horn, P.S., Nunnink, S.E., Baker, D.G., 2009. The association of posttraumatic stress disorder and metabolic syndrome: A study of increased health risk in veterans. BMC Med. 7. https://doi.org/10.1186/1741-7015-7-1

Herr, N., Bode, C., Duerschmied, D., 2017. The effects of serotonin in immune cells. Front. Cardiovasc. Med. 4, 48. https://doi.org/10.3389/fcvm.2017.00048

Herrera, B.S., Hasturk, H., Kantarci, A., Freire, M.O., Nguyen, O., Kansal, S., van Dyke, T.E., 2015. Impact of resolvin E1 on murine neutrophil phagocytosis in type 2 diabetes. Infect. Immun. 83, 792–801. https://doi.org/10.1128/IAI.02444-14

Herz, J., Filiano, A.J., Smith, A., Yogev, N., Kipnis, J., 2017. Myeloid cells in the central nervous system. Immunity 46, 943–956. https://doi.org/10.1016/j.immuni.2017.06.007

Ho, V.T., Shimbo, D., Duer-Hefele, J., Whang, W., Chang, M., Edmondson, D., 2016. Posttraumatic stress disorder symptoms and hypercoagulability during emergency department evaluation for acute coronary syndrome. IJC Metab. Endocr. 11, 1–2. https://doi.org/10.1016/j.ijcme.2016.03.002

Hoarau, J.-J., Krejbich-Trotot, P., Jaffar-Bandjee, M.-C., Das, T., Thon-Hon, G.-V., Kumar, S., W. Neal, J., Gasque, P., 2011. Activation and control of CNS innate immune responses in health and diseases: A balancing act finely tuned by neuroimmune regulators (NIReg). CNS Neurol. Disord. - Drug Targets 10, 25–43. https://doi.org/10.2174/187152711794488601

Hoban, A.E., Stilling, R.M., Moloney, G., Shanahan, F., Dinan, T.G., Clarke, G., Cryan, J.F., 2018. The microbiome regulates amygdala-dependent fear recall. Mol. Psychiatry 23, 1134–1144. https://doi.org/10.1038/mp.2017.100

Hodes, G.E., Ménard, C., Russo, S.J., 2016. Integrating Interleukin-6 into depression diagnosis

and treatment. Neurobiol. Stress 4, 15–22. https://doi.org/10.1016/j.ynstr.2016.03.003

Hodes, G.E., Pfau, M.L., Leboeuf, M., Golden, S.A., Christoffel, D.J., Bregman, D., Rebusi, N., Heshmati, M., Aleyasin, H., Warren, B.L., Labonté, B., Horn, S., Lapidus, K.A., Stelzhammer, V., Wong, E.H.F., Bahn, S., Krishnan, V., Bolaños-Guzman, C.A., Murrough, J.W., Merad, M., Russo, S.J., 2014. Individual differences in the peripheral immune system promote resilience versus susceptibility to social stress. Proc. Natl. Acad. Sci. 111, 16136–16141. https://doi.org/10.1073/PNAS.1415191111

Hofmann, A.F., 1999. The continuing importance of bile acids in liver and intestinal disease. Arch. Intern. Med. 159, 2647–2658. https://doi.org/10.1001/archinte.159.22.2647

Hoge, C.W., Riviere, L.A., Wilk, J.E., Herrell, R.K., Weathers, F.W., 2014. The prevalence of post-traumatic stress disorder (PTSD) in US combat soldiers: a head-to-head comparison of DSM-5 versus DSM-IV-TR symptom criteria with the PTSD checklist. The Lancet Psychiatry 1, 269–277. https://doi.org/10.1016/S2215-0366(14)70235-4

Hoisington, A.J., Billera, D.M., Bates, K.L., Stamper, C.E., Stearns-Yoder, K.A., Lowry, C.A., Brenner, L.A., 2018a. Exploring service dogs for rehabilitation of veterans with PTSD: A microbiome perspective. Rehabil. Psychol. 63, 575–587. https://doi.org/10.1037/rep0000237

Hoisington, A.J., Lowry, C., Stearns-Yoder, K., Brenner, L., Postolache, T., 2018b. Biological signature of an immunomodulatory probiotic intervention for veterans with mild TBI & PTSD. Arch. Phys. Med. Rehabil. 99, e130. https://doi.org/10.1016/j.apmr.2018.08.008

Holdcroft, A., 1975. Prostaglandins—A review. Anaesth. Intensive Care 3, 105–113. https://doi.org/10.1177/0310057X7500300204

Honda, K.L., Lamon-Fava, S., Matthan, N.R., Wu, D., Lichtenstein, A.H., 2015. EPA and DHA exposure alters the inflammatory response but not the surface expression of toll-like receptor 4 in macrophages. Lipids 50, 121–129. https://doi.org/10.1007/s11745-014-3971-y

Hoppen, T.H., Morina, N., 2019. The prevalence of PTSD and major depression in the global population of adult war survivors: a meta-analytically informed estimate in absolute numbers. Eur. J. Psychotraumatol. 10, 1578637. https://doi.org/10.1080/20008198.2019.1578637

Hopper, J.W., Spinazzola, J., Simpson, W.B., van der Kolk, B.A., 2006. Preliminary evidence of parasympathetic influence on basal heart rate in posttraumatic stress disorder. J. Psychosom.

Res. 60, 83–90. https://doi.org/10.1016/j.jpsychores.2005.06.002

Hornigold, D.C., Roth, E., Howard, V., Will, S., Oldham, S., Coghlan, M.P., Blouet, C., Trevaskis, J.L., 2018. A GLP-1:CCK fusion peptide harnesses the synergistic effects on metabolism of CCK-1 and GLP-1 receptor agonism in mice. Appetite 127, 334–340. https://doi.org/10.1016/j.appet.2018.05.131

Houlden, A., Goldrick, M., Brough, D., Vizi, E.S., Lénárt, N., Martinecz, B., Roberts, I.S., Denes, A., 2016. Brain injury induces specific changes in the caecal microbiota of mice via altered autonomic activity and mucoprotein production. Brain. Behav. Immun. 57, 10–20. https://doi.org/10.1016/J.BBI.2016.04.003

Hovhannisyan, L.P., Mkrtchyan, G.M., Sukiasian, S.H., Boyajyan, A.S., 2010. Alterations in the complement cascade in post-traumatic stress disorder. Allergy, Asthma Clin. Immunol. 6, 3. https://doi.org/10.1186/1710-1492-6-3

Howard, B.M., Kornblith, L.Z., Christie, S.A., Conroy, A.S., Nelson, M.F., Campion, E.M., Callcut, R.A., Calfee, C.S., Lamere, B.J., Fadrosh, D.W., Lynch, S., Cohen, M.J., 2017. Characterizing the gut microbiome in trauma: significant changes in microbial diversity occur early after severe injury. Trauma Surg. Acute Care Open 2, e000108. https://doi.org/10.1136/tsaco-2017-000108

Howard, N.C., Khader, S.A., 2020. Immunometabolism during *Mycobacterium tuberculosis* infection. Trends Microbiol. 28, 832–850. https://doi.org/10.1016/j.tim.2020.04.010

Hsieh, M.H., Jan, R.L., Wu, L.S.H., Chen, P.C., Kao, H.F., Kuo, W.S., Wang, J.Y., 2018. *Lactobacillus gasseri* attenuates allergic airway inflammation through PPARγ activation in dendritic cells. J. Mol. Med. 96, 39–51. https://doi.org/10.1007/s00109-017-1598-1

Hu, J., Lin, S., Zheng, B., Cheung, P.C.K., 2018. Short-chain fatty acids in control of energy metabolism. Crit. Rev. Food Sci. Nutr. 58, 1243–1249. https://doi.org/10.1080/10408398.2016.1245650

Hu, K., Sjölander, A., Lu, D., Walker, A.K., Sloan, E.K., Fall, K., Valdimarsdóttir, U., Hall, P., Smedby, K.E., Fang, F., 2020. Aspirin and other non-steroidal anti-inflammatory drugs and depression, anxiety, and stress-related disorders following a cancer diagnosis: A nationwide register-based cohort study. BMC Med. 18, 238. https://doi.org/10.1186/s12916-020-01709-4

Huang, C.T., Workman, C.J., Flies, D., Pan, X., Marson, A.L., Zhou, G., Hipkiss, E.L., Ravi, S.,

Kowalski, J., Levitsky, H.I., Powell, J.D., Pardoll, D.M., Drake, C.G., Vignali, D.A.A., 2004. Role of LAG-3 in regulatory T cells. Immunity 21, 503–513. https://doi.org/10.1016/j.immuni.2004.08.010

Huang, D.W., Sherman, B.T., Lempicki, R.A., 2009a. Systematic and integrative analysis of large gene lists using DAVID bioinformatics resources. Nat. Protoc. 4, 44–57. https://doi.org/10.1038/nprot.2008.211

Huang, D.W., Sherman, B.T., Lempicki, R.A., 2009b. Bioinformatics enrichment tools: Paths toward the comprehensive functional analysis of large gene lists. Nucleic Acids Res. 37, 1–13. https://doi.org/10.1093/nar/gkn923

Huang, E.Y., Inoue, T., Leone, V.A., Dalal, S., Touw, K., Wang, Y., Musch, M.W., Theriault, B., Higuchi, K., Donovan, S., Gilbert, J., Chang, E.B., 2015. Using corticosteroids to reshape the gut microbiome: implications for inflammatory bowel diseases. Inflamm. Bowel Dis. 21, 963–972. https://doi.org/10.1097/MIB.0000000000000332

Huang, W., Rha, G.B., Han, M.-J., Eum, S.Y., András, I.E., Zhong, Y., Hennig, B., Toborek, M., 2008. PPARα and PPARγ effectively protect against HIV-induced inflammatory responses in brain endothelial cells. J. Neurochem. 107, 497–509. https://doi.org/10.1111/j.1471-4159.2008.05626.x

Huang, Y., Shi, Xing, Li, Z., Shen, Y., Shi, Xinxin, Wang, L., Li, G., Yuan, Y., Wang, J., Zhang, Y., Zhao, L., Zhang, M., Kang, Y., Liang, Y., 2018. Possible association of Firmicutes in the gut microbiota of patients with major depressive disorder. Neuropsychiatr. Dis. Treat. 14, 3329–3337. https://doi.org/10.2147/NDT.S188340

Hubbard, T.D., Murray, I.A., Bisson, W.H., Lahoti, T.S., Gowda, K., Amin, S.G., Patterson, A.D., Perdew, G.H., 2015. Adaptation of the human aryl hydrocarbon receptor to sense microbiota-derived indoles. Sci. Rep. 5, 12689. https://doi.org/10.1038/srep12689

Hübner, M., Mantziari, S., Demartines, N., Pralong, F., Coti-Bertrand, P., Schäfer, M., 2016. Postoperative albumin drop is a marker for surgical stress and a predictor for clinical outcome: A pilot study. Gastroenterol. Res. Pract. 2016, 8743187. https://doi.org/10.1155/2016/8743187

Hughes, C.S., Foehr, S., Garfield, D.A., Furlong, E.E., Steinmetz, L.M., Krijgsveld, J., 2014. Ultrasensitive proteome analysis using paramagnetic bead technology. Mol. Syst. Biol. 10, 757. https://doi.org/10.15252/msb.20145625

Huntley, R.P., Sawford, T., Mutowo-Meullenet, P., Shypitsyna, A., Bonilla, C., Martin, M.J., O'Donovan, C., 2015. The GOA database: Gene Ontology annotation updates for 2015. Nucleic Acids Res. 43, D1057–D1063. https://doi.org/10.1093/nar/gku1113

Huo, R., Zeng, B., Zeng, L., Cheng, K., Li, B., Luo, Y., Wang, H., Zhou, C., Fang, L., Li, W., Niu, R., Wei, H., Xie, P., 2017. Microbiota modulate anxiety-like behavior and endocrine abnormalities in hypothalamic-pituitary-adrenal axis. Front. Cell. Infect. Microbiol. 7, 489. https://doi.org/10.3389/fcimb.2017.00489

Hurst, N.R., Kendig, D.M., Murthy, K.S., Grider, J.R., 2014. The short chain fatty acids, butyrate and propionate, have differential effects on the motility of the guinea pig colon. Neurogastroenterol. Motil. 26, 1586–1596. https://doi.org/10.1111/nmo.12425

Hussain, M.M., 2013. Metabolism: gut microbiota modulates diurnal secretion of glucocorticoids. Nat. Rev. Endocrinol. 9, 444–446. https://doi.org/10.1038/nrendo.2013.129

Ichimura, T., Uchiyama, J., Kunihiro, O., Itoh, M., Horigome, T., Omata, S., Shinkai, F., Kaji, H., Isobe, T., 1995. Identification of the site of interaction of the 14-3-3 protein with phosphorylated tryptophan hydroxylase. J. Biol. Chem. 270, 28515–28518. https://doi.org/10.1074/jbc.270.48.28515

Iwasaki, A., Kelsall, B.L., 1999. Freshly isolated peyer's patch, but not spleen, dendritic cells produce interleukin 10 and induce the differentiation of T helper type 2 cells. J. Exp. Med. 190, 229–239. https://doi.org/10.1084/jem.190.2.229

Iwasaki, Y., Sendo, M., Dezaki, K., Hira, T., Sato, T., Nakata, M., Goswami, C., Aoki, R., Arai, T., Kumari, P., Hayakawa, M., Masuda, C., Okada, T., Hara, H., Drucker, D.J., Yamada, Y., Tokuda, M., Yada, T., 2018. GLP-1 release and vagal afferent activation mediate the beneficial metabolic and chronotherapeutic effects of D-allulose. Nat. Commun. 9, 113. https://doi.org/10.1038/s41467-017-02488-y

Jacob, P.J., Manju, S.L., Ethiraj, K.R., Elias, G., 2018. Safer anti-inflammatory therapy through dual COX-2/5-LOX inhibitors: A structure-based approach. Eur. J. Pharm. Sci. 121, 356–381. https://doi.org/10.1016/j.ejps.2018.06.003

Jang, S., Uematsu, S., Akira, S., Salgame, P., 2004. IL-6 and IL-10 induction from dendritic cells in response to *Mycobacterium tuberculosis* is predominantly dependent on TLR2-mediated recognition. J. Immunol. 173, 3392–3397. https://doi.org/10.4049/jimmunol.173.5.3392

Jenness, J.L., Miller, A.B., Rosen, M.L., McLaughlin, K.A., 2018. Extinction learning as a

potential mechanism linking high vagal tone with lower PTSD symptoms among abused youth. J. Abnorm. Child Psychol. 1–12. https://doi.org/10.1007/s10802-018-0464-0

Jeong, S.Y., Lim, S.Y., Schevzov, G., Gunning, P.W., Helfman, D.M., 2017. Loss of Tpm4.1 leads to disruption of cell-cell adhesions and invasive behavior in breast epithelial cells via increased Rac1 signaling. Oncotarget 8, 33544–33559. https://doi.org/10.18632/oncotarget.16825

Jiang, H., Zhang, X., Yu, Z., Zhang, Z., Deng, M., Zhao, J., Ruan, B., 2018. Altered gut microbiota profile in patients with generalized anxiety disorder. J. Psychiatr. Res. 104, 130–136. https://doi.org/10.1016/J.JPSYCHIRES.2018.07.007

Jin, M., 2019. Unique roles of tryptophanyl-tRNA synthetase in immune control and its therapeutic implications. Exp. Mol. Med. https://doi.org/10.1038/s12276-018-0196-9

Johnson, J.D., O'Connor, K.A., Deak, T., Stark, M., Watkins, L.R., Maier, S.F., 2002. Prior stressor exposure sensitizes LPS-induced cytokine production. Brain. Behav. Immun. 16, 461–476. https://doi.org/10.1006/brbi.2001.0638

Jones, B.J., Tan, T., Bloom, S.R., 2012. Minireview: Glucagon in stress and energy homeostasis. Endocrinology 153, 1049–1054. https://doi.org/10.1210/en.2011-1979

Jones, P.M., Bennett, M.J., 2017. Disorders of mitochondrial fatty acid β-oxidation, in: Biomarkers in Inborn Errors of Metabolism. Elsevier, pp. 87–101. https://doi.org/10.1016/b978-0-12-802896-4.00005-5

Jones, S.P., Franco, N.F., Varney, B., Sundaram, G., Brown, D.A., de Bie, J., Lim, C.K., Guillemin, G.J., Brew, B.J., 2015. Expression of the kynurenine pathway in human peripheral blood mononuclear cells: Implications for inflammatory and neurodegenerative disease. PLoS One 10, e0131389. https://doi.org/10.1371/journal.pone.0131389

Jonkers, D., Penders, J., Masclee, A., Pierik, M., 2012. Probiotics in the management of inflammatory bowel disease. Drugs 72, 803–823. https://doi.org/10.2165/11632710-000000000-00000

Judd, L.L., Paulus, M.P., Wells, K.B., Rapaport, M.H., 1996. Socioeconomic burden of subsyndromal depressive symptoms and major depression in a sample of the general population. Am. J. Psychiatry 153, 1411–1417. https://doi.org/10.1176/ajp.153.11.1411

Jumeau, C., Awad, F., Assrawi, E., Cobret, L., Duquesnoy, P., Giurgea, I., Valeyre, D., Grateau, G., Amselem, S., Bernaudin, J.F., Karabina, S.A., 2019. Expression of SAA1, SAA2 and

SAA4 genes in human primary monocytes and monocyte-derived macrophages. PLoS One 14, e0217005. https://doi.org/10.1371/journal.pone.0217005

Just, S., Mondot, S., Ecker, J., Wegner, K., Rath, E., Gau, L., Streidl, T., Hery-Arnaud, G., Schmidt, S., Lesker, T.R., Bieth, V., Dunkel, A., Strowig, T., Hofmann, T., Haller, D., Liebisch, G., Gérard, P., Rohn, S., Lepage, P., Clavel, T., 2018. The gut microbiota drives the impact of bile acids and fat source in diet on mouse metabolism. Microbiome 6, 134. https://doi.org/10.1186/s40168-018-0510-8

Kabouridis, P.S., Lasrado, R., McCallum, S., Chng, S.H., Snippert, H.J., Clevers, H., Pettersson, S., Pachnis, V., 2015. Microbiota controls the homeostasis of glial cells in the gut lamina propria. Neuron 85, 289–295. https://doi.org/10.1016/j.neuron.2014.12.037

Kaelberer, M.M., Buchanan, K.L., Klein, M.E., Barth, B.B., Montoya, M.M., Shen, X., Bohórquez, D. V, 2018. A gut-brain neural circuit for nutrient sensory transduction. Science 361, eaat5236. https://doi.org/10.1126/science.aat5236

Kalkman, H.O., Feuerbach, D., 2016. Antidepressant therapies inhibit inflammation and microglial M1-polarization. Pharmacol. Ther. 163, 82–93. https://doi.org/10.1016/j.pharmthera.2016.04.001

Kambara, K., Ohashi, W., Tomita, K., Takashina, M., Fujisaka, S., Hayashi, R., Mori, H., Tobe, K., Hattori, Y., 2015. In vivo depletion of CD206+ M2 macrophages exaggerates lung injury in endotoxemic mice. Am. J. Pathol. 185, 162–171. https://doi.org/10.1016/j.ajpath.2014.09.005

Kanehisa, M., Goto, S., 2000. KEGG: Kyoto encyclopedia of genes and genomes. Nucleic Acids Res. 28, 27–30. https://doi.org/10.1093/nar/28.1.27

Kang, J.W., Lee, S.M., 2016. Resolvin D1 protects the liver from ischemia/reperfusion injury by enhancing: M2 macrophage polarization and efferocytosis. Biochim. Biophys. Acta - Mol. Cell Biol. Lipids 1861, 1025–1035. https://doi.org/10.1016/j.bbalip.2016.06.002

Kang, Kyuho, Park, S.H., Chen, J., Qiao, Y., Giannopoulou, E., Berg, K., Hanidu, A., Li, J., Nabozny, G., Kang, Keunsoo, Park-Min, K.H., Ivashkiv, L.B., 2017. Interferon-γ represses M2 gene expression in human macrophages by disassembling enhancers bound by the transcription factor MAF. Immunity 47, 235-250.e4. https://doi.org/10.1016/j.immuni.2017.07.017

Karabatsiakis, A., Hamuni, G., Wilker, S., Kolassa, S., Renu, D., Kadereit, S., Schauer, M.,

Hennessy, T., Kolassa, I.-T., 2015. Metabolite profiling in posttraumatic stress disorder. J. Mol. psychiatry 3, 2. https://doi.org/10.1186/s40303-015-0007-3

Karbach, S.H., Schönfelder, T., Brandão, I., Wilms, E., Hörmann, N., Jäckel, S., Schüler, R., Finger, S., Knorr, M., Lagrange, J., Brandt, M., Waisman, A., Kossmann, S., Schäfer, K., Münzel, T., Reinhardt, C., Wenzel, P., 2016. Gut microbiota promote angiotensin II-induced arterial hypertension and vascular dysfunction. J. Am. Heart Assoc. 5, e003698. https://doi.org/10.1161/JAHA.116.003698

Karl, J.P., Margolis, L.M., Madslien, E.H., Murphy, N.E., Castellani, J.W., Gundersen, Y., Hoke, A. V., Levangie, M.W., Kumar, R., Chakraborty, N., Gautam, A., Hammamieh, R., Martini, S., Montain, S.J., Pasiakos, S.M., 2017. Changes in intestinal microbiota composition and metabolism coincide with increased intestinal permeability in young adults under prolonged physiological stress. Am. J. Physiol. Liver Physiol. 312, G559–G571. https://doi.org/10.1152/ajpgi.00066.2017

Katsu, M., Niizuma, K., Yoshioka, H., Okami, N., Sakata, H., Chan, P.H., 2010. Hemoglobin-induced oxidative stress contributes to matrix metalloproteinase activation and blood-brain barrier dysfunction in vivo. J. Cereb. Blood Flow Metab. 30, 1939–1950. https://doi.org/10.1038/jcbfm.2010.45

Kawecki, C., Lenting, P.J., Denis, C. V., 2017. von Willebrand factor and inflammation. J. Thromb. Haemost. 15, 1285–1294. https://doi.org/10.1111/jth.13696

Kaysen, G.A., Dubin, J.A., Müller, H.G., Rosales, L., Levin, N.W., Mitch, W.E., 2004. Inflammation and reduced albumin synthesis associated with stable decline in serum albumin in hemodialysis patients. Kidney Int. 65, 1408–1415. https://doi.org/10.1111/j.1523-1755.2004.00520.x

Kazemi, A., Noorbala, A.A., Azam, K., Eskandari, M.H., Djafarian, K., 2018. Effect of probiotic and prebiotic vs placebo on psychological outcomes in patients with major depressive disorder: a randomized clinical trial. Clin. Nutr. 38, 522–528. https://doi.org/10.1016/j.clnu.2018.04.010

Keaton, S.A., Madaj, Z.B., Heilman, P., Smart, L.A., Grit, J., Gibbons, R., Postolache, T.T., Roaten, K., Achtyes, E.D., Brundin, L., 2019. An inflammatory profile linked to increased suicide risk. J. Affect. Disord. 247, 57–65. https://doi.org/10.1016/j.jad.2018.12.100

Kelbich, P., Radovnický, T., Selke-Krulichová, I., Lodin, J., Matuchová, I., Sameš, M.,

Procházka, J., Krejsek, J., Hanuljaková, E., Hejčl, A., 2020. Can aspartate aminotransferase in the cerebrospinal fluid be a reliable predictive parameter? Brain Sci. 10, 1–7. https://doi.org/10.3390/brainsci10100698

Kellermayer, R., Mir, S.A. V, Nagy-Szakal, D., Cox, S.B., Dowd, S.E., Kaplan, J.L., Sun, Y., Reddy, S., Bronsky, J., Winter, H.S., 2012. Microbiota separation and C-reactive protein elevation in treatment-naïve pediatric granulomatous Crohn disease. J. Pediatr. Gastroenterol. Nutr. 55, 243–250. https://doi.org/10.1097/MPG.0b013e3182617c16

Kessler, R.C., 2000. Posttraumatic stress disorder: The burden to the individual and to society, in: Journal of Clinical Psychiatry. pp. 4–12.

Kessler, R.C., Aguilar-Gaxiola, S., Alonso, J., Benjet, C., Bromet, E.J., Cardoso, G., Degenhardt, L., de Girolamo, G., Dinolova, R. V., Ferry, F., Florescu, S., Gureje, O., Haro, J.M., Huang, Y., Karam, E.G., Kawakami, N., Lee, S., Lepine, J.P., Levinson, D., Navarro-Mateu, F., Pennell, B.E., Piazza, M., Posada-Villa, J., Scott, K.M., Stein, D.J., Ten Have, M., Torres, Y., Viana, M.C., Petukhova, M. V., Sampson, N.A., Zaslavsky, A.M., Koenen, K.C., 2017. Trauma and PTSD in the WHO world mental health surveys. Eur. J. Psychotraumatol. 8, 1353383. https://doi.org/10.1080/20008198.2017.1353383

Kessler, R.C., Berglund, P., Demler, O., Jin, R., Merikangas, K.R., Walters, E.E., 2005. Lifetime prevalence and age-of-onset distributions of DSM-IV disorders in the National Comorbidity Survey Replication. Arch. Gen. Psychiatry 62, 593–602. https://doi.org/10.1001/archpsyc.62.6.593

Kessler, R.C., Sonnega, A., Bromet, E., Hughes, M., Nelson, C.B., 1995. Posttraumatic stress disorder in the national comorbidity survey. Arch. Gen. Psychiatry 52, 1048–1060. https://doi.org/10.1001/archpsyc.1995.03950240066012

Kidani, Y., Bensinger, S.J., 2012. Liver X receptor and peroxisome proliferator-activated receptor as integrators of lipid homeostasis and immunity. Immunol. Rev. 249, 72–83. https://doi.org/10.1111/j.1600-065X.2012.01153.x

Kierdorf, K., Masuda, T., Jordão, M.J.C., Prinz, M., 2019. Macrophages at CNS interfaces: ontogeny and function in health and disease. Nat. Rev. Neurosci. 20, 547–562. https://doi.org/10.1038/s41583-019-0201-x

Kilkenny, C., Browne, W.J., Cuthill, I.C., Emerson, M., Altman, D.G., 2010. Improving bioscience research reporting: the ARRIVE guidelines for reporting animal research. PLoS

Biol. 8, e1000412. https://doi.org/10.1371/journal.pbio.1000412

Kim, B.K., Fonda, J.R., Hauger, R.L., Pinna, G., Anderson, G.M., Valovski, I.T., Rasmusson, A.M., 2020. Composite contributions of cerebrospinal fluid GABAergic neurosteroids, neuropeptide Y and interleukin-6 to PTSD symptom severity in men with PTSD. Neurobiol. Stress 12, 100220. https://doi.org/10.1016/j.ynstr.2020.100220

Kim, H.-G., Cheon, E.-J., Bai, D.-S., Lee, Y.H., Koo, B.-H., 2018. Stress and heart rate variability: a meta-analysis and review of the literature. Psychiatry Investig. 15, 235–245. https://doi.org/10.30773/pi.2017.08.17

Kim, H.G., Cheon, E.J., Bai, D.S., Lee, Y.H., Koo, B.H., 2018. Stress and heart rate variability: A meta-analysis and review of the literature. Psychiatry Investig. 15, 235–245. https://doi.org/10.30773/pi.2017.08.17

Kim, J.H., Lee, Y.J., Park, B., 2019. Higher monocyte count with normal white blood cell count is positively associated with 10-year cardiovascular disease risk determined by Framingham risk score among community-dwelling Korean individuals. Medicine (Baltimore). 98, e15340. https://doi.org/10.1097/MD.0000000000015340

Kim, Y.-K., Jeon, S.W., 2018. Neuroinflammation and the immune-kynurenine pathway in anxiety disorders. Curr. Neuropharmacol. 16, 574–582. https://doi.org/10.2174/1570159x15666170913110426

Kim, Y.S., Lee, H.-M., Kim, J.K., Yang, C.-S., Kim, T.S., Jung, M., Jin, H.S., Kim, S., Jang, J., Oh, G.T., Kim, J.-M., Jo, E.-K., 2017. PPAR-α Activation Mediates Innate Host Defense through Induction of TFEB and Lipid Catabolism. J. Immunol. 198, 3283–3295. https://doi.org/10.4049/jimmunol.1601920

Kimura, I., Inoue, D., Maeda, T., Hara, T., Ichimura, A., Miyauchi, S., Kobayashi, M., Hirasawa, A., Tsujimoto, G., 2011. Short-chain fatty acids and ketones directly regulate sympathetic nervous system via G protein-coupled receptor 41 (GPR41). Proc. Natl. Acad. Sci. 108, 8030–8035. https://doi.org/10.1073/pnas.1016088108

Kishino, S., Takeuchi, M., Park, S.B., Hirata, A., Kitamura, N., Kunisawa, J., Kiyono, H., Iwamoto, R., Isobe, Y., Arita, M., Arai, H., Ueda, K., Shima, J., Takahashi, S., Yokozeki, K., Shimizu, S., Ogawa, J., 2013. Polyunsaturated fatty acid saturation by gut lactic acid bacteria affecting host lipid composition. Proc. Natl. Acad. Sci. U. S. A. 110, 17808–17813. https://doi.org/10.1073/pnas.1312937110

Kleen, T.-O., Galdon, A.A., MacDonald, A.S., Dalgleish, A.G., 2020. Mitigating coronavirus induced dysfunctional immunity for at-risk populations in COVID-19: Trained immunity, BCG and “new old friends.” Front. Immunol. 11, 2059. https://doi.org/10.3389/fimmu.2020.02059

Klinkenberg, S., Aalbers, M.W., Vles, J.S.H., Cornips, E.M.J., Rijkers, K., Leenen, L., Kessels, F.G.H., Aldenkamp, A.P., Majoie, M., 2012. Vagus nerve stimulation in children with intractable epilepsy: A randomized controlled trial. Dev. Med. Child Neurol. 54, 855–861. https://doi.org/10.1111/j.1469-8749.2012.04305.x

Klinkenberg, S., van den Borne, C.J.H., Aalbers, M.W., Verschuure, P., Kessels, A.G., Leenen, L., Rijkers, K., Aldenkamp, A.P., Vles, J.S.H., Majoie, H.J.M., 2014. The effects of vagus nerve stimulation on tryptophan metabolites in children with intractable epilepsy. Epilepsy Behav. 37, 133–138. https://doi.org/10.1016/j.yebeh.2014.06.001

Knoop, K.A., McDonald, K.G., Kulkarni, D.H., Newberry, R.D., 2016. Antibiotics promote inflammation through the translocation of native commensal colonic bacteria. Gut 65, 1100–1109. https://doi.org/10.1136/gutjnl-2014-309059

Knottnerus, S.J.G., Pras-Raves, M.L., van der Ham, M., Ferdinandusse, S., Houtkooper, R.H., Schielen, P.C.J.I., Visser, G., Wijburg, F.A., de Sain-van der Velden, M.G.M., 2020. Prediction of VLCAD deficiency phenotype by a metabolic fingerprint in newborn screening bloodspots. Biochim. Biophys. Acta - Mol. Basis Dis. 1866, 165725. https://doi.org/10.1016/j.bbadis.2020.165725

Knowles, K.A., Sripada, R.K., Defever, M., Rauch, S.A.M., 2019. Comorbid mood and anxiety disorders and severity of posttraumatic stress disorder symptoms in treatment-seeking veterans. Psychol. Trauma Theory, Res. Pract. Policy 11, 451–458. https://doi.org/10.1037/tra0000383

Kocher, F., Amann, A., Zimmer, K., Geisler, S., Fuchs, D., Pichler, R., Wolf, D., Kurz, K., Seeber, A., Pircher, A., 2021. High indoleamine-2,3-dioxygenase 1 (IDO) activity is linked to primary resistance to immunotherapy in non-small cell lung cancer (NSCLC). Transl. Lung Cancer Res. 10, 304–313. https://doi.org/10.21037/tlcr-20-380

Koeken, V.A.C.M., Charlotte, L., Mourits, V.P., Moorlag, S.J.C.F.M., Walk, J., Cirovic, B., Arts, R.J.W., Jaeger, M., Dijkstra, H., Lemmers, H., Joosten, L.A.B., Benn, C.S., van Crevel, R., Netea, M.G., 2020. BCG vaccination in humans inhibits systemic inflammation

in a sex-dependent manner. J. Clin. Invest. 130, 5591–5602. https://doi.org/10.1172/JCI133935

Koenen, K.C., Moffitt, T.E., Poulton, R., Martin, J., Caspi, A., 2007. Early childhood factors associated with the development of post-traumatic stress disorder: results from a longitudinal birth cohort. Psychol. Med. 37, 181–192. https://doi.org/10.1017/S0033291706009019

Koenen, K.C., Ratanatharathorn, A., Ng, L., McLaughlin, K.A., Bromet, E.J., Stein, D.J., Karam, E.G., Meron Ruscio, A., Benjet, C., Scott, K., Atwoli, L., Petukhova, M., Lim, C.C.W., Aguilar-Gaxiola, S., Al-Hamzawi, A., Alonso, J., Bunting, B., Ciutan, M., De Girolamo, G., Degenhardt, L., Gureje, O., Haro, J.M., Huang, Y., Kawakami, N., Lee, S., Navarro-Mateu, F., Pennell, B.E., Piazza, M., Sampson, N., Ten Have, M., Torres, Y., Viana, M.C., Williams, D., Xavier, M., Kessler, R.C., 2017. Posttraumatic stress disorder in the World Mental Health Surveys. Psychol. Med. 47, 2260–2274. https://doi.org/10.1017/S0033291717000708

Koh, A., De Vadder, F., Kovatcheva-Datchary, P., Bäckhed, F., 2016. From dietary fiber to host physiology: short-chain fatty acids as key bacterial metabolites. Cell 165, 1332–1345. https://doi.org/10.1016/j.cell.2016.05.041

Köhler, J., Maletzki, C., Koczan, D., Frank, M., Springer, A., Steffen, C., Revenko, A.S., MacLeod, A.R., Mikkat, S., Kreikemeyer, B., Oehmcke-Hecht, S., 2020. Kininogen supports inflammation and bacterial spreading during *Streptococccus Pyogenes* Sepsis. EBioMedicine 58, 102908. https://doi.org/10.1016/j.ebiom.2020.102908

Kolářová, H., Ambrůzová, B., Švihálková Šindlerová, L., Klinke, A., Kubala, L., 2014. Modulation of endothelial glycocalyx structure under inflammatory conditions. Mediators Inflamm. 2014, 694312. https://doi.org/10.1155/2014/694312

Kolmeder, C.A., Salojärvi, J., Ritari, J., de Been, M., Raes, J., Falony, G., Vieira-Silva, S., Kekkonen, R.A., Corthals, G.L., Palva, A., Salonen, A., de Vos, W.M., 2016. Faecal metaproteomic analysis reveals a personalized and stable functional microbiome and limited effects of a probiotic intervention in adults. PLoS One 11, e0153294. https://doi.org/10.1371/journal.pone.0153294

Konieczna, P., Groeger, D., Ziegler, M., Frei, R., Ferstl, R., Shanahan, F., Quigley, E.M.M., Kiely, B., Akdis, C.A., O'Mahony, L., 2012. *Bifidobacterium infantis* 35624 administration

induces Foxp3 T regulatory cells in human peripheral blood: potential role for myeloid and plasmacytoid dendritic cells. Gut 61, 354–366. https://doi.org/10.1136/gutjnl-2011-300936

Koning, N., Swaab, D.F., Hoek, R.M., Huitinga, I., 2009. Distribution of the immune inhibitory molecules CD200 and CD200R in the normal central nervous system and multiple sclerosis lesions suggests neuron-glia and glia-glia interactions. J. Neuropathol. Exp. Neurol. 68, 159–167. https://doi.org/10.1097/NEN.0b013e3181964113

Konnopka, A., König, H., 2020. Economic burden of anxiety disorders: A systematic review and meta-analysis. Pharmacoeconomics 38, 25–37. https://doi.org/10.1007/s40273-019-00849-7

Konstandi, M., Sotiropoulos, I., Matsubara, T., Malliou, F., Katsogridaki, A., Andriopoulou, C.E., Gonzalez, F.J., 2019. Adrenoceptor-stimulated inflammatory response in stress-induced serum amyloid A synthesis. Psychopharmacology (Berl). 236, 1687–1699. https://doi.org/10.1007/s00213-018-5149-4

Koo, M.S., Subbian, S., Kaplan, G., 2012. Strain specific transcriptional response in *Mycobacterium tuberculosis* infected macrophages. Cell Commun. Signal. 10, 2. https://doi.org/10.1186/1478-811X-10-2

Korbecki, J., Bobiński, R., Dutka, M., 2019. Self-regulation of the inflammatory response by peroxisome proliferator-activated receptors. Inflamm. Res. 68, 443–458. https://doi.org/10.1007/s00011-019-01231-1

Korf-Klingebiel, M., Reboll, M.R., Klede, S., Brod, T., Pich, A., Polten, F., Napp, L.C., Bauersachs, J., Ganser, A., Brinkmann, E., Reimann, I., Kempf, T., Niessen, H.W., Mizrahi, J., Schönfeld, H.J., Iglesias, A., Bobadilla, M., Wang, Y., Wollert, K.C., 2015. Myeloid-derived growth factor (C19orf10) mediates cardiac repair following myocardial infarction. Nat. Med. 21, 140–149. https://doi.org/10.1038/nm.3778

Kroner, E.E., Peskar, B.A., Fischer, H., Ferber, E., 1981. Control of arachidonic acid accumulation in bone marrow-derived macrophages by acyltransferases. J. Biol. Chem. 256, 3690–3697. https://doi.org/10.1016/s0021-9258(19)69510-4

Kuan, P.F., Yang, X., Clouston, S., Ren, X., Kotov, R., Waszczuk, M., Singh, P.K., Glenn, S.T., Gomez, E.C., Wang, J., Bromet, E., Luft, B.J., 2019. Cell type-specific gene expression patterns associated with posttraumatic stress disorder in World Trade Center responders. Transl. Psychiatry 9, 1. https://doi.org/10.1038/s41398-018-0355-8

Kuehnel, M.P., Reiss, M., Anand, P.K., Treede, I., Holzer, D., Hoffmann, E., Klapperstueck, M.,

Steinberg, T.H., Markwardt, F., Griffiths, G., 2009. Sphingosine-1-phosphate receptors stimulate macrophage plasma-membrane actin assembly via ADP release, ATP synthesis and P2X7R activation. J. Cell Sci. 122, 505–512. https://doi.org/10.1242/jcs.034207

Kurihara, T., Warr, G., Loy, J., Bravo, R., 1997. Defects in macrophage recruitment and host defense in mice lacking the CCR2 chemokine receptor. J. Exp. Med. 186, 1757–1762. https://doi.org/10.1084/jem.186.10.1757

Labelle, E.F., Polyak, E., 1998. Norepinephrine stimulates arachidonic acid release from vascular smooth muscle via activation of cPLA2. Am. J. Physiol. - Cell Physiol. 274, C1129–C1137. https://doi.org/10.1152/ajpcell.1998.274.4.c1129

Lacombe, M.L., Tokarska-Schlattner, M., Boissan, M., Schlattner, U., 2018. The mitochondrial nucleoside diphosphate kinase (NDPK-D/NME4), a moonlighting protein for cell homeostasis. Lab. Investig. 98, 582–588. https://doi.org/10.1038/s41374-017-0004-5

Lahey, T., Laddy, D., Hill, K., Schaeffer, J., Hogg, A., Keeble, J., Dagg, B., Ho, M.M., Arbeit, R.D., von Reyn, C.F., 2016. Immunogenicity and protective efficacy of the DAR-901 booster vaccine in a murine model of tuberculosis. PLoS One 11, e0168521. https://doi.org/10.1371/journal.pone.0168521

Lambert, S., Bowers, S.J., Olker, C.J., Song, E., Wright, K.P., Fleshner, M., Lowry, C.A., Vitaterna, M.H., Turek, F.W., 2017. *Mycobacterium vaccae* enhances sleep and counteracts effects of stress and sleep disruption in mice, in: Society for Neuroscience, Online. 241.19.

Langgartner, D., Lowry, C.A., Reber, S.O., 2019. Old Friends, immunoregulation, and stress resilience. Pflugers Arch. Eur. J. Physiol. https://doi.org/10.1007/s00424-018-2228-7

Langgartner, D., Palmer, A., Rittlinger, A., Reber, S.O., Huber-Lang, M., 2018. Effects of prior psychosocial trauma on subsequent immune response after experimental thorax trauma. SHOCK 49, 690–697. https://doi.org/10.1097/SHK.0000000000000973

Langgartner, D., Peterlik, D., Foertsch, S., Füchsl, A.M., Brokmann, P., Flor, P.J., Shen, Z., Fox, J.G., Uschold-Schmidt, N., Lowry, C.A., Reber, S.O., 2017. Individual differences in stress vulnerability: The role of gut pathobionts in stress-induced colitis. Brain. Behav. Immun. 64, 23–32. https://doi.org/10.1016/j.bbi.2016.12.019

Lanis, J.M., Alexeev, E.E., Curtis, V.F., Kitzenberg, D.A., Kao, D.J., Battista, K.D., Gerich, M.E., Glover, L.E., Kominsky, D.J., Colgan, S.P., 2017. Tryptophan metabolite activation of the aryl hydrocarbon receptor regulates IL-10 receptor expression on intestinal epithelia.

Mucosal Immunol. 10, 1133–1144. https://doi.org/10.1038/mi.2016.133

Lapthorne, S., MacSharry, J., Scully, P., Nally, K., Shanahan, F., 2012. Differential intestinal M-cell gene expression response to gut commensals. Immunology 136, 312–324. https://doi.org/10.1111/j.1365-2567.2012.03581.x

Larraufie, P., Martin-Gallausiaux, C., Lapaque, N., Dore, J., Gribble, F.M., Reimann, F., Blottiere, H.M., 2018. SCFAs strongly stimulate PYY production in human enteroendocrine cells. Sci. Rep. 8, 74. https://doi.org/10.1038/s41598-017-18259-0

Lathrop, S.K., Bloom, S.M., Rao, S.M., Nutsch, K., Lio, C.W., Santacruz, N., Peterson, D.A., Stappenbeck, T.S., Hsieh, C.S., 2011. Peripheral education of the immune system by colonic commensal microbiota. Nature 478, 250–254. https://doi.org/10.1038/nature10434

Latorre, R., Sternini, C., De Giorgio, R., Greenwood-Van Meerveld, B., 2016. Enteroendocrine cells: a review of their role in brain-gut communication. Neurogastroenterol. Motil. 28, 620–630. https://doi.org/10.1111/nmo.12754

Le Bert, N., Chain, B.M., Rook, G.A.W., Noursadeghi, M., 2011. DC priming by M. vaccae inhibits Th2 responses in contrast to specific TLR2 priming and is associated with selective activation of the CREB pathway. PLoS One 6, e18346. https://doi.org/10.1371/journal.pone.0018346

Leclercq, S., Forsythe, P., Bienenstock, J., 2016. Posttraumatic stress disorder: does the gut microbiome hold the key? Can. J. Psychiatry 61, 204–213. https://doi.org/10.1177/0706743716635535

Lee, A.H., Ledderose, C., Li, X., Slubowski, C.J., Sueyoshi, K., Staudenmaier, L., Bao, Y., Zhang, J., Junger, W.G., 2018. Adenosine triphosphate release is required for toll-like receptor-induced monocyte/macrophage activation, inflammasome signaling, interleukin-1β production, and the host immune response to infection. Crit. Care Med. 46, e1183–e1189. https://doi.org/10.1097/CCM.0000000000003446

Lee, A.R., Kim, J.H., Cho, E., Kim, M., Park, M., 2017. Dorsal and ventral hippocampus differentiate in functional pathways and differentially associate with neurological disease-related genes during postnatal development. Front. Mol. Neurosci. 10. https://doi.org/10.3389/fnmol.2017.00331

Lee, H.M., Wu, W., Wysoczynski, M., Liu, R., Zuba-Surma, E.K., Kucia, M., Ratajczak, J., Ratajczak, M.Z., 2009. Impaired mobilization of hematopoietic stem/progenitor cells in C5-

deficient mice supports the pivotal involvement of innate immunity in this process and reveals novel promobilization effects of granulocytes. Leukemia 23, 2052–2062. https://doi.org/10.1038/leu.2009.158

Lehmann, M.L., Poffenberger, C.N., Elkahloun, A.G., Herkenham, M., 2020. Analysis of cerebrovascular dysfunction caused by chronic social defeat in mice. Brain. Behav. Immun. 88, 735–747. https://doi.org/10.1016/j.bbi.2020.05.030

Lehmann, M.L., Weigel, T.K., Poffenberger, C.N., Herkenham, M., 2019. The behavioral sequelae of social defeat require microglia and are driven by oxidative stress in mice. J. Neurosci. 39, 5594–5605. https://doi.org/10.1523/JNEUROSCI.0184-19.2019

Lew, L.-C., Hor, Y.-Y., Yusoff, N.A.A., Choi, S.-B., Yusoff, M.S.B., Roslan, N.S., Ahmad, A., Mohammad, J.A.M., Abdullah, M.F.I.L., Zakaria, N., Wahid, N., Sun, Z., Kwok, L.-Y., Zhang, H., Liong, M.-T., 2018. Probiotic *Lactobacillus plantarum* P8 alleviated stress and anxiety while enhancing memory and cognition in stressed adults: A randomised, double-blind, placebo-controlled study. Clin. Nutr. 38, 2053-2064. https://doi.org/10.1016/J.CLNU.2018.09.010

Li, B., Guo, K., Zeng, L., Zeng, B., Huo, R., Luo, Y., Wang, H., Dong, M., Zheng, P., Zhou, C., Chen, J., Liu, Y., Liu, Z., Fang, L., Wei, H., Xie, P., 2018a. Metabolite identification in fecal microbiota transplantation mouse livers and combined proteomics with chronic unpredictive mild stress mouse livers. Transl. Psychiatry 8, 34. https://doi.org/10.1038/s41398-017-0078-2

Li, B., Selmi, C., Tang, R., Gershwin, M.E., Ma, X., 2018b. The microbiome and autoimmunity: a paradigm from the gut–liver axis. Cell. Mol. Immunol. 15, 595–609. https://doi.org/10.1038/cmi.2018.7

Li, C., Wu, X., Liu, S., Shen, D., Zhu, J., Liu, K., 2020. Role of resolvins in the inflammatory resolution of neurological diseases. Front. Pharmacol. 11, 612. https://doi.org/10.3389/fphar.2020.00612

Li, C.Y., Dempsey, J.L., Wang, D., Lee, S., Weigel, K.M., Fei, Q., Bhatt, D.K., Prasad, B., Raftery, D., Gu, H., Cui, J.Y., 2018a. PBDEs altered gut microbiome and bile acid homeostasis in male C57BL/6 mice. Drug Metab. Dispos. 46, 1226–1240. https://doi.org/10.1124/dmd.118.081547

Li, C.Y., Dempsey, J.L., Wang, D., Lee, S., Weigel, K.M., Fei, Q., Bhatt, D.K., Prasad, B.,

Raftery, D., Gu, H., Cui, J.Y., 2018b. PBDEs altered gut microbiome and bile acid homeostasis in male C57BL/6 mice. Drug Metab. Dispos. 46, 1226–1240. https://doi.org/10.1124/dmd.118.081547

Li, H., Liu, F., Lu, J., Shi, J., Guan, J., Yan, F., Li, B., Huo, G., 2020. Probiotic mixture of *Lactobacillus plantarum* strains improves lipid metabolism and gut microbiota structure in high fat diet-fed mice. Front. Microbiol. 11, 512. https://doi.org/10.3389/fmicb.2020.00512

Li, L., Tumen, B., Li, P.F., Liu, C., Li, S.H., Ning, K.J., Jiang, J.P., 2018c. Mechanisms of anti-inflammation of taurochenodeoxycholic acid based on network pharmacology. Yaoxue Xuebao 53, 2064–2075. https://doi.org/10.16438/J.0513-4870.2018-0600

Li, M., Cai, S.Y., Boyer, J.L., 2017. Mechanisms of bile acid mediated inflammation in the liver. Mol. Aspects Med. 56, 45–53. https://doi.org/10.1016/j.mam.2017.06.001

Li, M., van Esch, B.C.A.M., Henricks, P.A.J., Folkerts, G., Garssen, J., 2018d. The anti-inflammatory effects of short chain fatty acids on lipopolysaccharide- or tumor necrosis factor α-stimulated endothelial cells via activation of GPR41/43 and inhibition of HDACs. Front. Pharmacol. 9, 533. https://doi.org/10.3389/fphar.2018.00533

Li, T., Chiang, J.Y.L., 2009. Regulation of bile acid and cholesterol metabolism by PPARs. PPAR Res. 2009, 501739. https://doi.org/10.1155/2009/501739

Li, X., Ding, Y., Ma, Y., Liu, Y., Wang, Q., Song, J., Yang, Y., 2015. Very long-chain acyl-coenzyme A dehydrogenase deficiency in Chinese patients: Eight case reports, including one case of prenatal diagnosis. Eur. J. Med. Genet. 58, 134–139. https://doi.org/10.1016/j.ejmg.2015.01.005

Li, Z., Chalazonitis, A., Huang, Y. -y., Mann, J.J., Margolis, K.G., Yang, Q.M., Kim, D.O., Cote, F., Mallet, J., Gershon, M.D., 2011. Essential roles of enteric neuronal serotonin in gastrointestinal motility and the development/survival of enteric dopaminergic neurons. J. Neurosci. 31, 8998–9009. https://doi.org/10.1523/JNEUROSCI.6684-10.2011

Liang, J., Huang, H.-I., Benzatti, F.P., Karlsson, A.B., Zhang, J.J., Youssef, N., Ma, A., Hale, L.P., Hammer, G.E., 2016. Inflammatory Th1 and Th17 in the intestine are each driven by functionally specialized dendritic cells with distinct requirements for MyD88. Cell Rep. 17, 1330–1343. https://doi.org/10.1016/j.celrep.2016.09.091

Liang, S., Wang, T., Hu, X., Luo, J., Li, W., Wu, X., Duan, Y., Jin, F., 2015. Administration of *Lactobacillus helveticus* NS8 improves behavioral, cognitive, and biochemical aberrations

caused by chronic restraint stress. Neuroscience 310, 561–577. https://doi.org/10.1016/J.NEUROSCIENCE.2015.09.033

Lim, H.Y., Müller, N., Herold, M.J., Van Den Brandt, J., Reichardt, H.M., 2007. Glucocorticoids exert opposing effects on macrophage function dependent on their concentration. Immunology 122, 47–53. https://doi.org/10.1111/j.1365-2567.2007.02611.x

Lin, H.M., Barnett, M.P.G., Roy, N.C., Joyce, N.I., Zhu, S., Armstrong, K., Helsby, N.A., Ferguson, L.R., Rowan, D.D., 2010. Metabolomic analysis identifies inflammatory and noninflammatory metabolic effects of genetic modification in a mouse model of Crohn?s disease. J. Proteome Res. 9, 1965–1975. https://doi.org/10.1021/pr901130s

Lin, Z., Wang, Z., Li, G., Li, B., Xie, W., Xiang, D., 2016. Fibulin-3 may improve vascular health through inhibition of MMP-2/9 and oxidative stress in spontaneously hypertensive rats. Mol. Med. Rep. 13, 3805–3812. https://doi.org/10.3892/mmr.2016.5036

Linan-Rico, A., Ochoa-Cortes, F., Beyder, A., Soghomonyan, S., Zuleta-Alarcon, A., Coppola, V., Christofi, F.L., 2016. Mechanosensory signaling in enterochromaffin cells and 5-HT release: Potential implications for gut inflammation. Front. Neurosci. 10, 564. https://doi.org/10.3389/fnins.2016.00564

Linares, I., Farrokhi, K., Echeverri, J., Kaths, J.M., Kollmann, D., Hamar, M., Urbanellis, P., Ganesh, S., Adeyi, O.A., Yip, P., Selzner, M., Selzner, N., 2018. PPAR-gamma activation is associated with reduced liver ischemia-reperfusion injury and altered tissue-resident macrophages polarization in a mouse model. PLoS One 13, e0195212. https://doi.org/10.1371/journal.pone.0195212

Lischke, A., Jacksteit, R., Mau-Moeller, A., Pahnke, R., Hamm, A.O., Weippert, M., 2018. Heart rate variability is associated with psychosocial stress in distinct social domains. J. Psychosom. Res. 106, 56–61. https://doi.org/10.1016/j.jpsychores.2018.01.005

Liu, H., Petukhova, M. V., Sampson, N.A., Aguilar-Gaxiola, S., Alonso, J., Andrade, L.H., Bromet, E.J., De Girolamo, G., Haro, J.M., Hinkov, H., Kawakami, N., Koenen, K.C., Kovess-Masfety, V., Lee, S., Medina-Mora, M.E., Navarro-Mateu, F., O'Neill, S., Piazza, M., Posada-Villa, J., Scott, K.M., Shahly, V., Stein, D.J., Ten Have, M., Torres, Y., Gureje, O., Zaslavsky, A.M., Kessler, R.C., Al-Hamzawi, A., Al-Kaisy, M.S., Benjet, C., Borges, G., Bruffaerts, R., Bunting, B., De Almeida, J.M.C., Cardoso, G., Chatterji, S., Cia, A.H., Degenhardt, L., De Jonge, P., Demyttenaere, K., Fayyad, J., Florescu, S., He, Y., Hu, C.Y.,

Huang, Y., Karam, A.N., Karam, E.G., Kiejna, A., Lepine, J.P., Levinson, D., McGrath, J., Moskalewicz, J., Pennell, B.E., Slade, T., Stagnaro, J.C., Viana, M.C., Whiteford, H., Williams, D.R., Wojtyniak, B., 2017. Association of DSM-IV posttraumatic stress disorder with traumatic experience type and history in the World Health Organization World Mental Health surveys. JAMA Psychiatry 74, 270–281. https://doi.org/10.1001/jamapsychiatry.2016.3783

Liu, Y., Firoz Mian, M., McVey Neufeld, K.-A., Forsythe, P., 2020. CD4+CD25+ T cells are essential for behavioral effects of *Lactobacillus rhamnosus* JB-1 in male BALB/c mice. Brain. Behav. Immun. 88, 451–460. https://doi.org/10.1016/j.bbi.2020.04.014

Lloyd-Price, J., Abu-Ali, G., Huttenhower, C., 2016. The healthy human microbiome. Genome Med. 8, 51. https://doi.org/10.1186/s13073-016-0307-y

Long-Smith, C., O'Riordan, K.J., Clarke, G., Stanton, C., Dinan, T.G., Cryan, J.F., 2020. Microbiota-gut-brain axis: New therapeutic opportunities. Annu. Rev. Pharmacol. Toxicol. 60, 477–502. https://doi.org/10.1146/annurev-pharmtox-010919-023628

Lonsdale-Eccles, J.D., Grab, D.J., 2002. Trypanosome hydrolases and the blood-brain barrier. Trends Parasitol. 18, 17–19. https://doi.org/10.1016/S1471-4922(01)02120-1

Lopetuso, L.R., Scaldaferri, F., Petito, V., Gasbarrini, A., 2013. Commensal Clostridia: leading players in the maintenance of gut homeostasis. Gut Pathog. 5, 23. https://doi.org/10.1186/1757-4749-5-23

Lotto, V., Choi, S.W., Friso, S., 2011. Vitamin B6: A challenging link between nutrition and inflammation in CVD. Br. J. Nutr. 106, 183–195. https://doi.org/10.1017/S0007114511000407

Loupy, K.M., Arnold, M.R., Hassell, J.E., Lieb, M.W., Milton, L.N., Cler, K.E., Fox, J.H., Siebler, P.H., Schmidt, D., Noronha, S.I.S.R., Day, H.E.W., Lowry, C.A., 2018. Evidence that preimmunization with a heat-killed preparation of *Mycobacterium vaccae* reduces corticotropin-releasing hormone mRNA expression in the extended amygdala in a fear-potentiated startle paradigm. Brain. Behav. Immun. 77, 127–140. https://doi.org/10.1016/j.bbi.2018.12.015

Loupy, K.M., Cler, K.E., Marquart, B.M., Yifru, T.W., D'Angelo, H.M., Arnold, M.R., Elsayed, A.I., Gebert, M.J., Fierer, N., Fonken, L.K., Frank, M.G., Zambrano, C.A., Maier, S.F., Lowry, C.A., 2021. Comparing the effects of two different strains of *Mycobacterium*

vaccae, M. vaccae NCTC 11659 and *M. vaccae* ATCC 15483, on stress-resilient behaviors and lipid-immune signaling in rats. Brain. Behav. Immun. 91, 212–229. https://doi.org/10.1016/j.bbi.2020.09.030

Loupy, K.M., Lee, T., Zambrano, C.A., Elsayed, A.I., D'Angelo, H.M., Fonken, L.K., Frank, M.G., Maier, S.F., Lowry, C.A., 2020. Alzheimer's disease: protective effects of *Mycobacterium vaccae*, a soil-derived mycobacterium with anti-inflammatory and anti-tubercular properties, on the proteomic profiles of plasma and cerebrospinal fluid in rats. J. Alzheimer's Dis. 78, 965–987. https://doi.org/10.3233/JAD-200568

Loupy, K.M., Lowry, C.A., 2020. Posttraumatic stress disorder and the gut microbiome, in: Burnet, P.W.J. (Ed.), The Oxford Handbook of the Microbiome-Gut-Brain Axis. Oxford University Press. https://doi.org/10.1093/oxfordhb/9780190931544.013.10

Lovett-Racke, A.E., Hussain, R.Z., Northrop, S., Choy, J., Rocchini, A., Matthes, L., Chavis, J.A., Diab, A., Drew, P.D., Racke, M.K., 2004. Peroxisome proliferator-activated receptor α agonists as therapy for autoimmune disease. J. Immunol. 172, 5790–5798. https://doi.org/10.4049/jimmunol.172.9.5790

Lowry, C.A., Hollis, J.H., de Vries, A., Pan, B., Brunet, L.R., Hunt, J.R.F., Paton, J.F.R., van Kampen, E., Knight, D.M., Evans, A.K., Rook, G.A.W., Lightman, S.L., 2007. Identification of an immune-responsive mesolimbocortical serotonergic system: potential role in regulation of emotional behavior. Neuroscience 146, 756–772. https://doi.org/10.1016/j.neuroscience.2007.01.067

Lowry, C.A., Smith, D.G., Siebler, P.H., Schmidt, D., Stamper, C.E., Hassell, J.E., Yamashita, P.S., Fox, J.H., Reber, S.O., Brenner, L.A., Hoisington, A.J., Postolache, T.T., Kinney, K.A., Marciani, D., Hernandez, M., Hemmings, S.M.J., Malan-Muller, S., Wright, K.P., Knight, R., Raison, C.L., Rook, G.A.W., 2016. The microbiota, immunoregulation, and mental health: implications for public health. Curr. Environ. Heal. Reports 3, 270–286. https://doi.org/10.1007/s40572-016-0100-5

Lubbers, R., van Essen, M.F., van Kooten, C., Trouw, L.A., 2017. Production of complement components by cells of the immune system. Clin. Exp. Immunol. 188, 183–194. https://doi.org/10.1111/cei.12952

Luissint, A.-C., Parkos, C.A., Nusrat, A., 2016. Inflammation and the intestinal barrier: leukocyte-epithelial cell interactions, cell junction remodeling, and mucosal repair.

Gastroenterology 151, 616–32. https://doi.org/10.1053/j.gastro.2016.07.008

Luo, A., Leach, S.T., Barres, R., Hesson, L.B., Grimm, M.C., Simar, D., 2017. The microbiota and epigenetic regulation of T helper 17/Regulatory T cells: in search of a balanced immune system. Front. Immunol. 8, 417. https://doi.org/10.3389/fimmu.2017.00417

Lüthi, A., Laurent, J.P., Figurovt, A., Mullert, D., Schachnert, M., 1994. Hippocampal long-term potentiation and neural cell adhesion molecules L1 and NCAM. Nature 372, 777–779. https://doi.org/10.1038/372777a0

Lynall, M.E., Turner, L., Bhatti, J., Cavanagh, J., de Boer, P., Mondelli, V., Jones, D., Drevets, W.C., Cowen, P., Harrison, N.A., Pariante, C.M., Pointon, L., Clatworthy, M.R., Bullmore, E., 2020. Peripheral blood cell–stratified subgroups of inflamed depression. Biol. Psychiatry 88, 185–196. https://doi.org/10.1016/j.biopsych.2019.11.017

Lyte, M., Bailey, M.T., 1997. Neuroendocrine–bacterial interactions in a neurotoxin-induced model of trauma. J. Surg. Res. 70, 195–201. https://doi.org/10.1006/jsre.1997.5130

Lyte, M., Ernst, S., 1992. Catecholamine induced growth of gram negative bacteria. Life Sci. 50, 203–12.

Ma, C., Han, M., Heinrich, B., Fu, Q., Zhang, Q., Sandhu, M., Agdashian, D., Terabe, M., Berzofsky, J.A., Fako, V., Ritz, T., Longerich, T., Theriot, C.M., McCulloch, J.A., Roy, S., Yuan, W., Thovarai, V., Sen, S.K., Ruchirawat, M., Korangy, F., Wang, X.W., Trinchieri, G., Greten, T.F., 2018. Gut microbiome–mediated bile acid metabolism regulates liver cancer via NKT cells. Science 360, eaan5931. https://doi.org/10.1126/science.aan5931

Ma, K., Guo, L., Xu, A. mechanism for stress-induced depression assessed by sequencing miRNA and mRNA in medial prefrontal cortex, Cui, S., Wang, J.H., 2016. Molecular mechanism for stress-induced depression assessed by sequencing miRNA and mRNA in medial prefrontal cortex. PLoS One 11, e0159093. https://doi.org/10.1371/journal.pone.0159093

Macfarlane, D.P., Forbes, S., Walker, B.R., 2008. Glucocorticoids and fatty acid metabolism in humans: Fuelling fat redistribution in the metabolic syndrome. J. Endocrinol. 197, 189–204. https://doi.org/10.1677/JOE-08-0054

Maeda, N., Nigou, J., Herrmann, J.L., Jackson, M., Amara, A., Lagrange, P.H., Puzo, G., Gicquel, B., Neyrolles, O., 2003. The cell surface receptor DC-SIGN discriminates between *Mycobacterium* species through selective recognition of the mannose caps on

lipoarabinomannan. J. Biol. Chem. 278, 5513–5516. https://doi.org/10.1074/jbc.C200586200

Magee, P., Pearson, S., Whittingham-Dowd, J., Allen, J., 2012. PPARγ as a molecular target of EPA anti-inflammatory activity during TNF-α-impaired skeletal muscle cell differentiation. J. Nutr. Biochem. 23, 1440–1448. https://doi.org/10.1016/j.jnutbio.2011.09.005

Maguire, E.M., Pearce, S.W.A., Xiao, Q., 2019. Foam cell formation: A new target for fighting atherosclerosis and cardiovascular disease. Vascul. Pharmacol. 112, 54–71. https://doi.org/10.1016/j.vph.2018.08.002

Maier, S.F., Ryan, S.M., Barksdale, C.M., Kalin, N.H., 1986. Stressor controllability and the pituitary-adrenal system. Behav. Neurosci. 100, 669–674. https://doi.org/10.1037//0735-7044.100.5.669

Maier, S.F., Seligman, M.E., 1976. Learned helplessness: Theory and evidence. J. Exp. Psychol. Gen. 105, 3–46. https://doi.org/10.1037/0096-3445.105.1.3

Maier, S.F., Watkins, L.R., 2005. Stressor controllability and learned helplessness: The roles of the dorsal raphe nucleus, serotonin, and corticotropin-releasing factor. Neurosci. Biobehav. Rev. 29, 829–841. https://doi.org/10.1016/j.neubiorev.2005.03.021

Malan-Muller, S., Valles-Colomer, M., Raes, J., Lowry, C.A., Seedat, S., Hemmings, S.M.J., 2018. The gut microbiome and mental health: Implications for anxiety- and trauma-related disorders. Omi. A J. Integr. Biol. 22, 90–107. https://doi.org/10.1089/omi.2017.0077

Manfredo Vieira, S., Hiltensperger, M., Kumar, V., Zegarra-Ruiz, D., Dehner, C., Khan, N., Costa, F.R.C., Tiniakou, E., Greiling, T., Ruff, W., Barbieri, A., Kriegel, C., Mehta, S.S., Knight, J.R., Jain, D., Goodman, A.L., Kriegel, M.A., 2018. Translocation of a gut pathobiont drives autoimmunity in mice and humans. Science. 359, 1156–1161. https://doi.org/10.1126/science.aar7201

Marchesi, J.R., 2010. Prokaryotic and eukaryotic diversity of the human gut, in: Advances in Applied Microbiology. pp. 43–62. https://doi.org/10.1016/S0065-2164(10)72002-5

Marcon, R., Bento, A.F., Dutra, R.C., Bicca, M.A., Leite, D.F.P., Calixto, J.B., 2013. Maresin 1, a proresolving lipid mediator derived from omega-3 polyunsaturated fatty acids, exerts protective actions in murine models of colitis. J. Immunol. 191, 4288–4298. https://doi.org/10.4049/jimmunol.1202743

Margolis, K.G., Li, Z., Stevanovic, K., Saurman, V., Israelyan, N., Anderson, G.M., Snyder, I.,

Veenstra-VanderWeele, J., Blakely, R.D., Gershon, M.D., 2016. Serotonin transporter variant drives preventable gastrointestinal abnormalities in development and function. J. Clin. Invest. 126, 2221–2235. https://doi.org/10.1172/JCI84877

Martel-Pelletier, J., Lajeunesse, D., Reboul, P., Pelletier, J.P., 2003. Therapeutic role of dual inhibitors of 5-LOX and COX, selective and non-selective non-steroidal anti-inflammatory drugs. Ann. Rheum. Dis. 62, 501–509. https://doi.org/10.1136/ard.62.6.501

Martin, G., Kolida, S., Marchesi, J.R., Want, E., Sidaway, J.E., Swann, J.R., 2018. In vitro modeling of bile acid processing by the human fecal microbiota. Front. Microbiol. 9, 1153. https://doi.org/10.3389/fmicb.2018.01153

Martinez, F.O., Gordon, S., 2014. The M1 and M2 paradigm of macrophage activation: Time for reassessment. F1000Prime Rep. 6. https://doi.org/10.12703/P6-13

Martinez, F.O., Gordon, S., Locati, M., Mantovani, A., 2006. Transcriptional profiling of the human monocyte-to-macrophage differentiation and polarization: New molecules and patterns of gene expression. J. Immunol. 177, 7303–7311. https://doi.org/10.4049/jimmunol.177.10.7303

Masaki, T., Chiba, S., Tatsukawa, H., Yasuda, T., Noguchi, H., Seike, M., Yoshimatsu, H., 2004. Adiponectin protects LPS-induced liver injury through modulation of TNF-α in KK-Ay obese mice. Hepatology 40, 177–184. https://doi.org/10.1002/hep.20282

Mashego, M.R., Rumbold, K., De Mey, M., Vandamme, E., Soetaert, W., Heijnen, J.J., 2007. Microbial metabolomics: past, present and future methodologies. Biotechnol. Lett. 29, 1–16. https://doi.org/10.1007/s10529-006-9218-0

Maslanik, T., Mahaffey, L., Tannura, K., Beninson, L., Greenwood, B.N., Fleshner, M., 2013. The inflammasome and danger associated molecular patterns (DAMPs) are implicated in cytokine and chemokine responses following stressor exposure. Brain. Behav. Immun. 28, 54–62. https://doi.org/10.1016/j.bbi.2012.10.014

Maslanik, T., Tannura, K., Mahaffey, L., Loughridge, A.B., Beninson, L., Benninson, L., Ursell, L., Greenwood, B.N., Knight, R., Fleshner, M., 2012. Commensal bacteria and MAMPs are necessary for stress-induced increases in IL-1β and IL-18 but not IL-6, IL-10 or MCP-1. PLoS One 7, e50636. https://doi.org/10.1371/journal.pone.0050636

Matsumoto, J., Dohgu, S., Takata, F., Iwao, T., Kimura, I., Tomohiro, M., Aono, K., Kataoka, Y., Yamauchi, A., 2020. Serum amyloid A-induced blood-brain barrier dysfunction

associated with decreased claudin-5 expression in rat brain endothelial cells and its inhibition by high-density lipoprotein in vitro. Neurosci. Lett. 738, 135352. https://doi.org/10.1016/j.neulet.2020.135352

Matsumura, K., Noguchi, H., Nishi, D., Hamazaki, K., Hamazaki, T., Matsuoka, Y.J., 2017. Effects of omega-3 polyunsaturated fatty acids on psychophysiological symptoms of post-traumatic stress disorder in accident survivors: A randomized, double-blind, placebo-controlled trial. J. Affect. Disord. 224, 27–31. https://doi.org/10.1016/j.jad.2016.05.054

Matsuoka, Y.J., Hamazaki, K., Nishi, D., Hamazaki, T., 2016. Change in blood levels of eicosapentaenoic acid and posttraumatic stress symptom: A secondary analysis of data from a placebo-controlled trial of omega3 supplements. J. Affect. Disord. 205, 289–291. https://doi.org/10.1016/j.jad.2016.08.005

Matt, S.M., Allen, J.M., Lawson, M.A., Mailing, L.J., Woods, J.A., Johnson, R.W., 2018. Butyrate and dietary soluble fiber improve neuroinflammation associated with aging in mice. Front. Immunol. 9, 1832. https://doi.org/10.3389/fimmu.2018.01832

Mayer, E.A., 2011. Gut feelings: the emerging biology of gut-brain communication. Nat. Rev. Neurosci. 12, 453–66. https://doi.org/10.1038/nrn3071

Mazidi, M., Rezaie, P., Ferns, G.A., Vatanparast, H., 2017. Impact of probiotic administration on serum C-reactive protein concentrations: systematic review and meta-analysis of randomized control trials. Nutrients 9, 20. https://doi.org/10.3390/nu9010020

McCorry, L.K., 2007. Physiology of the autonomic nervous system. Am. J. Pharm. Educ. 71, 78.

McIntyre, C.K., 2018. Is there a role for vagus nerve stimulation in the treatment of posttraumatic stress disorder? Bioelectron. Med. 1, 95–99. https://doi.org/10.2217/bem-2018-0002

McLaughlin, K.A., Conron, K.J., Koenen, K.C., Gilman, S.E., 2010. Childhood adversity, adult stressful life events, and risk of past-year psychiatric disorder: A test of the stress sensitization hypothesis in a population-based sample of adults. Psychol. Med. 40, 1647–1658. https://doi.org/10.1017/S0033291709992121

McLaughlin, K.A., Rith-Najarian, L., Dirks, M.A., Sheridan, M.A., 2015. Low vagal tone magnifies the association between psychosocial stress exposure and internalizing psychopathology in adolescents. J. Clin. child Adolesc. Psychol. 44, 314–328. https://doi.org/10.1080/15374416.2013.843464

McMenamin, C., Schon-Hegrad, M., Oliver, J., Girn, B., Holt, P.G., 1991. Regulation of IgE responses to inhaled antigens: Cellular mechanisms underlying allergic sensitization versus tolerence induction. Int. Arch. Allergy Immunol. 94, 78–82. https://doi.org/10.1159/000235331

Meddings, J.B., Swain, M.G., 2000. Environmental stress-induced gastrointestinal permeability is mediated by endogenous glucocorticoids in the rat. Gastroenterology 119, 1019–1028. https://doi.org/10.1053/gast.2000.18152

Melamud, E., Vastag, L., Rabinowitz, J.D., 2010. Metabolomic analysis and visualization engine for LC - MS data. Anal. Chem. 82, 9818–9826. https://doi.org/10.1021/ac1021166

Mellon, S.H., Bersani, F.S., Lindqvist, D., Hammamieh, R., Donohue, D., Dean, K., Jett, M., Yehuda, R., Flory, J., Reus, V.I., Bierer, L.M., Makotkine, I., Amara, D.A., Haase, C.H., Coy, M., Doyle, F.J., Marmar, C., Wolkowitz, O.M., 2019. Metabolomic analysis of male combat veterans with post traumatic stress disorder. PLoS One 14, e0213839. https://doi.org/10.1371/journal.pone.0213839

Mellon, S.H., Gautam, A., Hammamieh, R., Jett, M., Wolkowitz, O.M., 2018. Metabolism, metabolomics, and inflammation in posttraumatic stress disorder. Biol. Psychiatry 83, 866–875. https://doi.org/10.1016/j.biopsych.2018.02.007

Menard, C., Pfau, M.L., Hodes, G.E., Kana, V., Wang, V.X., Bouchard, S., Takahashi, A., Flanigan, M.E., Aleyasin, H., Leclair, K.B., Janssen, W.G., Labonté, B., Parise, E.M., Lorsch, Z.S., Golden, S.A., Heshmati, M., Tamminga, C., Turecki, G., Campbell, M., Fayad, Z.A., Tang, C.Y., Merad, M., Russo, S.J., 2017a. Social stress induces neurovascular pathology promoting depression. Nat. Neurosci. 20, 1752–1760. https://doi.org/10.1038/s41593-017-0010-3

Menard, C., Pfau, M.L., Hodes, G.E., Russo, S.J., 2017b. Immune and neuroendocrine mechanisms of stress vulnerability and resilience. Neuropsychopharmacology 42, 62–80. https://doi.org/10.1038/npp.2016.90

Mencarelli, A., Distrutti, E., Renga, B., D'Amore, C., Cipriani, S., Palladino, G., Donini, A., Ricci, P., Fiorucci, S., 2011. Probiotics modulate intestinal expression of nuclear receptor and provide counter-regulatory signals to inflammation-driven adipose tissue activation. PLoS One 6, e22978. https://doi.org/10.1371/journal.pone.0022978

Ménégaut, L., Jalil, A., Thomas, C., Masson, D., 2019. Macrophage fatty acid metabolism and

atherosclerosis: The rise of PUFAs. Atherosclerosis 291, 52–61. https://doi.org/10.1016/j.atherosclerosis.2019.10.002

Messaoud, A., Mensi, R., Douki, W., Neffati, F., Najjar, M.F., Gobbi, G., Valtorta, F., Gaha, L., Comai, S., 2019. Reduced peripheral availability of tryptophan and increased activation of the kynurenine pathway and cortisol correlate with major depression and suicide. World J. Biol. Psychiatry 20, 703–711. https://doi.org/10.1080/15622975.2018.1468031

Michopoulos, V., Powers, A., Gillespie, C.F., Ressler, K.J., Jovanovic, T., 2017. Inflammation in fear- and anxiety-based disorders: PTSD, GAD, and beyond. Neuropsychopharmacology 42, 254–270. https://doi.org/10.1038/npp.2016.146

Michopoulos, V., Rothbaum, A.O., Jovanovic, T., Almli, L.M., Bradley, B., Rothbaum, B.O., Gillespie, C.F., Ressler, K.J., 2015. Association of CRP genetic variation and CRP level with elevated PTSD symptoms and physiological responses in a civilian population with high levels of trauma. Am. J. Psychiatry 172, 353–62. https://doi.org/10.1176/appi.ajp.2014.14020263

Michopoulos, V., Vester, A., Neigh, G., 2016. Posttraumatic stress disorder: A metabolic disorder in disguise? Exp. Neurol. 284, 220–229. https://doi.org/10.1016/j.expneurol.2016.05.038

Miller, A.H., Raison, C.L., 2016. The role of inflammation in depression: From evolutionary imperative to modern treatment target. Nat. Rev. Immunol. 16, 22–34. https://doi.org/10.1038/nri.2015.5

Miller, S.J., Zaloga, G.P., Hoggatt, A.M., Labarrere, C., Faulk, W.P., 2005. Short-chain fatty acids modulate gene expression for vascular endothelial cell adhesion molecules. Nutrition 21, 740–748. https://doi.org/10.1016/j.nut.2004.11.011

Mills, D.E., Huang, Y.S., Narce, M., Poisson, J.P., 1994. Psychosocial stress, catecholamines, and essential fatty acid metabolism in rats. Proc. Soc. Exp. Biol. Med. 205, 56–61. https://doi.org/10.3181/00379727-205-43677

Mizuno, K., Ueno, Y., 2017. Autonomic nervous system and the liver. Hepatol. Res. 47, 160–165. https://doi.org/10.1111/hepr.12760

Mogk, S., Meiwes, A., Shtopel, S., Schraermeyer, U., Lazarus, M., Kubata, B., Wolburg, H., Duszenko, M., 2014. Cyclical appearance of African trypanosomes in the cerebrospinal fluid: New insights in how trypanosomes enter the CNS. PLoS One 9, e91372.

https://doi.org/10.1371/journal.pone.0091372

Mohamed, H., Miloud, B., Zohra, F., García-Arenzana, J.M., Veloso, A., Rodríguez-Couto, S., 2017. Isolation and characterization of Actinobacteria from Algerian Sahara soils with antimicrobial activities. Int. J. Mol. Cell. Med. 6, 109–120. https://doi.org/10.22088/acadpub.BUMS.6.2.5

Montenegro-Burke, J.R., Sutton, J.A., Rogers, L.M., Milne, G.L., McLean, J.A., Aronoff, D.M., 2016. Lipid profiling of polarized human monocyte-derived macrophages. Prostaglandins Other Lipid Mediat. 127, 1–8. https://doi.org/10.1016/j.prostaglandins.2016.11.002

Moon, P., Minhas, P.S., 2018. Reexamining IFN-γ stimulation of de novo NAD+ in monocyte-derived macrophages. Int. J. Tryptophan Res. 11, 12–19. https://doi.org/10.1177/1178646918773067

Moore, B.A., Stewart, T.M.R., Hill, C., Vanner, S.J., 2002. TNBS ileitis evokes hyperexcitability and changes in ionic membrane properties of nociceptive DRG neurons. Am. J. Physiol. Liver Physiol. 282, G1045–G1051. https://doi.org/10.1152/ajpgi.00406.2001

Morán-Salvador, E., Titos, E., Rius, B., González-Périz, A., García-Alonso, V., López-Vicario, C., Miquel, R., Barak, Y., Arroyo, V., Clària, J., 2013. Cell-specific PPARγ deficiency establishes anti-inflammatory and anti-fibrogenic properties for this nuclear receptor in non-parenchymal liver cells. J. Hepatol. 59, 1045–1053. https://doi.org/10.1016/j.jhep.2013.06.023

Morath, J., Gola, H., Sommershof, A., Hamuni, G., Kolassa, S., Catani, C., Adenauer, H., Ruf-Leuschner, M., Schauer, M., Elbert, T., Groettrup, M., Kolassa, I.-T., 2014. The effect of trauma-focused therapy on the altered T cell distribution in individuals with PTSD: Evidence from a randomized controlled trial. J. Psychiatr. Res. 54, 1–10. https://doi.org/10.1016/j.jpsychires.2014.03.016

Morgan, X.C., Tickle, T.L., Sokol, H., Gevers, D., Devaney, K.L., Ward, D. V, Reyes, J.A., Shah, S.A., LeLeiko, N., Snapper, S.B., Bousvaros, A., Korzenik, J., Sands, B.E., Xavier, R.J., Huttenhower, C., 2012. Dysfunction of the intestinal microbiome in inflammatory bowel disease and treatment. Genome Biol. 13, R79. https://doi.org/10.1186/gb-2012-13-9-r79

Mosser, D.M., Hamidzadeh, K., Goncalves, R., 2020. Macrophages and the maintenance of homeostasis. Cell. Mol. Immunol. 18, 579–587. https://doi.org/10.1038/s41423-020-00541-

3

Mottahedin, A., Joakim Ek, C., Truvé, K., Hagberg, H., Mallard, C., 2019. Choroid plexus transcriptome and ultrastructure analysis reveals a TLR2-specific chemotaxis signature and cytoskeleton remodeling in leukocyte trafficking. Brain. Behav. Immun. 79, 216–227. https://doi.org/10.1016/j.bbi.2019.02.004

Moya-Pérez, A., Perez-Villalba, A., Benítez-Páez, A., Campillo, I., Sanz, Y., 2017. *Bifidobacterium* CECT 7765 modulates early stress-induced immune, neuroendocrine and behavioral alterations in mice. Brain. Behav. Immun. 65, 43–56. https://doi.org/10.1016/j.bbi.2017.05.011

Müller, N., 2019. COX-2 inhibitors, aspirin, and other potential anti-inflammatory treatments for psychiatric disorders. Front. Psychiatry 10, 375. https://doi.org/10.3389/fpsyt.2019.00375

Muñoz, L., Borrero, M.-J., Úbeda, M., Conde, E., del Campo, R., Rodríguez-Serrano, M., Lario, M., Sánchez-Díaz, A.-M., Pastor, O., Díaz, D., García-Bermejo, L., Monserrat, J., Álvarez-Mon, M., Albillos, A., 2018. Intestinal immune dysregulation driven by dysbiosis promotes barrier disruption and bacterial translocation in rats with cirrhosis. Hepatology 70, 925–938. https://doi.org/10.1002/hep.30349

Murakami, Y., Saito, K., 2013. Species and cell types difference in tryptophan metabolism. Int. J. Tryptophan Res. 6, 47–54. https://doi.org/10.4137/IJTR.S11558

Musaeus, C.S., Gleerup, H.S., Høgh, P., Waldemar, G., Hasselbalch, S.G., Simonsen, A.H., 2020. Cerebrospinal fluid/plasma albumin ratio as a biomarker for blood-brain barrier impairment across neurodegenerative dementias. J. Alzheimer's Dis. 75, 429–436. https://doi.org/10.3233/JAD-200168

Nair, V.R., Franco, L.H., Zacharia, V.M., Khan, H.S., Stamm, C.E., You, W., Marciano, D.K., Yagita, H., Levine, B., Shiloh, M.U., 2016. Microfold cells actively translocate *Mycobacterium tuberculosis* to initiate infection. Cell Rep. 16, 1253–1258. https://doi.org/10.1016/j.celrep.2016.06.080

National Center for Posttraumatic Stress Disorder., 2018. How common is PTSD in adults? https://www.ptsd.va.gov/understand/common/common_adults.asp.

National Research Council, 2011. Guide for the care and use of laboratory animals: Eighth edition. Washington, DC: The National Academies Press. https://doi.org/10.17226/12910

Needleman, P., Truk, J., Jakschik, B.A., Morrison, A.R., Lefkowith, J.B., 1986. Arachidonic acid

metabolism. Annu. Rev. Biochem. 55, 69–102. https://doi.org/10.1146/annurev.bi.55.070186.000441

Nemkov, T., Hansen, K.C., D'Alessandro, A., 2017. A three-minute method for high-throughput quantitative metabolomics and quantitative tracing experiments of central carbon and nitrogen pathways. Rapid Commun. Mass Spectrom. 31, 663–673. https://doi.org/10.1002/rcm.7834

Nemkov, T., Reisz, J.A., Gehrke, S., Hansen, K.C., D'Alessandro, A., 2019. High-throughput metabolomics: Isocratic and gradient mass spectrometry-based methods, in: Methods in Molecular Biology. Humana Press Inc., pp. 13–26. https://doi.org/10.1007/978-1-4939-9236-2_2

Nepelska, M., De Wouters, T., Jacouton, E., Béguet-Crespel, F., Lapaque, N., Doré, J., Arulampalam, V., Blottière, H.M., 2017. Commensal gut bacteria modulate phosphorylation-dependent PPARγ transcriptional activity in human intestinal epithelial cells. Sci. Rep. 7, 1–13. https://doi.org/10.1038/srep43199

Neufeld-Cohen, A., Kelly, P.A.T., Paul, E.D., Carter, R.N., Skinner, E., Olverman, H.J., Vaughan, J.M., Issler, O., Kuperman, Y., Lowry, C.A., Vale, W.W., Seckl, J.R., Chen, A., Jamieson, P.M., 2012. Chronic activation of corticotropin-releasing factor type 2 receptors reveals a key role for 5-HT1A receptor responsiveness in mediating behavioral and serotonergic responses to stressful challenge. Biol. Psychiatry 72, 437–447. https://doi.org/10.1016/J.BIOPSYCH.2012.05.005

Neumeier, M., Weigert, J., Schäffler, A., Weiss, T.S., Schmidl, C., Büttner, R., Bollheimer, C., Aslanidis, C., Schölmerich, J., Buechler, C., 2006. Aldehyde oxidase 1 is highly abundant in hepatic steatosis and is downregulated by adiponectin and fenofibric acid in hepatocytes in vitro. Biochem. Biophys. Res. Commun. 350, 731–735. https://doi.org/10.1016/j.bbrc.2006.09.101

Newman, K.D., Mhalhal, T.R., Washington, M.C., Heath, J.C., Sayegh, A.I., 2017. Peptide tyrosine tyrosine 3-36 reduces meal size and activates the enteric neurons in male Sprague–Dawley rats. Dig. Dis. Sci. 62, 3350–3358. https://doi.org/10.1007/s10620-017-4788-3

Neylan, T.C., Sun, B., Rempel, H., Ross, J., Lenoci, M., O'Donovan, A., Pulliam, L., 2011. Suppressed monocyte gene expression profile in men versus women with PTSD. Brain. Behav. Immun. 25, 524–531. https://doi.org/10.1016/j.bbi.2010.12.001

Nicoletti, C., Regoli, M., Bertelli, E., 2009. Dendritic cells in the gut: to sample and to exclude? Mucosal Immunol. 2, 462–462. https://doi.org/10.1038/mi.2009.92

Nie, A., Sun, B., Fu, Z., Yu, D., 2019. Roles of aminoacyl-tRNA synthetases in immune regulation and immune diseases. Cell Death Dis. 10, 901. https://doi.org/10.1038/s41419-019-2145-5

Nighot, M., Al-Sadi, R., Guo, S., Rawat, M., Nighot, P., Watterson, M.D., Ma, T.Y., 2017. Lipopolysaccharide-induced increase in intestinal epithelial tight permeability is mediated by toll-like receptor 4/myeloid differentiation primary response 88 (MyD88) activation of myosin light chain kinase expression. Am. J. Pathol. 187, 2698–2710. https://doi.org/10.1016/J.AJPATH.2017.08.005

Niraula, A., Wang, Y., Godbout, J.P., Sheridan, J.F., 2018. Corticosterone production during repeated social defeat causes monocyte mobilization from the bone marrow, glucocorticoid resistance, and neurovascular adhesion molecule expression. J. Neurosci. 38, 2328–2340. https://doi.org/10.1523/JNEUROSCI.2568-17.2018

Niraula, A., Witcher, K.G., Sheridan, J.F., Godbout, J.P., 2019. Interleukin-6 induced by social stress promotes a unique transcriptional signature in the monocytes that facilitate anxiety. Biol. Psychiatry 85, 679–689. https://doi.org/10.1016/j.biopsych.2018.09.030

Nishihara, H., Soldati, S., Mossu, A., Rosito, M., Rudolph, H., Muller, W.A., Latorre, D., Sallusto, F., Sospedra, M., Martin, R., Ishikawa, H., Tenenbaum, T., Schroten, H., Gosselet, F., Engelhardt, B., 2020. Human CD4+ T cell subsets differ in their abilities to cross endothelial and epithelial brain barriers in vitro. Fluids Barriers CNS 17, 3. https://doi.org/10.1186/s12987-019-0165-2

Nishioka, T., Shimizu, J., Iida, R., Yamazaki, S., Sakaguchi, S., 2006. CD4 + CD25 + Foxp3 + T cells and CD4 + CD25 − Foxp3 + T cells in aged mice. J. Immunol. 176, 6586–6593. https://doi.org/10.4049/jimmunol.176.11.6586

Nishitsuji, K., Xiao, J., Nagatomo, R., Umemoto, H., Morimoto, Y., Akatsu, H., Inoue, K., Tsuneyama, K., 2017. Analysis of the gut microbiome and plasma short-chain fatty acid profiles in a spontaneous mouse model of metabolic syndrome. Sci. Rep. 7, 15876. https://doi.org/10.1038/s41598-017-16189-5

Noble, L.J., Gonzalez, I.J., Meruva, V.B., Callahan, K.A., Belfort, B.D., Ramanathan, K.R., Meyers, E., Kilgard, M.P., Rennaker, R.L., McIntyre, C.K., 2017. Effects of vagus nerve

stimulation on extinction of conditioned fear and post-traumatic stress disorder symptoms in rats. Transl. Psychiatry 7, e1217. https://doi.org/10.1038/tp.2017.191

Noble, L.J., Meruva, V.B., Hays, S.A., Rennaker, R.L., Kilgard, M.P., McIntyre, C.K., 2019. Vagus nerve stimulation promotes generalization of conditioned fear extinction and reduces anxiety in rats. Brain Stimul. 12, 9–18. https://doi.org/10.1016/J.BRS.2018.09.013

Noguera, J.C., Aira, M., Pérez-Losada, M., Domínguez, J., Velando, A., 2018. Glucocorticoids modulate gastrointestinal microbiome in a wild bird. R. Soc. Open Sci. 5, 171743. https://doi.org/10.1098/rsos.171743

Nordahl, E.A., Rydengård, V., Mörgelin, M., Schmidtchen, A., 2005. Domain 5 of high molecular weight kininogen is antibacterial. J. Biol. Chem. 280, 34832–34839. https://doi.org/10.1074/jbc.M507249200

Norris, P.C., Dennis, E.A., 2014. A lipidomic perspective on inflammatory macrophage eicosanoid signaling. Adv. Biol. Regul. 54, 99–110. https://doi.org/10.1016/j.jbior.2013.09.009

Nouioui, I., Brunet, L.R., Simpson, D., Klenk, H.P., Goodfellow, M., 2018. Description of a novel species of fast growing mycobacterium: *Mycobacterium kyogaense* sp. nov., a scotochromogenic strain received as *Mycobacterium vaccae*. Int. J. Syst. Evol. Microbiol. 68, 3726–3734. https://doi.org/10.1099/ijsem.0.003039

Nowak, W., Grendas, L.N., Sanmarco, L.M., Estecho, I.G., Arena, Á.R., Eberhardt, N., Rodante, D.E., Aoki, M.P., Daray, F.M., Carrera Silva, E.A., Errasti, A.E., 2019. Pro-inflammatory monocyte profile in patients with major depressive disorder and suicide behaviour and how ketamine induces anti-inflammatory M2 macrophages by NMDAR and mTOR. EBioMedicine 50, 290–305. https://doi.org/10.1016/j.ebiom.2019.10.063

O'Brien, M.E.R., Anderson, H., Kaukel, E., O'Byrne, K., Pawlicki, M., Von Pawel, J., Reck, M., SR-ON-12 Study Group, 2004. SRL172 (killed *Mycobacterium vaccae*) in addition to standard chemotherapy improves quality of life without affecting survival, in patients with advanced non-small-cell lung cancer: phase III results. Ann. Oncol. Off. J. Eur. Soc. Med. Oncol. 15, 906–914.

O'Donovan, A., Cohen, B.E., Seal, K.H., Bertenthal, D., Margaretten, M., Nishimi, K., Neylan, T.C., 2015. Elevated risk for autoimmune disorders in Iraq and Afghanistan veterans with posttraumatic stress disorder. Biol. Psychiatry 77, 365–374.

https://doi.org/10.1016/j.biopsych.2014.06.015

O'Donovan, A., Neylan, T.C., Metzler, T., Cohen, B.E., 2012. Lifetime exposure to traumatic psychological stress is associated with elevated inflammation in the Heart and Soul Study. Brain. Behav. Immun. 26, 642–649. https://doi.org/10.1016/j.bbi.2012.02.003

O'Farrell, K., Harkin, A., 2017. Stress-related regulation of the kynurenine pathway: Relevance to neuropsychiatric and degenerative disorders. Neuropharmacology 112, 307–323. https://doi.org/10.1016/j.neuropharm.2015.12.004

O'Mahony, S.M., Marchesi, J.R., Scully, P., Codling, C., Ceolho, A.-M., Quigley, E.M.M., Cryan, J.F., Dinan, T.G., 2009. Early life stress alters behavior, immunity, and microbiota in rats: implications for irritable bowel syndrome and psychiatric illnesses. Biol. Psychiatry 65, 263–267. https://doi.org/10.1016/j.biopsych.2008.06.026

O'Neill, L.A.J., Kishton, R.J., Rathmell, J., 2016. A guide to immunometabolism for immunologists. Nat. Rev. Immunol. 16, 553–565. https://doi.org/10.1038/nri.2016.70

Oganesyan, L.P., Mkrtchyan, G.M., Sukiasyan, S.H., Boyajyan, A.S., 2009. Classic and alternative complement cascades in post-traumatic stress disorder. Bull. Exp. Biol. Med. 148, 859–861. https://doi.org/10.1007/s10517-010-0836-0

Oh, D.Y., Dowling, D.J., Ahmed, S., Choi, H., Brightman, S., Bergelson, I., Berger, S.T., Sauld, J.F., Pettengill, M., Kho, A.T., Pollack, H.J., Steen, H., Levy, O., 2016. Adjuvant-induced human monocyte secretome profiles reveal adjuvant- and age-specific protein signatures. Mol. Cell. Proteomics 15, 1877–1894. https://doi.org/10.1074/mcp.M115.055541

Ohnmacht, C., Park, J.-H., Cording, S., Wing, J.B., Atarashi, K., Obata, Y., Gaboriau-Routhiau, V., Marques, R., Dulauroy, S., Fedoseeva, M., Busslinger, M., Cerf-Bensussan, N., Boneca, I.G., Voehringer, D., Hase, K., Honda, K., Sakaguchi, S., Eberl, G., 2015. The microbiota regulates type 2 immunity through RORγt^+ T cells. Science (80-.). 349, 989–993. https://doi.org/10.1126/science.aac4263

Olff, M., van Zuiden, M., 2017. Neuroendocrine and neuroimmune markers in PTSD: pre-, peri- and post-trauma glucocorticoid and inflammatory dysregulation. Curr. Opin. Psychol. 14, 132–137. https://doi.org/10.1016/J.COPSYC.2017.01.001

Onodera, T., Fukuhara, A., Shin, J., Hayakawa, T., Otsuki, M., Shimomura, I., 2017. Eicosapentaenoic acid and 5-HEPE enhance macrophage-mediated Treg induction in mice. Sci. Rep. 7, 4560. https://doi.org/10.1038/s41598-017-04474-2

Opazo, M.C., Ortega-Rocha, E.M., Coronado-Arrázola, I., Bonifaz, L.C., Boudin, H., Neunlist, M., Bueno, S.M., Kalergis, A.M., Riedel, C.A., 2018. Intestinal microbiota influences non-intestinal related autoimmune diseases. Front. Microbiol. 9, 432. https://doi.org/10.3389/fmicb.2018.00432

Orecchioni, M., Ghosheh, Y., Pramod, A.B., Ley, K., 2019. Macrophage polarization: Different gene signatures in M1(Lps+) vs. Classically and M2(LPS-) vs. Alternatively activated macrophages. Front. Immunol. 10, 1084. https://doi.org/10.3389/fimmu.2019.01084

Oshima, Y., Watanabe, Tasuku, Endo, S., Hata, S., Watanabe, Tsuyoshi, Osada, K., Takenaka, A., 2018. Effects of eicosapentaenoic acid and docosahexaenoic acid on anxiety-like behavior in socially isolated rats. Biosci. Biotechnol. Biochem. 82, 716–723. https://doi.org/10.1080/09168451.2017.1403888

Pace, T.W.W., Mletzko, T.C., Alagbe, O., Musselman, D.L., Nemeroff, C.B., Miller, A.H., Heim, C.M., 2006. Increased stress-induced inflammatory responses in male patients with major depression and increased early life stress. Am. J. Psychiatry 163, 1630–1633. https://doi.org/10.1176/ajp.2006.163.9.1630

Palankar, R., Kohler, T.P., Krauel, K., Wesche, J., Hammerschmidt, S., Greinacher, A., 2018. Platelets kill bacteria by bridging innate and adaptive immunity via platelet factor 4 and FcγRIIA. J. Thromb. Haemost. 16, 1187–1197. https://doi.org/10.1111/jth.13955

Pan, X., Wang, Z., Wu, X., Wen, S.W., Liu, A., 2018. Salivary cortisol in post-traumatic stress disorder: a systematic review and meta-analysis. BMC Psychiatry 18, 324. https://doi.org/10.1186/s12888-018-1910-9

Park, J., Marvar, P.J., Liao, P., Kankam, M.L., Norrholm, S.D., Downey, R.M., McCullough, S.A., Le, N.-A., Rothbaum, B.O., 2017. Baroreflex dysfunction and augmented sympathetic nerve responses during mental stress in veterans with post-traumatic stress disorder. J. Physiol. 595, 4893–4908. https://doi.org/10.1113/JP274269

Parnell, E.A., Walch, E.M., Lo, D.D., 2017. Inducible colonic M cells are dependent on TNFR2 but not Ltβr, identifying distinct signalling requirements for constitutive versus inducible M cells. J. Crohns. Colitis 11, 751–760. https://doi.org/10.1093/ecco-jcc/jjw212

Pascovici, D., Handler, D.C.L., Wu, J.X., Haynes, P.A., 2016. Multiple testing corrections in quantitative proteomics: A useful but blunt tool. Proteomics 16, 2448–2453. https://doi.org/10.1002/pmic.201600044

Passlick, B., Flieger, D., Ziegler-Heitbrock, H., 1989. Identification and characterization of a novel monocyte subpopulation in human peripheral blood. Blood 74, 2527–2534. https://doi.org/10.1182/blood.v74.7.2527.2527

Paustian, C., Taylor, P., Johnson, T., Xu, M., Ramirez, N., Rosenthal, K.S., Shu, S., Cohen, P.A., Czerniecki, B.J., Koski, G.K., 2013. Extracellular ATP and toll-like receptor 2 agonists trigger in human monocytes an activation program that favors T helper 17. PLoS One 8, e54804. https://doi.org/10.1371/journal.pone.0054804

Pavlov, V.A., Tracey, K.J., 2012. The vagus nerve and the inflammatory reflex - Linking immunity and metabolism. Nat. Rev. Endocrinol. 8, 743–754. https://doi.org/10.1038/nrendo.2012.189

Pawlinski, R., Mackman, N., 2010. Cellular sources of tissue factor in endotoxemia and sepsis. Thromb. Res. 125, S70. https://doi.org/10.1016/j.thromres.2010.01.042

Pearson-Leary, J., Eacret, D., Chen, R., Takano, H., Nicholas, B., Bhatnagar, S., 2017. Inflammation and vascular remodeling in the ventral hippocampus contributes to vulnerability to stress. Transl. Psychiatry 7, e1160. https://doi.org/10.1038/tp.2017.122

Pellissier, S., Dantzer, C., Mondillon, L., Trocme, C., Gauchez, A.-S., Ducros, V., Mathieu, N., Toussaint, B., Fournier, A., Canini, F., Bonaz, B., 2014. Relationship between vagal tone, cortisol, TNF-alpha, epinephrine and negative affects in Crohn's disease and irritable bowel syndrome. PLoS One 9, e105328. https://doi.org/10.1371/journal.pone.0105328

Peña, J.A., Rogers, A.B., Ge, Z., Ng, V., Li, S.Y., Fox, J.G., Versalovic, J., 2005. Probiotic *Lactobacillus* spp. diminish *Helicobacter hepaticus*-induced inflammatory bowel disease in interleukin-10-deficient mice. Infect. Immun. 73, 912–925. https://doi.org/10.1128/IAI.73.2.912-920.2005

Penas, F., Mirkin, G.A., Vera, M., Cevey, Á., González, C.D., Gómez, M.I., Sales, M.E., Goren, N.B., 2015. Treatment in vitro with PPARα and PPARγ ligands drives M1-to-M2 polarization of macrophages from T. cruzi-infected mice. Biochim. Biophys. Acta - Mol. Basis Dis. 1852, 893–904. https://doi.org/10.1016/j.bbadis.2014.12.019

Peng, L., Li, Z.R., Green, R.S., Holzman, I.R., Lin, J., 2009. Butyrate enhances the intestinal barrier by facilitating tight junction assembly via activation of AMP-activated protein kinase in Caco-2 cell monolayers. J. Nutr. 139, 1619–1625. https://doi.org/10.3945/jn.109.104638

Peng, Z., Zhang, C., Yan, L., Zhang, Y., Yang, Z., Wang, J., Song, C., 2020. EPA is more effective than DHA to improve depression-like behavior, glia cell dysfunction and hippcampal apoptosis signaling in a chronic stress-induced rat model of depression. Int. J. Mol. Sci. 21, 1769. https://doi.org/10.3390/ijms21051769

Pennings, M., Meurs, I., Ye, D., Out, R., Hoekstra, M., Van Berkel, T.J.C., Eck, M. Van, 2006. Regulation of cholesterol homeostasis in macrophages and consequences for atherosclerotic lesion development. FEBS Lett. 580, 5588–5596. https://doi.org/10.1016/j.febslet.2006.08.022

Pepys, M.B., Hirschfield, G.M., 2003. C-reactive protein: a critical update. J. Clin. Invest. 111, 1805–1812. https://doi.org/10.1172/jci18921

Percie du Sert, N., Hurst, V., Ahluwalia, A., Alam, S., Avey, M.T., Baker, M., Browne, W.J., Clark, A., Cuthill, I.C., Dirnagl, U., Emerson, M., Garner, P., Holgate, S.T., Howells, D.W., Karp, N.A., Lazic, S.E., Lidster, K., MacCallum, C.J., Macleod, M., Pearl, E.J., Petersen, O.H., Rawle, F., Reynolds, P., Rooney, K., Sena, E.S., Silberberg, S.D., Steckler, T., Würbel, H., 2020. The ARRIVE guidelines 2.0: Updated guidelines for reporting animal research. PLOS Biol. 18, e3000410. https://doi.org/10.1371/journal.pbio.3000410

Perdigòn, G., Medina, M., Vintiñi, E., Valdez, J.C., 2000. Intestinal pathway of internalisation of lactic acid bacteria and gut mucosal immunostimulation. Int. J. Immunopathol. Pharmacol. 13, 141–150.

Perdomo, C., Zedler, U., Kühl, A.A., Lozza, L., Saikali, P., Sander, L.E., Vogelzang, A., Kaufmann, S.H.E., Kupz, A., 2016. Mucosal BCG vaccination induces protective lung-resident memory T cell populations against tuberculosis. MBio 7, e01686-16. https://doi.org/10.1128/mBio.01686-16

Perez-Burgos, A., Wang, B., Mao, Y.-K., Mistry, B., Neufeld, K.-A.M., Bienenstock, J., Kunze, W., 2013. Psychoactive bacteria *Lactobacillus rhamnosus* (JB-1) elicits rapid frequency facilitation in vagal afferents. Am. J. Physiol. Liver Physiol. 304, G211–G220. https://doi.org/10.1152/ajpgi.00128.2012

Pérgola, P.E., Alper, R.H., 1992. Effects of central serotonin on autonomic control of heart rate in intact and baroreceptor deficient rats. Brain Res. 582, 215–220. https://doi.org/10.1016/0006-8993(92)90135-V

Perry, R.J., Peng, L., Barry, N.A., Cline, G.W., Zhang, D., Cardone, R.L., Petersen, K.F.,

Kibbey, R.G., Goodman, A.L., Shulman, G.I., 2016. Acetate mediates a microbiome-brain-β-cell axis to promote metabolic syndrome. Nature 534, 213–217. https://doi.org/10.1038/nature18309

Pervanidou, P., Kolaitis, G., Charitaki, S., Lazaropoulou, C., Papassotiriou, I., Hindmarsh, P., Bakoula, C., Tsiantis, J., Chrousos, G.P., 2007. The natural history of neuroendocrine changes in pediatric posttraumatic stress disorder (PTSD) after motor vehicle accidents: progressive divergence of noradrenaline and cortisol concentrations over time. Biol. Psychiatry 62, 1095–1102. https://doi.org/10.1016/j.biopsych.2007.02.008

Petit, V., Parcelier, A., Mathé, C., Barroca, V., Torres, C., Lewandowski, D., Ferri, F., Gallouët, A.S., Dalloz, M., Dinet, O., Boschetti, G., Vozenin, M.C., Roméo, P.H., 2019. TRIM33 deficiency in monocytes and macrophages impairs resolution of colonic inflammation. EBioMedicine 44, 60–70. https://doi.org/10.1016/j.ebiom.2019.05.037

Piccini, A., Carta, S., Tassi, S., Lasiglié, D., Fossati, G., Rubartelli, A., 2008. ATP is released by monocytes stimulated with pathogen-sensing receptor ligands and induces IL-1β and IL-18 secretion in an autocrine way. Proc. Natl. Acad. Sci. U. S. A. 105, 8067–8072. https://doi.org/10.1073/pnas.0709684105

Pickens, C.A., Sordillo, L.M., Zhang, C., Fenton, J.I., 2017. Obesity is positively associated with arachidonic acid-derived 5- and 11-hydroxyeicosatetraenoic acid (HETE). Metabolism. 70, 177–191. https://doi.org/10.1016/j.metabol.2017.01.034

Pickens, C.A., Yin, Z., Sordillo, L.M., Fenton, J.I., 2019. Arachidonic acid-derived hydroxyeicosatetraenoic acids are positively associated with colon polyps in adult males: a cross-sectional study. Sci. Rep. 9, 12033. https://doi.org/10.1038/s41598-019-48381-0

Pinto-Sanchez, M.I., Hall, G.B., Ghajar, K., Nardelli, A., Bolino, C., Lau, J.T., Martin, F.-P., Cominetti, O., Welsh, C., Rieder, A., Traynor, J., Gregory, C., De Palma, G., Pigrau, M., Ford, A.C., Macri, J., Berger, B., Bergonzelli, G., Surette, M.G., Collins, S.M., Moayyedi, P., Bercik, P., 2017. Probiotic *Bifidobacterium longum* NCC3001 reduces depression scores and alters brain activity: a pilot study in patients with irritable bowel syndrome. Gastroenterology 153, 448–459.e8. https://doi.org/10.1053/j.gastro.2017.05.003

Pisani, V., Stefani, A., Pierantozzi, M., Natoli, S., Stanzione, P., Franciotta, D., Pisani, A., 2012. Increased blood-cerebrospinal fluid transfer of albumin in advanced Parkinson's disease. J. Neuroinflammation 9, 188. https://doi.org/10.1186/1742-2094-9-188

Pizurki, L., Zhou, Z., Glynos, K., Roussos, C., Papapetropoulos, A., 2003. Angiopoietin-1 inhibits endothelial permeability, neutrophil adherence and IL-8 production. Br. J. Pharmacol. 139, 329–336. https://doi.org/10.1038/sj.bjp.0705259

Polanski, M., Melican, N.S., Zhang, J., Weiner, H.L., 1997. Oral administration of the immunodominant B-chain of insulin reduces diabetes in a Co-transfer model of diabetes in the NOD mouse and is associated with a switch from Th1 to Th2 cytokines. J. Autoimmun. 10, 339–346. https://doi.org/10.1006/jaut.1997.0148

Powers, R.K., Culp-Hill, R., Ludwig, M.P., Smith, K.P., Waugh, K.A., Minter, R., Tuttle, K.D., Lewis, H.C., Rachubinski, A.L., Granrath, R.E., Carmona-Iragui, M., Wilkerson, R.B., Kahn, D.E., Joshi, M., Lleó, A., Blesa, R., Fortea, J., D'Alessandro, A., Costello, J.C., Sullivan, K.D., Espinosa, J.M., 2019. Trisomy 21 activates the kynurenine pathway via increased dosage of interferon receptors. Nat. Commun. 10, 4766. https://doi.org/10.1038/s41467-019-12739-9

Pradhananga, S., Lomax, A.E., Allen-Vercoe, E., Petrof, E.O., 2018. Secretions of intestinal microbiota increase the excitability of vagal afferent neurons via a protease activated receptor 2 (PAR2)-dependent pathway. J. Can. Assoc. Gastroenterol. 1, 408–408. https://doi.org/10.1093/jcag/gwy009.283

Pu, J., Liu, Y., Zhang, H., Tian, L., Gui, S., Yu, Y., Chen, X., Chen, Y., Yang, L., Ran, Y., Zhong, X., Xu, S., Song, X., Liu, L., Zheng, P., Wang, H., Xie, P., 2020. An integrated meta-analysis of peripheral blood metabolites and biological functions in major depressive disorder. Mol. Psychiatry 1–12. https://doi.org/10.1038/s41380-020-0645-4

Qi, C.C., Wang, Q.J., Ma, X. zhu, Chen, H.C., Gao, L.P., Yin, J., Jing, Y.H., 2018. Interaction of basolateral amygdala, ventral hippocampus and medial prefrontal cortex regulates the consolidation and extinction of social fear. Behav. Brain Funct. 14, 7. https://doi.org/10.1186/s12993-018-0139-6

Qin, J., Li, R., Raes, J., Arumugam, M., Burgdorf, K.S., Manichanh, C., Nielsen, T., Pons, N., Levenez, F., Yamada, T., Mende, D.R., Li, J., Xu, J., Li, Shaochuan, Li, D., Cao, J., Wang, B., Liang, H., Zheng, H., Xie, Y., Tap, J., Lepage, P., Bertalan, M., Batto, J.-M., Hansen, T., Le Paslier, D., Linneberg, A., Nielsen, H.B., Pelletier, E., Renault, P., Sicheritz-Ponten, T., Turner, K., Zhu, H., Yu, C., Li, Shengting, Jian, M., Zhou, Y., Li, Y., Zhang, X., Li, Songgang, Qin, N., Yang, H., Wang, Jian, Brunak, S., Doré, J., Guarner, F., Kristiansen, K.,

Pedersen, O., Parkhill, J., Weissenbach, J., Bork, P., Ehrlich, S.D., Wang, Jun, Blottiere, H., Borruel, N., Bruls, T., Casellas, F., Chervaux, C., Cultrone, A., Delorme, C., Denariaz, G., Dervyn, R., Forte, M., Friss, C., Guchte, M. van de, Guedon, E., Haimet, F., Jamet, A., Juste, C., Kaci, G., Kleerebezem, M., Knol, J., Kristensen, M., Layec, S., Roux, K. Le, Leclerc, M., Maguin, E., Minardi, R.M., Oozeer, R., Rescigno, M., Sanchez, N., Tims, S., Torrejon, T., Varela, E., Vos, W. de, Winogradsky, Y., Zoetendal, E., Bork, P., Ehrlich, S.D., Wang, Jun, 2010. A human gut microbial gene catalogue established by metagenomic sequencing. Nature 464, 59–65. https://doi.org/10.1038/nature08821

Ramírez-Pérez, O., Cruz-Ramón, V., Chinchilla-López, P., Méndez-Sánchez, N., 2017. The role of the gut microbiota in bile acid metabolism. Ann. Hepatol. 16, 15–20. https://doi.org/10.5604/01.3001.0010.5494

Ramirez, S.H., Heilman, D., Morsey, B., Potula, R., Haorah, J., Persidsky, Y., 2008. Activation of peroxisome proliferator-activated receptor γ (PPARγ) suppresses Rho GTPases in human brain microvascular endothelial cells and inhibits adhesion and transendothelial migration of HIV-1 infected monocytes. J. Immunol. 180, 1854–1865. https://doi.org/10.4049/jimmunol.180.3.1854

Ransohoff, R.M., Cardona, A.E., 2010. The myeloid cells of the central nervous system parenchyma. Nature 468, 253–262. https://doi.org/10.1038/nature09615

Ratajczak, M.Z., Adamiak, M., Kucia, M., Tse, W., Ratajczak, J., Wiktor-Jedrzejczak, W., 2018. The emerging link between the complement cascade and purinergic signaling in stress hematopoiesis. Front. Immunol. 9, 1295. https://doi.org/10.3389/fimmu.2018.01295

Rattigan, K.M., Pountain, A.W., Regnault, C., Achcar, F., Vincent, I.M., Goodyear, C.S., Barrett, M.P., 2018. Metabolomic profiling of macrophages determines the discrete metabolomic signature and metabolomic interactome triggered by polarising immune stimuli. PLoS One 13, e0194126. https://doi.org/10.1371/journal.pone.0194126

Reader, B.F., Jarrett, B.L., McKim, D.B., Wohleb, E.S., Godbout, J.P., Sheridan, J.F., 2015. Peripheral and central effects of repeated social defeat stress: Monocyte trafficking, microglial activation, and anxiety. Neuroscience 289, 429–442. https://doi.org/10.1016/j.neuroscience.2015.01.001

Reber, S.O., 2012. Stress and animal models of inflammatory bowel disease—An update on the role of the hypothalamo–pituitary–adrenal axis. Psychoneuroendocrinology 37, 1–19.

https://doi.org/10.1016/j.psyneuen.2011.05.014

Reber, S.O., Langgartner, D., Foertsch, S., Postolache, T.T., Brenner, L.A., Guendel, H., Lowry, C.A., 2016a. Chronic subordinate colony housing paradigm: A mouse model for mechanisms of PTSD vulnerability, targeted prevention, and treatment. Psychoneuroendocrinology 74, 221–230. https://doi.org/10.1016/j.psyneuen.2016.08.031

Reber, S.O., Obermeier, F., Straub, H.R., Falk, W., Neumann, I.D., 2006. Chronic intermittent psychosocial stress (social defeat/overcrowding) in mice increases the severity of an acute DSS-induced colitis and impairs regeneration. Endocrinology 147, 4968–4976. https://doi.org/10.1210/en.2006-0347

Reber, S.O., Siebler, P.H., Donner, N.C., Morton, J.T., Smith, D.G., Kopelman, J.M., Lowe, K.R., Wheeler, K.J., Fox, J.H., Hassell, J.E., Greenwood, B.N., Jansch, C., Lechner, A., Schmidt, D., Uschold-Schmidt, N., Füchsl, A.M., Langgartner, D., Walker, F.R., Hale, M.W., Lopez Perez, G., Van Treuren, W., González, A., Halweg-Edwards, A.L., Fleshner, M., Raison, C.L., Rook, G.A.W., Peddada, S.D., Knight, R., Lowry, C.A., 2016b. Immunization with a heat-killed preparation of the environmental bacterium *Mycobacterium vaccae* promotes stress resilience in mice. Proc. Natl. Acad. Sci. 113, E3130–E3139. https://doi.org/10.1073/pnas.1600324113

Regan-Komito, D., Valaris, S., Kapellos, T.S., Recio, C., Taylor, L., Greaves, D.R., Iqbal, A.J., 2017. Absence of the non-signalling chemerin receptor CCRL2 exacerbates acute inflammatory responses in vivo. Front. Immunol. 8, 21. https://doi.org/10.3389/fimmu.2017.01621

Regan, T., Gill, A.C., Clohisey, S.M., Barnett, M.W., Pariante, C.M., Harrison, N.A., Hume, D.A., Bullmore, E.T., Freeman, T.C., 2018. Effects of anti-inflammatory drugs on the expression of tryptophan-metabolism genes by human macrophages. J. Leukoc. Biol. 103, 681–692. https://doi.org/10.1002/JLB.3A0617-261R

Reichmann, F., Hassan, A.M., Farzi, A., Jain, P., Schuligoi, R., Holzer, P., 2015. Dextran sulfate sodium-induced colitis alters stress-associated behaviour and neuropeptide gene expression in the amygdala-hippocampus network of mice. Sci. Rep. 5, 9970. https://doi.org/10.1038/srep09970

Reidelberger, R., Haver, A., Chelikani, P.K., 2013. Role of peptide YY(3-36) in the satiety produced by gastric delivery of macronutrients in rats. Am. J. Physiol. Endocrinol. Metab.

304, E944–E950. https://doi.org/10.1152/ajpendo.00075.2013

Reigstad, C.S., Salmonson, C.E., Rainey, J.F., Szurszewski, J.H., Linden, D.R., Sonnenburg, J.L., Farrugia, G., Kashyap, P.C., 2015. Gut microbes promote colonic serotonin production through an effect of short-chain fatty acids on enterochromaffin cells. FASEB J. 29, 1395–1403. https://doi.org/10.1096/fj.14-259598

Reilly, S.M., Ahmadian, M., Zamarron, B.F., Chang, L., Uhm, M., Poirier, B., Peng, X., Krause, D.M., Korytnaya, E., Neidert, A., Liddle, C., Yu, R.T., Lumeng, C.N., Oral, E.A., Downes, M., Evans, R.M., Saltiel, A.R., 2015. A subcutaneous adipose tissue-liver signalling axis controls hepatic gluconeogenesis. Nat. Commun. 6, 1–12. https://doi.org/10.1038/ncomms7047

Reisman, M., 2016. PTSD treatment for veterans: what's working, what's new, and what's next. P T. 41, 623–634.

Reisz, J.A., Zheng, C., D'Alessandro, A., Nemkov, T., 2019. Untargeted and semi-targeted lipid analysis of biological samples using mass spectrometry-based metabolomics, in: Methods in Molecular Biology. Humana Press Inc., pp. 121–135. https://doi.org/10.1007/978-1-4939-9236-2_8

Remmerie, A., Scott, C.L., 2018. Macrophages and lipid metabolism. Cell. Immunol. 330, 27–42. https://doi.org/10.1016/j.cellimm.2018.01.020

Ren, J., Zhao, Y., Huang, S., Lv, D., Yang, F., Lou, L., Zheng, Y., Zhang, J., Liu, S., Zhang, N., Bachert, C., 2018. Immunomodulatory effect of *Bifidobacterium breve* on experimental allergic rhinitis in BALB/c mice. Exp. Ther. Med. 16, 3996–4004. https://doi.org/10.3892/etm.2018.6704

Ricciotti, E., Fitzgerald, G.A., 2011. Prostaglandins and inflammation. Arterioscler. Thromb. Vasc. Biol. 31, 986–1000. https://doi.org/10.1161/ATVBAHA.110.207449

Ridlon, J.M., Kang, D.-J., Hylemon, P.B., 2006. Bile salt biotransformations by human intestinal bacteria. J. Lipid Res. 47, 241–259. https://doi.org/10.1194/jlr.R500013-JLR200

Ridlon, J.M., Kang, D.J., Hylemon, P.B., Bajaj, J.S., 2014. Bile acids and the gut microbiome. Curr. Opin. Gastroenterol. 30, 332–338. https://doi.org/10.1097/MOG.0000000000000057

Ristori, G., Faustman, D., Matarese, G., Romano, S., Salvetti, M., 2018. Bridging the gap between vaccination with Bacille Calmette-Guérin (BCG) and immunological tolerance: the cases of type 1 diabetes and multiple sclerosis. Curr. Opin. Immunol. 55, 89–96

https://doi.org/10.1016/j.coi.2018.09.016

Robicsek, O., Makhoul, B., Klein, E., Brenner, B., Sarig, G., 2011. Hypercoagulation in chronic post-traumatic stress disorder - PubMed. Isr. Med. Assoc. J. 13, 548–552.

Roehrig, C., 2016. Mental disorders top the list of the most costly conditions in the United States: $201 billion. Health Aff. 35, 1130–1135. https://doi.org/10.1377/hlthaff.2015.1659

Rogers, T.J., Christenson, J.L., Greene, L.I., O'Neill, K.I., Williams, M.M., Gordon, M.A., Nemkov, T., D'Alessandro, A., Degala, G.D., Shin, J., Tan, A.C., Cittelly, D.M., Lambert, J.R., Richer, J.K., 2019. Reversal of triple-negative breast cancer EMT by miR-200c decreases tryptophan catabolism and a program of immunosuppression. Mol. Cancer Res. 17, 30–41. https://doi.org/10.1158/1541-7786.MCR-18-0246

Rohleder, N., 2014. Stimulation of systemic low-grade inflammation by psychosocial stress. Psychosom. Med. https://doi.org/10.1097/PSY.0000000000000049

Rolland, B., Deguil, J., Jardri, R., Cottencin, O., Thomas, P., Bordet, R., 2013. Therapeutic prospects of PPARs in psychiatric disorders: A comprehensive review. Curr. Drug Targets 14, 724–732. https://doi.org/10.2174/1389450111314070002

Rook, G.A.W., 2013. Regulation of the immune system by biodiversity from the natural environment: An ecosystem service essential to health. Proc. Natl. Acad. Sci. U. S. A. 110, 18360–18367. https://doi.org/10.1073/pnas.1313731110

Rook, G.A.W., Adams, V., Hunt, J., Palmer, R., Martinelli, R., Brunet, L.R., 2004. Mycobacteria and other environmental organisms as immunomodulators for immunoregulatory disorders. Springer Semin. Immunopathol. 25, 237–255. https://doi.org/10.1007/s00281-003-0148-9

Rook, G.A.W., Brunet, L.R., 2005. Microbes, immunoregulation, and the gut. Gut 54, 317–320. https://doi.org/10.1136/gut.2004.053785

Rook, G.A.W., Lowry, C.A., 2008. The hygiene hypothesis and psychiatric disorders. Trends Immunol. 29, 150–158. https://doi.org/10.1016/J.IT.2008.01.002

Rook, G.A.W., Lowry, C.A., Raison, C.L., 2013a. Microbial "Old Friends", immunoregulation and stress resilience. Evol. Med. public Heal. 2013, 46–64. https://doi.org/10.1093/emph/eot004

Rook, G.A.W., Raison, C.L., Lowry, C.A., 2014. Microbial "old friends", immunoregulation and socioeconomic status. Clin. Exp. Immunol. 177, 1–12. https://doi.org/10.1111/cei.12269

Rook, G.A.W., Raison, C.L., Lowry, C.A., 2013b. Childhood microbial experience,

immunoregulation, inflammation and adult susceptibility to psychosocial stressors and depression in rich and poor countries. Evol. Med. Public Heal. 2013, 14–17. https://doi.org/10.1093/emph/eos005

Rosen, R.L., Levy-Carrick, N., Reibman, J., Xu, N., Shao, Y., Liu, M., Ferri, L., Kazeros, A., Caplan-Shaw, C.E., Pradhan, D.R., Marmor, M., Galatzer-Levy, I.R., 2017. Elevated C-reactive protein and posttraumatic stress pathology among survivors of the 9/11 World Trade Center attacks. J. Psychiatr. Res. 89, 14–21. https://doi.org/10.1016/j.jpsychires.2017.01.007

Rosman, L., Sico, J.J., Lampert, R., Gaffey, A.E., Ramsey, C.M., Dziura, J., Chui, P.W., Cavanagh, C.E., Brandt, C., Haskell, S., Burg, M.M., 2019. Posttraumatic stress disorder and risk for stroke in young and middle-aged adults: A 13-year cohort study. Stroke 50, 2996–3003. https://doi.org/10.1161/STROKEAHA.119.026854

Rothschild, D., Weissbrod, O., Barkan, E., Kurilshikov, A., Korem, T., Zeevi, D., Costea, P.I., Godneva, A., Kalka, I.N., Bar, N., Shilo, S., Lador, D., Vila, A.V., Zmora, N., Pevsner-Fischer, M., Israeli, D., Kosower, N., Malka, G., Wolf, B.C., Avnit-Sagi, T., Lotan-Pompan, M., Weinberger, A., Halpern, Z., Carmi, S., Fu, J., Wijmenga, C., Zhernakova, A., Elinav, E., Segal, E., 2018. Environment dominates over host genetics in shaping human gut microbiota. Nature 555, 210–215. https://doi.org/10.1038/nature25973

Rouillard, A.D., Gundersen, G.W., Fernandez, N.F., Wang, Z., Monteiro, C.D., McDermott, M.G., Ma'ayan, A., 2016. The Harmonizome: a collection of processed datasets gathered to serve and mine knowledge about genes and proteins. Database (Oxford). 2016, baw100. https://doi.org/10.1093/database/baw100

Rowland, I., Gibson, G., Heinken, A., Scott, K., Swann, J., Thiele, I., Tuohy, K., 2018. Gut microbiota functions: metabolism of nutrients and other food components. Eur. J. Nutr. 57, 1–24. https://doi.org/10.1007/s00394-017-1445-8

Ruddick, J.P., Evans, A.K., Nutt, D.J., Lightman, S.L., Rook, G.A.W., Lowry, C.A., 2006. Tryptophan metabolism in the central nervous system: Medical implications. Expert Rev. Mol. Med. 8, 1–27. https://doi.org/10.1017/S1462399406000068

Ruiz, A., Sarabia, C., Torres, M., Juárez, E., 2019. Resolvin D1 (RvD1) and maresin 1 (Mar1) contribute to human macrophage control of M. tuberculosis infection while resolving inflammation. Int. Immunopharmacol. 74, 105694.

https://doi.org/10.1016/j.intimp.2019.105694

Russ, T.C., Kivimäki, M., Morling, J.R., Starr, J.M., Stamatakis, E., Batty, G.D., 2015. Association between psychological distress and liver disease mortality: A meta-analysis of individual study participants. Gastroenterology 148, 958-966.e4. https://doi.org/10.1053/j.gastro.2015.02.004

Russell, S.L., Lamprecht, D.A., Mandizvo, T., Crossman, D.K., Wells, G., Steyn Correspondence, A.J.C., 2019. Compromised metabolic reprogramming is an early indicator of CD8 + T cell dysfunction during chronic *Mycobacterium tuberculosis* infection. CellReports 29, 3564-3579.e5. https://doi.org/10.1016/j.celrep.2019.11.034

Russell, W.R., Gratz, S.W., Duncan, S.H., Holtrop, G., Ince, J., Scobbie, L., Duncan, G., Johnstone, A.M., Lobley, G.E., Wallace, R.J., Duthie, G.G., Flint, H.J., 2011. High-protein, reduced-carbohydrate weight-loss diets promote metabolite profiles likely to be detrimental to colonic health. Am. J. Clin. Nutr. 93, 1062–1072. https://doi.org/10.3945/ajcn.110.002188

Ryan, K.K., Grayson, B.E., Jones, K.R., Schneider, A.L., Woods, S.C., Seeley, R.J., Herman, J.P., Ulrich-Lai, Y.M., 2012. Physiological responses to acute psychological stress are reduced by the PPARγ agonist rosiglitazone. Endocrinology 153, 1279–1287. https://doi.org/10.1210/en.2011-1689

Saez-Lara, M.J., Gomez-Llorente, C., Plaza-Diaz, J., Gil, A., 2015. The role of probiotic lactic acid bacteria and bifidobacteria in the prevention and treatment of inflammatory bowel disease and other related diseases: a systematic review of randomized human clinical trials. Biomed Res. Int. 2015, 1–15. https://doi.org/10.1155/2015/505878

Sanchez, J.I., Marzorati, M., Grootaert, C., Baran, M., Van Craeyveld, V., Courtin, C.M., Broekaert, W.F., Delcour, J.A., Verstraete, W., Van de Wiele, T., 2009. Arabinoxylan-oligosaccharides (AXOS) affect the protein/carbohydrate fermentation balance and microbial population dynamics of the Simulator of Human Intestinal Microbial Ecosystem. Microb. Biotechnol. 2, 101–113. https://doi.org/10.1111/j.1751-7915.2008.00064.x

Santisteban, M.M., Qi, Y., Zubcevic, J., Kim, S., Yang, T., Shenoy, V., Cole-Jeffrey, C.T., Lobaton, G.O., Stewart, D.C., Rubiano, A., Simmons, C.S., Garcia-Pereira, F., Johnson, R.D., Pepine, C.J., Raizada, M.K., 2017. Hypertension-linked pathophysiological alterations in the gut. Circ. Res. 120, 312–323. https://doi.org/10.1161/CIRCRESAHA.116.309006

Sarkar, A., Lehto, S.M., Harty, S., Dinan, T.G., Cryan, J.F., Burnet, P.W.J., 2016. Psychobiotics and the manipulation of bacteria–gut–brain signals. Trends Neurosci. 39, 763–781. https://doi.org/10.1016/j.tins.2016.09.002

Satyam, A., Graef, E.R., Lapchak, P.H., Tsokos, M.G., Dalle Lucca, J.J., Tsokos, G.C., 2019. Complement and coagulation cascades in trauma. Acute Med. Surg. 6, 329–335. https://doi.org/10.1002/ams2.426

Savignac, H.M., Kiely, B., Dinan, T.G., Cryan, J.F., 2014. Bifidobacteria exert strain-specific effects on stress-related behavior and physiology in BALB/c mice. Neurogastroenterol. Motil. 26, 1615–1627. https://doi.org/10.1111/nmo.12427

Savignac, H.M., Tramullas, M., Kiely, B., Dinan, T.G., Cryan, J.F., 2015. Bifidobacteria modulate cognitive processes in an anxious mouse strain. Behav. Brain Res. 287, 59–72. https://doi.org/10.1016/j.bbr.2015.02.044

Savino, F., Galliano, I., Garro, M., Savino, A., Daprà, V., Montanari, P., Bergallo, M., 2018. Regulatory T cells and Toll-like receptor 2 and 4 mRNA expression in infants with colic treated with *Lactobacillus reuteri* DSM17938. Benef. Microbes 1–10. https://doi.org/10.3920/BM2017.0194

Savitz, J., 2017. Role of kynurenine metabolism pathway activation in major depressive disorders, in: Current Topics in Behavioral Neurosciences. Springer Verlag, pp. 249–268. https://doi.org/10.1007/7854_2016_12

Sawicki, C.M., McKim, D.B., Wohleb, E.S., Jarrett, B.L., Reader, B.F., Norden, D.M., Godbout, J.P., Sheridan, J.F., 2015. Social defeat promotes a reactive endothelium in a brain region-dependent manner with increased expression of key adhesion molecules, selectins and chemokines associated with the recruitment of myeloid cells to the brain. Neuroscience 302, 151–164. https://doi.org/10.1016/j.neuroscience.2014.10.004

Saxena, P.R., Villalón, C.M., 1991. 5-Hydroxytryptamine: a chameleon in the heart. Trends Pharmacol. Sci. 12, 223–227. https://doi.org/10.1016/0165-6147(91)90556-8

Sayin, S.I., Wahlström, A., Felin, J., Jäntti, S., Marschall, H.-U., Bamberg, K., Angelin, B., Hyötyläinen, T., Orešič, M., Bäckhed, F., 2013. Gut microbiota regulates bile acid metabolism by reducing the levels of tauro-beta-muricholic acid, a naturally occurring FXR antagonist. Cell Metab. 17, 225–235. https://doi.org/10.1016/j.cmet.2013.01.003

Schäfer, T., Schwarz, M.A., 2019. The meaningfulness of effect sizes in psychological research:

Differences between sub-disciplines and the impact of potential biases. Front. Psychol. 10, 813. https://doi.org/10.3389/fpsyg.2019.00813

Schirmer, M., Smeekens, S.P., Vlamakis, H., Jaeger, M., Oosting, M., Franzosa, E.A., Ter Horst, R., Jansen, T., Jacobs, L., Bonder, M.J., Kurilshikov, A., Fu, J., Joosten, L.A.B., Zhernakova, A., Huttenhower, C., Wijmenga, C., Netea, M.G., Xavier, R.J., 2016. Linking the human gut microbiome to inflammatory cytokine production capacity. Cell 167, 1125-1136.e8. https://doi.org/10.1016/j.cell.2016.10.020

Schiweck, C., Claes, S., Van Oudenhove, L., Lafit, G., Vaessen, T., de Beeck, G.O., Berghmans, R., Wijkhuijs, A., Müller, N., Arolt, V., Drexhage, H., Vrieze, E., 2020. Childhood trauma, suicide risk and inflammatory phenotypes of depression: insights from monocyte gene expression. Transl. Psychiatry 10, 1–12. https://doi.org/10.1038/s41398-020-00979-z

Schmid, M., Gemperle, C., Rimann, N., Hersberger, M., 2016. Resolvin D1 polarizes primary human macrophages toward a proresolution phenotype through GPR32. J. Immunol. 196, 3429–3437. https://doi.org/10.4049/jimmunol.1501701

Schultebraucks, K., Qian, M., Abu-Amara, D., Dean, K., Laska, E., Siegel, C., Gautam, A., Guffanti, G., Hammamieh, R., Misganaw, B., Mellon, S.H., Wolkowitz, O.M., Blessing, E.M., Etkin, A., Ressler, K.J., Doyle, F.J., Jett, M., Marmar, C.R., 2020. Pre-deployment risk factors for PTSD in active-duty personnel deployed to Afghanistan: a machine-learning approach for analyzing multivariate predictors. Mol. Psychiatry. https://doi.org/10.1038/s41380-020-0789-2

Schwab, J.M., Chiang, N., Arita, M., Serhan, C.N., 2007. Resolvin E1 and protectin D1 activate inflammation-resolution programmes. Nature 447, 869–874. https://doi.org/10.1038/nature05877

Sefik, E., Geva-Zatorsky, N., Oh, S., Konnikova, L., Zemmour, D., McGuire, A.M., Burzyn, D., Ortiz-Lopez, A., Lobera, M., Yang, J., Ghosh, S., Earl, A., Snapper, S.B., Jupp, R., Kasper, D., Mathis, D., Benoist, C., 2015. Individual intestinal symbionts induce a distinct population of RORγ^+ regulatory T cells. Science 349, 993–7. https://doi.org/10.1126/science.aaa9420

Seligman, M.E., Maier, S.F., 1967. Failure to escape traumatic shock. J. Exp. Psychol. 74, 1–9. https://doi.org/10.1037/h0024514

Selkrig, J., Wong, P., Zhang, X., Pettersson, S., 2014. Metabolic tinkering by the gut

microbiome: Implications for brain development and function. Gut Microbes 5, 369. https://doi.org/10.4161/gmic.28681

Sender, R., Fuchs, S., Milo, R., 2016. Revised estimates for the number of human and bacteria cells in the body. PLoS Biol. 14, e1002533. https://doi.org/10.1371/journal.pbio.1002533

Serafini, G., Parisi, V.M., Aguglia, A., Amerio, A., Sampogna, G., Fiorillo, A., Pompili, M., Amore, M., 2020. A specific inflammatory profile underlying suicide risk? Systematic review of the main literature findings. Int. J. Environ. Res. Public Health 17, 2393. https://doi.org/10.3390/ijerph17072393

Serbina, N. V., Pamer, E.G., 2006. Monocyte emigration from bone marrow during bacterial infection requires signals mediated by chemokine receptor CCR2. Nat. Immunol. 7, 311–317. https://doi.org/10.1038/ni1309

Serhan, C.N., Levy, B.D., 2018. Resolvins in inflammation: Emergence of the pro-resolving superfamily of mediators. J. Clin. Invest. https://doi.org/10.1172/JCI97943

Shajib, M.S., Chauhan, U., Adeeb, S., Chetty, Y., Armstrong, D., Halder, S.L.S., Marshall, J.K., Khan, W.I., 2018. Characterization of serotonin signaling components in patients with inflammatory bowel disease. J. Can. Assoc. Gastroenterol. 2, 132–140. https://doi.org/10.1093/jcag/gwy039

Sharifov, O.F., Fedorov, V. V., Beloshapko, G.G., Glukhov, A. V., Yushmanova, A. V., Rosenshtraukh, L. V., 2004. Roles of adrenergic and cholinergic stimulation in spontaneous atrial fibrillation in dogs. J. Am. Coll. Cardiol. 43, 483–490. https://doi.org/10.1016/j.jacc.2003.09.030

Shashkin, P., Dragulev, B., Ley, K., 2005. Macrophage differentiation to foam cells. Curr. Pharm. Des. 11, 3061–3072. https://doi.org/10.2174/1381612054865064

Shechter, R., Schwartz, M., 2013. Harnessing monocyte-derived macrophages to control central nervous system pathologies: No longer if' but how'. J. Pathol. 229, 332–346. https://doi.org/10.1002/path.4106

Shen, Z.-H., Zhu, C.-X., Quan, Y.-S., Yang, Z.-Y., Wu, S., Luo, W.-W., Tan, B., Wang, X.-Y., 2018. Relationship between intestinal microbiota and ulcerative colitis: Mechanisms and clinical application of probiotics and fecal microbiota transplantation. World J. Gastroenterol. 24, 5–14. https://doi.org/10.3748/wjg.v24.i1.5

Shibata, Y., 2005. Splenic PGE2-releasing macrophages regulate Th1 and Th2 immune

responses in mice treated with heat-killed BCG. J. Leukoc. Biol. 78, 1281–1290. https://doi.org/10.1189/jlb.0605321

Shishehbor, M.H., Zhang, R., Medina, H., Brennan, M.L., Brennan, D.M., Ellis, S.G., Topol, E.J., Hazen, S.L., 2006. Systemic elevations of free radical oxidation products of arachidonic acid are associated with angiographic evidence of coronary artery disease. Free Radic. Biol. Med. 41, 1678–1683. https://doi.org/10.1016/j.freeradbiomed.2006.09.001

Sia, J.K., Rengarajan, J., 2019. Immunology of *Mycobacterium tuberculosis* infections. Microbiol. Spectr. 7, 10.1128. https://doi.org/10.1128/microbiolspec.gpp3-0022-2018

Siebler, P.H., Heinze, J.D., Kienzle, D.M., Hale, M.W., Lukkes, J.L., Donner, N.C., Kopelman, J.M., Rodriguez, O.A., Lowry, C.A., 2018. Acute administration of the nonpathogenic, saprophytic bacterium, *Mycobacterium vaccae*, induces activation of serotonergic neurons in the dorsal raphe nucleus and antidepressant-like behavior in association with mild hypothermia. Cell. Mol. Neurobiol. 38, 289–304. https://doi.org/10.1007/s10571-017-0564-3

Silvennoinen, R., Quesada, H., Kareinen, I., Julve, J., Kaipiainen, L., Gylling, H., Blanco-Vaca, F., Escola-Gil, J.C., Kovanen, P.T., Lee-Rueckert, M., 2015. Chronic intermittent psychological stress promotes macrophage reverse cholesterol transport by impairing bile acid absorption in mice. Physiol. Rep. 3, e12402. https://doi.org/10.14814/phy2.12402

Simeonova, D., Ivanovska, M., Murdjeva, M., Carvalho, A.F., Maes, M., 2018. Recognizing the leaky gut as a trans-diagnostic target for neuro-immune disorders using clinical chemistry and molecular immunology assays. Curr. Top. Med. Chem. 18, 1641–1655. https://doi.org/10.2174/1568026618666181115100610

Singh, N., Gurav, A., Sivaprakasam, S., Brady, E., Padia, R., Shi, H., Thangaraju, M., Prasad, P.D., Manicassamy, S., Munn, D.H., Lee, J.R., Offermanns, S., Ganapathy, V., 2014. Activation of Gpr109a, receptor for niacin and the commensal metabolite butyrate, suppresses colonic inflammation and carcinogenesis. Immunity 40, 128–139. https://doi.org/10.1016/j.immuni.2013.12.007

Sintiprungrat, K., Singhto, N., Sinchaikul, S., Chen, S.T., Thongboonkerd, V., 2010. Alterations in cellular proteome and secretome upon differentiation from monocyte to macrophage by treatment with phorbol myristate acetate: Insights into biological processes. J. Proteomics 73, 602–618. https://doi.org/10.1016/j.jprot.2009.08.001

Smith, D.G., Martinelli, R., Besra, G.S., Illarionov, P.A., Szatmari, I., Brazda, P., Allen, M.A., Xu, W., Wang, X., Nagy, L., Dowell, R.D., Rook, G.A.W., Rosa Brunet, L., Lowry, C.A., 2019. Identification and characterization of a novel anti-inflammatory lipid isolated from *Mycobacterium vaccae*, a soil-derived bacterium with immunoregulatory and stress resilience properties. Psychopharmacology (Berl). 236, 1653–1670. https://doi.org/10.1007/s00213-019-05253-9

Smith, P.M., Howitt, M.R., Panikov, N., Michaud, M., Gallini, C.A., Bohlooly-Y, M., Glickman, J.N., Garrett, W.S., 2013. The microbial metabolites, short-chain fatty acids, regulate colonic Treg cell homeostasis. Science. 341, 569–73. https://doi.org/10.1126/science.1241165

Smith, S.A., Travers, R.J., Morrissey, J.H., 2015. How it all starts: Initiation of the clotting cascade. Crit. Rev. Biochem. Mol. Biol. 50, 326–336. https://doi.org/10.3109/10409238.2015.1050550

Smith, Z.Z., Kubiak, R.A., Arnold, M.R., Loupy, K.M., Taylor, J.A., Crist, T.G., Bernier, A.E., D'Angelo, H.M., Heinze, J.D., Lowry, C.A., Barth, D.S., 2020. Effects of immunization with heat-killed *Mycobacterium vaccae* on autism spectrum disorder-like behavior and epileptogenesis in a rat model of comorbid autism and epilepsy. Brain. Behav. Immun. 88, 763–780. https://doi.org/10.1016/j.bbi.2020.05.034

Sokol, H., Mahlaoui, N., Aguilar, C., Bach, P., Join-Lambert, O., Garraffo, A., Seksik, P., Danion, F., Jegou, S., Straube, M., Lenoir, C., Neven, B., Moshous, D., Blanche, S., Pigneur, B., Goulet, O., Ruemmele, F., Suarez, F., Beaugerie, L., Pannier, S., Mazingue, F., Lortholary, O., Galicier, L., Picard, C., de Saint Basile, G., Latour, S., Fischer, A., 2018. Intestinal dysbiosis in inflammatory bowel disease associated with primary immunodeficiency. J. Allergy Clin. Immunol. 143, 775–778.e6. https://doi.org/10.1016/j.jaci.2018.09.021

Sommershof, A., Aichinger, H., Engler, H., Adenauer, H., Catani, C., Boneberg, E.-M., Elbert, T., Groettrup, M., Kolassa, I.-T., 2009. Substantial reduction of naïve and regulatory T cells following traumatic stress. Brain. Behav. Immun. 23, 1117–1124. https://doi.org/10.1016/j.bbi.2009.07.003

Song, C., Hsu, K., Yamen, E., Yan, W., Fock, J., Witting, P.K., Geczy, C.L., Freedman, S. Ben, 2009. Serum amyloid A induction of cytokines in monocytes/macrophages and

lymphocytes. Atherosclerosis 207, 374–383. https://doi.org/10.1016/j.atherosclerosis.2009.05.007

Song, H., Fang, F., Tomasson, G., Arnberg, F.K., Mataix-Cols, D., Fernández de la Cruz, L., Almqvist, C., Fall, K., Valdimarsdóttir, U.A., 2018. Association of stress-related disorders with subsequent autoimmune disease. JAMA 319, 2388. https://doi.org/10.1001/jama.2018.7028

Song, J., Li, C., Lv, Y., Zhang, Y., Amakye, W., Mao, L., 2017. DHA increases adiponectin expression more effectively than EPA at relative low concentrations by regulating PPARγ and its phosphorylation at Ser273 in 3T3-L1 adipocytes. Nutr. Metab. (Lond). 14, 52. https://doi.org/10.1186/S12986-017-0209-Z

Sorgi, C.A., Zarini, S., Martin, S.A., Sanchez, R.L., Scandiuzzi, R.F., Gijón, M.A., Guijas, C., Flamand, N., Murphy, R.C., Faccioli, L.H., 2017. Dormant 5-lipoxygenase in inflammatory macrophages is triggered by exogenous arachidonic acid. Sci. Rep. 7, 1–13. https://doi.org/10.1038/s41598-017-11496-3

Soto, M., Herzog, C., Pacheco, J.A., Fujisaka, S., Bullock, K., Clish, C.B., Kahn, C.R., 2018. Gut microbiota modulate neurobehavior through changes in brain insulin sensitivity and metabolism. Mol. Psychiatry 23, 2287–2301. https://doi.org/10.1038/s41380-018-0086-5

Souza, R.R., Robertson, N.M., Mathew, E., Tabet, M.N., Bucksot, J.E., Pruitt, D.T., Rennaker, R.L., Hays, S.A., McIntyre, C.K., Kilgard, M.P., 2020. Efficient parameters of vagus nerve stimulation to enhance extinction learning in an extinction-resistant rat model of PTSD. Prog. Neuro-Psychopharmacology Biol. Psychiatry 99, 109848. https://doi.org/10.1016/j.pnpbp.2019.109848

Souza, R.R., Robertson, N.M., Pruitt, D.T., Gonzales, P.A., Hays, S.A., Rennaker, R.L., Kilgard, M.P., McIntyre, C.K., 2019. Vagus nerve stimulation reverses the extinction impairments in a model of PTSD with prolonged and repeated trauma. Stress 22, 509–520. https://doi.org/10.1080/10253890.2019.1602604

Spadoni, I., Zagato, E., Bertocchi, A., Paolinelli, R., Hot, E., Di Sabatino, A., Caprioli, F., Bottiglieri, L., Oldani, A., Viale, G., Penna, G., Dejana, E., Rescigno, M., 2015. A gut-vascular barrier controls the systemic dissemination of bacteria. Science (80-.). 350, 830–834. https://doi.org/10.1126/science.aad0135

Speaker, K.J., Cox, S.S., Paton, M.M., Serebrakian, A., Maslanik, T., Greenwood, B.N.,

Fleshner, M., 2014. Six weeks of voluntary wheel running modulates inflammatory protein (MCP-1, IL-6, and IL-10) and DAMP (Hsp72) responses to acute stress in white adipose tissue of lean rats. Brain. Behav. Immun. 39, 87–98. https://doi.org/10.1016/j.bbi.2013.10.028

Stafforini, D., Elstad, M., McIntyre, T., Zimmerman, G., Prescott, S., 1990. Human macrophages secret platelet-activating factor acetylhydrolase. J. Biol. Chemsitry 265, 9682–9687.

Stankiewicz, A.M., Goscik, J., Swiergiel, A.H., Majewska, A., Wieczorek, M., Juszczak, G.R., Lisowski, P., 2014. Social stress increases expression of hemoglobin genes in mouse prefrontal cortex. BMC Neurosci. 15, 130. https://doi.org/10.1186/s12868-014-0130-6

Steinmann, U., Borkowski, J., Wolburg, H., Schröppel, B., Findeisen, P., Weiss, C., Ishikawa, H., Schwerk, C., Schroten, H., Tenenbaum, T., 2013. Transmigration of polymorphnuclear neutrophils and monocytes through the human blood-cerebrospinal fluid barrier after bacterial infection in vitro. J. Neuroinflammation 10, 832. https://doi.org/10.1186/1742-2094-10-31

Stenman, L.K., Patterson, E., Meunier, J., Roman, F.J., Lehtinen, M.J., 2020. Strain specific stress-modulating effects of candidate probiotics: A systematic screening in a mouse model of chronic restraint stress. Behav. Brain Res. 379, 112376. https://doi.org/10.1016/j.bbr.2019.112376

Stevens, B.R., Goel, R., Seungbum, K., Richards, E.M., Holbert, R.C., Pepine, C.J., Raizada, M.K., 2018. Increased human intestinal barrier permeability plasma biomarkers zonulin and FABP2 correlated with plasma LPS and altered gut microbiome in anxiety or depression. Gut 67, 1555–1557. https://doi.org/10.1136/gutjnl-2017-314759

Stocker, S.D., Muntzel, M.S., 2013. Recording sympathetic nerve activity chronically in rats: Surgery techniques, assessment of nerve activity, and quantification. Am. J. Physiol. - Hear. Circ. Physiol. 305, H1407. https://doi.org/10.1152/ajpheart.00173.2013

Strandwitz, P., 2018. Neurotransmitter modulation by the gut microbiota. Brain Res. 1693, 128–133. https://doi.org/10.1016/j.brainres.2018.03.015

Straub, A.C., Lohman, A.W., Billaud, M., Johnstone, S.R., Dwyer, S.T., Lee, M.Y., Bortz, P.S., Best, A.K., Columbus, L., Gaston, B., Isakson, B.E., 2012. Endothelial cell expression of haemoglobin α regulates nitric oxide signalling. Nature 491, 473–477. https://doi.org/10.1038/nature11626

Strauss-Ayali, D., Conrad, S.M., Mosser, D.M., 2007. Monocyte subpopulations and their differentiation patterns during infection. J. Leukoc. Biol. 82, 244–252. https://doi.org/10.1189/jlb.0307191

Strominger, I., Elyahu, Y., Berner, O., Reckhow, J., Mittal, K., Nemirovsky, A., Monsonego, A., 2018. The choroid plexus functions as a niche for T-cell stimulation within the central nervous system. Front. Immunol. 9, 16. https://doi.org/10.3389/fimmu.2018.01066

Suchard, M.S., Savulescu, D.M., 2021. Nicotinamide pathways as the root cause of sepsis – an evolutionary perspective on macrophage energetic shifts. FEBS J. febs.15807. https://doi.org/10.1111/febs.15807

Suez, J., Korem, T., Zeevi, D., Zilberman-Schapira, G., Thaiss, C.A., Maza, O., Israeli, D., Zmora, N., Gilad, S., Weinberger, A., Kuperman, Y., Harmelin, A., Kolodkin-Gal, I., Shapiro, H., Halpern, Z., Segal, E., Elinav, E., 2014. Artificial sweeteners induce glucose intolerance by altering the gut microbiota. Nature 514, 181–186. https://doi.org/10.1038/nature13793

Suga, T., Yamaguchi, H., Sato, T., Maekawa, M., Goto, J., Mano, N., 2017. Preference of conjugated bile acids over unconjugated bile acids as substrates for OATP1B1 and OATP1B3. PLoS One 12, e0169719. https://doi.org/10.1371/journal.pone.0169719

Sumiyoshi, M., Satomi, J., Kitazato, K.T., Yagi, K., Shimada, K., Kurashiki, Y., Korai, M., Miyamoto, T., Suzue, R., Kuwayama, K., Nagahiro, S., 2015. PPARγ-dependent and -independent inhibition of the HMGB1/TLR9 pathway by eicosapentaenoic acid attenuates ischemic brain damage in ovariectomized rats. J. Stroke Cerebrovasc. Dis. 24, 1187–1195. https://doi.org/10.1016/j.jstrokecerebrovasdis.2015.01.009

Sun, D., Li, W., Li, S., Cen, Y., Xu, Q., Li, Y., Sun, Y., Qi, Y., Lin, Y., Yang, T., Xu, P., Lu, Q., 2016. Fecal microbiota transplantation as a novel therapy for ulcerative colitis: a systematic review and meta-analysis. Medicine (Baltimore). 95, e3765. https://doi.org/10.1097/MD.0000000000003765

Sun, Y., Zhang, M., Chen, C., Gillilland, M., Sun, X., El–Zaatari, M., Huffnagle, G.B., Young, V.B., Zhang, J., Hong, S., Chang, Y., Gumucio, D.L., Owyang, C., Kao, J.Y., 2013. Stress-induced corticotropin-releasing hormone-mediated NLRP6 inflammasome inhibition and transmissible enteritis in mice. Gastroenterology 144, 1478-1487.e8. https://doi.org/10.1053/j.gastro.2013.02.038

Sunderkötter, C., Nikolic, T., Dillon, M.J., van Rooijen, N., Stehling, M., Drevets, D.A., Leenen, P.J.M., 2004. Subpopulations of mouse blood monocytes differ in maturation stage and inflammatory response. J. Immunol. 172, 4410–4417. https://doi.org/10.4049/jimmunol.172.7.4410

Suneson, K., Lindahl, J., Hårsmar, S.C., Söderberg, G., Lindqvist, D., 2021. Inflammatory depression—mechanisms and non-pharmacological interventions. Int. J. Mol. Sci. 22, 1–20. https://doi.org/10.3390/ijms22041640

Suwal, S., Wu, Q., Liu, W., Liu, Q., Sun, H., Liang, M., Gao, J., Zhang, B., Kou, Y., Liu, Z., Wei, Y., Wang, Y., Zheng, K., 2018. The probiotic effectiveness in preventing experimental colitis is correlated with host gut microbiota. Front. Microbiol. 9, 2675. https://doi.org/10.3389/fmicb.2018.02675

Sytnyk, V., Leshchyns'ka, I., Schachner, M., 2017. Neural cell adhesion molecules of the immunoglobulin superfamily regulate synapse formation, maintenance, and function. Trends Neurosci. 40, 295–308. https://doi.org/10.1016/j.tins.2017.03.003

Szklarczyk, D., Gable, A.L., Lyon, D., Junge, A., Wyder, S., Huerta-Cepas, J., Simonovic, M., Doncheva, N.T., Morris, J.H., Bork, P., Jensen, L.J., Von Mering, C., 2019. STRING v11: Protein-protein association networks with increased coverage, supporting functional discovery in genome-wide experimental datasets. Nucleic Acids Res. 47, D607–D613. https://doi.org/10.1093/nar/gky1131

Tahara, Y., Yamazaki, M., Sukigara, H., Motohashi, H., Sasaki, H., Miyakawa, H., Haraguchi, A., Ikeda, Y., Fukuda, S., Shibata, S., 2018. Gut microbiota-derived short chain fatty acids induce circadian clock entrainment in mouse peripheral tissue. Sci. Rep. 8, 1395. https://doi.org/10.1038/s41598-018-19836-7

Takano, M., Uramoto, M., Otani, M., Matsuura, K., Sano, K., Matsuyama, S., 2014. Secretomic analysis of mouse choroid plexus cell line ECPC-4 using two-dimensional gel electrophoresis coupled to mass spectrometry. J. Proteomics Bioinform. 07, 347–352. https://doi.org/10.4172/jpb.1000338

Talebian, R., Hashem, O., Gruber, R., 2020. Taurocholic acid lowers the inflammatory response of gingival fibroblasts, epithelial ceand macrophages. J. Oral Sci. 62, 335–339. https://doi.org/10.2334/josnusd.19-0342

Tanca, A., Abbondio, M., Palomba, A., Fraumene, C., Manghina, V., Cucca, F., Fiorillo, E.,

Uzzau, S., 2017. Potential and active functions in the gut microbiota of a healthy human cohort. Microbiome 5, 79. https://doi.org/10.1186/s40168-017-0293-3

Tang, T., Scambler, T.E., Smallie, T., Cunliffe, H.E., Ross, E.A., Rosner, D.R., O'Neil, J.D., Clark, A.R., 2017. Macrophage responses to lipopolysaccharide are modulated by a feedback loop involving prostaglandin E2, dual specificity phosphatase 1 and tristetraprolin. Sci. Rep. 7, 1–13. https://doi.org/10.1038/s41598-017-04100-1

Tang, Z.-Z., Chen, G., Hong, Q., Huang, S., Smith, H.M., Shah, R.D., Scholz, M., Ferguson, J.F., 2019. Multi-omic analysis of the microbiome and metabolome in healthy subjects reveals microbiome-dependent relationships between diet and metabolites. Front. Genet. 10, 454. https://doi.org/10.3389/fgene.2019.00454

Tasnim, N., Abulizi, N., Pither, J., Hart, M.M., Gibson, D.L., 2017. Linking the gut microbial ecosystem with the environment: does gut health depend on where we live? Front. Microbiol. 8, 1935. https://doi.org/10.3389/fmicb.2017.01935

Tejera, N., Boeglin, W.E., Suzuki, T., Schneider, C., 2012. COX-2-dependent and -independent biosynthesis of dihydroxy-arachidonic acids in activated human leukocytes. J. Lipid Res. 53, 87–94. https://doi.org/10.1194/jlr.M017822

Terra, X., Montagut, G., Bustos, M., Llopiz, N., Ardèvol, A., Bladé, C., Fernández-Larrea, J., Pujadas, G., Salvadó, J., Arola, L., Blay, M., 2009. Grape-seed procyanidins prevent low-grade inflammation by modulating cytokine expression in rats fed a high-fat diet. J. Nutr. Biochem. 20, 210–218. https://doi.org/10.1016/j.jnutbio.2008.02.005

The UniProt Consortium, 2019. UniProt: a worldwide hub of protein knowledge. Nucleic Acids Res. 47, D506–D515. https://doi.org/10.1093/nar/gky1049

Thevaranjan, N., Puchta, A., Schulz, C., Naidoo, A., Szamosi, J.C., Verschoor, C.P., Loukov, D., Schenck, L.P., Jury, J., Foley, K.P., Schertzer, J.D., Larché, M.J., Davidson, D.J., Verdú, E.F., Surette, M.G., Bowdish, D.M.E., 2017. Age-associated microbial dysbiosis promotes intestinal permeability, systemic inflammation, and macrophage dysfunction. Cell Host Microbe 21, 455–466.e4. https://doi.org/10.1016/J.CHOM.2017.03.002

Thomas, T., Stefanoni, D., Reisz, J.A., Nemkov, T., Bertolone, L., Francis, R.O., Hudson, K.E., Zimring, J.C., Hansen, K.C., Hod, E.A., Spitalnik, S.L., D'Alessandro, A., 2020. COVID-19 infection alters kynurenine and fatty acid metabolism, correlating with IL-6 levels and renal status. JCI Insight 5, e140327. https://doi.org/10.1172/JCI.INSIGHT.140327

Thompson, R.S., Vargas, F., Dorrestein, P.C., Chichlowski, M., Berg, B.M., Fleshner, M., 2020. Dietary prebiotics alter novel microbial dependent fecal metabolites that improve sleep. Sci. Rep. 10, 1–14. https://doi.org/10.1038/s41598-020-60679-y

Tientcheu, L.D., Koch, A., Ndengane, M., Andoseh, G., Kampmann, B., Wilkinson, R.J., 2017. Immunological consequences of strain variation within the *Mycobacterium tuberculosis* complex. Eur. J. Immunol. 47, 432–445. https://doi.org/10.1002/eji.201646562

Tillisch, K., Labus, J., Kilpatrick, L., Jiang, Z., Stains, J., Ebrat, B., Guyonnet, D., Legrain–Raspaud, S., Trotin, B., Naliboff, B., Mayer, E.A., 2013. Consumption of fermented milk product with probiotic modulates brain activity. Gastroenterology 144, 1394–1401. https://doi.org/10.1053/j.gastro.2013.02.043

Trefely, S., Lovell, C.D., Snyder, N.W., Wellen, K.E., 2020. Compartmentalised acyl-CoA metabolism and roles in chromatin regulation. Mol. Metab. 38, 100941. https://doi.org/10.1016/j.molmet.2020.01.005

Tsou, C.L., Peters, W., Si, Y., Slaymaker, S., Aslanian, A.M., Weisberg, S.P., Mack, M., Charo, I.F., 2007a. Critical roles for CCR2 and MCP-3 in monocyte mobilization from bone marrow and recruitment to inflammatory sites. J. Clin. Invest. 117, 902–909. https://doi.org/10.1172/JCI29919

Turdi, S., Yuan, M., Leedy, G.M., Wu, Z., Ren, J., 2012. Chronic social stress induces cardiomyocyte contractile dysfunction and intracellular Ca 2+ derangement in rats. Physiol. Behav. 105, 498–509. https://doi.org/10.1016/j.physbeh.2011.09.012

Turnbaugh, P.J., Ley, R.E., Hamady, M., Fraser-Liggett, C.M., Knight, R., Gordon, J.I., 2007. The human microbiome project. Nature 449, 804–10. https://doi.org/10.1038/nature06244

Tursich, M., Neufeld, R.W.J., Frewen, P.A., Harricharan, S., Kibler, J.L., Rhind, S.G., Lanius, R.A., 2014. Association of trauma exposure with proinflammatory activity: a transdiagnostic meta-analysis. Transl. Psychiatry 4, e413–e413. https://doi.org/10.1038/tp.2014.56

Tytgat, H.L.P., van Teijlingen, N.H., Sullan, R.M.A., Douillard, F.P., Rasinkangas, P., Messing, M., Reunanen, J., Satokari, R., Vanderleyden, J., Dufrêne, Y.F., Geijtenbeek, T.B.H., de Vos, W.M., Lebeer, S., 2016. Probiotic gut microbiota isolate interacts with dendritic cells via glycosylated heterotrimeric pili. PLoS One 11, e0151824. https://doi.org/10.1371/journal.pone.0151824

Uche, U.U., Piccirillo, A.R., Kataoka, S., Grebinoski, S.J., D'Cruz, L.M., Kane, L.P., 2018. PIK3IP1/TrIP restricts activation of T cells through inhibition of PI3K/Akt. J. Exp. Med. 215, 3165–3179. https://doi.org/10.1084/jem.20172018

Ulmer, C.S., Hall, M.H., Dennis, P.A., Beckham, J.C., Germain, A., 2018. Posttraumatic stress disorder diagnosis is associated with reduced parasympathetic activity during sleep in US veterans and military service members of the Iraq and Afghanistan wars. Sleep 41. https://doi.org/10.1093/sleep/zsy174

Umamaheswaran, S., Dasari, S.K., Yang, P., Lutgendorf, S.K., Sood, A.K., 2018. Stress, inflammation, and eicosanoids: an emerging perspective. Cancer Metastasis Rev. 37, 203–211. https://doi.org/10.1007/s10555-018-9741-1

Uppalapati, D., Das, N.R., Gangwal, R.P., Damre, M. V., Sangamwar, A.T., Sharma, S.S., 2014. Neuroprotective potential of peroxisome proliferator activated receptor-α agonist in cognitive impairment in Parkinson's disease: Behavioral, biochemical, and PBPK profile. PPAR Res. 2014, 1–9. https://doi.org/10.1155/2014/753587

Valdes, A.M., Walter, J., Segal, E., Spector, T.D., 2018. Role of the gut microbiota in nutrition and health. BMJ 361, k2179. https://doi.org/10.1136/bmj.k2179

Valles-Colomer, M., Falony, G., Darzi, Y., Tigchelaar, E.F., Wang, J., Tito, R.Y., Schiweck, C., Kurilshikov, A., Joossens, M., Wijmenga, C., Claes, S., Van Oudenhove, L., Zhernakova, A., Vieira-Silva, S., Raes, J., 2019. The neuroactive potential of the human gut microbiota in quality of life and depression. Nat. Microbiol. 4, 623–632. https://doi.org/10.1038/s41564-018-0337-x

van de Wouw, M., Boehme, M., Dinan, T.G., Cryan, J.F., 2019. Monocyte mobilisation, microbiota & mental illness. Brain. Behav. Immun. 81, 74–91. https://doi.org/10.1016/j.bbi.2019.07.019

van de Wouw, M., Boehme, M., Lyte, J.M., Wiley, N., Strain, C., O'Sullivan, O., Clarke, G., Stanton, C., Dinan, T.G., Cryan, J.F., 2018. Short-chain fatty acids: microbial metabolites that alleviate stress-induced brain-gut axis alterations. J. Physiol. 596, 4923–4944. https://doi.org/10.1113/JP276431

Van Den Abbeele, P., Belzer, C., Goossens, M., Kleerebezem, M., De Vos, W.M., Thas, O., De Weirdt, R., Kerckhof, F.M., Van De Wiele, T., 2013. Butyrate-producing Clostridium cluster XIVa species specifically colonize mucins in an in vitro gut model. ISME J. 7, 949–

961. https://doi.org/10.1038/ismej.2012.158

van der Kolk, B., Greenberg, M., Boyd, H., Krystal, J., 1985. Inescapable shock, neurotransmitters, and addiction to trauma: Toward a psychobiology of post traumatic stress. Biol. Psychiatry 20, 314–325. https://doi.org/10.1016/0006-3223(85)90061-7

Van Der Kooij, M.A., Jene, T., Treccani, G., Miederer, I., Hasch, A., Voelxen, N., Walenta, S., Müller, M.B., 2018. Chronic social stress-induced hyperglycemia in mice couples individual stress susceptibility to impaired spatial memory. Proc. Natl. Acad. Sci. U. S. A. 115, E10187–E10196. https://doi.org/10.1073/pnas.1804412115

Van Ginderachter, J.A., Meerschaut, S., Liu, Y., Brys, L., De Groeve, K., Ghassabeh, G.H., Raes, G., De Baetselier, P., 2006. Peroxisome proliferator-activated receptor γ (PPARγ) ligands reverse CTL suppression by alternatively activated (M2) macrophages in cancer. Blood 108, 525–535. https://doi.org/10.1182/blood-2005-09-3777

van Zuiden, M., Heijnen, C.J., Maas, M., Amarouchi, K., Vermetten, E., Geuze, E., Kavelaars, A., 2012. Glucocorticoid sensitivity of leukocytes predicts PTSD, depressive and fatigue symptoms after military deployment: A prospective study. Psychoneuroendocrinology 37, 1822–1836. https://doi.org/10.1016/j.psyneuen.2012.03.018

Vandal, O.H., Gelb, M.H., Ehrt, S., Nathan, C.F., 2006. Cytosolic phospholipase A2 enzymes are not required by mouse bone marrow-derived macrophages for the control of *Mycobacterium tuberculosis* in vitro. Infect. Immun. 74, 1751–1756. https://doi.org/10.1128/IAI.74.3.1751-1756.2006

Vargas-Caraveo, A., Sayd, A., Maus, S.R., Caso, J.R., Madrigal, J.L.M., García-Bueno, B., Leza, J.C., 2017. Lipopolysaccharide enters the rat brain by a lipoprotein-mediated transport mechanism in physiological conditions. Sci. Rep. 7, 13113. https://doi.org/10.1038/s41598-017-13302-6

Verbitsky, A., Dopfel, D., Zhang, N., 2020. Rodent models of post-traumatic stress disorder: behavioral assessment. Transl. Psychiatry 10. https://doi.org/10.1038/s41398-020-0806-x

Verdú, E.F., Bercik, P., Verma-Gandhu, M., Huang, X.-X., Blennerhassett, P., Jackson, W., Mao, Y., Wang, L., Rochat, F., Collins, S.M., 2006. Specific probiotic therapy attenuates antibiotic induced visceral hypersensitivity in mice. Gut 55, 182–190. https://doi.org/10.1136/gut.2005.066100

Verma, R., Lee, C., Jeun, E.-J., Yi, J., Kim, K.S., Ghosh, A., Byun, S., Lee, C.-G., Kang, H.-J.,

Kim, G.-C., Jun, C.-D., Jan, G., Suh, C.-H., Jung, J.-Y., Sprent, J., Rudra, D., De Castro, C., Molinaro, A., Surh, C.D., Im, S.-H., 2018. Cell surface polysaccharides of *Bifidobacterium bifidum* induce the generation of Foxp3+ regulatory T cells. Sci. Immunol. 3, eaat6975. https://doi.org/10.1126/sciimmunol.aat6975

Vicente, R., Quentin, J., Mausset-Bonnefont, A.-L., Chuchana, P., Martire, D., Cren, M., Jorgensen, C., Louis-Plence, P., 2016. Nonclassical CD4 + CD49b + regulatory T cells as a better alternative to conventional CD4 + CD25 + T cells to dampen arthritis severity . J. Immunol. 196, 298–309. https://doi.org/10.4049/jimmunol.1501069

Viola, A., Munari, F., Sánchez-Rodríguez, R., Scolaro, T., Castegna, A., 2019. The metabolic signature of macrophage responses. Front. Immunol. 10, 1462. https://doi.org/10.3389/fimmu.2019.01462

Višnjić, D., Batinić, D., Banfić, H., 1997. Arachidonic acid mediates interferon-γ-induced sphingomyelin hydrolysis and monocytic marker expression in HL-60 cell line. Blood 89, 81–91. https://doi.org/10.1182/blood.v89.1.81

Vital, M., Howe, A.C., Tiedje, J.M., 2014. Revealing the bacterial butyrate synthesis pathways by analyzing (meta)genomic data. MBio 5, e00889. https://doi.org/10.1128/mBio.00889-14

Von Känel, R., 2015. Acute mental stress and hemostasis: When physiology becomes vascular harm. Thromb. Res. 135, S52–S55. https://doi.org/10.1016/S0049-3848(15)50444-1

Von Känel, R., Hepp, U., Buddeberg, C., Keel, M., Mica, L., Aschbacher, K., Schnyder, U., 2006. Altered blood coagulation in patients with posttraumatic stress disorder. Psychosom. Med. 68, 598–604. https://doi.org/10.1097/01.psy.0000221229.43272.9d

Von Reyn, C.F., Mtei, L., Arbeit, R.D., Waddell, R., Cole, B., MacKenzie, T., Matee, M., Bakari, M., Tvaroha, S., Adams, L. V., Horsburgh, C.R., Pallangyo, K., 2010. Prevention of tuberculosis in Bacille Calmette-Guérin-primed, HIV-infected adults boosted with an inactivated whole-cell mycobacterial vaccine. AIDS 24, 675–685. https://doi.org/10.1097/QAD.0b013e3283350f1b

Vrieling, F., Kostidis, S., Spaink, H.P., Haks, M.C., Mayboroda, O.A., Ottenhoff, T.H.M., Joosten, S.A., 2020. Analyzing the impact of *Mycobacterium tuberculosis* infection on primary human macrophages by combined exploratory and targeted metabolomics. Sci. Rep. 10, 7085. https://doi.org/10.1038/s41598-020-62911-1

Vu-Dac, N., Chopin-Delannoy, S., Gervois, P., Bonnelye, E., Martin, G., Fruchart, J.C., Laudet,

V., Staels, B., 1998. The nuclear receptors peroxisome proliferator-activated receptor α and rev-erbα mediate the species-specific regulation of apolipoprotein A-I expression by fibrates. J. Biol. Chem. 273, 25713–25720. https://doi.org/10.1074/jbc.273.40.25713

Vukojevic, V., Mastrandreas, P., Arnold, A., Peter, F., Kolassa, I.-T., Wilker, S., Elbert, T., de Quervain, D.J.-F., Papassotiropoulos, A., Stetak, A., 2020. Evolutionary conserved role of neural cell adhesion molecule-1 in memory. Transl. Psychiatry 10, 217. https://doi.org/10.1038/s41398-020-00899-y

Vuola, J.M., Ristola, M.A., Cole, B., Järviluoma, A., Tvaroha, S., Rönkkö, T., Rautio, O., Arbeit, R.D., Von Reyn, C.F., 2003. Immunogenicity of an inactivated mycobacterial vaccine for the prevention of HIV-associated tuberculosis: A randomized, controlled trial. AIDS 17, 2351–2355. https://doi.org/10.1097/00002030-200311070-00010

Wa, Y., Yin, B., He, Y., Xi, W., Huang, Y., Wang, C., Guo, F., Gu, R., 2019. Effects of single probiotic- And combined probiotic-fermented milk on lipid metabolism in hyperlipidemic rats. Front. Microbiol. 10, 1312. https://doi.org/10.3389/fmicb.2019.01312

Waddell, R.D., Chintu, C., Lein, A.D., Zumla, A., Karagas, M.R., Baboo, K.S., Habbema, J.D.F., Tosteson, A.N.A., Morin, P., Tvaroha, S., Arbeit, R.D., Mwinga, A., von Reyn, C.F., 2000. Safety and immunogenicity of a five-dose series of inactivated *Mycobacterium vaccae* vaccination for the prevention of HIV-associated tuberculosis. Clin. Infect. Dis. 30, S309–S315. https://doi.org/10.1086/313880

Wallner, S., Grandl, M., Konovalova, T., Sigrüner, A., Kopf, T., Peer, M., Orsó, E., Liebisch, G., Schmitz, G., 2014. Monocyte to macrophage differentiation goes along with modulation of the plasmalogen pattern through transcriptional regulation. PLoS One 9, e94102. https://doi.org/10.1371/journal.pone.0094102

Wammers, M., Schupp, A.K., Bode, J.G., Ehlting, C., Wolf, S., Deenen, R., Köhrer, K., Häussinger, D., Graf, D., 2018. Reprogramming of pro-inflammatory human macrophages to an anti-inflammatory phenotype by bile acids. Sci. Rep. 8, 255. https://doi.org/10.1038/s41598-017-18305-x

Wang, C., Li, L., Guan, H., Tong, S., Liu, M., Liu, C., Zhang, Z., Du, C., Li, P., 2013. Effects of taurocholic acid on immunoregulation in mice. Int. Immunopharmacol. 15, 217–222. https://doi.org/10.1016/j.intimp.2012.12.006

Wang, C.W., Colas, R.A., Dalli, J., Arnardottir, H.H., Nguyen, D., Hasturk, H., Chiang, N., Van

Dyke, T.E., Serhan, C.N., 2016. Maresin 1 biosynthesis and proresolving anti-infective functions with human-localized aggressive periodontitis leukocytes. Infect. Immun. 84, 658–665. https://doi.org/10.1128/IAI.01131-15

Wang, J., Ji, H., Wang, S., Liu, H., Zhang, W., Zhang, D., Wang, Y., 2018. Probiotic *Lactobacillus plantarum* promotes intestinal barrier function by strengthening the epithelium and modulating gut microbiota. Front. Microbiol. 9, 1953. https://doi.org/10.3389/fmicb.2018.01953

Wang, L., Li, L., Zhou, X., Pandya, S., Baser, O., 2016. A real-world evaluation of the clinical and economic burden of United States veteran patients with post-traumatic stress disorder. Value Heal. 19, A524. https://doi.org/10.1016/j.jval.2016.09.1030

Wang, R.X., Lee, J.S., Campbell, E.L., Colgan, S.P., 2020. Microbiota-derived butyrate dynamically regulates intestinal homeostasis through regulation of actin-associated protein synaptopodin. Proc. Natl. Acad. Sci. U. S. A. 117, 11648–11657. https://doi.org/10.1073/pnas.1917597117

Wang, Y., Xie, J., Li, Y., Dong, S., Liu, H., Chen, J., Wang, Yan, Zhao, S., Zhang, Y., Zhang, H., 2016. Probiotic *Lactobacillus casei* Zhang reduces pro-inflammatory cytokine production and hepatic inflammation in a rat model of acute liver failure. Eur. J. Nutr. 55, 821–831. https://doi.org/10.1007/s00394-015-0904-3

Wasilewski, A., Zielińska, M., Storr, M., Fichna, J., 2015. Beneficial effects of probiotics, prebiotics, synbiotics, and psychobiotics in inflammatory bowel disease. Inflamm. Bowel Dis. 21, 1674–1682. https://doi.org/10.1097/MIB.0000000000000364

Watts, S.W., Morrison, S.F., Davis, R.P., Barman, S.M., 2012. Serotonin and blood pressure regulation. Pharmacol. Rev. 64, 359–388. https://doi.org/10.1124/pr.111.004697

Weber, M.D., Frank, M.G., Tracey, K.J., Watkins, L.R., Maier, S.F., 2015. Stress induces the danger-associated molecular pattern HMGB-1 in the hippocampus of male sprague dawley rats: A priming stimulus of microglia and the NLRP3 inflammasome. J. Neurosci. 35, 316–324. https://doi.org/10.1523/JNEUROSCI.3561-14.2015

Weber, M.D., Godbout, J.P., Sheridan, J.F., 2017. Repeated social defeat, neuroinflammation, and behavior: monocytes carry the signal. Neuropsychopharmacology 42, 46–61. https://doi.org/10.1038/npp.2016.102

Weidner, M.T., Lardenoije, R., Eijssen, L., Mogavero, F., De Groodt, L.P.M.T., Popp, S., Palme,

R., Förstner, K.U., Strekalova, T., Steinbusch, H.W.M., Schmitt-Böhrer, A.G., Glennon, J.C., Waider, J., van den Hove, D.L.A., Lesch, K.-P., 2019. Identification of cholecystokinin by genome-wide profiling as potential mediator of serotonin-dependent behavioral effects of maternal separation in the amygdala. Front. Neurosci. 13, 460. https://doi.org/10.3389/fnins.2019.00460

Weiss, J.M., Simson, P.G., 1986. Depression in an animal model: focus on the locus ceruleus. Ciba Found. Symp. 123, 191–215. https://doi.org/10.1002/9780470513361.ch11

Welcome, M.O., Mastorakis, N.E., 2020. Stress-induced blood brain barrier disruption: Molecular mechanisms and signaling pathways. Pharmacol. Res. 157, 104769. https://doi.org/10.1016/j.phrs.2020.104769

Werz, O., Gerstmeier, J., Libreros, S., De La Rosa, X., Werner, M., Norris, P.C., Chiang, N., Serhan, C.N., 2018. Human macrophages differentially produce specific resolvin or leukotriene signals that depend on bacterial pathogenicity. Nat. Commun. 9, 59. https://doi.org/10.1038/s41467-017-02538-5

Wettschureck, N., Strilic, B., Offermanns, S., 2019. Passing the vascular barrier: Endothelial signaling processes controlling extravasation. Physiol. Rev. 99, 1467–1525. https://doi.org/10.1152/physrev.00037.2018

Whitaker, A.M., Gilpin, N.W., Edwards, S., 2014. Animal models of post-traumatic stress disorder and recent neurobiological insights. Behav. Pharmacol. 25, 398–409. https://doi.org/10.1097/FBP.0000000000000069

Wichmann, S., Kirschbaum, C., Böhme, C., Petrowski, K., 2017. Cortisol stress response in post-traumatic stress disorder, panic disorder, and major depressive disorder patients. Psychoneuroendocrinology 83, 135–141. https://doi.org/10.1016/j.psyneuen.2017.06.005

Wikoff, W.R., Anfora, A.T., Liu, J., Schultz, P.G., Lesley, S.A., Peters, E.C., Siuzdak, G., 2009. Metabolomics analysis reveals large effects of gut microflora on mammalian blood metabolites. Proc. Natl. Acad. Sci. U. S. A. 106, 3698–3703. https://doi.org/10.1073/pnas.0812874106

Williams, L.L., Kiecolt-Glaser, J.K., Horrocks, L.A., Hillhouse, J.T., Glaser, R., 1992. Quantitative association between altered plasma esterified omega-6 fatty acid proportions and psychological stress. Prostaglandins, Leukot. Essent. Fat. Acids 47, 165–170. https://doi.org/10.1016/0952-3278(92)90155-C

Wilmanski, T., Rappaport, N., Earls, J.C., Magis, A.T., Manor, O., Lovejoy, J., Omenn, G.S., Hood, L., Gibbons, S.M., Price, N.D., 2019. Blood metabolome predicts gut microbiome α-diversity in humans. Nat. Biotechnol. 37, 1217–1228. https://doi.org/10.1038/s41587-019-0233-9

Wiśniewski, J.R., Gaugaz, F.Z., 2015. Fast and sensitive total protein and peptide assays for proteomic analysis. Anal. Chem. 87, 4110–4116. https://doi.org/10.1021/ac504689z

Wittbrodt, M.T., Gurel, N.Z., Nye, J.A., Ladd, S., Shandhi, M.M.H., Huang, M., Shah, A.J., Pearce, B.D., Alam, Z.S., Rapaport, M.H., Murrah, N., Ko, Y.A., Haffer, A.A., Shallenberger, L.H., Vaccarino, V., Inan, O.T., Bremner, J.D., 2020. Non-invasive vagal nerve stimulation decreases brain activity during trauma scripts. Brain Stimul. 13, 1333–1348. https://doi.org/10.1016/j.brs.2020.07.002

Wohleb, E.S., Hanke, M.L., Corona, A.W., Powell, N.D., Stiner, L.M., Bailey, M.T., Nelson, R.J., Godbout, J.P., Sheridan, J.F., 2011. β-Adrenergic receptor antagonism prevents anxiety-like behavior and microglial reactivity induced by repeated social defeat. J. Neurosci. 31, 6277–6288. https://doi.org/10.1523/JNEUROSCI.0450-11.2011

Wohleb, E.S., McKim, D.B., Shea, D.T., Powell, N.D., Tarr, A.J., Sheridan, J.F., Godbout, J.P., 2014. Re-establishment of anxiety in stress-sensitized mice is caused by monocyte trafficking from the spleen to the brain. Biol. Psychiatry 75, 970–981. https://doi.org/10.1016/j.biopsych.2013.11.029

Wohleb, E.S., McKim, D.B., Sheridan, J.F., Godbout, J.P., 2015. Monocyte trafficking to the brain with stress and inflammation: A novel axis of immune-to-brain communication that influences mood and behavior. Front. Neurosci. 8, 447. https://doi.org/10.3389/fnins.2014.00447

Wohleb, E.S., Powell, N.D., Godbout, J.P., Sheridan, J.F., 2013. Stress-induced recruitment of bone marrow-derived monocytes to the brain promotes anxiety-like behavior. J. Neurosci. 33, 13820–13833. https://doi.org/10.1523/JNEUROSCI.1671-13.2013

Wolska, A., Dunbar, R.L., Freeman, L.A., Ueda, M., Amar, M.J., Sviridov, D.O., Remaley, A.T., 2017. Apolipoprotein C-II: New findings related to genetics, biochemistry, and role in triglyceride metabolism. Atherosclerosis 267, 49–60. https://doi.org/10.1016/j.atherosclerosis.2017.10.025

Won, E., Kim, Y.-K., 2016. Stress, the autonomic nervous system, and the immune-kynurenine

pathway in the etiology of depression. Curr. Neuropharmacol. 14, 665–673. https://doi.org/10.2174/1570159x14666151208113006

Wong, D.L., 2006. Epinephrine biosynthesis: hormonal and neural control during stress. Cell. Mol. Neurobiol. 26, 891–900. https://doi.org/10.1007/s10571-006-9056-6

Wong, M.-L., Inserra, A., Lewis, M.D., Mastronardi, C.A., Leong, L., Choo, J., Kentish, S., Xie, P., Morrison, M., Wesselingh, S.L., Rogers, G.B., Licinio, J., 2016. Inflammasome signaling affects anxiety- and depressive-like behavior and gut microbiome composition. Mol. Psychiatry 21, 797–805. https://doi.org/10.1038/mp.2016.46

Wood, S.K., Wood, C.S., Lombard, C.M., Lee, C.S., Zhang, X.Y., Finnell, J.E., Valentino, R.J., 2015. Inflammatory factors mediate vulnerability to a social stress-induced depressive-like phenotype in passive coping rats. Biol. Psychiatry 78, 38–48. https://doi.org/10.1016/j.biopsych.2014.10.026

Wright, G.J., Puklavec, M.J., Willis, A.C., Hoek, R.M., Sedgwick, J.D., Brown, M.H., Barclay, A.N., 2000. Lymphoid/neuronal cell surface OX2 glycoprotein recognizes a novel receptor on macrophages implicated in the control of their function. Immunity 13, 233–242. https://doi.org/10.1016/S1074-7613(00)00023-6

Wu, G., Fang, Y.Z., Yang, S., Lupton, J.R., Turner, N.D., 2004. Glutathione metabolism and its implications for health. J. Nutr. 134, 489–492. https://doi.org/10.1093/jn/134.3.489

Wu, T., Levine, S.J., Lawrence, M.G., Logun, C., Angus, C.W., Shelhamer, J.H., 1994. Interferon-γ induces the synthesis and activation of cytosolic phospholipase A2. J. Clin. Invest. 93, 571–577. https://doi.org/10.1172/JCI117009

Xiao, G., Tsai, A.L., Palmer, G., Boyar, W.C., Marshall, P.J., Kulmacz, R.J., 1997. Analysis of hydroperoxide-induced tyrosyl radicals and lipoxygenase activity in aspirin-treated human prostaglandin H synthase-2. Biochemistry 36, 1836–1845. https://doi.org/10.1021/bi962476u

Xiao, M.F., Xu, J.C., Tereshchenko, Y., Novak, D., Schachner, M., Kleene, R., 2009. Neural cell adhesion molecule modulates dopaminergic signaling and behavior by regulating dopamine D2 receptor internalization. J. Neurosci. 29, 14752–14763. https://doi.org/10.1523/JNEUROSCI.4860-09.2009

Xu, G., Li, Y., Ma, C., Wang, C., Sun, Z., Shen, Y., Liu, L., Li, S., Zhang, X., Cong, B., 2019. Restraint stress induced hyperpermeability and damage of the blood-brain barrier in the

amygdala of adult rats. Front. Mol. Neurosci. 12, 32. https://doi.org/10.3389/fnmol.2019.00032

Xu, M., Cen, M., Shen, Y., Zhu, Y., Cheng, · Fangli, Tang, L., Hu, W., Dai, N., 2021. Deoxycholic acid-induced gut dysbiosis disrupts bile acid enterohepatic circulation and promotes intestinal inflammation. Dig. Dis. Sci. 66, 568–576. https://doi.org/10.1007/s10620-020-06208-3

Xu, M., Wang, C., Krolick, K.N., Shi, H., Zhu, J., 2020. Difference in post-stress recovery of the gut microbiome and its altered metabolism after chronic adolescent stress in rats. Sci. Rep. 10, 1–10. https://doi.org/10.1038/s41598-020-60862-1

Xu, Y., Zhou, H., Zhu, Q., 2017. The impact of microbiota-gut-brain axis on diabetic cognition impairment. Front. Aging Neurosci. 9, 106. https://doi.org/10.3389/fnagi.2017.00106

Yagnik, D., 2014. Macrophage derived platelet activating factor implicated in the resolution phase of gouty inflammation. Int. J. Inflam. 2014, 526496. https://doi.org/10.1155/2014/526496

Yamano, T., Tanida, M., Niijima, A., Maeda, K., Okumura, N., Fukushima, Y., Nagai, K., 2006. Effects of the probiotic strain *Lactobacillus johnsonii* strain La1 on autonomic nerves and blood glucose in rats. Life Sci. 79, 1963–1967. https://doi.org/10.1016/J.LFS.2006.06.038

Yamashiro, K., Tanaka, R., Urabe, T., Ueno, Y., Yamashiro, Y., Nomoto, K., Takahashi, T., Tsuji, H., Asahara, T., Hattori, N., 2017. Gut dysbiosis is associated with metabolism and systemic inflammation in patients with ischemic stroke. PLoS One 12, e0171521. https://doi.org/10.1371/journal.pone.0171521

Yang, C., Fujita, Y., Ren, Q., Ma, M., Dong, C., Hashimoto, K., 2017. *Bifidobacterium* in the gut microbiota confer resilience to chronic social defeat stress in mice. Sci. Rep. 7, 45942. https://doi.org/10.1038/srep45942

Yang, C., Shirayama, Y., Zhang, J.C., Ren, Q., Hashimoto, K., 2015. Peripheral interleukin-6 promotes resilience versus susceptibility to inescapable electric stress. Acta Neuropsychiatr. 27, 312–316. https://doi.org/10.1017/neu.2015.36

Yang, Y., Feng, Y., Zhang, X., Nakajima, T., Tanaka, N., Sugiyama, E., Kamijo, Y., Aoyama, T., 2016. Activation of PPARα by fatty acid accumulation enhances fatty acid degradation and sulfatide synthesis. Tohoku J. Exp. Med. 240, 113–122. https://doi.org/10.1620/tjem.240.113

Yano, J.M., Yu, K., Donaldson, G.P., Shastri, G.G., Ann, P., Ma, L., Nagler, C.R., Ismagilov, R.F., Mazmanian, S.K., Hsiao, E.Y., 2015. Indigenous bacteria from the gut microbiota regulate host serotonin biosynthesis. Cell 161, 264–76. https://doi.org/10.1016/j.cell.2015.02.047

Yaribeygi, H., Panahi, Y., Sahraei, H., Johnston, T.P., Sahebkar, A., 2017. The impact of stress on body function: a review. EXCLI J. 16, 1057–1072. https://doi.org/10.17179/excli2017-480

Yehuda, R., Boisoneau, D., Lowy, M.T., Giller, E.L., 1995. Dose-response changes in plasma cortisol and lymphocyte glucocorticoid receptors following dexamethasone administration in combat veterans with and without posttraumatic stress disorder. Arch. Gen. Psychiatry 52, 583–593.

Yehuda, R., Pratchett, L.C., Elmes, M.W., Lehrner, A., Daskalakis, N.P., Koch, E., Makotkine, I., Flory, J.D., Bierer, L.M., 2014. Glucocorticoid-related predictors and correlates of post-traumatic stress disorder treatment response in combat veterans. Interface Focus 4, 20140048. https://doi.org/10.1098/rsfs.2014.0048

Yildiz, S., Mazel-Sanchez, B., Kandasamy, M., Manicassamy, B., Schmolke, M., 2018. Influenza A virus infection impacts systemic microbiota dynamics and causes quantitative enteric dysbiosis. Microbiome 6, 9. https://doi.org/10.1186/s40168-017-0386-z

Ylikoski, J., Lehtimäki, J., Pirvola, U., Mäkitie, A., Aarnisalo, A., Hyvärinen, P., Ylikoski, M., 2017. Non-invasive vagus nerve stimulation reduces sympathetic preponderance in patients with tinnitus. Acta Otolaryngol. 137, 426–431. https://doi.org/10.1080/00016489.2016.1269197

Yu, H., Rao, X., Zhang, K., 2017. Nucleoside diphosphate kinase (Ndk): A pleiotropic effector manipulating bacterial virulence and adaptive responses. Microbiol. Res. 205, 125–134. https://doi.org/10.1016/j.micres.2017.09.001

Yu, M., Jia, H., Zhou, C., Yang, Y., Zhao, Y., Yang, M., Zou, Z., 2017. Variations in gut microbiota and fecal metabolic phenotype associated with depression by 16S rRNA gene sequencing and LC/MS-based metabolomics. J. Pharm. Biomed. Anal. 138, 231–239. https://doi.org/10.1016/j.jpba.2017.02.008

Yuksel, Z.S., Buber, E., Kocagoz, T., Alp, A., Saribas, Z., Acan, N.L., 2011. Mycobacterial strains that stimulate the immune system most efficiently as candidates for the treatment of

bladder cancer. J. Mol. Microbiol. Biotechnol. 20, 24–28. https://doi.org/10.1159/000324331

Zarrinpar, A., Chaix, A., Xu, Z.Z., Chang, M.W., Marotz, C.A., Saghatelian, A., Knight, R., Panda, S., 2018. Antibiotic-induced microbiome depletion alters metabolic homeostasis by affecting gut signaling and colonic metabolism. Nat. Commun. 9, 2872. https://doi.org/10.1038/s41467-018-05336-9

Zelkas, L., Raghupathi, R., Lumsden, A.L., Martin, A.M., Sun, E., Spencer, N.J., Young, R.L., Keating, D.J., 2015. Serotonin-secreting enteroendocrine cells respond via diverse mechanisms to acute and chronic changes in glucose availability. Nutr. Metab. (Lond). 12, 55. https://doi.org/10.1186/s12986-015-0051-0

Zeng, H., Chi, H., 2015. Metabolic control of regulatory T cell development and function. Trends Immunol. 36, 3–12. https://doi.org/10.1016/J.IT.2014.08.003

Zhang, C., Wang, Y., Wang, D., Zhang, J., Zhang, F., 2018. NSAID exposure and risk of Alzheimer's disease: An updated meta-analysis from cohort studies. Front. Aging Neurosci. 10, 83. https://doi.org/10.3389/fnagi.2018.00083

Zhang, J., Song, L., Wang, Y., Liu, C., Zhang, L., Zhu, S., Liu, S., Duan, L., 2019. Beneficial effect of butyrate-producing Lachnospiraceae on stress-induced visceral hypersensitivity in rats. J. Gastroenterol. Hepatol. 34, 1368–1376. https://doi.org/10.1111/jgh.14536

Zhang, K., Fujita, Y., Chang, L., Qu, Y., Pu, Y., Wang, S., Shirayama, Y., Hashimoto, K., 2019. Abnormal composition of gut microbiota is associated with resilience versus susceptibility to inescapable electric stress. Transl. Psychiatry 9, 231. https://doi.org/10.1038/s41398-019-0571-x

Zhang, L., Jiang, Y., Cui, Z., Yang, W., Yue, L., Ma, Y., Shi, S., Wang, Chunfang, Wang, Chunfeng, Qian, A., 2016. *Mycobacterium vaccae* induces a strong Th1 response that subsequently declines in C57BL/6 mice. J. Vet. Sci. 17, 505–513. https://doi.org/10.4142/jvs.2016.17.4.505

Zhang, X., Osaka, T., Tsuneda, S., 2015. Bacterial metabolites directly modulate farnesoid X receptor activity. Nutr. Metab. (Lond). 12, 48. https://doi.org/10.1186/s12986-015-0045-y

Zhang, Z., Lei, Y., Yan, C., Mei, X., Jiang, T., Ma, Z., Wang, Q., 2019. Probenecid relieves cerebral dysfunction of sepsis by inhibiting pannexin 1-dependent ATP release. Inflammation 42, 1082–1092. https://doi.org/10.1007/s10753-019-00969-4

Zhao, F., Feng, J., Li, J., Zhao, L., Liu, Y., Chen, H., Jin, Y., Zhu, B., Wei, Y., 2018. Alterations of the gut microbiota in Hashimoto's Thyroiditis patients. Thyroid 28, 175–186. https://doi.org/10.1089/thy.2017.0395

Zhao, R.J., Wang, H., 2011. Chemerin/ChemR23 signaling axis is involved in the endothelial protection by KATP channel opener iptakalim. Acta Pharmacol. Sin. 32, 573–580. https://doi.org/10.1038/aps.2011.19

Zhao, X., Zhang, J., Yi, S., Xixi, L., Guo, Z., Zhou, X., Mu, J., Yi, R., 2019. *Lactobacillus plantarum* CQPC02 Prevents Obesity in Mice through the PPAR-α Signaling Pathway. Biomolecules 9, 407.

Zheng, G., Victor Fon, G., Meixner, W., Creekmore, A., Zong, Y., K. Dame, M., Colacino, J., Dedhia, P.H., Hong, S., Wiley, J.W., 2017. Chronic stress and intestinal barrier dysfunction: Glucocorticoid receptor and transcription repressor HES1 regulate tight junction protein Claudin-1 promoter. Sci. Rep. 7, 4502. https://doi.org/10.1038/s41598-017-04755-w

Zhou, G.X., Liu, Z.J., 2017. Potential roles of neutrophils in regulating intestinal mucosal inflammation of inflammatory bowel disease. J. Dig. Dis. 18, 495–503. https://doi.org/10.1111/1751-2980.12540

Ziegler, M.E., Souda, P., Jin, Y.P., Whitelegge, J.P., Reed, E.F., 2012. Characterization of the endothelial cell cytoskeleton following HLA class I ligation. PLoS One 7, e29472. https://doi.org/10.1371/journal.pone.0029472

Zijlmans, M.A.C., Korpela, K., Riksen-Walraven, J.M., de Vos, W.M., de Weerth, C., 2015. Maternal prenatal stress is associated with the infant intestinal microbiota. Psychoneuroendocrinology 53, 233–245. https://doi.org/10.1016/J.PSYNEUEN.2015.01.006

Zlotnik, A., Klin, Y., Kotz, R., Dubilet, M., Boyko, M., Ohayon, S., Shapira, Y., Teichberg, V.I., 2010. Regulation of blood L-glutamate levels by stress as a possible brain defense mechanism. Exp. Neurol. 224, 465–471. https://doi.org/10.1016/j.expneurol.2010.05.009

Zuany-Amorim, C., Sawicka, E., Manlius, C., Le Moine, A., Brunet, L.R., Kemeny, D.M., Bowen, G., Rook, G.A.W., Walker, C., 2002. Suppression of airway eosinophilia by killed *Mycobacterium vaccae*-induced allergen-specific regulatory T-cells. Nat. Med. 8, 625–629. https://doi.org/10.1038/nm0602-625

Zúñiga, J., Cancino, M., Medina, F., Varela, P., Vargas, R., Tapia, G., Videla, L.A., Fernández,

V., 2011. N-3 PUFA supplementation triggers PPAR-α activation and PPAR-α/NF-κB interaction: Anti-inflammatory implications in liver ischemia-reperfusion injury. PLoS One 6, e28502. https://doi.org/10.1371/journal.pone.0028502

Zuo, H., Ueland, P.M., Ulvik, A., Eussen, S.J.P.M., Vollset, S.E., Nygård, O., Midttun, Ø., Theofylaktopoulou, D., Meyer, K., Tell, G.S., 2016. Plasma biomarkers of inflammation, the kynurenine pathway, and risks of all-cause, cancer, and cardiovascular disease mortality: The Hordaland Health Study. Am. J. Epidemiol. 183, 249–258. https://doi.org/10.1093/aje/kwv242

Zuo, Z., Qi, F., Yang, J., Wang, X., Wu, Y., Wen, Y., Yuan, Q., Zou, J., Guo, K., Yao, Z. Bin, 2017. Immunization with Bacillus Calmette-Guérin (BCG) alleviates neuroinflammation and cognitive deficits in APP/PS1 mice via the recruitment of inflammation-resolving monocytes to the brain. Neurobiol. Dis. 101, 27–39. https://doi.org/10.1016/j.nbd.2017.02.001

Appendix 1. Chapter 2 supplementary material

Supplementary figures

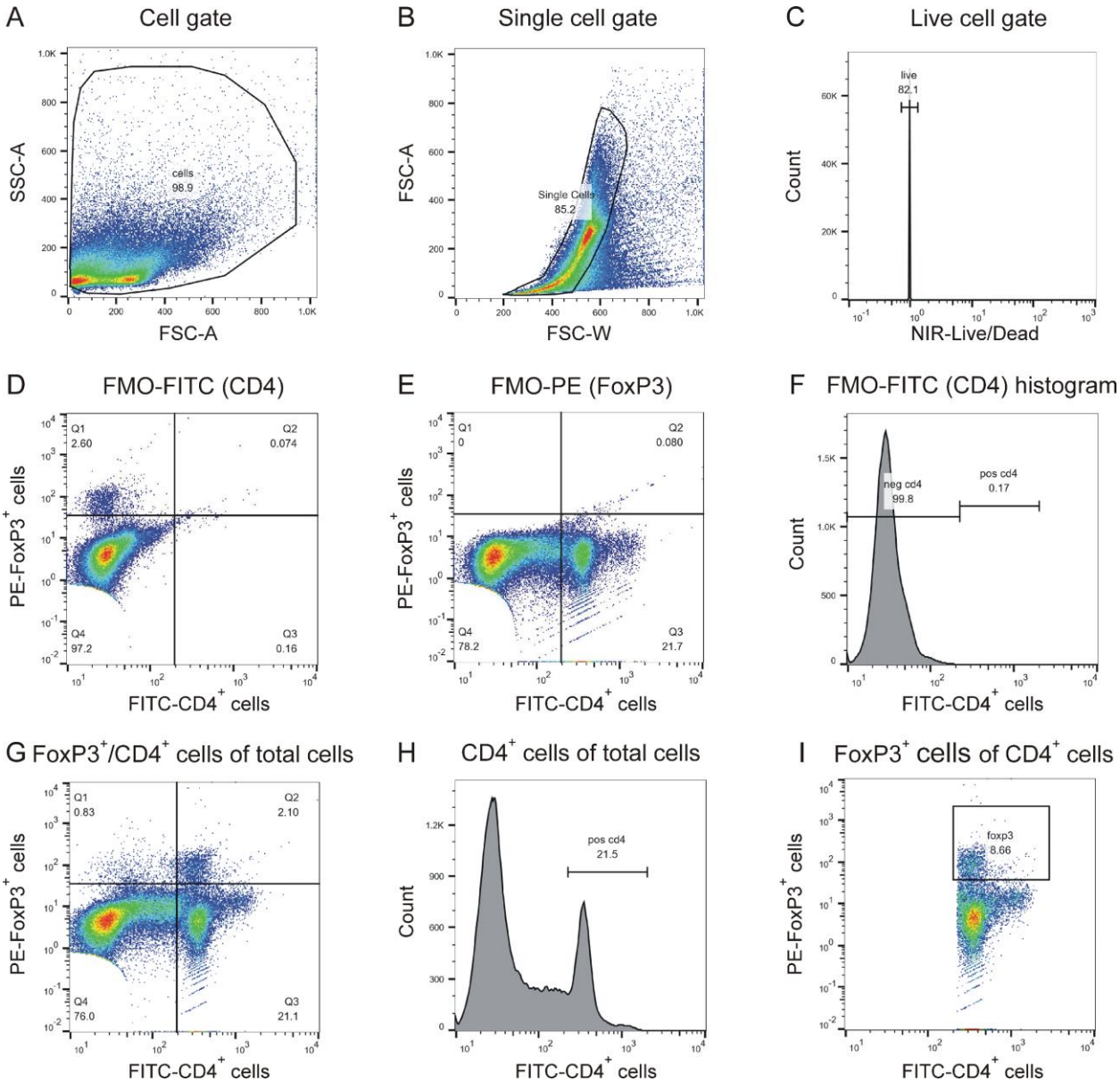

Supplementary Figure 2.1 Gating strategy for flow cytometry analysis using FlowJo software, including (A) cell gating, (B) single cell gating, (C) live cell gating, (D) fluorescence minus one (FMO) gating for FITC (CD4), (E) FMO gating for PE (FoxP3), (F) FMO gating for FITC (CD4) histogram gate, (G) double-label $FoxP3^+/CD4^+$ cell gating, (H) $CD4^+$ gating only, and (I) $FoxP3^+$ cells as percent of $CD4^+$ cell population.

Abbreviations: CD, cluster of differentiation; FITC, fluorescein isothiocyanate; FMO, fluorescence minus one; FoxP3, forkhead box P3; FSC-A, forward scatter area; FSC-W, forward scatter width; NIR, near infrared; PE, phycoerythrin.

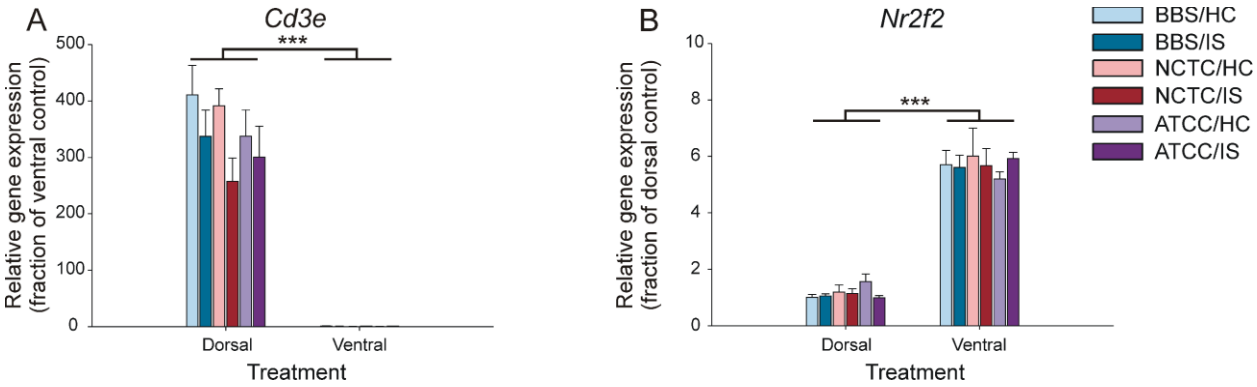

Supplementary Figure 2.2 High relative mRNA expression of *Cd3e* in the dorsal hippocampus and high relative mRNA expression of *Nr2f2* in the ventral hippocampus validate our hippocampal dissections.

Data represent (A) dorsal *Cd3e* and (B) ventral *Nr2f2* hippocampus markers in dorsal and ventral hippocampus dissections. Expression of *Cd3e* is represented as fraction of ventral control (BBS/HC) and expression of *Nr2f2* is represented as fraction of dorsal control (BBS/HC). High relative mRNA expression of *Cd3e* in the dorsal hippocampus and high relative mRNA expression of *Nr2f2* in the ventral hippocampus validate our hippocampal dissections. Sample sizes: *Cd3e*, dorsal (BBS/HC, $n = 7$; BBS/IS, $n = 8$; NCTC/HC, $n = 7$; NCTC/IS, $n = 8$; ATCC/HC, $n = 8$; ATCC/IS, $n = 8$;); *Cd3e*, ventral (BBS/HC, $n = 6$; BBS/IS, $n = 6$; NCTC/HC, $n = 5$; NCTC/IS, $n = 7$; ATCC/HC, $n = 8$; ATCC/IS, $n = 7$); *Nr2f2*, dorsal (BBS/HC, $n = 6$; BBS/IS, $n = 7$; NCTC/HC, $n = 7$; NCTC/IS, $n = 8$; ATCC/HC, $n = 8$; ATCC/IS, $n = 7$); *Nr2f2*, ventral (BBS/HC, $n = 6$; BBS/IS, $n = 6$; NCTC/HC, $n = 6$; NCTC/IS, $n = 7$; ATCC/HC, $n = 7$; ATCC/IS, $n = 7$). Expression of *Cd3e* and *Nr2f2* mRNA was measured using quantitative real-time polymerase chain reaction (RT-qPCR), with beta-actin as a reference. Bars represent the mean + SEM. ***$p < 0.001$. Abbreviations: ATCC, *M. vaccae* ATCC 15483; BBS, borate-buffered saline; *Cd*, cluster of differentiation; HC, home cage control conditions; IS, inescapable tail shock; NCTC, *M. vaccae* NCTC 11659; *Nr2f2*, nuclear receptor subfamily 2, group F, member 2.

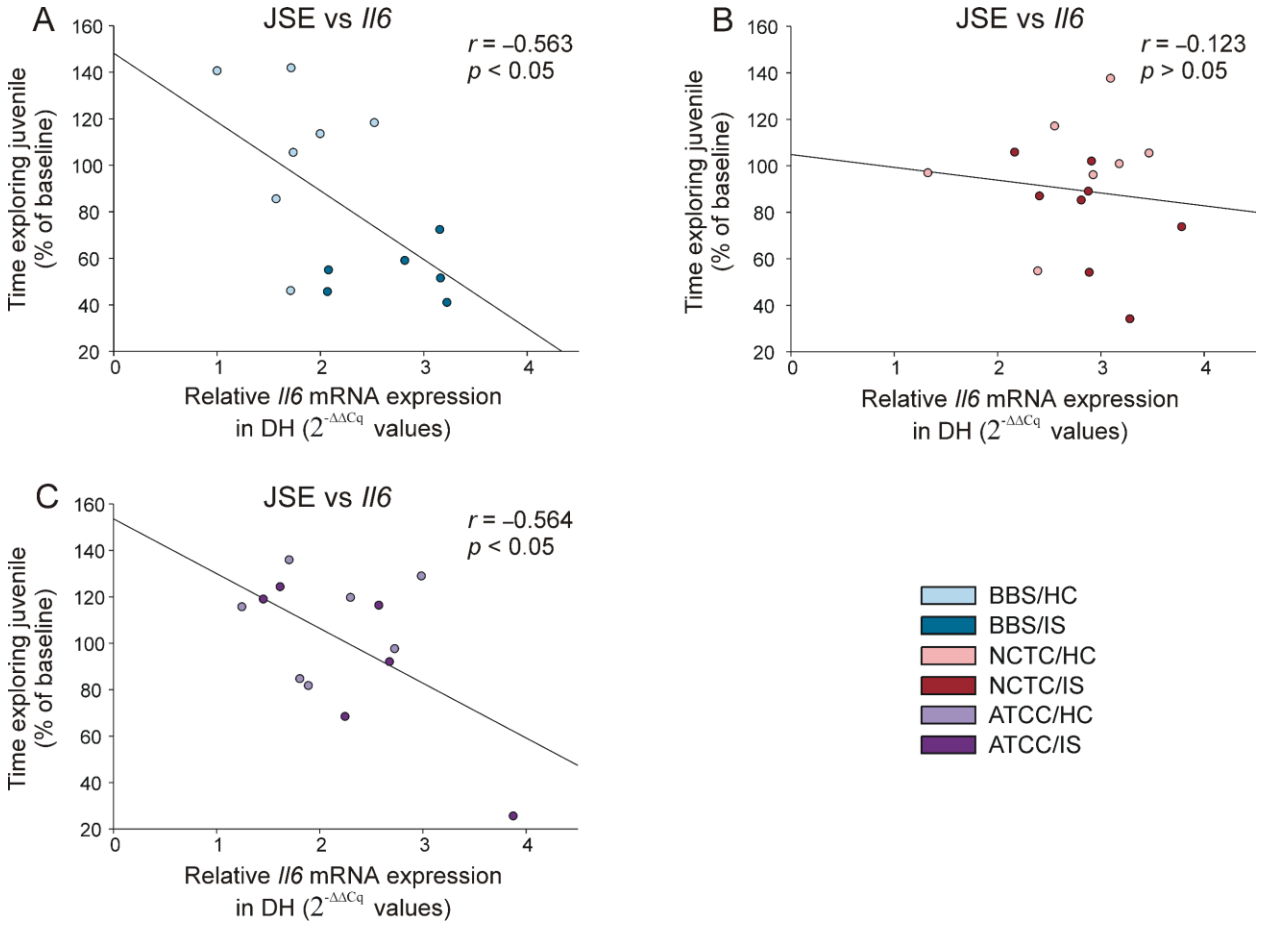

Supplementary Figure 2.3 JSE behavior negatively correlates with *Il6* mRNA in the dorsal hippocampus among BBS-treated animals only and animals immunized with *M. vaccae* ATCC 15483 only, but not with animals immunized with *M. vaccae* NCTC 11659 only.

Sample sizes: *Il6* (BBS/HC, *n* = 7; BBS/IS, *n* = 8; NCTC/HC, *n* = 7; NCTC/IS, *n* = 8; ATCC/HC, *n* = 8; ATCC/IS, *n* = 8); JSE (BBS/HC, *n* = 8; BBS/IS, *n* = 6; NCTC/HC, *n* = 8; NCTC/IS, *n* = 8; ATCC/HC, *n* = 7; ATCC/IS, *n* = 6). Expression of *Il6* mRNA was measured using quantitative real-time polymerase chain reaction (RT-qPCR), with beta-actin as a reference, and data are presented as raw $2^{-\Delta\Delta Cq}$ values. Data for JSE behavior are presented as percent baseline. Pearson's correlation coefficient and *p*-values are given. Abbreviations: ATCC, *M. vaccae* ATCC 15483; BBS, borate-buffered saline; DH, dorsal hippocampus; HC, home cage control conditions; *Il*, interleukin; IS, inescapable tail shock; JSE, juvenile social exploration; NCTC, *M. vaccae* NCTC 11659

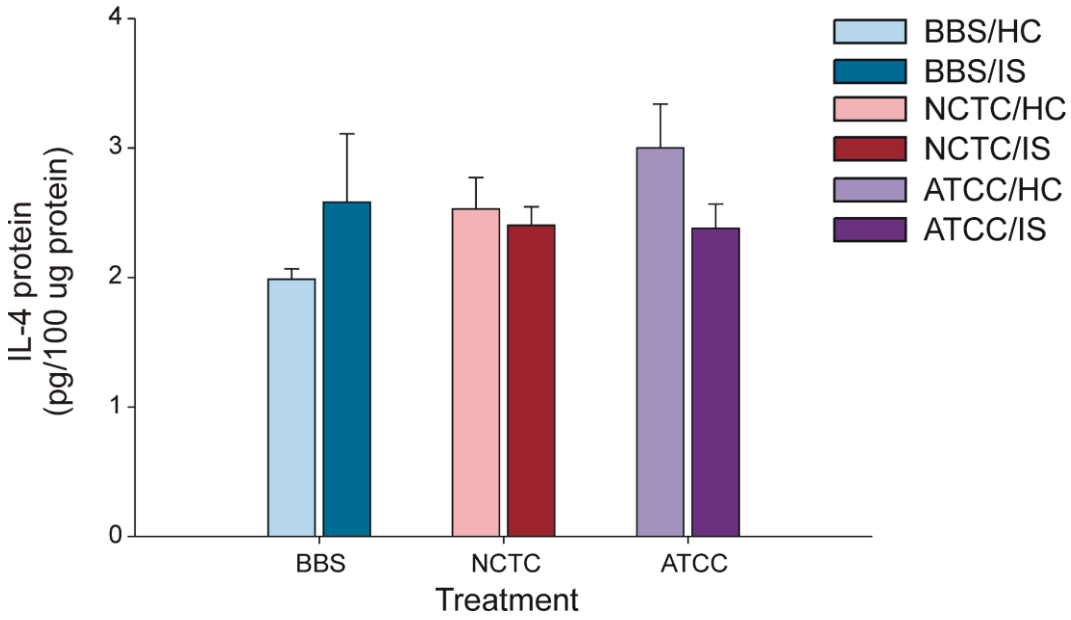

Supplementary Figure 2.4 Neither immunization with *M. vaccae* NCTC 11659 (NCTC) nor *M. vaccae* ATCC 15483 (ATCC) alters IL-4 protein in the dorsal hippocampus among home cage control animals or rats exposed to inescapable tail shock stress (IS).

Sample sizes: BBS/HC, $n = 6$; BBS/IS, $n = 8$; NCTC/HC, $n = 7$; NCTC/IS, $n = 8$; ATCC/HC, $n = 8$; ATCC/IS, $n = 8$. Bars represent the mean + SEM. Post hoc testing was conducted using Fisher's least significant difference (LSD) test. *$p < 0.05$. Abbreviations: ATCC, *M. vaccae* ATCC 15483; BBS, borate-buffered saline; HC, home cage control conditions; IL, interleukin; IS, inescapable tail shock; NCTC, *M. vaccae* NCTC 11659.

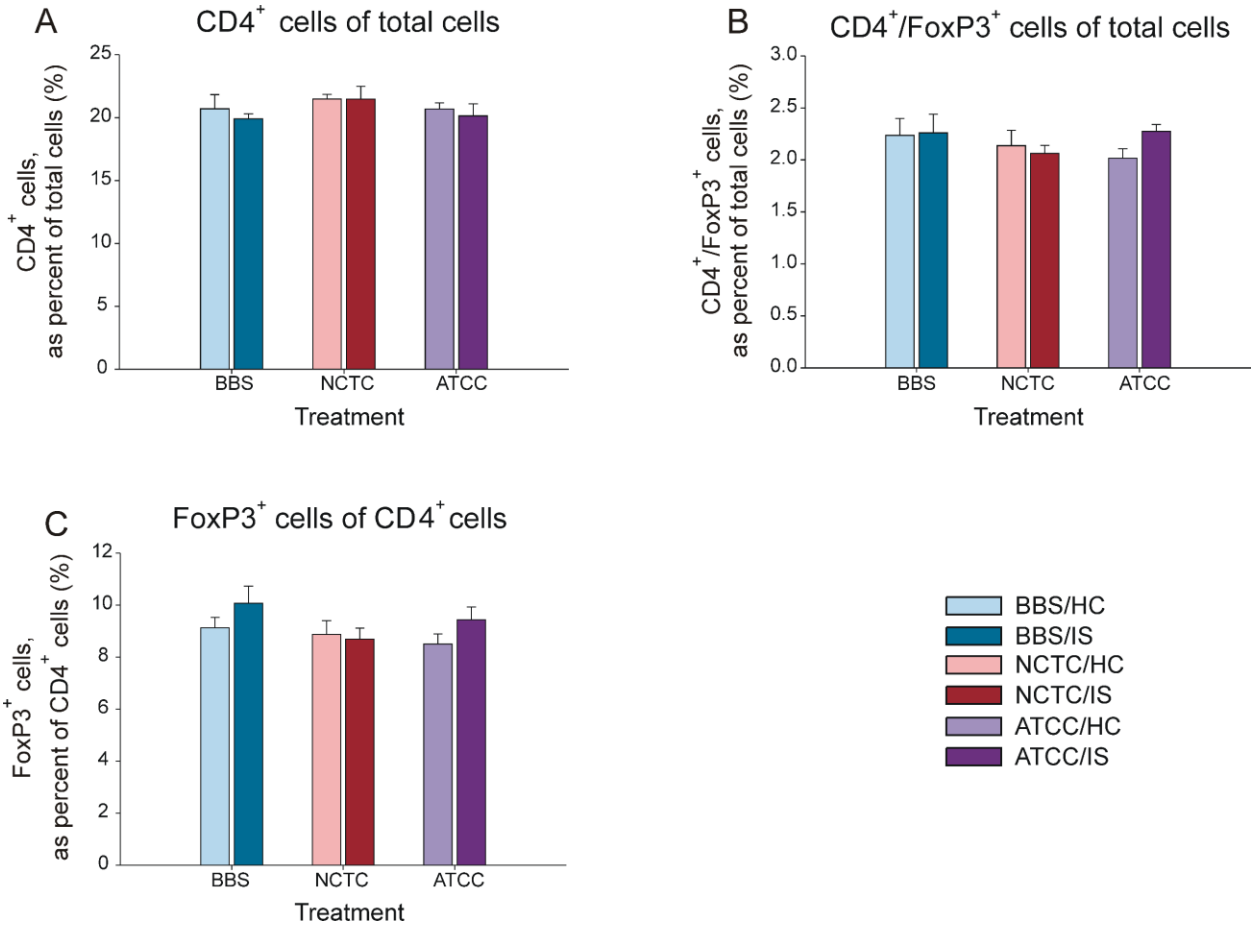

Supplementary Figure 2.5 Neither immunization with either *M. vaccae* NCTC 11659 (NCTC) nor *M. vaccae* ATCC 15483 (ATCC) alters the abundance of $CD4^+$ cells or $CD4^+/FoxP3^+$ regulatory T cells in the spleen.

Sample sizes: $CD4^+$ cells as percent of total cells (BBS/HC, *n* = 8; BBS/IS, *n* = 7; NCTC/HC, *n* = 7; NCTC/IS, *n* = 8; ATCC/HC, *n* = 8; ATCC/IS, *n* = 8); $CD4^+/FoxP3^+$ cells as percent of total cells (BBS/HC, *n* = 8; BBS/IS, *n* = 8; ATCC/HC, *n* = 8; ATCC/IS, *n* = 7; NCTC/HC, *n* = 8; NCTC/IS, *n* = 8); $FoxP3^+$ cells as percent of $CD4^+$ cells (BBS/HC, *n* = 8; BBS/IS, *n* = 8; NCTC/HC, *n* = 8; NCTC/IS, *n* = 8; ATCC/HC, *n* = 8; ATCC/IS, *n* = 8). Bars represent the mean + SEM. There were no differences among any of the groups. Abbreviations: ATCC, *M. vaccae* ATCC 15483; BBS, borate-buffered saline; CD, cluster of differentiation; FoxP3, forkhead box P3; HC, home cage control conditions; IS, inescapable tail shock; NCTC, *M. vaccae* NCTC 11659.

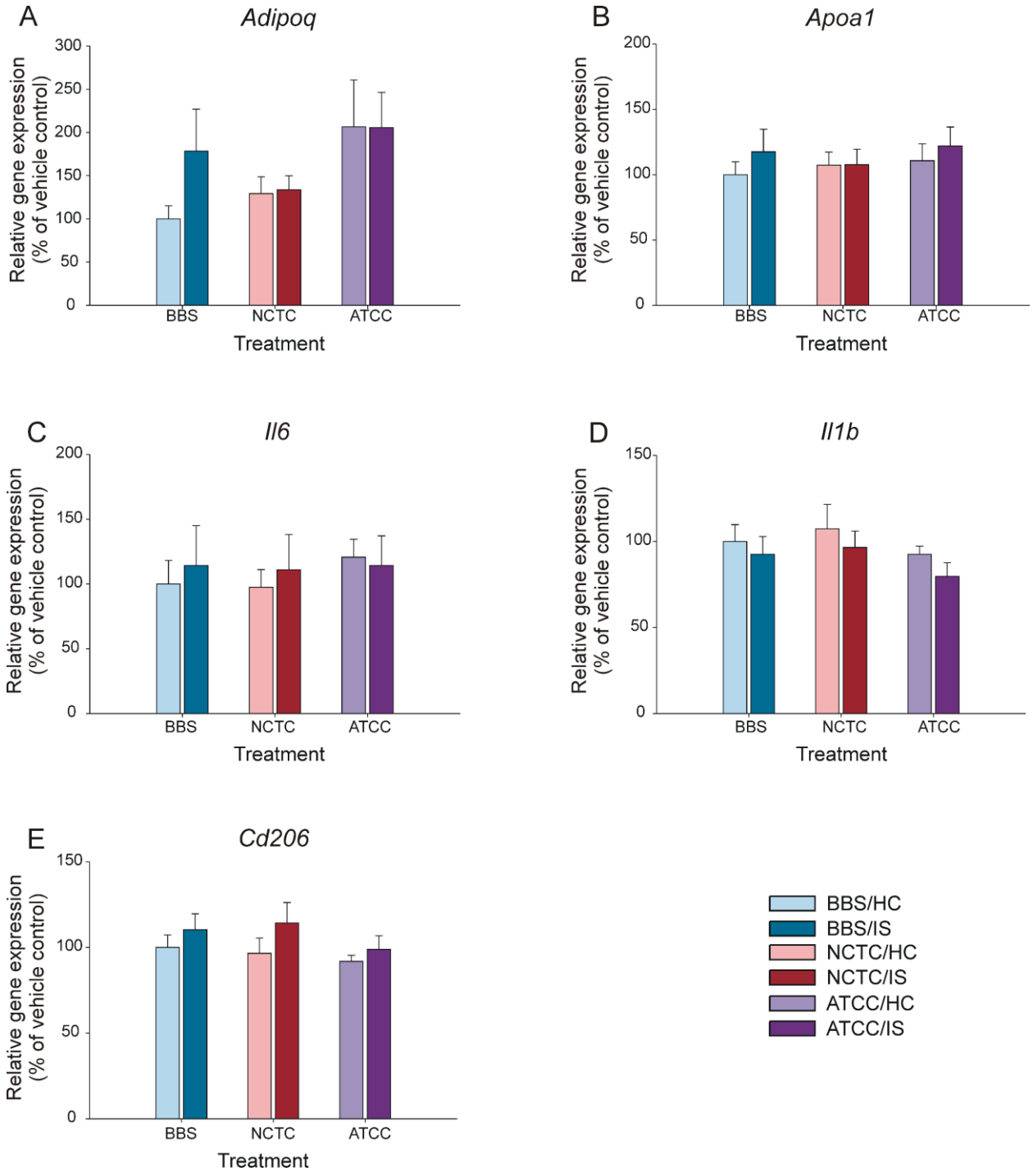

Supplementary Figure 2.6 Neither immunization with *M. vaccae* NCTC 11659 (NCTC) nor *M. vaccae* ATCC 15483 (ATCC) alters a subset of lipid and immune signaling genes in the liver.

Data represent mRNA expression of (A) *Adipoq*, (B) *Apoa1*, (C) *Il6*, (D) *Il1b*, and (E) *Cd206* in the right median lobe of the liver. Sample sizes: *Adipoq* (BBS/HC, *n* = 7; BBS/IS, *n* = 8; NCTC/HC, *n* = 8; NCTC/IS, *n* = 7; ATCC/HC, *n* = 8; ATCC/IS, *n* = 8); *Apoa1* (BBS/HC, *n* = 8; BBS/IS, *n* = 8; NCTC/HC, *n* = 8; NCTC/IS, *n* = 8; ATCC/HC, *n* = 8; ATCC/IS, *n* = 8); *Il6*

(BBS/HC, *n* = 7; BBS/IS, *n* = 7; NCTC/HC, *n* = 8; NCTC/IS, *n* = 7; ATCC/HC, *n* = 8; ATCC/IS, *n* = 8); *Il1b* (BBS/HC, *n* = 8; BBS/IS, *n* = 8; NCTC/HC, *n* = 8; NCTC/IS, *n* = 8; ATCC/HC, *n* = 7; ATCC/IS, *n* = 8); *Cd206* (BBS/HC, *n* = 8; BBS/IS, *n* = 8; NCTC/HC, *n* = 8; NCTC/IS, *n* = 8; ATCC/HC, *n* = 8; ATCC/IS, *n* = 8). Expression of *Adipoq*, *Apoa1*, *Il6*, *Il1b*, and *Cd206* mRNA was measured using quantitative real-time polymerase chain reaction (RT-qPCR), with beta-actin as a reference. Bars represent the mean + SEM. Abbreviations: *Adipoq*, adiponectin; *Apoa1*, apolipoprotein A-I; ATCC, *M. vaccae* ATCC 15483; BBS, borate-buffered saline; *Cd*, cluster of differentiation; HC, home cage control conditions; *Il*, interleukin; IS, inescapable tail shock; NCTC, *M. vaccae* NCTC 11659.

Supplementary tables

Supplementary Table 2.1 List of primer sequences and corresponding tissue analyzed by RT-qPCR.

Gene[1]	Primer Sequence 5' → 3'	Tissue
Actb	F: TTCCTTCCTGGGTATGGAAT	Dorsal and ventral hippocampus; liver
	R: GAGGAGCAATGATCTTGATC	
Adipoq	F: ATCCTGGTCACAATGGGATAC	Liver
	R: CCTTAGGACCAAGAACACCTG	
Apoa1	F: AGGATTTCGCCACTGTGTATG	Liver
	R: GTTGTCCAGGAGATTCAGGTTC	
Cd200	F: CTCTCTATGTACAGCCCATAG	Dorsal hippocampus
	R: GGGAGTGACTCTCAGTACTAT	
Cd200r1	F: TAGAGGGGGTGACCAATTAT	Dorsal hippocampus
	R: TACATTTTCTGCAGCCACTG	
Cd206 (Mrc1)	F: GGGGTTGTTGCTGTTGATGT	Dorsal hippocampus; liver
	R: GCTCGAAACGGAAAAGGTTC	
Cd3e	F: AAAGCCAGAGTGTGCGAGAA	Dorsal and ventral hippocampus
	R: CCTTCCTTTTCTTGCTCCAG	
Crp	F: TTTGTGCTATCTCCAGAACAGATCA	Liver
	R: GCCCGCCAGTTCAAAACAT	
Il1b	F: CCTTGTGCAAGTGTCTGAAG	Dorsal hippocampus; liver
	R: GGGCTTGGAAGCAATCCTTA	
Il4	F: GAACTCACTGAGAAGCTGCA	Dorsal hippocampus; liver
	R: GAAGTGCAGGACTGCAAGTA	
Il6	F: AGAAAAGAGTTGTGCAATGGCA	

	R: GGCAAATTTCCTGGTTATATCC	Dorsal hippocampus
Nfkbia	F: CACCAACTACAACGGCCACA	Dorsal hippocampus
	R: GCTCCTGAGCGTTGACATCA	
Nr2f2	F: TGTTCACCTCAGATGCCTGT	Dorsal and ventral hippocampus
	R: AGGGAGACGAAGCAAAAGCT	
Ppara	F: TGCTGAAGTACGGTGTGTATG	Liver
	R: CTTTAGGAACTCTCGGGTGATG	
Ppard	F: CCTTCTCCAAGCACATCTACAA	Liver
	R: TGATGAAGGGTGCGTTATGG	
Pparg	F: CGGTTGATTTCTCCAGCATTTC	Liver
	R:CTACTTTGATCGCACTTTGGTATTC	

[1]Abbreviations: *Actb*, beta actin; *Adipoq*, adiponectin; *Apoa1*, apolipoprotein A-I; *Cd*, cluster of differentiation; *Cd200r1*, CD200 receptor 1; *Cd206* (*Mrc1*), CD206 (mannose receptor C-type 1); *Cd3e*, CD3, epsilon chain; *Crp*, C-reactive protein; *Il*, interleukin; *Nfkbia*, NF-κB inhibitor α; *Nr2f2*, nuclear receptor 2, factor 2; *Ppara*, peroxisome proliferator-activated receptor α; *Ppard*, peroxisome proliferator-activated receptor δ; *Pparg*, peroxisome proliferator-activated receptor γ.

Supplementary Table 2.2 Group means ± standard deviations[1] for each study measurement and effect sizes for measurements with significant effects of treatment, stress, or treatment x stress.

Measure	BBS/HC	BBS/IS	NCTC/HC	NCTC/IS	ATCC/HC	ATCC/IS	η^2_p treatment	η^2_p stress	η^2_p treatment x stress	Cohen's d for pairwise comparisons
JSE (time exploring juvenile as % baseline)	107 ± 30.9	54.1 ± 11.0	96.5 ± 26.9	78.9 ± 24.2	109 ± 21.4	91.0 ± 38.3	0.088	0.26	0.098	BBS/IS vs BBS/HC: –2.28
***Il6* mRNA DH**	1.75 ± 0.46	2.69 ± 0.62	2.70 ± 0.71	2.89 ± 0.49	2.17 ± 0.61	2.54 ± 0.81	0.147	0.154	0.069	NCTC/HC vs BBS/HC: 1.59; BBS/IS vs BBS/HC: 1.72
***Il1b* mRNA DH**	3.60 ± 1.4	4.95 ± 4.1	3.48 ± 0.98	3.82 ± 1.5	5.10 ± 1.3	3.70 ± 2.2	na	na	na	na
***Nfkbia* mRNA DH**	1.66 ± 0.46	1.84 ± 0.45	1.97 ± 0.45	1.94 ± 0.48	1.96 ± 0.42	1.72 ± 0.57	na	na	na	na
***Il4* mRNA DH**	3.44 ± 2.1	3.87 ± 1.6	2.56 ± 1.0	3.30 ± 0.58	4.28 ± 3.4	2.72 ± 1.2	na	na	na	na
***Cd206* mRNA DH**	3.36 ± 2.8	1.62 ± 0.40	1.66 ± 0.36	1.73 ± 0.29	4.61 ± 3.5	1.86 ± 0.59	0.114	0.149	0.099	ATCC/IS vs ATCC/HC: –1.10
***Cd200* mRNA DH**	1.58 ± 0.37	1.45 ± 0.16	1.50 ± 0.26	1.21 ± 0.097	1.50 ± 0.36	1.45 ± 0.42	na	na	na	na

***Cd200r1* mRNA DH**	5.84 ± 2.1	3.49 ± 0.75	5.11 ± 2.5	3.92 ± 1.5	6.51 ± 2.7	3.95 ± 1.1	0.031	0.247	0.029	BBS/IS vs BBS/HC: –1.49; ATCC/IS vs ATCC/HC: –1.24
IL-4 protein DH	1.99 ± 0.20	2.58 ± 1.2	2.53 ± 0.64	2.40 ± 0.41	3.00 ± 0.90	2.38 ± 0.50	na	na	na	na
% CD4+ cells of total cells	20.7 ± 3.2	19.9 ± 1.0	21.5 ± 0.95	21.5 ± 2.9	20.7 ± 1.4	20.1 ± 2.7	na	na	na	na
% CD4+/FoxP3+ cells of total cells	2.24 ± 0.46	2.26 ± 0.51	2.14 ± 0.42	2.06 ± 0.21	2.02 ± 0.26	2.27 ± 0.18	na	na	na	na
% FoxP3+ cells of CD4+ cells	9.13 ± 1.1	10.1 ± 1.9	8.88 ± 1.5	8.69 ± 1.2	8.50 ± 1.1	9.44 ± 1.39	na	na	na	na
***Ppara* mRNA liver**	2.38 ± 1.2	2.90 ± 1.9	1.86 ± 0.62	3.19 ± 1.8	3.20 ± 1.7	2.65 ± 1.9	na	na	na	na
***Ppard* mRNA liver**	3.27 ± 1.7	2.53 ± 0.93	2.89 ± 1.0	2.24 ± 1.2	3.09 ± 1.5	2.50 ± 1.8	na	na	na	na
***Pparg* mRNA liver**	4.93 ± 1.3	3.19 ± 1.3	3.54 ± 1.3	2.91 ± 1.4	3.46 ± 0.86	2.02 ± 0.84	0.193	0.247	0.043	NCTC/HC vs BBS/HC: –1.07; ATCC/HC vs BBS/HC: –1.33; BBS/IS vs BBS/HC: –1.33; ATCC/IS vs ATCC/HC: –1.69
***Crp* mRNA liver**	6.14 ± 1.2	7.72 ± 3.4	6.05 ± 1.3	6.56 ± 1.6	5.60 ± 0.85	9.09 ± 3.0	0.044	0.182	0.088	ATCC/IS vs ATCC/HC: 1.58
***Nfkbia* mRNA liver**	2.01 ± 0.46	2.13 ± 0.50	2.72 ± 1.1	1.80 ± 0.22	2.30 ± 0.43	1.75 ± 0.56	0.031	0.131	0.121	NCTC/IS vs NCTC/HC: –1.16
***Il4* mRNA liver**	28.6 ± 46	46.5 ± 63	7.36 ± 5.4	60.0 ± 56	28.7 ± 30	44.2 ± 60	na	na	na	na
***Adipoq* mRNA liver**	5.13 ± 2.0	9.15 ± 7.0	6.63 ± 2.8	6.9 ± 2.2	10.6 ± 7.9	10.5 ± 5.9	na	na	na	na
***Apoa1* mRNA liver**	5.25 ± 1.5	6.17 ± 2.6	5.63 ± 1.5	5.65 ± 1.7	5.81 ± 1.9	6.40 ± 2.2	na	na	na	na
***Il6* mRNA liver**	8.13 ± 3.9	9.28 ± 6.6	7.91 ± 3.1	9.02 ± 5.8	9.80 ± 3.2	9.28 ± 5.3	na	na	na	na
***Il1b* mRNA liver**	1.98 ± 0.55	1.84 ± 0.57	2.13 ± 0.79	1.91 ± 0.53	1.83 ± 0.26	1.58 ± 0.44	na	na	na	na
***Cd206* mRNA liver**	1.68 ± 0.35	1.85 ± 0.44	1.62 ± 0.43	1.92 ± 0.56	1.54 ± 0.17	1.66 ± 0.38	na	na	na	na

Supplementary Table 2.3 Functional enrichment pathway analysis for a subset of genes that hierarchically clustered together based on correlation of mRNA expression.

Pathway[1]	Genes involved[2]	Percent	Fold enrichment	*P*-value	Benjamini-Hotchberg adjusted *p*-value
PPAR signaling pathway	*Adipoq, Apoa1, Ppara*	60	60	0.00058	0.014*
Adipocytokine signaling pathway	*Adipoq, Nfkbia, Ppara*	60	62	0.00055	0.026*
Measles	*Il4, Nfkbia*	40	23	0.068	0.39
Non-alcoholic fatty liver disease (NAFLD)	*Adipoq, Ppara*	40	19	0.081	0.4
Hepatitis C	*Nfkbia, Ppara*	40	24	0.065	0.42
cAMP signaling pathway	*Nfkbia, Ppara*	40	16	0.097	0.43
Insulin resistance	*Nfkbia, Ppara*	40	28	0.056	0.43
Leishmaniasis	*Il4, Nfkbia*	40	43	0.037	0.46
T cell receptor signaling pathway	*Il4, Nfkbia*	40	30	0.053	0.49

[1]Functional enrichment pathway analysis provided by DAVID bioinformatics resource.
[2]Abbreviations: *Apoa1*, apolipoprotein A-I; *Adipoq*, adiponectin; *Il*, interleukin; *Nfkbia*, NF-κB inhibitor α; *Ppara*, peroxisome proliferator-activated receptor α.
*$p < 0.05$ after Benjamini-Hotchberg correction.

Supplementary Table 2.4 PTSD-relevant findings following immunization with *Mycobacterium vaccae* NCTC 11659.

PTSD Symptom based on DSM-5	Effects of *M. vaccae* NCTC 11659 in rodent models
Intrusions	N.A.
Avoidance (avoiding people, situations circumstances resembling or associated with the event)	Decreased stress-induced anxiety-like defensive behavioral responses (avoidance) (Amoroso et al., 2020; Frank et al., 2018b; Reber et al., 2016a) and current study

Negative alterations in mood and cognition	Prevention of surgery-induced microglial priming and cognitive impairment (Fonken et al., 2018)
Alterations in arousal or reactivity (hypervigilance for threat, exaggerated startle response, irritability, difficulty concentration, sleep problems)	Enhanced fear extinction in fear-potentiated startle (Fox et al., 2017; Hassell et al., 2019) Prevention of stress-induced cortical hyperarousal (Bowers et al., 2019) Prevention of stress-induced sleep and behavioral impairments (Bowers et al., 2017, 2019, 2018; Lambert et al., 2017)

Abbreviations: DSM-5, Diagnostic and Statistical Manual of Mental Disorders, 5th Edition; N.A., not applicable; NCTC, National Collection of Type Cultures; PTSD, posttraumatic stress disorder.

Appendix 2. Chapter 3 supplementary material

Supplementary tables

Supplementary Table 3.1 Functional enrichment annotations for genes whose protein abundance was upregulated or downregulated, respectively, in the plasma of home cage animals eight days after the final immunization with *M. vaccae* ATCC 15483*[1].

Effects of *M. vaccae* ATCC 15483 on plasma functional enrichment					
Upregulated by immunization with *M. vaccae* ATCC 15483					
Pathway	**Genes involved**	**Percent**	**Fold enrichment**	***P*-value**	**Benjamini-Hotchberg corrected**
none listed	na	na	na	na	na
Gene ontology, biological process					
negative regulation of blood coagulation	*Kng1*, *Kng2*	66.7	974.2	0.0014	0.024
vasodilation	*Kng1*, *Kng2*	66.7	467.6	0.0028	0.025
acute-phase response	*Kng1*, *Kng2*	66.7	307.6	0.0043	0.026
negative regulation of cell adhesion	*Kng1*, *Kng2*	66.7	285.1	0.0047	0.021
negative regulation of endopeptidase activity	*Kng1*, *Kng2*	66.7	79	0.017	0.059
positive regulation of cytosolic calcium ion concentration	*Kng1*, *Kng2*	66.7	74.9	0.018	0.052
Gene ontology, cellular component					
extracellular space	*Igfbp6*, *Kng1*, *Kng2*	100	14.1	0.005	0.04
blood microparticle	*Kng1*, *Kng2*	66.7	104.6	0.013	0.05
cell	*Kng1*, *Kng2*	66.7	103.8	0.013	0.034
extracellular exosome	*Igfbp6*, *Kng1*, *Kng2*	100	7	0.02	0.04
Gene ontology, molecular function					
cysteine-type endopeptidase inhibitor activity	*Kng1*, *Kng2*	66.7	258.1	0.0052	0.026
receptor binding	*Kng1*, *Kng2*	66.7	30.7	0.043	0.1
Downregulated by immunization with *M. vaccae* ATCC 15483					

Pathway	Genes involved	Percent	Fold enrichment	*P*-value	Benjamini-Hotchberg corrected
none listed	na	na	na	na	na
Gene ontology, biological process					
none listed	na	na	na	na	na
Gene ontology, cellular component					
extracellular space	*C4bpb, Efemp1, Pf4, Serpina3l*	57.1	9.4	0.0032	0.068
vesicle	*Pf4*, *Ywhag*	28.6	38.3	0.043	0.38
Gene ontology, molecular function					
actin binding	*Tpm1, Ywhag*	28.6	26.7	0.058	0.73

*There were no enriched pathways nor gene ontology annotations in the plasma proteome eight days after the final immunization with *M. vaccae* NCTC 11659.
[1]Functional enrichment annotations provided by DAVID bioinformatics resource.
[2]Abbreviations: *C4bpb*, complement C4b-binding protein beta chain (C4BPb); *Efemp1*, fibulin-3 (FIBL-3); *Igfbp6*, insulin-like growth factor-binding protein 6 (IGFBP-6); *Kng1*, T-kininogen 1 (KNG1); *Kng2*, T-kininogen 2 (KNG2); *Pf4*, platelet factor 4 (PF-4); *Serpina3l*, serine protease inhibitor A3L (Serpin A3L); *Tpm1*, tropomyosin alpha-1 chain (Tpm1); *Ywhag*, 14-3-3 protein gamma (YWHAG).

Supplementary Table 3.2 Functional enrichment annotations for genes whose protein abundance was upregulated or downregulated, respectively, in the plasma of BBS-treated animals 24 hours after IS[1].

Plasma functional enrichment					
Upregulated by stress in BBS-treated animals					
Pathway	**Genes involved**	**Percent**	**Fold enrichment**	***P*-value**	**Benjamini-Hochberg corrected**
complement and coagulation cascades	*C1s, C5, C9, C4bpa, C4bpb, Fgb, Fgg, Kng1, Vwf*	25.7	46.1	4.30E-12	2.30E-10
pertussis	*C1s, C5, C9, C4bpa, C4bpb*	11.4	20.2	0.00082	0..022

platelet activation	*Actb*, *Fgb*, *Fgg*, *Vwf*	11.4	10.9	0.0047	0.085
Staphylococcus aureus infection	*C1s*, *C5*, *Fgg*	8.6	20.5	8.40E-03	0.11
cardiac muscle contraction	*Myh6/7*, *Mlc1/3/4*, *Tpm1*	8.6	14.2	0.017	0.15
hypertrophic cardiomyopathy	*Actb*, *Mlc1/3/4*, *Tpm1*	8.6	13.8	0.018	0.15
dilated cardiomyopathy	*Actb*, *Mlc1/3/4*, *Tpm1*	8.6	13.2	1.90E-02	0.15
Tight junction	*Actb*, *Myh1/2*, *Myh4*	8.6	12	2.30E-02	0.16
systemic lupus erythematosus	*C1s*, *C5*, *C9*	8.6	8.4	0.045	0.26
adrenergic signaling in cardiomyocytes	*Myh6/7*, *Mlc1/3/4*, *Tpm1*	8.6	8.0	0.049	0.26
prion diseases	*C5*, *C9*	5.7	22.4	0.082	0.4
Gene ontology, biological process (top 16 based on *p*-value)					
complement activation, classical pathway	*C1s*, *C5*, *C9*, *C4bpa*, *C4bpb*, *Igh-1a*	17.1	86.2	6.10E-09	8.30E-07
acute-phase response	*Itih4*, *Kng1*, *Kng2*, *Lbp*, *Orm1*, *Saa4*	17.1	83.9	7.00E-09	8.30E-07
muscle contraction	*Myh1/2*, *Myh4*, *Myh6/7*, *Myl1/34*, *Tpm1*	1.43	53.1	2.00E-06	0.00015
striated muscle contraction	*Aldoa*, *Myh1*, *Myh4*, *Myh6/7*	11.4	141.7	2.50E-06	0.00015
innate immune response	*C1s*, *C4bpa*, *C4bpb*, *Fgb*, *Igh-1a*, *Lbp*	17.1	12.2	0.00010	0.0048

negative regulation of endopeptidase activity	*C5*, *Itih4*, *Kng1*, *Kng2*, *Serpina3n*	14.3	18.0	0.00015	0.0057
ventricular cardiac tissue morphogenesis	*Myh6/7*, *Myl1/3/4*, *Tpm1*	8.6	61.3	0.0010	0.034
platelet aggregation	*Actb*, *Fgb*, *Fgg*	8.6	38.9	0.0025	0.075
cardiac muscle contraction	*Myh6/7*, *Myl1/3/4*, *Tpm1*	8.6	32.5	0.0036	0.094
negative regulation of complement activation, classical pathway	*C4bpa*, *C4bpb*	5.7	354.2	0.0055	0.13
blood coagulation, fibrin clot formation	*Fgb*, *Fgg*	5.7	212.5	0.091	0.20
muscle filament sliding	*Myh6/7*, *Tpm1*	5.7	177.1	0.011	0.20
complement activation, alternative pathway	*C5*, *C9*	5.7	177.1	0.011	0.20
regulation of ATPase activity	*Myh6/7*, *Tpm1*	5.7	151.8	0.013	0.21
cellular response to interleukin-1	*Fgb*, *Fgg*, *Serpina3n*	8.6	16.3	0.014	0.21
response to lipopolysaccharide	*Aldoa*, *Lbp*, *Orm1*, *Serpina3n*	11.4	7.6	0.014	0.21
Gene ontology, cellular component (top 10 based on *p*-value)					
blood microparticle	*Acta1*, *Actb*, *C1s*, *C9*, *C4bpa*, *Cfhr1*, *Fgb*, *Fgg*, *Igh-1a*, *Itih4*, *Kng1*, *Kng2*, *Orm1*	37.1	60	7.90E-19	6.80E-17
extracellular exosome	*Acta1*, *Actb*, *Aldoa*, *Angptl6*, *C1s*, *C5*, *C9*, *Cfhr1*, *Fgb*, *Fgg*, *Fgl1*, *Igfbp6*,	60	4.3	1.00E-09	4.40E-08

	Itih4, *Kng1*, *Kng2*, *Lbp*, *Orm1*, *Pkm*, *Pygm*, *Vwf*, *Ywhag*				
extracellular space	*Acta1*, *Actb*, *Aldoa*, *C5*, *C4bpa*, *C4bpb*, *Fgb*, *Fgg*, *Igfbp6*, *Kng1*, *Kng2*, *Lbp*, *Orm1*, *Prg4*, *Serpina3n*, *Vwf*	45.7	6.6	1.70E-09	4.80E-08
muscle myosin complex	*Myh1*, *Myh4*, *Myh6/7*	8.6	272.4	4.60E-05	0.001
myosin complex	*Myh1*, *Myh4*, *Myh6/7*, *Myl1/34*	11.4	42.7	0.0001	0.002
stress fiber	*Acta1*, *Actb*, *Myh6/7*, *Tpm1*	11.4	31.6	0.00025	0.0036
extracellular region	*C1s*, *C9*, *C4bpa*, *C4bpb*, *Serpina3n*, *Saa4*, *Vwf*	20	5.3	0.00150	0.018
myofibril	*Myh4*, *Myh6/7*, *Tpm1*	8.6	40.9	0.0023	0.025
myelin sheath	*Actb*, *Aldoa*, *Pkm*, *Ywhag*	11.4	11.4	0.005	0.045
other organism cell	*C4bpa*, *C4bpb*	5.7	363.1	0.0053	0.046
Gene ontology, molecular function (top 10 based on *p*-value)					

microfilament motor activity	*Myh1*, *Myh4*, *Myh6*/7	8.6	90.7	0.00046	0.029
actin binding	*Myh1*, *Myh4*, *Myh6/7*, *Tpm1*, *Ywhag*	14.3	11.5	0.00075	0.029
receptor binding	*Fgb*, *Fgg*, *Kng1*, *Kng2*, *Lbp*	14.3	8.0	0.0029	0.071
motor activity	*Myh1*, *Myl1/3/4*, *Myh4*	8.6	31.9	0.0037	0.071
protein homodimerization activity	*Abcb9*, *Fgg*, *Myh6/7*, *Pygm*, *Tpm1*, *Vwf*	17.1	4.3	0.010	0.16
protease binding	*Aldoa*, *Kng1*, *Vwf*	8.6	14.1	0.018	0.23
ATP binding	*Abcb9*, *Acta1*, *Actb*, *Myh1*, *Myh4*, *Myh6*, *Pkm*	20	2.9	0.027	0.29
ATPase activity	*Myh1*, *Myh4*, *Myh6/7*	8.6	9.7	0.036	0.34
cysteine-type endopeptidase inhibitor activity	*Kng1*, *Kng2*	5.7	26.7	0.070	0.60
identical protein binding	*Actb*, *C1s*, *Myh6/7*, *Vwf*	11.4	3.5	0.093	0.66
Downregulated by stress in BBS-treated animals					
Pathway	**Genes involved**	**Percent**	**Fold enrichment**	***P*-value**	**Benjamini-Hochberg corrected**
complement and coagulation cascades	*C4a*, *C8a*, *Mbl1*	9.7	23.1	0.0062	0.085
PPAR signaling pathway	*Apoa1*, *Apoa2*, *Pltp*	9.7	21.6	0.0071	0.085
vitamin digestion and absorption	*Apoa1*, *Apoa4*	6.5	50.3	0.036	0.29
African trypanosomiasis	*Apoa1*, *Hba1*	6.5	29.1	0.062	0.30

fat digestion and absorption	*Apoa1*, *Apoa4*	6.5	29.1	0.062	0.30
Staphylococcus aureus infection	*C4a*, *Mbl1*	6.5	20.5	0.087	0.35
Gene ontology, biological process (top 15 based on *p*-value)					
phospholipid efflux	*Apoa1*, *Apoa2*, *Apoa4*, *Apoc2*, *Apoe*	16.1	215.9	5.10E-09	1.70E-06
cholesterol efflux	*Apoa1*, *Apoa2*, *Apoc2*, *Apoc2*, *Apoe*	16.1	112	8.90E-08	1.50E-05
positive regulation of cholesterol esterification	*Apoa1*, *Apoa2*, *Apoa4*, *Apoe*	12.9	302.3	2.00E-07	1.70E-05
high density lipoprotein particle assembly	*Apoa1*, *Apoa2*, *Apoa4*, *Apoe*	12.9	302.3	2.00E-07	1.70E-05
reverse cholesterol transport	*Apoa1*, *Apoa2*, *Apoa4*, *Apoe*	12.9	201.6	7.90E-07	4.40E-05
high density lipoprotein particle remodeling	*Apoa1*, *Apoa2*, *Apoe*, *Pltp*	12.9	201.6	7.90E-07	4.40E-05
phosphatidylcholine metabolic process	*Apoa1*, *Apoa4*, *Gpld1*, *Pon1*	12.9	172.8	1.30E-06	6.30E-05
cholesterol metabolic process	*Apoa1*, *Apoa2*, *Apoa4*, *Apoe*, *Pon1*	16.1	48.8	2.70E-06	0.00011
triglyceride homeostasis	*Apoa1*, *Apoa4*, *Apoc2*, *Apoe*	12.9	93	0.000009	0.00035
lipoprotein metabolic process	*Apoa1*, *Apoa2*, *Apoa4*, *Apoe*	12.9	89.6	1.00E-05	0.00035
high density lipoprotein particle clearance	*Apoa2*, *Apoc2*, *Apoe*	9.7	362.8	2.50E-05	0.00074

complement activation, classical pathway	*C4a*, *Igg-2a*, *Igkc*, *Mbl1*	12.9	65.4	0.000027	0.00076
very-low-density lipoprotein particle remodeling	*Apoa1*, *Apoa4*, *Apoe*	9.7	259.1	0.000051	0.00120
regulation of intestinal cholesterol absorption	*Apoa1*, *Apoa2*, *Apoa4*	9.7	259.1	5.10E-05	0.00120
negative regulation of endopeptidase activity	*A1i3*, *C4a*, *C4b*, *Mug1*, *Serpina3c*	16.1	20.4	0.000085	0.00190
Gene ontology, cellular component (top 10 based on *p*-value)					
blood microparticle	*Alb*, *Apoa1*, *Apoa2*, *Apoa4*, *Apoe*, *C4b*, *C8a*, *Hba1*, *Igg-2a*, *Igkc*, *Mug1*, *Pon1*	38.7	62.8	1.40E-17	8.70E-16
extracellular space	*Alb*, *Apoa1*, *Apoa2*, *Apoa4*, *Apoc2*, *Apoe*, *Ai13*, *C4a*, *C4b*, *C8a*, *Efemp1*, *Gpld1*, *Gpx3*, *Igkc*, *Mbl1*, *Mug1*, *Pf4*, *Pltp*, *Pon1*, *Psap*, *Serpina3c*	67.7	9.9	4.90E-17	1.50E-15
high-density lipoprotein particle	*Apoa1*, *Apoa2*, *Apoa4*, *Apoe*, *Gpld1*, *Pon1*	19.4	217.9	4.00E-11	8.50E-10

extracellular exosome	*Alb*, *Apoa1*, *Apoa2*, *Apoa4*, *Apoc2*, *Apoe*, *C4b*, *C8a*, *Efemp1*, *Gpld1*, *Gpx3*, *Hba1*, *Igkc*, *Igfals*, *Mbl1*, *Mug1*, *Pglyrp2*, *Pon1*, *Psap*, *Rarres2*, *Tpm4*	64.5	4.7	3.90E-10	6.30E-09
chylomicron	*Apoa1*, *Apoa2*, *Apoa4*, *Apoc2*, *Apoe*	16.1	280.6	1.60E-09	2.00E-08
very-low-density lipoprotein particle	*Apoa1*, *Apoa2*, *Apoa4*, *Apoc2*, *Apoe*	16.1	181.6	1.10E-08	1.20E-07
spherical high-density lipoprotein particle	*Apoa1*, *Apoa2*, *Apoc2*, *Pon1*	12.9	352.8	1.20E-07	1.10E-06
extracellular region	*Alb*, *Apoa1*, *Apoe*, *A1i3*, *C4a*, *C8a*, *Gpld1*, *Rarres2*	25.8	6.9	9.10E-05	0.00073
discoidal high-density lipoprotein particle	*Apoa1*, *Apoe*	6.5	411.6	0.0047	0.033
intermediate-density lipoprotein particle	*Apoc2*, *Apoe*	6.5	308.7	0.0062	0.040
Gene ontology, molecular function (top 10 based on *p*-value)					
phosphatidylcholine-sterol O-acyltransferase activator activity	*Apoa1*, *Apoa2*, *Apoa4*, *Apoe*	12.9	444	4.70E-08	4.20E-06

cholesterol transporter activity	*Apoa1*, *Apoa2*, *Apoa4*, *Apoe*	12.9	170.8	1.30E-06	5.90E-05
lipid binding	*Apoa1*, *Apoa2*, *Apoa4*, *Apoc2*, *Apoe*, *Pltp*	19.4	26.9	2.20E-06	6.40E-05
endopeptidase inhibitor activity	*A1i3*, *C4a*, *C4b*, *Mug1*	12.9	74	1.90E-05	0.00041
cholesterol binding	*Apoa1*, *Apoa2*, *Apoa4*, *Apoe*	12.9	63.4	3.00E-05	0.00053
lipase inhibitor binding	*Apoa1*, *Apoa2*, *Apoc2*	9.7	277.5	4.40E-05	0.00064
lipid transporter activity	*Apoa1*, *Apoa2*, *Apoe*	9.7	111	0.00030	0.003800
phospholipid binding	*Apoa1*, *Apoa2*, *Apoe*, *Pon1*	12.9	27.4	0.00037	0.00410
phosphatidylcholine binding	*Apoa1*, *Apoa2*, *Apoa4*	9.7	83.3	0.00055	0.00530
beta-amyloid binding	*Apoa1*, *Apoe*, *Hba1*	9.7	52	0.0014	0.01200

[1]Functional enrichment annotations provided by DAVID bioinformatics resource.
[2]Abbreviations: *Alb*, albumin; *Acta1*, alpha-actin 1/2 (α-actin 1/2); *Actb*, beta-actin (β-actin); *Aldoa*, fructose-bisphosphate aldolase A (AldoA); *Ali3*, alpha-1-inhibitor 3 (alpha 1 I3); *Apoa1*, apolipoprotein A-I (ApoA-I); *Apoa2*, apolipoprotein A-II (ApoA-II); *Apoc2*, apolipoprotein C-II (ApoC-II); *Apoe*, apolipoprotein E (ApoE); *Cfhr1*, complement component factor h-like 1 (CFHL1); *Colec10*, collectin liver protein 1 (CL-L1); *C1s*, complement C1s subcomponent (C1s); *C4a*, complement C4a (C4a); *C4b*, complement C4b (C4b); *C4bpa*, complement C4b-binding protein alpha chain (C4Bpa); *C9*, complement C9 (C9); *Efemp1*, fibulin-3 (FIBL-3); *Fgb*, fibrinogen beta chain (FGB); *Fgg*, fibrinogen gamma chain (FGG); *Gpld1*, phosphatidylinositol-glycan-specific phospholipase D (PI-G PLD); *Gpx3*, glutathione peroxidase matching isoforms 3, 5, and 6 (GPx3/5/6); *Igfals*, insulin-like growth factor-binding protein complex acid labile subunit (IGFALS); *Igg-2a*, Ig-gamma-2A chain C region (IgG-2a); *Igh-1a*, immunoglobulin heavy chain 1a (IgH-1a); *Igkc*, Ig kappa chain C region (IgK); *Itih4*, inter-alpha trypsin inhibitor heavy chain 4 (ITIH4); *Kng1*, T-kininogen 1 (KNG1); *Kng2*, T-kininogen 2 (KNG2); *Lbp*, lipopolysaccharide binding protein (LBP); *Loxl1*, lysyl oxidase-like 1 (LOXL1); *Mbl1*, mannose-binding protein A (MBP-A); *Mug1*, murinoglobulin 1 (Mug1); *Myh1/2*, myosin heavy chain matching isoforms 1 and 2 (MyHC-1/2); *Myh4*, myosin heavy chain 4 (MyHC-4); *Myh6/7*, myosin heavy chain matching isoforms 6 and 7 (MyHC-6/7); *Myl2/3/4*, myosin light

chain matching isoforms 1, 3, and 4 (MyLC-1/3/4); *Orm1*, alpha-1-acid glycoprotein (AGP); *Pf4*, platelet factor 4 (PF-4); *Pglyrp2*, peptidoglycan recognition protein 2 (PGLYRP2); *Pltp*, phospholipid transfer protein (PLTP); *Pon1*, serum paraoxonase/arylesterase (PON 1); *Psap*, sulfated glycoprotein 1 (SGP-1); *Pygm*, glycogen phosphorylase (PYG); *Serpina3c*, serine protease inhibitor A3C (Serpin A3C); *Serpina3n*, serine protease inhibitor A3N (Serpin A3N); *Tpm1*, tropomyosin 1; *Tpm4*, tropomyosin 4; *Vwf*, von Willebrand factor (VWF); *Ywhag*, 14-3-3 protein gamma (YWHAG).

Supplementary Table 3.3 Functional enrichment annotations for genes whose protein abundance in the plasma was differentially altered between animals immunized with *M. vaccae* NCTC 11659 and BBS-treated animals, 24 hours after IS[1].

Effects of *M. vaccae* NCTC 11659 on plasma functional enrichment					
Stress-induced increase prevented by immunization with *M. vaccae* NCTC 11659					
Pathway	**Genes involved**	**Percent**	**Fold enrichment**	***P*-value**	**Benjamini-Hochberg corrected**
complement and coagulation cascades	*C5*, *C9*, *Vwf*	27.3	64.6	5.00E-04	0.015
prion diseases	*C5*, *C9*	18.2	93.9	0.017	0.25
systemic lupus erythematosus	*C5*, *C9*	18.2	23.5	0.066	0.51
platelet activation	*Actb*, *Vwf*	18.2	23	0.068	0.51
Gene ontology, biological process					
complement activation, classical pathway	*C5*, *C9*, *Igh-1a*	27.3	142.2	0.00015	0.011
complement activation, alternative pathway	*C5*, *C9*	18.2	584.5	0.0031	0.11
response to immobilization stress	*Actb*, *Vwf*	18.2	83.5	0.021	0.53
blood coagulation	*C9*, *Vwf*	18.2	53.1	0.033	0.62
negative regulation of endopeptidase activity	*C5*, *Kng2*	18.2	23.7	0.073	1.0
Gene ontology, cellular component					
blood microparticle	*Actb*, *C9*, *Igh-1a*, *Kng2*	36.4	57.1	2.9E-05	0.0013
extracellular space	*Actb*, *C5*, *Igfbp6*, *Kng2*, *Prg4*, *Vwf*	54.5	7.7	0.00033	0.0074
extracellular exosome	*Actb*, *Angptl6*, *C5*, *C9*,	63.6	4.5	0.0011	0.016

	Igfbp6, Kng2, Vwf				
cell	*C5, Kng2*	18.2	28.3	0.062	0.61
endoplasmic reticulum	*Abac9, Trappc4, Vwf*	27.3	6.2	0.070	0.61
Gene ontology, molecular function					
none listed	na	na	na	na	na
Stress-induced increase promoted by immunization with *M. vaccae* NCTC 11659					
Pathway	**Genes involved**	**Percent**	**Fold enrichment**	***P*-value**	**Benjamini-Hochberg corrected**
complement and coagulation cascades	*C4, Fga*	20	35.9	0.046	0.73
Gene ontology, biological process					
response to growth hormone	*Fga, Hp*	20	185.6	0.0095	0.55
negative regulation of endothelial cell apoptotic process	*Angpt1, Fga*	20	129.9	0.014	0.55
response to X-ray	*Fga, Hp*	20	125.7	0.014	0.55
acute-phase response	*Fga, Hp*	20	102.5	0.017	0.55
response to heat	*Ckm, Hp*	20	50	0.035	0.88
organ regeneration	*Angpt1, Hp*	20	42.8	0.041	0.88
defense response to bacterium	*Hp, Lyz2*	20	29.3	0.059	1.0
positive regulation of ERK1 and ERK2 cascade	*Angpt1, Fga*	20	20.9	0.082	1.0
response to estradiol	*Fga, Gc*	20	19.4	0.088	1.0
Gene ontology, cellular component					
extracellular space	*Angpt1, Ckm, C4, Fga, Gc, Hp, Lyz2*	70	10.9	3.10E-06	0.00011
blood microparticle	*Fga, Gc, Hp*	30	52.3	0.0011	0.02
extracellular exosome	*Angpt1, Gc, Hp, Lyz2, Pygm*	50	3.9	0.018	0.22
microvillus	*Angpt1, Lyz2*	20	58.8	0.03	0.27
Gene ontology, molecular function					

none listed	na	na	na	na	na
Stress-induced decrease prevented by immunization with *M. vaccae* NCTC 11659					
Pathway	**Genes involved**	**Percent**	**Fold enrichment**	***P*-value**	**Benjamini-Hochberg corrected**
complement and coagulation cascades	*C4a, Mbl1*	14.3	47.8	0.034	0.32
Staphylococcus aureus infection	*C4a, Mbl1*	14.3	35.9	0.046	0.32
Gene ontology, biological process					
inflammatory response	*A1i3, C4a, C4b, Mug1, Pf4, Rarres2*	42.9	25.3	1.6E-06	0.00017
negative regulation of endopeptidase activity	*A1i3, C4a, C4b, Mug1*	28.6	33.9	0.00014	0.0088
complement activation	*C4a, C4b*	14.3	167	0.011	0.41
complement activation, classical pathway	*C4a, Mbl1*	14.3	67.7	0.027	0.75
Gene ontology, cellular component					
extracellular space	*Alb, A1i3, C4a, C4b, Efemp1, Mbl1, Mug1, Pf4, Psap*	64.3	9	5.90E-07	2.40E-05
blood microparticle	*Alb, C4b, Hba1, Mug1*	28.6	44.8	6.90E-05	0.0014
extracellular exosome	*Alb, C4b, Efemp1, Hba1, Igfals, Mug1, Psap, Rarres2, Tpm4*	64.3	4.5	0.00011	0.0015
extracellular region	*Alb, A1i3, C4a, Rarres2*	28.6	7.4	0.012	0.12
basement membrane	*Alb, Efemp1*	14.3	28.4	0.063	0.51
Gene ontology, molecular function					

endopeptidase inhibitor activity	*A1i3*, *C4a*, *C4b*, *Mug1*	28.6	158.6	1.5E-06	0.00007
peptidase inhibitor activity	*A1i3*, *Mug1*	14.3	108.1	0.017	0.36
oxygen binding	*Alb*, *Hba1*	14.3	79.3	0.023	0.36
serine-type endopeptidase inhibitor activity	*A1i3*, *Mug1*	14.3	22.7	0.079	0.93
Stress-induced decrease promoted by immunization with *M. vaccae* NCTC 11659					
Pathway	**Genes involved**	**Percent**	**Fold enrichment**	***P*-value**	**Benjamini-Hochberg corrected**
none listed	na	na	na	na	na
Gene ontology, biological process					
none listed	na	na	na	na	na
Gene ontology, cellular component					
extracellular space	*A1i3* (unchar. Protein G3V9J1), *Apom*, *Chga*, *Jchain*, *Trfc*	83.3	11.7	0.00012	0.0048
extracellular region	*A1i3* (unchar. Protein G3V9J1), *Apom*, *Trfc*	50	13	0.014	0.25
extracellular exosome	*Angtpl6*, *Apom*, *Jchain*, *Trfc*	66.7	4.7	0.023	0.25
secretory granule	*Angtpl6*, *Chga*	33.3	58.2	0.028	0.25
blood microparticle	*Jchain*, *Trfc*	33.3	52.3	3.10E-02	0.25
Gene ontology, molecular function					
none listed	na	na	na	na	na

[1]Functional enrichment annotations provided by DAVID bioinformatics resource.
[2]Abbreviations: *Actb*, β-actin; *Alb*, albumin; *Ali3*, alpha-1-inhibitor 3 (alpha 1 I3; matched by UniProt as uncharacterized protein G3V9J1); *Angpt1*, angiopoietin-1 (ANG-1); *Angptl6*, angiopoietin-like protein 6 (ANGL-6); *Apom*, apolipoprotein M; *Cdh17*, cadherin-17; *Chga*,

chromogranin-A (CgA); *Ckm*, creatine kinase M-type (M-CK); *C4a*, complement C4a (C4a); *C4b*, complement C4b (C4b); *C5*, complement component C5 (C5); *C9*, complement C9 (C9); *Efemp1*, fibulin-3 (FIBL-3); *Fga*, fibrinogen alpha chain (FGA); *Gc*, vitamin D-binding protein (VDB); *Hp*, haptoglobin; *Igfbp6*, insulin-like growth factor-binding protein 6 (IGFBP-6); *Igh-1a*, immunoglobulin heavy chain 1a (IgH-1a); *Jchain*, immunoglobulin joining chain (J-chain); *Kng2*, T-kininogen 2 (KNG2); *Lyz2*, lysozyme; *Mbl1*, mannose-binding protein A (MBP-A); *Mug1*, murinoglobulin 1 (Mug1); *Mylpf*, myosin regulatory light chain 2 (MyLC-2); *Prg4*, proteoglycan 4; *Psap*, sulfated glycoprotein 1 (SGP-1); *Rarres2*, retinoic acid receptor responder 2 (also known as chemerin); *Trfc*, transferrin receptor protein 1 (TfR1); *Vwf*, von Willebrand factor (VWF).

Supplementary Table 3.4 Functional enrichment annotations for genes whose protein abundance in the plasma was differentially altered between animals immunized with *M. vaccae* ATCC 15483 and BBS-treated animals, 24 hours after IS[1].

Effects of *M. vaccae* ATCC 15483 on plasma functional enrichment					
Stress-induced increase prevented by immunization with *M. vaccae* ATCC 15483					
Pathway	**Genes involved**	**Percent**	**Fold enrichment**	***P*-value**	**Benjamini-Hochberg corrected**
complement and coagulation cascades	*C5, C9, Vwf*	33.3	64.6	0.00050	0.02
prion diseases	*C5, C9*	22.2	93.9	0.017	0.33
systemic lupus erythematosus	*C5, C9*	22.2	23.5	0.066	0.66
platelet activation	*Actb, Vwf*	22.2	23	0.068	0.66
Gene ontology, biological process					
complement activation, classical pathway	*C5, C9, Igh-1a*	33.3	158	0.00012	0.0088
complement activation, alternative pathway	*C9, Igh-1a*	22.2	649.4	0.0027	0.10
response to immobilization stress	*C5, C9*	22.2	92.8	0.019	0.46
blood coagulation	*Actb, Vwf*	22.2	59	0.03	0.54
liver development	*C9, Vwf*	22.2	26.9	0.064	0.80
negative regulation of endopeptidase activity	*Pkm, Vwf*	22.2	26.3	0.066	0.80
Gene ontology, cellular component					
blood microparticle	*Actb, C9, Igh-1a, Kng2*	44.4	78.5	8.7E-06	0.00034
extracellular exosome	*Actb, C5, C9, Igfbp6,*	77.8	6.1	5.2E-05	0.0010

	Kng2, Pkm, Vwf				
extracellular space	*Actb, C5, Igfbp6, Kng2, Vwf*	55.6	8.8	0.00075	0.0097
cell	*C5, Kng2*	22.2	38.9	0.044	0.43
myelin sheath	*Actb, Pkm*	22.2	24.2	0.07	0.54
extracellular matrix	*Pkm, Vwf*	22.2	18.2	0.092	0.54
external side of plasma membrane	*Igh-1a, Vwf*	22.2	17.3	0.097	0.54
Gene ontology, molecular function					
none listed	na	na	na	na	na
Stress-induced increase promoted by immunization with *M. vaccae* ATCC 15483					
Pathway	**Genes involved**	**Percent**	**Fold enrichment**	***P*-value**	**Benjamini-Hochberg corrected**
oocyte meiosis	*Calm1/2/3, Ywhae*	16.7	19.9	0.083	1.0
neurotrophin signaling pathway	*Calm1/2/3, Ywhae*	16.7	17.6	0.094	1.0
Gene ontology, biological process					
substantia nigra development	*Calm1/2/3, Ywhae*	16.7	81.2	0.022	1.0
Gene ontology, cellular component					
extracellular exosome	*Calm1/2/3, Masp2, Proz, Sbsn, Ywhae*	41.7	3.2	0.043	0.98
extracellular region	*Apoa5, Masp2, Proz*	25	7.1	0.054	0.98
Gene ontology, molecular function					
calcium ion binding	*Calm1/2/3, Masp2, Mylpf, Proz*	33.3	12	0.0022	0.11
calcium-dependent protein binding	*Calm1/2/3, Masp2*	16.7	57.8	0.03	0.75
ion channel binding	*Calm1/2/3, Ywhae*	16.7	32.8	0.052	0.87

serine-type endopeptidase activity	*Masp2*, *Proz*	16.7	19.7	0.085	1.0
Stress-induced decrease prevented by immunization with *M. vaccae* ATCC 15483					
Pathway	**Genes involved**	**Percent**	**Fold enrichment**	***P*-value**	**Benjamini-Hochberg corrected**
complement and coagulation cascades	*C4a*, *C8a*, *Mbl1*	21.4	40.4	0.0017	0.031
Staphylococcus aureus infection	*C4a*, *Mbl1*	14.3	35.9	0.048	0.43
Gene ontology, biological process					
complement activation	*C4a*, *C4b*, *C8a*	21.4	269.8	4.5E-05	0.0057
inflammatory response	*C4a*, *C4b*, *Pf4*, *Rarres2*	28.6	18.2	0.00094	0.060
negative regulation of plasma lipoprotein particle oxidation	*Apoa4*, *Pon1*	14.3	899.2	0.0021	0.087
phosphatidylcholine metabolic process	*Apoa4*, *Pon1*	14.3	192.7	0.0095	0.22
positive regulation of cholesterol efflux	*Pon1*, *Pltp*	14.3	192.7	0.0095	0.22
response to stilbenoid	*Apoa4*, *Hba1*	14.3	168.6	0.011	0.22
hydrogen peroxide catabolic process	*Apoa4*, *Hba1*	14.3	149.9	11	0.22
complement activation, classical pathway	*C4a*, *Mbl1*	14.3	72.9	0.025	0.40
cholesterol metabolic process	*Apoa4*, *Pon1*	14.3	43.5	0.042	0.59
lipid metabolic process	*Pon1*, *Pltp*	14.3	30.3	0.059	0.75
negative regulation of endopeptidase activity	*C4a*, *C4b*	14.3	18.2	0.097	1.0
Gene ontology, cellular component					
extracellular space	*Apoa4*, *C4a*, *C4b*, *C8a*, *Efemp1*, *Mbl1*, *Pon1*, *Pltp*, *Pf4*	64.3	9.0	5.9E-07	0.00002
blood microparticle	*Apoa4*, *C4b*, *C8a*, *Hba1*, *Pon1*	35.7	56.1	1.1E-06	0.00002

extracellular exosome	*Apoa4*, *C4b*, *C8a*, *Efemp1*, *Hba1*, *Pon1*, *Rarres2*, *Tpm4*	57.1	4.0	0.00094	0.012
high-density lipoprotein particle	*Apoa4*, *Pon1*	14.3	155.6	0.012	0.11
collagen trimer	*Colec10*, *Mbl1*	14.3	44.1	0.041	0.31
extracellular region	*C4a*, *C8a*, *Rarres2*	21.4	5.6	0.087	0.55
Gene ontology, molecular function					
complement binding	*C4b*, *C8a*	14,.3	297.3	0.0062	0.25
calcium ion binding	*Cdh17*, *Efemp1*, *Mbl1*, *Pon1*	28.6	6.8	0.015	0.25
mannose binding	*Colec10*, *Mbl1*	14.3	103.4	0.018	0.25
endopeptidase inhibitor activity	*C4a*, *C4b*	14.3	79.3	0.023	0.25
lipid binding	*Apoa4*, *Pltp*	14.3	19.2	0.093	0.82
Stress-induced decrease promoted by immunization with *M. vaccae* ATCC 15483					
Pathway	**Genes involved**	**Percent**	**Fold enrichment**	***P*-value**	**Benjamini-Hochberg corrected**
none listed	na	na	na	na	na
Gene ontology, biological process					
positive regulation of B cell activation	*Ighg1*, *Igh-1a*, unchar. protein M0RA79	30	239.1	5.40E-05	0.0017
phagocytosis, recognition	*Ighg1*, *Igh-1a*, unchar. protein M0RA79	30	202.3	7.60E-05	0.0017
phagocytosis, engulfment	*Ighg1*, *Igh-1a*, unchar. protein M0RA79	30	150.3	0.00014	0.0018

complement activation, classical pathway	*Ighg1*, *Igh-1a*, unchar. protein M0RA79	30	142.2	0.00015	0.0018
B cell receptor signaling pathway	*Ighg1*, *Igh-1a*, unchar. protein M0RA79	30	114.4	0.00024	0.0022
defense response to bacterium	*Ighg1*, *Igh-1a*, unchar. protein M0RA79	30	39.6	0.002	0.015
innate immune response	*Ighg1*, *Igh-1a*, unchar. protein M0RA79	30	20.2	0.0074	0.049
lipoprotein metabolic process	*Apoc1*, *Apom*	20	129.9	0.014	0.07
cholesterol efflux	*Apoc1*, *Apom*	20	129.9	0.014	0.07
negative regulation of endopeptidase activity	*A1i3* (unchar. protein G3V9J1), *Serpina3m*	20	23.7	0.073	0.34
Gene ontology, cellular component					
blood microparticle	*Cd5l*, *Ighg1*, *Igh-1a*, unchar. protein M0RA79	40	62.8	2.1E-05	0.00019
immunoglobulin complex, circulating	*Ighg1*, *Igh-1a*, unchar. protein M0RA79	30	370.4	2.2E-05	0.00019
extracellular space	*A1i3* (unchar. protein G3V9J1), *Ces1c*, *Igfbp6*, *Ighg1*, *Serpina3m*	60	8.4	0.00018	0.001

external side of plasma membrane	*Ighg1*, *Igh-1a*, unchar. protein M0RA79	30	20.8	0.007	0.023
very-low-density lipoprotein particle	*Apoc1*, *Apom*	20	217.9	0.0082	0.023
high-density lipoprotein particle	*Apoc1*, *Apom*	20	217.9	0.0082	0.023
extracellular exosome	*Cd5l*, *Ighg1*, *Apoc1*, *Apom*, *Igfbp6*	50	3.5	0.029	0.07
extracellular region	A1i3 (unchar. protein G3V9J1), *Apoc1*, *Apom*	30	7.8	0.045	0.095
Gene ontology, molecular function					
immunoglobulin receptor binding	*Ighg1*, *Igh-1a*, unchar. protein M0RA79	30	262.9	4.40E-05	0.00071
antigen binding	*Ighg1*, *Igh-1a*, unchar. protein M0RA79	30	113.5	0.00024	0.0019
serine-type endopeptidase inhibitor activity	*A1i3* (unchar. protein G3V9J1), *Serpina3m*	20	31.7	0.055	0.30

[1]Functional enrichment annotations provided by DAVID bioinformatics resource.
[2]Abbreviations: *Actb*, β-actin*; Ali3*, alpha-1-inhibitor 3 (alpha 1 I3); *Apoa5*, apolipoprotein A-V (ApoA-V); *Apom*, apolipoprotein M; *Calm1/2/3*, calmodulin matching isoforms 1, 2, and 3 (CaM); *Cd5l*, CD5 molecule like (CD5L); *Ces1c*, carboxylesterase 1C (Ces1C); *Ckm*, creatine kinase M-type (M-CK); *Colec10*, collectin liver protein 1 (CL-L1); *Colec11*, collectin 11; *C4b*, complement C4b (C4b); *C5*, complement component C5 (C5); *C9*, complement C9 (C9); *Efemp1*, fibulin-3 (FIBL-3); *Igfbp6*, insulin-like growth factor-binding protein 6 (IGFBP-6); *Ighg1*, Ig gamma-1 chain C region (IgG-1); *Igh-1a*, immunoglobulin heavy chain 1a (IgH-1a); *Masp2*, mannan-binding lectin serine protease 2 (MASP-2); *Mbl1*, mannose-binding protein A (MBP-A); *Mylpf*, myosin regulatory light chain 2 (MyLC-2); *Pf4*, platelet factor 4 (PF-4); *Pltp*, phospholipid transfer protein (PLTP); *Pon1*, serum paraoxonase/arylesterase (PON 1); *Proz*, protein Z; *Rarres2*, retinoic acid receptor responder 2 (also known as chemerin); *Sbsn*,

suprabasin; *Serpina3m*, serine protease inhibitor A3M (Serpin A3M); *Vwf*, von Willebrand factor (VWF); *Ywhae*, 14-3-3 protein epsilon (YWHAE).

Supplementary Table 3.5 Proteins in the plasma that correlated with juvenile social exploration after exposure to inescapable tail shock (% of baseline exploration), ordered by *p*-value*.

Protein name	Pearson's *r*	FDR-adjusted *p*-value
pyruvate kinase (PKM)	-0.542	0.029
complement C4b-binding protein alpha chain (C4BPa)	-0.514	0.046
T-kininogen 2 (KNG2)	-0.496	0.047
tropomyosin alpha-1 chain (Tpm1)	-0.493	0.047
T-kininogen 1 (KNG1)	-0.486	0.047
myosin light chain isoforms 1, 3, and 4 (MyLC-1/3/4)	-0.482	0.047
glycogen phosphorylase (PYG)	-0.467	0.054
serum amyloid A protein (SAA4)	-0.471	0.054
myosin regulatory light chain 2 (MyLC-2)	-0.481	0.058
myosin heavy chain 1/2 (MyHC-1/2)	-0.437	0.074
myosin heavy chain 4 (MyHC-4)	-0.432	0.074
serine protease inhibitor A3N (Serpin A3N)	-0.433	0.074
serine protease inhibitor A3K (Serpin A3K)	0.430	0.074
lipopolysaccharide binding protein (LBP)	-0.435	0.074
α-actin 1/2	-0.424	0.078
lysyl oxidase-like 1 (LOXL1)	0.422	0.078

*Sample sizes: JSE (BBS/HC, *n* = 8; BBS/IS, *n* = 6; NCTC/HC, *n* = 8; NCTC/IS, *n* = 8; ATCC/HC, *n* = 7; ATCC/IS, *n* = 6); PKM, C4BPa, KNG2, Tpm1, KNG1, MyLC-1/3/4, PYG, SAA4, MYHC-1/2, MyHC-4, Serpin A3N, Serpin A3K, LBP, α-actin 1/2, and LOXL1 (BBS/HC, *n* = 8; BBS/IS, *n* = 6; NCTC/HC, *n* = 8; NCTC/IS, *n* = 8; ATCC/HC, *n* = 7; ATCC/IS, *n* = 8); MyLC-2 (BBS/HC, *n* = 7; BBS/IS, *n* = 6; NCTC/HC, *n* = 7; NCTC/IS, *n* = 7; ATCC/HC, *n* = 7; ATCC/IS, *n* = 7).

Appendix 3. Chapter 4 supplementary material

Supplementary figures

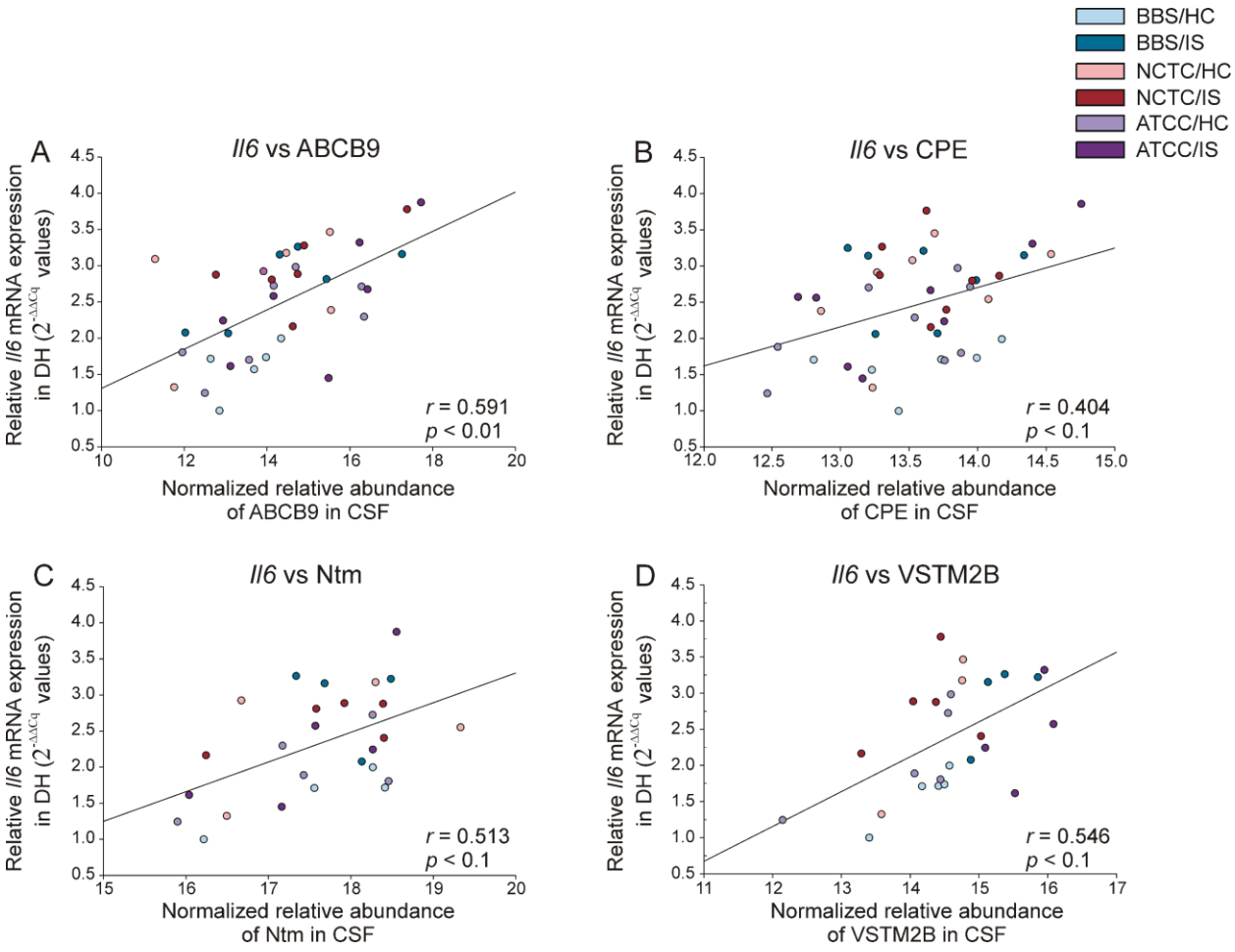

Supplementary Figure 4.1 Correlations between abundances of CSF proteins and hippocampal *Il6* mRNA expression. *Il6* mRNA expression in the dorsal hippocampus (DH) correlated with (A) ATP-binding cassette sub-family B member 9 (ABCB9), (B) carboxypeptidase E (CPE), (C) neurotrimin (Ntm), and (D) V-set and transmembrane domain containing 2B (VSTM2B) in the CSF.

Sample sizes: *Il6* (BBS/HC, *n* = 7; BBS/IS, *n* = 8; NCTC/HC, *n* = 7; NCTC/IS, *n* = 8; ATCC/HC, *n* = 8; ATCC/IS, *n* = 8); ABCB9 (BBS/HC, *n* = 6; BBS/IS, *n* = 6; NCTC/HC, *n* = 7; NCTC/IS, *n* = 6; ATCC/HC, *n* = 7; ATCC/IS, *n* = 7); CPE (BBS/HC, *n* = 7; BBS/IS, *n* = 7; NCTC/HC, *n* = 8; NCTC/IS, *n* = 7; ATCC/HC, *n* = 8; ATCC/IS, *n* = 8); Ntm (BBS/HC, *n* = 4; BBS/IS, *n* = 4; NCTC/HC, *n* = 5; NCTC/IS, *n* = 5; ATCC/HC, *n* = 5; ATCC/IS, *n* = 5); VSTM2B (BBS/HC, *n* = 5; BBS/IS, *n* = 4; NCTC/HC, *n* = 4; NCTC/IS, *n* = 5; ATCC/HC, *n* = 5; ATCC/IS, *n* = 4). Expression of *Il6* mRNA was measured using quantitative real-time polymerase chain reaction (RT-qPCR), with beta-actin as a reference, and data are presented as raw 2-ΔΔCq values. *Il6* was correlated with normalized protein values. Pearson's correlation

coefficient *r* and false discovery rate (FDR)-adjusted *p*-values are given. Abbreviations: ABCB9, ATP-binding cassette sub-family B member 9; ATCC, *M. vaccae* ATCC 15483; BBS, borate-buffered saline; CPE, carboxypeptidase E; CSF, cerebrospinal fluid; DH, dorsal hippocampus; HC, home cage control conditions; *Il*, interleukin; IS, inescapable tail shock; NCTC, *M. vaccae* NCTC 11659; Ntm, neurotrimin; VSTM2B, V-set and transmembrane domain containing 2B.

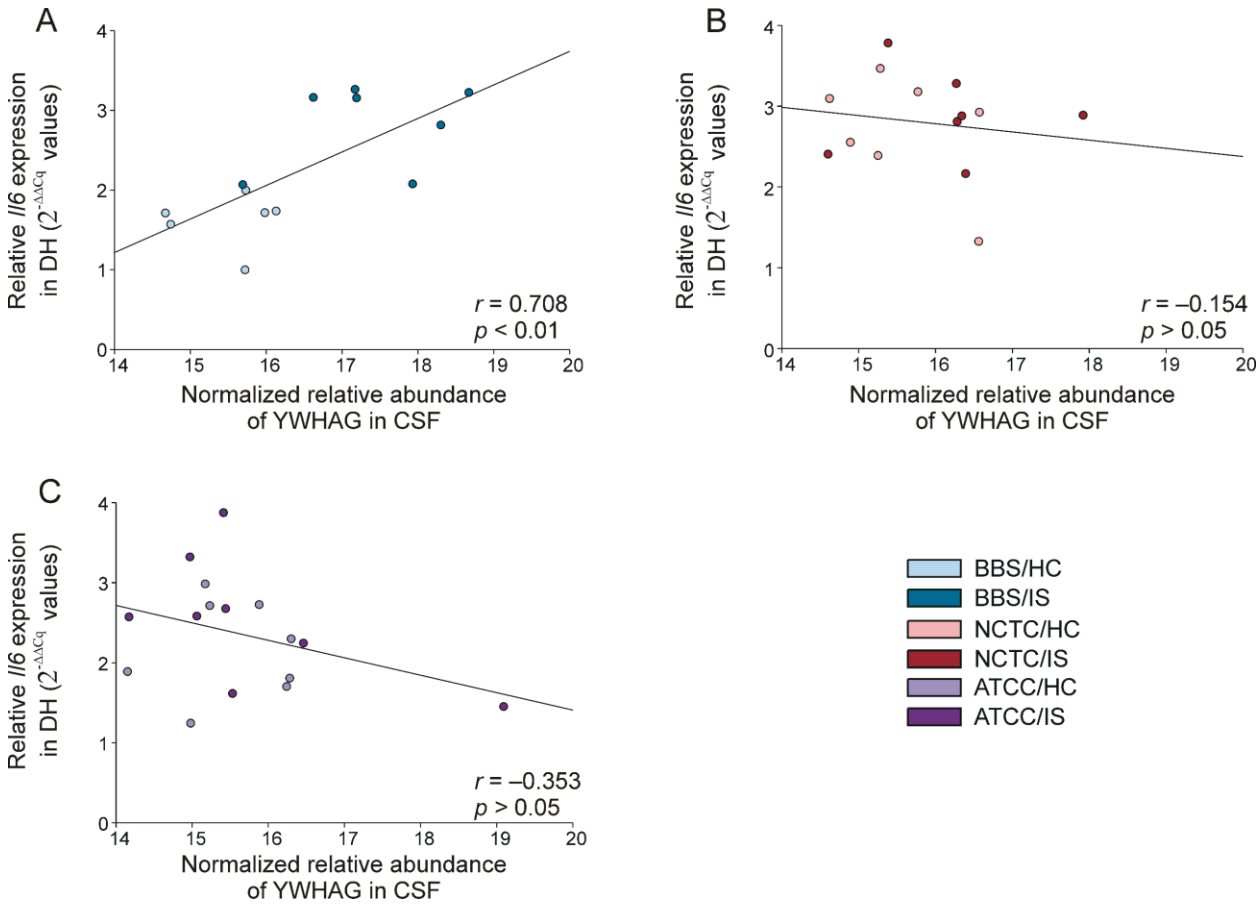

Supplementary Figure 4.2 Correlations between abundances of 14-3-3 protein gamma (YWHAG) in the CSF and hippocampal *Il6* mRNA expression in borate-buffered saline (BBS) or *M. vaccae* immunized rats.

Il6 mRNA expression in the dorsal hippocampus (DH) correlated with 14-3-3 protein gamma (YWHAG) in the CSF among (A) BBS-treated animals, but not among animals previously immunized with (B) *M. vaccae* NCTC 11659 or (C) *M. vaccae* ATCC 15483. Sample sizes: *Il6* (BBS/HC, *n* = 7; BBS/IS, *n* = 7; NCTC/HC, *n* = 7; NCTC/IS, *n* = 8; ATCC/HC, *n* = 8; ATCC/IS, *n* = 8); YWHAG (BBS/HC, *n* = 6; BBS/IS, *n* = 6; NCTC/HC, *n* = 8; NCTC/IS, *n* = 7; ATCC/HC, *n* = 7; ATCC/IS, *n* = 7). Expression of *Il6* mRNA was measured using quantitative real-time polymerase chain reaction (RT-qPCR), with beta-actin as a reference, and data are presented as raw 2-ΔΔCq values. *Il6* was correlated with normalized protein values. Pearson's correlation coefficient *r* and *p*-values are given. Abbreviations: ATCC, *M. vaccae* ATCC 15483; BBS, borate-buffered saline; CSF, cerebrospinal fluid; DH, dorsal hippocampus; HC, home cage

control conditions; *Il*, interleukin; IS, inescapable tail shock; NCTC, *M. vaccae* NCTC 11659; YWHAG, 14-3-3 protein gamma.

Supplementary tables

Supplementary Table 4.1 Functional enrichment annotations for genes whose protein abundance was upregulated or downregulated, respectively, in the CSF of home cage animals eight days after the final immunization with *M. vaccae* NCTC 11659*[1].

Effects of *M. vaccae* NCTC 11659 on CSF functional enrichment in home cage control animals					
Upregulated by immunization with *M. vaccae* NCTC 11659					
Pathway	**Genes involved**	**Percent**	**Fold enrichment**	***P*-value**	**Benjamini-Hochberg corrected**
none listed	na	na	na	na	na
Gene ontology, biological process					
positive regulation of lipoprotein lipase activity	*Apoa1, Apoc2*	40	701.4	0.0023	0.19
positive regulation of triglyceride catabolic process	*Apoa1, Apoc2*	40	701.4	0.0023	0.19
positive regulation of fatty acid biosynthetic process	*Apoa1, Apoc2*	40	584.5	0.0027	0.12
phospholipid efflux	*Apoa1, Apoc2*	40	501.1	0.0032	0.091
triglyceride homeostasis	*Apoa1, Apoc2*	40	269.8	0.0059	0.13
cholesterol efflux	*Apoa1, Apoc2*	40	259.8	0.0061	0.11
negative regulation of endopeptidase activity	*A1m, C4a*	40	47.4	0.033	0.4
Gene ontology, cellular component					
extracellular space	*Apoa1, Apoc2, A1m, C4a*	80	11.3	0.0014	0.057
spherical high-density (HDL) lipoprotein particle	*Apoa1, Apoc2*	40	1058.3	0.0015	0.032
chylomicron	*Apoa1, Apoc2*	40	673.5	0.0024	0.033
very-low-density (VLDL) lipoprotein particle	*Apoa1, Apoc2*	40	435.8	0.0037	0.039
extracellular vesicle	*Apoa1, Vcl*	40	148.2	0.011	0.089

Gene ontology, molecular function					
lipase inhibitor activity	*Apoa1, Apoc2*	40	1110	0.0014	0.051
lipid binding	*Apoa1, Apoc2*	40	53.7	0.029	0.42
Downregulated by immunization with *M. vaccae* NCTC 11659					
Pathway	**Genes involved**	**Percent**	**Fold enrichment**	***P*-value**	**Benjamini-Hochberg corrected**
none listed	na	na	na	na	na
Gene ontology, biological process					
none listed	na	na	na	na	na
Gene ontology, cellular component					
extracellular space	*Serpina3c, Vnn3*	100	14.1	0.071	0.071
Gene ontology, molecular function					
none listed	na	na	na	na	na

*There were no enriched pathways nor gene ontology annotations in the CSF proteome eight days after the final immunization with *M. vaccae* ATCC 15483 in home cage animals.
[1]Functional enrichment annotations provided by DAVID bioinformatics resource.
[2]Abbreviations: *A1m*, alpha-1-macroglobulin (alpha-1-M); *Apoa1*, apolipoprotein A-I (ApoA-I); *Apoc2*, apolipoprotein C-II (ApoC-II); *C4a*, complement C4a (C4a); *Serpina3c*, serine proteinase inhibitor, clade A, member 3C (Serpin A3C); *Vcl*, vinculin; *Vnn3*, vascular non-inflammatory molecule 3 (vanin-3).

Supplementary Table 4.2 Functional enrichment annotations for genes whose protein abundance was upregulated or downregulated, respectively, in the CSF of BBS-treated animals 24 hours after IS[1].

CSF functional enrichment					
Upregulated by stress in BBS-treated animals					
Pathway	**Genes involved**	**Percent**	**Fold enrichment**	***P*-value**	**Benjamini-Hochberg corrected**
African trypanosomiasis	*Hbb-b1, Hbb-b2*	13.3	51	0.034	0.50
malaria	*Hbb-b1, Hbb-b2*	13.3	32.8	0.052	0.50
Gene ontology, biological process					

acute-phase response	*Kng1*, *Kng2*, *Orm1*, *Saa4*	26.7	131.8	2.6E-06	0.00035
oxygen transport	*Hbb-b1*, *Hbb-b2*, *Hbe1*	20	208.7	7.7E-05	0.0051
negative regulation of endopeptidase activity	*Kng1*, *Kng2*, *Serpina3n*	20	25.4	0.0052	0.23
negative regulation of blood coagulation	*Kng1*, *Kng2*	13.3	208.7	0.0089	0.23
nucleoside trisphosphate biosynthetic process	*Ak1*, *Nme1/2*	13.3	208.7	0.0089	0.23
nucleoside diphosphate phosphorylation	*Ak1*, *Nme1/2*	13.3	139.2	0.013	0.29
vasodilation	*Kng1*, *Kng2*	13.3	100.2	0.018	0.34
cellular response to glucocorticoid stimulus	*Orm1*, *Serpina3n*	13.3	69.6	0.026	0.43
negative regulation of cell adhesion	*Kng1*, *Kng2*	13.3	61.1	0.03	0.44
response to drug	*Ak1*, *Apoc2*, *Orm1*	20	7.1	0.057	0.74
Gene ontology, cellular component					
blood microparticle	*Hbb-b2*, *Hbe1*, *Kng1*, *Kng2*, *Orm1*	33.3	52.3	1.5E-06	0.000073
hemoglobin complex	*Hbb-b1*, *Hbb-b2*, *Hbe1*	20	246.9	5.5E-05	0.0014
extracellular exosome	*Ak1*, *Apoc2*, *Kng1*, *Kng2*, *Nme1/2*, *Orm1*, *Ywhag*	46.7	3.3	0.0091	0.15
extracellular space	*Apoc2*, *Kng1*, *Kng2*, *Orm1*, *Serpina3n*	33.3	4.7	0.014	0.17
cell	*Kng1*, *Kng2*	13.3	20.8	0.086	0.85
Gene ontology, molecular function					
oxygen transporter activity	*Hbb-b1*, *Hbb-b2*, *Hbe1*	20	213.5	7.2E-05	0.0031
oxygen binding	*Hbb-b1*, *Hbb-b2*, *Hbe1*	20	128.1	0.0002	0.0044

heme binding	*Hbb-b1*, *Hbb-b2*, *Hbe1*	20	23.1	0.0061	0.088
iron ion binding	*Hbb-b1*, *Hbb-b2*, *Hbe1*	20	19	0.0089	0.096
nucleoside diphosphate kinase activity	*Ak1*, *Nme1/2*	13.3	134.8	0.014	0.12
cysteine-type endopeptidase inhibitor activity	*Kng1*, *Kng2*	13.3	59.6	0.031	0.22
drug binding	*Nme1/2*, *Orm1*	13.3	22.7	0.078	0.48
Downregulated by stress in BBS-treated animals					
Pathway	**Genes involved**	**Percent**	**Fold enrichment**	***P*-value**	**Benjamini-Hochberg corrected**
none listed	na	na	na	na	na
Gene ontology, biological process					
cell adhesion	*Ncam1*, *Ntm*	25	19.2	0.086	1
Gene ontology, cellular component					
extracellular space	*Alb*, *Chga*, *Ntm*, *Ogn*, *Pla2g7*	62.5	8.8	0.00075	0.024
extracellular exosome	*Alb*, *Ncam1*, *Ogn*, *Pik3ip1*	50	3.5	0.065	0.67
myelin sheath	*Alb*, *Ncam1*	25	24.2	0.07	0.55
Gene ontology, molecular function					
heparin binding	*Ncam1*, *Ogn*	25	38	0.043	0.6

[1]Functional enrichment annotations provided by DAVID bioinformatics resource.
[2]Abbreviations: *Ak1*, adenylate kinase isoenzyme 1 (AK1); *Alb*, albumin; *Apoc2*, apolipoprotein C-II (ApoC-II); *Chga*, chromogranin A (CgA); *Hbb-b1*, hemoglobin subunit beta 1 (HBB-1); *Hbb-b2*, hemoglobin subunit beta 2 (HBB-2); *Hbe1*, hemoglobin subunit epsilon 1 (HBE-1); *Kng1*, T-kininogen 1 (also mapped as *Kngl1l* by DAVID); *Kng2*, T-kininogen 2 (also mapped as kininogen-1 by UniProt and *Map1* gene by DAVID); *Ncam1*, neural cell adhesion molecule 1 (NCAM1); *Nme1/2*, NME/NM23 nucleoside diphosphate kinase 1 gene, encoding NDK A/B, nucleoside; *Ntm*, neurotrimin (Ntm); *Ogn*, osteoglycin (Ogn); *Orm1*, alpha-1-acid glycoprotein (AGP); *Pik3ip1*, phosphoinositide-3-kinase-interacting protein 1 (PIK3IP1); *Pla2g7*, platelet-activating factor acetylhydrolase (PAF-AH); *Saa4*, serum amyloid A protein (SAA4); *Serpina3n*, serine protease inhibitor A3N (Serpin A3N); *Ywhag*, 14-3-3 protein gamma (YWHAG).

Supplementary Table 4.3 Functional enrichment annotations for genes whose protein abundance in the cerebrospinal fluid was differentially altered between animals immunized with *M. vaccae* NCTC 11659 and BBS-treated animals, 24 hours after IS[1].

Effects of *M. vaccae* NCTC 11659 on CSF functional enrichment in animals exposed to IS					
Stress-induced increase prevented by immunization with *M. vaccae* NCTC 11659					
Pathway	**Genes involved**	**Percent**	**Fold enrichment**	***P*-value**	**Benjamini-Hochberg corrected**
African trypanosomiasis	*Hbb-b1*, *Hbb-b2*	20	68	0.024	0.23
malaria	*Hbb-b1*, *Hbb-b2*	20	43.8	0.038	0.23
Gene ontology, biological process					
oxygen transport	*Hbb-b1*, *Hbb-b2*, *Hbe1*	30	324.7	2.8E-05	0.0024
nucleoside triphosphate biosynthetic process	*Ak1*, *Nme1/2*	20	324.7	0.0055	0.23
nucleoside diphosphate phosphorylation	*Ak1*, *Nme1/2*	20	216.5	0.0082	0.23
acute-phase response	*Kng1*, *Saa4*	20	102.5	0.017	0.37
Gene ontology, cellular component					
hemoglobin complex	*Hbb-b1*, *Hbb-b2*, *Hbe1*	30	370.4	2.2E-05	0.00075
blood microparticle	*Hbb-b2*, *Hbe1*, *Kng1*	30	47.1	0.0014	0.024
extracellular exosome	*Apoc2*, *Ak1*, *Kng1*, *Nme1/2*, *Ywhag*	50	3.5	0.029	0.33
myelin sheath	*Nme1/2*, *Ywhag*	20	19.4	0.089	0.76
Gene ontology, molecular function					
oxygen transporter activity	*Hbb-b1*, *Hbb-b2*, *Hbe1*	30	0.000023	346.9	0.00081
oxygen binding	*Hbb-b1*, *Hbb-b2*, *Hbe1*	30	0.000066	208.1	0.0011
heme binding	*Hbb-b1*, *Hbb-b2*, *Hbe1*	30	0.0020	37.6	0.023

iron ion binding	*Hbb-b1*, *Hbb-b2*, *Hbe1*	30	0.0030	30.9	0.026
nucleoside diphosphate kinase activity	*Ak1*, *Nme1/2*	20	0.0080	219.1	0.056
Stress-induced increase promoted by immunization with *M. vaccae* NCTC 11659					
Pathway	**Genes involved**	**Percent**	**Fold enrichment**	***P*-value**	**Benjamini-Hochberg corrected**
none listed	na	na	na	na	na
Gene ontology, biological process					
negative regulation of endopeptidase activity	*A2m*, *Serpina3c*	50	59.2	0.025	0.95
Gene ontology, cellular component					
none listed	na	na	na	na	na
Gene ontology, molecular function					
serine-type endopeptidase inhibitor activity	*A2m*, *Serpina3c*	50	79.3	0.19	0.38
Stress-induced decrease prevented by immunization with *M. vaccae* NCTC 11659					
Pathway	**Genes involved**	**Percent**	**Fold enrichment**	***P*-value**	**Benjamini-Hochberg corrected**
none listed	na	na	na	na	na
Gene ontology, biological process					
none listed	na	na	na	na	na
Gene ontology, cellular component					
extracellular space	*Alb*, *Chga*, *Ntm*, *Ogn*, *Pla2g7*	71.4	10.1	0.00034	0.0095
Gene ontology, molecular function					
none listed	na	na	na	na	na
Stress-induced decrease promoted by immunization with *M. vaccae* NCTC 11659					
Pathway	**Genes involved**	**Percent**	**Fold enrichment**	***P*-value**	**Benjamini-Hochberg corrected**
none listed	na	na	na	na	na
Gene ontology, biological process					
none listed	na	na	na	na	na

Gene ontology, cellular component					
extracellular space	*Ahsg, LOC259246, RGD1310507*	100	14.1	0.005	0.045
extracellular region	*LOC259246, RGD1310507*	66.7	17.3	0.076	0.34
Gene ontology, molecular function					
none listed	na	na	na	na	na

[1]Functional enrichment annotations provided by DAVID bioinformatics resource.
[2]Abbreviations: *Ahsg*, alpha-2-HC-glycoprotein (also known as 59 kDa bone sialic acid-containing protein; BSP); *Alb*, albumin; *A2m*, alpha-2-macroglobulin (alpha-2-M); *Chga*, chromogranin-A (CgA); *Cryab*, alpha-crystallin B chain (Cryab); *Hbb-b1*, hemoglobin subunit beta 1 (HBB-1); *Hbb-b2*, hemoglobin subunit beta 2 (HBB-2); *Hbe1*, hemoglobin subunit epsilon 1 (HBE-1); *Kng1*, T-kininogen 1 (also mapped as *Kngl1l* by DAVID); *LOC259246*, major urinary protein (also known as alpha-2u globulin PGCL1; MUP) *Ntm*, neurotrimin (Ntm); *Ogn*, osteoglycin (Ogn); *Pla2g7*, platelet-activating factor acetylhydrolase (PAF-AH); *RGD1310507*, uncharacterized protein A0A0G2K896 (similar to RIKEN cDNA); *Saa4*, serum amyloid A protein (SAA4); *Serpina3c*, serine proteinase inhibitor, clade A, member 3C (Serpin A3C).

Supplementary Table 4.4 Functional enrichment annotations for genes whose protein abundance in the cerebrospinal fluid was differentially altered between animals immunized with *M. vaccae* ATCC 15483 and BBS-treated animals, 24 hours after IS[1].

Effects of *M. vaccae* ATCC 15483 on CSF functional enrichment in animals exposed to IS					
Stress-induced increase prevented by immunization with *M. vaccae* ATCC 15483					
Pathway	**Genes involved**	**Percent**	**Fold enrichment**	***P*-value**	**Benjamini-Hochberg corrected**
African trypanosomiasis	*Hbb-b1, Hbb-b2*	22.2	68	0.024	0.23
Malaria	*Hbb-b1, Hbb-b2*	22.2	43.8	0.038	0.23
Gene ontology, biological process					
acute-phase response	*Kng1, Kng2, Saa4*	33.3	153.8	0.00013	0.01
nucleoside triphosphate biosynthetic process	*Ak1, Nme1/2*	22.2	324.7	0.0055	0.13
negative regulation of blood coagulation	*Kng1, Kng2*	22.2	324.7	0.0055	0.13
oxygen transport	*Hbb-b1, Hbb-b2*	22.2	216.5	0.0082	0.13

nucleoside diphosphate phosphorylation	*Ak1*, *Nme1/2*	22.2	216.5	0.0082	0.13
vasodilation	*Kng1*, *Kng2*	22.2	155.9	0.011	0.16
negative regulation of cell adhesion	*Kng1*, *Kng2*	22.2	95	0.019	0.22
negative regulation of endopeptidase activity	*Kng1*, *Kng2*	22.2	26.3	0.066	0.63
positive regulation of cytosolic calcium ion concentration	*Kng1*, *Kng2*	22.2	25	0.069	0.63
Gene ontology, cellular component					
blood microparticle	*Hbb-b2*, *Kng1*, *Kng2*	33.3	52.3	0.0011	0.036
extracellular exosome	*Apoc2*, *Kng1*, *Kng2*, *Ywhag*	66.7	4.7	0.0023	0.038
hemoglobin complex	*Hbb-b1*, *Hbb-b2*	22.2	274.4	0.0065	0.071
cell	*Kng1*, *Kng2*	22.2	34.6	0.05	0.41
myelin sheath	*Nme1/2*, *Ywhag*	22.2	21.5	0.08	0.53
Gene ontology, molecular function					
oxygen transporter activity	*Hbb-b1*, *Hbb-b2*	22.2	231.2	0.0075	0.14
nucleoside diphosphate kinase activity	*Ak1*, *Nme1/2*	22.2	219.1	0.008	0.14
oxygen binding	*Hbb-b1*, *Hbb-b2*	22.2	138.8	0.013	0.14
cysteine-type endopeptidase inhibitor activity	*Kng1*, *Kng2*	22.2	96.8	0.018	0.15
heme binding	*Hbb-b1*, *Hbb-b2*	22.2	25.1	0.068	0.46
iron ion binding	*Hbb-b1*, *Hbb-b2*	22.2	20.6	0.082	0.46
Stress-induced increase promoted by immunization with *M. vaccae* ATCC 15483					
Pathway	**Genes involved**	**Percent**	**Fold enrichment**	***P*-value**	**Benjamini-Hochberg corrected**
cell adhesion molecules	*Cd99*, *Cntn2*	100	45.1	0.022	0.044
Gene ontology, biological process					
none listed	na	na	na	na	na
Gene ontology, cellular component					
none listed	na	na	na	na	na

Gene ontology, molecular function					
none listed	na	na	na	na	na
Stress-induced decrease prevented by immunization with *M. vaccae* ATCC 15483					
Pathway	**Genes involved**	**Percent**	**Fold enrichment**	***P*-value**	**Benjamini-Hochberg corrected**
none listed	na	na	na	na	na
Gene ontology, biological process					
none listed	na	na	na	na	na
Gene ontology, cellular component					
extracellular space	*Alb, Chga, Ntm, Ogn, Pla2g7*	71.4	10.1	0.00034	0.0095
Gene ontology, molecular function					
none listed	na	na	na	na	na
Stress-induced decrease promoted by immunization with *M. vaccae* ATCC 15483					
Pathway	**Genes involved**	**Percent**	**Fold enrichment**	***P*-value**	**Benjamini-Hochberg corrected**
none listed	na	na	na	na	na
Gene ontology, biological process					
negative regulation of ERK1 and ERK2 cascade	*Fbln1, Igf1*	40	107.9	0.015	0.89
positive regulation of fibroblast proliferation	*Fbln1, Igf1*	40	100.2	0.016	0.69
epithelial cell differentiation	*Aldoc, Ces1c*	40	89.9	0.018	0.58
response to hypoxia	*Aldoc, Igf1*	40	26	0.06	0.9
response to organic cyclic compound	*Aldoc, Igf1*	40	25.8	0.061	0.84
aging	*Aldoc, Igf1*	40	22.3	0.07	0.83
Gene ontology, cellular component					
Extracellular space	*Cesc1, Fbln1, Igf1*	60	8.4	0.027	0.46
axon	*Aldoc, Pvalb*	40	20.5	0.076	0.58
Gene ontology, molecular function					
integrin binding	*Fbln1, Igf1*	40	66.6	0.024	0.41

[1]Functional enrichment annotations provided by DAVID bioinformatics resource.

[2]Abbreviations: *Alb*, albumin; *Aldoc*, fructose-bisphosphate aldolase C (AldoC); *Apoc2*, apolipoprotein C-II (ApoC-II); *Cd*, cluster of differentiation; *Ces1c*, carboxylesterase 1C (Ces1C); *Chga*, chromogranin-A (CgA); *Cntn2*, contactin-2 (CNTN2); *Cryab*, alpha-crystallin B chain (Cryab); *Fbln1*, fibulin-1 (FIBL-1); *Hbb-b1*, hemoglobin subunit beta 1 (HBB-1); *Hbb-b2*, hemoglobin subunit beta 2 (HBB-2); *Hbe1*, hemoglobin subunit epsilon 1 (HBE-1); *Igf1*, insulin-like growth factor I (IGF-I); *Kng1*, T-kininogen 1 (also mapped as *Kngl1l* by DAVID); *Kng2*, T-kininogen 2 (also mapped as kininogen-1 by UniProt and *Map1* gene by DAVID); *Ntm*, neurotrimin (Ntm); *Ogn*, osteoglycin (Ogn); *Pla2g7*, platelet-activating factor acetylhydrolase (PAF-AH); *Pvalb*, parvalbumin alpha (Pvalb); *Saa4*, serum amyloid A protein (SAA4); *Ywhag*, 14-3-3 protein gamma (YWHAG).

Supplementary Table 4.5 Proteins in the CSF that correlated with *Il6* mRNA in the dorsal hippocampus, ordered by *p*-value*.

Protein name	Pearson's *r*	FDR-adjusted *p*-value
sulfhydryl oxidase 1 (rQSOX)	0.588	0.0044
ATP-binding cassette sub-family B member 9 (ABCB9)	0.591	0.0062
insulin-like growth factor-binding protein 5 (IGFBP-5)	0.643	0.0062
neuronal pentraxin receptor (NPTXR)	0.555	0.0062
Ig gamma-2C chain C region (IgG-2c)	-0.532	0.010
glutathione peroxidase 1 (GPx1)	-0.610	0.027
aspartate aminotransferase (AST)	0.493	0.035
augurin	0.505	0.041
elongation factor 1-alpha 1 (EF-1-alpha-1)	-0.578	0.041
YIP1 family member 3 (YIPF3)	0.455	0.052
beta-1,3-N-acetylglucosaminyltransferase lunatic fringe (LFNG)	0.506	0.067
neural cell adhesion molecule 2 (NCAM2)	0.461	0.076

V-set and transmembrane domain containing 2B (VSTM2B)	0.546	0.076
pro-melanin-concentrating hormone (pro-MCH)	0.456	0.079
fibulin-5	0.517	0.081
G-protein coupled receptor 158 (GPCR158)	0.412	0.081
myeloid-derived growth factor (MYDGF)	-0.422	0.081
neurotrimin (Ntm)	0.513	0.081
uncharacterized protein with UniProt ID A0A0G2JXF0	-0.415	0.081
carboxypeptidase C (CPE)	0.404	0.089

* Sample sizes: *Il6* (BBS/HC, *n* = 7; BBS/IS, *n* = 8; NCTC/HC, *n* = 7; NCTC/IS, *n* = 8; ATCC/HC, *n* = 8; ATCC/IS, *n* = 8); rQSOX (BBS/HC, *n* = 7; BBS/IS, *n* = 7; NCTC/HC, *n* = 8; NCTC/IS, *n* = 7; ATCC/HC, *n* = 8; ATCC/IS, *n* = 8); ABCB9 (BBS/HC, *n* = 6; BBS/IS, *n* = 6; NCTC/HC, *n* = 7; NCTC/IS, *n* = 6; ATCC/HC, *n* = 7; ATCC/IS, *n* = 7); IGFBP-5 (BBS/HC, *n* = 5; BBS/IS, *n* = 5; NCTC/HC, *n* = 6; NCTC/IS, *n* = 5; ATCC/HC, *n* = 6; ATCC/IS, *n* = 6); NPTXR (BBS/HC, *n* = 7; BBS/IS, *n* = 7; NCTC/HC, *n* = 8; NCTC/IS, *n* = 7; ATCC/HC, *n* = 8; ATCC/IS, *n* = 8); IgG-2c (BBS/HC, *n* = 7; BBS/IS, *n* = 7; NCTC/HC, *n* = 8; NCTC/IS, *n* = 7; ATCC/HC, *n* = 8; ATCC/IS, *n* = 8); GPx1 (BBS/HC, *n* = 4; BBS/IS, *n* = 4; NCTC/HC, *n* = 5; NCTC/IS, *n* = 5; ATCC/HC, *n* = 5; ATCC/IS, *n* = 5); AST (BBS/HC, *n* = 7; BBS/IS, *n* = 6; NCTC/HC, *n* = 7; NCTC/IS, *n* = 7; ATCC/HC, *n* = 8; ATCC/IS, *n* = 8); augurin (BBS/HC, *n* = 6; BBS/IS, *n* = 6; NCTC/HC, *n* = 7; NCTC/IS, *n* = 6; ATCC/HC, *n* = 7; ATCC/IS, *n* = 7); EF-1-alpha-1 (BBS/HC, *n* = 5; BBS/IS, *n* = 5; NCTC/HC, *n* = 5; NCTC/IS, *n* = 4; ATCC/HC, *n* = 5; ATCC/IS, *n* = 5); YIPF3 (BBS/HC, *n* = 7; BBS/IS, *n* = 7; NCTC/HC, *n* = 8; NCTC/IS, *n* = 7; ATCC/HC, *n* = 8; ATCC/IS, *n* = 8); LFNG (BBS/HC, *n* = 5; BBS/IS, *n* = 6; NCTC/HC, *n* = 6; NCTC/IS, *n* = 5; ATCC/HC, *n* = 6; ATCC/IS, *n* = 6); NCAM2 (BBS/HC, *n* = 6; BBS/IS, *n* = 6; NCTC/HC, *n* = 7; NCTC/IS, *n* = 6; ATCC/HC, *n* = 7; ATCC/IS, *n* = 7); VSTM2B (BBS/HC, *n* = 5; BBS/IS, *n* = 4; NCTC/HC, *n* = 4; NCTC/IS, *n* = 5; ATCC/HC, *n* = 5; ATCC/IS, *n* = 4); pro-MCH (BBS/HC, *n* = 6; BBS/IS, *n* = 6; NCTC/HC, *n* = 7; NCTC/IS, *n* = 6; ATCC/HC, *n* = 7; ATCC/IS, *n* = 7); fibulin-5 (BBS/HC, *n* = 4; BBS/IS, *n* = 5; NCTC/HC, *n* = 5; NCTC/IS, *n* = 5; ATCC/HC, *n* = 5; ATCC/IS, *n* = 5); GPCR158 (BBS/HC, *n* = 7; BBS/IS, *n* = 7; NCTC/HC, *n* = 8; NCTC/IS, *n* = 7; ATCC/HC, *n* = 8; ATCC/IS, *n* = 8); MYDGF (BBS/HC, *n* = 7; BBS/IS, *n* = 7; NCTC/HC, *n* = 8; NCTC/IS, *n* = 6; ATCC/HC, *n* = 8; ATCC/IS, *n* = 8); Ntm (BBS/HC, *n* = 4; BBS/IS, *n* = 4; NCTC/HC, *n* = 5; NCTC/IS, *n* = 5; ATCC/HC, *n* = 5; ATCC/IS, *n* = 5); uncharacterized protein with UniProt ID A0A0G2JXF0 (BBS/HC, *n* = 7; BBS/IS, *n* = 7; NCTC/HC, *n* = 8; NCTC/IS, *n* = 7; ATCC/HC, *n* = 8; ATCC/IS, *n* = 8); CPE (BBS/HC, *n* = 7; BBS/IS, *n* = 7; NCTC/HC, *n* = 8; NCTC/IS, *n* = 7; ATCC/HC, *n* = 8; ATCC/IS, *n* = 8).

Appendix 4. Chapter 5 supplementary material

Supplementary figures

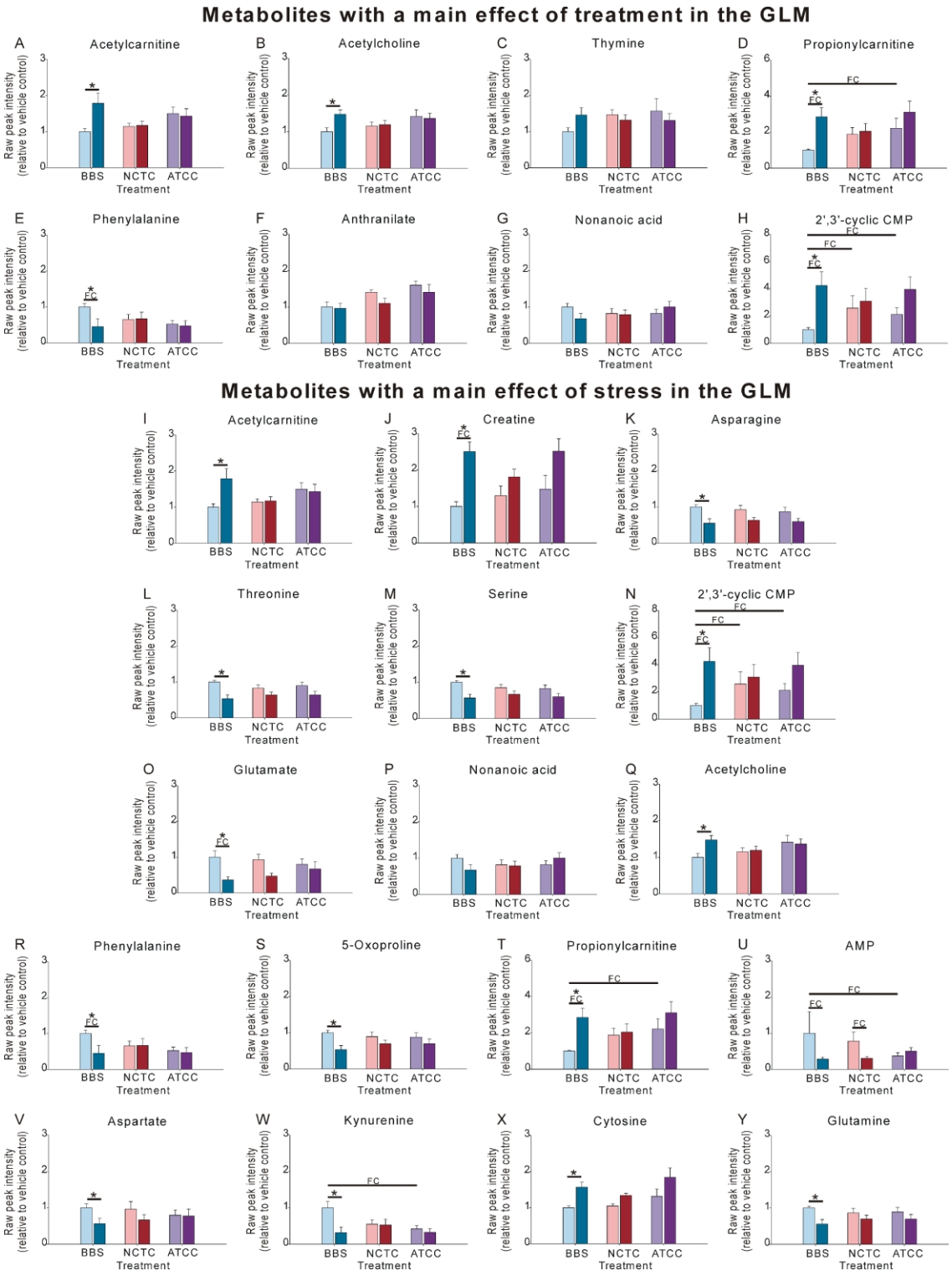

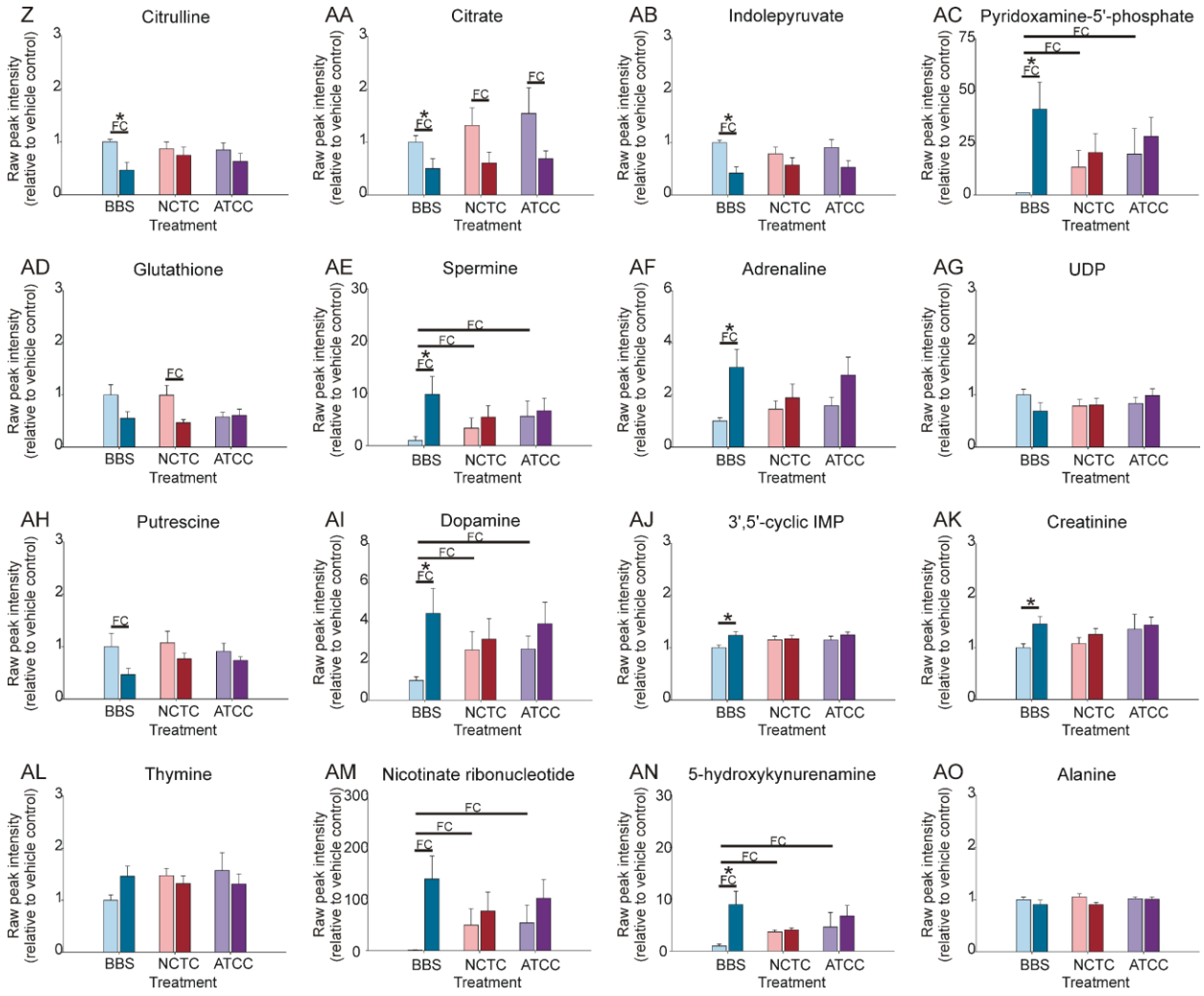

Metabolites with an interaction effect of treatment x stress in the GLM

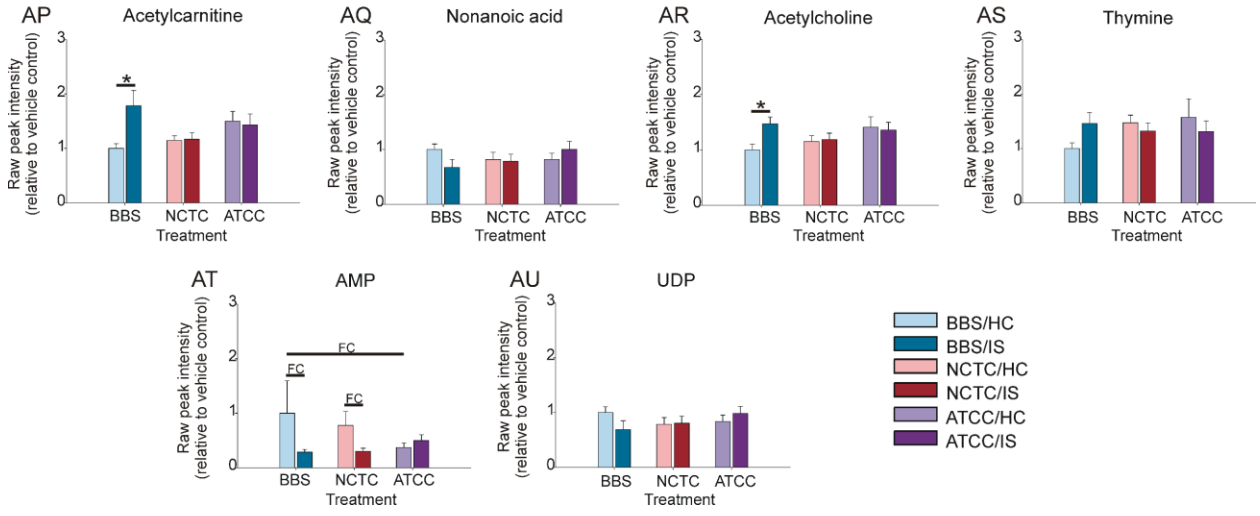

Supplementary Figure 5.1 Plasma metabolites whose abundances were altered by a main effect of treatment, a main effect of stress, or an interaction effect of treatment x stress in the generalized linear model (GLM), ordered within each subheading by *p*-value.

There was a main effect of treatment on (A) acetylcarnitine (acyl-C2), (B) acetylcholine, (C) thymine, (D) propionylcarnitine (acyl-C3), (E) phenylalanine, (F) anthranilate (G) nonanoic acid (pelargonate), and (H) 2',3'-cyclic CMP; there was a main effect of stress on (I) acetylcarnitine (acyl-C2), (J) creatine, (K) asparagine, (L) threonine, (M) serine, (N) 2',3'-cyclic CMP, (O) glutamate, (P) nonanoic acid (pelargonate), (Q) acetylcholine, (R) phenylalanine, (S) 5-oxoproline, (T) propionylcarnitine (acyl-C3) (U) AMP, (V) aspartate, (W) kynurenine, (X) cytosine, (Y) glutamine, (Z) citrulline, (AA) citrate, (AB) indolepyruvate, (AC) pyridoxamine-5'-phosphate, (AD) glutathione, (AE) spermine, (AF) adrenaline, (AG) UDP, (AH) putrescine, (AI) dopamine, (AJ) 3',5'-cyclic IMP, (AK) creatinine, (AL) thymine, (AM) nicotinate ribonucleotide, (AN) 5-hydroxykynurenamine, and (AO) alanine; and there was an interaction effect of treatment x stress on (AP) acetylcarnitine (acyl-C2), (AQ) nonanoic acid (pelargonate), (AR) acetylcholine, (AS) thymine, (AT) AMP, and (AU) UDP. Bars represent the mean + standard error of the mean (SEM) of raw peak intensities of metabolites relative to vehicle control (BBS/HC). Sample sizes: BBS/HC, $n = 8$; BBS/IS, $n = 6$; NCTC/HC, $n = 8$; NCTC/IS, $n = 8$; ATCC/HC, $n = 7$; ATCC/IS, $n = 8$. FC, fold change difference. *FDR-adjusted $p < 0.1$. Abbreviations: AMP, adenosine monophosphate; ATCC, *M. vaccae* ATCC 15483; BBS, borate-buffered saline; CMP, cytidine monophosphate; HC, home cage control conditions; IMP, inosine monophosphate; IS, inescapable tail shock; NCTC, *M. vaccae* NCTC 11659; UDP, uridine diphosphate.

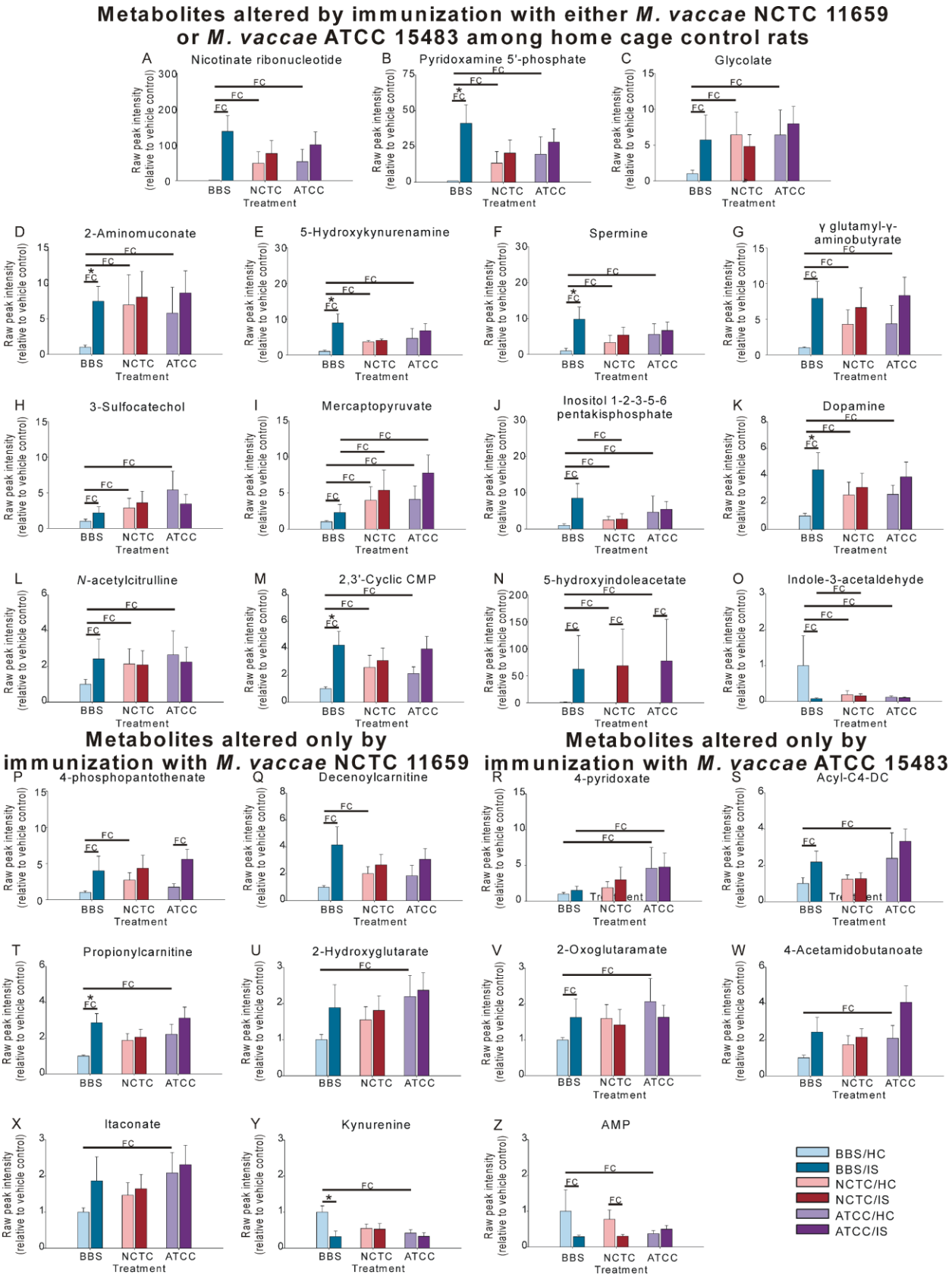
Metabolites altered by immunization with either M. vaccae NCTC 11659 or M. vaccae ATCC 15483 among home cage control rats
A Nicotinate ribonucleotide
B Pyridoxamine 5'-phosphate
C Glycolate
D 2-Aminomuconate
E 5-Hydroxykynurenamine
F Spermine
G γ glutamyl-γ-aminobutyrate
H 3-Sulfocatechol
I Mercaptopyruvate
J Inositol 1-2-3-5-6 pentakisphosphate
K Dopamine
L N-acetylcitrulline
M 2,3'-Cyclic CMP
N 5-hydroxyindoleacetate
O Indole-3-acetaldehyde
Metabolites altered only by immunization with M. vaccae NCTC 11659
P 4-phosphopantothenate
Q Decenoylcarnitine
T Propionylcarnitine
U 2-Hydroxyglutarate
X Itaconate
Y Kynurenine
Metabolites altered only by immunization with M. vaccae ATCC 15483
R 4-pyridoxate
S Acyl-C4-DC
V 2-Oxoglutaramate
W 4-Acetamidobutanoate
Z AMP
Raw peak intensity (relative to vehicle control)
Treatment
BBS
NCTC
ATCC
FC
BBS/HC
BBS/IS
NCTC/HC
NCTC/IS
ATCC/HC
ATCC/IS

Supplementary Figure 5.2 Plasma metabolites whose abundances were altered by immunization with either *M. vaccae* NCTC 11659 (NCTC) or *M. vaccae* ATCC 15483 (ATCC) among home cage control rats, ordered within each subheading by fold change (averaged across the two treatment groups if altered by both *M. vaccae* strains).

Immunization with either *M. vaccae* NCTC 11659 or *M. vaccae* ATCC 15483 altered the abundance of (A) nicotinate ribonucleotide, (B) pyridoxamine 5'-phosphate, (C) glycolate, (D) 2-aminomuconate, (E) 5-hydroxykynurenamine, (F) spermine, (G) γ-glutamyl-γ-aminobutyrate, (H) 3-sulfocatechol, (I) mercaptopyruvate, (J) inositol 1-2-3-5-6-pentakisphosphate, (K) dopamine, (L) *N*-acetylcitrulline, (M) 2',3'-cyclic CMP, (N) 5-hydroxyindoleacetate, and (O) indole-3-acetaldehyde; immunization with *M. vaccae* NCTC 11659 uniquely altered (P) 4-phosphopantothenate and (Q) decenoylcarnitine (acyl-C10:1); and immunization with *M. vaccae* ATCC 15483 uniquely altered (R) 4-pyridoxate, (S) acyl-C4-DC, (T) propionylcarnitine (acyl-C3), (U) 2-hydroxyglutarate/citramalate, (V) 2-oxoglutaramate, (W) 4-acetamidobutanoate, (X) itaconate, (Y) kynurenine, and (Z) AMP. Bars represent the mean + standard error of the mean (SEM) of raw peak intensities of metabolites relative to vehicle control (BBS/HC). Sample sizes: BBS/HC, $n = 8$; BBS/IS, $n = 6$; NCTC/HC, $n = 8$; NCTC/IS, $n = 8$; ATCC/HC, $n = 7$; ATCC/IS, $n = 8$. FC, fold change difference. *FDR-adjusted $p < 0.1$. Abbreviations: acyl-C4-DC, acyl-C4-dicarboxylcarnitine; AMP, adenosine monophosphate; ATCC, *M. vaccae* ATCC 15483; BBS, borate-buffered saline; HC, home cage control conditions; IS, inescapable tail shock; NCTC, *M. vaccae* NCTC 11659.

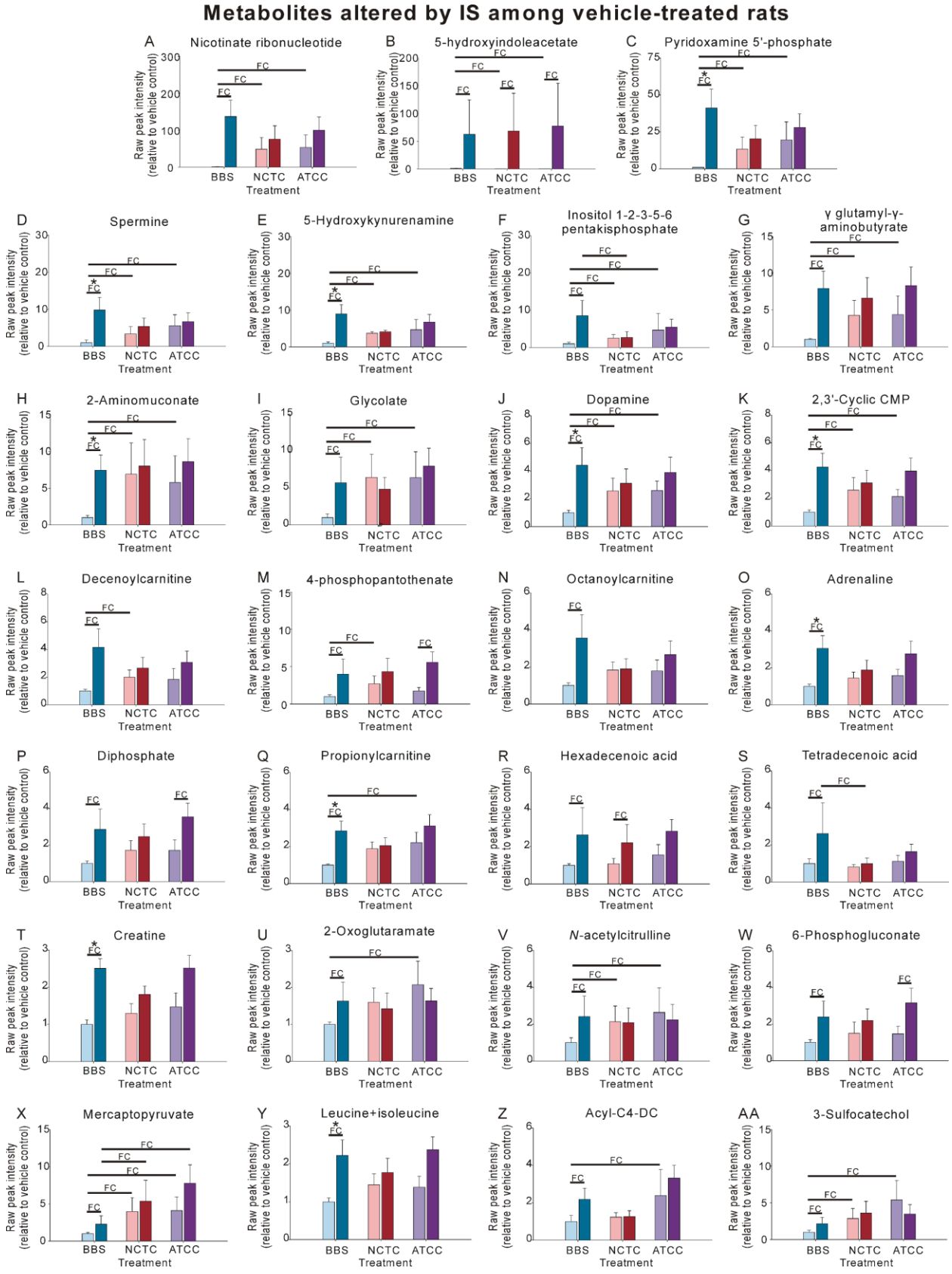
Metabolites altered by IS among vehicle-treated rats
A Nicotinate ribonucleotide
B 5-hydroxyindoleacetate
C Pyridoxamine 5'-phosphate
D Spermine
E 5-Hydroxykynurenamine
F Inositol 1-2-3-5-6 pentakisphosphate
G γ glutamyl-γ-aminobutyrate
H 2-Aminomuconate
I Glycolate
J Dopamine
K 2,3'-Cyclic CMP
L Decenoylcarnitine
M 4-phosphopantothenate
N Octanoylcarnitine
O Adrenaline
P Diphosphate
Q Propionylcarnitine
R Hexadecenoic acid
S Tetradecenoic acid
T Creatine
U 2-Oxoglutaramate
V N-acetylcitrulline
W 6-Phosphogluconate
X Mercaptopyruvate
Y Leucine+isoleucine
Z Acyl-C4-DC
AA 3-Sulfocatechol
Raw peak intensity (relative to vehicle control)
BBS
NCTC
ATCC
Treatment
FC
*

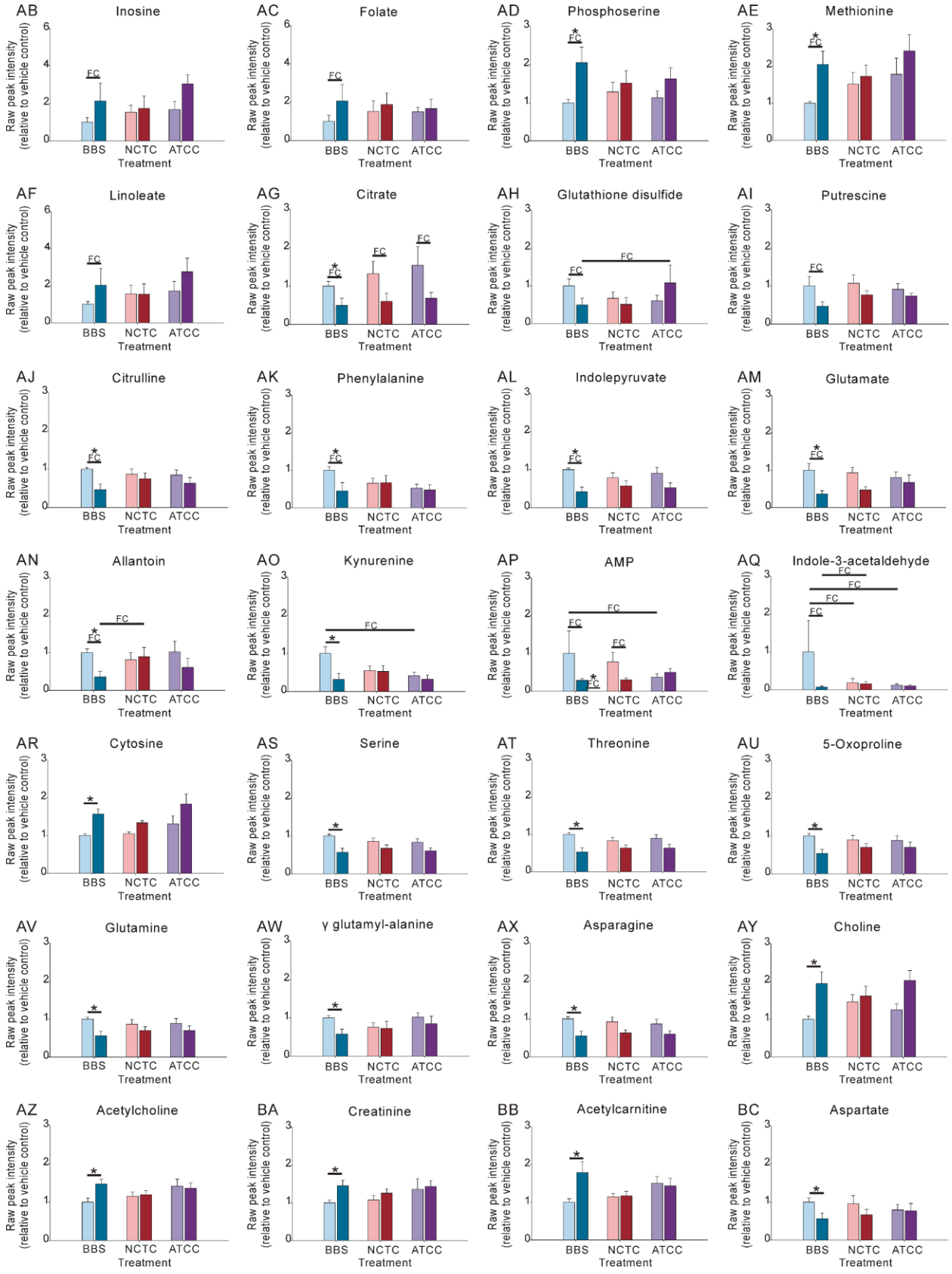
AB Inosine
AC Folate
AD Phosphoserine
AE Methionine
AF Linoleate
AG Citrate
AH Glutathione disulfide
AI Putrescine
AJ Citrulline
AK Phenylalanine
AL Indolepyruvate
AM Glutamate
AN Allantoin
AO Kynurenine
AP AMP
AQ Indole-3-acetaldehyde
AR Cytosine
AS Serine
AT Threonine
AU 5-Oxoproline
AV Glutamine
AW γ glutamyl-alanine
AX Asparagine
AY Choline
AZ Acetylcholine
BA Creatinine
BB Acetylcarnitine
BC Aspartate
Raw peak intensity (relative to vehicle control)
BBS
NCTC
ATCC
Treatment
FC
*

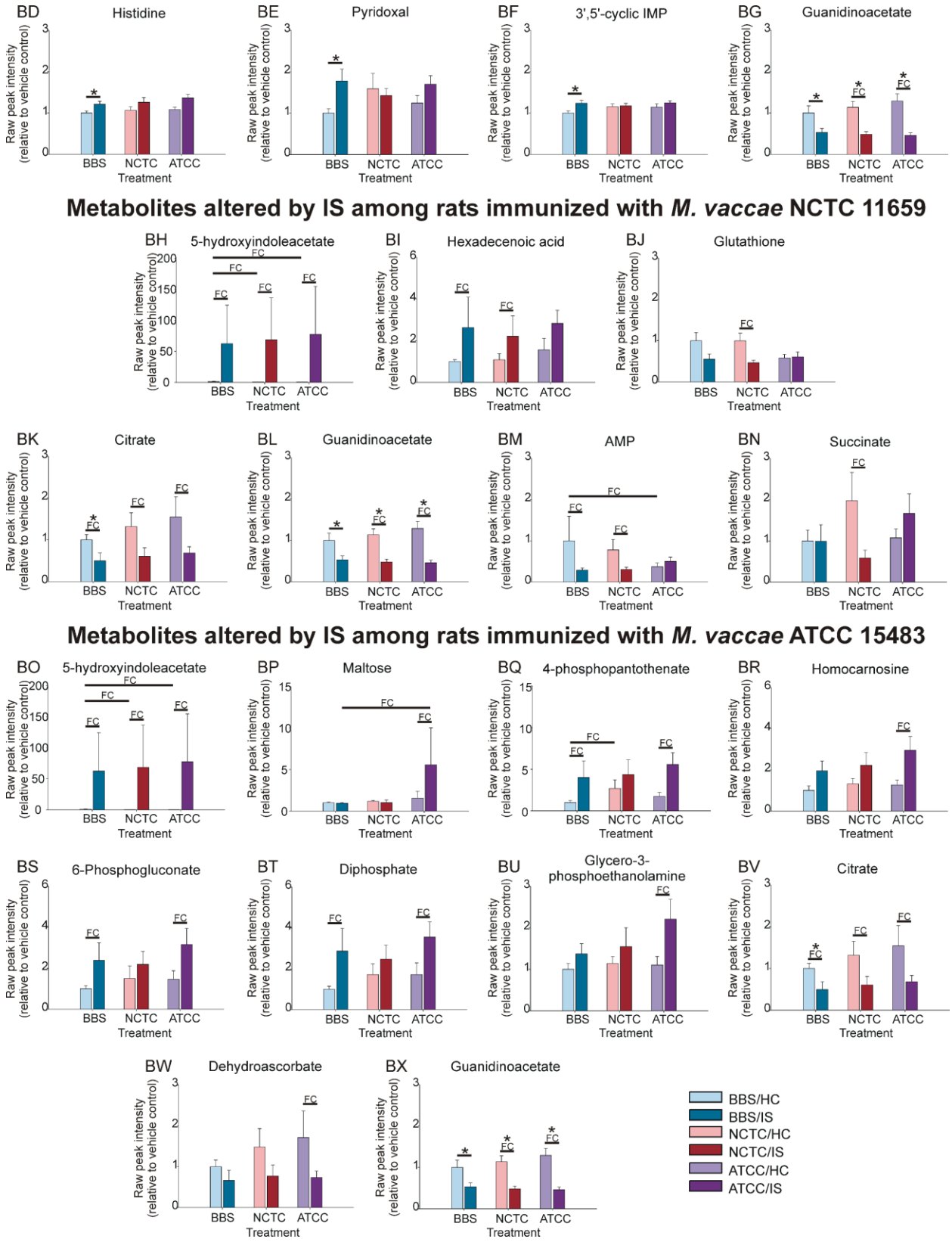
BD Histidine
BE Pyridoxal
BF 3',5'-cyclic IMP
BG Guanidinoacetate
Raw peak intensity (relative to vehicle control)
BBS NCTC ATCC
Treatment
Metabolites altered by IS among rats immunized with M. vaccae NCTC 11659
BH 5-hydroxyindoleacetate
BI Hexadecenoic acid
BJ Glutathione
BK Citrate
BL Guanidinoacetate
BM AMP
BN Succinate
Metabolites altered by IS among rats immunized with M. vaccae ATCC 15483
BO 5-hydroxyindoleacetate
BP Maltose
BQ 4-phosphopantothenate
BR Homocarnosine
BS 6-Phosphogluconate
BT Diphosphate
BU Glycero-3-phosphoethanolamine
BV Citrate
BW Dehydroascorbate
BX Guanidinoacetate
FC
*
BBS/HC
BBS/IS
NCTC/HC
NCTC/IS
ATCC/HC
ATCC/IS

Supplementary Figure 5.3 Plasma metabolites whose abundances were altered by inescapable tail shock stress (IS) among vehicle-treated rats, animals immunized with *M. vaccae* NCTC 11659, and animals immunized with *M. vaccae* ATCC 15483, ordered within each subheading by fold change first and then by *p*-value.

Among vehicle-treated rats, IS altered the abundance of (A) nicotinate ribonucleotide, (B) 5-hydroxyindoleacetate, (C) pyridoxamine 5'-phosphate, (D) spermine, (E) 5-hydroxykynurenamine, (F) inositol 1-2-3-5-6-pentakisphosphate, (G) γ-glutamyl-γ-aminobutyrate, (H) 2-aminomuconate, (I) glycolate, (J) dopamine, (K) 2',3'-cyclic CMP, (L) decenoylcarnitine (acyl-C10:1), (M) 4-phosphopantothenate, (N) octanoylcarnitine (acyl-C8), (O) adrenaline, (P) diphosphate, (Q) propionylcarnitine (acyl-C3), (R) hexadecenoic acid, (S) tetradecenoic acid, (T) creatine, (U) 2-oxoglutaramate, (V) *N*-acetylcitrulline, (W) 6-phospho-D-gluconate, (X) mercaptopyruvate, (Y) leucine and isoleucine, (Z) acyl-C4-DC, (AA) 3-sulfocatechol, (AB) inosine, (AC) folate, (AD) phosphoserine, (AE) methionine, (AF) linoleate, (AG) citrate, (AH) glutathione disulfide, (AI) putrescine, (AJ) citrulline, (AK) phenylalanine, (AL) indolepyruvate, (AM) glutamate, (AN) allantoin, (AO) kynurenine, (AP) AMP, (AQ) indole-3-acetaldehyde, (AR) cytosine, (AS) serine, (AT) threonine, (AU) 5-oxoproline, (AV) glutamine, (AW) γ-glutamyl-alanine, (AX) asparagine, (AY) choline, (AZ) acetylcholine, (BA) creatinine, (BB) acetylcarnitine (acyl-C2), (BC) aspartate, (BD) histidine, (BE) pyridoxal, (BF) 3',5'-cyclic IMP, and (BG) guanidinoacetate; among rats immunized with *M. vaccae* NCTC 11659, IS altered the abundance of (BH) 5-hydroxyindoleacetate, (BI) hexadecenoic acid, (BJ) glutathione, (BK) citrate, (BL) guanidinoacetate, (BM) AMP, and (BN) succinate; among rats immunized with *M. vaccae* ATCC 15483, IS altered the abundance of (BO) 5-hydroxyindoleacetate, (BP) maltose, (BQ) 4-phosphopanthothenate, (BR) homocarnosine, (BS) 6-phosphogluconate, (BT) diphosphate, (BU) glycero-3-phosphoethanolamine, (BV) citrate, (BW) dehydroascorbate, and (BX) guanidinoacetate. Bars represent the mean + standard error of the mean (SEM) of raw peak intensities of metabolites relative to vehicle control (BBS/HC). Sample sizes: BBS/HC, $n = 8$; BBS/IS, $n = 6$; NCTC/HC, $n = 8$; NCTC/IS, $n = 8$; ATCC/HC, $n = 7$; ATCC/IS, $n = 8$. FC, fold change difference. *FDR-adjusted $p < 0.1$. Abbreviations: acyl-C4-DC, acyl-C4-dicarboxylcarnitine; AMP, adenosine monophosphate; ATCC, *M. vaccae* ATCC 15483; BBS, borate-buffered saline; CMP, cytidine monophosphate; HC, home cage control conditions; IMP, inosine monophosphate; IS, inescapable tail shock; NCTC, *M. vaccae* NCTC 11659; UDP, uridine diphosphate.

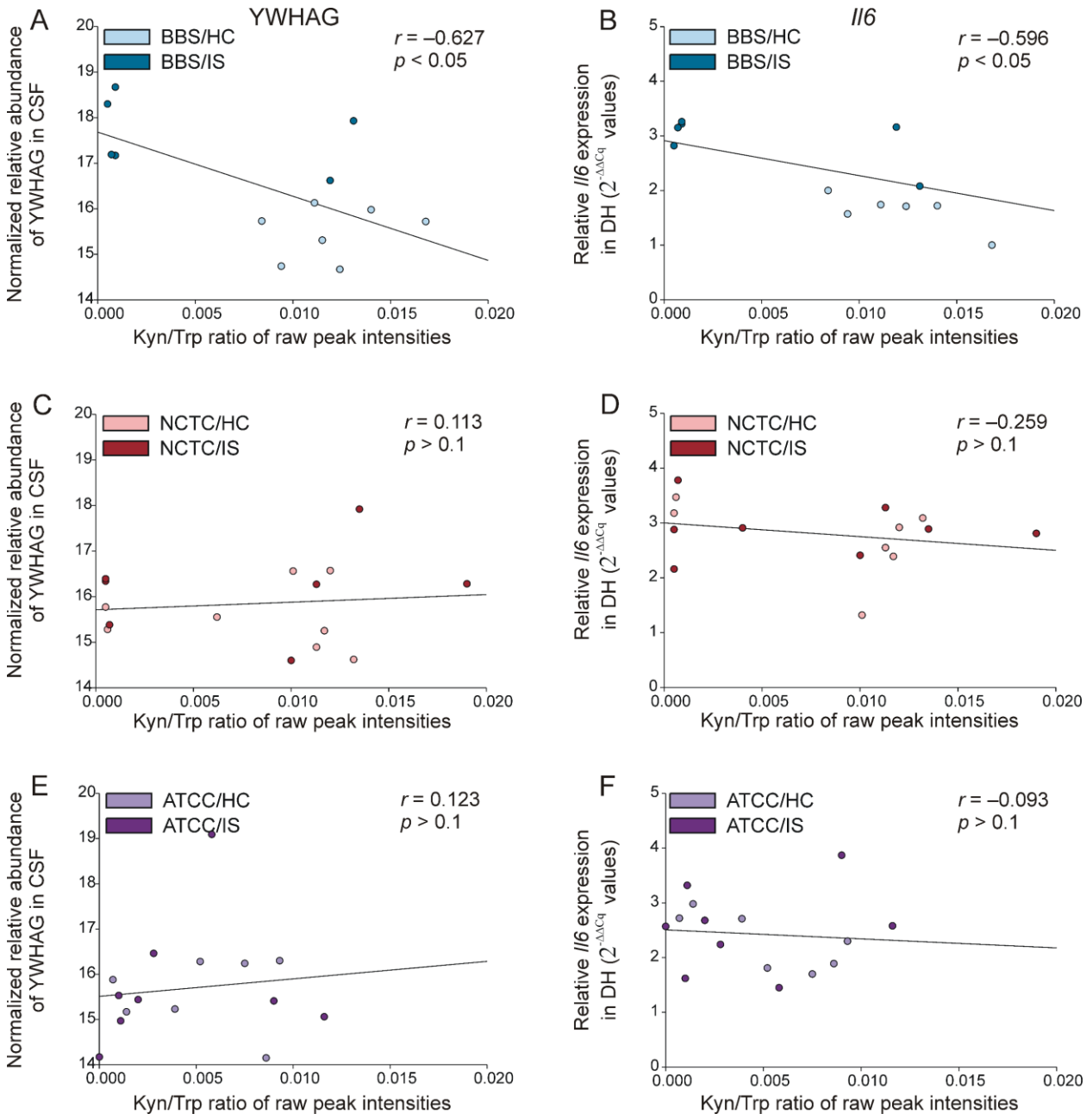

Supplementary Figure 5.4 Relative abundance of YWHAG in CSF and mRNA expression of *Il6* in the dorsal hippocampus (DH) correlated with kynurenine/tryptophan (Kyn/Trp) ratios in plasma among (A, B) BBS-treated animals, but not among animals previously immunized with (C, D) *M. vaccae* NCTC 11659 or (E, F) *M. vaccae* ATCC 15483.

Sample sizes: Kyn/Trp ratios (BBS/HC, *n* = 8; BBS/IS, *n* = 6; NCTC/HC, *n* = 8; NCTC/IS, *n* = 8; ATCC/HC, *n* = 7; ATCC/IS, *n* = 8); *Il6* (BBS/HC, *n* = 7; BBS/IS, *n* = 7; NCTC/HC, *n* = 7; NCTC/IS, *n* = 8; ATCC/HC, *n* = 8; ATCC/IS, *n* = 8); YWHAG (BBS/HC, *n* = 6; BBS/IS, *n* = 6; NCTC/HC, *n* = 8; NCTC/IS, *n* = 7; ATCC/HC, *n* = 7; ATCC/IS, *n* = 7). Expression of *Il6* mRNA was measured using quantitative real-time polymerase chain reaction (RT-qPCR), with beta-actin as a reference, and data are presented as raw 2-ΔΔCq values. Pearson's correlation

coefficient *r* and *p*-values are given. Abbreviations: ATCC, *M. vaccae* ATCC 15483; BBS, borate-buffered saline; CSF, cerebrospinal fluid; DH, dorsal hippocampus; HC, home cage control conditions; *Il*, interleukin; IS, inescapable tail shock; Kyn, kynurenine; NCTC, *M. vaccae* NCTC 11659; Trp, tryptophan; YWHAG, 14-3-3 protein gamma.

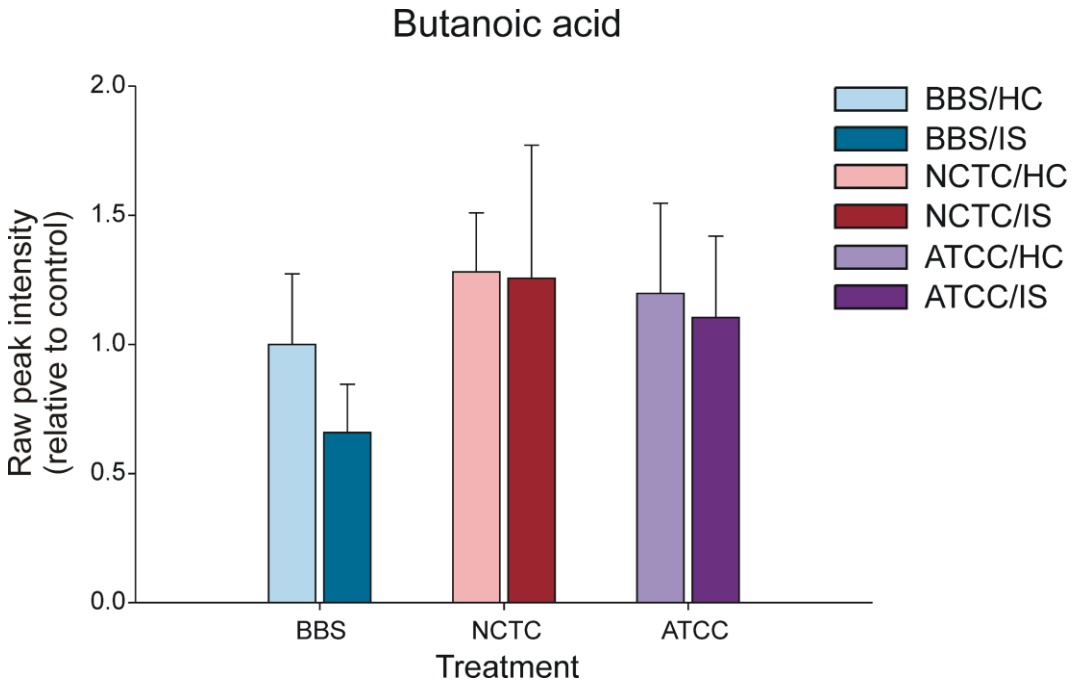

Supplementary Figure 5.5 Effects of immunization with either *M. vaccae* NCTC 11659 (NCTC) or *M. vaccae* ATCC 15483 (ATCC) and inescapable tail shock (IS) on abundances of butanoic acid (butyrate) in the plasma.

Bars represent the mean + standard error of the mean (SEM) of raw peak intensities of butanoic acid relative to vehicle control (BBS/HC). Sample sizes: BBS/HC, *n* = 8; BBS/IS, *n* = 6; NCTC/HC, *n* = 8; NCTC/IS, *n* = 8; ATCC/HC, *n* = 7; ATCC/IS, *n* = 8. There were no significant differences between the groups based on fold change analysis or independent samples *t*-tests using FDR-adjusted *p*-values. Abbreviations: ATCC, *M. vaccae* ATCC 15483; BBS, borate-buffered saline; HC, home cage control conditions; IS, inescapable tail shock; NCTC, *M. vaccae* NCTC 11659.

Supplementary tables

Supplementary Table 5.1 List of metabolites whose abundance was altered by a main effect of treatment (*M. vaccae* NCTC 11659, *M. vaccae* ATCC 15483, or BBS), a main effect of stress (IS or HC), and interaction effects of treatment x stress in the generalized linear model, ordered by *p*-value.

Effect of treatment	
Metabolite	***p*-value**
acetylcarnitine (acyl-C2)	0.0176

acetylcholine	0.0350
thymine	0.0538
acyl-C3 (propionylcarnitine)	0.0629
phenylalanine	0.0731
anthranilate	0.0760
nonanoic acid (pelargonate)	0.0774
2',3'-cyclic CMP	0.0780
Effect of stress	
Metabolite	***p*-value**
acetylcarnitine (acyl-C2)	0.0117
creatine	0.0142
asparagine	0.0147
threonine	0.0152
serine	0.0161
2',3'-cyclic CMP	0.0211
glutamate	0.0246
nonanoic acid (pelargonate)	0.0269
acetylcholine	0.0280
phenylalanine	0.0285
5-oxoproline	0.0299
propionylcarnitine (acyl-C3)	0.0323
AMP	0.0362
aspartate	0.0369
kynurenine	0.0381
cytosine	0.0382
glutamine	0.0389
citrulline	0.0401
citrate	0.0405
indolepyruvate	0.0406
pyridoxamine-5'-phosphate	0.0410
glutathione	0.0460
spermine	0.0497
adrenaline	0.0507
UDP	0.0742
putrescine	0.0749
dopamine	0.0766
3',5'-cyclic IMP	0.0771
creatinine	0.0845
thymine	0.0894
nicotinate ribonucleotide	0.0913
5-hydroxykynurenamine	0.0951

alanine	0.0995
Effect of treatment x stress	
Metabolite	***p*-value**
acetylcarnitine (acyl-C2)	0.0257
nonanoic acid (pelargonate)	0.0403
acetylcholine	0.0658
thymine	0.0786
AMP	0.0883
UDP	0.0980

Supplementary Table 5.2 Effects of immunization with either *M. vaccae* NCTC 11659 or *M. vaccae* ATCC 15483 on the plasma metabolome in home cage control animals, ordered by fold change.

Immunization with *M. vaccae* NCTC 11659		
Metabolite	**Fold change**	**Log2(fold change)**
nicotinate ribonucleotide	48.8	5.61
pyridoxamine 5'-phosphate	13.3	3.74
2-aminomuconate	6.96	2.80
glycolate	6.46	2.69
5-hydroxykynurenamine	5.70	2.51
γ-glutamyl-γ-aminobutyrate	4.27	2.10
mercaptopyruvate	3.97	1.99
spermine	3.35	1.75
3-sulfocatechol	2.87	1.52
4-phosphopantothenate	2.69	1.43
2',3'-cyclic CMP	2.58	1.37
dopamine	2.57	1.36
inositol 1-2-3-5-6-pentakisphosphate	2.48	1.31
N-acetylcitrulline	2.13	1.09
decenoylcarnitine (acyl-C10:1)	2.00	1.00
5-hydroxyindoleacetate	0.392	-1.35
indole-3-acetaldehyde	0.189	-2.40
Immunization with *M. vaccae* ATCC 15483		
Metabolite	**Fold change**	**Log2(fold change)**
nicotinate D-ribonucleotide	53.3	5.74
pyridoxamine 5'-phosphate	19.6	4.29
glycolate	6.43	2.68
2-aminomuconate	5.81	2.54
spermine	5.60	2.49

3-sulfocatechol	5.39	2.43
5-hydroxykynurenamine	4.65	2.22
inositol 1-2-3-5-6-pentakisphosphate	4.64	2.22
4-pyridoxate	4.59	2.20
γ-glutamyl-γ-aminobutyrate	4.36	2.13
mercaptopyruvate	4.11	2.04
N-acetylcitrulline	2.64	1.40
dopamine	2.60	1.38
acyl-C4-DC	2.39	1.25
propionylcarnitine (acyl-C3)	2.22	1.15
2-hydroxyglutarate/citramalate	2.19	1.13
2',3'-cyclic CMP	2.12	1.08
itaconate	2.08	1.06
2-oxoglutaramate	2.08	1.05
4-acetamidobutanoate	2.07	1.05
kynurenine	0.419	-1.26
5-hydroxyindoleacetate	0.392	-1.35
AMP	0.371	-1.43
indole-3-acetaldehyde	0.122	-3.04

Supplementary Table 5.3 Effects of inescapable tail shock stress (IS) on the plasma metabolome in borate-buffered saline (BBS)-treated animals, ordered by fold change and FDR-adjusted *p*-value.

Metabolite	Fold change	Log2(fold change)
nicotinate ribonucleotide	137	7.10
5-hydroxyindoleacetate	62.5	5.97
pyridoxamine 5'-phosphate	41.2	5.36
spermine	9.82	3.30
5-hydroxykynurenamine	8.96	3.16
inositol 1-2-3-5-6-pentakisphosphate	8.53	3.09
γ-glutamyl-γ-aminobutyrate	7.93	2.99
2-aminomuconate	7.47	2.90
glycolate	5.73	2.52
dopamine	4.43	2.15
2',3'-cyclic CMP	4.24	2.09
decenoylcarnitine (acyl-C10:1)	4.15	2.05
D-4-phosphopantothenate	4.02	2.01
octanoylcarnitine (acyl-C8)	3.57	1.83
adrenaline	3.06	1.61

diphosphate	2.86	1.52
propionylcarnitine (acyl-C3)	2.86	1.51
hexadecenoic acid	2.63	1.39
tetradecenoic acid	2.62	1.39
creatine	2.51	1.33
2-oxoglutaramate	2.42	1.28
N-acetylcitrulline	2.42	1.27
6-phospho-gluconate	2.39	1.26
mercaptopyruvate	2.27	1.19
leucine and isoleucine	2.22	1.15
acyl-C4-DC	2.18	1.13
3-sulfocatechol	2.18	1.12
inosine	2.13	1.09
folate	2.08	1.06
phosphoserine	2.05	1.04
methionine	2.04	1.03
linoleate	2.03	1.02
citrate	0.498	-1.01
glutathione disulfide	0.496	-1.01
putrescine	0.467	-1.10
citrulline	0.464	-1.11
phenylalanine	0.449	-1.15
indolepyruvate	0.418	-1.26
glutamate	0.363	-1.46
allantoin	0.360	-1.47
kynurenine	0.319	-1.65
AMP	0.287	-1.80
indole-3-acetaldehyde	0.0772	-3.69

Metabolite	***t*-statistic**	**FDR-adjusted *p*-value**
creatine	5.43	0.0233
cytosine	4.49	0.0318
indolepyruvate	-4.48	0.0318
adrenaline	4.24	0.0318
propionylcarnitine (acyl-C3)	4.20	0.0318
serine	-4.16	0.0318
threonine	-4.10	0.0318
5-oxoproline	-3.92	0.0332
allantoin	-3.92	0.0332
citrulline	-3.88	0.0332

glutamine	-3.75	0.0374
pyridoxamine 5'-phosphate	3.70	0.0374
γ-glutamyl-alanine	-3.66	0.0374
kynurenine	-3.63	0.0374
asparagine	-3.55	0.0407
choline	3.49	0.0416
5-hydroxykynurenamine	3.47	0.0416
methionine	3.32	0.0513
phenylalanine	-3.18	0.0624
glutamate	-3.16	0.0624
leucine and isoleucine	3.09	0.0666
2',3'-cyclic CMP	3.07	0.0666
2-aminomuconate	3.03	0.0692
citrate	-3.00	0.0693
acetylcholine	2.98	0.0693
creatinine	2.94	0.0721
acetylcarnitine (acyl-C2)	2.82	0.0844
dopamine	2.78	0.0844
aspartate	-2.78	0.0844
histidine	2.75	0.0844
pyridoxal	2.75	0.0844
3',5'-cyclic IMP	2.74	0.0844
phosphoserine	2.73	0.0844
spermine	2.62	0.0978
guanidinoacetate	-2.62	0.0978

Supplementary Table 5.4 Pathway analysis of metabolites altered in the plasma after IS exposure in BBS-treated animals, as ordered by *p*-value.

Pathway	Total	Expected	Hits*	Raw *p*-value	FDR-adjusted *p*-value	Impact
aminoacyl-tRNA biosynthesis	48	1.59	10	0.0000016	0.00013	0.17
alanine, aspartate and glutamate metabolism	28	0.93	6	0.00021	0.0089	0.53
arginine biosynthesis	14	0.46	4	0.00084	0.023	0.35
tryptophan metabolism	41	1.36	6	0.0018	0.038	0.14
glyoxylate and dicarboxylate metabolism	32	1.06	5	0.0033	0.056	0.15
glycine, serine and threonine metabolism	34	1.13	5	0.0044	0.061	0.30

histidine metabolism	16	0.53	3	0.014	0.14	0.22
nitrogen metabolism	6	0.20	2	0.015	0.14	0.00
D-glutamine and D-glutamate metabolism	6	0.20	2	0.015	0.14	0.50
cysteine and methionine metabolism	33	1.09	4	0.021	0.18	0.15
valine, leucine and isoleucine biosynthesis	8	0.27	2	0.027	0.20	0.00
beta-alanine metabolism	21	0.70	3	0.030	0.21	0.06
vitamin B6 metabolism	9	0.30	2	0.033	0.21	0.54
arginine and proline metabolism	38	1.26	4	0.034	0.21	0.12
glutathione metabolism	28	0.93	3	0.063	0.35	0.05
nicotinate and nicotinamide metabolism	15	0.50	2	0.086	0.45	0.19
phenylalanine, tyrosine and tryptophan biosynthesis	4	0.13	1	0.13	0.60	0.50
pantothenate and CoA biosynthesis	19	0.63	2	0.13	0.60	0.02
linoleic acid metabolism	5	0.17	1	0.16	0.69	1.00
purine metabolism	66	2.19	4	0.17	0.72	0.06
one carbon pool by folate	9	0.30	1	0.26	1.00	0.00
phenylalanine metabolism	12	0.40	1	0.33	1.00	0.36
butanoate metabolism	15	0.50	1	0.40	1.00	0.00
tyrosine metabolism	42	1.39	2	0.41	1.00	0.14
citrate cycle (TCA cycle)	20	0.66	1	0.49	1.00	0.09
sphingolipid metabolism	21	0.70	1	0.51	1.00	0.00
pentose phosphate pathway	21	0.70	1	0.51	1.00	0.13
folate biosynthesis	27	0.89	1	0.60	1.00	0.00
porphyrin and chlorophyll metabolism	30	0.99	1	0.64	1.00	0.00
biosynthesis of unsaturated fatty acids	36	1.19	1	0.71	1.00	0.00
pyrimidine metabolism	39	1.29	1	0.74	1.00	0.00
valine, leucine and isoleucine degradation	40	1.33	1	0.74	1.00	0.00

*acyl-C4-DC, decenoylcarnitine (acyl-C10:1), and octanoylcarnitine (acyl-C8) were not annotated in MetaboAnalyst for pathway analysis.

Supplementary Table 5.5 Effects of IS, among animals immunized with either *M. vaccae* NCTC 11659 or *M. vaccae* ATCC 15483, on the plasma metabolome, ordered by fold change.

Effects of IS among animals immunized with *M. vaccae* NCTC 11659		
Metabolite	**Fold change**	**Log2(fold change)**
5-hydroxyindoleacetate	175	7.45
hexadecenoic acid	2.05	1.03
glutathione	0.469	-1.09
citrate	0.458	-1.13
guanidinoacetate	0.424	-1.24
AMP	0.390	-1.36
succinate	0.296	-1.76
Effects of IS among animals immunized with *M. vaccae* ATCC 15483		
Metabolite	**Fold change**	**Log2(fold change)**
5-hydroxyindoleacetate	198	7.63
maltose	3.57	1.83
4-phosphopantothenate	3.21	1.68
homocarnosine	2.32	1.21
6-phospho-gluconate	2.15	1.11
diphosphate	2.07	1.05
glycero-3-phosphoethanolamine	2.00	1.00
citrate	0.44	-1.17
dehydroascorbate	0.43	-1.21
guanidinoacetate	0.36	-1.49

Supplementary Table 5.6 Effects of immunization with either *M. vaccae* NCTC 11659 or *M. vaccae* ATCC 15483, on the plasma metabolome of animals exposed to IS, ordered by fold change.

Immunization with *M. vaccae* NCTC 11659		
Metabolite	**Fold change**	**Log2(fold change)**
allantoin	2.5	1.31
mercaptopyruvate	2.4	1.24
indole-3-acetaldehyde	2.05	1.03
pyridoxamine 5'-phosphate	0.49	-1.02
tetradecenoic acid	0.38	-1.40
inositol 1-2-3-5-6-pentakisphosphate	0.32	-1.66
Immunization with *M. vaccae* ATCC 15483		
Metabolite	**Fold change**	**Log2(fold change)**
maltose	5.8	2.55

mercaptopyruvate	3.4	1.77
4-pyridoxate	3.16	1.66
tryptophanamide	2.19	1.13
glutathione disulfide	2.17	1.12

Supplementary Table 5.7 Correlations between adrenaline and metabolites involved in tryptophan metabolism that were significantly altered in the GLM or pairwise comparisons.

Correlation with adrenaline	Pearson's *r*
tryptophan	0.671***
kynurenine	–0.690***
kynurenine/tryptophan	–0.654***
5-hydroxyindoleacetate	0.018
5-hydroxykynurenamine	0.686***
2-aminomuconate	0.653***
anthranilate	–0.250
indole-3-acetylaldehyde	–0.001
indolepyruvate	–0.774***

Appendix 5. Chapter 6 supplementary material

Supplementary figures

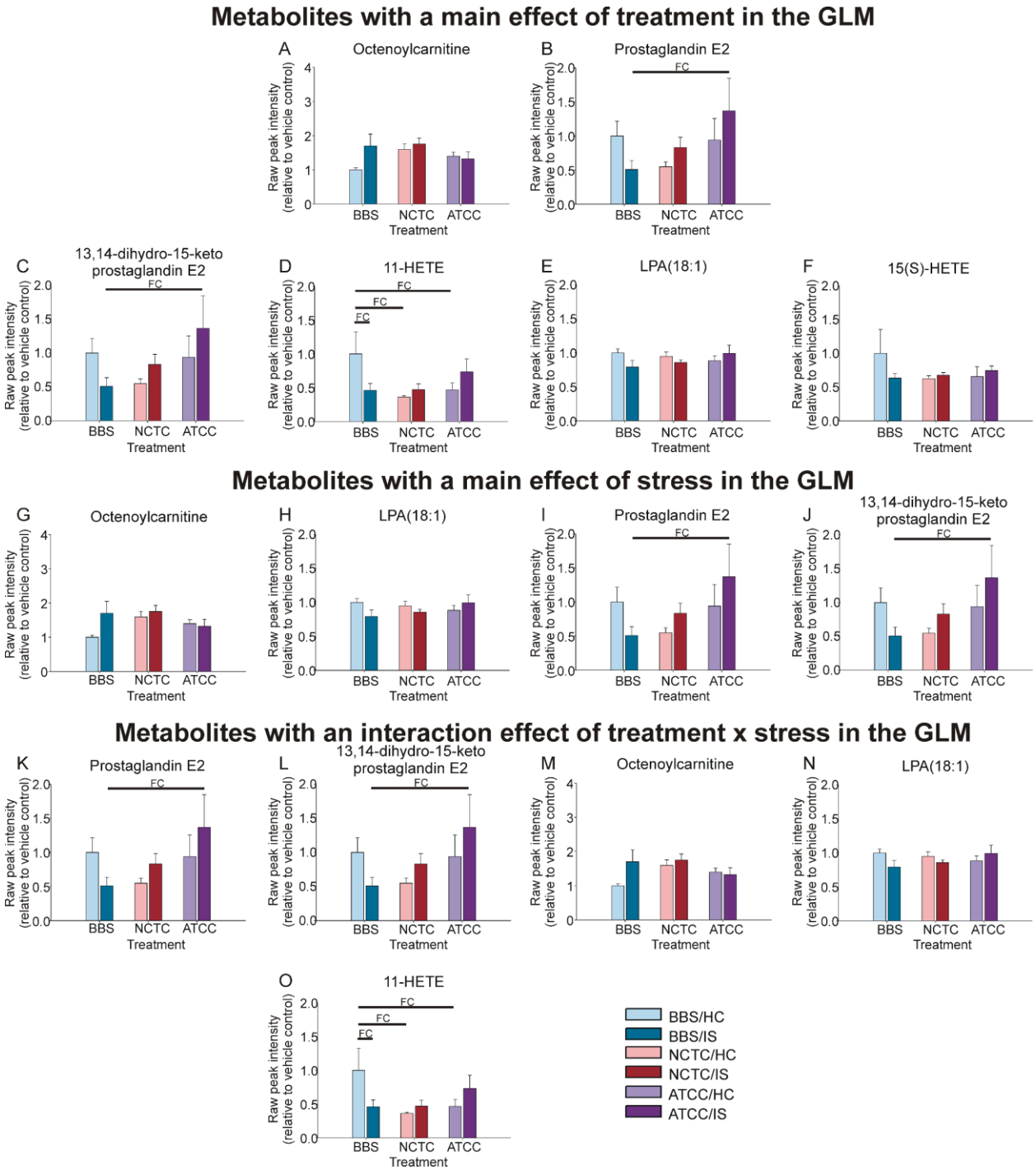

Supplementary Figure 6.1 Plasma lipids whose abundances were altered by a main effect of treatment, a main effect of stress, or an interaction effect of treatment x stress in the generalized linear model (GLM), ordered within each subheading by *p*-value.

There was a main effect of treatment on (A) octenoylcarnitine (acyl-C8:1), (B) prostaglandin E2, (C) 13,14-dihydro-15-keto prostaglandin E2, (D) 11-HETE, (E) LPA(18:1), and (F) 15(S)-HETE; there was a main effect of stress on (G) octenoylcarnitine (acyl-C8:1), (H) LPA(18:1), (I) prostaglandin E2, and (J) 13,14-dihydro-15-keto prostaglandin E2; and there was an interaction effect of treatment x stress on (K) prostaglandin E2, (L) 13,14-dihydro-15-keto prostaglandin E2, (M) octenoylcarnitine (acyl-C8:1), (N) LPA(18:1), and (O) 11-HETE. Bars represent the mean + standard error of the mean (SEM) of raw peak intensities of metabolites relative to vehicle control (BBS/HC). Sample sizes: BBS/HC, *n* = 8; BBS/IS, *n* = 6; NCTC/HC, *n* = 8; NCTC/IS, *n* = 8; ATCC/HC, *n* = 7; ATCC/IS, *n* = 8. FC, fold change difference. Abbreviations: ATCC, *M. vaccae* ATCC 15483; BBS, borate-buffered saline; HC, home cage control conditions; HETE, hydroxyeicosatetraenoic acid; IS, inescapable tail shock; LPA, lysophosphatidic acid; NCTC, *M. vaccae* NCTC 11659.

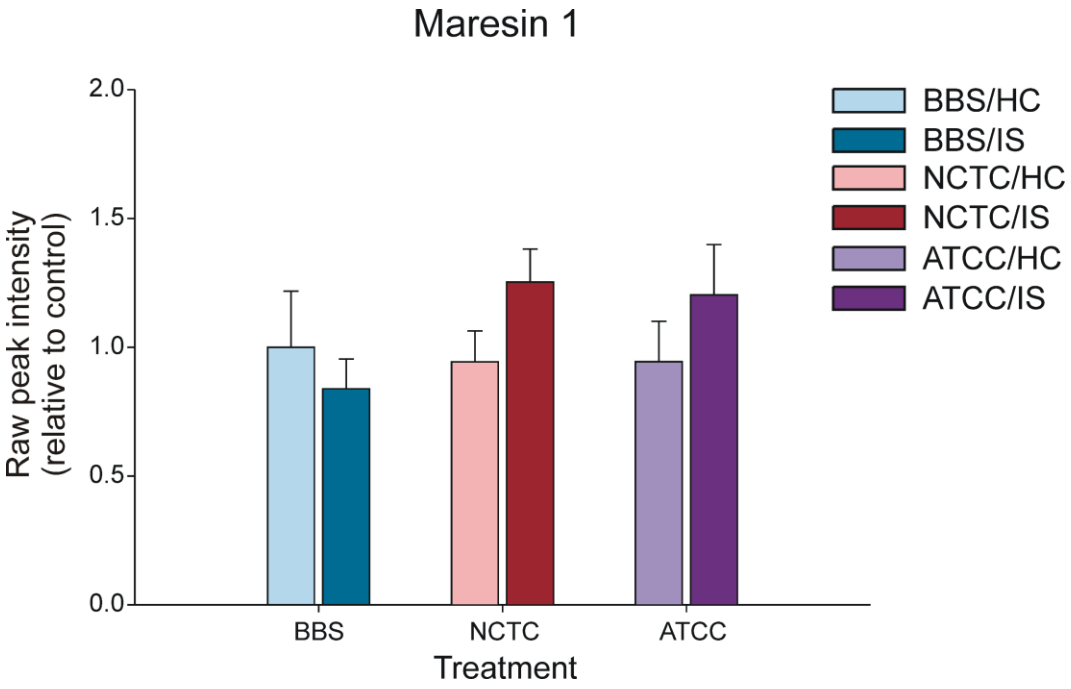

Supplementary Figure 6.2 Effects of immunization with either *M. vaccae* NCTC 11659 (NCTC) or *M. vaccae* ATCC 15483 (ATCC) and inescapable tail shock (IS) on abundances of maresin 1 in the plasma. Bars represent the mean + standard error of the mean (SEM) of raw peak intensities of maresin 1 relative to vehicle control (BBS/HC).

Sample sizes: BBS/HC, *n* = 8; BBS/IS, *n* = 6; NCTC/HC, *n* = 8; NCTC/IS, *n* = 8; ATCC/HC, *n* = 7; ATCC/IS, *n* = 8. There were no significant differences between the groups based on fold change analysis or independent samples *t*-tests using FDR-adjusted *p*-values. Abbreviations: ATCC, *M. vaccae* ATCC 15483; BBS, borate-buffered saline; HC, home cage control conditions; IS, inescapable tail shock; NCTC, *M. vaccae* NCTC 11659.

Supplementary tables

Supplementary Table 6.1 List of lipids whose abundance was altered by a main effect of treatment (*M. vaccae* NCTC 11659, *M. vaccae* ATCC 15483, or BBS), a main effect of stress (IS or HC), and interaction effects of treatment x stress in the generalized linear model, ordered by *p*-value.

Effect of treatment	
Lipid	***p*-value**
octenoylcarnitine (acyl-C8:1)	0.0357
prostaglandin E2	0.0836
13,14-dihydro-15-keto prostaglandin E2	0.0836
11-HETE	0.0893
LPA(18:1)	0.0948
15(S)-HETE	0.0997
Effect of stress	
Lipid	***p*-value**
octenoylcarnitine (acyl-C8:1)	0.0140
LPA(18:1)	0.0308
prostaglandin E2	0.0372
13,14-dihydro-15-keto prostaglandin E2	0.0372
Effect of treatment x stress	
Lipid	***p*-value**
prostaglandin E2	0.0241
13,14-dihydro-15-keto prostaglandin E2	0.0241
octenoylcarnitine (acyl-C8:1)	0.0329
LPA(18:1)	0.0583
11-HETE	0.0799

Supplementary Table 6.2 Pathway analysis of lipids altered in the plasma by pairwise comparisons.

Effect of *M. vaccae* NCTC 11659 among home cage control animals						
Pathway	**Total**	**Expected**	**Hits**	**Lipids**	**Raw *p*-value**	**FDR-adjusted *p*-value**
primary bile acid biosynthesis	46	0.244	2	taurocholic acid; chenodeoxycholic acid	0.0227	1
taurine and hypotaurine metabolism	8	0.0424	1	taurocholic acid	0.0417	1

Effect of *M. vaccae* ATCC 15483 among home cage control animals						
Pathway	**Total**	**Expected**	**Hits**	**Lipids**	**Raw *p*-value**	**FDR-adjusted *p*-value**
biosynthesis of unsaturated fatty acids	36	0.1193	2	arachidonic acid; n-3 DPA	0.0053	0.44447
arachidonic acid metabolism	36	0.1193	1	arachidonic acid	0.1139	1
Effect of IS among vehicle-treated animals						
Pathway	**Total**	**Expected**	**Hits**	**Lipids**	**Raw *p*-value**	**FDR-adjusted *p*-value**
Biosynthesis of unsaturated fatty acids	36	0.04771	1	arachidonic acid	0.0472	1
Arachidonic acid metabolism	36	0.04771	1	arachidonic acid	0.0472	1
Effect of IS among animals immunized with *M. vaccae* NCTC 11659						
Pathway	**Total**	**Expected**	**Hits**	**Lipids**	**Raw *p*-value**	**FDR-adjusted *p*-value**
primary bile acid biosynthesis	46	0.122	1	chenodeoxycholic acid	0.117	1
Effect of IS among animals immunized with *M. vaccae* ATCC 15483						
Pathway	**Total**	**Expected**	**Hits**	**Lipids**	**Raw *p*-value**	**FDR-adjusted *p*-value**
na	–	–	–	–	–	–

Supplementary Table 6.3 Effects of immunization with either *M. vaccae* NCTC 11659 or *M. vaccae* ATCC 15483, on the plasma lipidome of animals exposed to IS, ordered by fold change.

Immunization with *M. vaccae* NCTC 11659		
Metabolite	**Fold change**	**Log2(fold change)**
taurochenodeoxycholic acid	2.1	1.06
deoxycholic acid	2.0	1.03
Immunization with *M. vaccae* ATCC 15483		
Metabolite	**Fold change**	**Log2(fold change)**
prostaglandin E2	2.7	1.43
13,14-dihydro-15-keto prostaglandin E2	2.7	1.43
18-HEPE	2.15	1.10
13,14-dihydro-15-keto prostaglandin D2	2.02	1.01